

600833

APL-TDR-64-53

295-P-4.00

INVESTIGATION OF POWER CONVERSION
AND
GENERATION TECHNIQUES

TECHNICAL DOCUMENTARY REPORT NO. APL-TDR-64-53

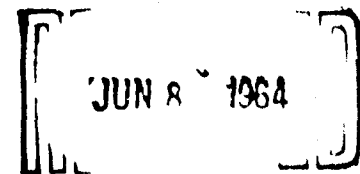
MAY 15, 1964

Research and Technology Division
Air Force Systems Command
Wright-Patterson Air Force Base, Ohio

Project No. 8128, Task No. 812808

(Prepared under Contract No. AF33(657)-11049 by
North American Aviation, Inc., Los Angeles Division
Los Angeles, California 90009

J. J. Pierro, J. E. Phillips, E. Cima, L. Luera
S. J. Nalbandian, R. L. Montague, L. Opel, M. Hansen
H. Rosenfeld, D. Dickson, and J. A. Korbanski, Authors)



HIA F

NOTICES

When Government drawings, specifications, or other data are used for any purpose other than in connection with a definitely related Government procurement operation, the United States Government thereby incurs no responsibility nor any obligation whatsoever; and the fact that the Government may have formulated, furnished, or in any way supplied the said drawings, specifications, or other data, is not to be regarded by implication or otherwise as in any manner licensing the holder or any other person or corporation, or conveying any rights or permission to manufacture, use, or sell any patented invention that may in any way be related thereto.

Qualified requesters may obtain copies of this report from the Defense Documentation Center (DDC), (formerly ASTIA), Cameron Station, Bldg. 5, 5010 Duke Street, Alexandria 4, Virginia

This report has been released to the Office of Technical Services, U.S. Department of Commerce, Washington 25, D.C., for sale to the general public.

Copies of this report should not be returned to the Aeronautical Systems Division unless return is required by security considerations, contractual obligations, or notice on a specific document.

APL-TDR-64-53

**INVESTIGATION OF POWER CONVERSION
AND
GENERATION TECHNIQUES**

TECHNICAL DOCUMENTARY REPORT NO. APL-TDR-64-53

MAY 15, 1964

**Research and Technology Division
Air Force Systems Command
Wright-Patterson Air Force Base, Ohio**

Project No. 8128, Task No. 812808

**(Prepared under Contract No. AF33(657)-11049 by
North American Aviation, Inc., Los Angeles Division
Los Angeles, California 90009**

**J. J. Pierro, J. E. Phillips, E. Cima, L. Luera
S. J. Nalbandian, R. L. Montague, L. Opel, M. Hansen
H. Rosenfeld, D. Dickson, and J. A. Korbanski, Authors)**

FOREWORD

This report was prepared by J. E. Phillips, Emil Cima, and Larry Luera, of the Los Angeles Division of North American Aviation, Inc., on Air Force Contract No. AF33(657)-11049. The study effort was administered under the direction of the Research and Technology Division, Wright-Patterson Air Force Base, with Captain Harold L. Briggs as the Project Officer. The analytical effort upon which the report is based was accomplished or directed by the Energy Conversion Group of the Research and Development Division of North American Aviation. Experimental analyses were performed by the Electrical Laboratory of North American Aviation, Inc.

Mr. J. J. Pierro, Principal Scientist of Avionics and Mr. W. Daniels, Jr., Manager of Applied Science were responsible for the work covered under Contract No. AF33(657)-11049. Research started on April 15, 1963 and was completed on February 15, 1964.

Special recognition is due Ron Montague for the static transistor converter designs and to Matt Hansen and Larry Opel for assistance in the area of electromagnetic techniques and generator design. Floyd Pixley and H. Harvey of the Laboratory gave admirable assistance in performing the core loss and transistor response tests.

J. E. Phillips
Emil Cima
Larry Luera

ABSTRACT

Contract objectives called for an analytic and experimental investigation of techniques whereby an efficient and lightweight power conversion unit can be provided. The conversion unit is to be used to supply high-frequency electric power to accelerate plasmas in an electric propulsion engine. Various conversion and power generation techniques were reviewed in the early part of the study before approaches and concepts were established. In addition to the converter concepts, an additional investigation of high-frequency power generation was performed. After the preliminary investigation, an analysis of possible approaches for conversion of 60 KW of SNAP 8 type of power and 300 KW of SPUR type of power was made and conceptual designs established. Three converter techniques in addition to a high-frequency generator concept were evaluated; namely, a motor-generator unit, a static transistor unit and a static tube unit.

Parametric data was derived and is included in this report to show component losses, size and weight. Problem areas under each conversion technique have been outlined and areas for future applied research recommended.

PUBLICATION REVIEW

The content of this report represents the scientific findings of an Air Force sponsored program. Publication of this technical documentary report does not constitute Air Force approval of the findings. It is published only for the exchange and stimulation of ideas.

TABLE OF CONTENTS

Section		Page
	INTRODUCTION	1
	PROGRAM SUMMARY	2
I	HIGH-FREQUENCY POWER GENERATION TECHNIQUES	14
	ELECTROMAGNETIC GENERATORS	14
	ELECTROSTATIC GENERATORS	29
	ROTARY CONVERTER TECHNIQUES	33
	STATIC CONVERTER TECHNIQUES	34
II	CONCEPTUAL CONVERTER DESIGNS	62
	STATIC TRANSISTOR CONVERTER DESIGNS	63
	STATIC TUBE CONVERTER DESIGNS	88
	MOTOR-GENERATOR DESIGN CONCEPT	111
III	HIGH-FREQUENCY GENERATOR CONCEPT	136
IV	RELATED STUDIES	154
	ENVIRONMENT	154
	APPROACH TO SYSTEM COOLING	159
	ANALYSIS OF MATERIALS	176
	RADIATION RESISTANCE OF CONVERTER COMPONENTS	197
	RELIABILITY	205
V	EXPERIMENTAL STUDIES	209
VI	CONCLUSIONS AND RECOMMENDATIONS	241
	BIBLIOGRAPHY	245
	APPENDIX	247
	TRANSFORMER DESIGN ANALYSIS	249
	ANALYSIS OF SCR FREQUENCY POWER CONVERTER	252
	TRANSISTOR POWER CAPABILITIES	256

LIST OF ILLUSTRATIONS

<u>FIGURE NO.</u>	<u>TITLE</u>	<u>PAGE</u>
1.	Comparison of Weight vs. Frequency for 60 KW and 300 Converter Units.	4
2.	Comparison of Efficiency vs. Frequency for 60 KW and 300 KW Converter Units.	5
3.	Comparison of Weight and Efficiency vs. Frequency for High-Frequency Generator.	7
4.	Analysis of System Weight vs. Temperature for 60 KW Converters.	8
5.	Analysis of System Weight vs. Temperature for 300 KW Converter.	9
6.	Analysis of System Weight vs. Temperature for High Frequency Generator.	11
7.	Comparison of High Frequency (50 to 200 KC) Generator with SPUR Type Generator Plus Static Converter Unit.	12
8.	Weight vs. Frequency Comparison of High Frequency (50 to 200 KC) Generator with SPUR Type Generator Plus Static Converter Unit.	13
9.	Power vs. Frequency for Rotating Generators.	16
10.	Estimated Weight vs. Frequency for Rotating Generators	17
11.	Electromagnetic Generator Concept (Perspective)	18
12.	Generator Concept "A".	19
13.	Generator Concept "B".	21
14.	Generator Concept "C".	22
15.	Flux Switch Generator Concept "D".	23
16.	Generator Concepts "E" and "F".	25
17.	Specific Weights of Practical Electrostatic and Electromagnetic Designs.	30
18.	Electrostatic Generator Techniques.	31
19.	Comparison of Semiconductor Devices.	35

LIST OF ILLUSTRATIONS (Continued)

<u>FIGURE NO.</u>	<u>TITLE</u>	<u>PAGE</u>
20.	SCR Frequency Chager Techniques.	37
21.	SCR Inverter Schemes.	39
22.	Transistor Inverter Techniques.	41
23.	High Voltage Dual Transformer Converter.	42
24.	Other Inverter Schemes.	44
25.	RF Generator Tube System Schematic.	49
26.	Basic RF Generator Tank Circuits.	50
27.	Power Supply Rectifier Circuits for RF Generator.	53
28.	RF Tubes Available for Oscillator Use.	54
29.	Magnetic Multiplier Techniques.	56
30.	Transformer Parameter Analysis.	60
31.	60 KW Static Transistor Converter (Perspective)	64
32.	Preliminary Schematic of 60 KW Static Transistor 1 ϕ .	67
33.	Preliminary Schematic of 60 KW Static Transistor 3 ϕ .	68
34.	Preliminary Schematic of 300 KW Static Transistor 1 ϕ .	73
35.	Preliminary Schematic of 300 KW Static Transistor 3 ϕ .	74
36.	Preliminary Mechanical Design of 60 KW, 1 ϕ , 200 KC Static Transistor Converter (Typical of 50 and 800 KC Designs.	79
37.	Preliminary Mechanical Design of 60 KW, 3 ϕ , 200 KC Static Transistor Converter (Typical of 50 and 800 KC Designs.	80
38.	Preliminary Mechanical Design of 300 KW, 1 ϕ , 200 KC Static Transistor Converter (Typical of 50 and 800 KC Designs.	81

LIST OF ILLUSTRATIONS(Continued)

<u>FIGURE NO.</u>	<u>TITLE</u>	<u>PAGE</u>
39.	Preliminary Mechanical Design of 300 KW, 3 ϕ , 200 KC Static Transistor Converter (Typical of 50 and 800 KC Designs.	82
40.	Thermal Flow Diagram for Static Transistor Converter.	85
41.	Thermal Flow Diagram for 60 KW and 300 KW Static Transistor Converter.	86
42.	Analysis of System Weight vs. Temperature for Static Transistor Converter (60 KW and 300 KW).	87
43.	Static Tube Converter Unit (Perspective).	89
44.	Preliminary Schematic of Static Tube 1 ϕ Converter.	91
45.	Preliminary Schematic of Static Tube 3 ϕ Converter.	92
46.	Thyatron Control Technique.	96
47.	Preliminary Mechanical Design of 60 KW, 1 ϕ , 200 KC Static Tube Converter (Typical of 50 KC and 800 KC).	101
48.	Preliminary Mechanical Design of 60 KW, 3 ϕ , 200 KC Static Tube Converter (Typical of 50 KC and 800 KC).	104
49.	Preliminary Mechanical Design of 300 KW, 1 ϕ , 200 KC Static Tube Converter (Typical of 50 KC and 800 KC).	105
50.	Preliminary Mechanical Design of 300 KW, 3 ϕ , 200 KC Static Tube Converter (Typical of 50 KC and 800 KC).	106
51.	Analysis of System Weight vs. Temperature for Static Tube Converter (60 KW and 300 KW).	107
52.	Thermal Flow Diagram of 60 KW Static Tube Converter.	109
53.	Thermal Flow Diagram of 300 KW Static Tube Converter.	110
54.	Motor Generator Unit (Perspective).	112
55.	Details of Basic Generator Concept.	116
56.	NADYNE Synchronous Motor Details.	118

LIST OF ILLUSTRATIONS(Continued)

<u>FIGURE NO.</u>	<u>TITLE</u>	<u>PAGE</u>
57.	Preliminary Mechanical Design of 60 KW, 1 ϕ , 50 KC Motor Generator.	121
58.	Preliminary Mechanical Design of 60 KW, 1 ϕ , 100 KC Motor Generator.	122
59.	Preliminary Mechanical Design of 60 KW, 1 ϕ , 200 KC Motor Generator.	123
60.	Preliminary Mechanical Design of 60 KW, 3 ϕ , 50 KC Motor Generator (Typical of 100 KC and 200 KC).	124
61.	Preliminary Mechanical Design of 300 KW, 1 ϕ , 50 KC Motor Generator.	128
62.	Preliminary Mechanical Design of 300 KW, 1 ϕ , 100 KC Motor Generator.	129
63.	Preliminary Mechanical Design of 300 KW, 1 ϕ , 200 KC Motor Generator.	130
64.	Preliminary Mechanical Design of 300 KW, 3 ϕ , 50 KC Motor Generator (Typical of 100 KC and 200 KC).	131
65.	Analysis of System Weight vs. Temperature for Motor Generator (2 figures) (60 KW and 300 KW).	132
66.	Thermal Flow Diagram for 60 KW and 300 KW Motor Generator.	133
67.	Efficiency vs. Temperature for a Motor-Generator Converters.	134
68.	Basic High-Frequency Generator Configuration (Perspective).	137
69.	Preliminary Mechanical Design of 50 KC High-Frequency Generator.	140
70.	Preliminary Mechanical Design of 100 KC High-Frequency Generator.	141
71.	Preliminary Mechanical Design of 200 KC High-Frequency Generator.	143
72.	Analysis of System Weight vs. Temperature for High-Frequency Generator.	147
73.	Thermal Flow Diagram for High-Frequency Generator.	148

LIST OF ILLUSTRATIONS(Continued)

<u>FIGURE NO.</u>	<u>TITLE</u>	<u>PAGE</u>
74.	Efficiency vs. Temperature for High-Frequency Generator Concept.	150
75.	Efficiency vs. Weight for Various Generator Materials.	151
76.	Weight vs. Temperature for HYMU 80 Material.	153
77.	Weight vs. Temperature for Silicon Steel.	153
78.	Proton Intensity with Typical Earth Orbits.	157
79.	Analysis of Cooling System Weight vs. System Operating Temperature.	160
80.	Typical Space Cooling System.	161
81.	Space Radiator Design Technique.	161
82.	Analysis of Radiator Area vs. Temperature.	163
83.	Fluid Flow Rate vs. Fluid Temperature Rise of OS-124.	169
84.	Typical Transformer Construction Showing Cooling Provisions.	171
85.	Transistor Cooling Concept.	173
86.	Transistor Mounting Considerations.	174
87.	Flux Density vs. Temperature for Various Materials.	177
88.	Hysteresis Loops of Various Magnetic Materials.	179
89.	Variation of Physical and Magnetic Properties of Electrical Steels.	180
90.	Flux Density vs. Core Loss for Various Materials.	182
91.	Flux Density vs. Core Loss for Various Materials.	183
92.	Core Loss vs. Temperature and Flux Density for 3-1/4% Silicon Steel.	185
93.	Core Loss vs. Temperature and Lamination Thickness for Various Materials.	186

LIST OF ILLUSTRATIONS(Continued)

<u>FIGURE NO.</u>	<u>TITLE</u>	<u>PAGE</u>
94.	Iron Loss Data for Generator Designs.	187
95.	Comparison of Yield Strength and Flux Densities.	190
96.	Yield Stress vs. Temperature for Magnetic Steels.	191
97.	Relative Radiation Tolerance of Various Materials.	198
98.	Radiation Tolerance of Capacitors and Resistors.	203
99.	Reliability Required for Various Mission.	206
100.	Core Loss vs. Frequency for Various Transformer Materials.	211
101.	Core Loss vs. Frequency for Various Transformer Materials. Including Ferrites.	212
102.	Transformer Core Output Voltage Waveforms.	215
103.	Transformer Core Output Voltage Waveforms (Including Ferrites).	218
104.	Laboratory Core Loss Test Circuits.	219
105.	Laboratory Test Set-up (50 KC).	220
106.	Laboratory Test Set-up (100 KC - 800 KC).	222
107.	Laboratory Test Set-up Showing Cores.	223
108.	Current Sharing Waveforms.	225
109A.	Frequency Response Waveforms (5 Parallel Transistors).	228
109B.	Frequency Response Waveforms (5 Parallel Transistors).	229
110A.	Frequency Response Waveforms (10 Parallel Transistors).	230
110B.	Frequency Response Waveforms (10 Parallel Transistors).	231
111A.	Frequency Response Waveforms (20 Farallel Transistors).	232
111B.	Frequency Response Waveforms (20 Parallel Transistors).	233
112.	Test Circuit Schematic.	236
113.	Test Set-up Showing Mounted Transistors.	238
114.	Test Set-up Showing Transistor and Instrumentation.	239

LIST OF ILLUSTRATIONS (Continued)

<u>FIGURE NO.</u>	<u>TITLE</u>	<u>PAGE</u>
115.	Test Set-up Showing Power Supplies.	240
116.	Schematic of 60 KW, 50 KC, SCR Inverter.	253
117.	Power-Frequency Material Relationship (1963).	257

LIST OF TABLES

TABLE NO.	TITLE	PAGE
1.	Summary of 60 KW Static Transistor Converter Parametric Data.	65
2.	Summary of 300 KW Static Transistor Converter Parametric Data.	71
3.	Preliminary Component List for 60 KW, 1 ϕ , Static Transistor Converter.	75
4.	Preliminary Component List for 60 KW, 3 ϕ , Static Transistor Converter.	76
5.	Preliminary Component List for 300 KW, 1 ϕ , Static Transistor Converter.	77
6.	Preliminary Component List for 300 KW, 3 ϕ , Static Transistor Converter.	78
7.	Summary of 60 KW Static Tube Converter Parametric Data.	90
8.	Summary of 300 KW Static Tube Converter Parametric Data.	93
9.	Preliminary Component List for 60 KW, 1 ϕ , Static Tube Converter.	97
10.	Preliminary Component List for 60 KW, 3 ϕ , Static Tube Converter.	98
11.	Preliminary Component List for 300 KW, 1 ϕ , Static Tube Converter.	99
12.	Preliminary Component List for 300 KW, 3 ϕ , Static Tube Converter.	100
13.	Summary of 60 KW Motor-Generator Parametric Data.	113
14.	Summary of 300 KW Motor-Generator Parametric Data.	114
15.	60 KW Motor-Generator Design Data (1 ϕ).	119
16.	60 KW Motor-Generator Design Data (3 ϕ).	120

LIST OF TABLES (Continued)

TABLE NO.	TITLE	PAGE
17	300 KW Motor-Generator Design Data (1 ϕ)	126
18	300 KW Motor-Generator Design Data (3 ϕ)	127
19	Summary of High-Frequency Generator Parametric Data	138
20	High-Frequency Generator Design Data	139
21	Summary of Coolants	164
22	Properties of Organic Coolants	166
23	Properties of Inorganic Coolants	167
24	Maximum Temperature of Transformer Insulations	195
25	Percentage Change in DC Magnetic Properties as Result of Irradiation	202
26	Parametric Data on Core Tests	213
27	Parametric Data on Core Tests	214
28	Current Sharing Results	226
29	Test Instrumentation	237
30	Preliminary Component List for SCR Converter	254

INTRODUCTION

A need exists for efficient and lightweight power conversion units for use with space power systems currently being developed. One of the several areas in which converters are needed is for supplying high-frequency, high-voltage power to accelerate plasma in an electric propulsion engine. The objective of this ten-month study effort, which began 15 April 1963, was to analytically investigate techniques for providing such specialized power requirements and to formulate conceptual designs for both 60 KW and 300 KW units. A second part of the study involved an analysis of component designs for the generation of high frequency electrical power.

Areas of general analysis included rotary-mechanical, frequency-changer, transformer and logical combinations of these converter devices. In arriving at specific conceptual converter and high frequency generator designs, related areas of materials, environment, cooling, and reliability were studied. Two areas of experimental investigation to support analytic effort included measurement of magnetic core loss magnitude at high frequencies and determination of transistor response in a high-frequency, power-chopper circuit.

Parametric data is included in this report in order that a comparison of motor-generator, static tube and static transistor converter techniques can be made in the frequency range of 50 to 800 kilocycles and the power range of 60 to 300 kilowatts.

Problem areas for each conversion technique are analyzed and areas for future applied science research are recommended.

PROGRAM SUMMARY

The investigation of techniques for converting power from SNAP 8 and SPUR type power systems for use in high-voltage, high-frequency electromagnetic propulsion units covered a variety of AC to AC power conversion methods. (The high frequency range in this study is from 50 KC to 800 KC and represents a power frequency range higher than that considered in conventional power systems. The expression "high frequency" is not to be mistaken for the HF frequency range of five to fifty MC used in communications.) Analysis of these conversion methods lead to the formulation of several techniques which appear most feasible for use in converting electric power at these levels and frequencies to high-frequency (50 KC to 800 KC), high-voltage power. Each of these techniques discussed in this report along with conceptual designs for three specific converter systems to meet the 60 KW and 300 KW power requirements. The three converter designs are: (1) a motor-generator concept, (2) a static transistor unit, and (3) a static tube concept.

A second part of the study involved analysis of techniques for generating high-frequency electric power directly from a turbine shaft output. A high-frequency electromagnetic generator was designed using a solid-rotor, static-winding technique and analyzed for use in meeting the requirements of the Work Statement. Parametric data and design drawings are included in the report to show the feasibility of such a machine.

General conclusions reached at the end of the study program are:

1. The transistor converter is lightest in weight and highest in efficiency both when considered as a separate unit and also when the total weight of converter and cooling system are considered. Total weight decreases with increasing temperature, but operating temperatures above 300°F coolant temperature produce very little weight decrease. From a reliability standpoint 300°F appears best.
2. The high-frequency (50 KC to 200 KC) generator concept is competitive with the transistorized converter design below about 50 KC, but not above. Even at frequencies up to 100 KC and above, a generator designed with an output frequency to match the requirement of an electromagnetic propulsion engine to be driven directly from the turbine should be considered since the absence of a converter unit increases the reliability of the conversion system and may be worth the additional weight in this frequency regime. Comparison of a turbine-driven generator with an output in the 50 KC to 200 KC range with a low frequency generator plus a converter is made later in this section.
3. The motor-generator converter is also competitive with the transistorized converter at the 50 KC level, but gets decidedly

heavier at the higher frequencies. The reliability of a motor-generator unit with its high temperature capability over a multi-transistor converter unit with temperature-limited transistors should be considered at the 50 KC to 100 KC level, even at the disadvantage of being heavier and less efficient than the transistorized converter.

4. Both the transistorized converter and the direct high-frequency generator offer a very important potential for application to lightweight ion engine systems as well as for the plasma engines of this study application. The high-frequency technique permits extremely lightweight transformer designs which, when applied to the ion engine system, may lead to less total weight than the more direct transformation and rectification of 1,000 or 3,200 cps power for DC ion engines. High-frequency power in the 60 to 300 KW power level is used in radio communication and also in induction heating techniques. In each of these areas the volume of equipment is not critical and in most instances efficiency of operation is not too critical. Nevertheless, r-f generation techniques appeared feasible in the early analysis and were explored further.

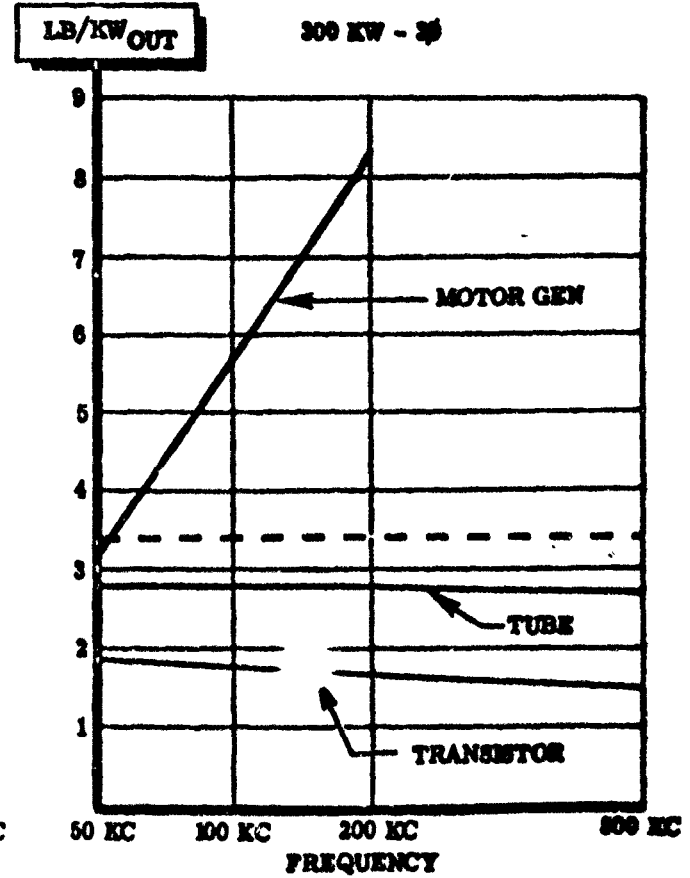
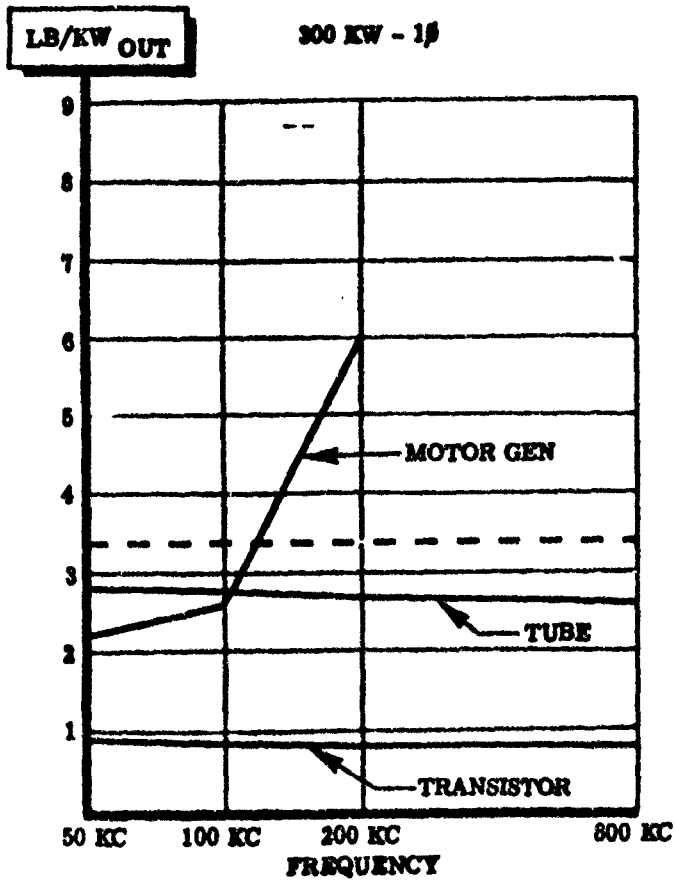
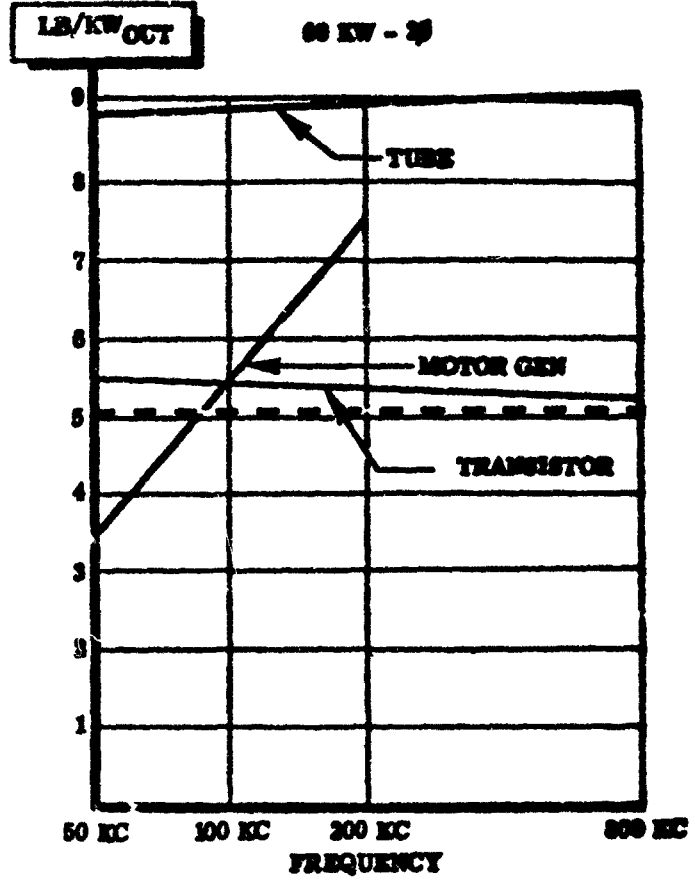
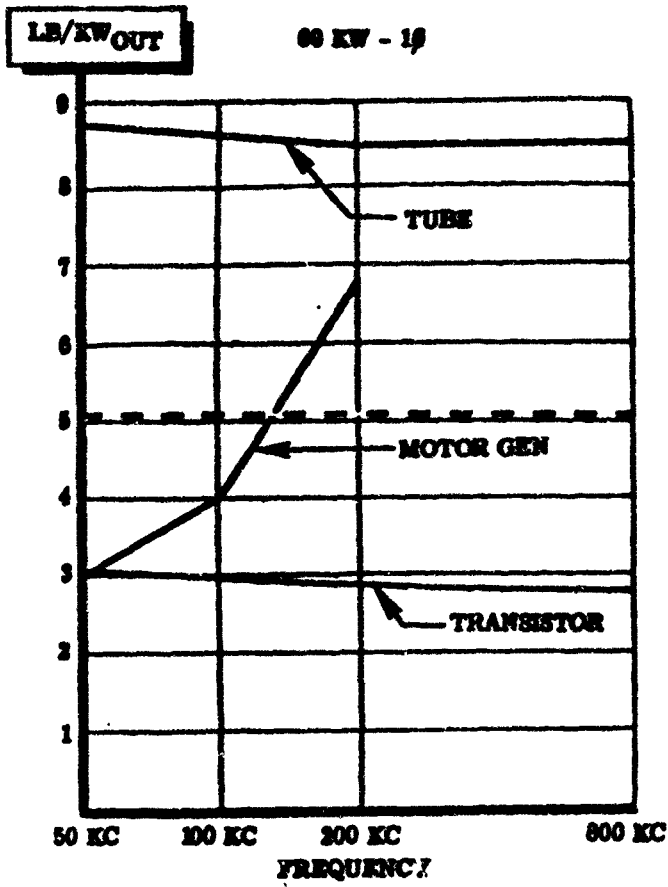
Parametric data on weight and efficiency versus frequency for converter and generator systems is summarized in this section. A more detailed discussion of (1) high-frequency generation and conversion techniques, (2) conceptual converter designs, and (3) conceptual high-frequency generator designs is presented in later sections.

Converter Weight Versus Frequency

Converter system weight as a function of frequency in the 50 to 800 kilocycle range is shown in Figure 1. This data for both single-phase and three-phase converter designs compares the three types of converter concepts which formed the major analytic effort of the study. The weight advantage of the static transistor converter over the other two concepts at each of the three conversion frequencies is quite evident. The motor-generator concept is competitive with the static transistor converter in weight only at the 50 kilocycle level, but gets decidedly heavier at the 200 kilocycle level. The motor-generator concept was not considered at the 300 kilocycle level because of the extreme number of poles and/or high rotor speed required for such a high-frequency output. The static tube converter is the heaviest of the three converter types, but like the static transistor unit is fairly independent of the frequency conversion level throughout the 50 to 300 kilocycle range. Weights for the transistor designs were considerably less than the overall component weight design objective of 300 pounds for the 60 KW unit and 1,000 pounds for the 300 KW unit.

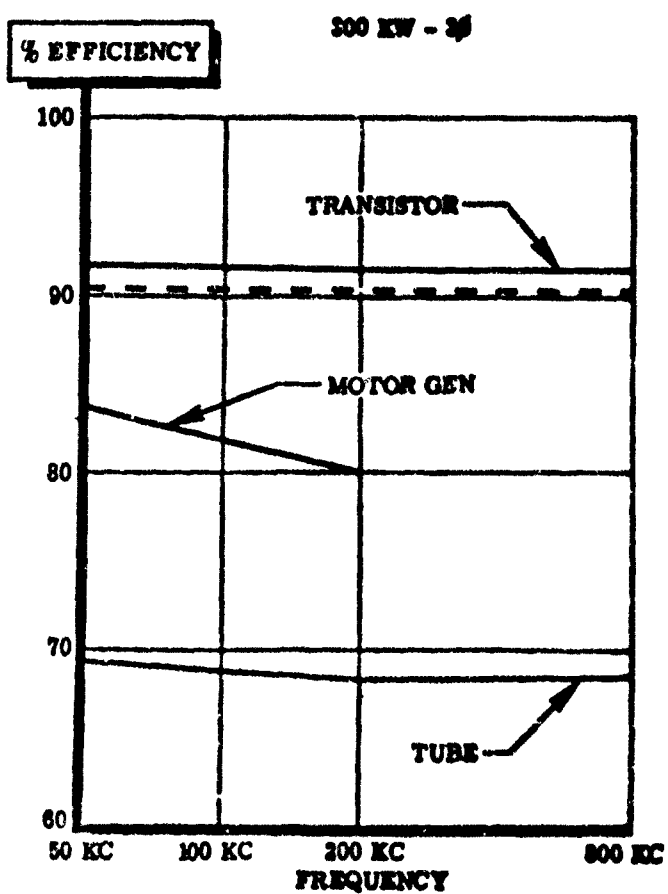
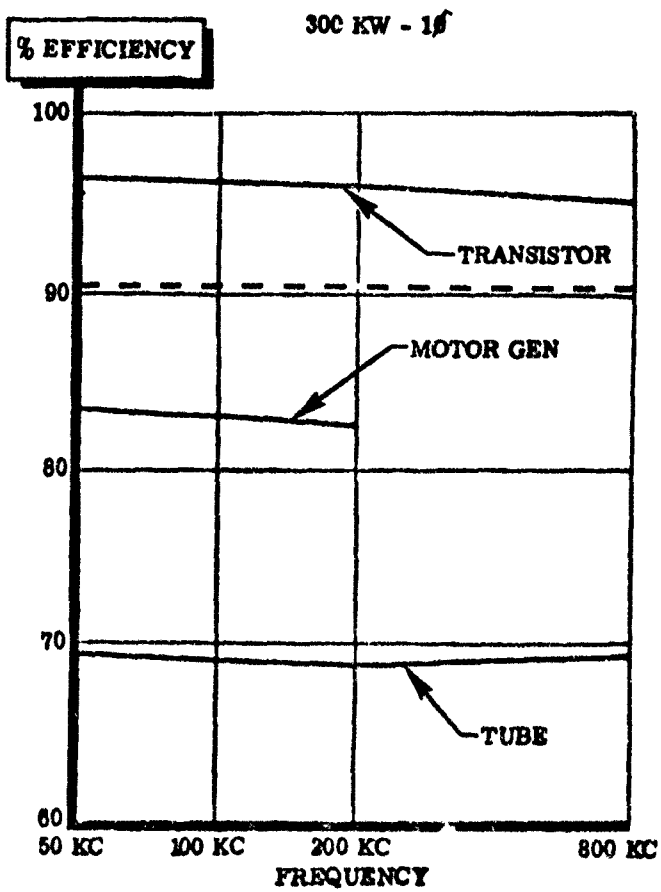
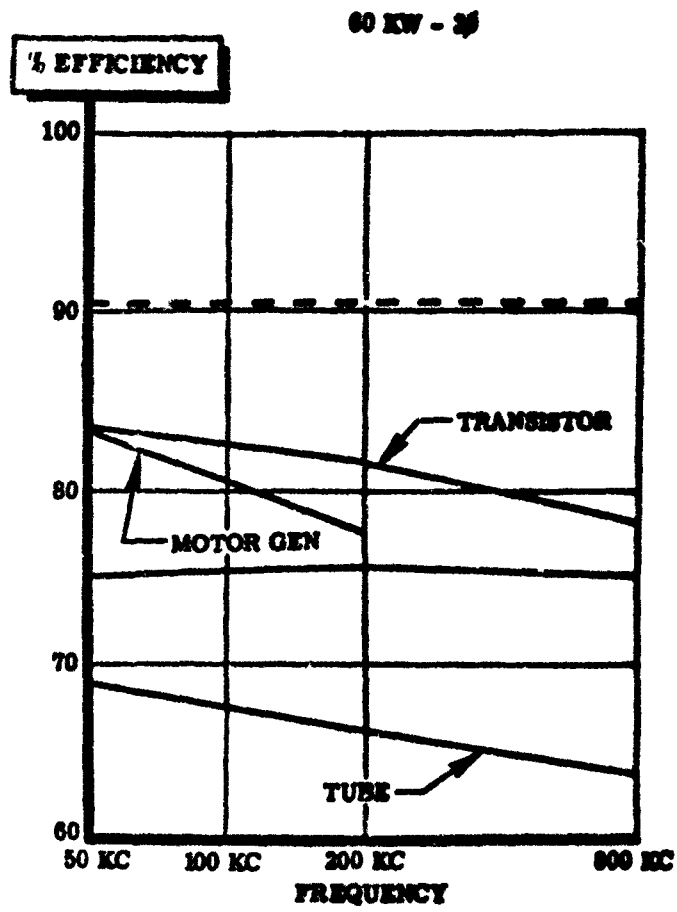
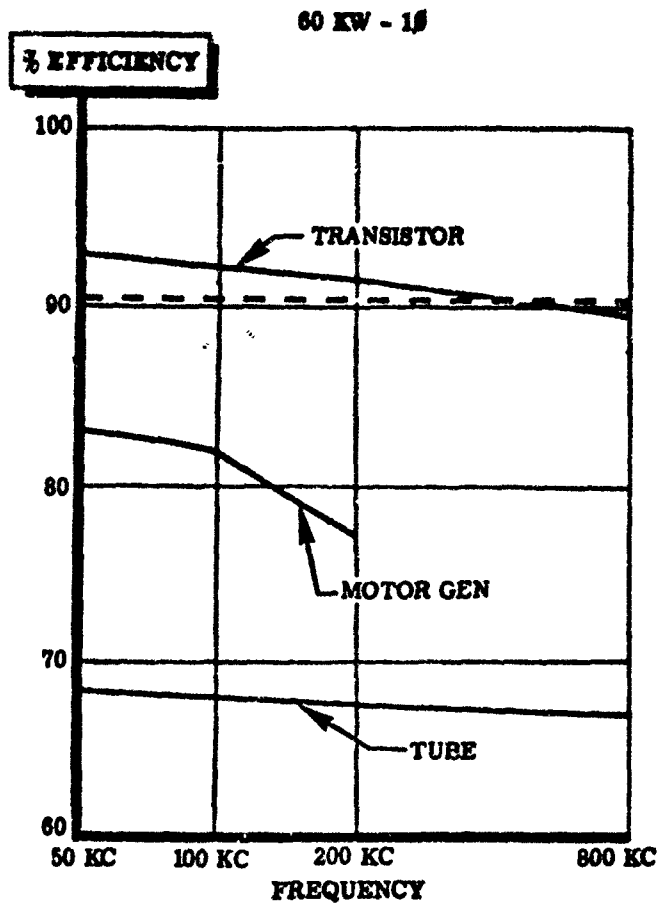
Converter Efficiency Versus Frequency

The three converter types analyzed during the study program are compared from an efficiency versus frequency standpoint in Figure 2. The static transistor concept is the most efficient of the three concepts with the



--- DESIGN OBJECTIVE

Figure 1. Comparison of Weight vs. Frequency for 60 KW and 300 KW Converter Units



--- DESIGN OBJECTIVE

Figure 2. Comparison of Efficiency vs. Frequency
for 60 KW and 300 KW Converter Units

static tube converter being the least efficient. To be noted is the fact that the efficiency of the 300 KW unit exceeds the design objective of 90 per cent and is greater than 96 per cent for the 300 KW single-phase design.

Generator Weight and Efficiency Versus Frequency

A portion of the study involved an analysis of high-frequency (50 KC to 800 KC) power generation by rotary-electromechanical techniques. A solid-rotor electromagnetic generator design was also analyzed for use in deriving high-voltage, high-frequency directly from a 500 hp, 24,000 rpm mechanical shaft. Figure 3 compares weight (lbs/KW out) versus frequency for the conceptual design in the 50 to 200 kilocycle frequency range and indicates the possibility of achieving a system design weight objective of 1,500 pounds or less. High-frequency (50 KC to 200 KC) generator efficiency ranges from above 95 per cent for the 50 kilocycle design to nearly 93 per cent for the 200 kilocycle design. This exceeds the 85 per cent design objective of the Work Statement.

Converter System Weight Versus Temperature

System weights for both 60 KW and 300 KW converter units are compared in Figures 4 and 5. Total system weight (including coolant system provisions) is extremely dependent on the operating temperature of the system. At the low temperature level, the static tube and the motor-generator units are quite heavy. As the operating temperature is increased towards the 1,000°F level, particularly at the 60 KW level, the system weight curves become more convergent and the heavier static tube and motor-generator converter designs become more competitive with the transistor design. At temperatures above 275°F, the static transistor and motor-generator unit (50 KC) meet the system weight objective of 300 pounds for both a single-phase and three-phase unit. The system weight comparative analysis for 300 KW converter designs shows a wider range of converter weights at the low temperature (200°F) level than for the 60 KW unit. The design objective of 1,500 pounds for this converter, to be used with a SPUR type power system, can be met in all the concepts except the 200 KC motor-generator.

The curves of Figures 4 and 5 resulted from cooling system studies performed during the program in which radiator, pump, coolant fluid, and coolant tube weights were analyzed for each of the converters and generators. These curves are based on the weight of a cooling system with a "heavy" radiator, one designed with adequate protection against meteorites. A radiator with less meteorite protection was considered in the weight analysis, but this concept was not used because of the desire to be conservative in assessing the cooling system weight penalty for each of the concepts. Total system weights are somewhat less when the lightweight radiator concept is used, but the weight trends do not change. A more complete picture of the effect of cooling system requirements on total system weight is given in the Related Studies section.

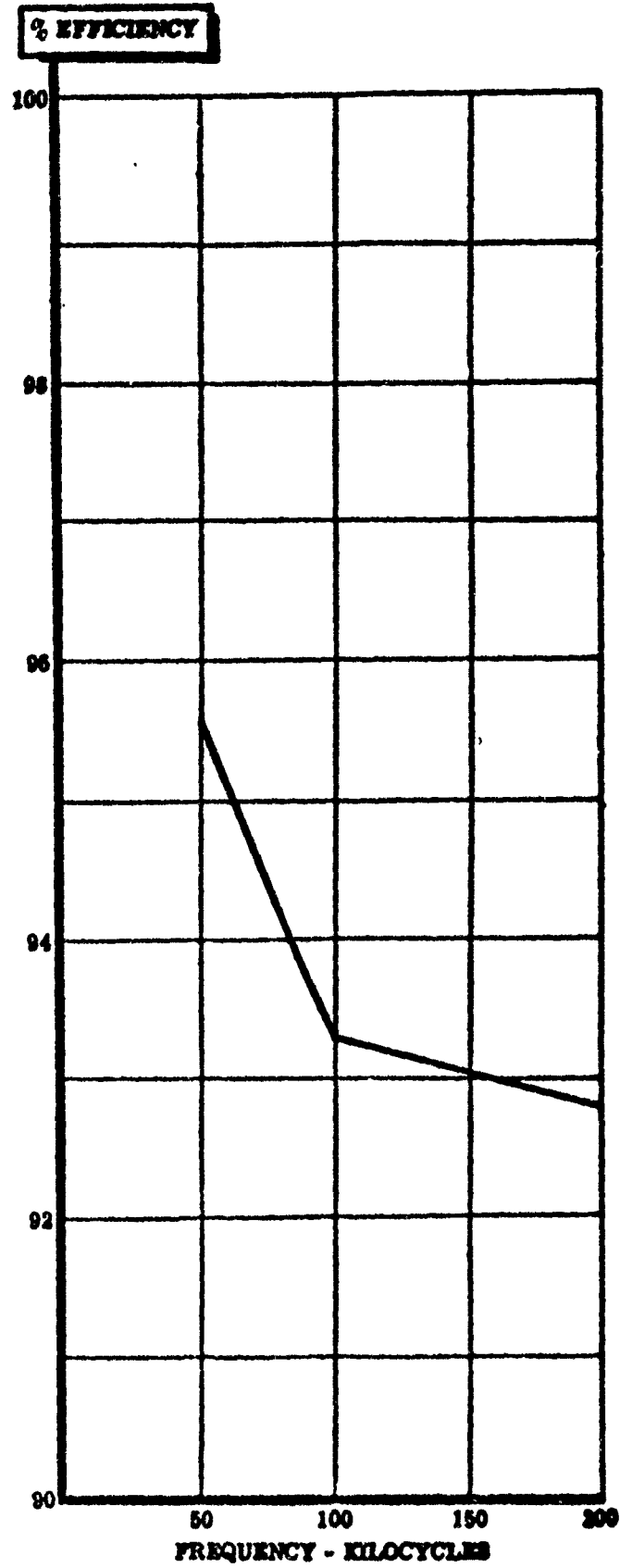
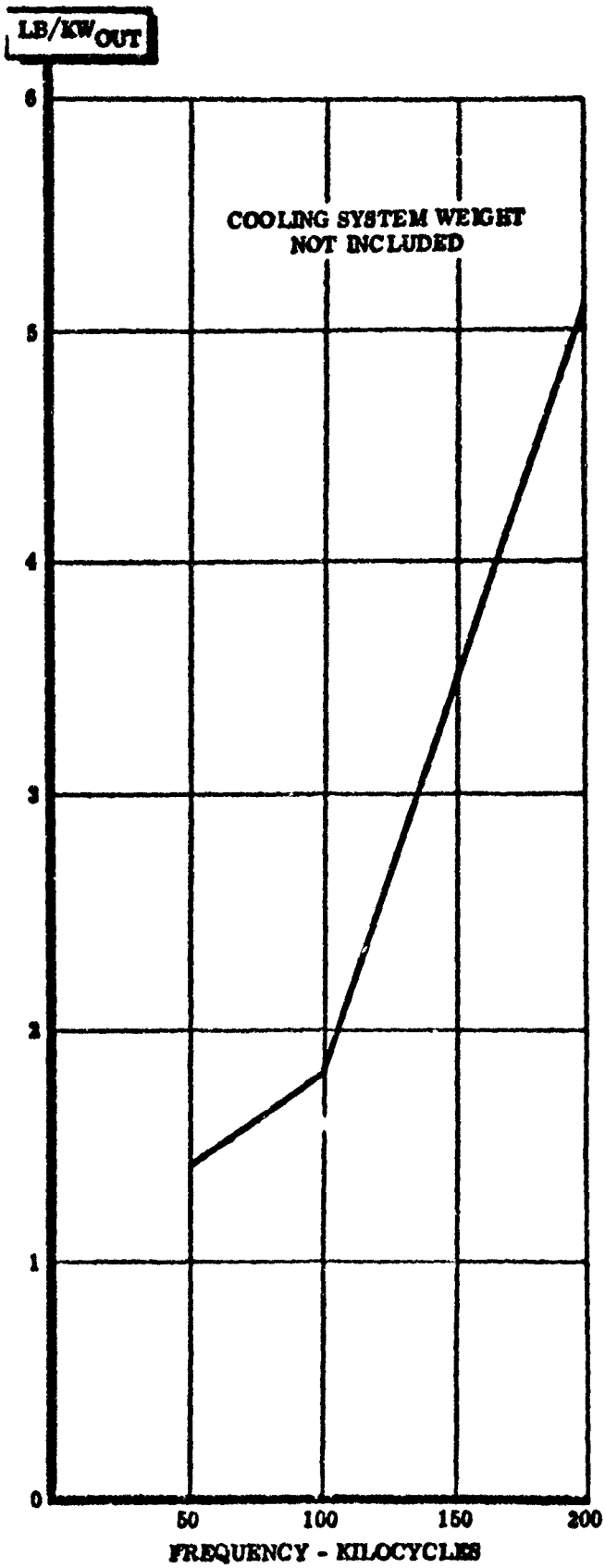


Figure 3. Comparison of Weight and Efficiency vs. Frequency for High Frequency (50 to 200 KC) Generator

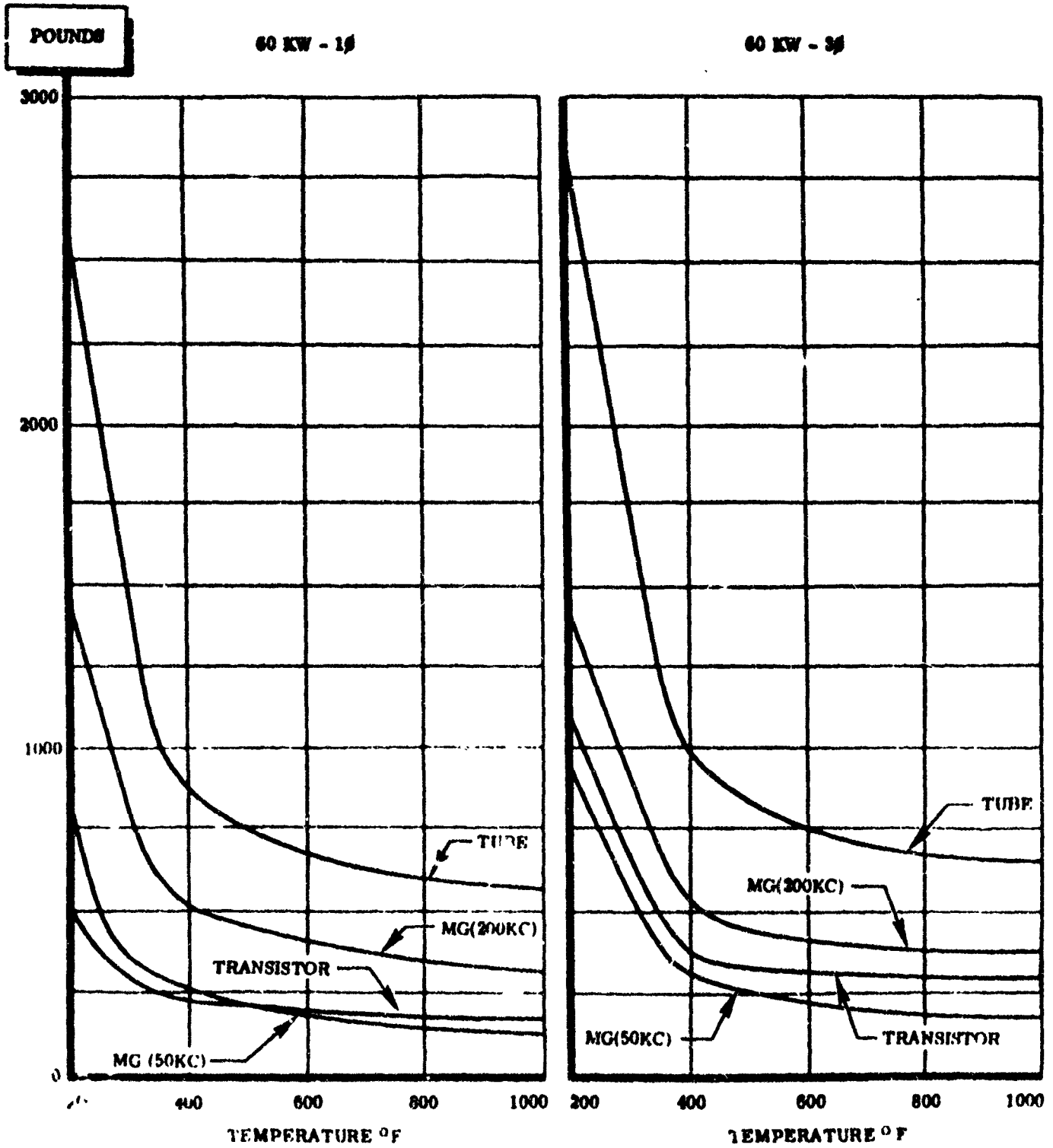


Figure 4. Analysis of System Weight vs. Temperature for 60 KW Converter (Includes Weight of Cooling System)

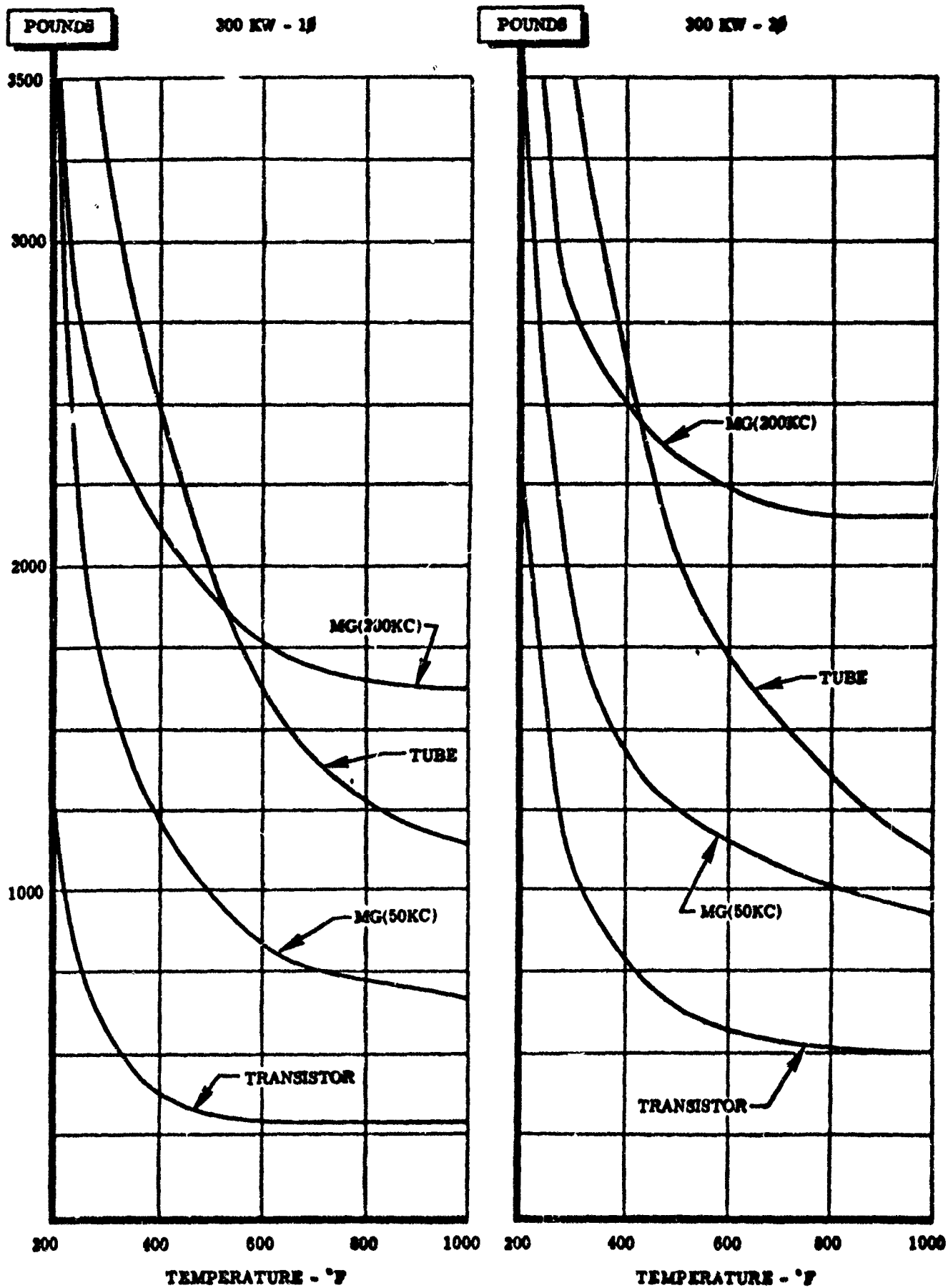


Figure 5. Analysis of System Weight vs. Temperature for 300 KW Converter (Includes Weight of Cooling System)

Total Generator System Weight Versus Temperature

Figure 6 summarizes generator configuration weights and cooling system weights in a plot of total generator system weight versus system operating temperature. The design objective for this portion of the study can easily be met, as shown by the curve at the 50 KC frequency. System weight also increases with frequency as shown. The feasibility of generating power at the required high-frequency (50 KC to 200 KC), high-voltage level and elimination of frequency and voltage multiplier devices is quite evident here.

The same feasibility applies to use of a high-voltage generator technique in conjunction with rectifiers to arrive at high-voltage DC power for use in an ion type engine. The main advantage in this technique would be in elimination of the transformer weight required in generating at a lower voltage and stepping up to the required high-voltage level.

High Frequency Generator Versus a SPUR Type Generator Plus Converter

The basic power supplies considered in this study were of the SNAP 8 and SPUR types and each generates low frequency (1 KC and 3.2 KC) power. Since high-frequency power is required for the electromagnetic engine of this study, it was early considered that the low specified frequency of power generation (1 KC and 3.2 KC) was not an optimum input frequency level. With this thought in mind, a parametric study was performed to compare the following conversion concepts for delivering high frequency (50 KC to 200 KC) power to an electromagnetic propulsion engine:

1. A high-frequency (50 KC to 200 KC) generator design concept of this study which delivers the required high-frequency, high-voltage power.
2. A SPUR type low frequency generator plus a converter design of this study.

Figure 7 compares the two conversion concepts on a lbs/KW out versus temperature basis. Weights include cooling system penalties for the SPUR type generator operating at two fixed temperature levels (600°F and 800°F) with the static transistor converter operating at various temperature levels. Also considered were the weights of two cooling system concepts, one based on a heavily-protected type of radiator and the other one a lightweight radiator. Significant is the fact that the high-frequency generator concept is lighter in weight than the SPUR type generator plus a converter over a major portion of the temperature spectrum. Figure 8 plots weight versus frequency to show the "breakover" points for the two concepts. A single generator unit producing the required high-frequency output is lighter in weight than the SPUR type generator plus a static transistor converter up to approximately 100 KC in a system utilizing the heavy radiator concept. Two operating temperature levels for the converter were considered (300°F and 600°F). This leads to the conclusion that below approximately 150 KC, the HF generator is the lightest and most efficient way to generate high frequency power. Above this frequency, a low frequency generator plus a transistor converter is lighter. Above 200 KC, only the converter approach is feasible due to the inability of generator designs investigated to operate above this frequency.

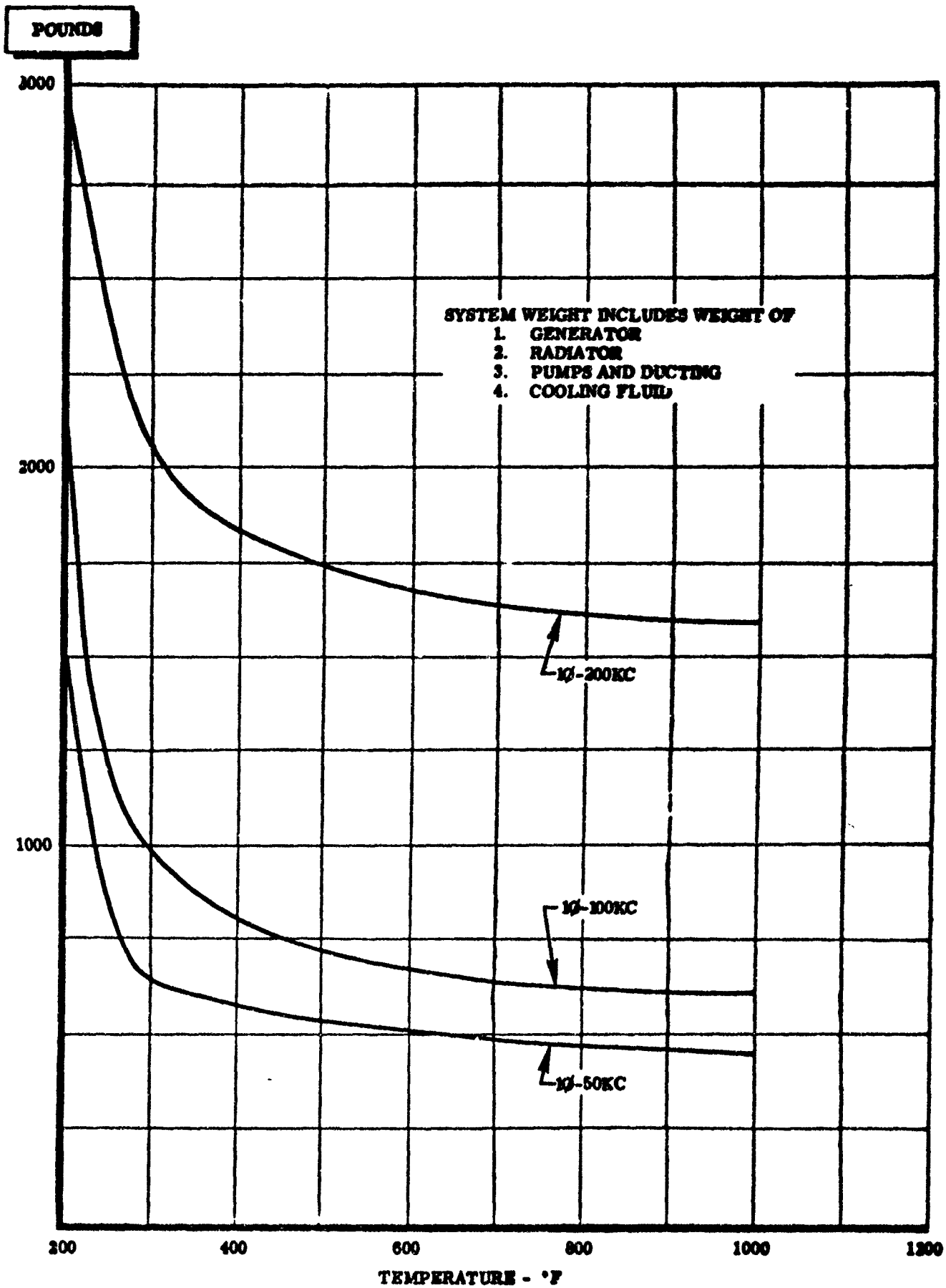


Figure 6. Generator System Weight vs. Temperature (Includes Weight of Cooling System)

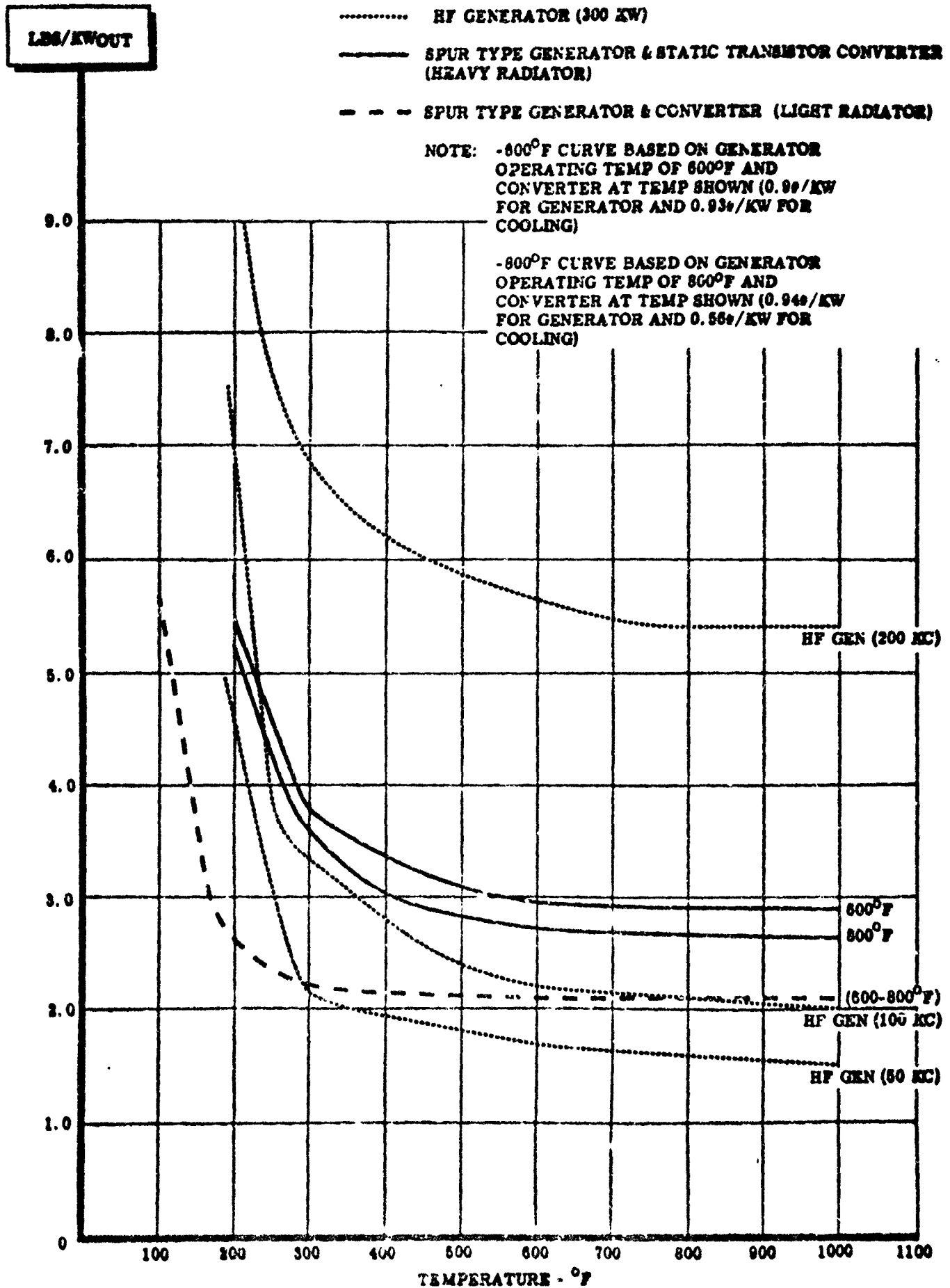


Figure 7. Comparison of High Frequency (50 to 200 KC) Generator with SPUR Type Generator Plus Static Converter Unit

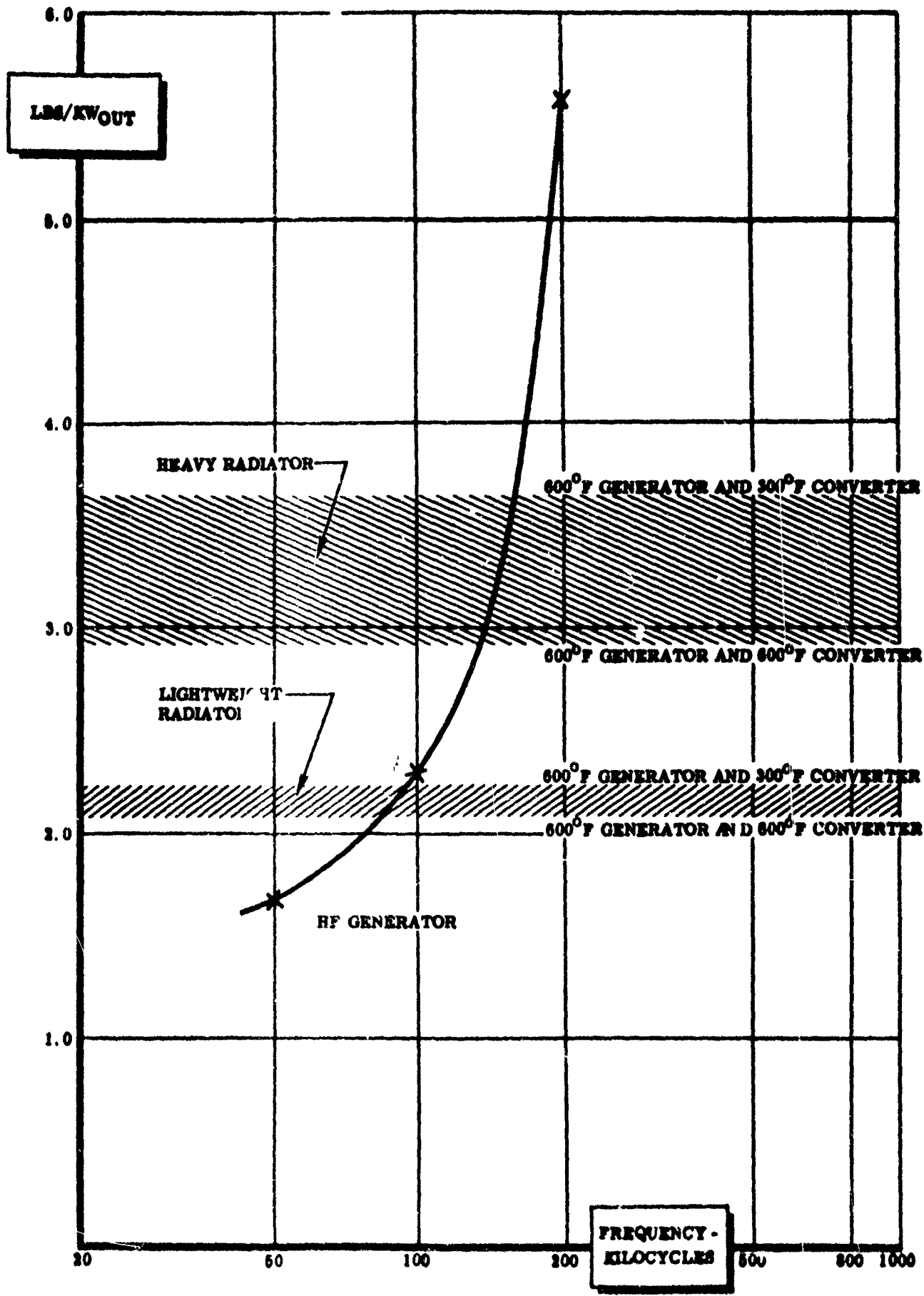


Figure 8. Weight vs. Frequency Comparison of High Frequency (50 to 200 KC) Generator With SPUR Type Generator Plus Static Converter Unit

Section I

HIGH FREQUENCY POWER GENERATION TECHNIQUES

ELECTROMAGNETIC GENERATORS

Electrical power of radio frequencies from 50 kilocycles to 200 kilocycles can be generated with solid rotor generator designs, converting mechanical energy to electrical energy by rotating a magnetic field through generator conductors.

The upper limit of generating frequency is determined by the maximum allowable material stress in the rotating part, the minimum practical dimensions of the magnetic poles, and the minimum space in which a generating winding may be placed to utilize the number of magnetic rotor poles.

The generator described as configuration B most readily allows the maximum freedom of the design limitations on the upper frequency limit and has capability for generating large power output.

Maximum number of rotor poles are obtained by separating the north and south poles axially, as the number of rotor teeth are one half that required if alternate polarity poles were not displaced axially. Maximum space is allowed for the stator generating winding by using a winding design requiring one-third of a slot per pole. This means stator diameter will have a frequency capability of three-times the same stator using a single slot per pole, because physical spacing is required between slots.

The generator magnetic-excitation circuit with its stationary excitation coils is similar to that used for the NADYNE generator, a North American conceived design. The use of stationary coils increases the upper generating frequency limit since rotor space is not used for excitation coils between poles. The use of stationary coils also increases the frequency capability by permitting the rotor to be rotated at greater surface speeds.

Generator configuration B is similar to the inductor type (homopolar double-ended) generator except that a laminated outer yoke is added to permit the flux to rotate with the rotor. The inductor generator would not be suitable without this modification since its losses would be quite high.

As the frequency increases, the unit volume core loss increases. In order to limit the unit core loss it becomes necessary to reduce the flux density of the generator stator iron circuit as frequency is increased. The reduced flux density requires an increase in the amount of stator iron required, resulting in increased weight for the frequency band being considered. Unfortunately, the presently available low loss magnetic materials saturate at low flux densities and have lower Curie temperatures than the nickel irons. As the percentage of AC stator iron is low compared to the total generator weight, the reduction in AC stator iron flux density is not

as severe a penalty as it might seem. The largest portion of the iron circuit is operating with DC flux and produces no loss under steady-state operating conditions.

SOLID-ROTOR TECHNIQUES

Five solid-rotor, homopolar type inductor generator concepts (A, B, C, E, & F) plus a flux-switch heteropolar type of machine (D), were evaluated and parametric data plotted to show power output versus frequency. This data is shown in Figure 9 and 10 and discussed in the section which follows. Data on Configuration B, a 24,000 rpm 300 KW design, shows a 1.2 lb/KW weight at the 50 KC frequency level increasing to approximately 4.6 lbs/KW at the 200 KC level. Plotted data shows that an increase of generator speed to 48,000 rpm leads to a 50 per cent reduction in generator specific weight at 200 KC (see Figure 10), but places an upper limit on power output from a single unit at less than 300 KW. For a 300 KW - 200 KC design at 48,000 rpm, it would be necessary to use multiple units at a net weight increase. The data shows Configuration B to be more suited, power wise, for the 50 KC to 200 KC range. Configuration A is suitable for 50 to 100 KC power generation. The plotted data also indicates a low power output limit for Configuration C and the flux-switch type of design. Configuration E is similar to Configuration B, but differs in structure. Configuration F is limited by its permanent magnet and is estimated to be capable of one-half the power generation capacity of Configuration B. Losses and efficiency have been determined for generator Configuration B for various iron hot spot temperatures and coolant temperatures. As the cooling ambient temperature increases, it is necessary to use magnetic materials with higher Curie temperatures. The survey of magnetic materials has shown that the losses increase in materials of higher Curie temperatures and result in lower efficiency at higher temperatures.

In summary, a rotary type of alternator with efficiency from 85 per cent to 95 per cent is feasible in a motor-generator type of converter design in the 100 to 200 KC frequency range. Likewise, a rotary alternator concept is feasible for power generation with a 24,000 rpm turbine prime mover.

Generator Configurations Considered

Configuration A - Configuration A consists of a north pole rotor and stator section and a south pole rotor and stator section. The rotor flux is unidirectional and its path is axially in the rotor to the poles, across the pole gap to stator, through the outer stator yoke to the other stator section across the pole gap, axially along the rotor to a concentric pole gap, axially along the frame to the other pole gap and then into the rotor. Each stator section is equivalent to an inductor-generator stator with one slot per pole where one-half of the slots in each stator section are inactive in producing voltage at any instant of time. Configuration A is limited in frequency by the maximum number of stator slots usable in a given diameter (see Figures 11 and 12).

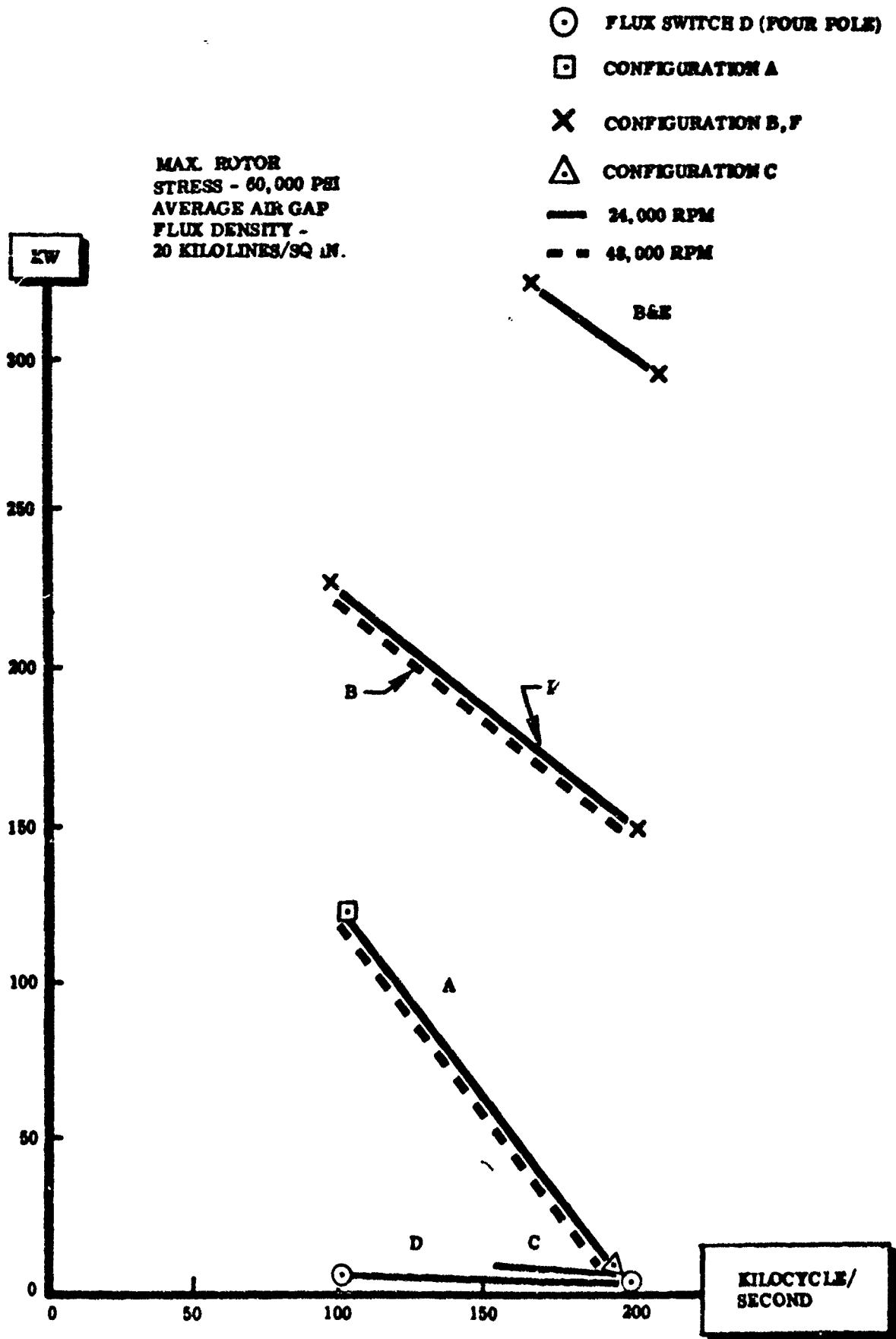


Figure 9. Power vs. Frequency for Rotating Generators

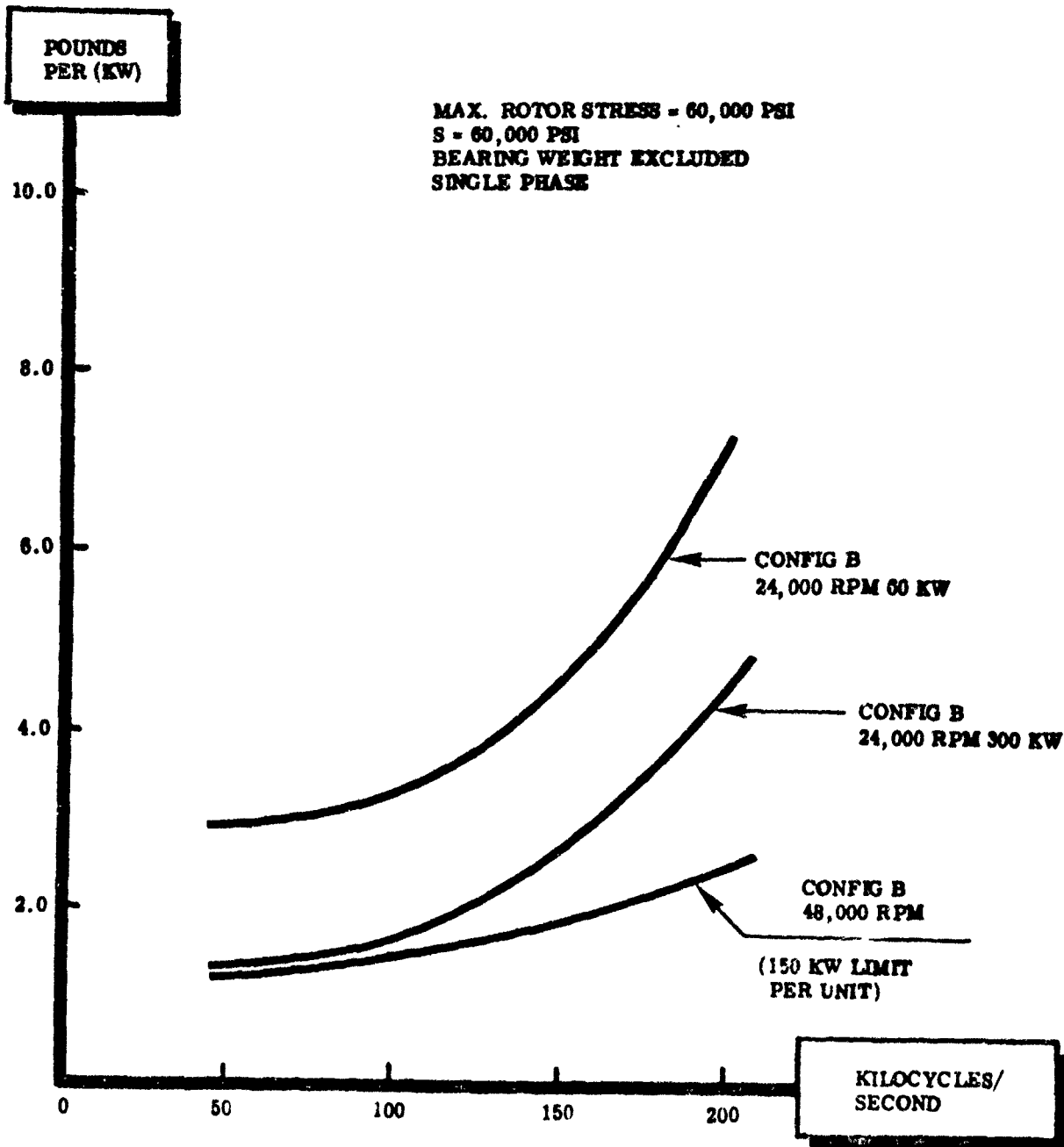
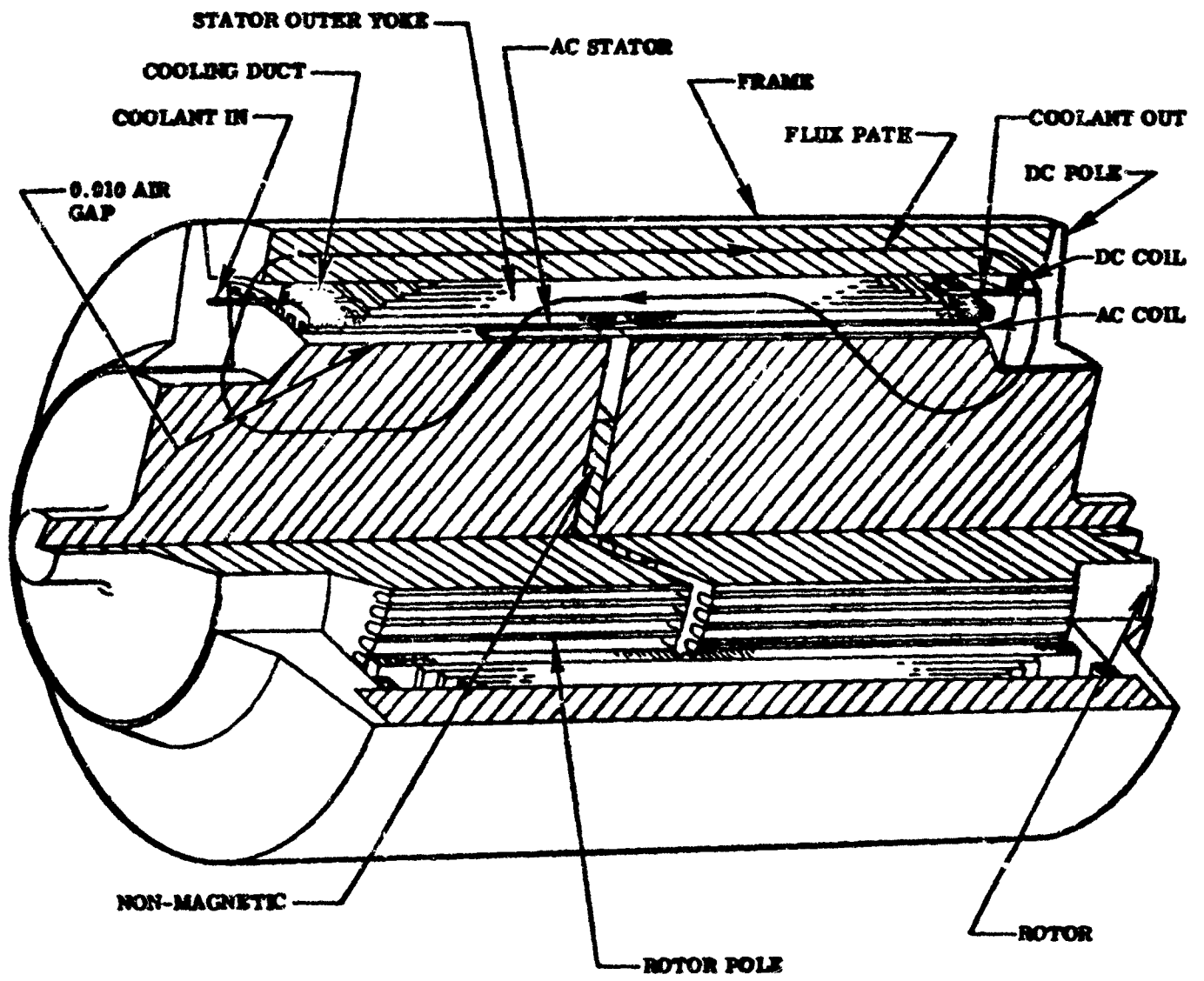


Figure 10. Estimated Weight vs. Frequency for Rotating Generators



GENERATOR CONFIGURATION B

Figure 11, Electromagnetic Generator Concept (Perspective)

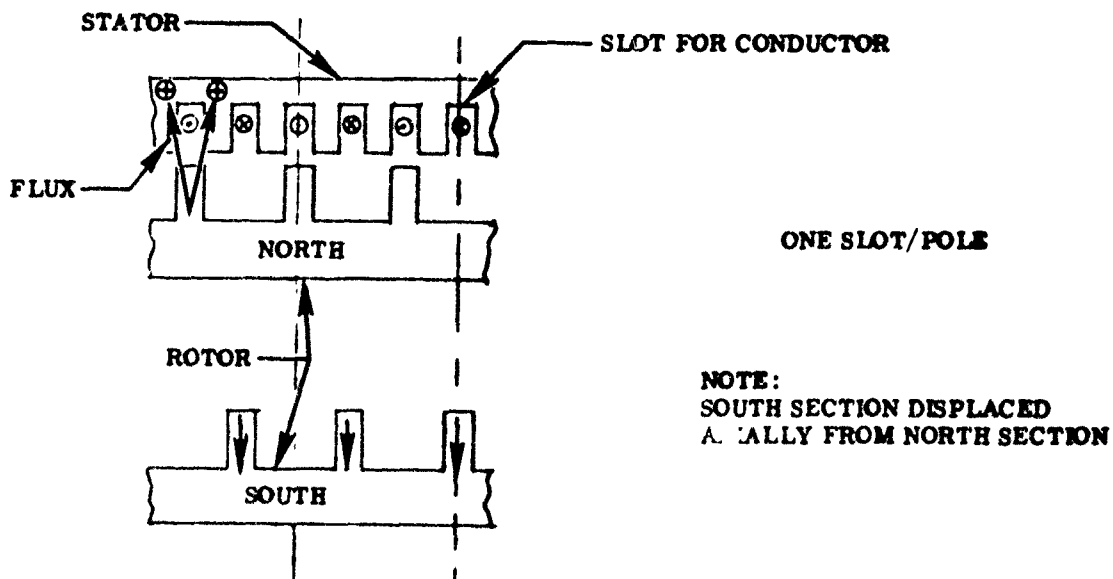
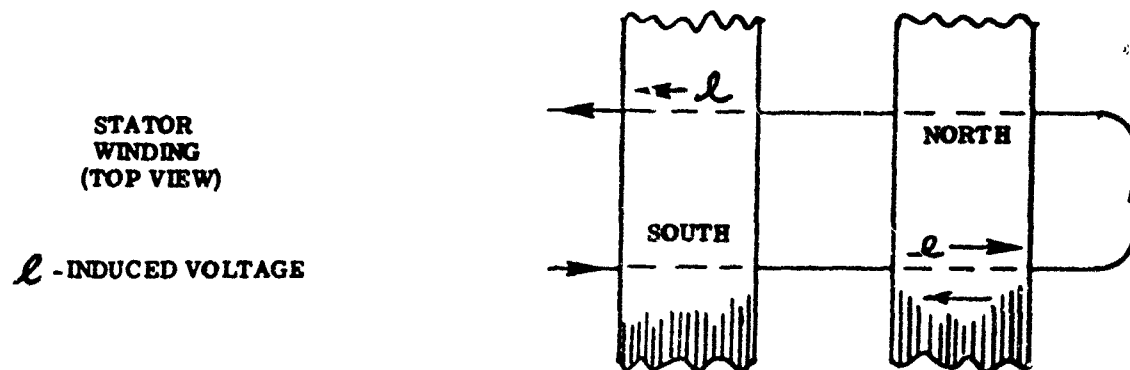
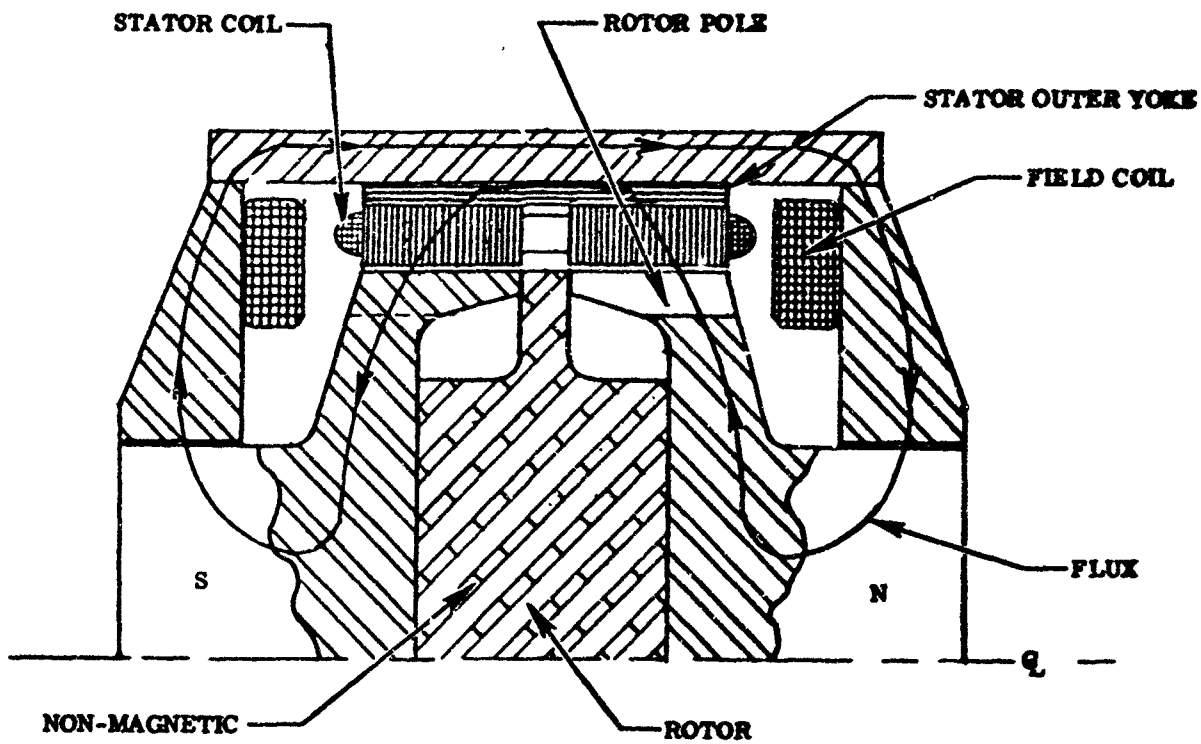


Figure 12. Generator Concept "A"

Configuration B - Configuration B is the same as Configuration A with the exception that the stator has one-third of a slot per pole. This permits generation of power at higher frequencies than possible with Configuration A, as the number of stator slots is one-third that of A. Configuration B requires three times as many conductors per slot as Configuration A to obtain the same voltage output (see Figures 11 and 13).

Configuration C - Generator C in Figure 14 is similar to generator Configuration A. In this configuration the poles in each half of the two axial rotor portions are in line with each other and not displaced 180 electrical degrees as in A and B generator configurations. The return conductor of the generator stator turn is located on the outside of the outer stator yoke iron so as not to have AC voltages induced in the return conductor of each stator turn. The required number of stator slots for a given frequency and speed is reduced to one-half that required for generator Configuration A by this means; therefore increasing the maximum possible frequency for generating power to higher frequencies than are possible with Configuration A.

Figures 12, 13, and 14 schematically show the AC generator stator winding and the relative positions of the rotor magnetic poles. The generator rotor pole sections are similar to the Inductor type generator. The excitation circuit is the same as for a NADYNE type of generator, a North American Aviation solid-rotor design. The generator may be modified to use permanent magnet type excitation by installing a permanent magnet in the nonmagnetic section of the rotor and eliminating the static excitation parts. A stationary permanent magnet may be installed in the static excitation magnetic circuit.

Demagnetization and Opposing Transformer Voltages in Generator C - The return conductor of the stator winding, located on the outside of the stator yoke iron along with the conductor in the slot, forms a turn around the stator which produces an MMF when a load current is flowing in the winding. This MMF produces a flux which will flow around the stator yoke and generate a transformer voltage. This voltage is in opposition to the generated voltage at a vector angle determined by the power factor of the circuit. To limit the reaction flux and its associated transformer voltage, the stator is divided into segments as shown in Figure 14. The amount of separation or gap is limited by the maximum stator flux densities allowable and the minimum iron sections allowable.

Flux Switch Configuration D - This concept, shown in Figure 15, generates voltage by switching the flux passing through the stator coil from a plus to a negative value. This is accomplished by changing the reluctance of the magnetic circuit by rotation of the rotor poles. The field MMF being constant, the flux changes as a function of the reluctance of the magnetic circuit. The flux switch has several disadvantages: (1) The flux from the field excitation circuits oppose each other in the stator coil reducing the alternating flux to one-half the excitation flux, (2) the stator coil maximum flux is one-half the total flux passing through each pole on the rotor, (3) the rotor flux alternates in each rotor pole, (4) the

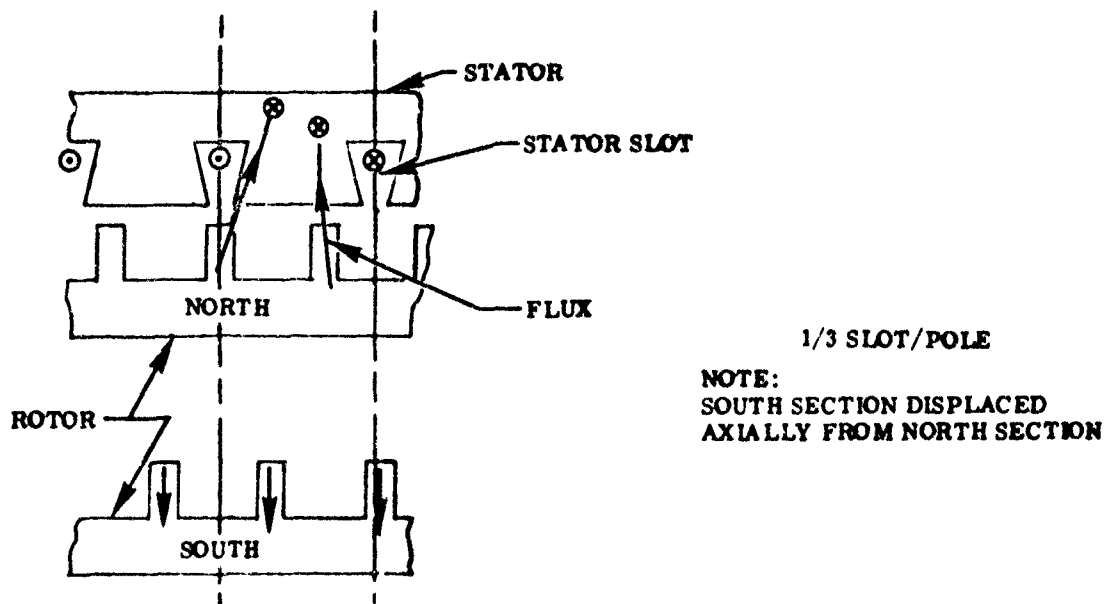
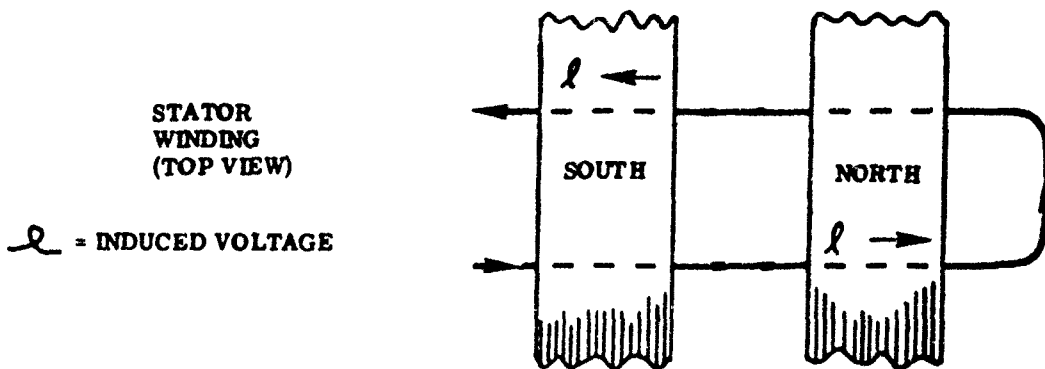
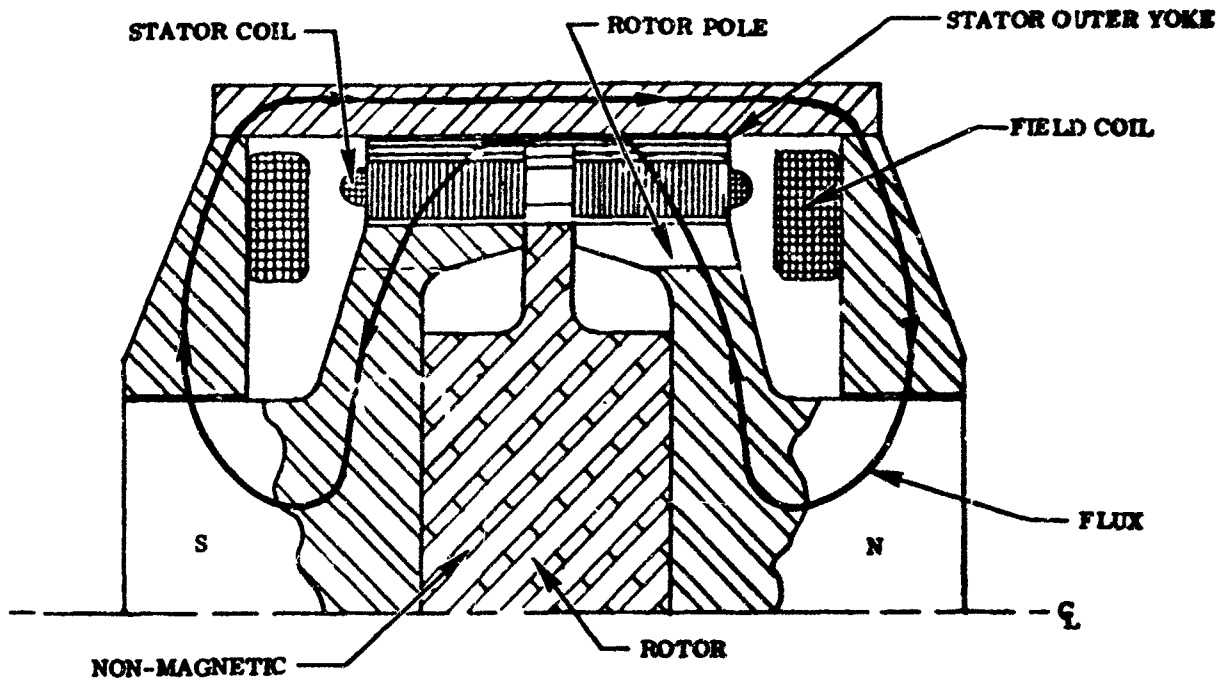


Figure 13. Generator Concept "B"

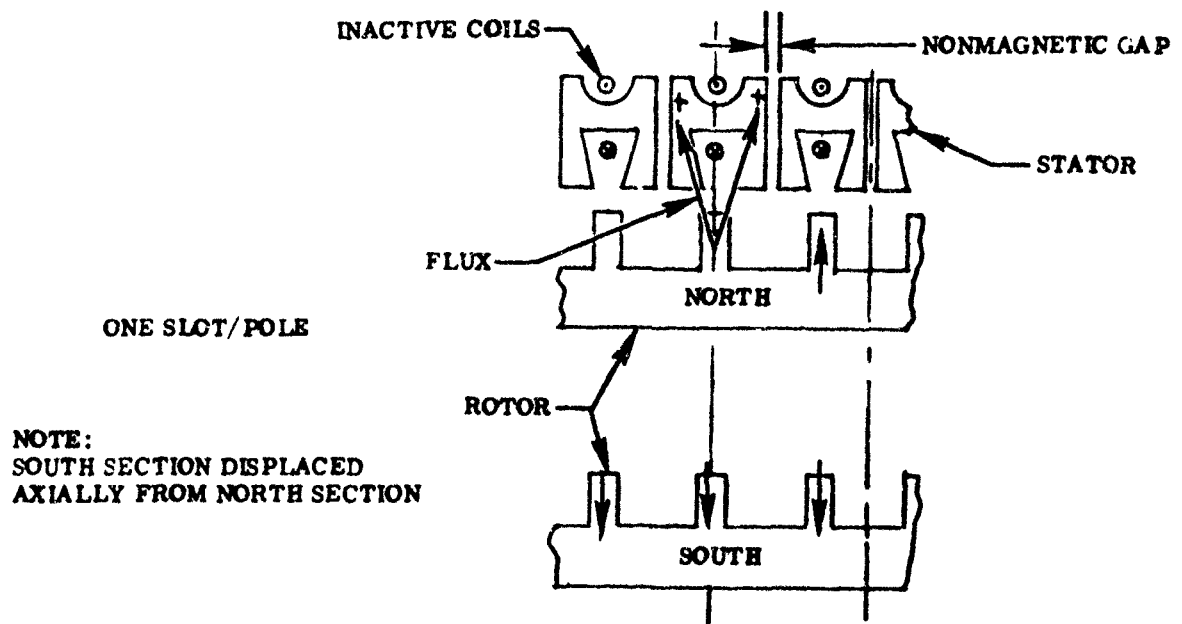
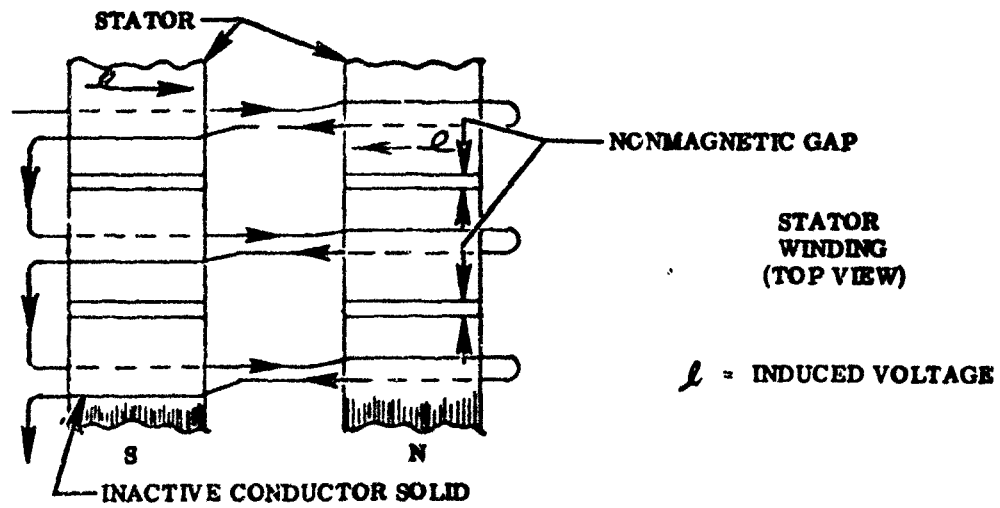
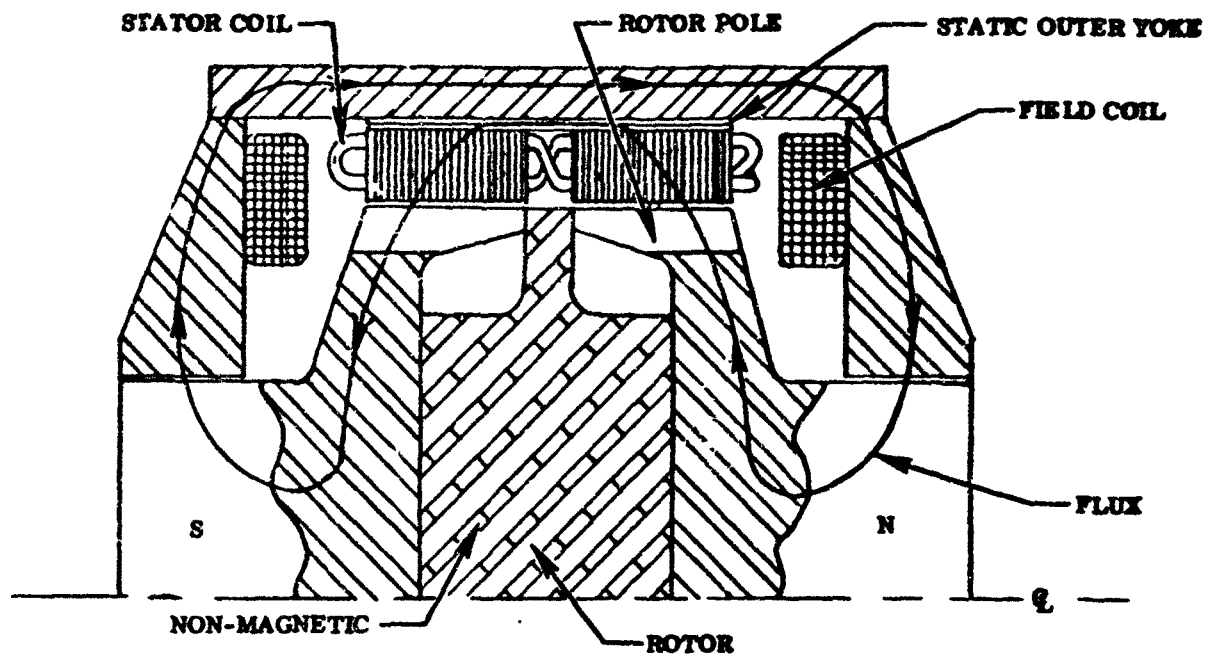


Figure 11. Generator Concept "C"

FLUX SWITCH GENERATOR

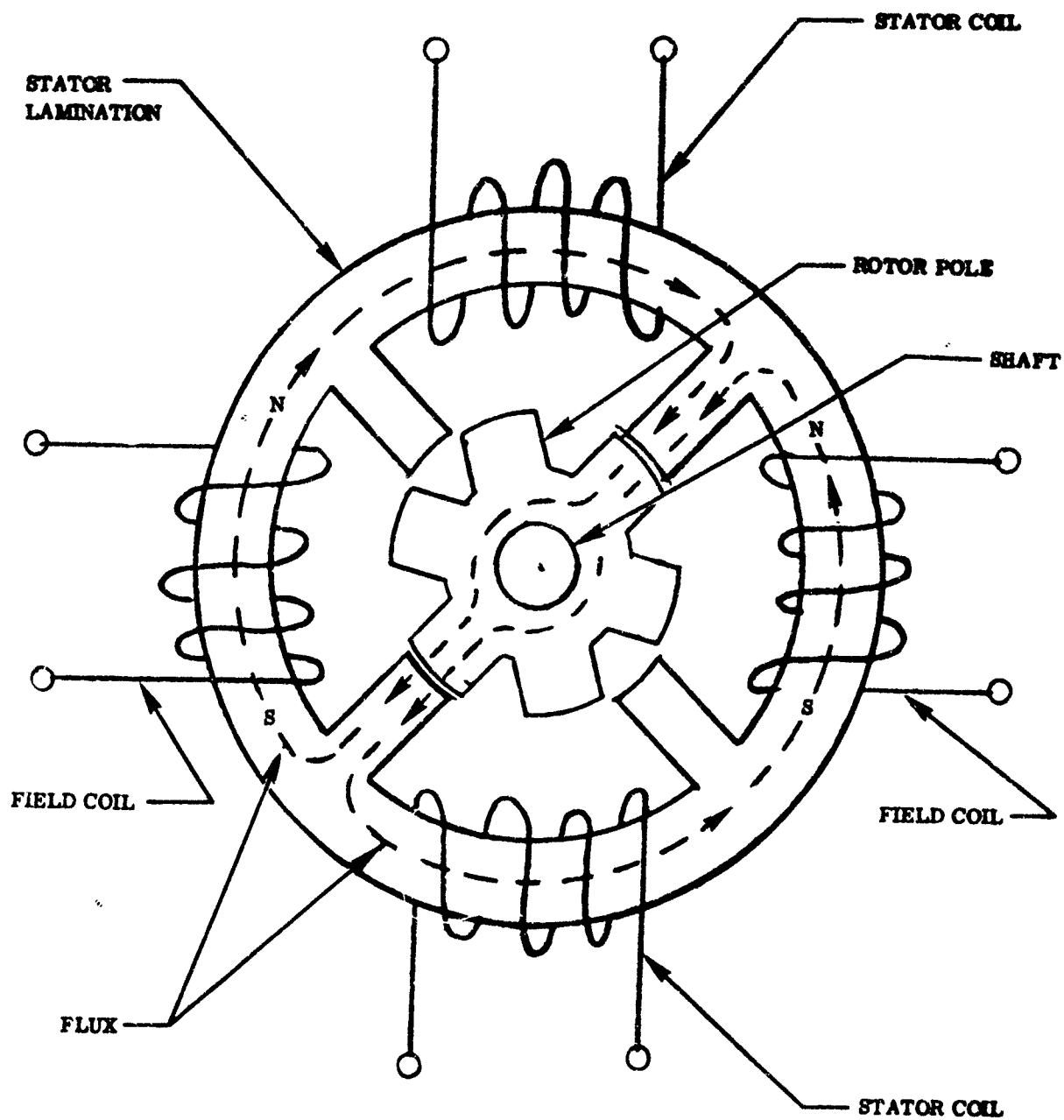


Figure 15. Flux Switch Generator Concept "D"

demagnetizing action of the stator is large, as the stator has a large number of turns compared to the rotor pole gap ampere turns, which limits the output power.

Configuration E - Configuration E is similar to Configuration A or B, and is shown in Figure 16. The field coils of A and B have been relocated to a position between stator sections. This eliminates the magnetic field poles and the need for the outer magnetic housing of generator A and B. The magnetic frame and poles are replaced by parts sufficient for mechanical purposes. The stator outer yoke is retained as a laminated core to permit rotation of the DC flux with rotor rotation. The stator portions are the same as for A and B Configurations. Data for A and B are applicable to Configuration E.

Configuration F - This configuration, also shown in Figure 16 is the same as Configuration E except the rotor center portion or complete rotor is a permanent magnet and replaces the field coil. A field coil may be retained and used for regulating the generator output. The PM material limits the power to about one-half that of Configuration B.

Other Generator Design Considerations

Power Output - The power output of each configuration has been calculated with the following parameters. the same for each configuration.

Average air gap flux density = 20 kilolines/square inch
RMS conductor current density = maximum of 6,400 amps/square inch
Rotor diameter - dependent upon RPM, but constant for each comparison
Single stator core axial length
RPM - dependent upon RPM, but constant for each comparison
RMS stator reaction ampere turns = equal or less than the field ampere turns of the pole air gap for the air gap flux density above.
Sinusoidal flux variation - assumed for each design comparison

Power Output Curves - The power output shown on the curves of Figure 9 approximates the maximum obtainable for the conditions of rpm and maximum rotor stress noted for the air gap flux density, conductor current densities and stator reaction ampere turns specified in the power output paragraph above. The curves show that the power output is increased by a decrease in rpm; the power output may also be increased by increased rotor stress, increased gap flux density, and optimization of design. A decrease in rpm results in a power increase through an increase in rotor-diameter and length, which results in a weight increase.

An increase in the rotor allowable stress for a given rpm permits the use of a larger diameter rotor. Assuming the same rotor flux density, the total flux of the generator increases as the diameter squared, or stress squared; the linear velocity increases with the diameter; therefore, the power output is increasing as the cube power of the rotor stress. An increase in the generator stator gap flux density also increases the power as it increases the total flux of the generator. This increase is limited by the saturation flux density of the rotor material.

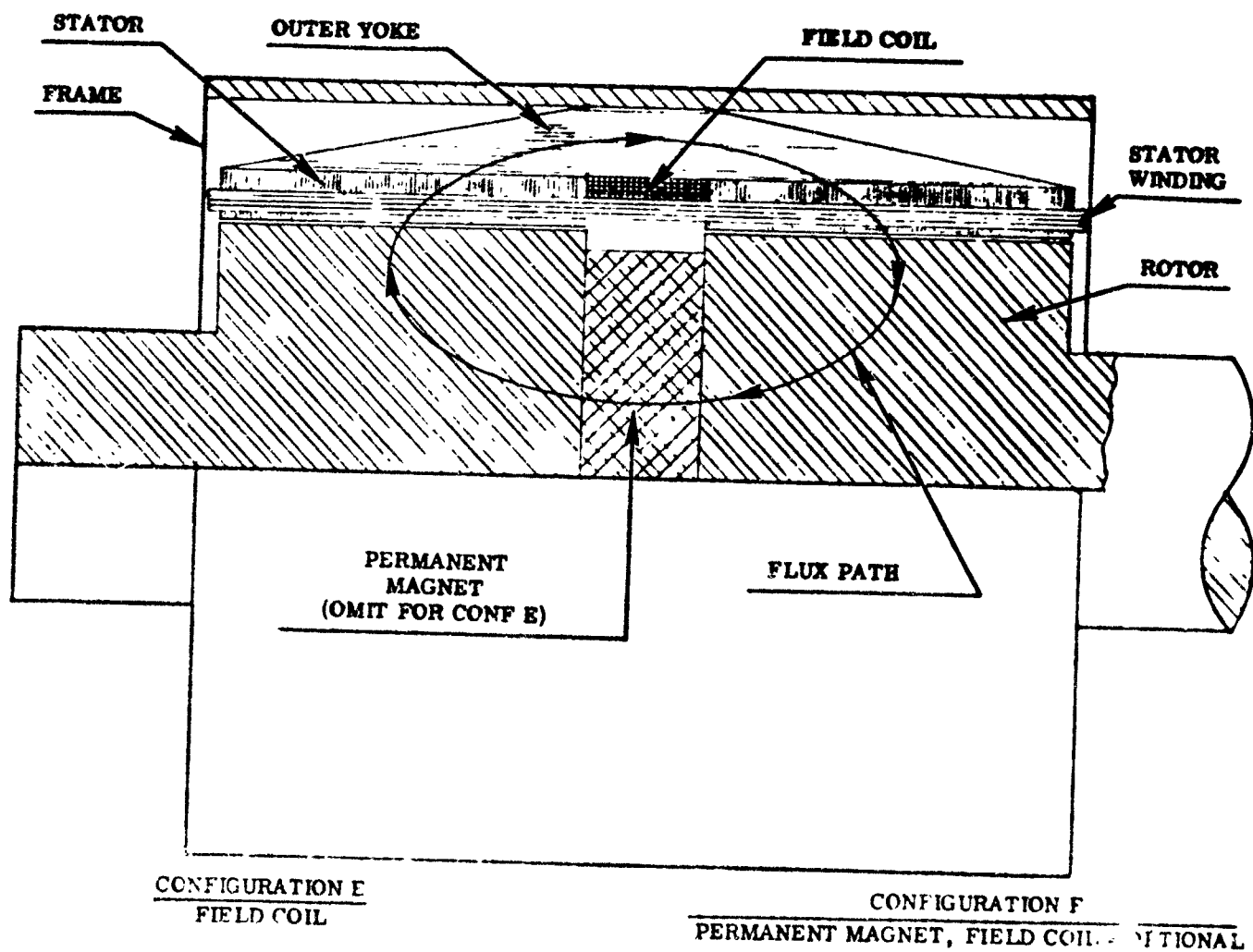


Figure 16. Generator Concepts "E" and "F"

Power Output vs. Frequency - Note that at the high power (50 to 800 KC) frequency considered, the obtainable power output decreases with increase in frequency. This is a result of being stress limited, because the large number of poles decreases the space available for conductors to produce a voltage output. Generator Configurations A, B, and E power outputs are limited by the maximum conduction current density since the conductor area is limited. The power output of Configuration F is limited by the allowable flux density and rotational stresses of the permanent magnet material. The high cobalt permanent magnet material values at 70°F have been used to determine the power output data. Configurations C and D are limited by the stator reaction ampere turns (MMF) and not by conductor density. The power from Configuration D may be increased by adding additional poles around the stator. These would have to be added in increments of four; the addition of these poles would not increase the power sufficiently to compete with A, B, or E Configurations.

Generator C (200 KC - 24,000 rpm) - A preliminary analysis of generator C assumed that limitations due to demagnetizing and transformer voltage from load current would be computed and added in before finalizing the design. This assumption resulted in favorable power outputs (over 200 KW at 200 KC). An analysis of transformer voltage for a generator C design of 200 KC, 24,000 rpm and an average air gap density of 20 kilolines/square inch showed a power limit of five KW for a transformer voltage equal to the terminal voltage. The power limit is approximately proportional to the air gap density, and if the air gap density were increased until the tooth flux density limited the flux, the power limit would be increased from five KW to ten KW at an average tooth flux density of 60 kilolines/square inch (9300 GAUSS).

Weight vs. Frequency - The weights have been estimated at 24,000 rpm and 48,000 rpm for generator Configuration B for the power output levels shown on Figure 9 and are plotted in Figure 10. The weights include all the parts shown in the generator cross-section drawing. A detailed weight estimate has been made on selected designs to evaluate the configurations considered. Higher power levels can be obtained at the higher rpm by ganging or using multiple units for less weight than the slower speed units.

Frequency vs. rpm and Poles - Consider the case of generating a 100 KC power output with a 3200 cps input:

Input:	300 KW 120/208 volts	3200 cps 1ϕ
Output:	10,100 volts	100 kilocycles/sec. 1ϕ

The input and output frequencies determine the range in speeds and number of poles which can be used for frequency conversion. The relationship of $f = \frac{PN}{120}$ poles exists for both motor and generator, where $f = \text{CPS}$, $p =$ number of poles, $N = \text{rpm}$. Therefore, the following combinations are considered:

<u>MOTOR FREQUENCY</u>	<u>MOTOR POLES</u>	<u>RPM</u>	<u>GENERATOR POLES</u>	<u>OUTPUT FREQUENCY</u>
3,200 CPS	2	192,000	62	99.2 KC
3,200 CPS	4	96,000	124	99.2 KC
3,200 CPS	6	64,000	186	99.2 KC
3,200 CPS	8	48,000	246	98.5 KC
3,200 CPS	16	24,000	492	98.5 KC

Rotor Diameter vs. rpm - The diameter of the rotor is limited by the allowable stress level for the rotor configuration and material. A solid rotor with no axial holes through it has the minimum internal stress generated by rotation for a given diameter. As a large diameter is desired in order to obtain a large number of poles, the diameter of solid rotors producing a maximum stress of 60,000 pounds per square inch at its center for the generator rpm has been established as a basepoint and are tabulated below. This diameter varies as the allowable stress to the one-half power. A stress of 60,000 psi is considered conservative for purposes of this study.

<u>RPM</u>	<u>PSI MAX. STRESS</u>	<u>ROTOR DIA. (INCHES)</u>
96,000	60,000	2.84
64,000	60,000	4.25
48,000	60,000	5.69
24,000	60,000	11.37
12,000	60,000	22.75

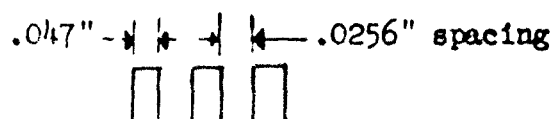
Pole Pitch - Consider 48,000 rpm and a rotor diameter of 5.69 inches with 246 poles.

$$\text{Pole Pitch} = \frac{\pi (5.69)}{246} = .0726 \text{ inches}$$

A pole span of 65 per cent of the pole pitch is reasonable; therefore, the pole width is $(.65)(.0726) = 0.0472$ inches.

The pole spacing conditions are as follows:

For alternate north-south pole rotor:



For alternate north pole rotor:



The resulting close spacing for an alternate North-south pole rotor would result in high leakage fluxes between North and South poles unless very small air gaps are used between rotor and stator. Therefore, this type is not as well suited to the frequency range of 50 KC to 200 KC as the homopolar type.

ELECTROSTATIC GENERATORS

Early in the preliminary phase of the study program, the plasma engine requirements of high voltage and relatively low current suggested the application of an electrostatic generator for mechanical to electrical energy conversion. The electrostatic generator is attractive for plasma engine power due to its high efficiency and its low power to mass ratio. Figure 17 compares the specific weight (lbs/KW) versus power output of a 90 per cent efficiency electromagnetic generator and a 98 per cent efficiency electrostatic generator. For the power level of this program, (300 KW), Figure 17 indicates approximately .75 lbs/KW. Other references reviewed indicate specific weights of .6 to .9 lbs/KW down to .2 and .4 lbs/KW.

Broadly classified, the electrostatic generator falls into two categories: (1) The Van de Graaff generator, which operates on the principle of charge transport by a moving belt, and (2) the variable capacitance type. For the plasma engine only the varying capacitance type appears feasible. Varying capacitance electrostatic generators may be classified into various types dependent upon type of excitation, AC or DC output, voltage doubling, bridge type, etc. Three types were considered in this study and are shown schematically in Figure 18. The Type I generator shown in Figure 18 is a variable capacitance, line-excited type of machine with AC excitation and AC output. A second type of electrostatic generator, the bridge type, utilizes a DC excitation voltage and produces an AC output. A third type of electrostatic generator as shown in Figure 18 is the voltage doubler or parametric generator. This generator delivers a DC output voltage from lower DC excitation voltage.

The efficiency of electrostatic generators approaches 100 per cent with experimentally verified efficiencies of 98 and 99 per cent obtained. These high efficiencies are the result of the elimination of losses inherent to the electromagnetic generator such as hysteresis, dielectric, eddy current, magnetic and windage (vacuum dielectric operation). In addition, the I^2R ohmic losses are a minimum due to the low required charging currents. The increased efficiency is important for a number of reasons. Energy is conserved, heat losses (which must be radiated to space) are at a minimum resulting in lighter weight radiators and the total system weight is reduced.

The utilization of the electrostatic generator for the particular application of this program would involve the solution of a number of problems, some inherent to the generator and some due to program requirements.

Some major problems requiring solution are:

1. Selection of generator type (possibly a hybrid type) which would provide the high frequency output power.
2. Conversion equipment to provide proper output loads for the generator. The electrostatic generator is inherently a high-voltage, low constant-current generator and thus requires a high impedance output load. The load represented by the plasma

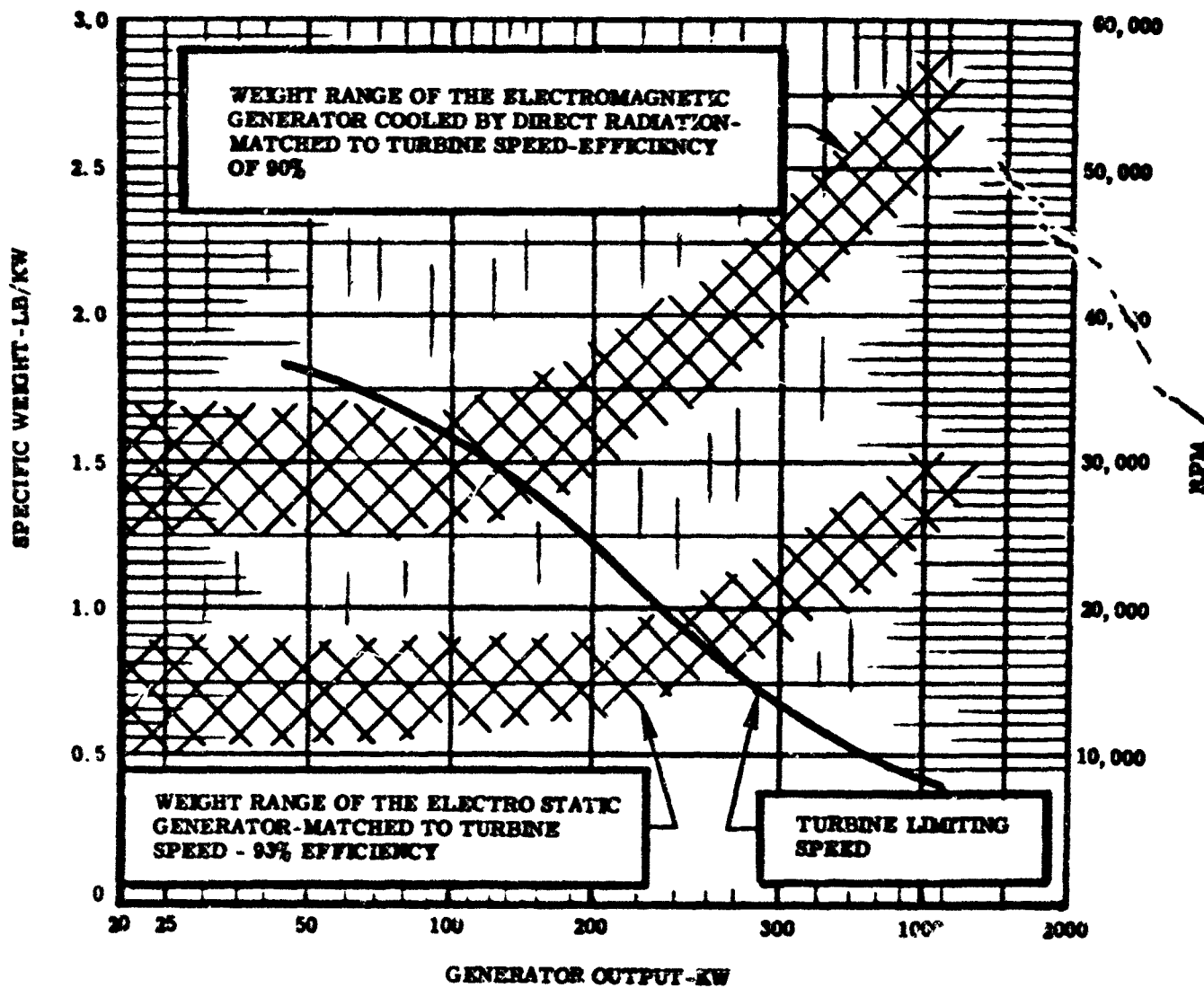
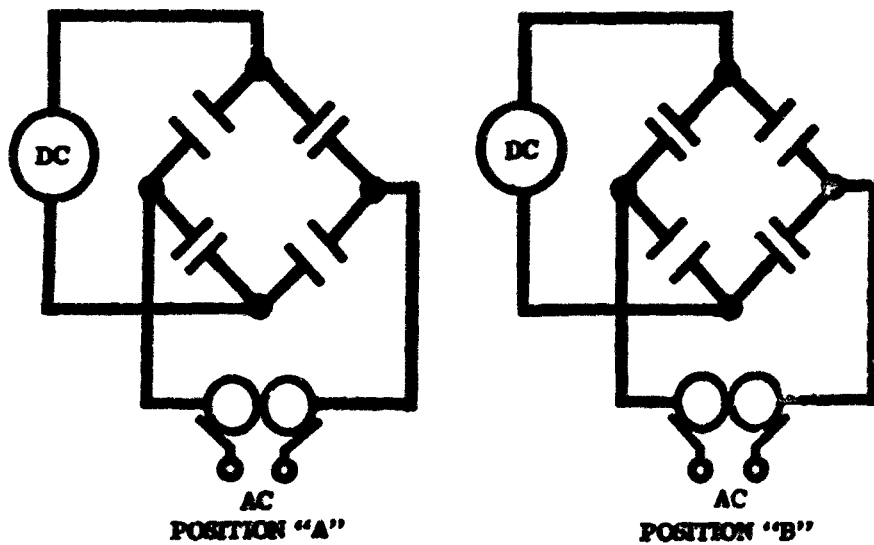
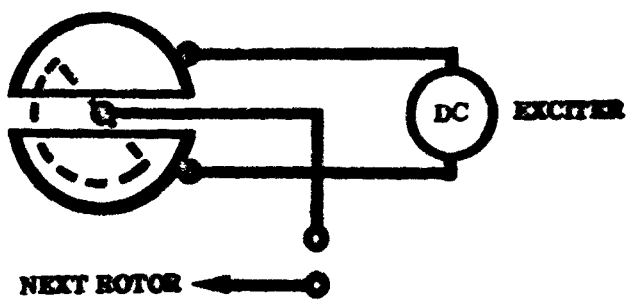


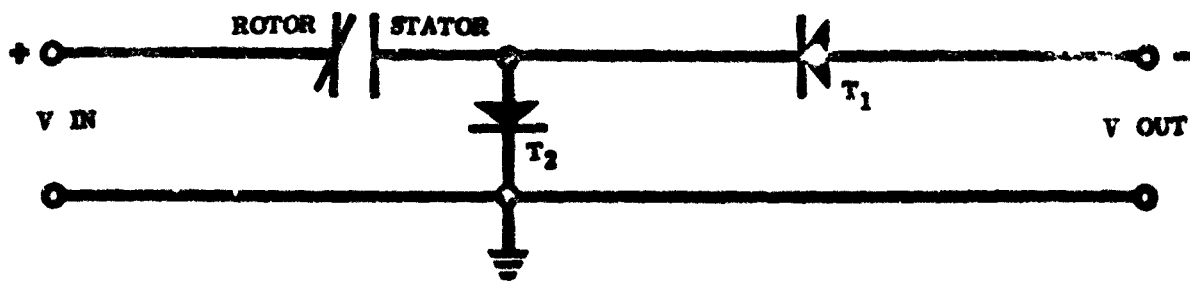
Figure 17. Specific Weights of Practical Electrostatic and Electromagnetic Generator Designs



TYPE I



TYPE II



TYPE III

Figure 18. Electrostatic Generator Techniques

engine is low (below 1,000 ohms) and this would result in low power transfer and very high excitation voltage unless some type of impedance matching device is used.

3. Bearing and seal problems. Since rotor weight is small, the electromagnetic bearing is one solution that should be investigated.
4. Manufacturing and fabrication problems involving rotating elements at very close spacing.
5. Electrical conversion equipment for excitation power supply.

ROTARY CONVERTER TECHNIQUES

A MOTOR-GENERATOR

The most common type of frequency changer or converter is a motor-generator set. Such a device possesses the main advantages of high power per unit weight and high temperature capability. Traditional designs are frequency limited for this particular application because of the number of poles required to produce the desired frequency.

With the advent of high-strength steels from which rotors can be manufactured has come an increased speed capability for generators. Coupled with this is the trend away from wound-rotor construction and toward solid-rotor types of machines. By use of solid-rotor techniques and increasing the speed of the rotor, an increased frequency output is possible from a motor-generator type of converter. High voltage, either three-phase or single-phase, is no problem for a motor-generator unit and is limited only by the insulation requirements.

For the high-frequency, high-voltage requirement of this study, the motor-generator is appealing in that there is no need for a transformer to gain the high output voltage of 10,100 volts. The motor-generator type of device is really limited only by the number of poles which can be included in the periphery of the rotor.

It is necessary in the three-phase application to consider three separate generator sections on a single rotor, each displaced by 120 electrical degrees.

STATIC CONVERTER TECHNIQUES

SEMICONDUCTOR TECHNIQUES

Several types of semiconductor devices were reviewed during the preliminary investigation phase for possible application in high-frequency and high-voltage conversion devices. These included:

- a. Silicon controlled rectifiers (SCR)
- b. Transistors
- c. Four-layer diodes
- d. Tunnel diodes

Each semiconductor device was investigated in terms of voltage, current and frequency capabilities today and in the future. Figure 19 is a comparison of these static devices. The first device to be investigated was the silicon controlled rectifier (SCR) because it is widely used today in converter systems. Although SCR's are capable of handling large currents and voltages (up to 235 amps at 600 volts) they are presently limited in frequency of operation to about 35 K cps. This frequency capability is expected to advance upward to around 70 to 100 K cps in the next few years. Based on this expected future capability a preliminary design of a single-phase SCR type of converter has been made and is compared with the transistor unit in the Appendix.

Transistor devices have high voltage, high current, and high frequency capability and appear the most promising for converter use. Several types of circuits using transistors were investigated, including power chopper, power square wave oscillation and an rf generator technique. Of these, the power chopper appeared the best; mainly, due to the fact that this circuit does not require a saturated-core transformer with its resulting large saturating current loss. In using a DC chopper technique with transistors or the silicon controlled rectifier, the DC magnetization of the transformer resulting from the large DC current in the primary winding must be considered. The tunnel diode is capable of switching large currents (1,000 amps or more) at a high frequency, but these devices are limited in voltage capability to .2-2 volts. This voltage feature makes tunnel diodes not too practical for use with high-voltage power sources. The four-layer diode is limited in current and frequency (ten amperes at 20 kilocycles per second).

Of the semiconductor devices studied, the SCR and transistor concepts were the most worthy of design analysis. A more detailed discussion of these two techniques plus tunnel diodes and four-layer diodes will be found in the section which follows.

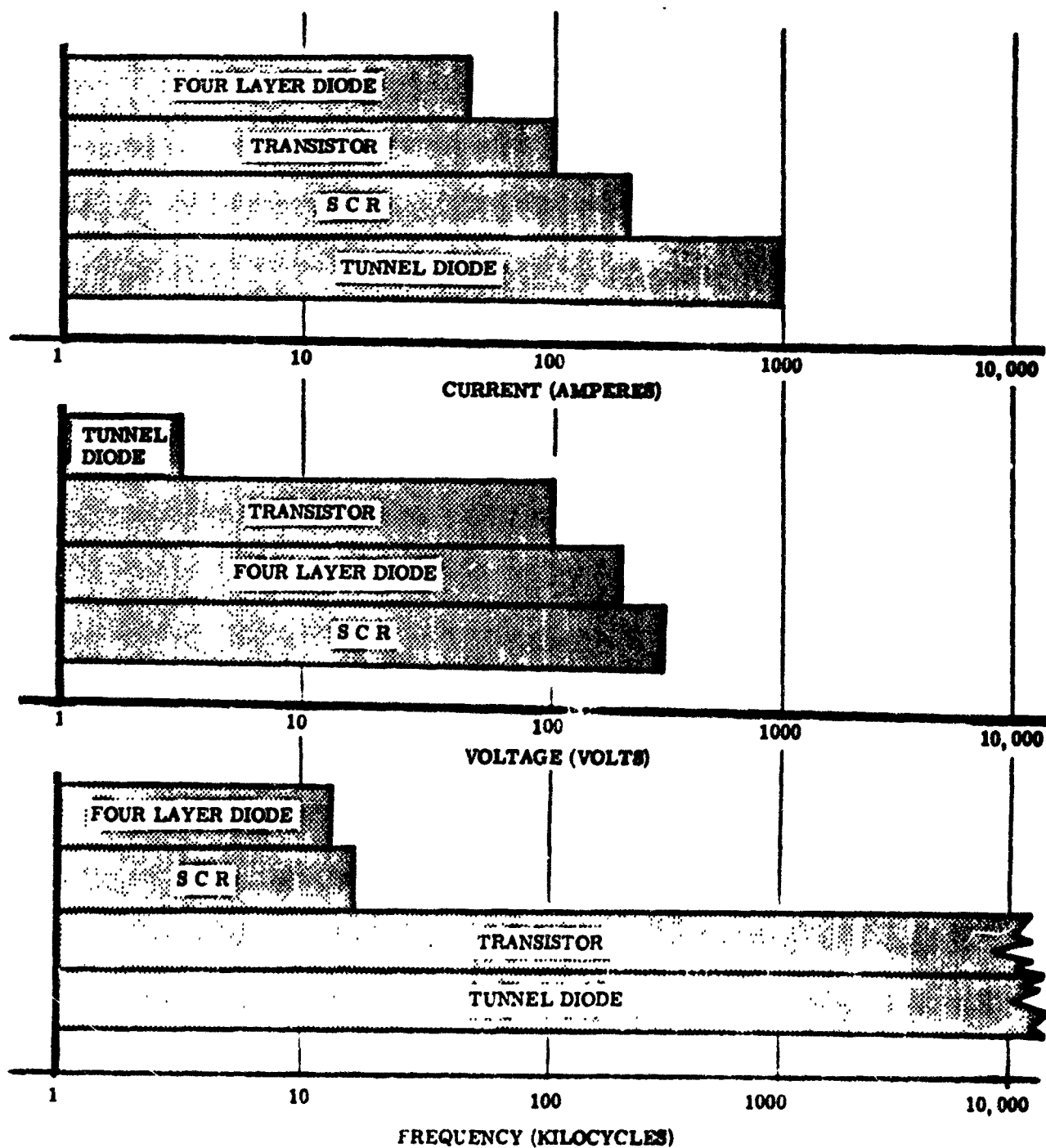


Figure 19. Comparison of Semiconductor Devices

Silicon Controlled Rectifier (SCR) Converters

SCR inverter circuits are of three main types: The power chopper which produces a square wave output, a sine wave inverter type, and a 3 ϕ AC to 1 ϕ AC direct converter. A direct AC converter frequency changer requires no input transformer for its operation, but can convert 3 ϕ alternating current directly into high frequency, high voltage, single-phase alternating current. In order to increase the output voltage, a step-up transformer is required.

The operation of a typical circuit for utilizing 3 ϕ , 120/208 V, 3200 cps power input as shown in Figure 20 is as follows. During the 120 electrical degrees that the line to neutral voltage of phase A of the supply to the frequency changer is higher than that of the other two phases, the two silicon controlled rectifiers connected to phase A of the supply alternately conduct current. The rate at which these two controlled rectifiers switch is determined by the timing of the firing pulses that are sent to their gate. The commutation or transfer of the load current from one rectifier to the other is accomplished by the commutating capacitor C.

During the next 120 electrical degrees, the line to neutral voltage of phase B of the supply is the highest and the two-controlled rectifiers connected to this phase take over the switching of the load current. The silicon-controlled rectifiers connected to phase A and C are idle during this period.

The output frequency is dependent on the frequency of the controlled rectifier firing, and this follows some reference such as an oscillator. During the operation of a frequency changer of this type, when one silicon-controlled rectifier is fired, the capacitor charges according to the time constant determined by the commutating capacitor C1, the inductance of the neutral choke L1, and the impedance of the load. A transformer voltage is then reproduced since the capacitor is in parallel with the transformer. When the second rectifier of the pair which is connected to the other half of the primary is fired, the capacitor discharges around the near short circuit path. The discharge current passes forward through the controlled rectifier turning it off. The capacitor now charges in the opposite direction until the first rectifier is again fired. This commutation process continues with the controlled rectifiers producing the high-frequency voltage in the output transformer.

In order for this circuit to commute, the total load must be capacitive or represent a leading power factor; the commutating capacitor being considered part of the load. If an inductance is added to the load, the capacitor value may have to be changed to keep the total power factor leading. This circuit can operate with a maximum power factor of .96, and a minimum of zero. In other words, the circuit can operate at no load with only the commutating capacitor. However, if the value of capacitance is large (approaching zero power factor), high voltage will appear across the power transformer and across the controlled rectifiers. These voltages are much in excess of the applied supply voltage and could easily exceed the ratings of the switching components.

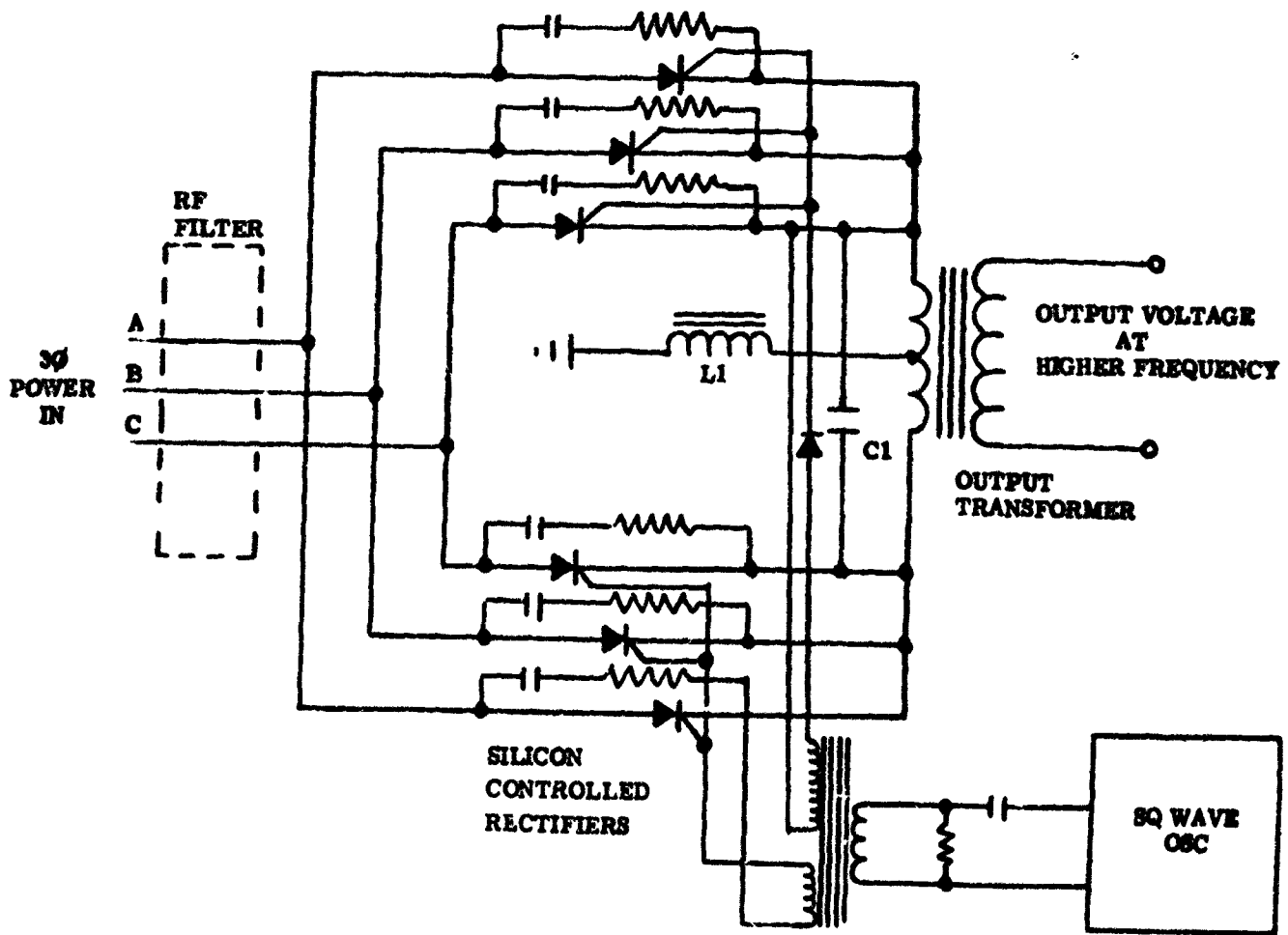


Figure 20. SCR Frequency Changer Technique

The operating frequency of this circuit is limited by the controlled rectifiers used. If the controlled rectifier is selected for a short turn-off time and the transformer leakage is kept to a minimum, operating frequencies up to 35,000 cycles per second and beyond could be realized. The switching power capability of SCR devices is also limited by frequency.

Direct Sine Wave Inverter

The operation of the direct sine wave inverter may be described as follows: The DC voltage is applied as shown in Figure 21A. Capacitors C_1 and C_2 are kept from charging because silicon controlled rectifiers CR1 and CR2 are in their blocking state. If a pulse is applied to both SCR gates, only SCR1 will fire as CR2 is reverse biased. As CR1 starts to conduct current, I_1 flows in the direction indicated through the load T_1 and charges capacitor C_2 to twice the applied voltage E . Since the voltage on C_2 is of the polarity shown, CR1 becomes back biased and returns to its blocking state. CR2 is now forward biased and begins to conduct, causing current I_2 to flow through the load T_1 in the direction shown and causing capacitor C_2 to discharge. When capacitor C_2 discharges completely, silicon controlled rectifier CR2 returns to its blocking state and CR1 starts to conduct repeating the cycle at half the rate of the applied gate pulses.

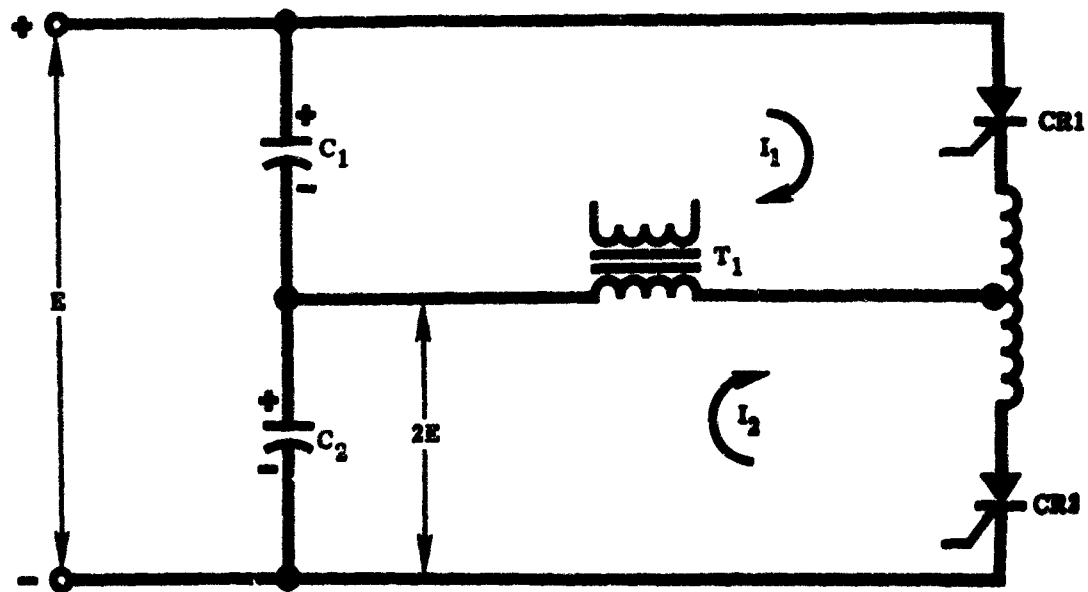
SCR Power Chopper

The operation of this circuit depends on the use of a gate-controlled silicon controlled rectifier, that is, an SCR which can be turned on with a positive pulse and turned off with a negative pulse. The circuit for the power chopper is shown in Figure 21B. A voltage V is applied with the polarity as shown and this causes capacitor C_1 to charge through resistor R_1 and output transformer T_1 . When the voltage of C_1 reaches the breakdown value of diode D_1 (20V to 40V), a positive pulse is applied through R_3 to the gate of silicon controlled rectifier CR1 causing it to conduct current I_1 through the load transformer T_1 . As CR1 starts to conduct, capacitor C_2 starts to charge through R_1 . When the voltage across C_2 reaches the breakdown voltage of diode D_2 , D_2 starts to conduct a current I_2 as shown causing CR1 to return to its blocking state. C_1 then starts to charge causing the cycle to repeat. This circuit then is free running compared to the sine wave inverter which has to be pulsed at a rate twice the output frequency.

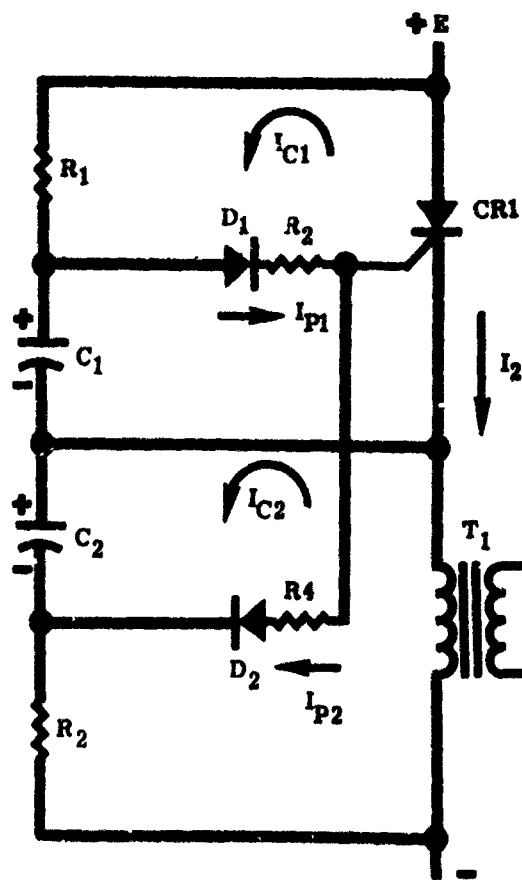
For this study the SCR power chopper circuit was chosen for detailed analysis and comparison with the transistor circuit and is described in the Appendix.

Transistor Type Inverter - With recent developments in high power, high-frequency transistors, it is now possible to design a DC to AC frequency converter with outputs of several thousand watts. These power transistors have remarkable frequency capabilities even into the megacycle range.

Transistor inverters may roughly be classified into three types, although all are based on rectifications of the incoming AC to DC, then



A SINE WAVE INVERTER



B POWER CHOPPER

Figure 21. SCR Inverter Schemes

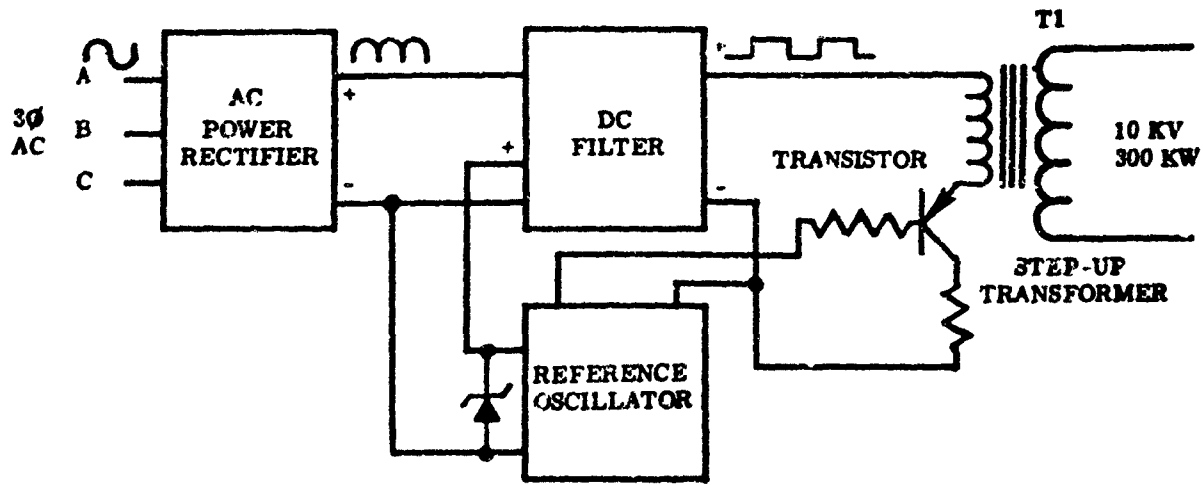
regenerating a new frequency. The first type might be called a power chopper. In this type of system the incoming alternating voltage is rectified, filtered, then switched by a power switch at the desired frequency as shown in Figure 22A. The step-up transformer T_1 transforms the output voltage to the desired level. The power switch in this case is a transistor or a group of transistors in parallel. The switch can be a silicon-controlled rectifier but due to the frequency limitation of silicon-controlled rectifiers, transistors must be used in this application with a corresponding loss in efficiency due to the additional power loss in each transistor.

One design aspect which must be considered in using the DC chopper technique is the DC magnetization of the transformer core resulting from the large DC current present in the primary windings. Three methods can be used to correct this DC magnetization effect and establish a "flux reset" in the transformer. One technique is the use of an air gap in the transformer which prevents the transformer core from saturating. Another technique is the use of an extra transformer winding of the proper polarity to cancel the unwanted field flux. The third technique is to use an increased amount of iron in the core. Any of these methods will result in a weight penalty. However, this penalty will be small due to the small size and weight of the transformer required at the high frequencies proposed in the inverter design. Selection of the technique to be used can easily be made in the prototype transformer design stage. Implementation of the "flux reset" technique (any one of the three mentioned) presents no real problem in the design.

The second type of transistor inverter might be called the power square wave oscillator. In this type of circuit the input 3ϕ alternating current is rectified, filtered, and used as the supply voltage for a square wave oscillator. The operation of this circuit (see Figure 22B) is as follows: Assume that transistor A is conducting and transistor B is off. The voltage E is now across winding (2) of the transformer, with the polarity as shown. Voltages of the same polarity are induced in the other winding; this results in a positive base voltage at B, and a negative base voltage at A. This maintains A conducting and B at cutoff.

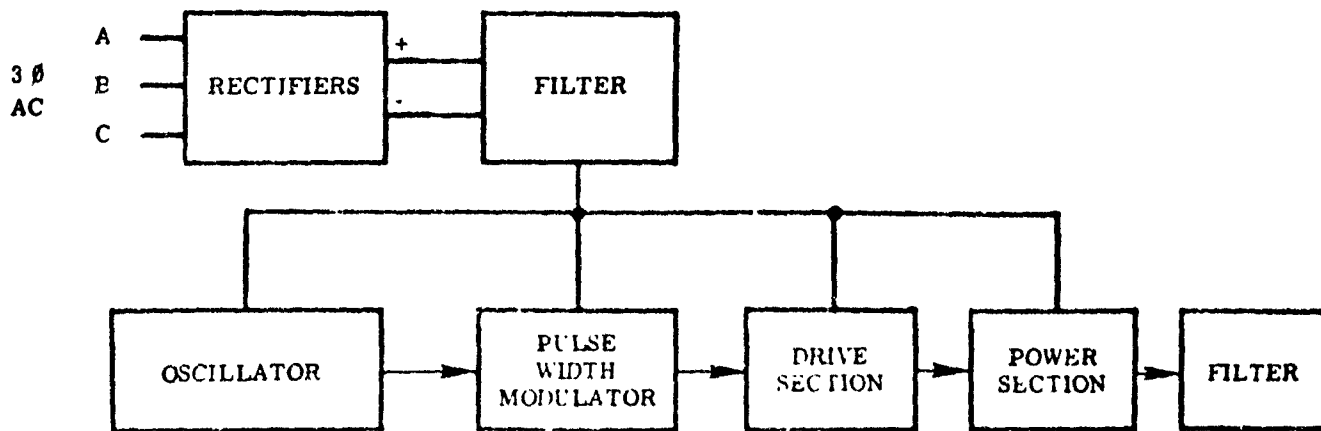
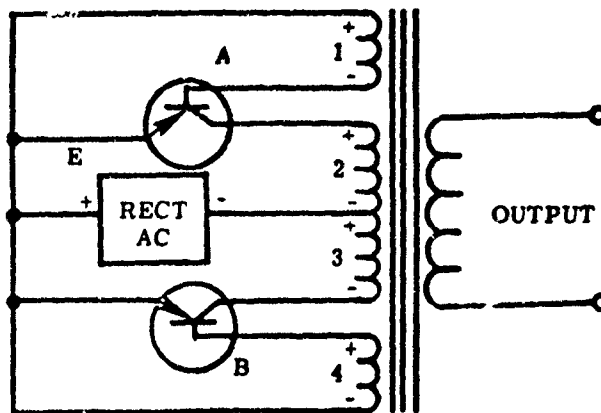
The voltage E across winding (2) produces an increase of flux in the core until it saturates. At saturation the current in winding (2) rapidly rises and the reactance drops, causing the voltage in the remaining windings to disappear. The negative base drive is removed from transistor A, so that it is nonconducting. The current of the winding is then zero, and the flux drops. The flux change induces voltage in the windings opposite in polarity to the previous condition. This causes transistor B to start conducting with transistor A maintained off. Voltage E is now across winding (3) and the cycle repeats itself in the reverse direction.

For high power output the circuit of Figure 23 can be used. It is essentially the same as Figure 22B except that it uses two transformers instead of one. By use of two transformers, the input transformer saturates; therefore, the extra current necessary at saturation is small compared to the load current. This allows the use of a small square-core driver to drive a much larger power. The output transformer then works linearly to step up the output voltage to the required level. The input voltage is divided equally across the four series primary, subjecting each transistor to only half of the supply voltage.



A
POWER CHOPPER TYPE FREQUENCY CHANGER

B
POWER SQUARE WAVE
OSCILLATOR
(DC TO AC CONVERTER)



C
RF POWER GENERATOR

Figure 22. Transistor Frequency Changer Techniques

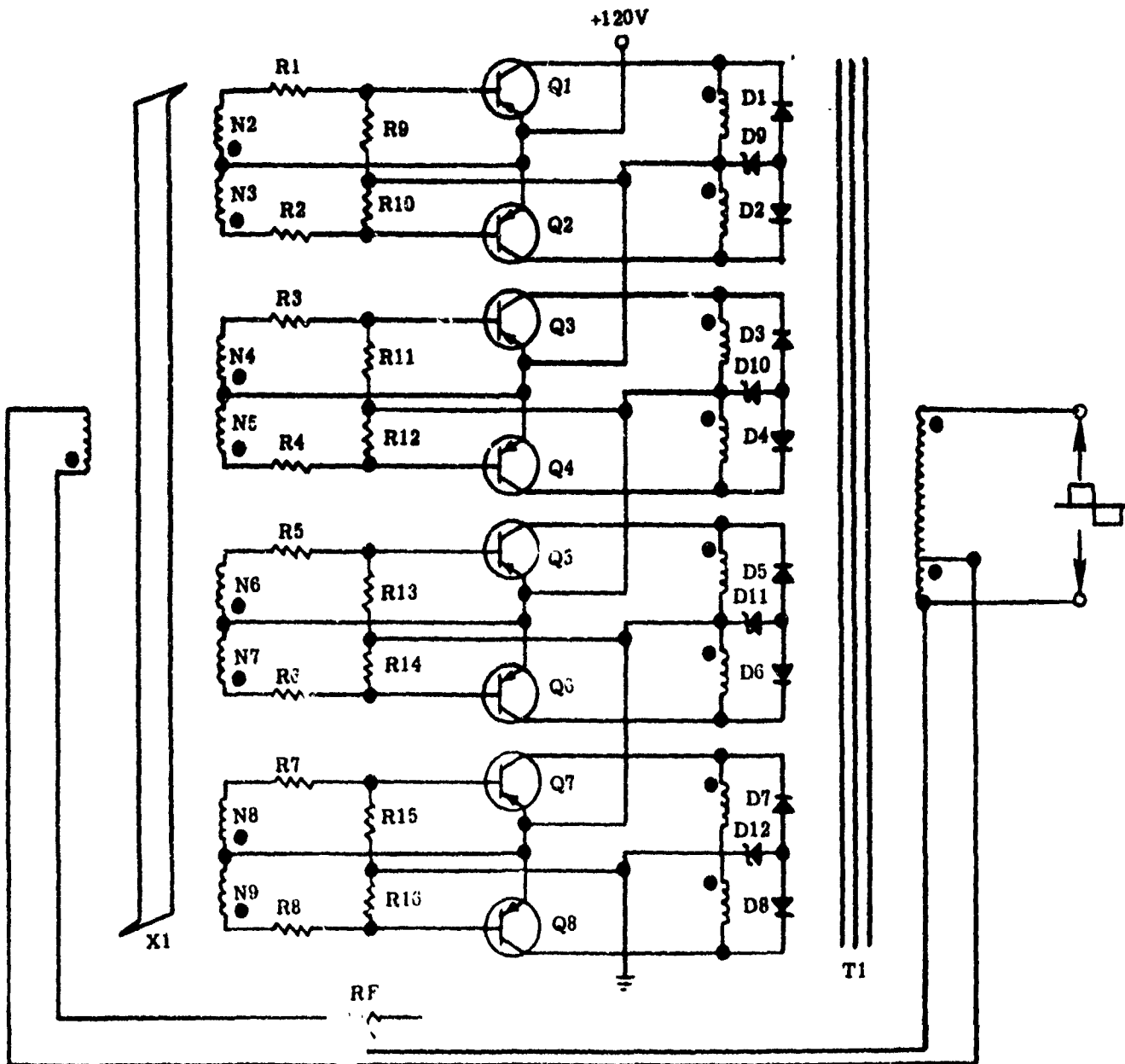


Figure 23. High Voltage Full Transformer Transistor Converter

The third type of transistor inverter could be called an LF power generator (refer to Figure 22C). The RF frequency is generated by a low level precision oscillator. The output of the oscillator is applied to a pulse width modulator, which regulates the output voltage by controlling the on-off time of the driver circuit and this actuates the power output stage. The duration of the square-wave voltage is controlled during each half cycle as it is applied to the driver section. For low line and high load conditions of the inverter, the square-wave voltage actuates the driver circuit during 180° of each half cycle of the inverter frequency at high line and low load conditions, the driver is actuated only for approximately 90° of each half cycle. This reduces the "on" time of the power switches resulting in reduction of output power at constant output voltage.

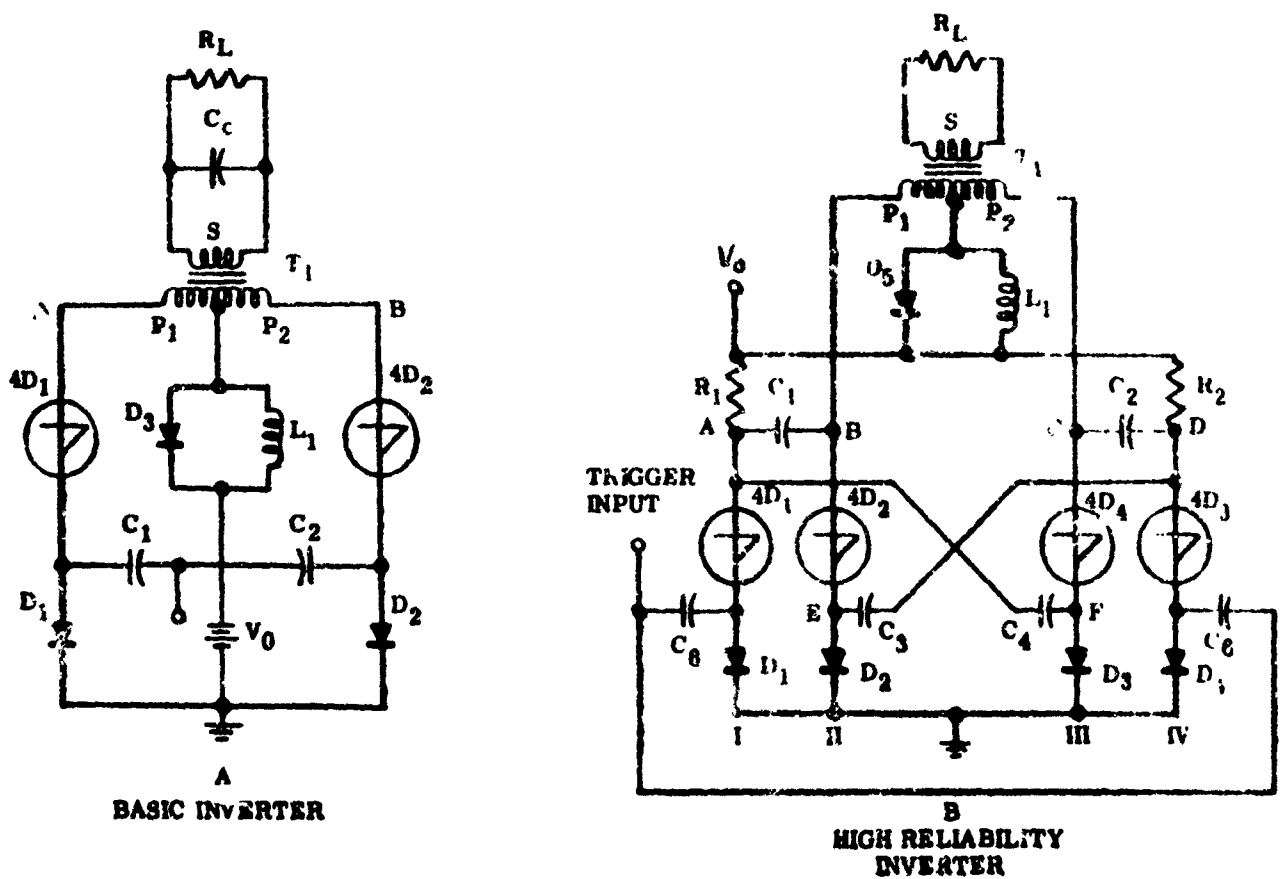
Shockley Four-Layer Diode Inverter - Simple, efficient and versatile solid-state inverters may be made using Shockley four-layer diodes. These inverters may be used for the generation of alternating current from a direct current source. With the addition of a transformer and rectifier, a direct current at a high voltage can be obtained. The alternating current is obtained by switching a constant current first into one side of a transformer and then into the other.

Two basic circuits are shown. The first is a high efficiency circuit requiring a minimum of components. The second circuit provides extra protection against lock-on from wide load changes, loads of varying power factor, or changes in supply voltage. Several types of four-layer diodes are available providing a range of current in the primary of the transformer from ma to amperes. Supply voltages up to 80 volts may be used with a single four-layer diode in each side of the inverter. Higher supply voltages may be employed by using several four-layer diodes in series.

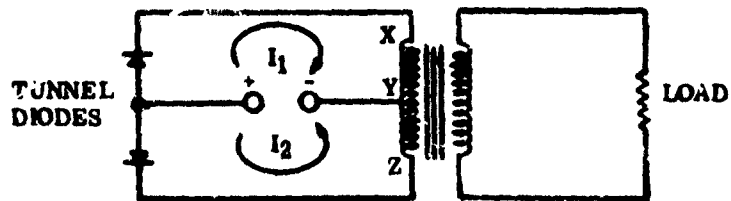
Figure 24A shows a high efficiency DC to AC power converter. The circuit alternately switches a fixed current (supplied through L_1) into the two halves (P_1 and P_2) of the primary of a center-tapped transformer (T_1). The frequency is controlled externally by pulses received at the trigger point. A cycle is completed for every two pulses received at the trigger point.

The circuit can be designed to operate at any frequency from a few hundred cycles to 20 kilocycles or more. The DC supply voltage may be from six volts to several hundred volts. The power output is limited by the maximum current which may be switched in the primary. The circuit efficiency is a function of DC supply voltage, with a practical maximum of 95 percent at higher supply voltages and a minimum value of 75 percent for a six volt DC supply. For supply voltages above 20 volts, efficiency is determined principally by losses in the transformer (T_1) and the coil (L_1).

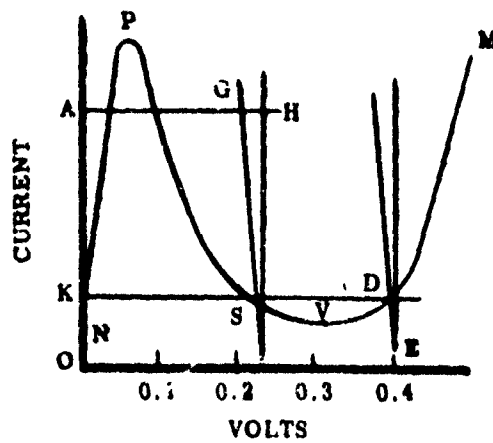
The circuit in Figure 24A operates as follows: When four-layer diode $4D_1$ is conducting, current from the DC supply is passed through the loop composed of L_1 , P_1 , and $4D_1$. This current is limited by the impedance reflected into P_1 from the secondary of the transformer. Point A will be at the holding voltage of $4D_1$ and D_1 in series (1 to 2 volts). The center tap of the transformer will be at V_0 , and point B will, by transformer coupling between P_1 and P_2 , be at a voltage of $2V_e$.



Shockley Four Layer Diode Inverter



G



D

OPERATING CHARACTERISTIC CURVE FOR THE INITIAL DIODE STATIC INVERTER TUNNEL DIODE INVERTER

Figure 24. Other Inverter Schemes

A negative pulse of sufficient amplitude applied to the trigger point will now switch $4D_2$ into its conducting state. The voltage on the commutating capacitor (C_c), which is coupled from the transformer secondary into the two primary legs, will drive point A negative by a voltage of $2V_s$, switching off $4D_1$. The DC supply current will thus be commutated from P_1 into P_2 . This current may be assumed to be constant during the switching transient due to the presence of L_1 . As the current and voltage reach their steady-state values, point B will be at 1 to 2 volts, point A will be at plus $2V_0$ volts.

The next negative trigger pulse will switch $4D_1$ on again, and the commutating capacitor will, through transformer action, switch $4D_2$ off, completing the cycle.

The inverter efficiency is particularly sensitive to certain design conditions. With proper care, however, a highly efficient, trouble-free circuit may be obtained. The switching voltage of $4D_1$ and $4D_2$ must be at least twice the DC supply voltage. A margin should be allowed to provide protection against false firing due to noise, high temperature or other problems peculiar to special application. The maximum primary current should be limited to twice the DC current rating of the four-layer diodes. Also, the inductance L_1 must be large enough to insure constant current during the switching transient. It must also be such that, in combination with the reflected R and C provided by the transformer, oscillations in the current do not occur which might turn the conducting diode off. For maximum efficiency the coil should have a high Q (low resistance).

The design of the transformer (T_1) is most important. A unity coupling coefficient for all values of primary current is required. Transformer efficiency must be high for maximum circuit efficiency. Saturation of the transformer will cause the inverter to lock-on (see below). Poor coupling reduces the range of load variation possible and requires a larger commutating capacitor. Poor coupling also tends to cause lock-on.

One of the standard problems of high efficiency parallel inverters is their tendency to lock-on; i.e., for both sides of the inverter to be turned on and stay on. Protection against this possibility may be provided by using a normally closed relay in place of L_1 and passing the DC supply current through both the relay contacts and the actuating coil. The relay should be selected to operate at a current level somewhat less than twice the normal circuit current. Solid-state protection against lock-on in place of the relay is discussed below.

The solid-state inverter circuit shown in Figure 24B provides unusually reliable performance under extreme conditions of load variation, load power factor, or supply voltage variations. The circuit is fail-safe in that the supply current drops to zero when the load is shorted. When the short is removed, normal operation is resumed. The circuit will continue normal despite large changes in supply voltage or poor load power factors. A modest loss of efficiency - ten per cent to fifteen per cent is required to obtain this protection when compared with the high efficiency circuit of Figure 24A.

Best Available Copy

The high reliability circuit uses outrigger stages which definitely turn off the adjacent conducting legs of the basic inverter when a trigger pulse is received, independent of the state of the other basic inverter leg. The onset of conduction in a given outrigger stage will also trigger the previously nonconducting inverter leg into the conducting state under normal operating conditions.

Design considerations for the basic inverter are the same as described above for Figure 24B. Note the absence of the commutating capacitor in the transformer secondary. This function is provided by the outrigger stages.

A Tunnel Diode Static Inverter - A simple static inverter circuit consisting of two tunnel diodes and a transformer wound on a square-loop magnetic core was reviewed earlier in this program. The techniques are feasible and are described in limited detail in this section. The circuit provides a practical method for stepping up voltages of the order of 0.2 volt to practical values.

In practice, the low voltage of a tunnel diode (a fraction of a volt per unit) constitutes a problem, since connecting many units in series to obtain useful voltage rapidly becomes uneconomical and unreliable. Based on this inherent problem, only a limited amount of study time was expended on the tunnel diode technique.

It would be highly desirable to use a single high-current unit, chop the current, pass it through a step-up transformer, and use the output either in its AC form or rectify it for DC applications. However, no static device at present is capable of being used as a chopper in such a circuit, because the saturation resistance of the high-power transistors and silicon-controlled rectifiers, while low, would still be much too high for efficient use in such a low-voltage circuit. Even mechanical devices would offer formidable contact problems.

As a solution to this problem, a high-power tunnel diode static inverter, using very high-current tunnel diodes and a square-loop magnetic core transformer is required. Tunnel diodes are not affected by temperature or radiation to the extent as are transistors and inasmuch as they are used as switches in a circuit which consists entirely of static components, the inverter should be both highly reliable and stable. The circuit employed is shown in Figure 24C and consists of two tunnel diodes and a square-loop magnetic core transformer. It depends for its operation on the tunnel diode characteristic, as shown in the Figure 24D.

The frequency of this circuit depends upon the size of the core, the number of turns on the primary windings and the input voltage.

Since the input voltage is limited to approximately 0.2 volt (for germanium) it is obvious that to obtain any appreciable power, the peak current of the tunnel diode must be very large. At the present state of the art, tunnel diodes are made in the *1,000 ampere range, but no theoretical peak current limit exists. Apparently, the peak current is only a function of cross-sectional area. Improved fabrication techniques should produce the large-area uniform junctions needed for peak currents

several orders of magnitude larger than those which are capable of being produced at present.

The efficiency obtained for this converter circuit will depend largely upon the ultimate characteristics of the improved tunnel diodes. Using tunnel diodes in converter circuits in thermionic and thermoelectric power supplies is appealing and should be the subject of further research.

*ASD Contract AF33(9657)-8964 with RCA

RF GENERATOR (VACUUM TUBE) SYSTEM CONCEPT

Vacuum tubes are used extensively as a prime source of r-f power in electronic heaters. Vacuum tube oscillators have frequency capabilities ranging from 100 KC to 1 MC and higher, with power outputs from 1 to 500 KW or more. Their greatest use is in the range from 150 to 500 KC at 5 to 100 KW. With these known characteristics, an r-f generator converter system appeared feasible for use in a converter system. A portion of this study was centered on the design of such a system.

In terms of electronics, r-f power generating equipment is not at all complex. Usually a power triode is used with three related circuits -- a power supply, a control circuit, and an output tank circuit. Energy from the power supply is changed into r-f energy by the oscillator-generator and then applied to the load through a tank circuit and matching device as shown in Figure 25. R-f power from a system such as this is used extensively for induction heating and makes use of Class C oscillator techniques.

A Typical RF System - An r-f power generation system is described in a section on Stator Tube Converter and uses a single high power oscillator tube with thyatron tubes for control of the output power level. Line power, such as would be available from the SNAP or SPUR system, goes to both the plate power and filament power circuits and to the control circuit. Control of the grid circuits of the thyatron tubes allows adjustment of the plate voltage of the oscillator, which in turn varies the power output to the load. Equipment protection features are required in an r-f power system in addition to cooling for the oscillator tube.

Figure 25 is a typical r-f generator system in which the source of r-f load (work coil) power is the tank and oscillator tube circuit. Here the tank circuit is simply a parallel circuit tuned to the required frequency with the tank capacitor storing energy in the form of kilovolt-amperes and then discharging it across the tank coil. The load (work coil) can be either part or all of the tank coil, or it can be the secondary of an r-f transformer. Various basic tank circuits used are shown in Figure 26. The following symbols are used:

V_T = tank voltage

Z_T = dynamic tank-circuit impedance

I_T = tank circulating current

C_T = tank capacitor, source of tank kilovolt-amperes

L_T = tank-coil inductance, including strays

R_T = tank-coil resistance, including strays

L_O = effective load (work coil) inductance under load

R_O = effective load (work coil) resistance under load

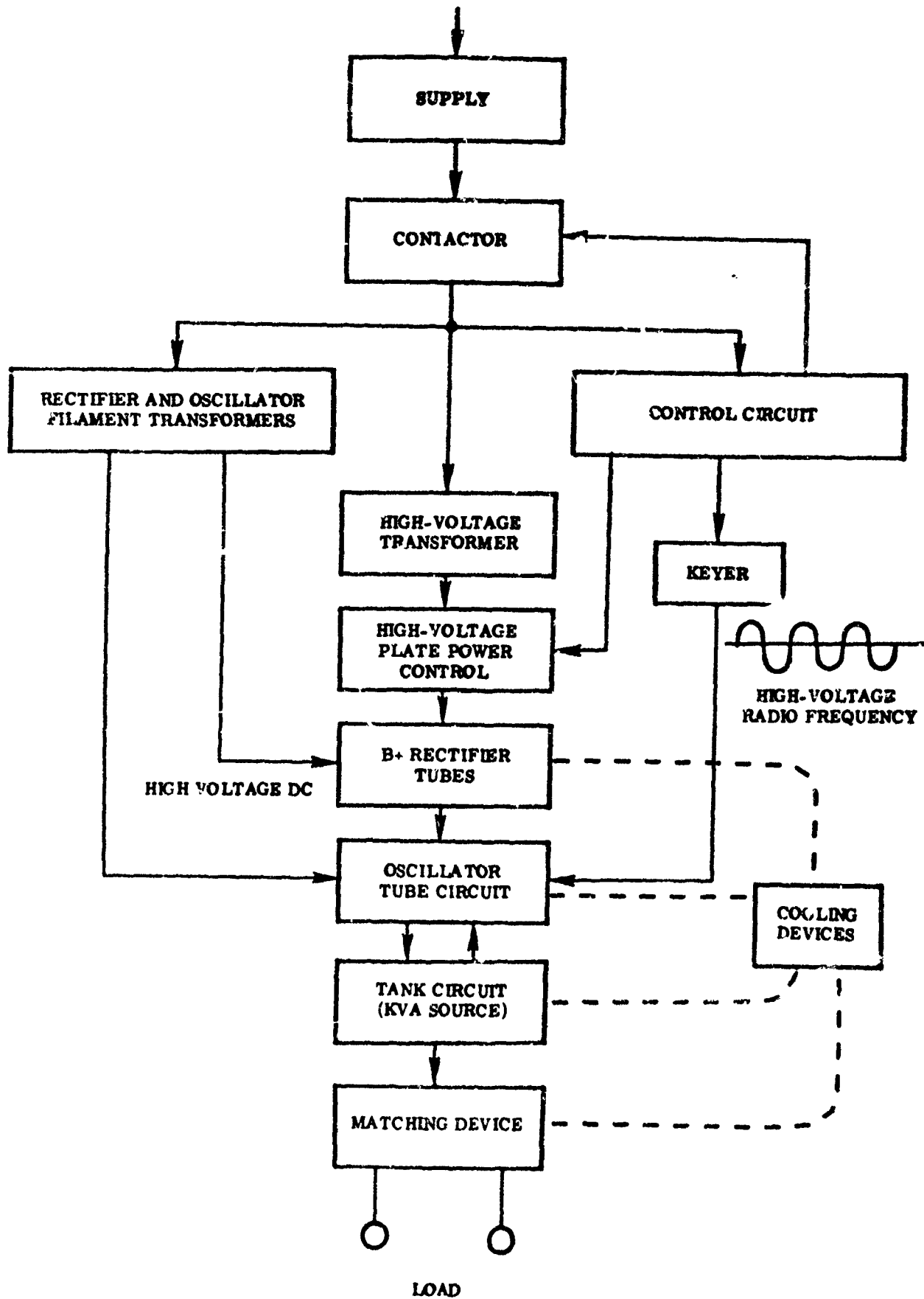
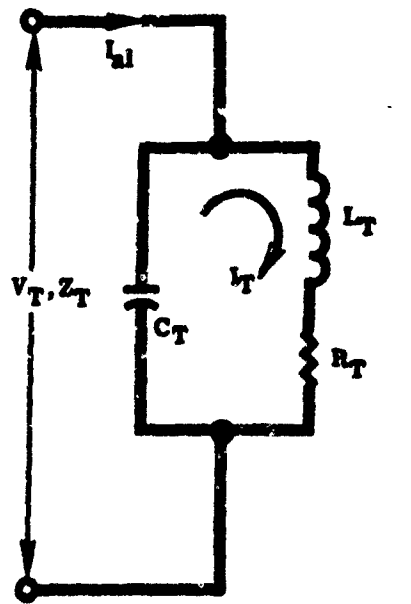
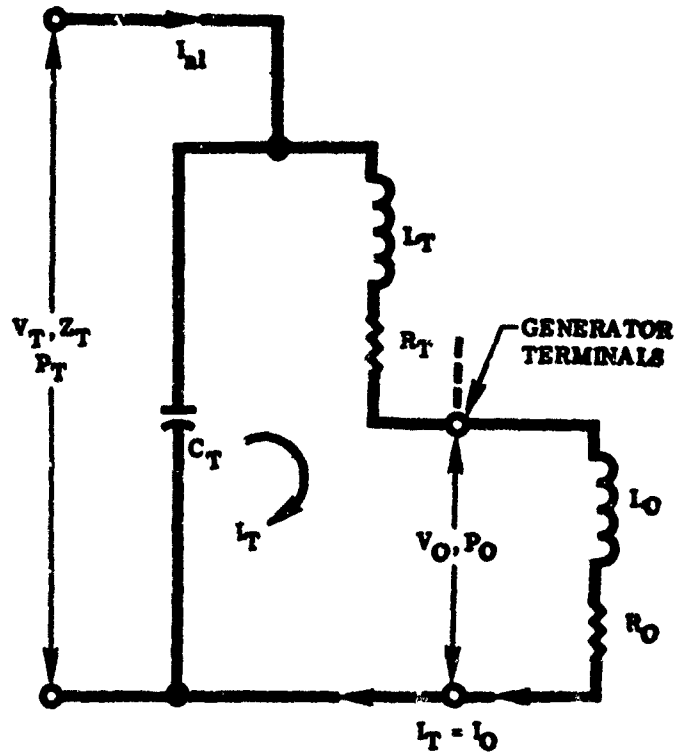


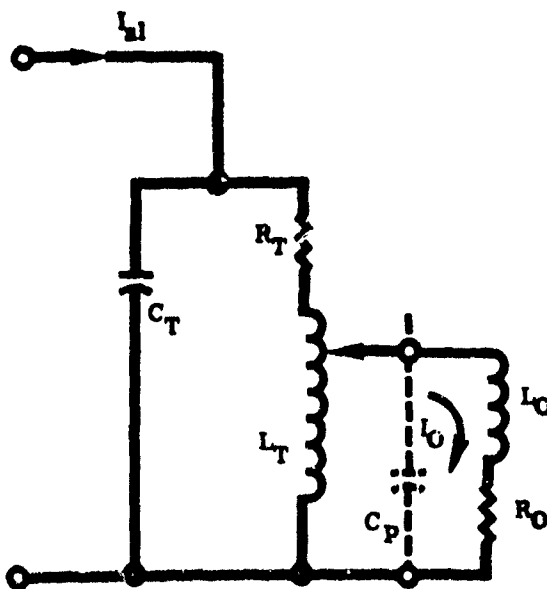
Figure 25. R F Generator Tube System Schematic



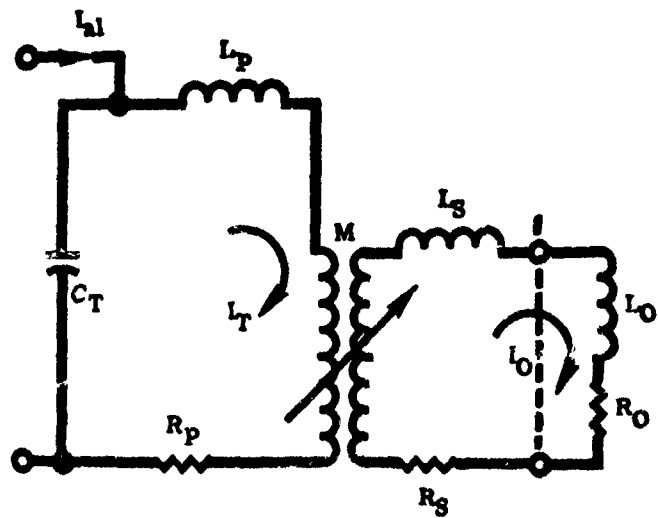
A BASIC R-F TANK CIRCUIT



B LOAD IN SERIES WITH TANK COIL



C LOAD TAPPED OFF TANK COIL (AUTO-TRANSFORMER)



D LOAD COUPLED TO TANK COIL (R-F TRANSFORMER)

Figure 26. Basic R F Generator Tank Circuits

- I_o = coil or load current
- V_o = coil or load voltage
- C_p = coil boosting or power factor correction capacitor
- L_p = transformer primary-winding inductance
- R_p = transformer primary-winding resistance
- M = mutual transformer inductance
- L_s = transformer secondary-winding inductance
- P_T = power into tank circuit (from tube)
- Q_T = effective tank circuit Q with loaded work coil
- R_s = coupled transformer secondary-winding resistance

The type of tank circuit used depends on range of generator applications. Where loads of the r-f power system may vary considerably, but coupling to the load is very low and Q_o values are not excessive, the coupled transformer circuit of Figure 26D is most suitable. If the impedance varies considerably, a variable coupling concept should be used. Ordinarily, the load impedance is low with a low Q value. This means a high value of I_o , usually higher than I_T , but it does not necessarily mean a high coil kilovolt-amperes if Q_o is low. This type of generator output is low-impedance or low KVA. Its main disadvantage is that transformer KVA losses vary between 75 to 85 per cent (variable coupling) and 60 to 75 per cent (fixed coupling).

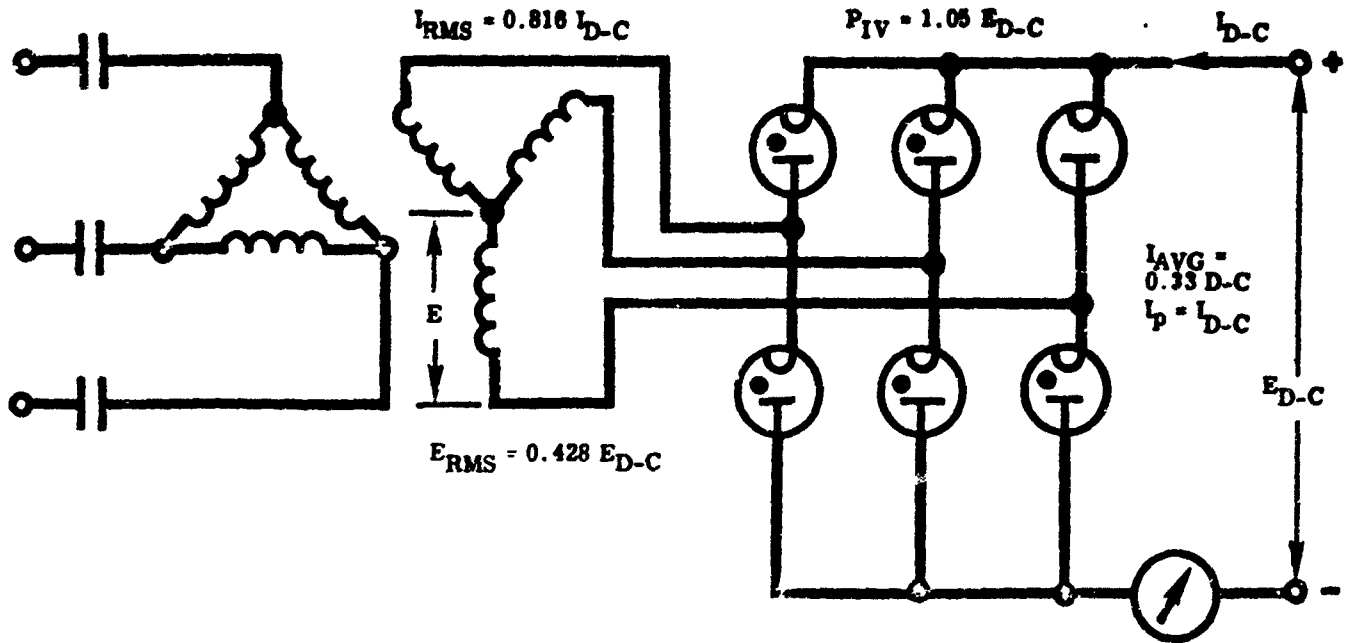
When the load impedance and Q values are high and many coil turns are required, the split tank-coil circuit of Figure 26B can be used. It provides a higher coil KVA, in fact the load in this configuration can serve as the complete tank coil if necessary. Current values are not so high as in coupled circuits. Figure 26C is a compromise between high and low impedance circuits and has a distinct advantage where automatic impedance matching is required.

Power losses in an r-f power system vary according to the Q of the load, the coupling coefficient of the transformer (if used) and the stray losses. The circuit of Figure 26D may be between 75 to 80 per cent efficient for Q's of five to ten, dropping to 65 to 70 per cent for Q's of 15 and 20. Circuit of Figure 26B usually has to work into a high Q coil resulting in a power efficiency of 70 to 80 per cent. Coil leads are very important in these circuits and should be kept to a minimum length. Due to high KVA required and the radio frequencies employed, the inductance of coil leads can cause considerable losses.

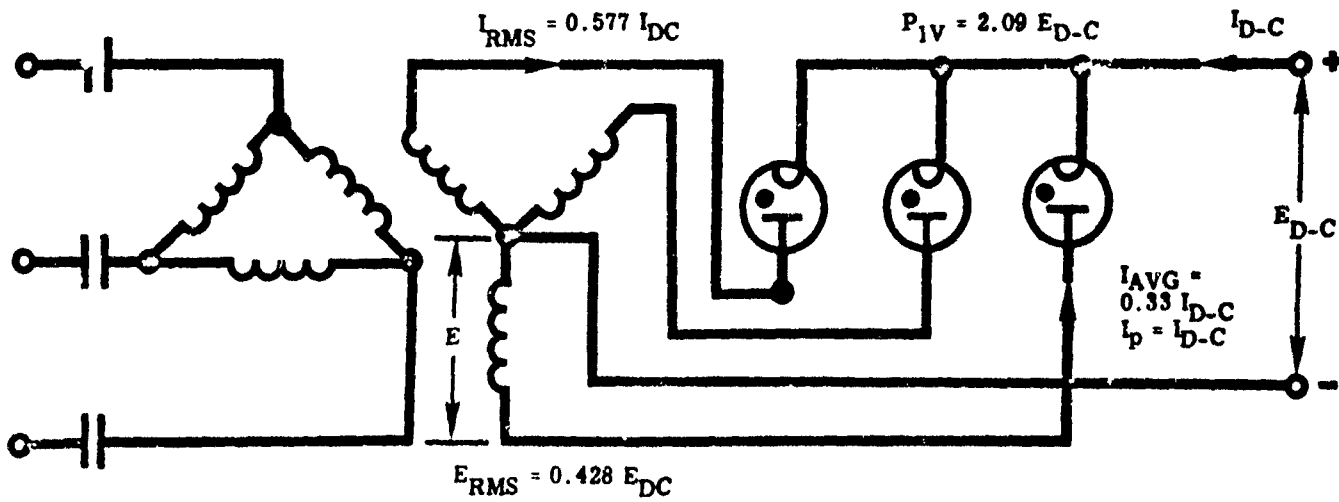
Generator Tube Power Supplies

The tube plate power supply is a source of DC voltage, usually between 3,000 to 12,000 volts and is capable of giving a DC plate current which may range from 200 ma to 20 amperes, depending on the tube power requirements. Most circuits include a high voltage transformer and rectifiers. For generators with outputs greater than 3 KW, circuits of Figure 27A and 27B are used. They present a balanced load to the supply line. The full wave circuit of Figure 27A has less than five per cent peak ripple voltage and requires no smoothing circuit.

Oscillator tubes of the type used in this particular circuit and typical of those shown in Figure 28 require liquid coolants. Liquid cooling of the oscillator anode is by means of a fluid coolant jacket around the tube in which a continuous flow of coolant is maintained. For application to a space system, a closed-loop type of cooling system with a circulating coolant would be required. The tubes supply a high impedance constant-current source of power and have to match into widely varying loads in a typical induction heating circuit. The design is usually rugged for industrial purposes and is based on triode principles. Filaments utilize thoriated tungsten and have high emission and long life. Most triodes operate in a Class C condition as oscillators at 70-80 efficiency.



A THREE-PHASE FULL WAVE SINGLE WYE



B THREE-PHASE HALF WAVE SINGLE WYE

Figure 27. Power Supply Rectifier Circuits for RF Generator

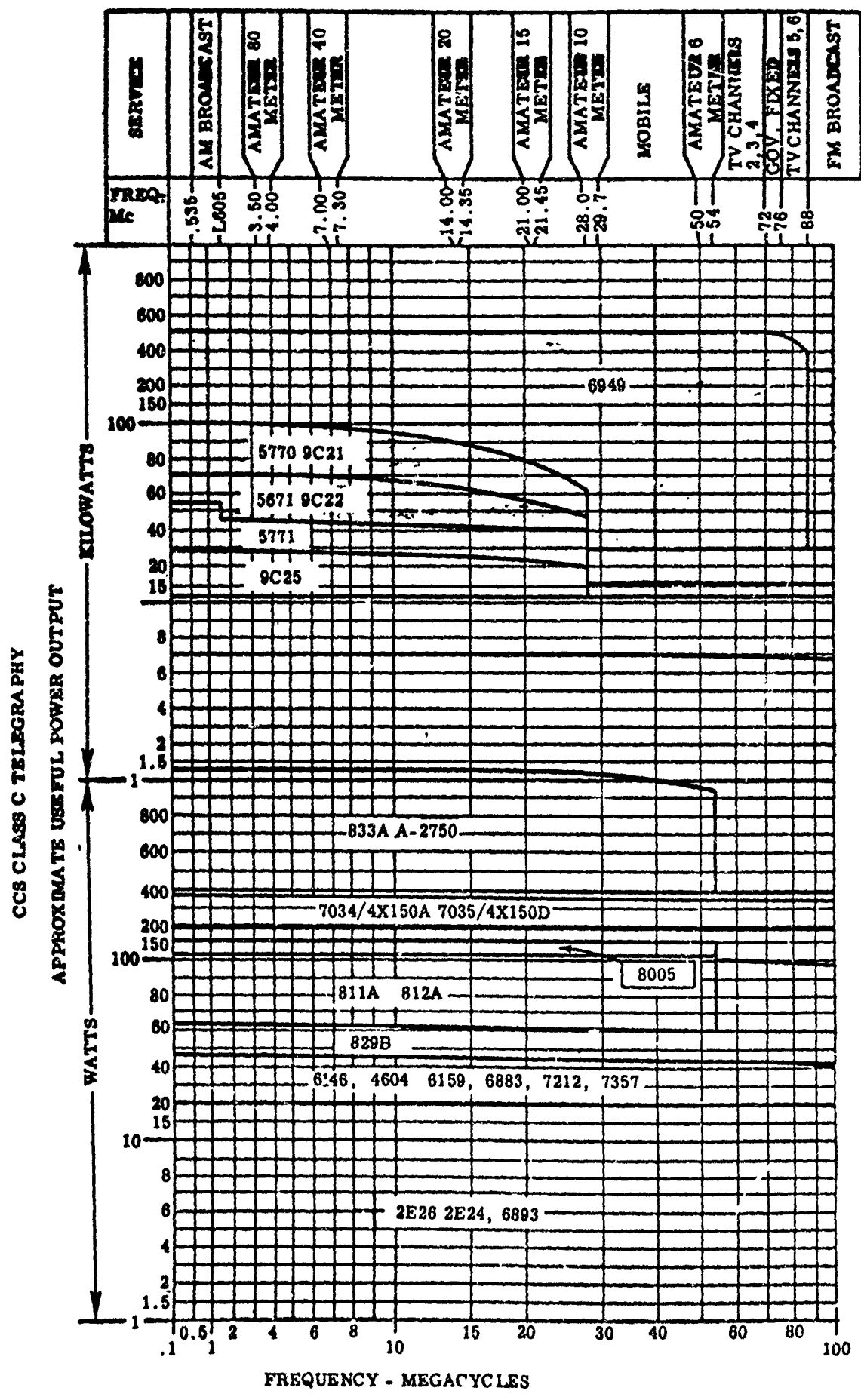


Figure 28. Available R F Tubes for Oscillator Use

FREQUENCY MULTIPLIERS

Another approach to high frequency power is use of magnetic-multiplier techniques. These were investigated and found to be feasible only in the lower frequency ranges (possible to 20 KC). Where the quality of power required is not too critical (as in the Litton accelerator), the reliability and long life of a magnetic type of frequency multiplier is worthy of consideration.

The size of magnetic multipliers in induction heating power systems is greater than an equivalent motor-generator set and the efficiency tends to be lower, but the device possesses advantages of simplicity, low maintenance cost, ruggedness and static operation. A two-stage frequency sextupler was one of the types analyzed during the study. (Figure 29 shows a typical magnetic multiplier). The discussion which follows gives an indication of the simplicity and performance of typical magnetic-multiplier systems.

The major undesirable features of magnetic frequency multipliers are the low input power factor and the relatively large size of equipment.

With the development of better core materials and circuits, a great improvement in these features has been achieved recently. Power at frequencies of two to six times the input frequency may be generated with reasonable efficiency.

Generally, in magnetic multiplier circuits, non-linear magnetic reactors are connected in a symmetrical multiphase fashion using the cores to produce harmonics, and using symmetrical interphase connections to isolate desired groups of harmonics without the use of filters. The synthesis and analysis of frequency multipliers is complicated both by the presence of non-linear elements and by the multiplicity of different linear network connections which can be used in harmonic isolation. Selection of a best circuit is related to economic and application factors; i.e., whether input power factor, saturating core cost, or output voltage level is most significant.

A Two-Stage Frequency Sextupler - Figure 29 illustrates an improved sextupler circuit using a doubler cascaded with a symmetrical frequency tripler. Here E_T is the output of the tripler stage and is the supply voltage to the doubler stage and has an almost rectangular wave shape. The load voltage E_L is also a near-rectangular wave shape. The doubler stage enters a current-limited mode of operation when load R becomes less than a certain critical value corresponding to a peak value of load current equal to the DC bias I_d on the doubler. Similarly, the tripler stage cannot supply an interstage current having a peak value greater than twice the DC bias I_d on the tripler. Thus if

$$I_d^1 = I_d \frac{N_1^1}{N_0^1}$$

then both the doubler stage and the tripler stage will become current limited for the same critical value of R, and the performance of the two-

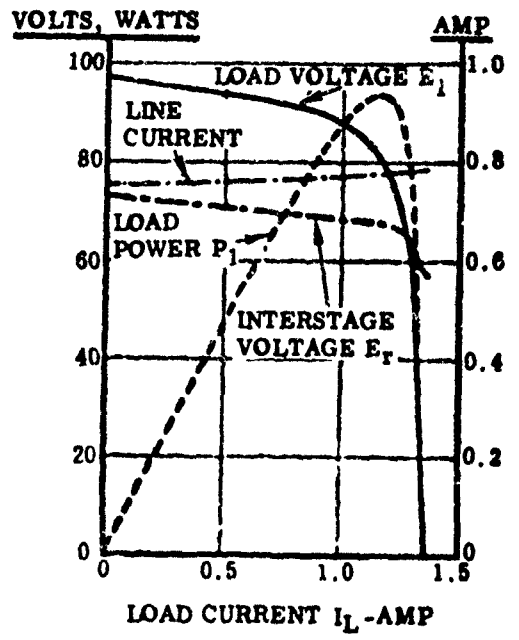
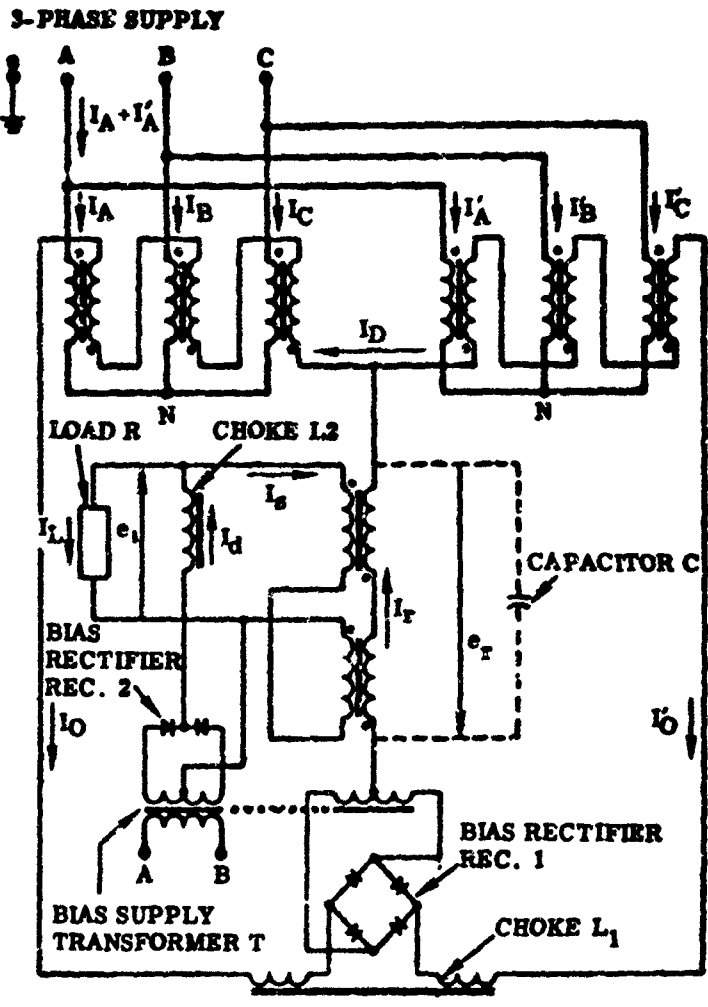


Figure 29. Magnetic Multiplier Technique

stage circuit will be optimum. During the current limited mode in which R is less than critical, the circuit becomes a source of sextuple frequency current with rectangular wave of magnitude I_d provided the equation above is satisfied. Performance data of this two-stage circuit is shown in Figure 29. It can be shown that the load voltage regulation of a two-stage circuit is better than that of the simple one-stage sextupler circuit. The performance of the sextupler can be improved by using an interstage capacitor C to correct the doubler stage power factor, but this distorts the interstage voltage EC and gives E a saw-toothed shape.

The following conclusions can be drawn from this part of the study:

1. If phase-changing transformers are included in the circuit to provide multiphase star outputs, any number of multiplications is possible. In practice, nine or eleven times appears to be a reasonable limit to any one stage. The output, of course, can be fed to another stage.
2. Upper limit in frequency is unknown (probably is near 20 KC).
3. At present, the size of multiplier devices in induction heating is greater than that of the equivalent motor-generator set and the efficiency tends to be lower.
4. The inherent advantages of simplicity, low maintenance cost, ruggedness, and static operation make these devices desirable for frequencies which are not too high.
5. The inherently low-input power factor requires considerable correction.

TRANSFORMERS

As a part of the investigation of converter devices, a review of transformer design techniques was made. The general transformer equation can be used to show how various parameters affect transformer size.

$$W_r = 1/45 f F_c F_1 B \lambda A_c A_1$$

where

- A_c = area of core window
- A_1 = core cross-sectional area
- W_r = load volt-amperes of transformer
- f = frequency in cycles per second
- F_c = winding space factor
- F_1 = core space factor

B = maximum flux density in kilolines per square inch

λ = current density in kiloamperes per square inch of conductor

Minimum size of transformer means using the best ratio of copper to core material. If the configuration of the transformer is held constant while other parameters are varied, then the effect of these parameters on transformer volume can be investigated. When all other size reduction methods have been considered, an optimum configuration can then be computed to give either minimum volume or minimum weight. To obtain an expression for volume, the equation can be rewritten:

$$A_c A_1 = \frac{45 W_r}{f F_c F_1 B \lambda}$$

$$V \propto a^3, \quad A_c \propto a^2, \quad A_1 \propto a^2$$

where

V = volume and a = any linear dimension of the transformer

then

$$V \propto (A_c A_1)^{3/4}$$

or

$$V \propto \left(\frac{45 W_r}{f F_c F_1 B \lambda} \right)^{3/4}$$

A configuration coefficient can then be defined such that

$$V = K \left(\frac{W_r}{f F_c F_1 B \lambda} \right)^{3/4}$$

We can now see which parameters to manipulate in order to reduce transformer size. To be considered at the same time are penalties in loss, regulation, and heating which occur.

From the above equation it becomes evident that:

1. Transformer output (W_r) should be kept to a minimum.
2. The transformer should be used at the highest frequency (f) possible.
3. Size is reduced by increasing the winding space factor (F_c) through improved insulations, and winding techniques (such as foil methods).

4. Use of better core materials (higher flux density B) is necessary.
5. Current densities (λ) should be the highest possible until loss, regulation, and heating become limiting factors.

Reducing the size of transformers complicates the problem of cooling because of increased losses and the fact that the increased heating is dissipated from a smaller volume. Figures 30A and 30B show how the loss and heat density are affected as size is reduced by increasing various parameters found in the denominator of the transformer volume equation. These curves give the ratio of loss and heat density in the transformer of reduced size to the loss or heat density of a standard design of the same configuration. It is assumed that the loss in the coil is equal to the loss in the core.

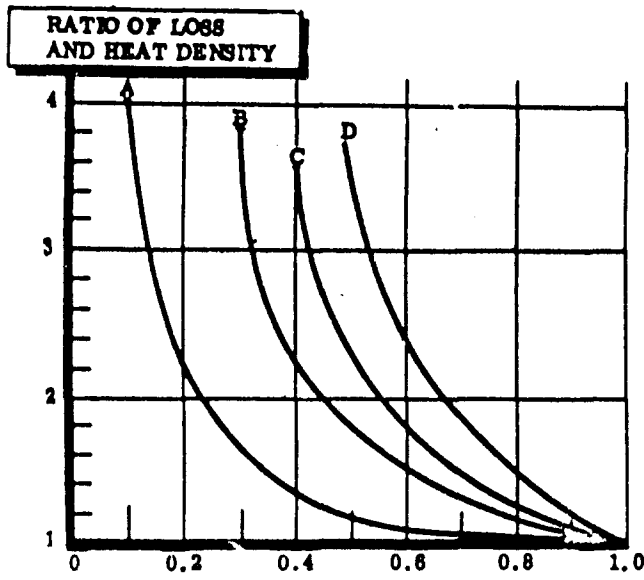
The watts per cubic inch dissipated as heat is designated as heat density. The temperature rise for any configuration will increase as the heat density increases, but it will not be directly proportional to the heat density. The heat distribution between core and coil will usually change as various parameters are changed. If the heat distribution remains the same within the transformer, then the temperature rise for a given heat density will be less with a small transformer than with a large one. Figure 30C shows how temperature rise increases as the transformer size is reduced. Experience has shown that transformer sizes can be reduced to less than one-half the size of conventional units if the higher heat density can be allowed in the smaller transformer.

This rise in temperature can be handled by two techniques. One method is to use high temperature insulation and let the transformer operate hot. Channels for heat flow to the common heat sink of the unit must be provided to limit the ultimate operating temperatures of the transformer. The other method for eliminating heat losses is by acceleration of heat flow by use of thermal conductors. These thermal conductors may be metallic or a circulating type of fluid system considered in this converter study and discussed in more detail in a later section.

Design of each of the transformers for this study has been based on providing minimum system weight. Cooling requirements have been considered as part of the total converter system weight in each instance. Cooling system studies have been performed and a cooling system weight penalty per kilowatt of loss has been established. This penalty is discussed and a curve shown in the section on Cooling.

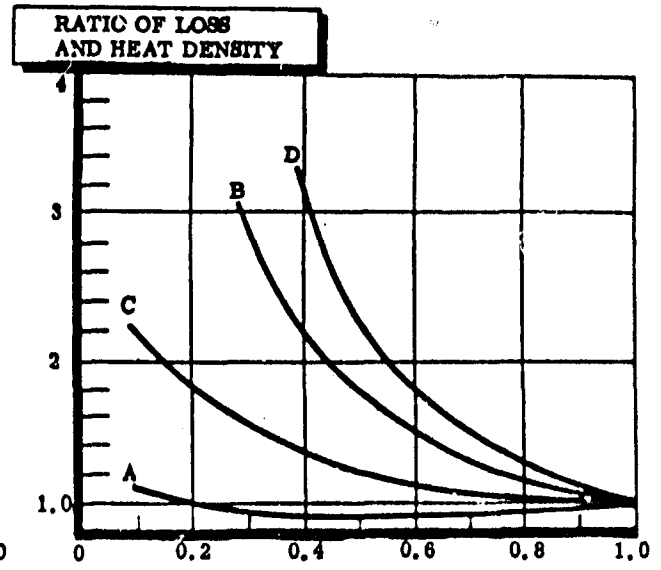
Design techniques for each power transformer include:

1. Ducting of coolant fluid over the core and through the coils to reduce the temperature drop.
2. Use of tape-wound cores with an inorganic binder because of cooling efficiency.
3. Use of advanced type of core materials.



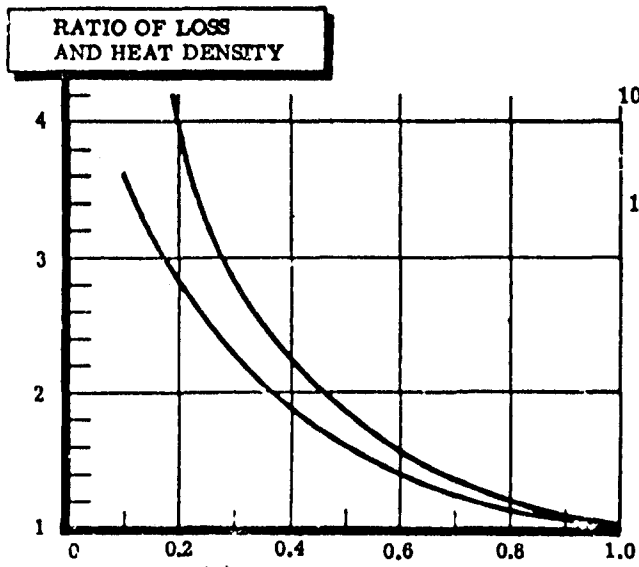
(A) RATIO OF VOLUME

- A - LOSS RATIO AS FREQUENCY INCREASES
- B - HEAT-DENSITY RATIO AS FREQUENCY IS INCREASED
- C - LOSS RATIO AS CURRENT DENSITY IS INCREASED
- D - HEAT-DENSITY RATIO AS CURRENT DENSITY IS INCREASED



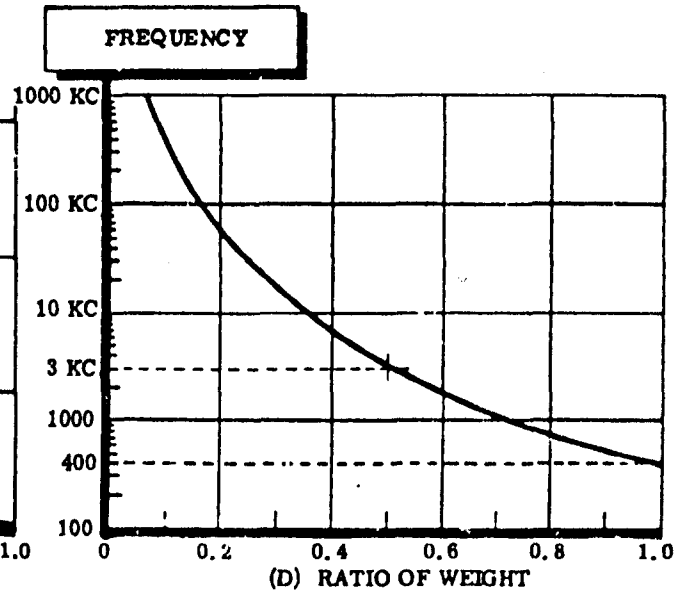
(B) RATIO OF VOLUME

- A - LOSS RATIO AS COIL SPACE FACTOR IS INCREASED
- B - HEAT DENSITY AS COIL SPACE FACTOR IS INCREASED
- C - LOSS RATIO AS CURRENT DENSITY AND FLUX DENSITY ARE INCREASED
- D - HEAT-DENSITY RATIO AS CURRENT DENSITY AND FLUX DENSITY ARE INCREASED



(C) RATIO OF VOLUME

- A - TEMPERATURE RISE WHEN TOTAL HEAT FLOW IS CONSTANT
- B - TEMPERATURE RISE WHEN TRANSFORMER IS REDUCED BY INCREASING CURRENT DENSITY AND FLUX DENSITY AT THE SAME RATE



(D) RATIO OF WEIGHT

- A - TRANSFORMER WEIGHT CHANGE AS FREQUENCY IS INCREASED

Figure 30. Transformer Parameter Analysis

4. All ducts and cooling plates are electrically insulated from the windings.
5. Assumed 100% conductivity for copper at the temperature at which losses are calculated.

Air core transformers eliminate the core loss problems of metallic core transformers, but coefficients of coupling for air core units are much less than iron core units. In a converter system where heat efficiencies are stressed, the low coupling of air core transformer (0.5 to 0.75) coefficient prevents their being selected for use. Coupling coefficients for transformers using cores of high permeability iron may be as high as 0.98.

Figure 30D indicates transformer weight changes as a function of frequency.

SECTION II

CONCEPTUAL CONVERTER DESIGNS

OBJECTIVE AND APPROACH

The objective of this part of the study program was to investigate approaches and establish conceptual component designs for the conversion of sinusoidal electrical power under the conditions stipulated below:

1. Conversion of 60 KW of electrical energy from 1000 cps, 3 ϕ , 43,6/75.8 volts to:
 - a. 50 KC, 3 ϕ , 5810/10,100 volts
50 KC, 1 ϕ , 10,100 volts
 - b. 200 KC, 3 ϕ , 5810/10,100 volts
200 KC, 1 ϕ , 10,100 volts
 - c. 800 KC, 3 ϕ , 5810/10,100 volts
800 KC, 1 ϕ , 10,100 volts

Design objectives included conversion efficiency of not less than 90% and over-all component weight of less than 300 pounds. Electrical power conforms basically to energy available from a SNAP 8 power supply.

2. Conversion of 300 KW electrical energy from 3200 cps, 3 ϕ , 120/208 volts to:
 - a. 50 KC, 3 ϕ , 5810/10,100 volts
50 KC, 1 ϕ , 10,100 volts
 - b. 200 KC, 3 ϕ , 5810/10,100 volts
200 KC, 1 ϕ , 10,100 volts
 - c. 800 KC, 3 ϕ , 5810/10,100 volts
800 KC, 1 ϕ , 10,100 volts

Design objectives included efficiency of not less than 90% and over-all component weight of less than 1000 pounds. Electrical power conforms basically to energy available from a SPUR type electrical generator.

Based on the preliminary investigations of converter techniques, three specific converter concepts were derived which follow and are discussed in this section. The concepts are:

1. Static transistor converter
2. Static tube converter
3. Motor-generator converter

STATIC TRANSISTOR CONVERTER DESIGNS

A 60 KW UNIT

The most promising of the three converter types for meeting the weight and efficiency objectives of this study is a static transistor type of unit. A transistorized 60 KW 1 ϕ power converter is illustrated in Figure 31 and shown schematically in Figure 32. Parametric data is summarized in Table I which follows.

As can be seen from Figure 31, the packaging concept is compact and the volume is slightly over two cubic feet. The static transistor converter concept as detailed in this section will fulfill the 50 KC, 200 KC, and 800 KC output frequency requirements and approaches the 90 per cent efficiency objective. The weight and volumes are fairly constant throughout the frequency range. Specific values are noted on Table 1.

Table I also summarizes parametric data for a 3 ϕ , 60 KW converter unit shown schematically in Figure 33. The three-phase unit is heavier than the single phase concept and is less efficient.

Operation of the single phase converter is based on a power chopper technique and is explained in the section which follows. The 43.6/75.8 volt, 3 ϕ , 1,000 cycle power is applied at the input terminals (Figure 32), and is converted to a pulsating DC voltage by diodes CR1 - CR6. Filter choke L1 and filter capacitors C3 and C6 smooth the rectified DC voltage. This filtered DC is then applied through output transformer T2 to the collectors of the power switching transistors Q3, Q5, Q7, Q9, Q10, and Q11. The switching rate of the power transistors is determined by the precision square wave oscillator Q1 and Q2. The output from the square wave oscillator is applied to the impedance matching transistor Q4. The output from Q4 is amplified by the driver transistors Q6 and Q8 and is applied to the power switching transistors. Transformer T1, filter choke L2 and filter capacitors C7 and C8 form the low-voltage power supply which furnishes the power for the square-wave oscillator and the driver transistors. Reference diode CR13 provides a regulated voltage for the oscillator.

The selection of transistors for the power switching section will depend on future current capabilities of power transistors. Serious limitation of present day semiconductor devices is in operating temperature (100°C). However, new materials, including gallium arsenide, are being developed which should raise their operating temperature capability in the future to 400°C.

If the power switching circuit was designed using state-of-the-art transistors, it would consist of 100 transistors. In order to compensate for the voltage limit of most power devices, two transistors would have to be used in series. Since most devices are presently limited to 20 amperes of current, this would require 50 pairs of transistors in parallel for the 60 KW unit.

A three-phase converter is shown schematically in Figure 33 with parametric data included in Table I. 43.6/75.8 volt, 3 ϕ , 1,000 cps power is applied

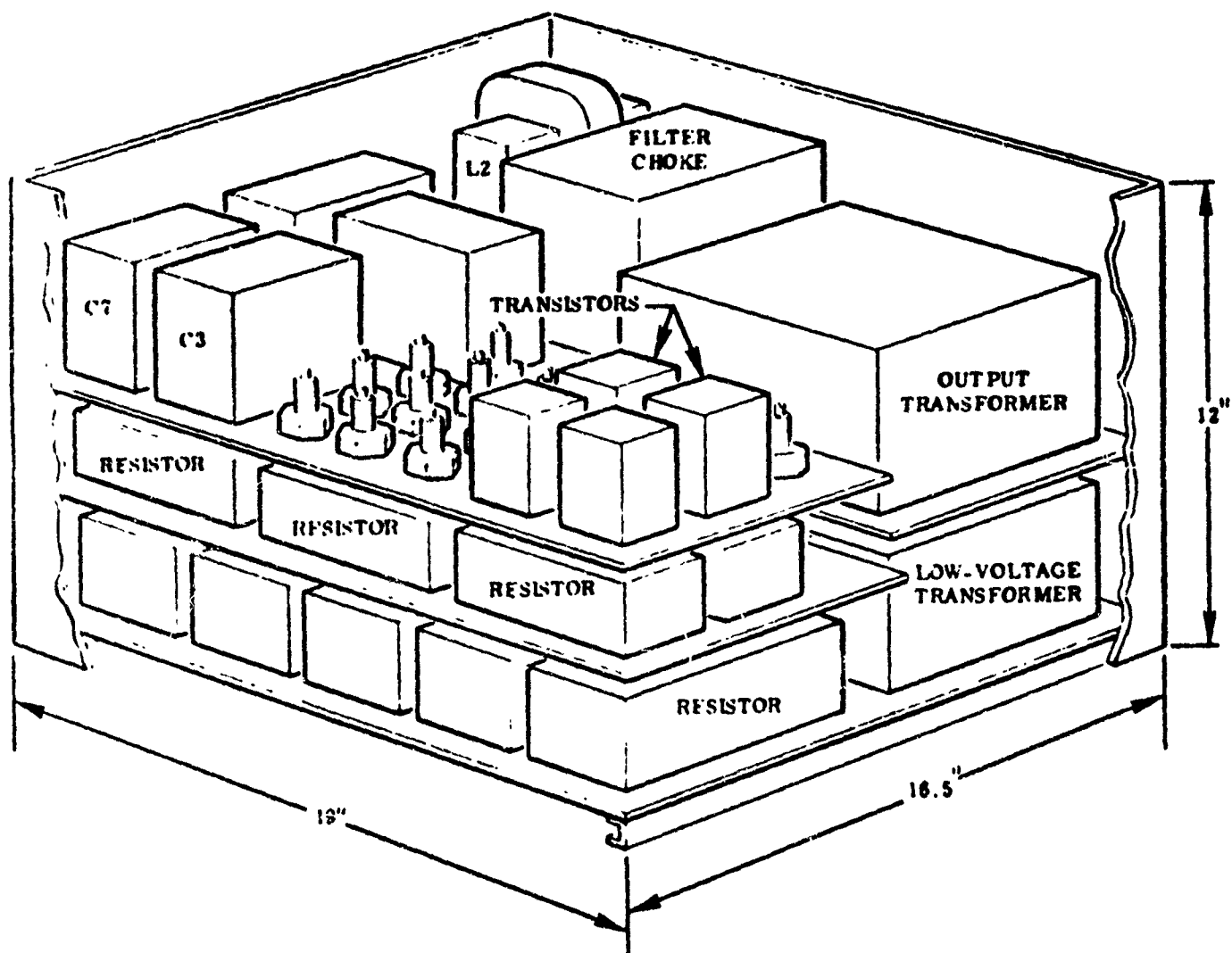


Figure 31. 60 KW Static Transistor Converter (Perspective)

TABLE 1

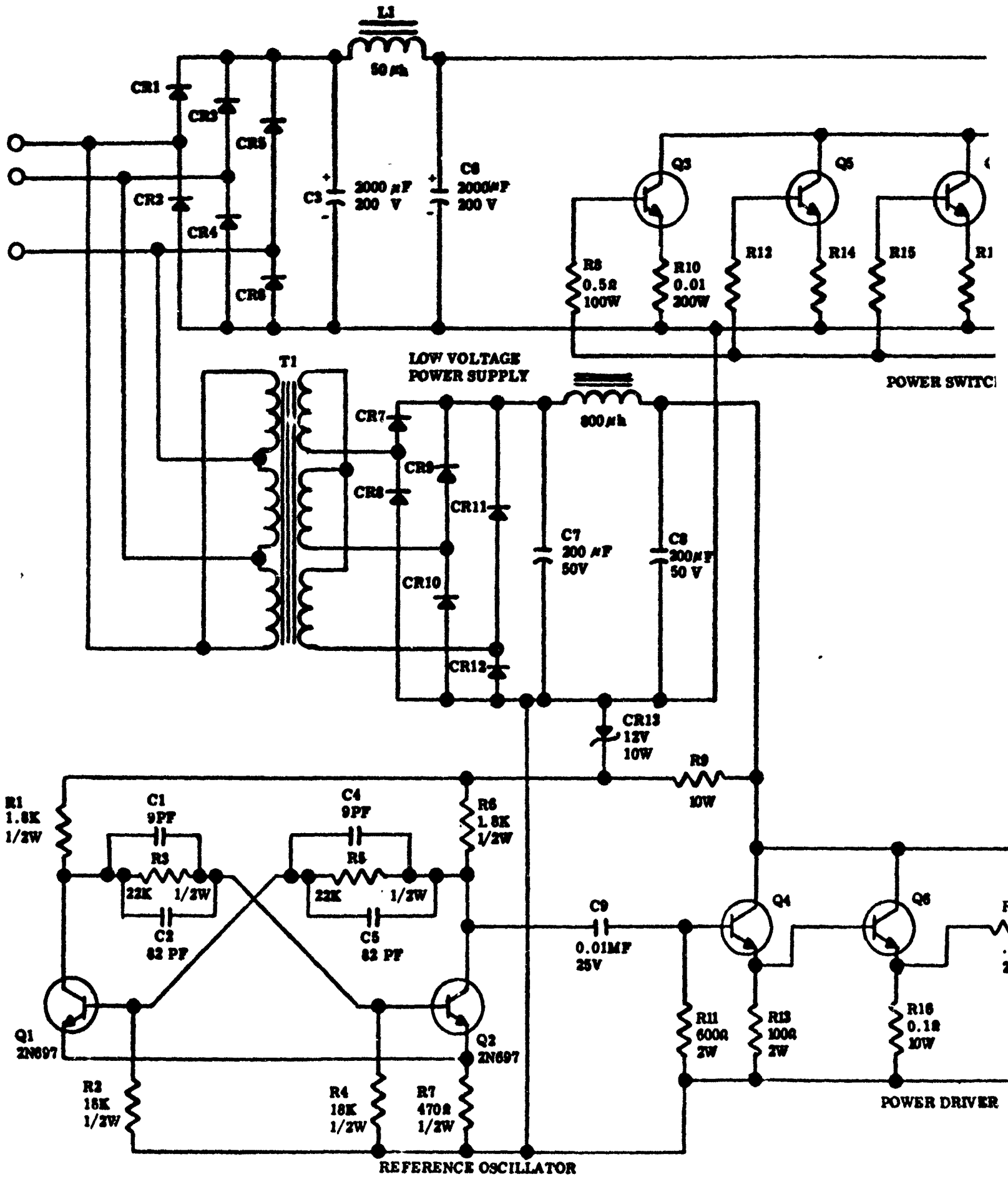
SUMMARY OF 60 KW STATIC TRANSISTOR CONVERTER PARAMETRIC DATA

1 ϕ	50 KC	200 KC	800 KC
WEIGHT (lbs)	168.9	161.5	154.1
KW RAD (Losses)	4.3	5.1	6.3
KW OUT	55.7	54.9	53.7
EFFICIENCY (%)	93.0	91.6	89.4
LENGTH (inches)	19	19	19
WIDTH (inches)	16.5	16.5	16.5
HEIGHT (inches)	12	12	12
VOLUME (cu. ft.)	2.2	2.2	2.2
LBS/KW RAD	38.2	31.7	31.5
LBS/KW OUT	3.02	2.91	2.87

3 ϕ	50 KC	200 KC	800 KC
WEIGHT (lbs)	275.8	258.2	244.0
KW RAD (Losses)	9.8	11.1	13.1
KW OUT	50.2	48.9	46.9
EFFICIENCY (%)	83.6	81.4	78.2
LENGTH (inches)	20	20	20
WIDTH (inches)	20	20	20
HEIGHT (inches)	15.5	16.4	17.2
VOLUME (cu. ft.)	3.5	3.8	4.0
LBS/KW RAD	28.5	23.1	18.6
LBS/KW OUT	5.5	5.29	5.20

NOTE: VALUES DO NOT INCLUDE COOLING SYSTEM WEIGHTS.

INPUT
45.0/75.8 V
1000 ~
3 φ
60 KW



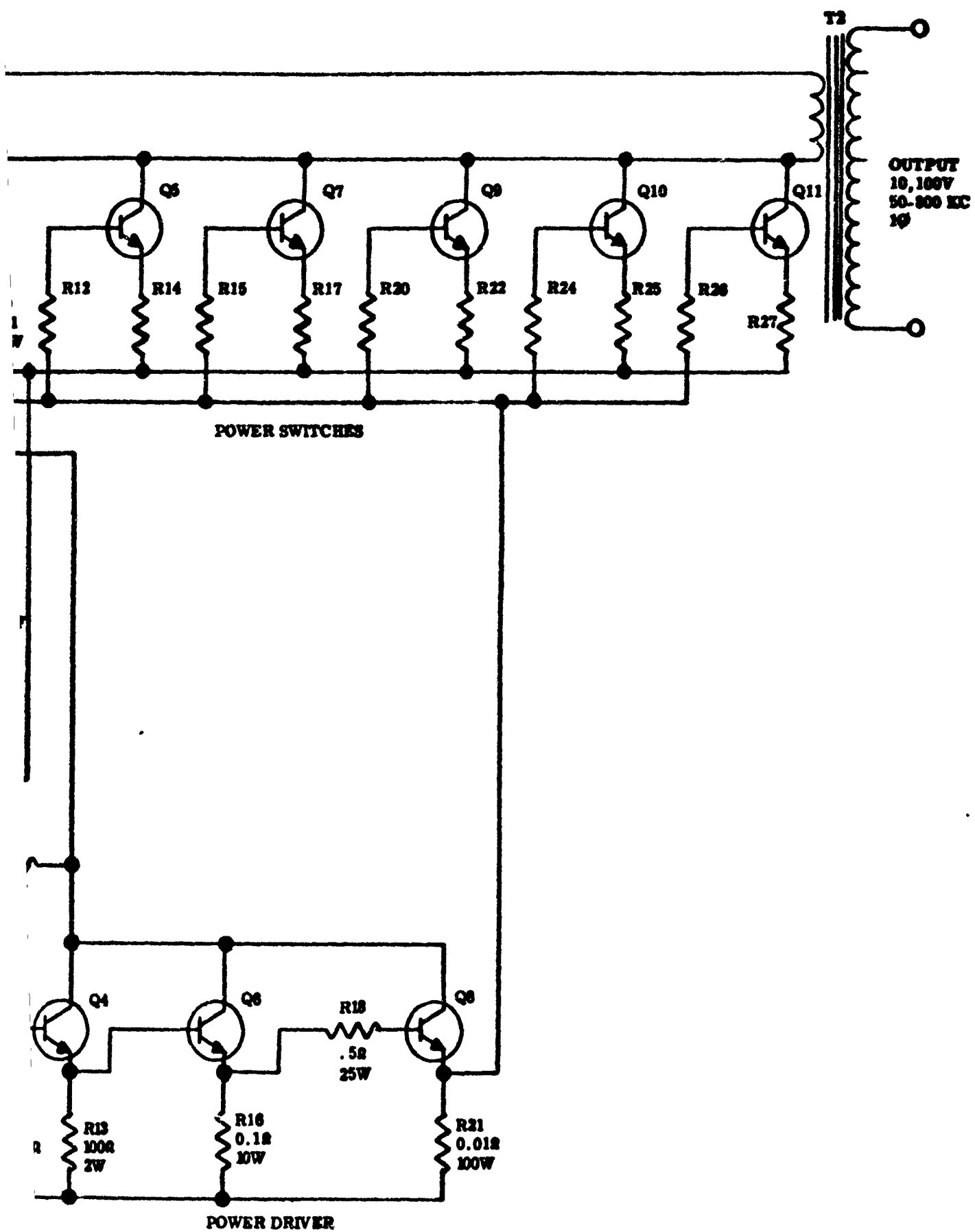
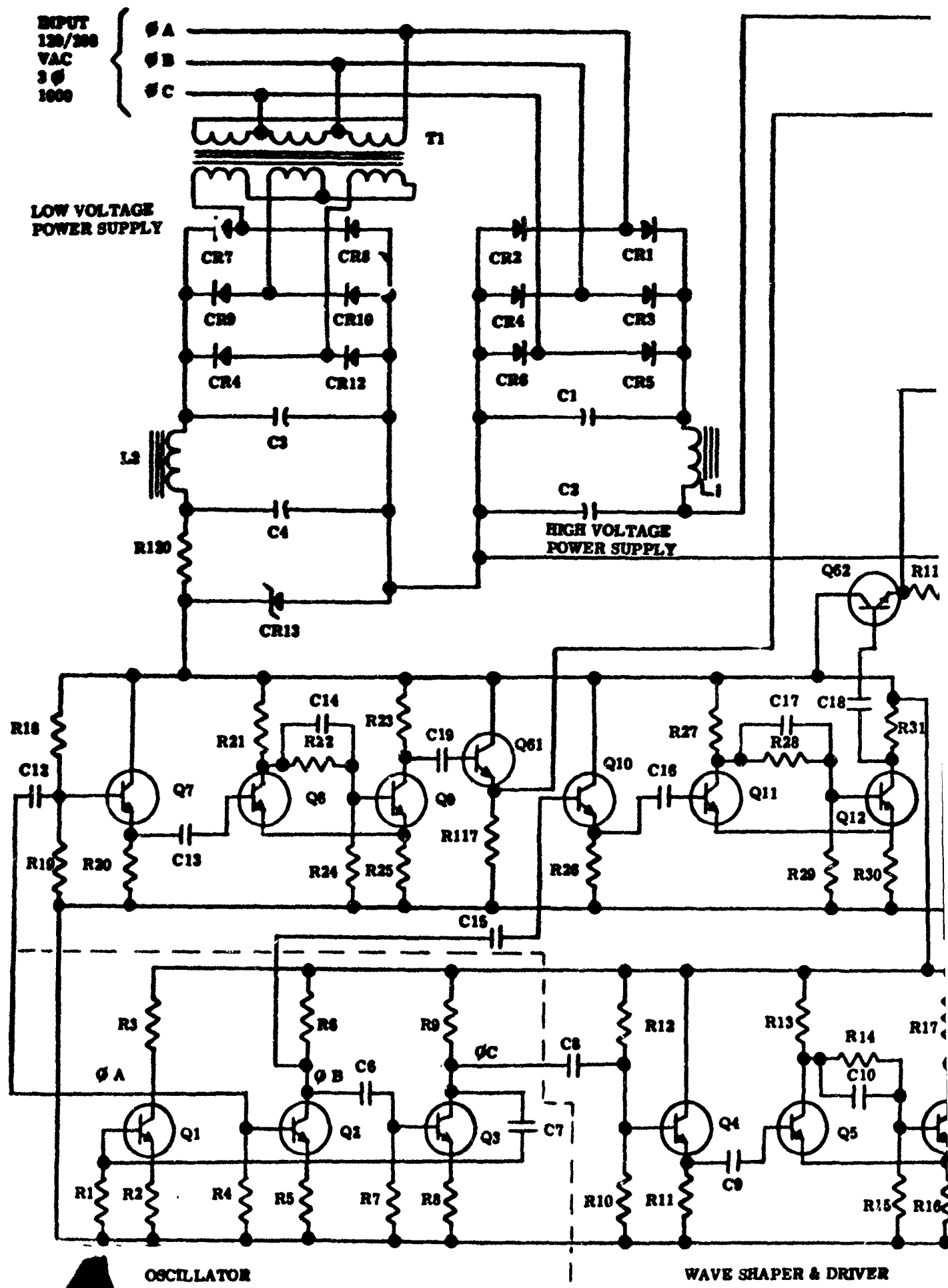


Figure 32. Preliminary Schematic of
60 KW Static Transistor
1 ϕ Converter



A

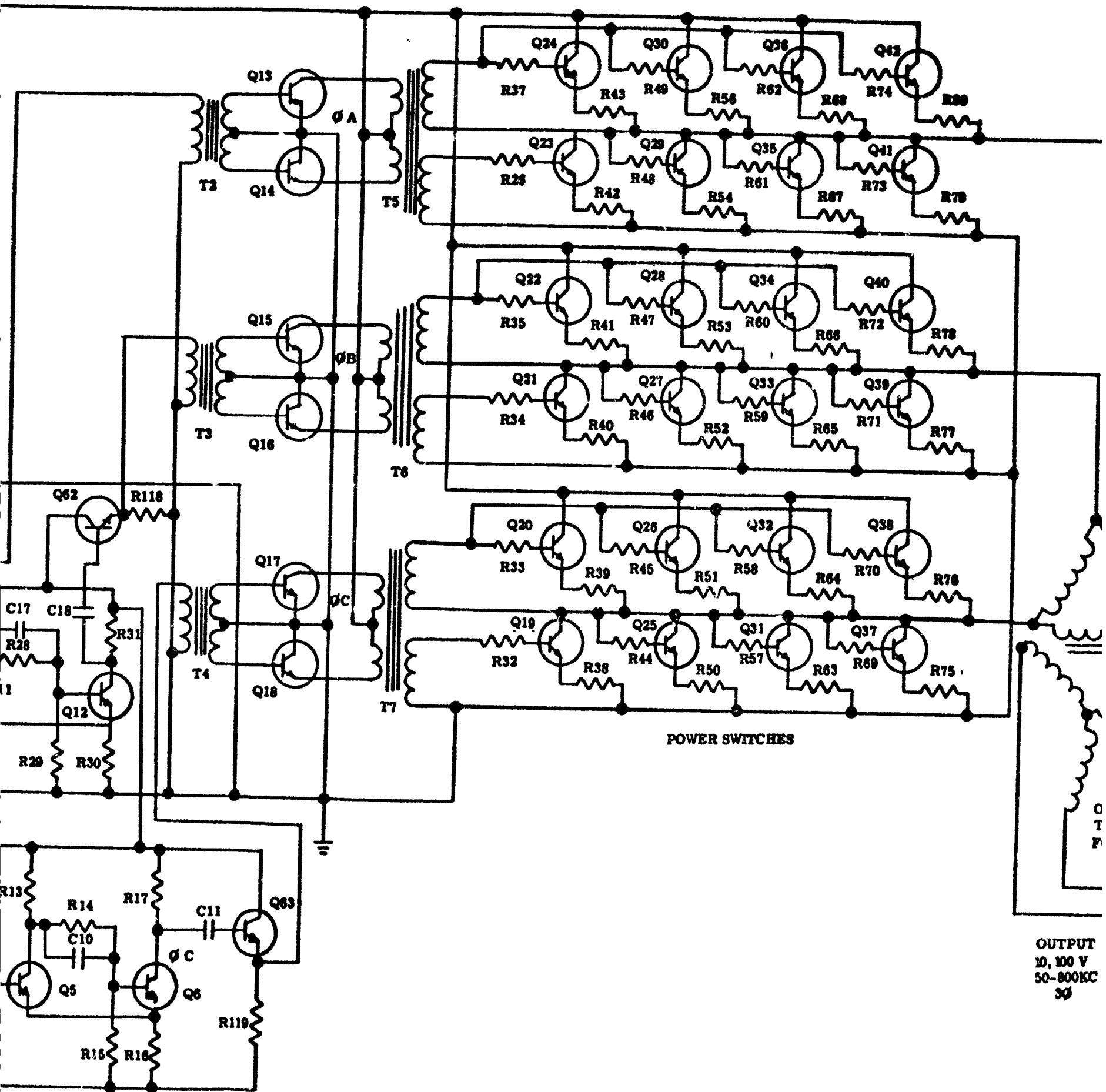
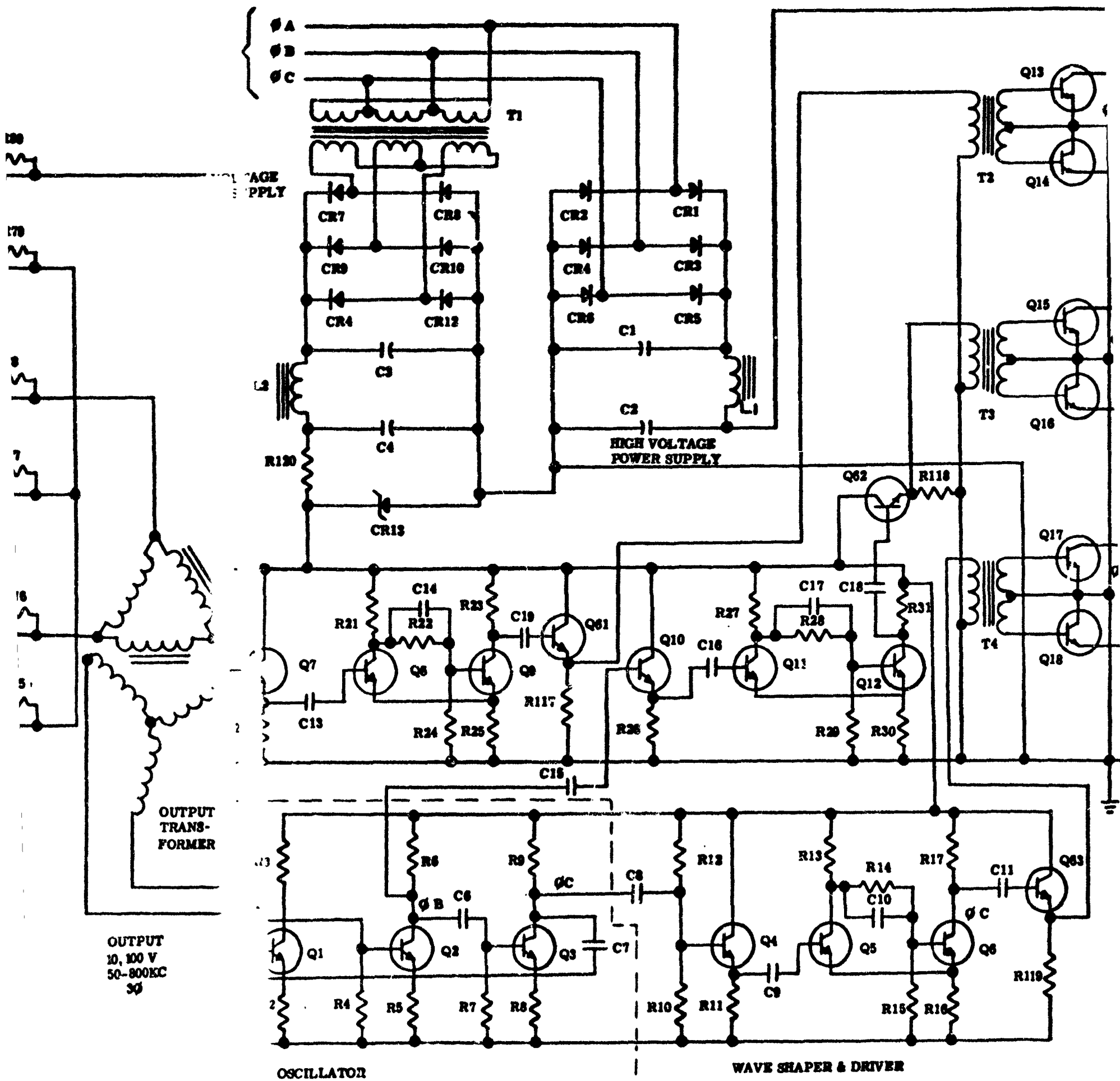


Figure 33. Preliminary Schematic
60 KW Static Transistor
3 ϕ Converter



Primary Schematic of Static Transistor Converter

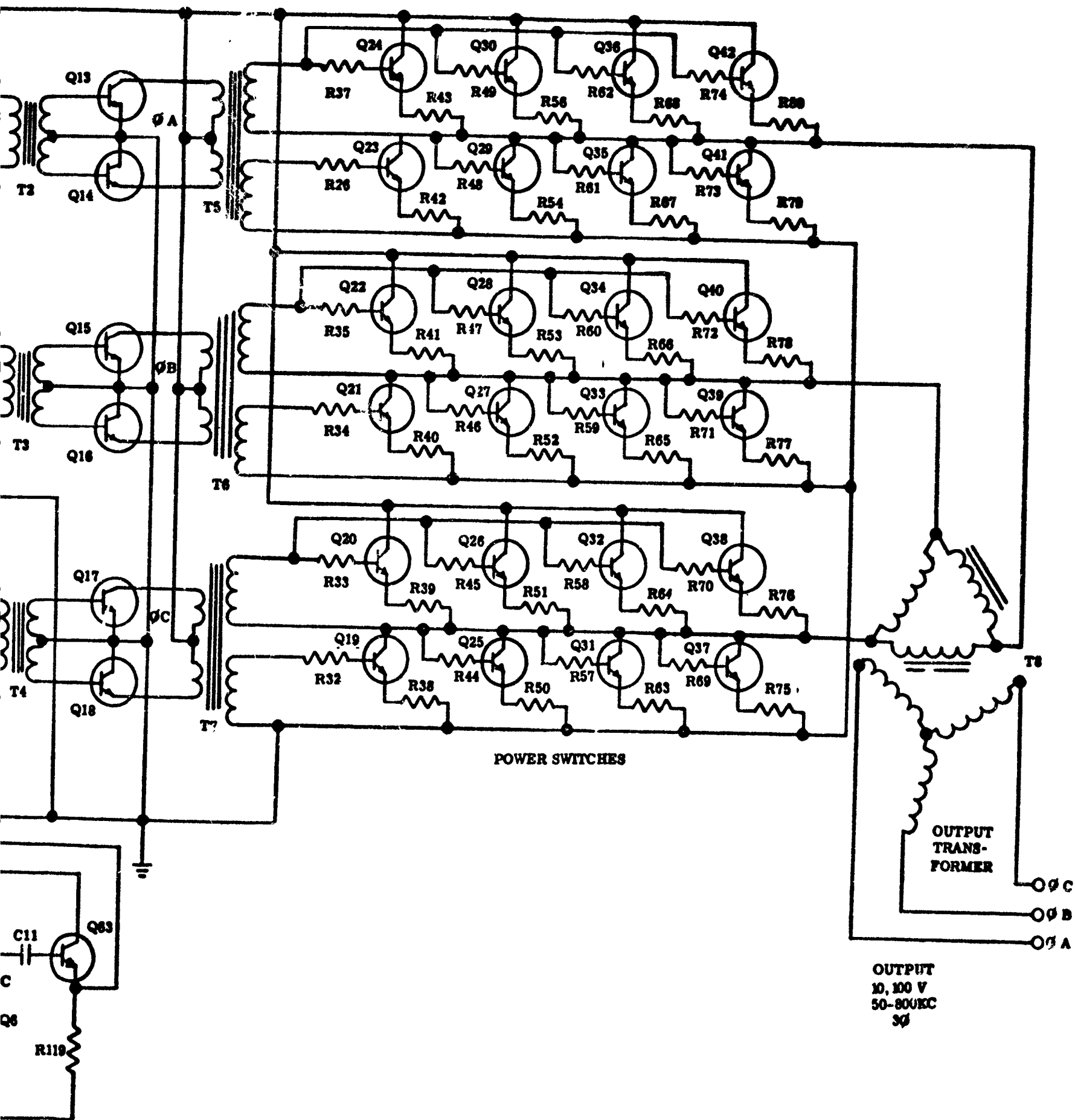


Figure 33. Preliminary Schematic of
60 KW Static Transistor
3 ϕ Converter

B

at the input terminal and is converted to a pulsating DC voltage by the power diodes CR1 - CR6. This DC voltage is then filtered by filter choke L1 and filter capacitors C₁ and C₂. This filtered DC is now applied directly to power transistors Q19 through Q60.

The switching rate of the power transistors in this concept is determined by three-phase sine wave oscillator. The ϕ A output from the oscillator is applied to the impedance matching transistor Q7. The output from Q7 is applied to a Schmitt trigger (square wave forming circuit) Q8 and Q9. The output from Q9 is then applied to the emitter follower Q61 which feeds transformer T2 and powers the push-pull driver Q13 and Q14.

The output from the push-pull driver is then applied through transformer T5 to drive the power transistors. The same pattern is followed with ϕ B and ϕ C. The final output is taken from three-phase output transformer T8.

Output Power Characteristics

Although the basic switching mode of the transistor power chopper gives a square wave output and this is the input to the primary of the step-up transformer, the output on the load side of the transformer is essentially a sine wave. This results from the action of a transformer on the incoming wave shape.

A 300 KW UNIT

A transistorized power converter for delivering 300 KW of single-phase high frequency power is shown schematically in Figure 34. Data for this concept is summarized in Table 2. The operation of the circuit is identical to that of the 60 KW unit and it differs from the 60 KW unit only in the number of transistors in the chopper circuit. The 300 KW input is 120/208 volts, 3 ϕ , 3,200 cps power, rather than the 43.6/75.8 volt, 1,000 cps power for the 60 KW unit. The filtered DC from the rectifier section is applied to one side of the output transformer T2. The other side of the output transformer is connected in series with this parallel group of power transistors which switch the DC voltage at a 50 to 800 kilocycle rate through the primary winding of T2. The output from the secondary winding of T2 is then stepped up to a value of 10,100 volts AC for the load.

The switching rate of the power transistors is determined by the precision square-wave oscillator. The output from the oscillator is fed to the driver transistors Q8 and Q10 through the impedance matching emitter-follower transistor Q4. The driver transistors and oscillator are powered by the low voltage power supply.

A three-phase design for the 300 KW (input) unit is shown in Figure 35 and is almost identical to the 3 ϕ , 60 KW unit. Major difference is in the number of power transistors in the power switch section.

Output Power Characteristics

As in the single-phase converter concept, the power chopper section of the three-phase converter gives a square wave output. The waveshape that appears across the output of the transformer and available to the load device is essentially a sine wave.

COMPONENT CHARACTERISTICS

Tables 3 - 6 which follow list the components of 60 and 300 KW converter designs for both single-phase and three-phase configurations. They are arranged in converter subsection headings and are identified on each of the schematic drawings. Weight, size and internal loss data have been listed and summarized as part of the study effort.

These static transistor converter concepts can be packaged within an aluminum structure for protection against radiation and space erosion. This structure will provide minimum weight to maximum strength plus good thermal conductance characteristics. A preliminary package design for a 60 KW, 1 ϕ 200 KC concept is typical of the other designs and is shown in Figure 36.

Figure 37 shows a 60 KW, 3 ϕ converter design for a 200 KC output. This concept is typical of a unit for 50 KC and 800 KC output. The 300 KW concepts are detailed in Figures 38 and 39.

The internal portion may be considered to be in a tray configuration, in which each tray holds a portion of the circuit. The trays are formed from aluminum sheets so that coolant tubes may be imbedded in them to form a cold-plate structure.

In order to isolate the transistors and diodes from the high power components, such as resistors and transformers, thin insulation barriers may be set up around the transistors. These barriers will consist of thin aluminum foil against thin glass or asbestos cloth. This will provide a means of controlling the temperature of the transistors and diodes which are the most heat sensitive of the electrical components. Since the parts are, in general, rather small in a transistor type of unit, there is greater flexibility in package design, and this concept can be packaged to match the generator configuration and the electric propulsion engine configuration.

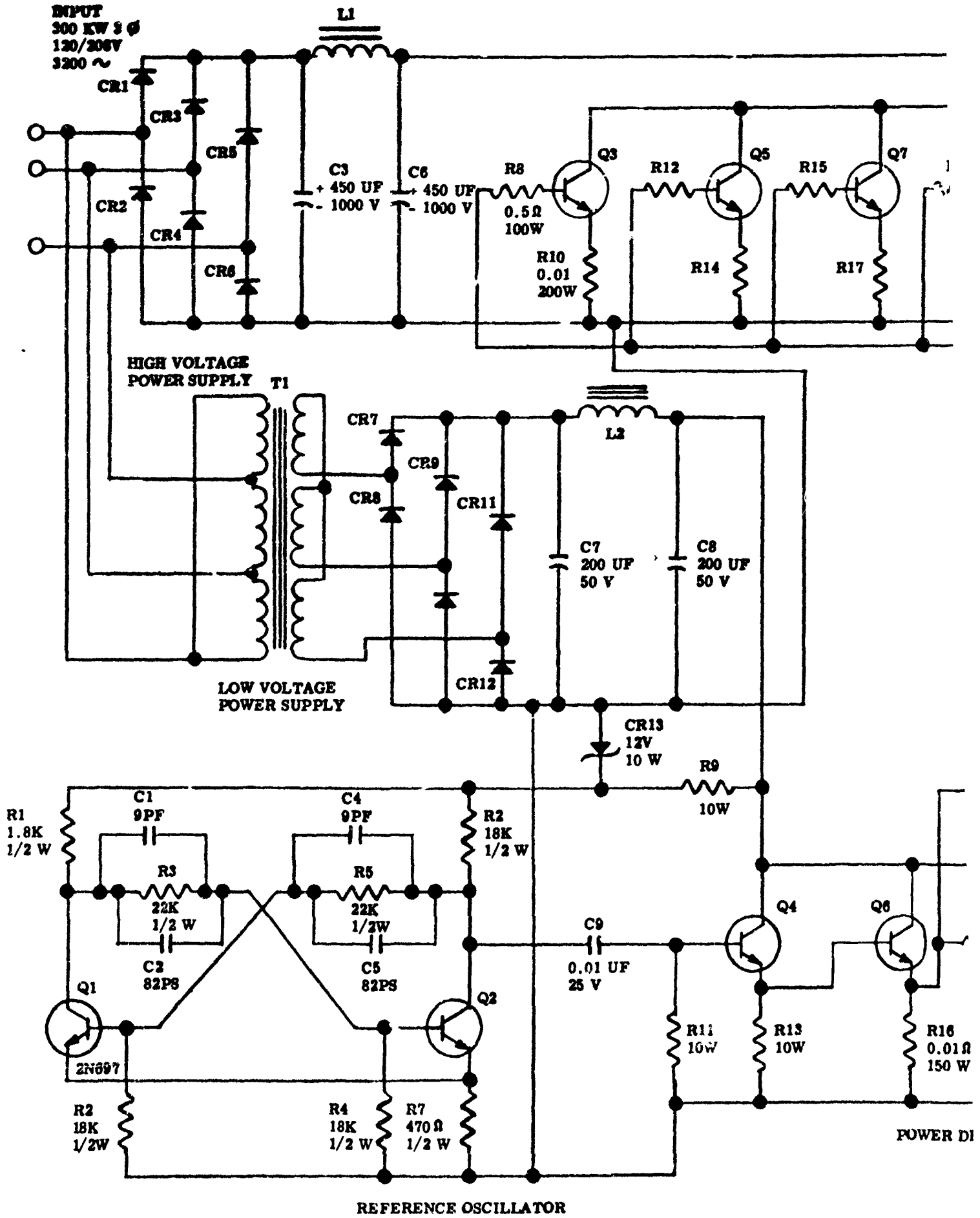
TABLE 2

SUMMARY OF 300 KW STATIC TRANSISTOR CONVERTER PARAMETRIC DATA

1 ϕ	50 KC	200 KC	800 KC
WEIGHT (lbs)	278.9	249.3	225.8
KW RAD (Losses)	10.7	11.9	14.4
KW OUT	289.3	288.1	285.6
EFFICIENCY (%)	96.4	96.0	95.0
LENGTH (inches)	24	24	24
WIDTH (inches)	19	19	19
HEIGHT (inches)	11.5	11.5	11.5
VOLUME (cu. ft.)	3.0	3.2	3.5
LBS/KW RAD	25.9	20.9	16.5
LBS/KW OUT	.93	.86	.79

3 ϕ	50 KC	200 KC	800 KC
WEIGHT (lbs)	518.9	451.0	402.7
KW RAD (Losses)	22.3	23.8	27.2
KW OUT	277.0	276.0	272.0
EFFICIENCY (%)	92.3	92.0	90.7
LENGTH (inches)	24.5	25.5	24.5
WIDTH (inches)	22.5	22.5	22.5
HEIGHT (inches)	18	18	18
VOLUME (cu. ft.)	5.7	6.0	6.5
LBS/KW RAD	10.3	7.9	7.4
LBS/KW OUT	1.86	1.63	1.48

NOTE: VALUES DO NOT INCLUDE COOLING SYSTEM WEIGHTS.



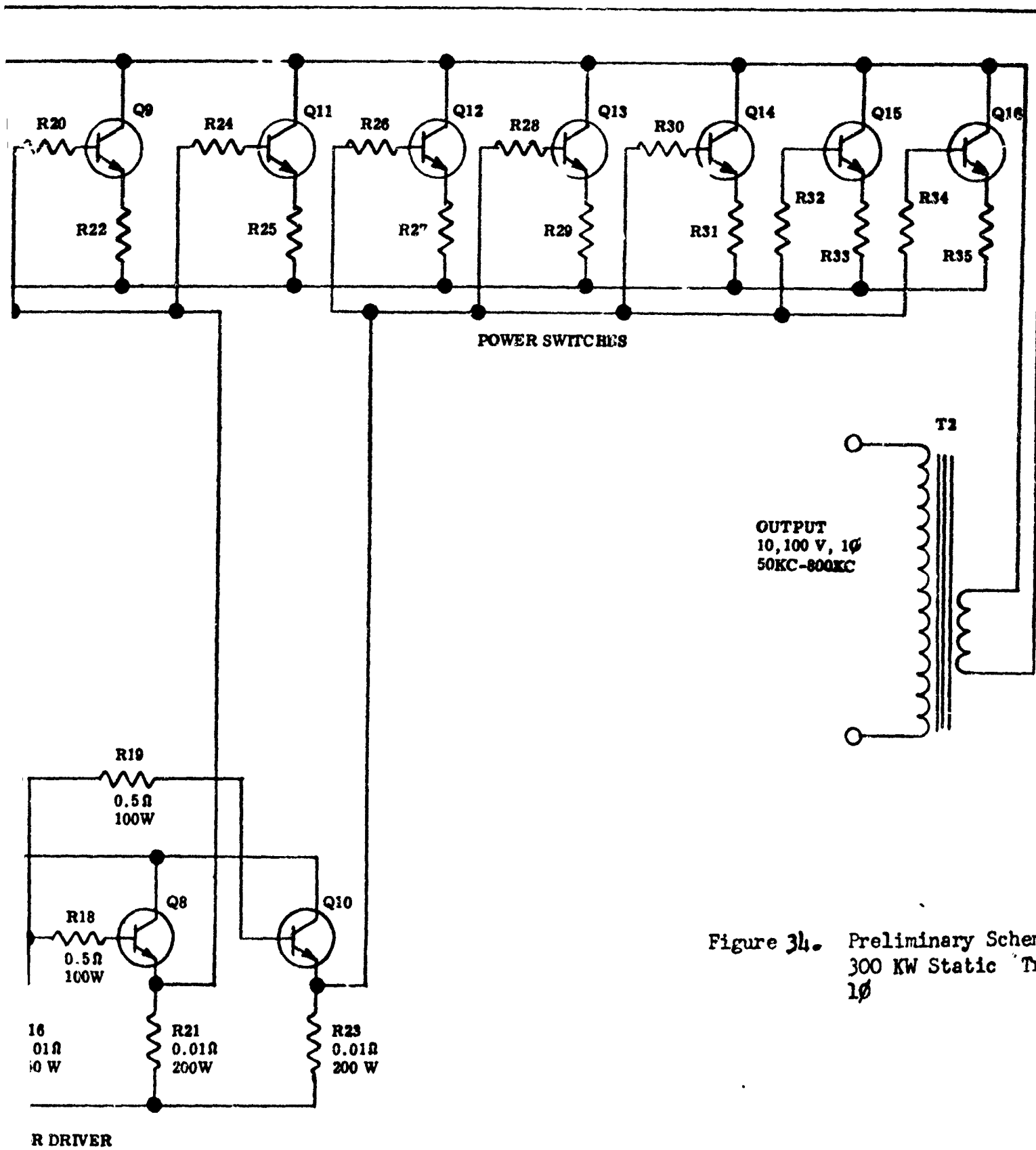
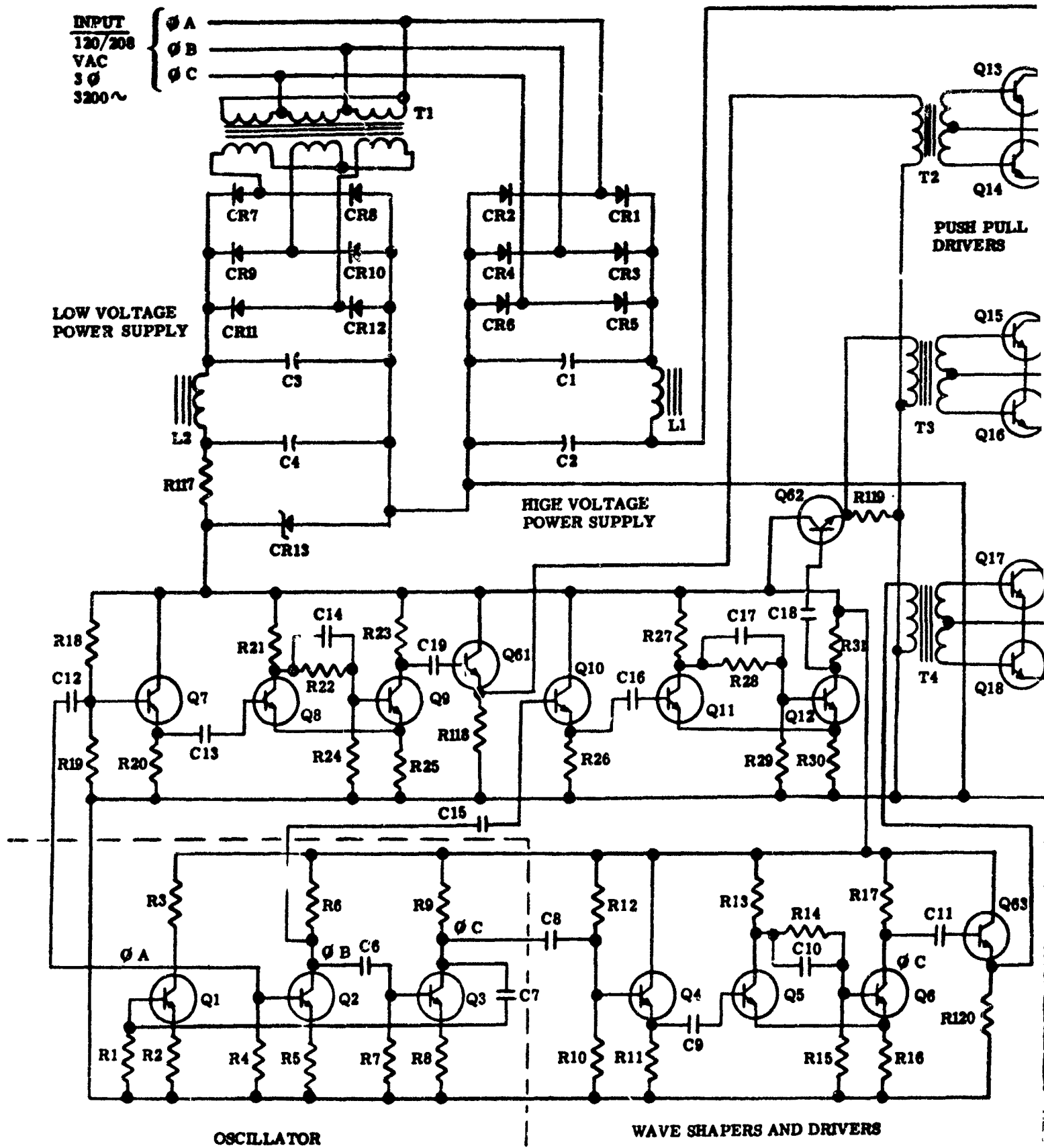


Figure 34. Preliminary Schematic of 300 KW Static Transistor 1φ



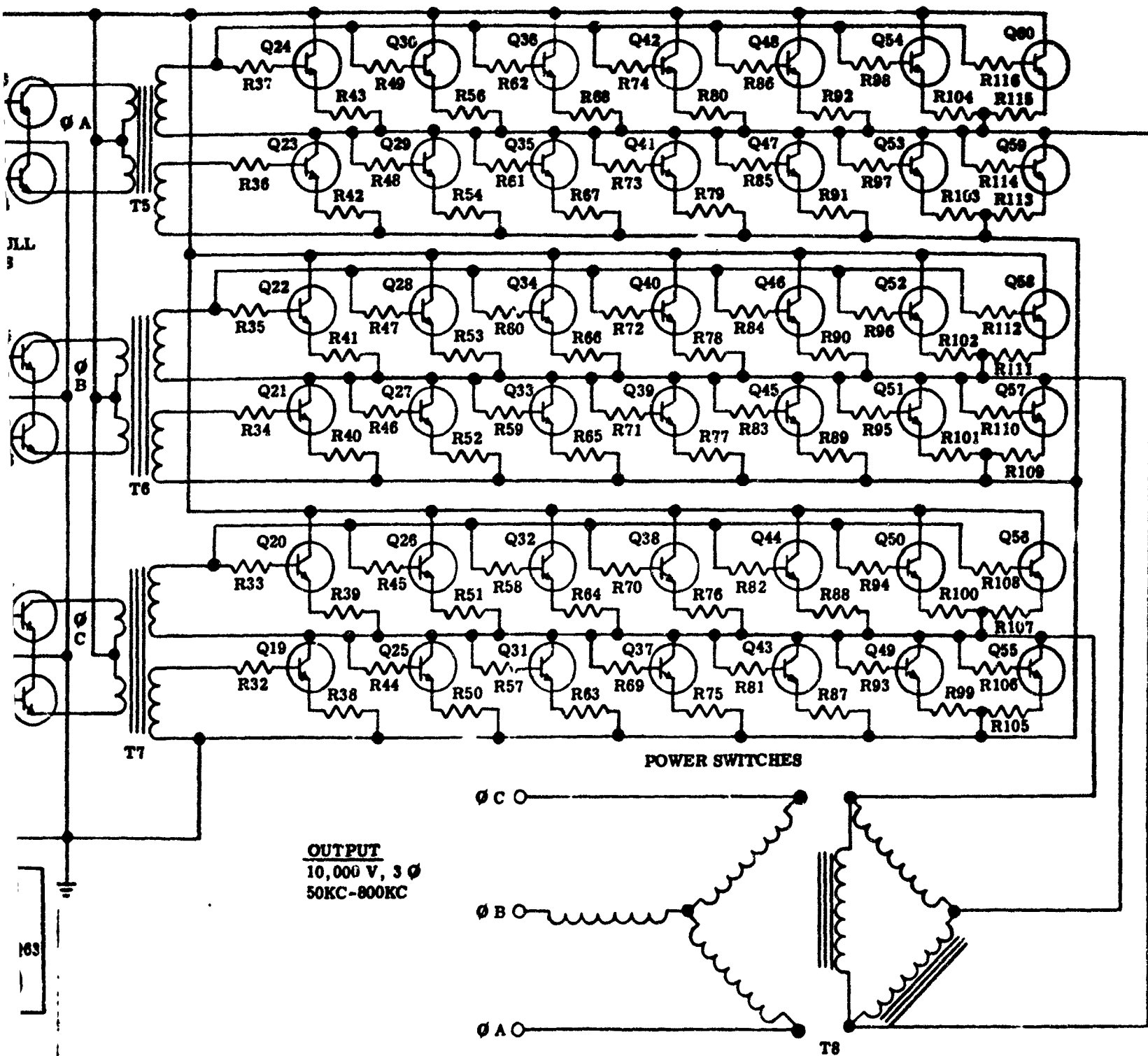


Figure 35. Preliminary Schematic of 300 KW Static Transistor Converter (3 Ø)

		50	
NO.	COMPONENTS	WT (LBS)	LOSSES (WATTS)
<u>POWER SUPPLY (LOW VOLTAGE)</u>			
6	Rectifier, semiconductor	3.0	144
1	Transformer, low voltage (T1)	2.4	207
2	Capacitor, filter	1.2	1
1	Filter Choke L-2	15.8	84
1	Diode, zener reference (CR13)	0.1	2
1	Resistor	0.2	5
<u>POWER SUPPLY (HIGH VOLTAGE)</u>			
6	Rectifier, semiconductor	5.0	1,440
2	Capacitor, filter	3.5	1
1	Filter Choke (L1)	22.0	258
<u>OSCILLATOR SECTION</u>			
2	Transistor, low power (Q1, Q2)	.1	1
7	Resistor	.1	2
5	Capacitor	.1	
<u>WAVE SHAPER AND DRIVER</u>			
1	Transistor, power (Q8)	.5	60
1	Transistor, med power (Q6)	.3	5
1	Transistor, low power (Q4)	.3	1
2	Resistor (10W)	.4	10
3	Resistor, power	2.7	175
<u>OUTPUT SECTION</u>			
6	Transistor, power	3.0	360
6	Resistor, power (200W)	8.4	600
6	Resistor, base drive	5.4	300
1	Transformer, output (A2)	18.0	680
<u>MISCELLANEOUS</u>			
	Mounting plate and Enclosure	43.1	
	Cooling ducts	2.8	
	Controls	10.0	
	Wire and Hardware	20.5	
TOTALS		168.9	4,336

TABLE 3

ST FOR A 60 KW STATIC TRANSISTOR CONVERTER (1φ)

50 KC			200 KC			800 KC		
SIZE (INCHES)	WT (LBS)	LOSSES (WATTS)	SIZE (INCHES)	WT (LBS)	LOSSES (WATTS)	SIZE (INCHES)	WT (LBS)	LOSSES (WATTS)
1 $\frac{1}{4}$ X 1 $\frac{1}{4}$ X 3	3.0	144	1 $\frac{1}{4}$ X 1 $\frac{1}{4}$ X 3	3.0	144	1 $\frac{1}{4}$ X 1 $\frac{1}{4}$ X 3	3.0	144
2 X 2 X 4	2.4	207	2 X 2 X 4	2.4	207	2 X 2 X 4	2.4	207
2 1/8 Dia. X 6	1.2	1	2 1/8 Dia. X 6	1.2	1	2 1/8 Dia. X 6	1.2	1
4 $\frac{1}{2}$ X 3-3/4 X 5-1/8	15.8	84	4 $\frac{1}{2}$ X 3 3/4 X 5 1/8	15.8	84	4 $\frac{1}{2}$ X 3 3/4 X 5 1/8	15.8	84
3/8 Dia. X 1	0.1	2	3/8 Dia. X 1	0.1	2	3/8 Dia. X 1	0.1	2
1/2 Dia. X 2	0.2	5	1/2 Dia. X 2	0.2	5	1/2 Dia. X 2	0.2	5
1-7/8 X 1-7/8 X 4-1/16	5.0	1,440	1-7/8 X 1-7/8 X 4-1/16	5.0	1,440	1-7/8 X 1-7/8 X 4-1/16	5.0	1,440
4 X 5 X 6 $\frac{1}{2}$	3.5	1	4 X 5 X 6 $\frac{1}{2}$	3.5	1	4 X 5 X 6 $\frac{1}{2}$	3.5	1
4 $\frac{1}{2}$ X 4 X 6-3/4	22.0	258	4 $\frac{1}{2}$ X 4 X 6-3/4	22.0	258	4 $\frac{1}{2}$ X 4 X 6-3/4	22.0	258
TO5	.1	1	TO5	.1	1	TO5	.1	1
$\frac{1}{2}$ W MIL-R-11C	.1	2	$\frac{1}{2}$ W MIL-R-11C	.1	2	$\frac{1}{2}$ W MIL-R-11C	.1	2
MIL-C-5B	.1		MIL-C-5B	.1		MIL-C-5B	.1	
1 $\frac{1}{4}$ X 1 $\frac{1}{4}$ X 2	.5	60	1 $\frac{1}{4}$ X 1 $\frac{1}{4}$ X 2	.5	60	1 $\frac{1}{4}$ X 1 $\frac{1}{4}$ X 2	.5	60
TO3	.3	5	TO3	.3	5	TO3	.3	5
TO3	.3	1	TO3	.3	1	TO3	.3	1
5/16 Dia. X 1-3/4	.4	10	5/16 Dia. X 1 3/4	.4	10	5/16 Dia. X 1 3/4	.4	10
2 $\frac{1}{4}$ X 3 X 7	2.7	175	2 $\frac{1}{4}$ X 3 X 7	2.7	175	2 $\frac{1}{4}$ X 3 X 7	2.7	175
1 $\frac{1}{4}$ X 1 $\frac{1}{4}$ X 2	3.0	360	1 $\frac{1}{4}$ X 1 $\frac{1}{4}$ X 2	3.0	360	1 $\frac{1}{4}$ X 1 $\frac{1}{4}$ X 2	3.0	360
2 $\frac{1}{4}$ X 3 X 7	8.4	600	2 $\frac{1}{4}$ X 3 X 7	8.4	600	2 $\frac{1}{4}$ X 3 X 7	8.4	600
1 $\frac{1}{2}$ X 2-1/8 X 5 $\frac{1}{2}$	5.4	300	1 $\frac{1}{2}$ X 2-1/8 X 5 $\frac{1}{2}$	5.4	300	1 $\frac{1}{2}$ X 2-1/8 X 5 $\frac{1}{2}$	5.4	300
4 X 5 X 7 $\frac{1}{2}$	13.2	1,400	3 $\frac{1}{2}$ X 4 X 6	7.6	2,675	2-3/4 X 3 $\frac{1}{2}$ X 4-3/4	7.6	2,675
	40.8			38.5			38.5	
	3.0			3.8			3.8	
	10.0			10.0			10.0	
	20.0			19.7			19.7	
	161.5	5,056		154.1	6,331		154.1	6,331

COMPONENT LIST FOR A

NO.	COMPONENTS	50 KC		
		WT (LBS)	LOSSES (WATTS)	
<u>POWER SUPPLY (LOW VOLTAGE)</u>				
6	Rectifier, semiconductor	3.0	144	1 1/8 X
2	Capacitor, filter	1.2	1	2-1/8
1	Filter Choke (L-2)	15.8	84	4 1/2 X
1	Diode, zener reference	.1	2	3/8 I
1	Resistor	.2	5	1/2 I
1	Transformer (T1)	2.4	207	2 X 2
<u>POWER SUPPLY (HIGH VOLTAGE)</u>				
6	Rectifier, semiconductor	5.0	1,440	1-7/8
2	Capacitor, filter	3.5	1	4 X 5
1	Filter Choke (L1)	22.0	258	4 1/2 X
<u>OSCILLATOR SECTION</u>				
3	Transistor	.2	2	TO5
3	Capacitor	.1		MIL-C
3	Resistor, base drive)			
6	Resistor)	.2	3	1/2 W MI
<u>WAVE SHAPER AND DRIVER</u>				
9	Transistor, low power	2.7	9	TO3
12	Capacitor	.4	1	MIL-C
3	Resistor (10W)	.6	15	5/16 I
3	Transistor, med power	.9	15	TO3
6	Transistor, high power	3.0	360	1 1/2 X 1
24	Resistor (1W)	.5	12	1W MI
<u>OUTPUT SECTION</u>				
24	Transistor, power	12.0	2,000	1 1/2 X 1
24	Resistor, emitter	34.0	2,400	2 1/4 X 3
1	Transformer, output	18.0	1,020	3-3/4
3	Transformer, driver	7.5	90	2 X 2 1/4
24	Resistor, base drive	21.5	1,200	1 1/2 X 2
3	Transformer - push-pull	6.0	615	2 1/2 X 3
<u>MISCELLANEOUS</u>				
	Mounting plate and Enclosure	76.9		
	Cooling Ducts	5.6		
	Controls	10.0		
	Wire and Hardware	22.5		
TOTALS		275.8	9,884	

TABLE 4

FOR A 60 KW STATIC TRANSISTOR CONVERTER (30)

SIZE (INCHES)	200 KC			800 KC		
	WT (LBS)	LOSSES (WATTS)	SIZE (INCHES)	WT (LBS)	LOSSES (WATTS)	SIZE (INCHES)
1 1/4 X 1 1/4 X 3	3.0	144	1 1/4 X 1 1/4 X 3	3.0	144	1 1/4 X 1 1/4 X 3
2-1/8 Dia. X 6	1.2	1	2-1/8 Dia. X 6	1.2	1	2-1/8 Dia. X 6
1 1/2 X 3-3/4 X 5-1/8	15.8	84	4 1/2 X 3-3/4 X 5-1/8	15.8	84	4 1/2 X 3-3/4 X 5-1/8
3/8 Dia. X 1	.1	2	3/8 Dia. X 1	.1	2	3/4 Dia. X 1
1/2 Dia. X 2	.2	5	1/2 Dia. X 2	.2	5	1/2 Dia. X 2
2 X 2 X 4	2.4	207	2 X 2 X 4	2.4	207	2 X 2 X 4
1-7/8 X 1-7/8 X 4-1/16	5.0	1,440	1-7/8 X 1-7/8 X 4-1/16	5.0	1,440	1-7/8 X 1-7/8 X 4-1/16
4 X 5 X 6 1/2	3.5	1	4 X 5 X 6 1/2	3.5	1	4 X 5 X 6 1/2
1 1/2 X 4 X 6-3/4	22.0	258	4 1/2 X 4 X 6-3/4	22.0	258	4 1/2 X 4 X 6-3/4
T05	.2	2	T05	.2	2	T05
MIL-C-5B	.1		MIL-C-5B	.1		MIL-C-5B
1/2 W MIL-R-11C	.2	3	1/2 W MIL-R-11C	.2	3	1/2 W MIL-R-11C
T03	2.7	9	T03	2.7	9	T03
MIL-C-25	.4	1	MIL-C-25	.4	1	MIL-C-25
5/16 Dia. X 1-3/4	.6	15	5/16 Dia. X 1-3/4	.6	15	5/16 Dia. X 1-3/4
T03	.9	15	T03	.9	15	T03
1 1/4 X 1 1/4 X 2	3.0	360	1 1/4 X 1 1/4 X 2	3.0	360	1 1/4 X 1 1/4 X 2
1 W MIL-R-11C	.5	12	1 W MIL-R-11C	.5	12	1 W MIL-R-11C
1 1/4 X 1 1/4 X 2	12.0	2,000	1 1/4 X 1 1/4 X 2	12.0	2,000	1 1/4 X 1 1/4 X 2
2 1/4 X 3 X 7	34.0	2,400	2 1/4 X 3 X 7	34.0	2,400	2 1/4 X 3 X 7
3 X 5 X 6	13.2	1,700	3 X 5 X 6	7.8	2,920	3 X 3 1/2 X 4 1/2
2 X 2 X 3	5.5	152	2 X 2 X 3	3.3	262	1 1/2 X 2 X 3
1 1/2 X 2-1/8 X 5 1/2	21.5	1,200	1 1/2 X 2-1/8 X 5 1/2	21.5	1,200	1 1/2 X 2-1/8 X 5 1/2
2 X 3 1/4 X 4-5/8	4.0	1,050	2 1/4 X 3 X 3 1/2	2.4	1,800	2 X 2 1/2 X 3
	68.1			62.0		
	6.1			7.5		
	10.0			10.0		
	22.0			21.7		
	258.2	11,061		244.0	13,141	

NO.	COMPONENTS	WT (LBS)	LOSSES (WATTS)
<u>POWER SUPPLY (LOW VOLTAGE)</u>			
6	Rectifier, semiconductor	3.0	344
1	Transformer, low voltage (T1)	3.4	430
2	Capacitor, filter	1.2	1
1	Filter Choke (L-2)	19.0	200
1	Diode, zener reference (CR13)	.1	2
1	Resistor (R9)	.3	6
<u>POWER SUPPLY (HIGH VOLTAGE)</u>			
6	Rectifier, semiconductor	5.0	2,004
2	Capacitor, filter	3.5	1
1	Filter Choke (L1)	25.0	650
<u>OSCILLATOR SECTION</u>			
2	Transistor, low power (Q1, Q2)	.1	1
7	Resistor	.1	2
5	Capacitor	.1	
<u>WAVE SHAPER AND DRIVER</u>			
2	Transistor, power (Q8) (Q10)	1.0	120
1	Transistor, med power (Q6)	.3	5
1	Transistor, low power (Q4)	.3	1
2	Resistor (10W)	.4	10
5	Resistor, power	5.0	325
<u>OUTPUT SECTION</u>			
10	Transistor, power	5.0	600
10	Resistor, power (200W)	14.0	1,000
10	Resistor, base drive (100W)	9.0	500
1	Transformer, output (T2)	90.0	4,472
<u>MISCELLANEOUS</u>			
	Mounting plate and Enclosure	51.4	
	Cooling ducts	4.7	
	Controls	12.0	
	Wire and Hardware	25.0	
TOTALS		278.9	10,674

LIST FOR A 300 KW STATIC TRANSISTOR CONVERTER (1φ)

50 KC			200 KC			800 KC		
LOSSES (WATTS)	SIZE (INCHES)	WT (LBS)	LOSSES (WATTS)	SIZE (INCHES)	WT (LBS)	LOSSES (WATTS)	SIZE (INCHES)	
344	1 1/4 X 1 1/4 X 3	3.0	344	1 1/4 X 1 1/4 X 3	3.0	344	1 1/4 X 1 1/4 X 3	
430	2 1/4 X 2 1/4 X 4 1/2	3.4	430	2 1/4 X 2 1/4 X 4 1/2	3.4	430	2 1/4 X 2 1/4 X 4 1/2	
1	2-1/8 Dia. X 6	1.2	1	2-1/8 Dia. X 6	1.2	1	2-1/8 Dia. X 6	
200	4 X 5 X 6	19.0	200	4 X 5 X 6	19.0	200	4 X 5 X 6	
2	3/8 Dia. X 1	.1	2	3/8 Dia. X 1	.1	2	3/8 Dia. X 1	
6	1/2 Dia. X 2	.3	6	1/2 Dia. X 2	.3	6	1/2 Dia. X 2	
2,004	1-7/8 X 1-7/8 X 4-1/16	5.0	2,004	1-7/8 X 1-7/8 X 4-1/16	5.0	2,004	1-7/8 X 1-7/8 X 4-1/16	
1	4 X 5 X 6 1/2	3.5	1	4 X 5 X 6 1/2	3.5	1	4 X 5 X 6 1/2	
650	7 X 4 X 6 1/2	25.0	650	7 X 4 X 6 1/2	25.0	650	7 X 4 X 6 1/2	
1	T05	.1	1	T05	.1	1	T05	
2	1/2W MIL-R-11C MIL-C-5B	.1 .1	2	1/2W MIL-R-11C MIL-C-5B	.1 .1	2	1/2W MIL-R-11C MIL-C-5B	
120	1 1/4 X 1 1/4 X 2	1.0	120	1 1/4 X 1 1/4 X 2	1.0	120	1 1/4 X 1 1/4 X 2	
5	T03	.3	5	T03	.3	5	T03	
1	T03	.3	1	T03	.3	1	T03	
10	5/16 Dia. X 1-3/4	.4	10	5/16 Dia. X 1-3/4	.4	10	5/16 Dia. X 1-3/4	
325	2 1/4 X 3 X 7	5.0	325	2 1/4 X 3 X 7	5.0	325	2 1/4 X 3 X 7	
600	1 1/4 X 1 1/4 X 2	5.0	600	1 1/4 X 1 1/4 X 2	5.0	600	1 1/4 X 1 1/4 X 2	
1,000	2 1/4 X 3 X 7	14.0	1,000	2 1/4 X 3 X 7	14.0	1,000	2 1/4 X 3 X 7	
500	1 1/2 X 2-1/8 X 5 1/2	9.0	500	1 1/2 X 2-1/8 X 5 1/2	9.0	500	1 1/2 X 2-1/8 X 5 1/2	
472	6 X 8 X 11 1/2	63.5	5,710	6 X 7 X 9 1/2	42.0	8,225	5 X 6 X 8 1/2	
		48.5			46.0			
		5.0			6.0			
		12.0			12.0			
		24.5			24.0			
574		249.3	11,912		225.8	14,427		

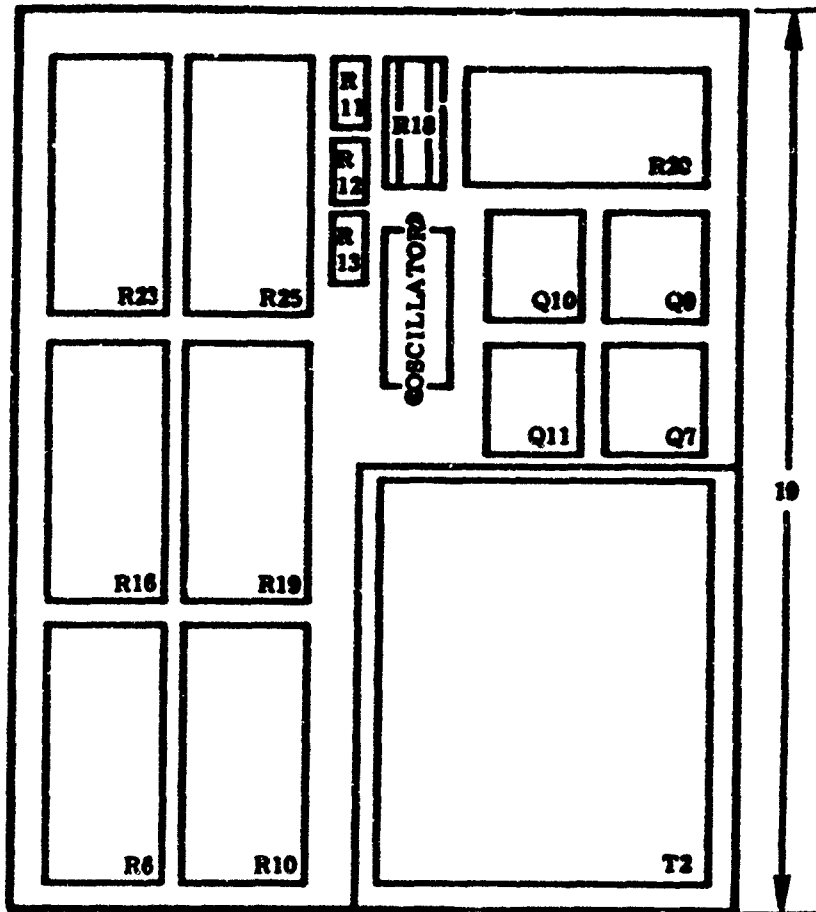
COMPONENT LIST FC

NO.	COMPONENTS	50 K		
		WT (LBS)	LOSSES (WATTS)	
<u>POWER SUPPLY (LOW VOLTAGE)</u>				
6	Rectifier, semiconductor	3.0	344	1 1/2
2	Capacitor, filter	1.2	1	2
1	Filter Choke (L-2)	19.0	200	4
1	Diode, zener reference	.1	2	3/4
1	Resistor	.3	6	1 1/2
1	Transformer	3.4	430	2 1/2
<u>POWER SUPPLY (HIGH VOLTAGE)</u>				
6	Rectifier, semiconductor	5.0	2,004	1-
2	Capacitor, filter	3.5	1	4
1	Filter Choke (L1)	25.0	650	7
<u>OSCILLATOR SECTION</u>				
3	Transistor	.2	2	TC
3	Capacitor	.1		MI
3	Resistor, base drive)	.2	3	1/
6	Resistor)			
<u>WAVE SHAPER AND DRIVER</u>				
9	Transistor, low power	2.7	9	TC
12	Capacitor	.4	1	MI
3	Resistor (10W)	.6	15	5/
3	Transistor, med power	.9	15	TO
6	Transistor, high power	3.0	360	1 1/2
24	Resistor (1W)	.5	12	1W
<u>OUTPUT SECTION</u>				
42	Transistor, power	21.0	4,000	1 1/2
42	Resistor, emitter	59.0	4,200	2 1/2
1	Transformer, output	90.0	6,300	6
3	Transformer, driver	37.4	450	3 1/2
42	Resistor, base drive	37.8	2,100	1 1/2
3	Transformer - push-pull	20.0	1,165	3 1/2
<u>MISCELLANEOUS</u>				
	Mounting plate and Enclosure	134.0		
	Cooling Ducts	9.6		
	Controls	12.0		
	Wire and Hardware	29.0		
TOTALS		518.9	22,270	

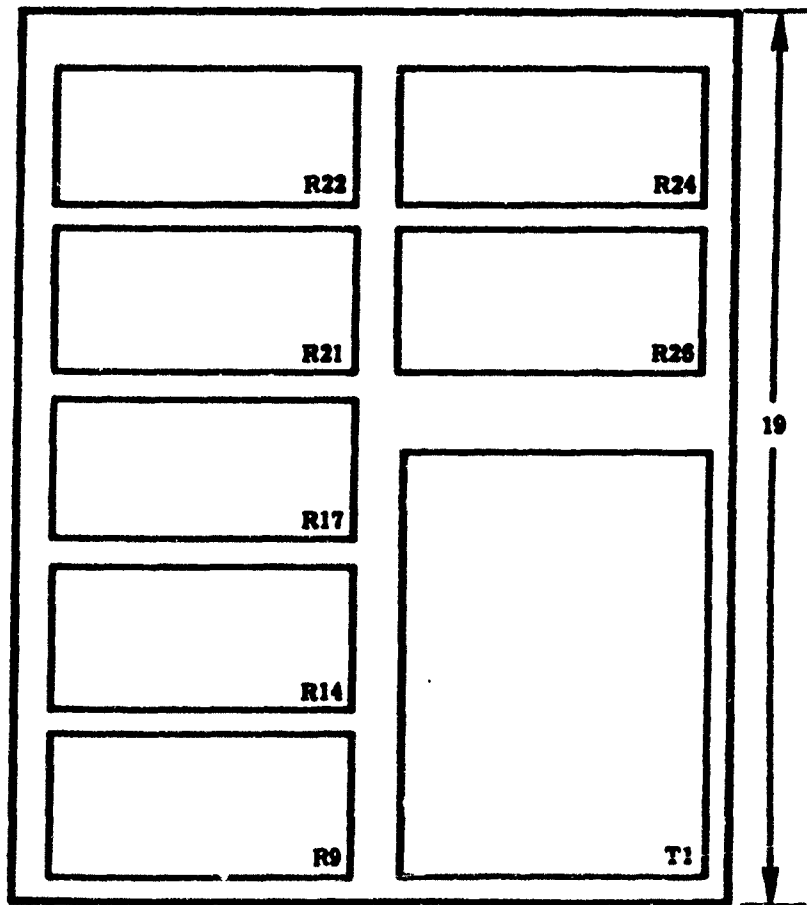
TABLE 6

FOR A 300 KW STATIC TRANSISTOR CONVERTER (3φ)

0 KC	200 KC			800 KC		
SIZE (INCHES)	WT (LBS)	LOSSES (WATTS)	SIZE (INCHES)	WT (LBS)	LOSSES (WATTS)	SIZE (INCHES)
1 1/8 X 1 1/8 X 3	3.0	344	1 1/8 X 1 1/8 X 3	3.0	344	1 1/8 X 1 1/8 X 3
2-1/8 Dia. X 6	1.2	1	2-1/8 Dia. X 6	1.2	1	2-1/8 Dia. X 6
4 X 5 X 6	19.0	200	4 X 5 X 6	19.0	200	4 X 5 X 6
3/8 Dia. X 1	.1	2	3/8 Dia. X 1	.1	2	3/8 Dia. X 1
1/2 Dia. X 2	.3	6	1/2 Dia. X 2	.3	6	1/2 Dia. X 2
2 1/8 X 2 1/8 X 4 1/2	3.4	430	2 1/8 X 2 1/8 X 4 1/2	3.4	430	2 1/8 X 2 1/8 X 4 1/2
1-7/8 X 1-7/8 X 4-1/16	5.0	2,004	1-7/8 X 1-7/8 X 4-1/16	5.0	2,004	1-7/8 X 1-7/8 X 4-1/16
4 X 5 X 6 1/2	3.5	1	4 X 5 X 6 1/2	3.5	1	4 X 5 X 6 1/2
7 X 4 X 6 1/2	25.0	650	7 X 4 X 6 1/2	25.0	650	7 X 4 X 6 1/2
T05	.2	2	T05	.2	2	T05
MIL-C-5B	.1		MIL-C-5B	.1		MIL-C-5B
1/2W MIL-R-11C	.2	3	1/2W MIL-R-11C	.2	3	1/2W MIL-R-11C
T03	2.7	9	T03	2.7	9	T03
MIL-C-25	.4	1	MIL-C-25	.4	1	MIL-C-25
5/16 Dia. X 1-3/4	.6	15	5/16 Dia. 1-3/4	.6	15	5/16 Dia. 1-3/4
T03	.9	15	T03	.9	15	T03
1 1/8 X 1 1/8 X 2	3.0	360	1 1/8 X 1 1/8 X 2	3.0	360	1 1/8 X 1 1/8 X 2
1W MIL-R-11C	.5	12	1W MIL-R-11C	.5	12	1W MIL-R-11C
1 1/8 X 1 1/8 X 2	21.0	4,000	1 1/8 X 1 1/8 X 2	21.0	4,000	1 1/8 X 1 1/8 X 2
2 1/8 X 3 X 7	59.0	4,200	2 1/8 X 3 X 7	59.0	4,200	2 1/8 X 3 X 7
6 X 8 X 11 1/2	63.5	7,400	6 X 7 X 9 1/2	42.0	9,600	5 X 6 X 8 1/2
3 1/2 X 4 1/8 X 5 1/4	26.3	700	3 1/4 X 3-3/4 X 4-5/8	17.8	1,480	2 1/2 X 3 1/8 X 4 1/2
1 1/2 X 2-1/8 X 5 1/2	37.8	2,100	1 1/2 X 2-1/8 X 5 1/2	37.8	2,100	1 1/2 X 2-1/8 X 5 1/2
3 1/2 X 5 X 7 1/4	15.0	1,370	3 1/2 X 4 1/2 X 6	9.0	1,780	2 1/2 X 3-7/8 X 6
	109.0			95.9		
	10.3			12.1		
	12.0			12.0		
	28.0			27.0		
	451.0	23,825		402.7	27,215	



VIEW B-B



VIEW A-A



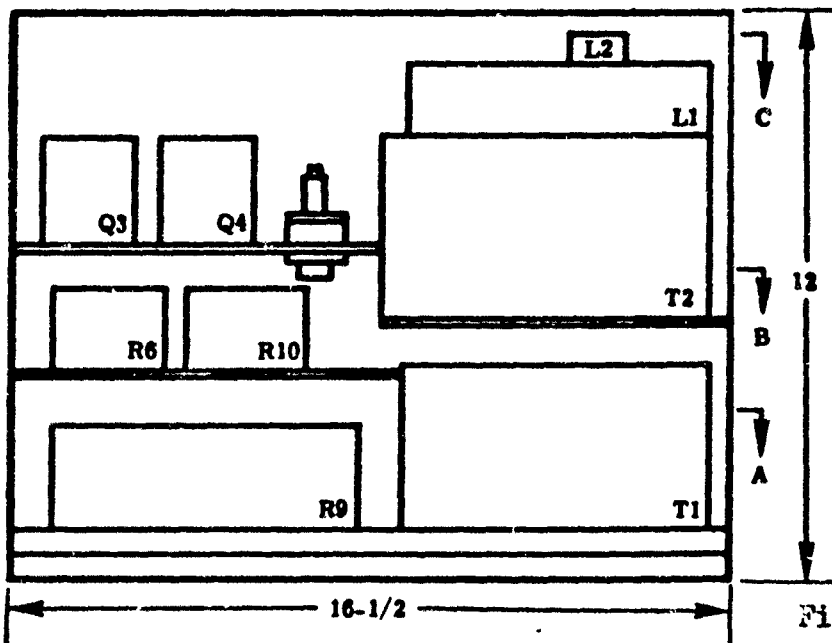
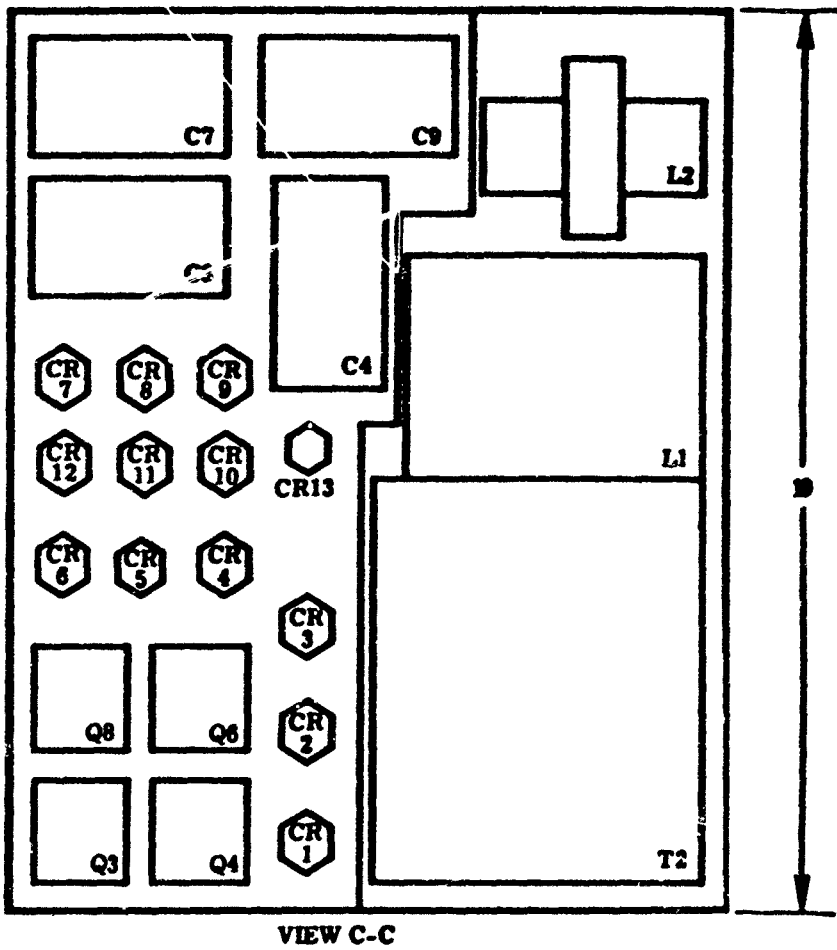
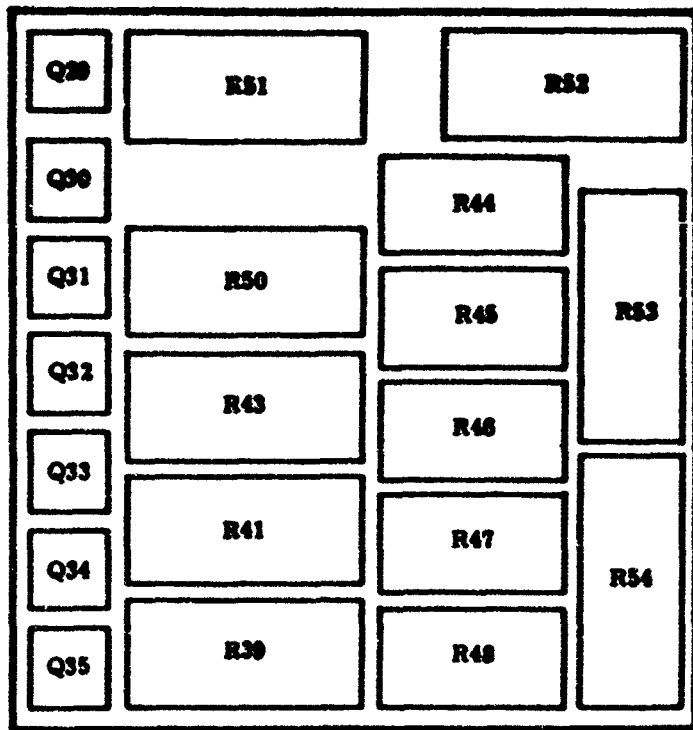
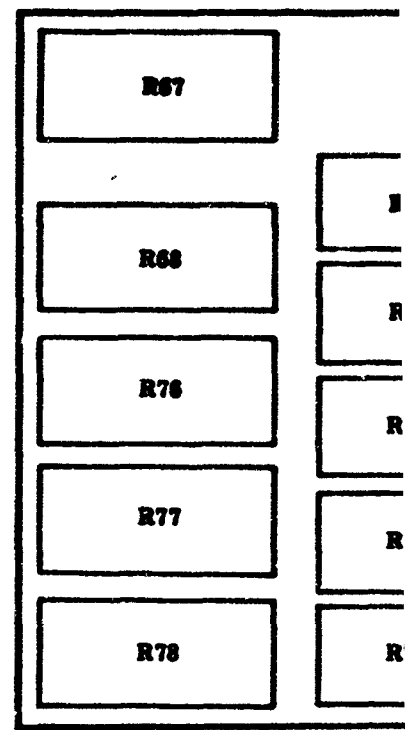


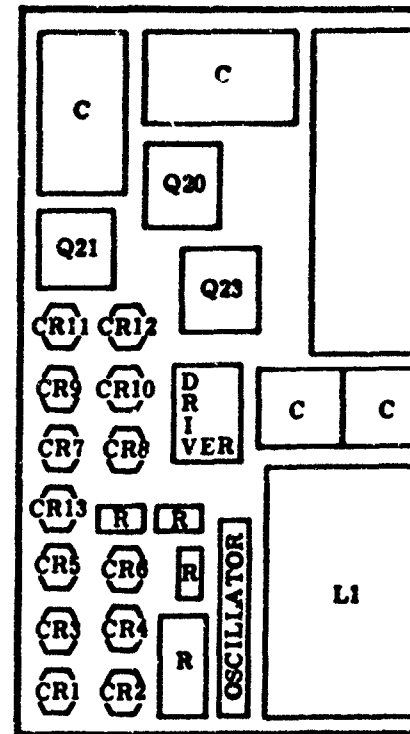
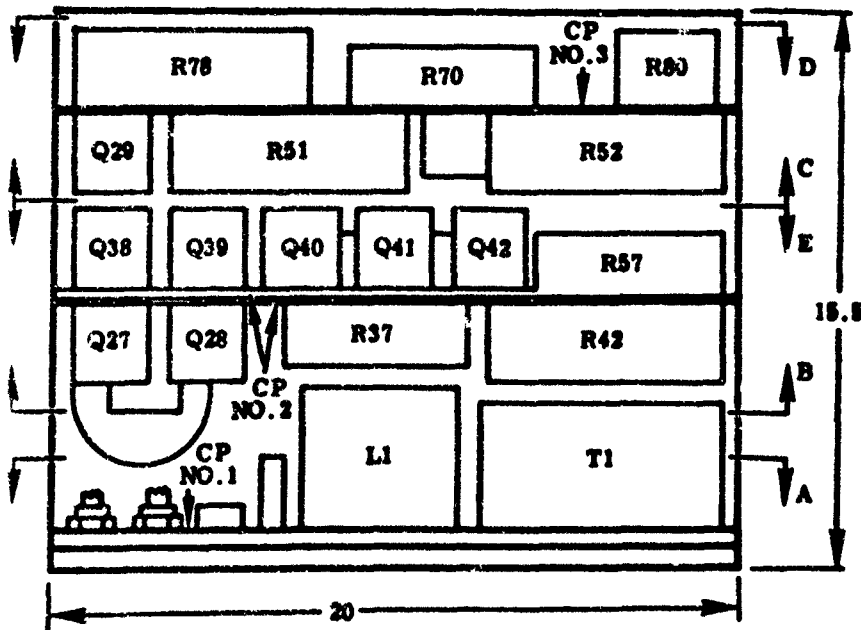
Figure 36. Preliminary Mechanical Design of 60 KW, 1 ϕ , 200 KC Static Transistor Converter—Typical of 50 and 800 KC Designs



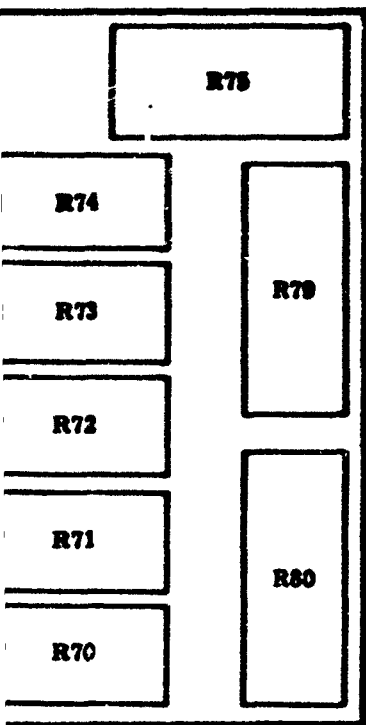
SECT C-C



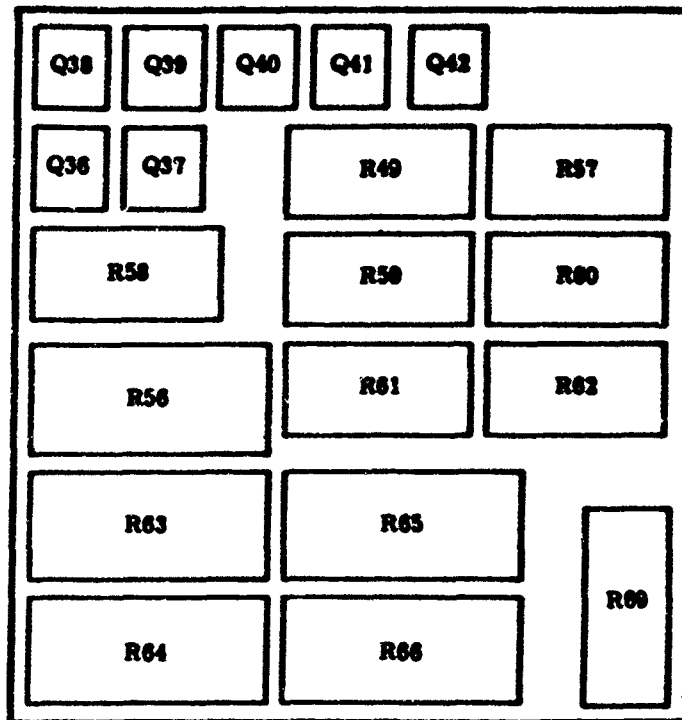
SECT D-I



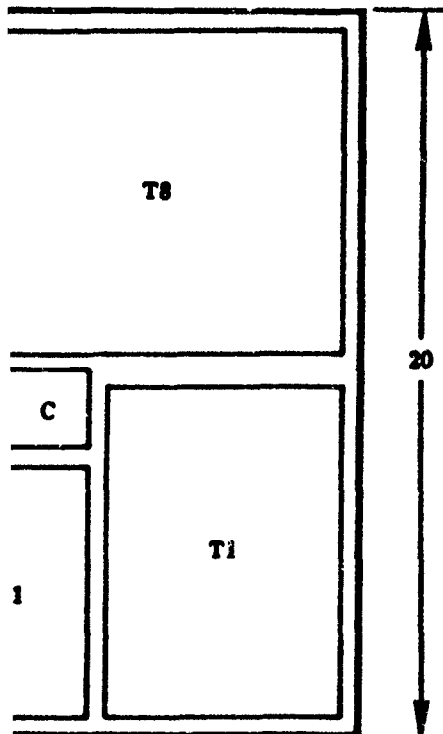
SECT A-A



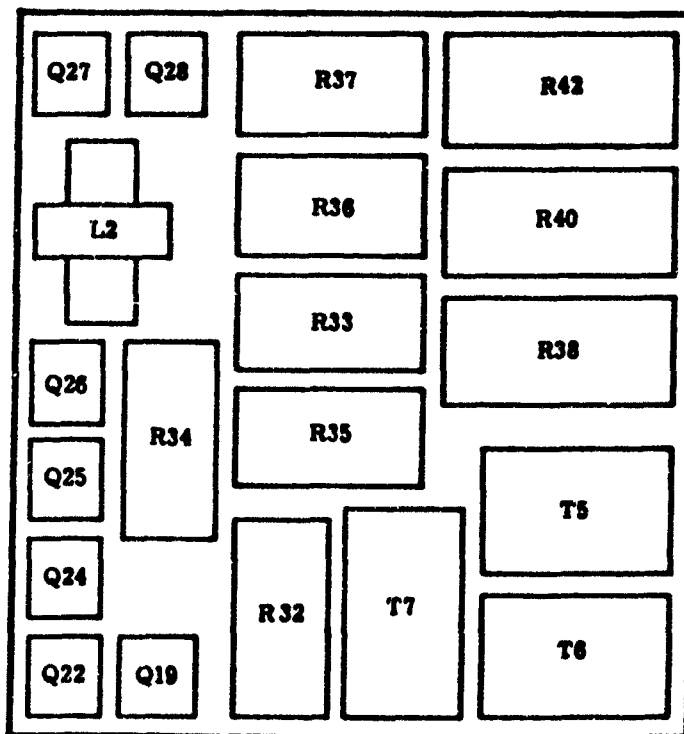
T D-D



VIEW E-E

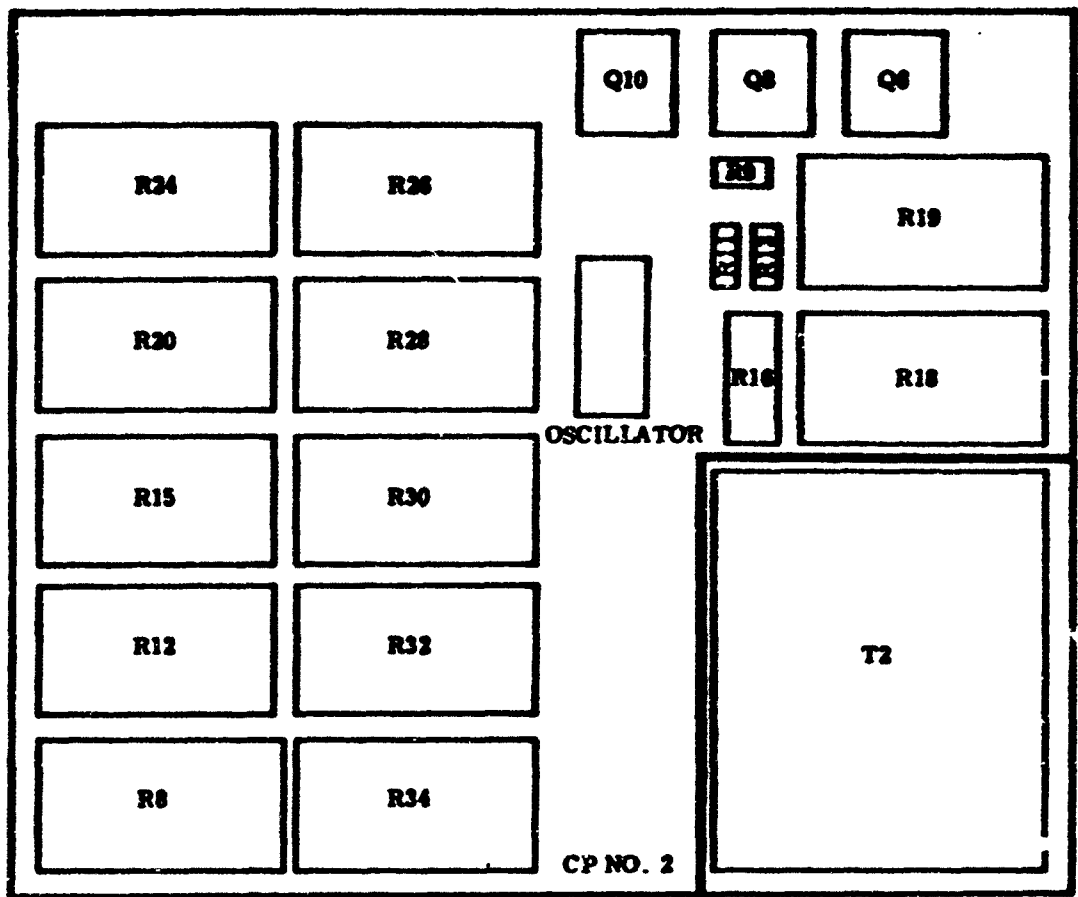


A-A

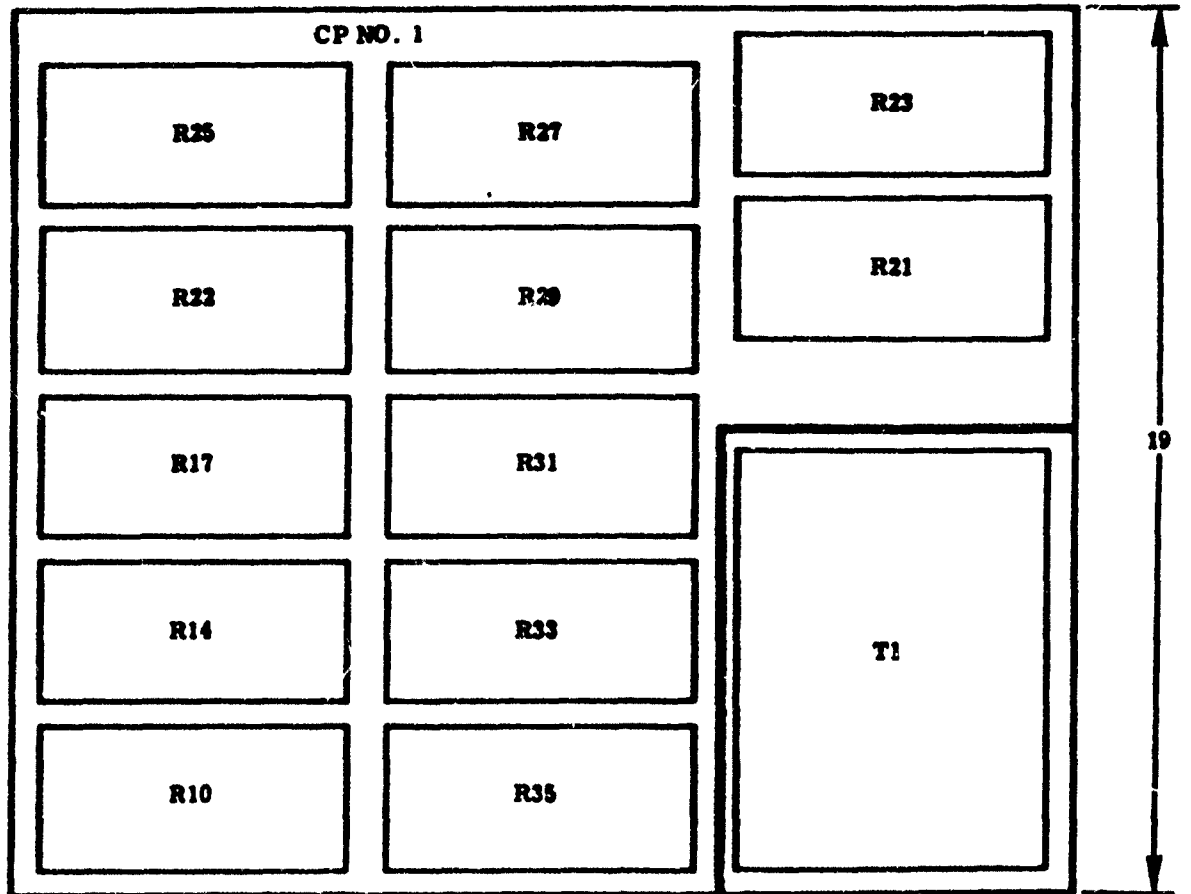


SECT B-B

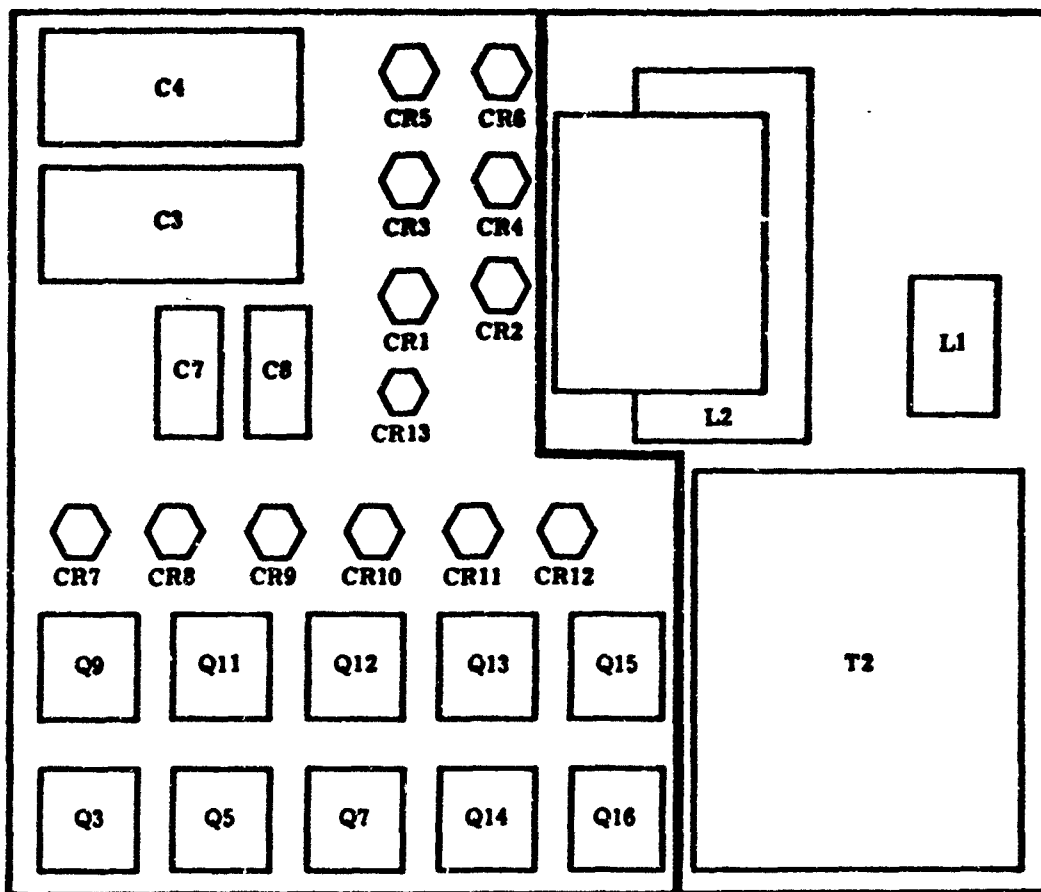
Figure 37. Preliminary Mechanical Design of 60 KW, 3 ϕ , 200 KC Static Transistor Converter--Typical of 50 and 800 KC Designs



VIEW B-B



VIEW A-A



VIEW C-C

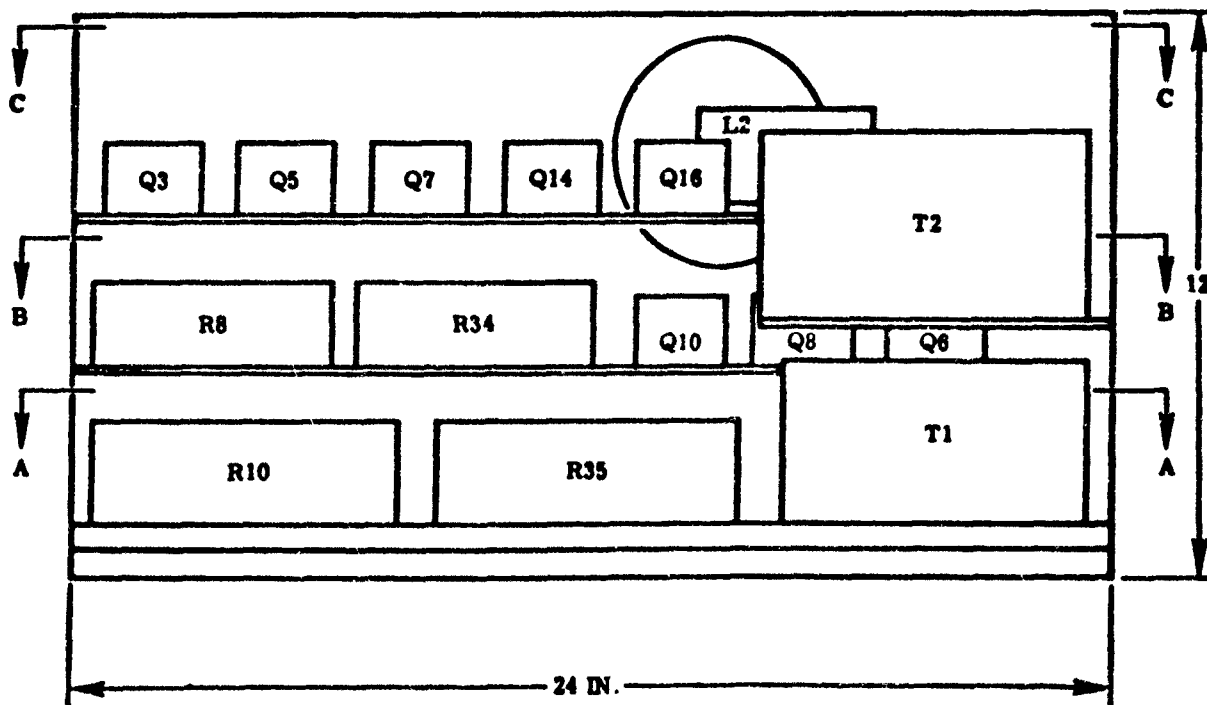
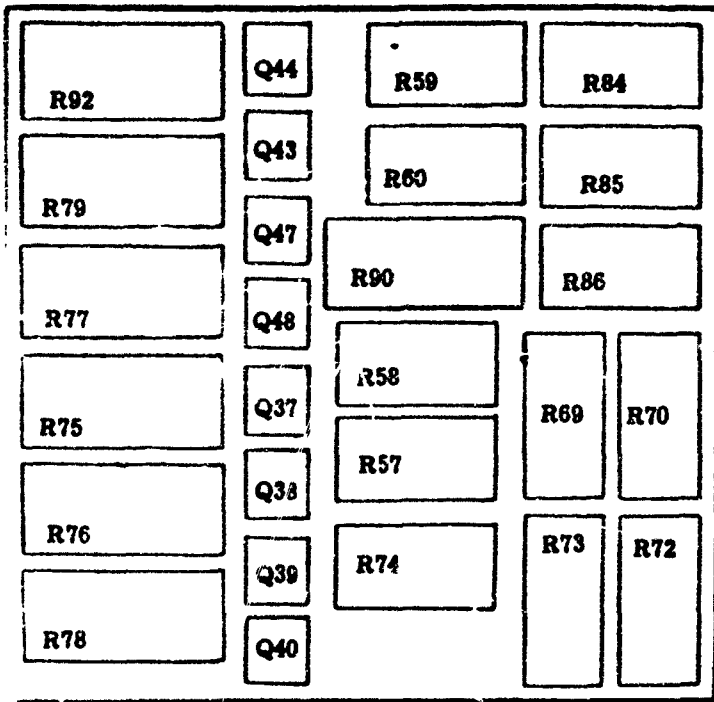
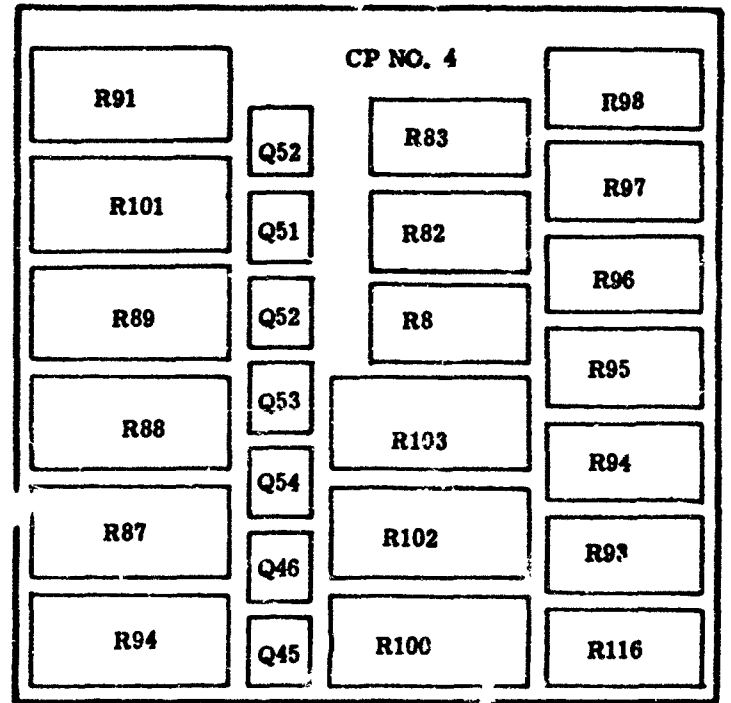


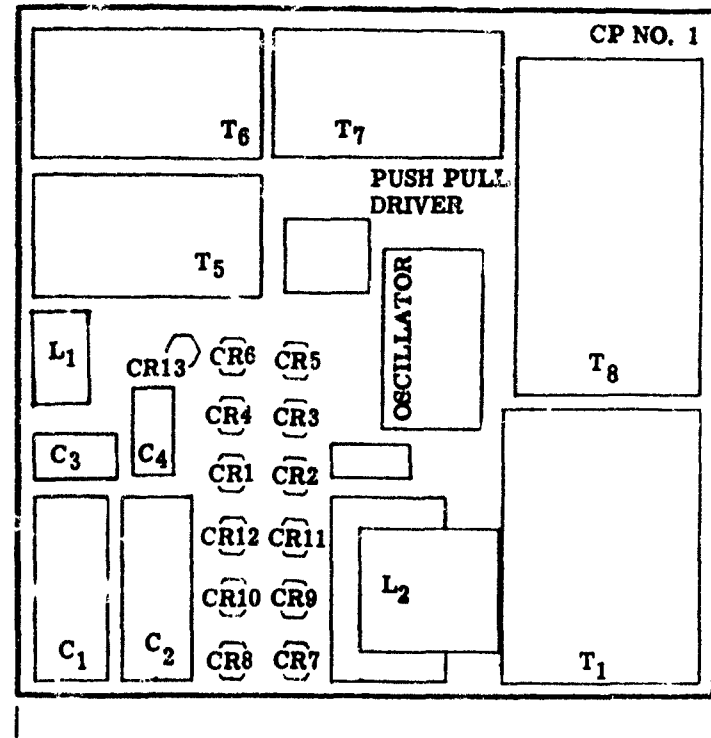
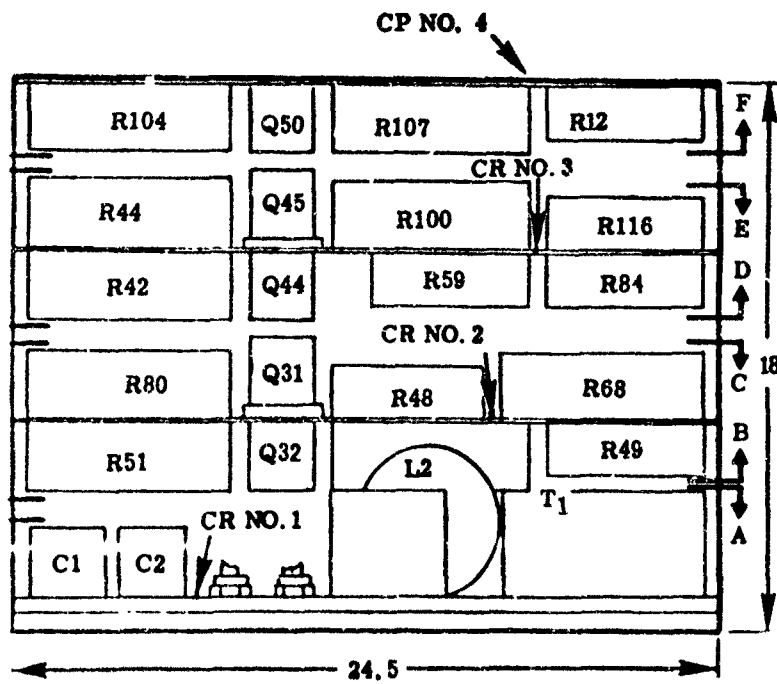
Figure 38. Preliminary Mechanical Design of 300 KW, 1 ϕ , Static (Transistor) Converter

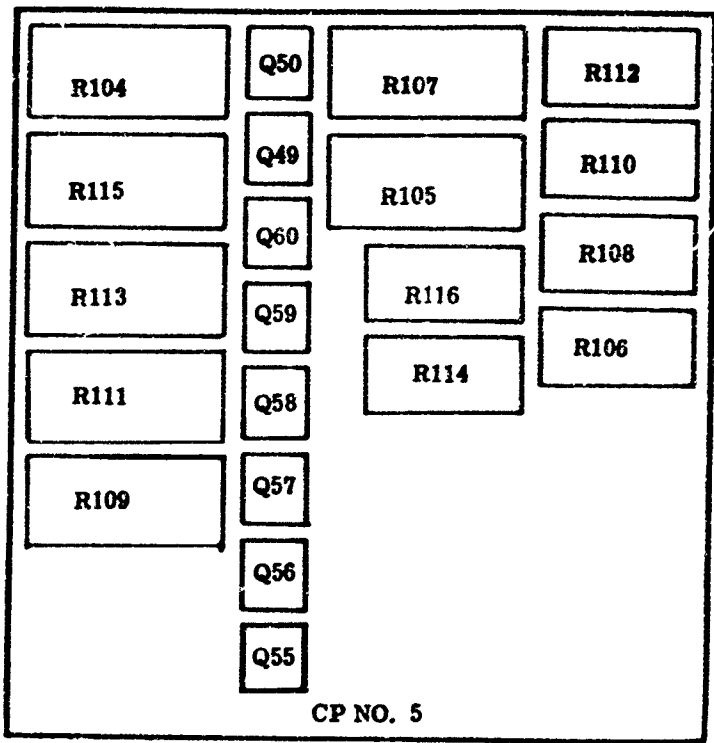


VIEW D - D

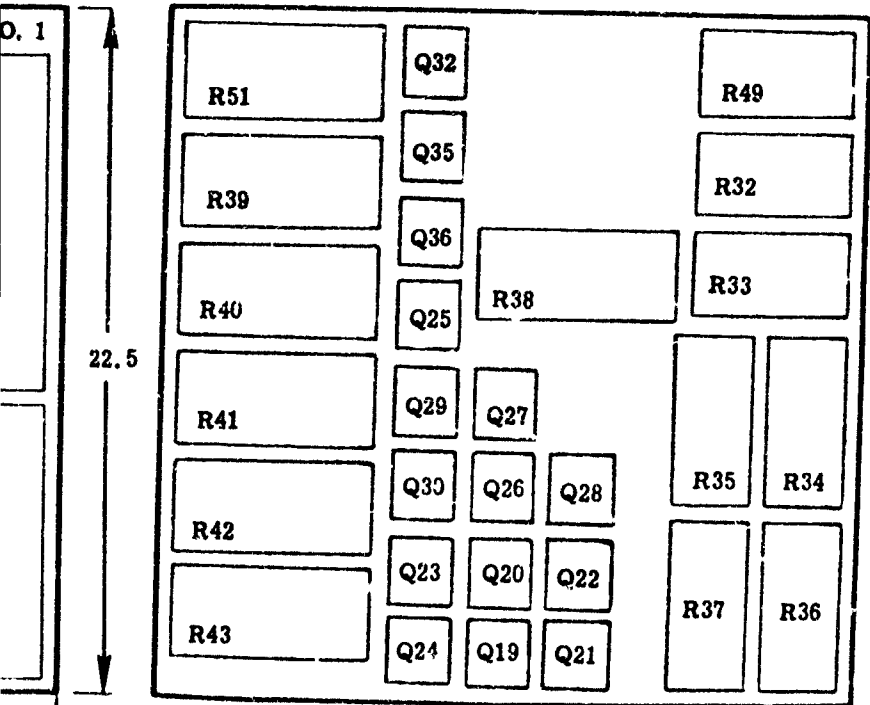


VIEW E - E

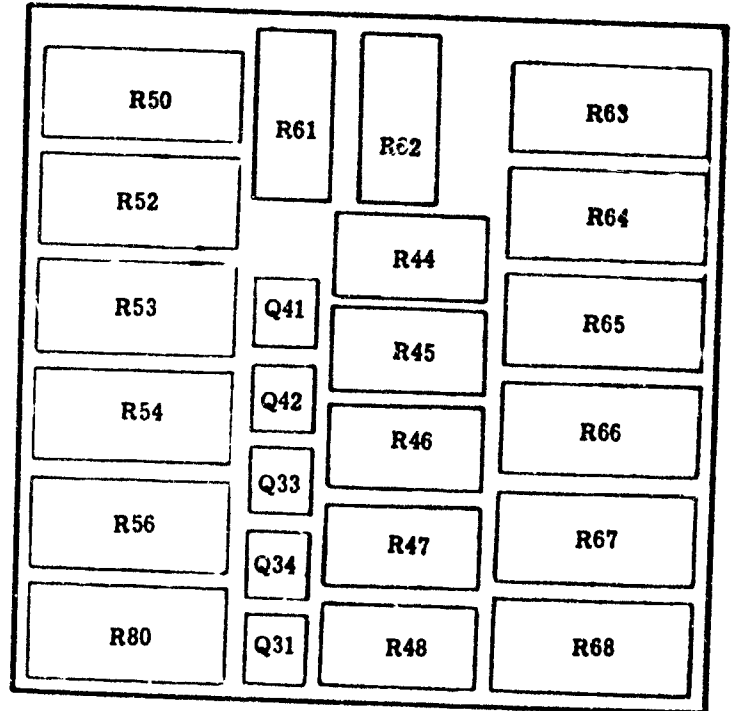




VIEW F - F

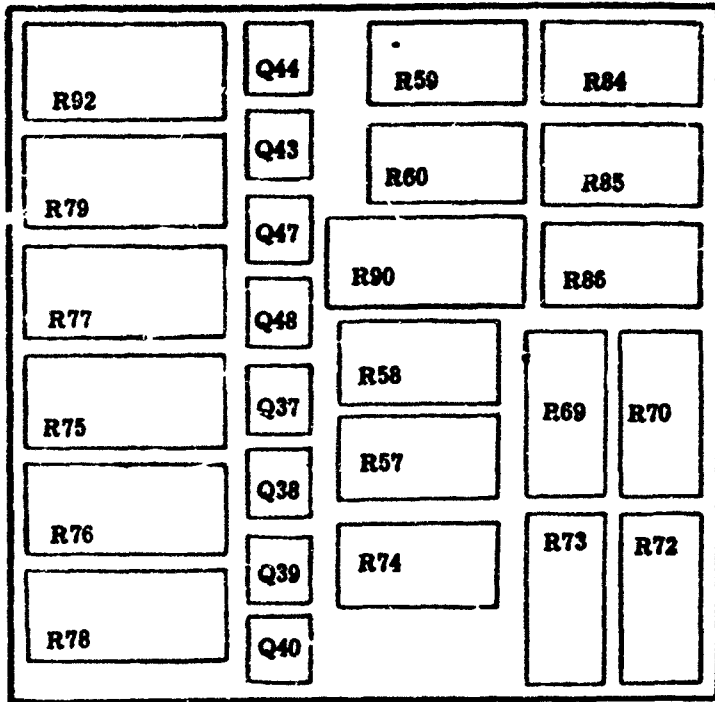


VIEW B - B

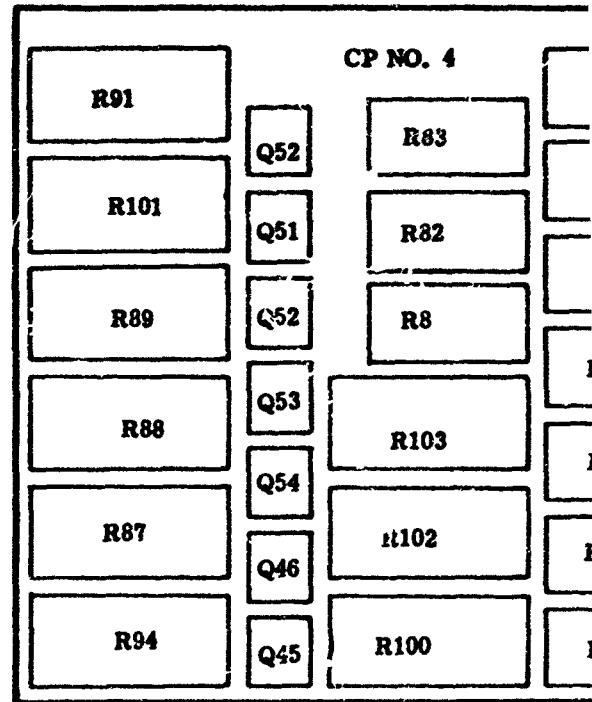


VIEW C - C

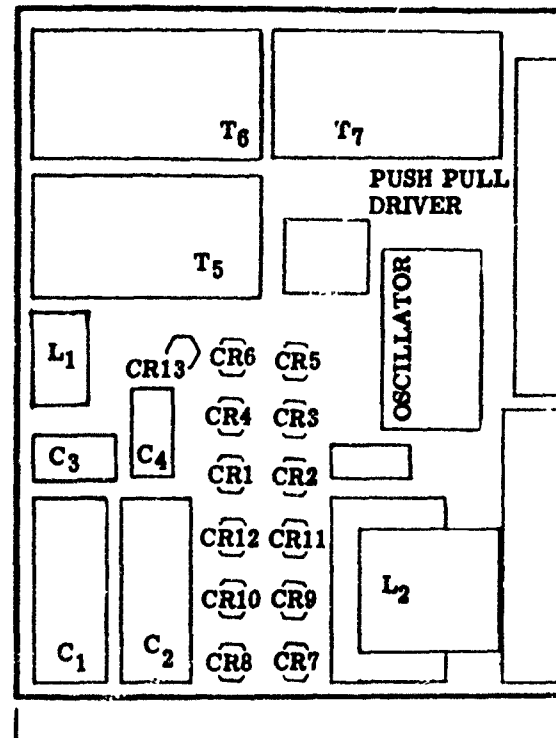
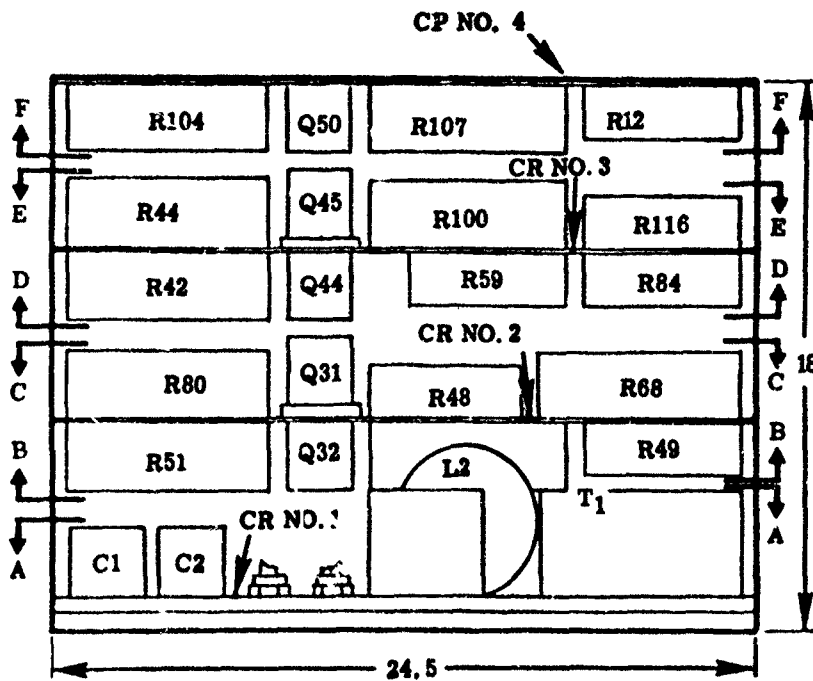
Figure 39. Preliminary Mechanical Design of 300 KW, 3 ϕ , 200 KC Static Transistor Converter Typical of 50 and 800 KC Units

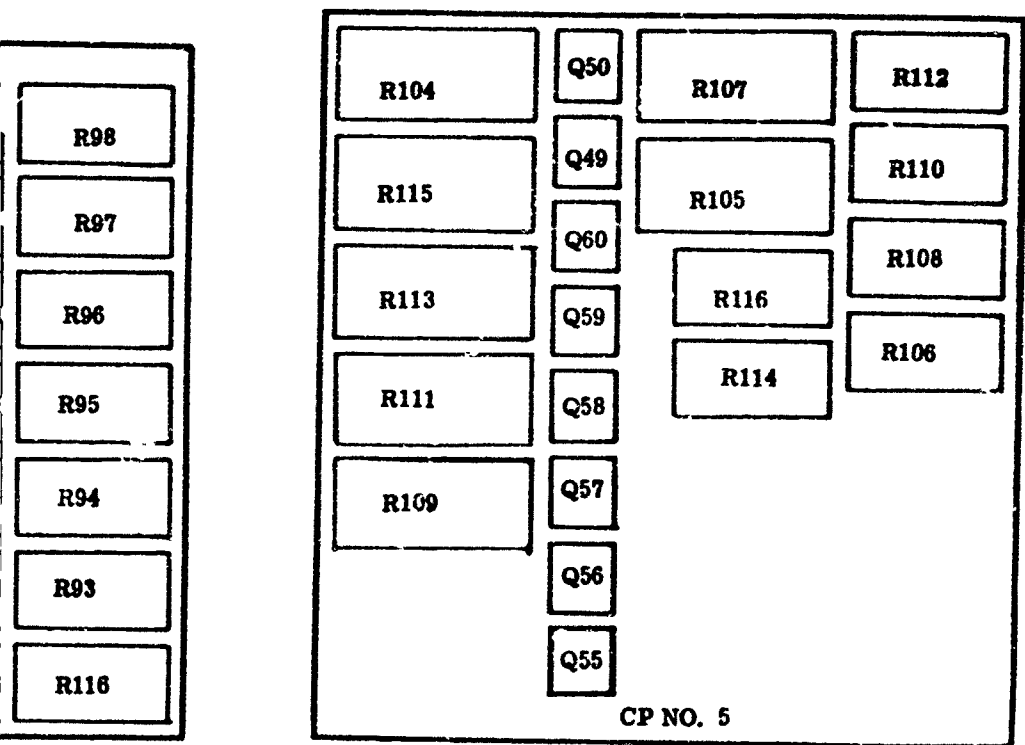


VIEW D - D

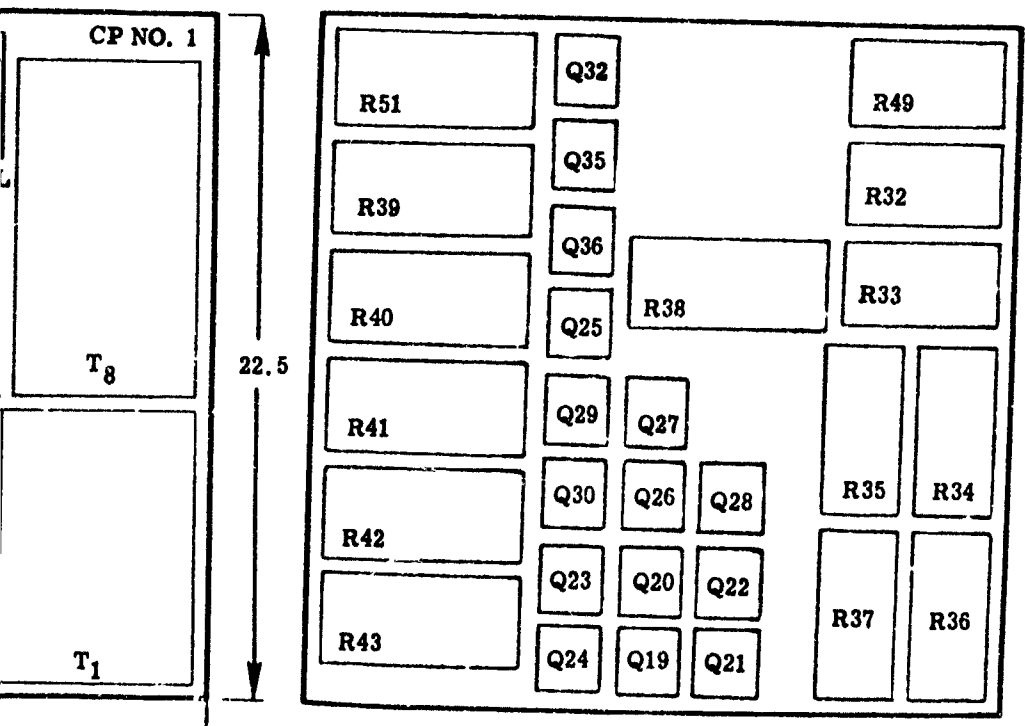


VIEW E - E

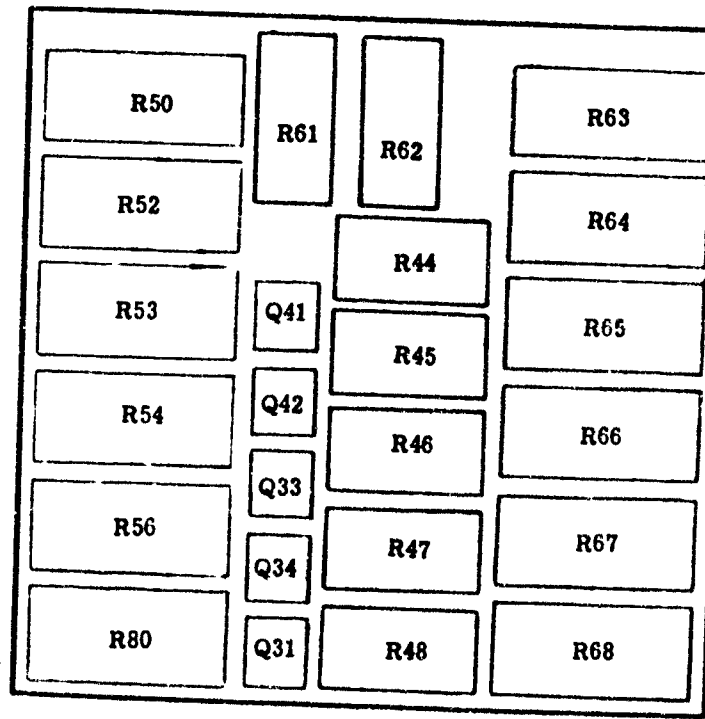




VIEW F - F



VIEW B - B



VIEW C - C

Figure 39. Preliminary Mechanical Design of 300 KW, 3 ϕ , 200 KC Static Transistor Converter Typical of 50 and 800 KC Unit

THERMAL DESIGN

For the purposes of a cooling analysis, it has been assumed that all transistors are mounted on a heat sink material which is part of the heat exchanger or cold plate. In the thermal analysis, thermal drop through electrical insulation, allowable junction temperatures of the transistors and internal heat flow from each device to the heat exchanger were considered. System cooling was approached by treating the shelves as a heat source. Each shelf has a certain number of computable heat losses by which the total shelf losses were derived. The 60 KW, 1 ϕ transistor converter has been packaged so that the magnetic components (transformers and coils) are in one area of the package and the non-magnetic components (transistors, diodes, capacitors, and resistors) are basically together in the remaining area of the package.

In this particular converter the heat losses of the magnetic and the non-magnetic components were approximately equal. Using the cold plate cooling technique, three cold plates were set up in parallel to cool the non-magnetic components, and the coolant tubes converge to a common tube and then flow to the magnetic components for further heat transfer. This allows a greater overall coolant temperature rise (ΔT).

Flow rate is determined by using the following equation: $W_p = AV$ a form of the continuity equation where A is the conduit area in square feet and V is the fluid velocity in feet/second. Knowing the flow rate required per shelf, the different area requirements can be obtained, giving us a total inlet coolant tube area requirement. This can be done by using values of A and V which will insure turbulent flow. By keeping the overall coolant tube area constant we can assume Δp to be zero; the only overall Δp is due to friction losses.

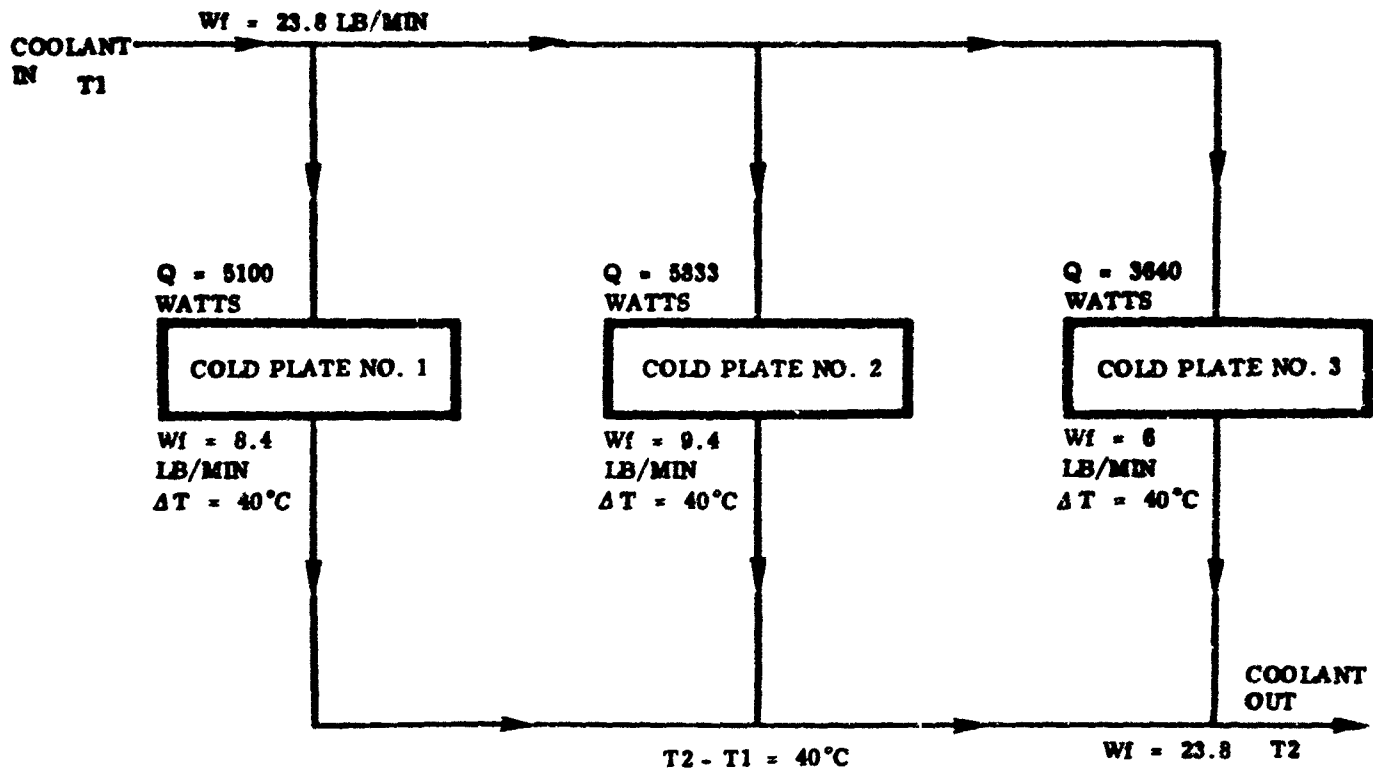
Figure 40 shows the system flow schematics for the single phase, 200 KC, 60 KW units and is typical of the 50 and 800 KC designs. A ΔT of approximately 24°C has been allowed across the non-magnetic components and approximately 26°C has been allowed across the magnetic components. It is now clear that a greater overall ΔT can be obtained with a smaller flow rate which is dependent upon the temperature range allowable, primarily by the semiconductor components. Figure 41 is the 300 KW analysis.

In the single phase systems, the output sections consist of several transistors in parallel. Since all the collectors are attached to a common lead, these transistors can be mounted directly to the cold plate without any insulating washers. This increases the thermal conductance and allows the transistors to dissipate more heat.

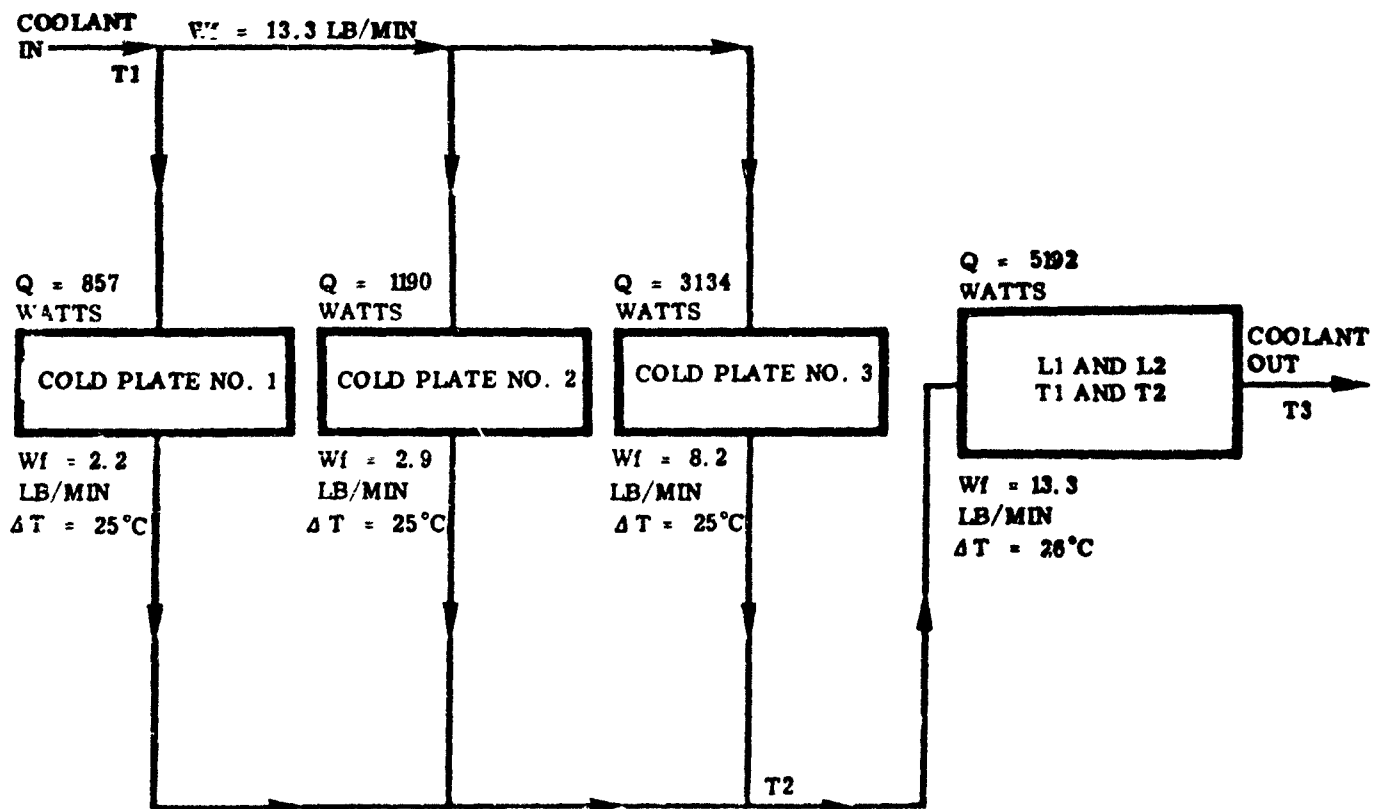
Knowing the heat losses present per shelf, Figure 83 was used to determine the coolant flow rate (W_p) required for each heat flow (q). A coolant temperature rise (ΔT) of 1.0°C was assumed for this design based on the probability that transistors will be available to operate at a high enough temperature to allow such a range.

Figure 42 shows the total lbs/KW out for both single and three-phase converter outputs at 50 KC, 200 KC and 800 KC. The curves show the trend

of system weight with temperature. Since present transistors are limited in temperature to about 300°F, this is the governing factor in determining the system operating point. From these curves, the optimum operating point from a weight basis is higher than the maximum transistor operating temperature (300°F). Lighter weight systems are possible only as transistor temperature capabilities are increased.



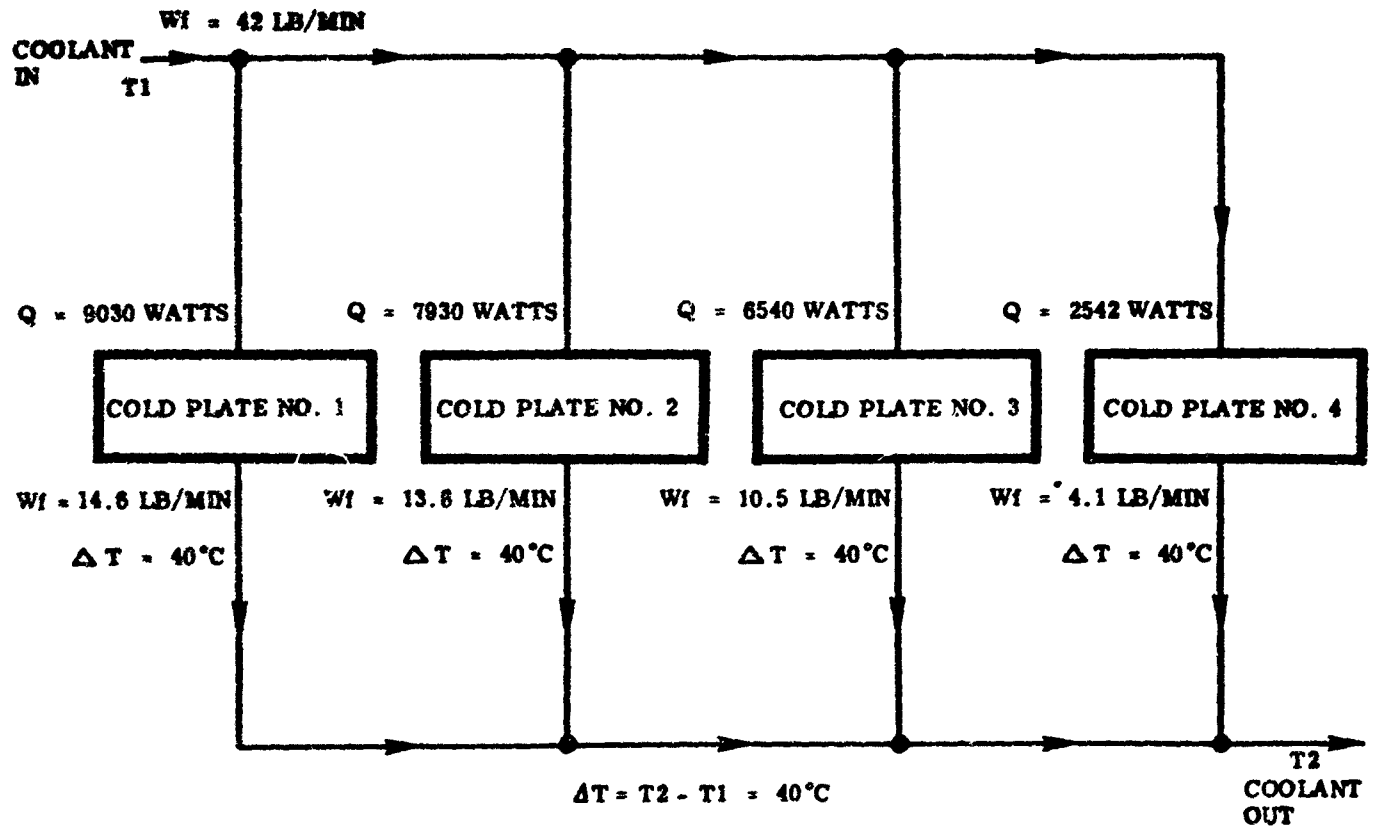
(A) 60KW, 3Ø, 200KC UNIT



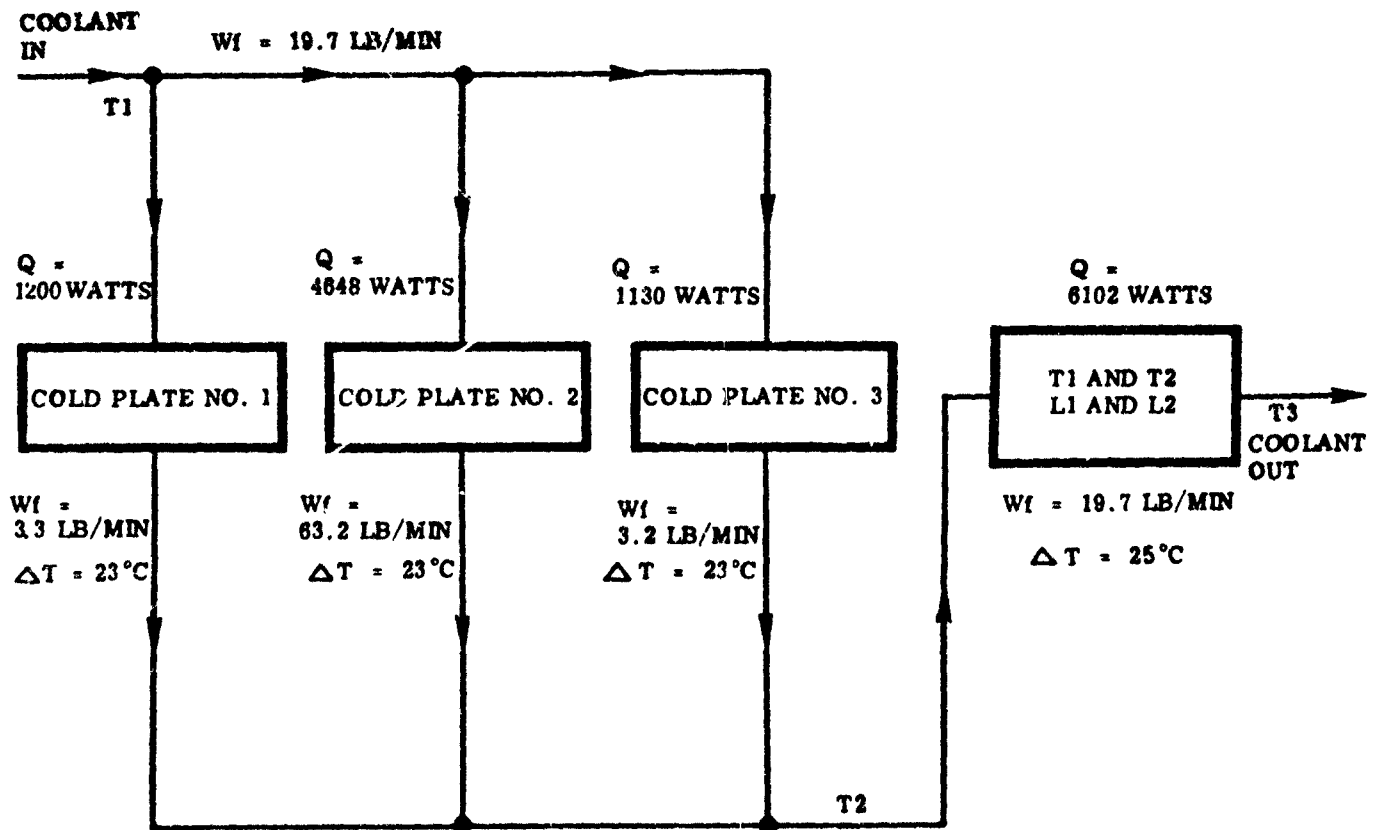
$$\Sigma \Delta T = (T_2 - T_1) + (T_3 - T_2) = 50^\circ\text{C}$$

(B) 60 KW, 1Ø, 200KC UNIT

Figure 40. Thermal Flow Diagram for 60 KW Static Transistor Converter Unit



(A) 300KW, 3φ, 200KC UNIT



$\Sigma \Delta T = (T_2 - T_1) + (T_3 - T_2) = 50^\circ\text{C}$

(B) 300 KW, 1φ, 200 KC UNIT

Figure h1. Thermal Flow Diagram for 300 KW Static Transistor Converter Unit

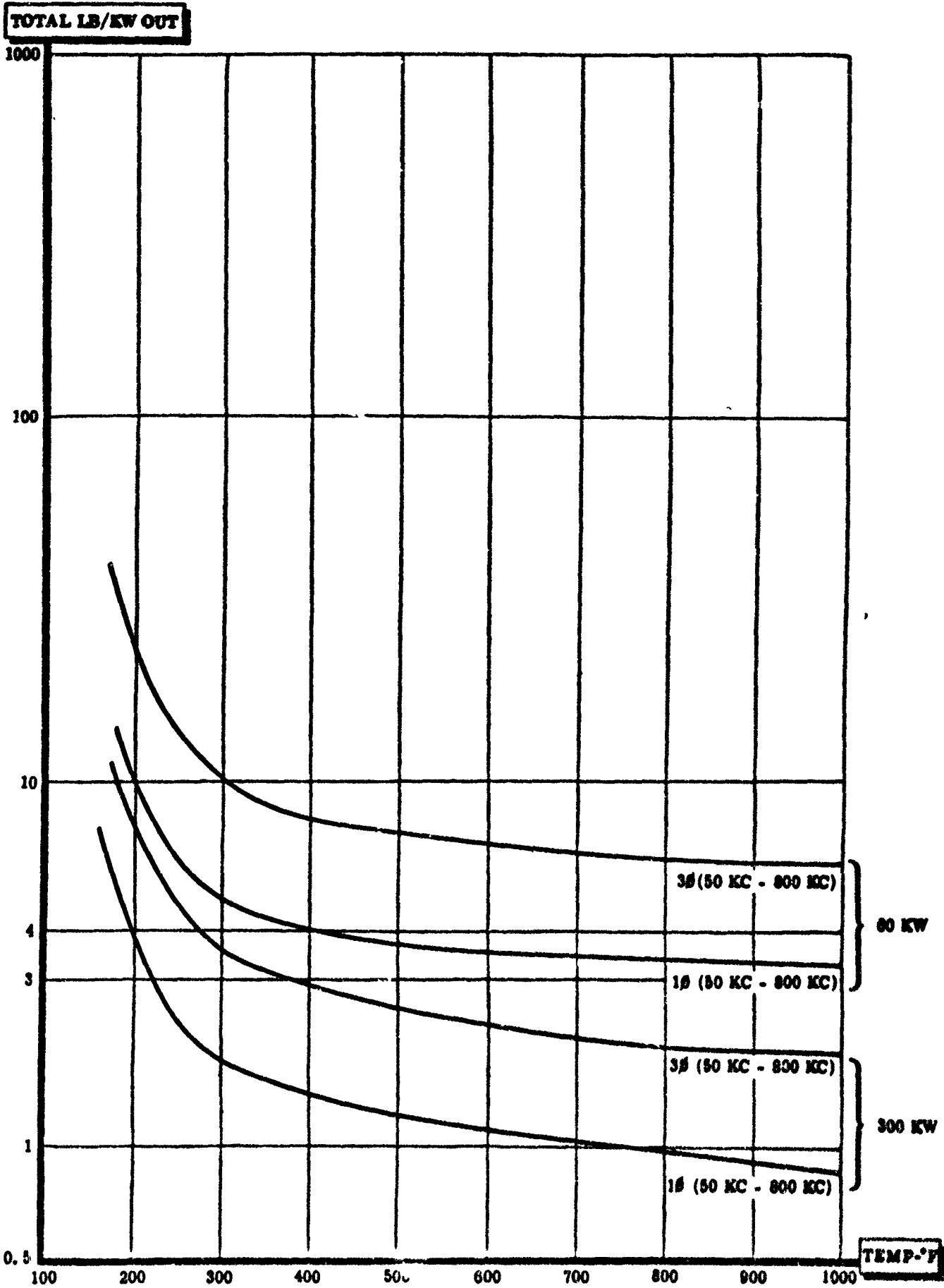


Figure 42. Analysis of System Weight Vs. Temperature For Static Transistor Converters

STATIC TUBE CONVERTER DESIGNS

A 60 KW UNIT

One design concept for a 60 KW (input) high-frequency static converter unit involves use of a vacuum tube type of r-f generator. A particular single-phase concept is shown in Figure 43. The system is fairly simple and involves use of a ceramic type power oscillator tube operating in Class C mode. Power in the 50 to 800 KC frequency range is generated in a resonant tank circuit. Transfer of high-frequency, high-voltage power to the single-phase load can be accomplished through a matching transformer. Weights, volumes, and efficiencies are shown in Table 7 for a single-phase concept. Figure 44 shows a schematic of this concept.

The high-voltage plate power for the oscillator tube is furnished by a typical series three-phase (quadrature operation) power supply composed of a high-voltage plate transformer, three thyratrons and three diodes. The DC output from the power supply is filtered and applied to the oscillator tube plate through two r-f isolators. Control of the grid circuit of the gas thyratrons (T1, T2, and T3) is provided by a phase-shifter technique which allows adjustment of the plate voltage and current to the oscillator. The net result is a means of varying the power output to the load.

A three-phase concept is shown in Figure 45. As can be seen from the figure, the three-phase concept involves a phase shifting of the output from a typical single-phase output into a composite three-phase output. This is done by a capacitive and resistive network.

Phase A of the output waveform is derived directly from the inverted waveform $+180^\circ$ of the transformer secondary. Phase B is shifted -60° electrically, and Phase C is shifted $+60^\circ$ electrically. The three outputs then form a composite three-phase voltage for use in the load. Power consumed in the phase-shifting capacitors and resistances is fairly low because of the low-current, high-voltage output requirement.

Weights, volumes, and efficiencies for a three-phase converter are summarized in Table 7. To be noted is the fact that weights and volumes for the three-phase unit are not much greater than those for the single-phase unit.

A 300 KW UNIT

The design of a single-phase 300 KW (input) static tube converter unit is based on the same schematic (Figure 44) as the 60 KW unit with a higher power input level being the major difference. Power input to this converter unit is also at a different voltage and frequency - 120/208 volts (3,200 cps) rather than the 43.6/75.3 volts (1,000 cps) of the 60 KW unit. Weights, volumes, and efficiencies for a 300 KW unit are summarized in Table 8.

A three-phase concept is shown in Figure 45. This concept also involves use of the single-phase concept with the addition of a phase-shifting network

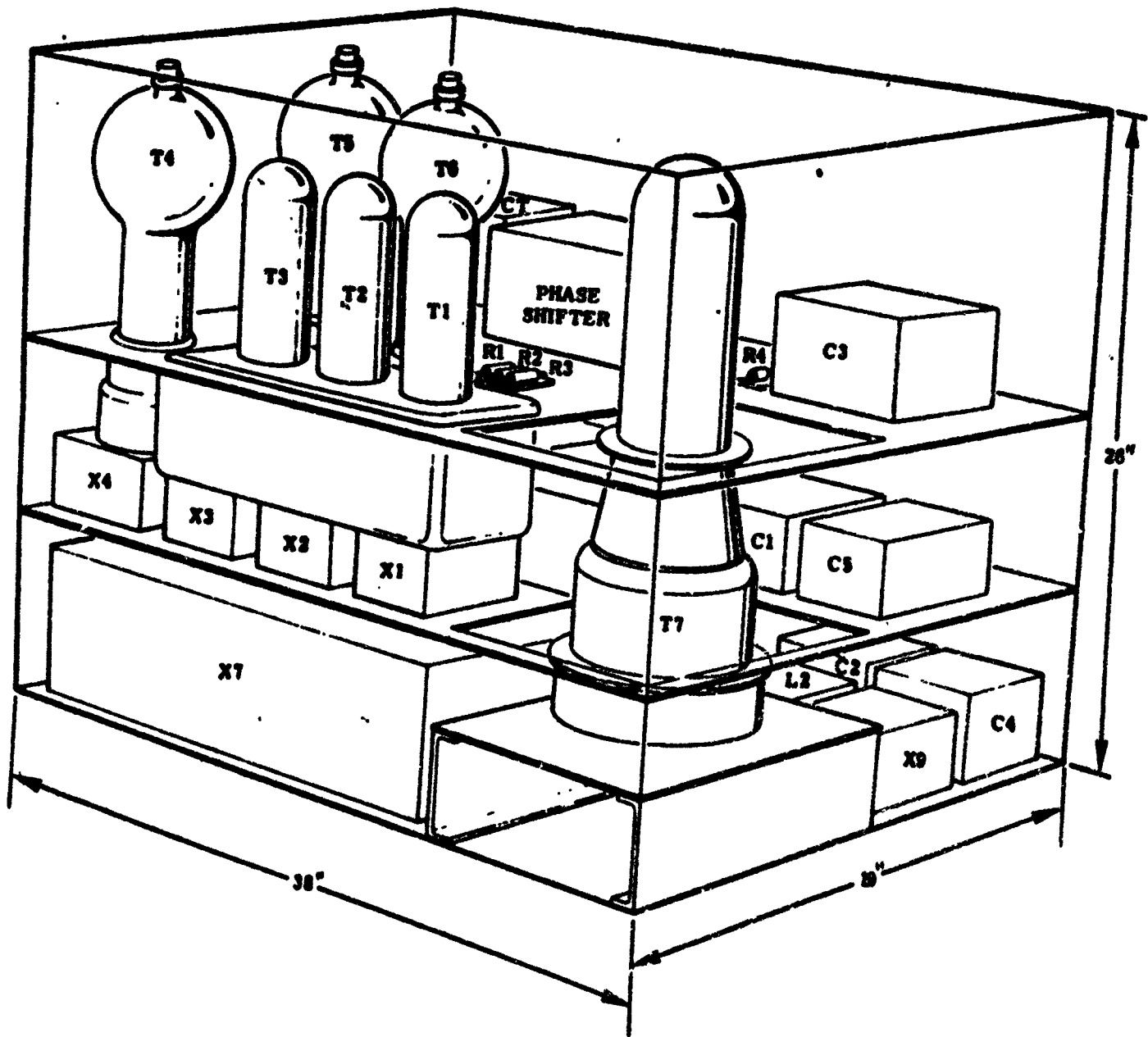


Figure 43. Static Tube Converter Unit (Perspective)

TABLE 7

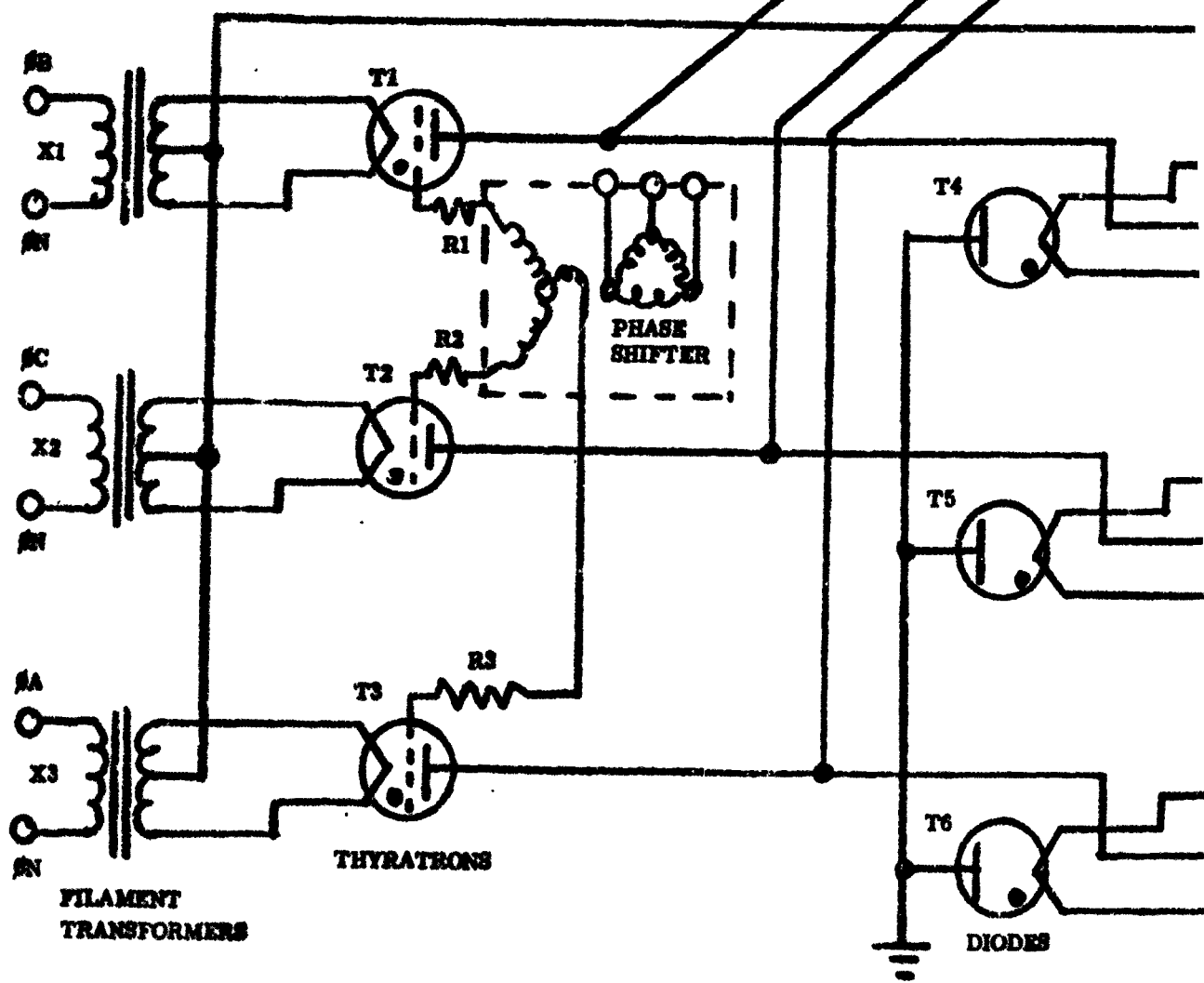
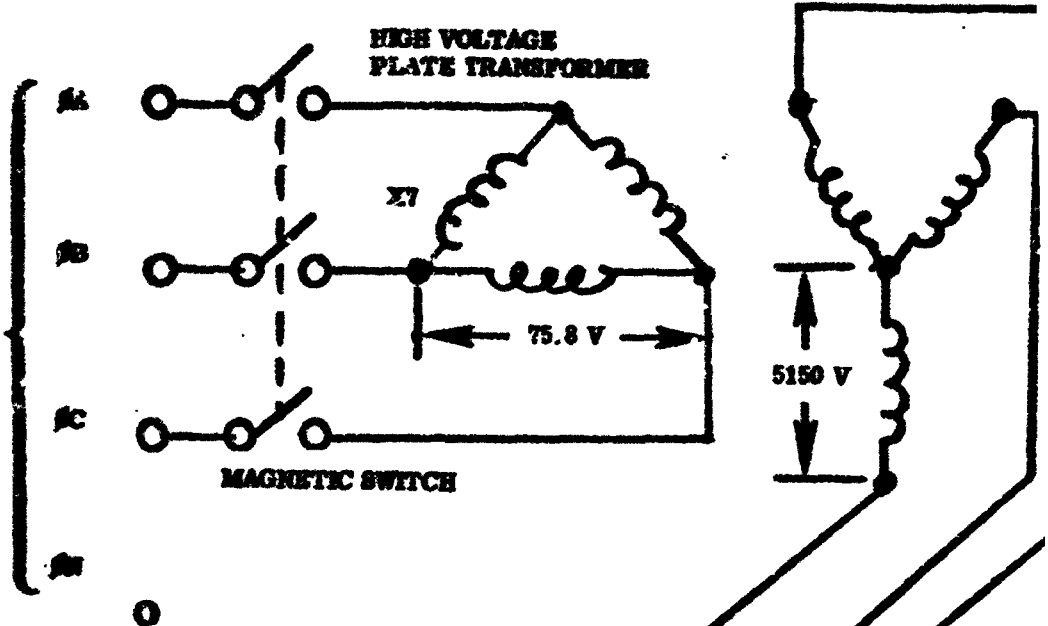
SUMMARY OF 60 KW STATIC TUBE CONVERTER PARAMETRIC DATA

1φ	50 KC	200 KC	800 KC
WEIGHT (lbs)	358	347	345
KW RAD (Losses)	18.9	19.5	19.9
KW OUT	41.2	40.5	40.1
EFFICIENCY (%)	68.6	67.5	66.9
LENGTH (inches)	26	26	26
WIDTH (inches)	19	19	19
HEIGHT (inches)	38	38	38
VOLUME (cu. ft.)	10.9	10.9	10.9
LBS/KW RAD	18.9	17.7	17.2
LBS/KW OUT	8.7	8.5	8.5

3φ	50 KC	200 KC	800 KC
WEIGHT (lbs)	363	353	349
KW RAD (losses)	18.8	20.0	21.8
KW OUT	41.2	39.9	38.2
EFFICIENCY (%)	68.7	66.6	63.7
LENGTH (inches)	34	34	34
WIDTH (inches)	23	23	23
HEIGHT (inches)	39	39	39
VOLUME (cu. ft.)	17.7	17.7	17.7
LBS/KW RAD	19.3	17.8	16.0
LBS/KW OUT	8.8	8.9	9.1

NOTE: VALUES DO NOT INCLUDE COOLING SYSTEM WEIGHT

INPUT
 45.8/75.8 V.
 1000 ~
 3 #
 OF
 120/200 V
 3200 ~



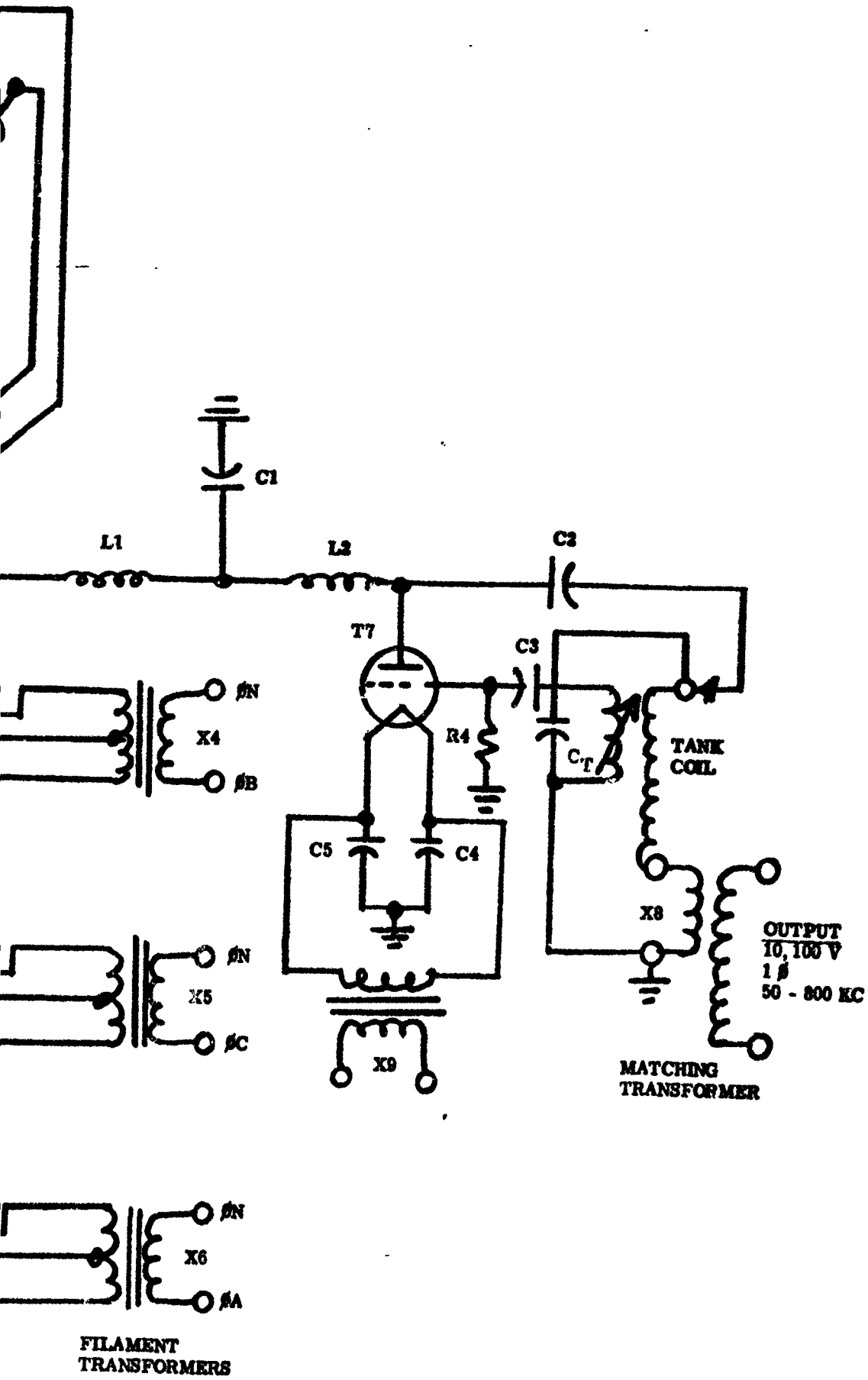
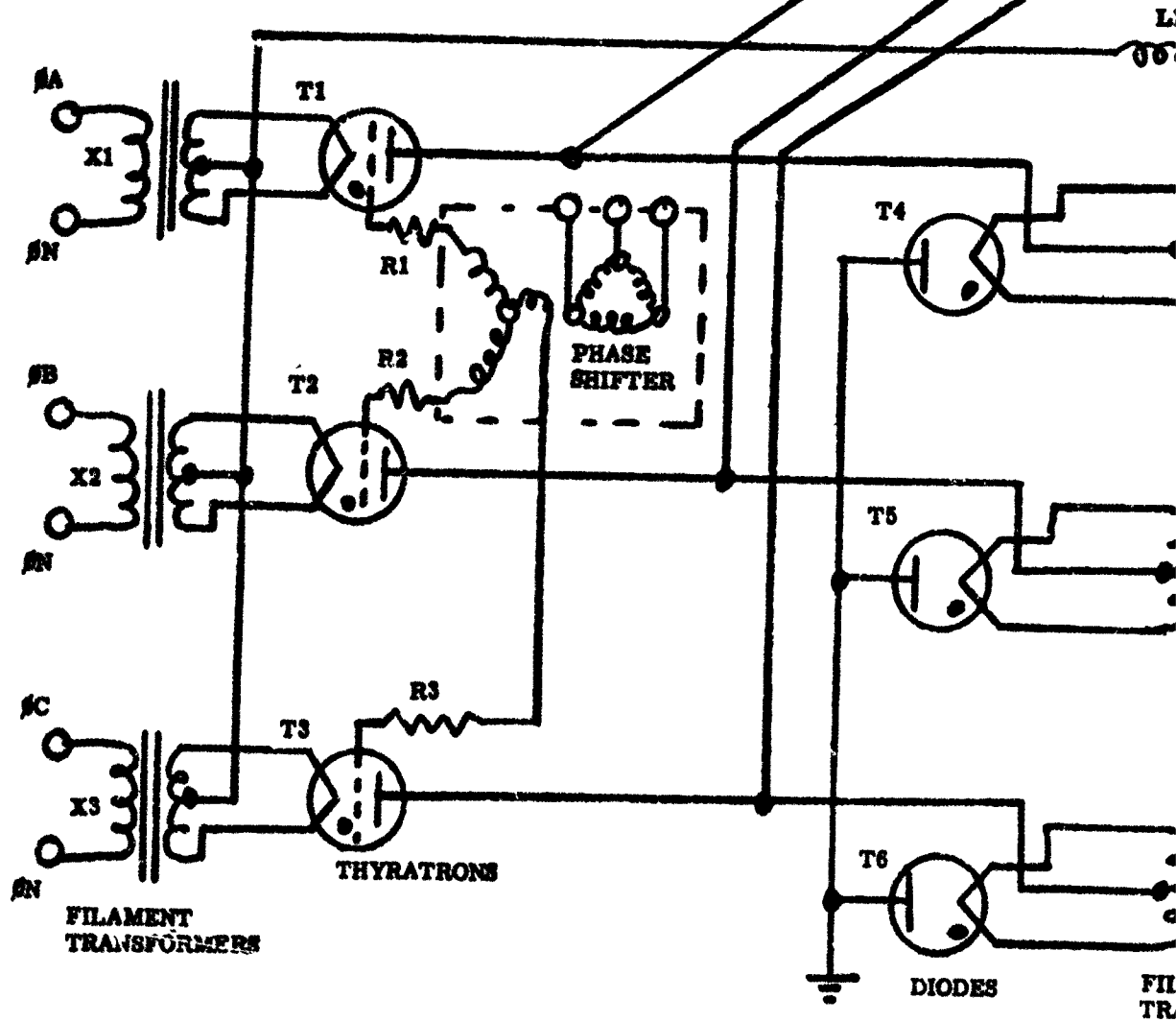
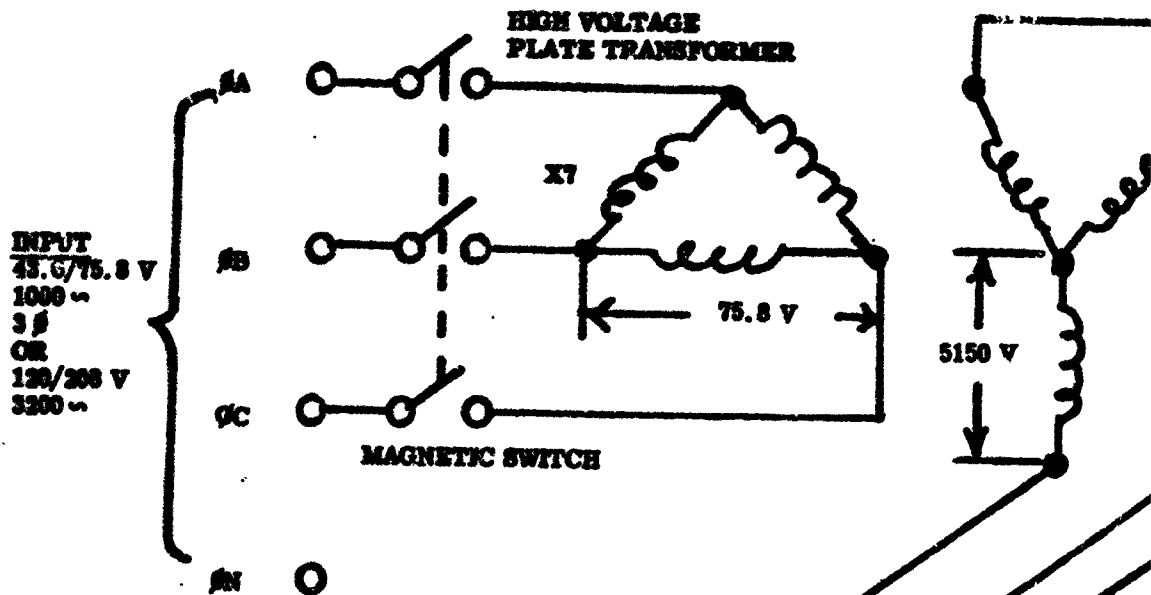


Figure 44. Preliminary Schematic of Static Tube 1 ϕ Converter



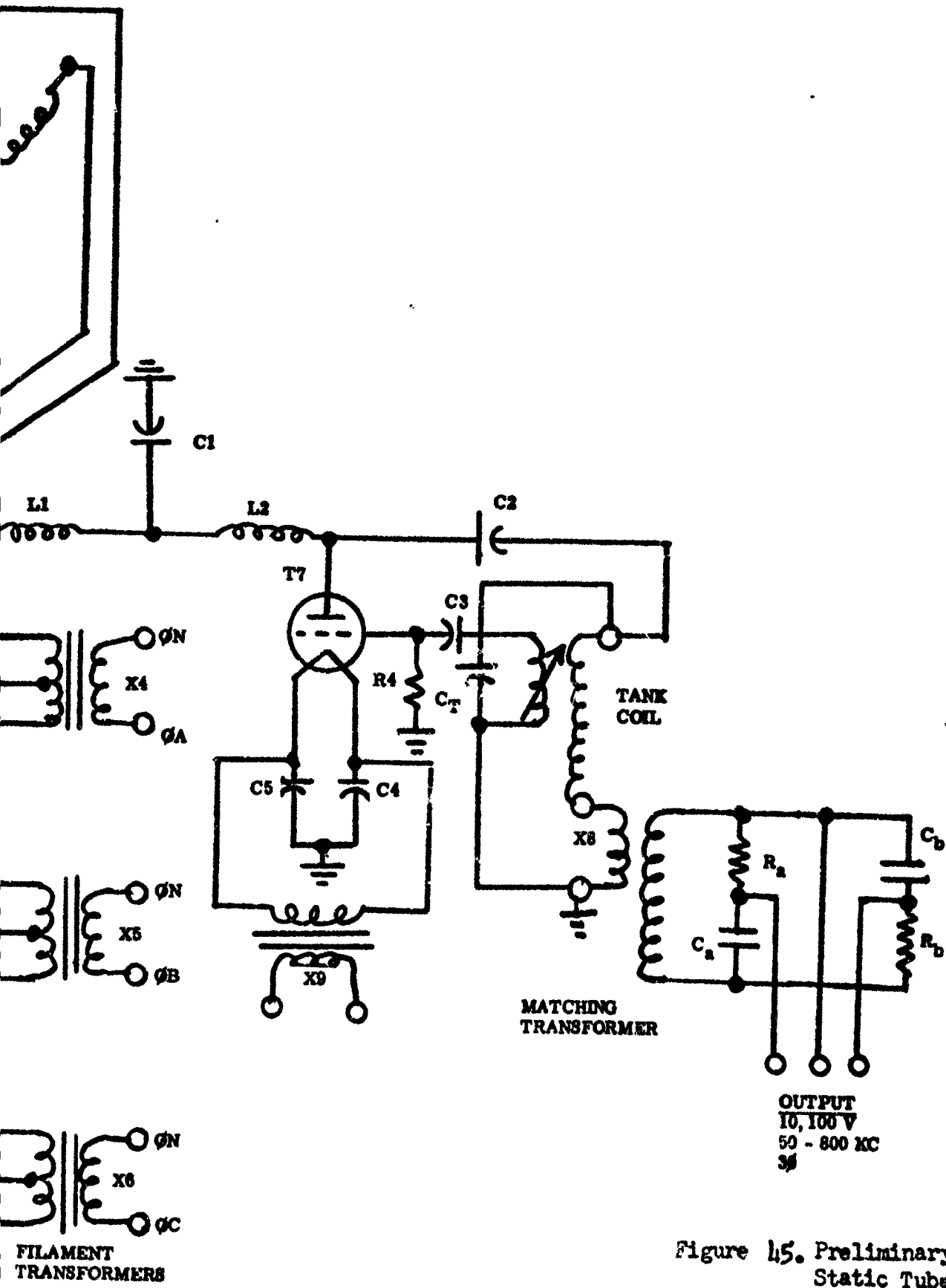


Figure 45. Preliminary Schematic of Static Tube 3 φ Converter

TABLE 8

SUMMARY OF 300 KW STATIC TUBE CONVERTER PARAMETRIC DATA

1φ	50 KC	200 KC	800 KC
WEIGHT (lbs)	577	555	549
KW RAD (losses)	91.2	92.6	91.4
KW OUT	208.8	207.4	208.6
EFFICIENCY (%)	69.6	69.1	69.5
LENGTH (inches)	26	26	26
WIDTH (inches)	19	19	19
HEIGHT (inches)	38	38	38
VOLUME (cu. ft.)	10.9	10.9	10.9
LBS/KW RAD	6.3	6.0	6.0
LBS/KW OUT	2.8	2.7	2.6

3φ	50 KC	200 KC	800 KC
WEIGHT (lbs)	592	573	562
KW RAD (losses)	91.5	94.3	94.1
KW OUT	208.6	205.7	205.9
EFFICIENCY (%)	69.5	68.6	68.7
LENGTH (inches)	34	34	34
WIDTH (inches)	23	23	23
HEIGHT (inches)	38	38	38
VOLUME (cu. ft.)	17.2	17.2	17.2
LBS/KW RAD	6.5	6.1	6.0
LBS/KW OUT	2.8	2.8	2.7

NOTE: WEIGHT FIGURES DO NOT INCLUDE COOLING SYSTEM WEIGHT

composed of resistors and capacitors. This phase-shifting network appears feasible for the 300 KW level because of the fact that the power is at a high-voltage, low-current level and I^2R losses will not be too great.

Output to the load is from a three-phase transformer. Control of the output power is through the individual grid circuits of each of the thyratrons of the power supply section where voltage and plate current to the oscillator can be raised or lowered. Components of a 300 KW, three-phase system plus weights, volumes, and efficiencies are summarized in Table 8 for each of three frequencies.

GENERAL DESIGN CONSIDERATIONS

Input characteristics to the power supply part of this converter are not too critical for this unit, since it is capable of handling fairly large transients. Tubes are most reliable when filament voltages are constant, so it is important that fluctuations in filament voltages be held to low level in order to achieve long tube life. Tube manufacturers state that filament voltages should be within one per cent either side of the nominal value for mercury-vapor rectifiers. Voltage-regulated transformers of the self-saturating type, with tuned primary windings can be used when needed to provide the constant filament voltage input. Initial oscillator tube filament current must be limited to a maximum value of approximately 1.5 times rated hot value. This is necessary since the cold filament resistance is usually as low as one-tenth its hot value, and the surge currents at switching could damage the filament.

The generator is designed with an isolating magnetic switch to isolate the power supply from the power source. The filament transformers must be isolated from the power source by a separate switch in order that filaments may be allowed to warm up before plate power is turned on. A protective device to prevent plate power turn on before coolant fluid flow has started is also a part of the design.

Several methods for control of power from an r-f generator are available such as: (1) Variable-coupling r-f output transformer, (2) saturable-reactor system in high voltage system, (3) saturable-reactor system in supply line, and (4) thyatron control. Variable coupling transformers are not attractive for this lightweight, high efficiency converter application, and the saturable reactor techniques are much too heavy to be considered. A thyatron technique has been used in this system. The main characteristic of the thyatron is that it will not conduct unless the grid voltage is at some value less negative than the critical grid voltage. If a constant DC bias is applied to the grid and an AC voltage superimposed on this, the thyatron will conduct at the point where the AC voltage exceeds the critical voltage. Once the tube has fired, it will continue to conduct even when the AC grid voltage falls below the critical voltage, and will stop conducting only when the plate voltage is less than the cathode voltage. If this AC grid voltage is made to alter its phase angle with respect to the plate voltage by a phasing network, the firing or conduction angle will be increased. This results in retarding the plate current and

voltage conducting point, as shown in Figure 46A. The resulting DC plate voltage along with the DC plate current is reduced and the total DC voltage to the oscillator tube plate is reduced. The r-f output of the generator is thereby reduced. The thyratron is stable and does not drift with time, but these tubes are sensitive to line voltage variations, which change the critical grid voltage. Figure 46B shows a typical phasing circuit, the output across x and y is connected across the grid and cathode with a bias voltage in series with the thyratron.

Component Characteristics - Tables 9 and 10 list individual components for 60 KW single-phase and three-phase converters and Tables 11 and 12 for 300 KW single-phase and three-phase converters. Components listed are also shown in the high voltage power supply, oscillator and output sections of the schematic diagrams (Figure 44 and 45). Weight, volume, and loss parametric data is listed for comparison with other converter techniques.

The thyratron and diode types considered for the high voltage power supply section are based on conventional units presently available for power supply use. Operating characteristics are typical of conventional units. Only the volume of the oscillator tube has been reduced somewhat to take advantage of expected improvements in state of the art for power tubes. The other tube dimensions used for packaging are realistic state of the art. The oscillator tube characteristics are similar to those of the RCA 5671 (9C22) for the 60 KW unit and the RCA 6949 for the 300 KW unit. As discussed in the section on Cooling, use of a coolant other than water and one compatible with liquid cooled tubes has been a basic design assumption.

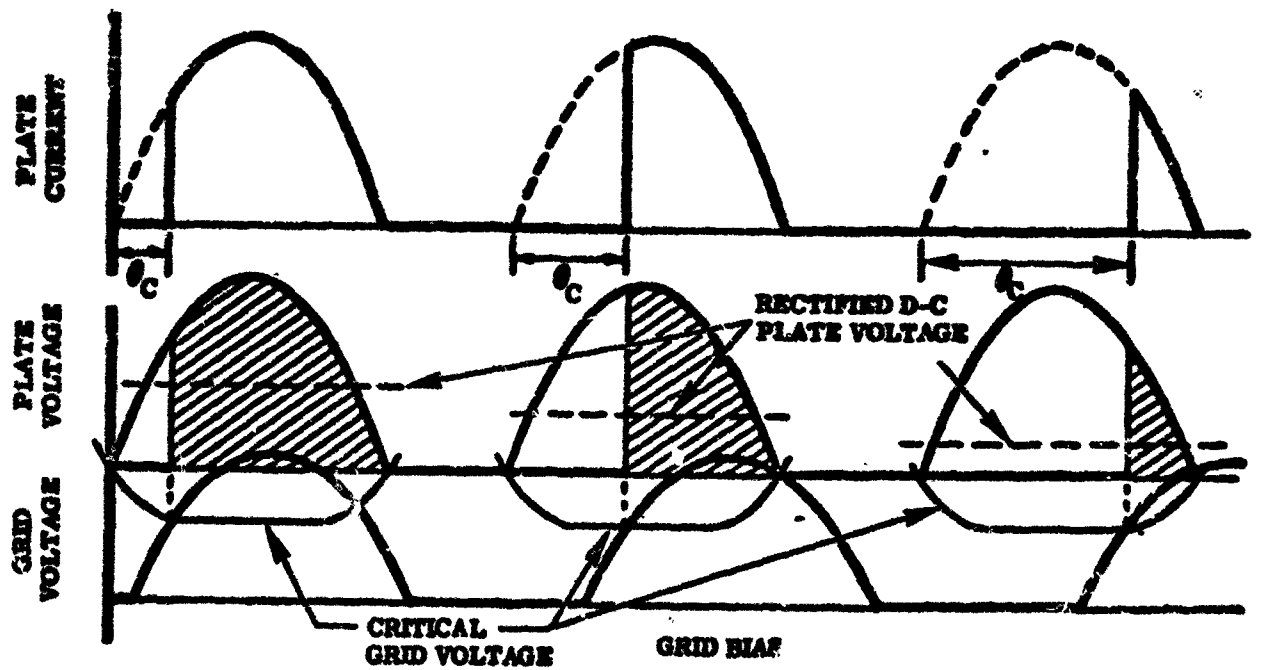
Transformer and choke units are based on conventional designs using low-loss magnetic cores with fluid coolant circulating between core and winding to remove excess heat. Heat loss data for each of the transformers is based on loss data extrapolated from available loss curves and test data derived during the experimental part of this study program.

Resistor and capacitor components are conventional designs with low-loss characteristics. Each has high temperature capabilities and is derated to achieve long life expectancy. Remaining parts of the unit include mounting structure, wire and hardware, and cooling ducts and these are listed so that a total weight can be calculated.

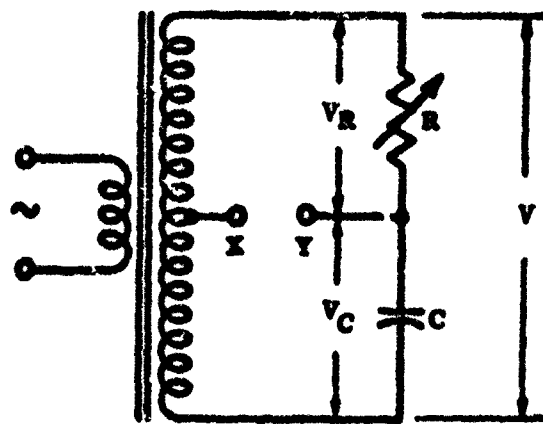
MECHANICAL DESIGN

The static tube converter unit can be packaged in an aluminum container for partial protection from a radiation environment, for mechanical support, and for limited protection from meteoroid damage. The container can be designed to serve as a heat sink. Typical structural design for a 60 KW, single-phase, 200 KC unit is shown in Figure 47, and is based on maximum system reliability, minimum weight, and minimum volume. Weight, dimensions and volume data is shown in Tables 7 and 8.

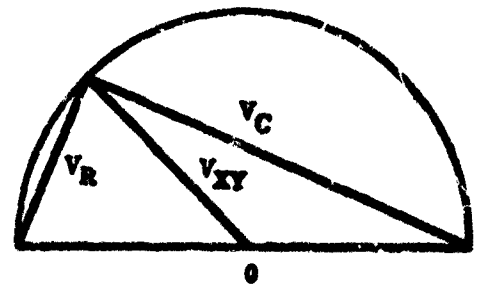
Each tube will be mounted on its own filament transformer for compactness and to make use of the transformer as a partial heat sink. Tube cooling will be by integral cooling ducts for the oscillators and cooling



A
EFFECT OF INCREASING CUTOFF OR PHASE-BACK ANGLE θ_c ON D-C PLATE VOLTAGE



B
PHASING CIRCUIT



C
VARIABLE-PHASE GRID VOLTAGE

Figure 46. Thyatron Control Techniques

PRELIMINARY COMPONENT LIST FOR A

NO.	COMPONENTS	50 KC		
		WT (LBS)	LOSSES (WATTS)	SIZE (IN)
<u>POWER SUPPLY (HIGH VOLTAGE)</u>				
1	High Voltage Transformer (X7) 1 KC, 3 ϕ , 60 KW	114	640	18x14x6
1	Magnetic Switch	10	100	5x3x4
3	Filament Transformers (X1, X2 & X3)	9	6	2 5/8x3 1/4
3	Filament Transformers (X4, X5 & X6)	8	12	5x5x3 3/8
3	Thyratrons (T1, T2, & T3)	3	1800	10 17/32x1
3	Diodes (T4, T5 & T6)	3	378	14 7/16x5
<u>OSCILLATOR SECTION</u>				
1	Oscillator Tube (T7) 80 ϕ x 56 KW	45	11,200	25x8 1/2 I
1	Filament Transformer (X9)	5	105	5x4x4
1	Phase Shifter	15	100	5x5 13/16x
1	Filter Choke (L1 & L2)	9	3200	
1	Filter Capacitor (C1)	3	--	6 1/2x5x4
2	Coupling Capacitors (C2 & C3)	4	120	6 1/2x5x4
2	Neutralizing Capacitors (C4 & C5)	1	--	6 1/2x5x4
1	Tank Coil Capacitor (Ct)	2	60	6 1/2x5x4
5	Resistors (R1, R2, R3, R4)	2	2	9/16x3/16
1	Tank Coil	2	100	
<u>OUTPUT SECTION</u>				
1	Matching Transformer (X8)	17	1030	10x4x3
<u>MISCELLANEOUS</u>				
-	Mounting structure	80	--	
-	Cooling ducts	5	--	
-	Controls	10	--	
-	Wire and Hardware	10	--	
TOTALS		358	18,853	

TABLE 3

FOR A 60 KW. STATIC CONVERTER TUBE (10)

SIZE (INCHES)	200 KC			800 KC		
	WT (LBS)	LOSSES (WATTS)	SIZE (INCHES)	WT (LBS)	LOSSES (WATTS)	SIZE (INCHES)
x6	114	640	18x14x6	114	640	18x14x6
31/16x3 3/16	10	100	5x3x4	10	100	5x3x4
	9	6	2 5/8x3 1/16x33/16	9	6	2 5/8x3 1/16x3 3/16
3/8	8	12	5x5x3 3/8	8	12	5x5x3 3/8
12x2 3/8 Dia 6x5 1/8 Dia	3	1800	10 17/32x2 3/8 Dia	3	1800	10 17/32x2 3/8 Dia
	3	378	14 7/16x5 1/8 Dia	3	378	14 7/16x5 1/8 Dia
1/2 Dia	45	11,200	25x8 1/2 Dia	45	11,200	25x8 1/2 Dia
1/16x4 11/16	5	105	5x5 13/16x4 11/16	5	105	
	15	100		15	100	
x4	9	3200	x4	9	3200	
x4	3	--	6 1/2x5x4	3	--	6 1/2x5x4
x4	4	120	6 1/2x5x4	4	120	6 1/2x5x4
x4	1	--	6 1/2x5x4	1	--	6 1/2x5x4
x4	2	60	6 1/2x5x4	2	60	6 1/2x5x4
/16 Dia	2	2	9/16x3/16 Dia	2	2	9/16x3/16 Dia
3	3	100	8x3x3	3	100	7x3x3
	6	1650		4	2050	
	80	--		80	--	
	5	--		5	--	
	10	--		10	--	
	10	--		10	--	
	347	19,473		345	19,953	

PRELIMINARY COMPONENT LIST FOR A 60 I

NO.	COMPONENT	50 KC		SIZE (INCHES)
		WT. (LBS)	LOSSES (WATTS)	
<u>POWER SUPPLY (HIGH VOLTAGE)</u>				
1	High Voltage Transformer (X7) 1 KC, 3 ϕ , 60 KW	114	640	18 X 14 X 6
1	Magnetic Switch	10	100	5 X 3 X 4
3	Filament Transformer (X1, X2 & X3)	9	6	2-5/8 X 3-1/16 X 3-3/16
3	Filament Transformer (X4, X5 & X6)	8	12	5 X 5 X 3-3/8
3	Thyratrons (T1, T2 & T3)	3	1,800	10-1/2 X 2-3/8 dia.
3	Diodes (T4, T5 & T6)	3	380	14-7/16 X 5-1/8 dia.
<u>OSCILLATOR SECTION</u>				
1	Oscillator Tube (T7) 8C ϕ X 56 KW	45	11,200	25 X 8-1/2 dia.
1	Filament Transformer (X9)	5	100	5 X 4 X 4
1	Phase Shifter	15	100	5 X 5-13/16 X 4-3/8
2	Filter Choke (L1 & L2)	9	3,200	5-1/2 X 5-1/2 X 4-1/2
1	Filter Capacitor (C1)	3	-	6-1/2 X 5 X 4
2	Coupling Capacitors (C2 & C3)	4	120	6-1/2 X 5 X 4
2	Neutralizing Capacitors (C4 & C5)	1	-	6-1/2 X 5 X 4
1	Tank Coil Capacitor (CT)	1	-	6-1/2 X 5 X 4
5	Resistors	2	-	6-1/2 X 5 X 4
1	Tank Coil	3	100	10 X 7 X 3
<u>OUTPUT SECTION</u>				
1	Matching Transformer	17	907	10 X 7 X 3
2	Resistors	1	20	2 X 1/2 dia.
2	Capacitors	4	25	6-1/2 X 5 X 4
<u>MISCELLANEOUS</u>				
-	Mounting Structure	80	-	
-	Cooling Ducts	5	-	
-	Controls	10	-	
-	Wire and Hardware	10	-	
TOTALS		363	18,770	

TABLE 10

60 KW STATIC TUBE CONVERTER (3 ϕ)

	200 KC			800 KC		
	WT. (LBS)	LOSSES (WATTS)	SIZE (INCHES)	WT. (LBS)	LOSSES (WATTS)	SIZE (INCHES)
	114	640	18 X 14 X 6	114	640	18 X 14 X 6
	10	100	5 X 3 X 4	10	100	5 X 3 X 4
-3/16	9	6	2-5/8 X 3-1/16 X 3-3/16	9	6	2-5/8 X 3-1/16 X 3-3/16
	8	12	5 X 5 X 3-3/8	8	12	5 X 5 X 3-3/8
.	3	1,800	10-1/2 X 2-3/8 dia.	3	1,800	10-1/2 X 2-3/8 dia.
a.	3	380	14-7/16 X 5-1/8	3	380	14-7/16 X 5-1/8 dia.
	45	11,200	25 X 8-1/2 dia.	45	11,200	25 X 8-1/2 dia.
	5	100	5 X 4 X 4	5	100	5 X 4 X 4
3	15	100	5 X 5-13/16 X 4-3/8	15	100	5 X 5-13/16 X 4-3/8
1/2	9	3,200	5-1/2 X 5-1/2 X 4-1/2	9	3,200	5-1/2 X 5-1/2 X 4-1/2
	3	-	6-1/2 X 5 X 4	3	-	6-1/2 X 5 X 4
	4	120	6-1/2 X 5 X 4	4	120	6-1/2 X 5 X 4
	1	-	6-1/2 X 5 X 4	1	-	6-1/2 X 5 X 4
	1	-	6-1/2 X 5 X 4	1	-	6-1/2 X 5 X 4
	2	-	6-1/2 X 5 X 4	1	-	6-1/2 X 5 X 4
	3	100	8 X 4 X 3	3	100	7 X 3 X 3
	7	2,180	8 X 4 X 3	3	3,920	7 X 3 X 3
	1	5	9/16 X 3/16 dia.	1	1.5	3/8 X 5/32
	4	25	6-1/2 X 5 X 4	4	25	6-1/2 X 5 X 4
	80	-		80	-	
	5	-		5	-	
	10	-		10	-	
	10	-		10	-	
	353	19,968		349	21,767	

PRELIMINARY COMPONENT LIST FO

NO.	COMPONENTS	50 KC		
		WT (LBS)	LOSSES (WATTS)	
<u>POWER SUPPLY (HIGH VOLTAGE)</u>				
1	Plate Transformer X7 3.2 KC, 3φ, 300 KW	99	8350	1.3x5x
1	Magnetic Switch	30	200	6x5x5
3	Filament Transformer	15	48	4x5x4
3	Filament Transformer	12	18	3x4x4
3	Thyratrons	12	14,000	14x5 1
3	Diodes	6	495	19x7 1
<u>OSCILLATOR SECTION</u>				
1	Oscillator Tube 80% x 290 KW	140	58,000	34x10
1	Filament Transformer	12	240	4x5x4
1	Phase Shifter	15	200	5x5 7/8
2	Filter Choke	35	7100	
1	Filter Capacitor	4	--	6 1/2x5
2	Coupling Capacitor	4	600	6 1/2x5
2	Neutralizing Capacitor	2	--	6 1/2x5
1	Tank Coil Capacitor	2	300	6 1/2x5
4	Resistors	2	2	9/16x3
1	Tank Coil	10	250	
<u>OUTPUT SECTION</u>				
1	Matching Transformer (X8) 1φ, 300 KW	36	1377	10x4
<u>MISCELLANEOUS</u>				
-	Mounting Structure	90	--	
-	Cooling Ducts	21	--	
-	Controls	10	--	
-	Wire and Hardware	20	--	
TOTALS		577	91,180	

TABLE 11 . . .

FOR A 300 KW STATIC TUBE CONVERTER (10)

SIZE (INCHES)	200 KC			800 KC		
	WT (LBS)	LOSSES (WATTS)	SIZE (INCHES)	WT (LBS)	LOSSES (WATTS)	SIZE (INCHES)
13x5x11	99	8350	13x5x11	99	8350	13x5x11
6x5	30	200	6x5x5	30	200	6x5x5
5x4	15	48	4x5x4	15	48	4x5x4
4x4	12	18	3x4x3	12	18	3x4x4
14x5 Dia	12	14,000	14x5 Dia	12	14,000	14x5 Dia
19x7 Dia	6	495	19x7 Dia	6	495	19x7 Dia
34x10 Dia	140	58,000	34x10 Dia	140	58,000	34x10 Dia
4x5x4	12	240	4x5x4	12	240	4x5x4
5x5 7/8x4 3/4	15	200	5x5 7/8x4 3/4	15	200	5x5 7/8x4 3/4
	35	7100		35	7100	
6 1/2x5x4	4	--	6 1/2x5x4	4	--	6 1/2x5x4
6 1/2x5x4	4	600	6 1/2x5x4	4	600	6 1/2x5x4
6 1/2x5x4	2	--	6 1/2x5x4	2	--	6 1/2x5x4
6 1/2x5x4	2	300	6 1/2x5x4	2	300	6 1/2x5x4
9/16x3/16 Dia	2	2	9/16x3/16 Dia	2	2	9/16x3/16 Dia
	10	250)		10	250)	
10x4x5			10x4x3.5			8x4x3.5
	14	2796)		8.6	1638)	
	90	--		90	--	
	20	--		20	--	
	10	--		10	--	
	20	--		20	--	
	555	92,599		549	91,531	

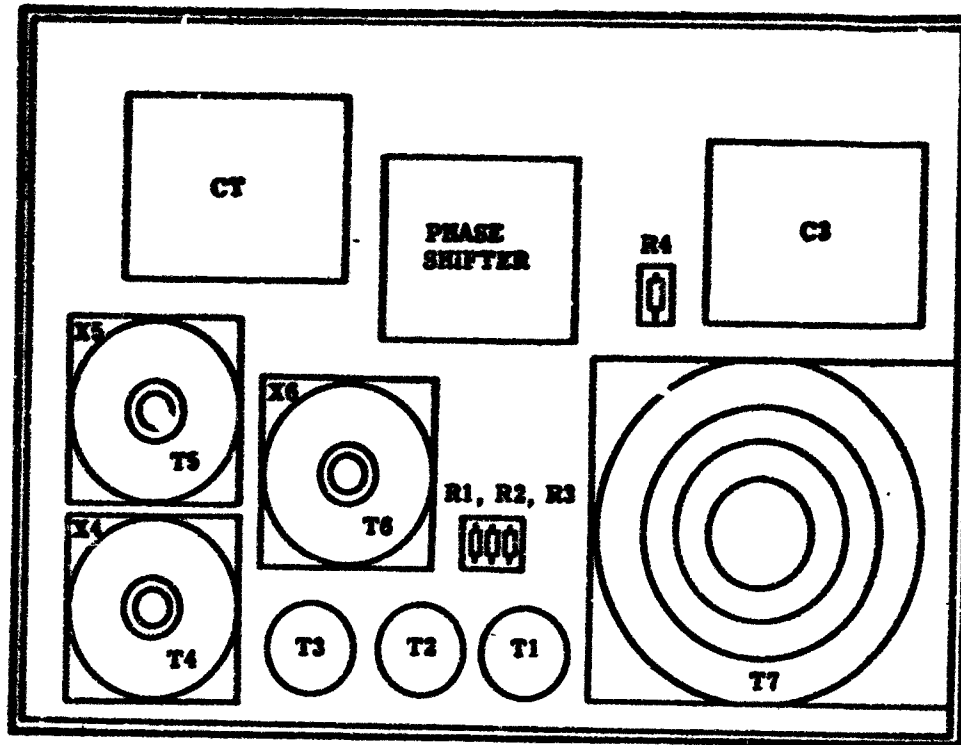
TABLE 12 . .

PRELIMINARY COMPONENT LIST FOR A 300 KW STATIC 'TUBE' CON

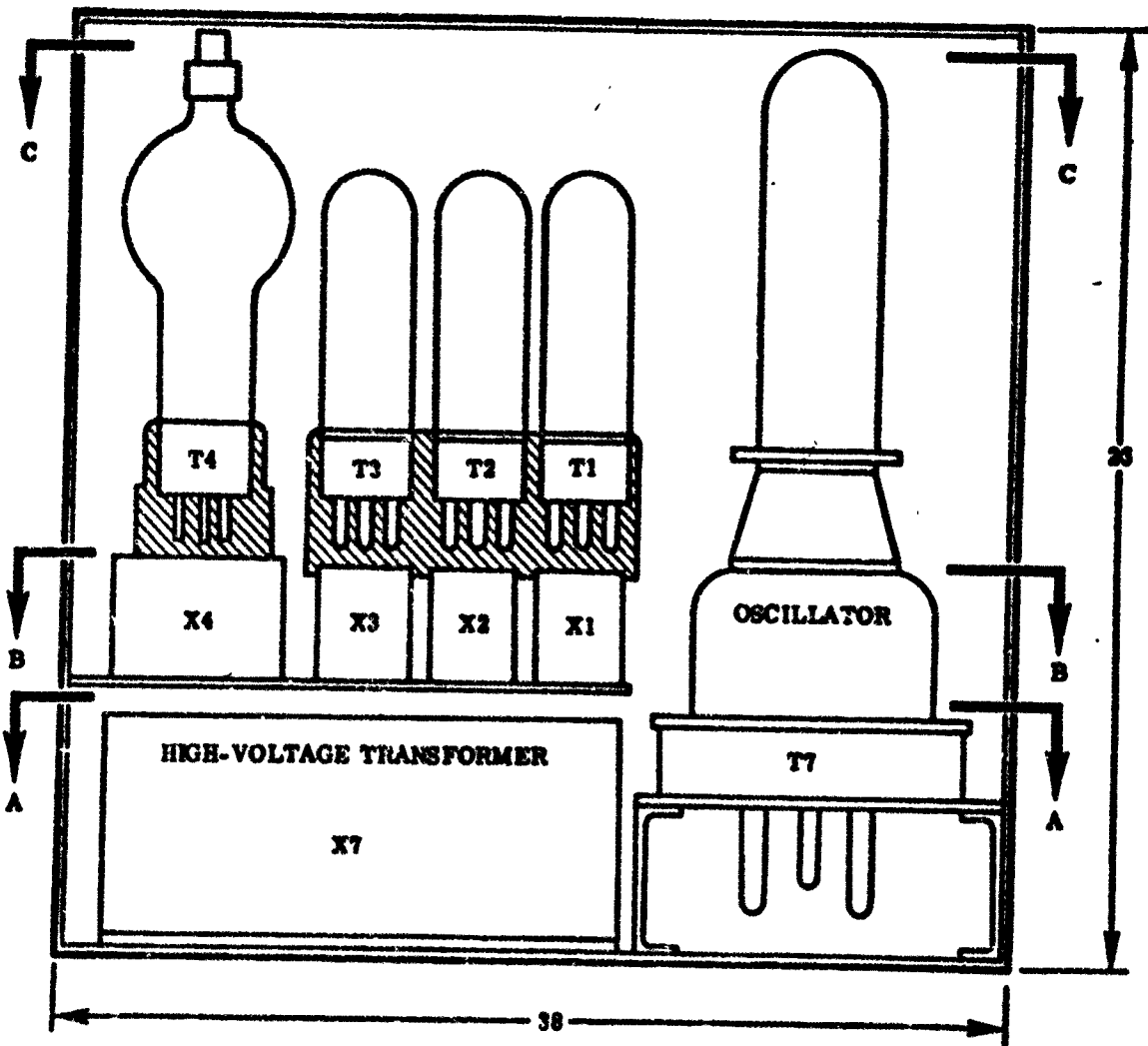
NO.	COMPONENTS	50 KC			200 J	
		WT (LBS)	LOSSES (WATTS)	SIZE (INCHES)	WT (LBS)	LOSSES (WATTS)
<u>POWER SUPPLY (HIGH VOLTAGE)</u>						
1	Plate Voltage Transformer	99	8350	12x19x5	99	8350
1	Magnetic Switch	30	200	6x5x5	30	200
3	Filament Transformer	15	48	4x5x4	15	48
3	Filament Transformer	12	18	4x3 $\frac{1}{2}$ x4	12	18
3	Thyratrons	12	14,000	21x7 Dia.	12	14,000
3	Diodes	6	495	14x3 Dia.	6	495
<u>OSCILLATOR SECTION</u>						
1	Oscillator Tube	140	58,000	36x10 Dia.	140	58,000
1	Filament Transformer	12	240	4x5x4	12	240
1	Phase Shifter	15	200	5 3/4 x5x5	15	200
2	Filter Choke	70.5	7,100	4 3/4 x5x5 7/8	70.5	7,100
1	Filter Capacitor	4	--	4x5x6 $\frac{1}{2}$	4	--
2	Coupling Capacitor	4	600	4x5x6 $\frac{1}{2}$	4	600
2	Neutralizing Capacitor	2	--	4x5x6 $\frac{1}{2}$	2	--
1	Tank Coil Capacitor	2	300	4x5x6 $\frac{1}{2}$	2	300
	Resistors	2	20	1 $\frac{1}{2}$ x $\frac{1}{2}$ Dia.	2	20
1	Tank Coil	10	250	4x4x4	10	250
<u>OUTPUT SECTION</u>						
1	Matching Transformer	45	1460	10x4 Dia.	40	1,240
2	Resistors	4	240	1 $\frac{1}{2}$ x2 1/8x5 $\frac{1}{2}$	2	60
2	Capacitors	4	120	4x5x6 $\frac{1}{2}$	4	120
<u>MISCELLANEOUS</u>						
-	Mounting Structure	90	--		90	--
-	Cooling Ducts	21	--		21	--
-	Controls	15	--		15	--
-	Wire and Hardware	20	--		20	--
TOTALS		634.5	91,781		627.5	94,281

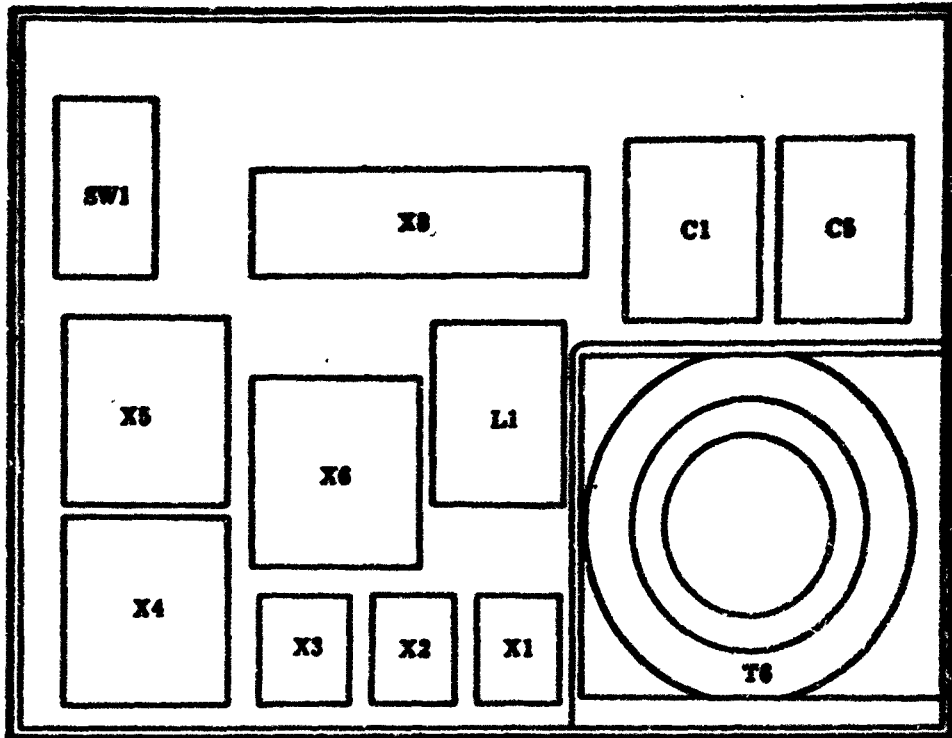
MENT LIST FOR A 300 KW STATIC TUBE CONVERTER (3φ)

0 KC	200 KC			800 KC		
SIZE (INCHES)	WT (LBS)	LOSSES (WATTS)	SIZE (INCHES)	WT (LBS)	LOSSES (WATTS)	SIZE (INCHES)
12x19x5	99	8350	12x19x5	99	8350	12x19x5
6x5x5	30	200	6x5x5	30	200	6x5x5
4x5x4	15	48	4x5x4	15	48	4x5x4
4x3½x4	12	18	4x3.5x4	12	18	4x3.5x4
21x7 Dia.	12	14,000	21x7 Dia.	12	14,000	21x7 Dia.
14x3 Dia.	6	495	14x3 Dia.	6	495	14x3 Dia.
36x10 Dia.	140	58,000	36x10 Dia.	140	58,000	36x10 Dia.
4x5x4	12	240	4x5x4	12	240	4x5x4
5 3/4 x5x5	15	200	5 3/4 x5x5	15	200	5 3/4 x5x5
4 3/4 x5x5 7/8	70.5	7,100	4 3/4 x5x5 7/8	70.5	7,100	4 3/4 x5x5 7/8
4x5x6½	4	--	4x5x6½	4	--	4x5x6½
4x5x6½	4	600	4x5x6½	4	600	4x5x6½
4x5x6½	2	--	4x5x6½	2	--	4x5x6½
4x5x6½	2	300	4x5x6½	2	300	4x5x6½
1½x½ Dia.	2	20	1½x½ Dia.	2	20	1½x½ Dia.
4x4x4	10	250	4x4x4	10	250	4x4x4
10x4 Dia.	40	4240	10x3 Dia.	26.6	3920	10x3 Dia.
1½x2 1/8x5½	2	60	1½x2 1/8 x5½	.5	17	1
4x5x6½	4	120	4x5x6½	4	120	2½
	90	--		90	--	
	21	--		21	--	
	15	--		15	--	
	20	--		20	--	
	627.5	94,281		610.6	93,964	

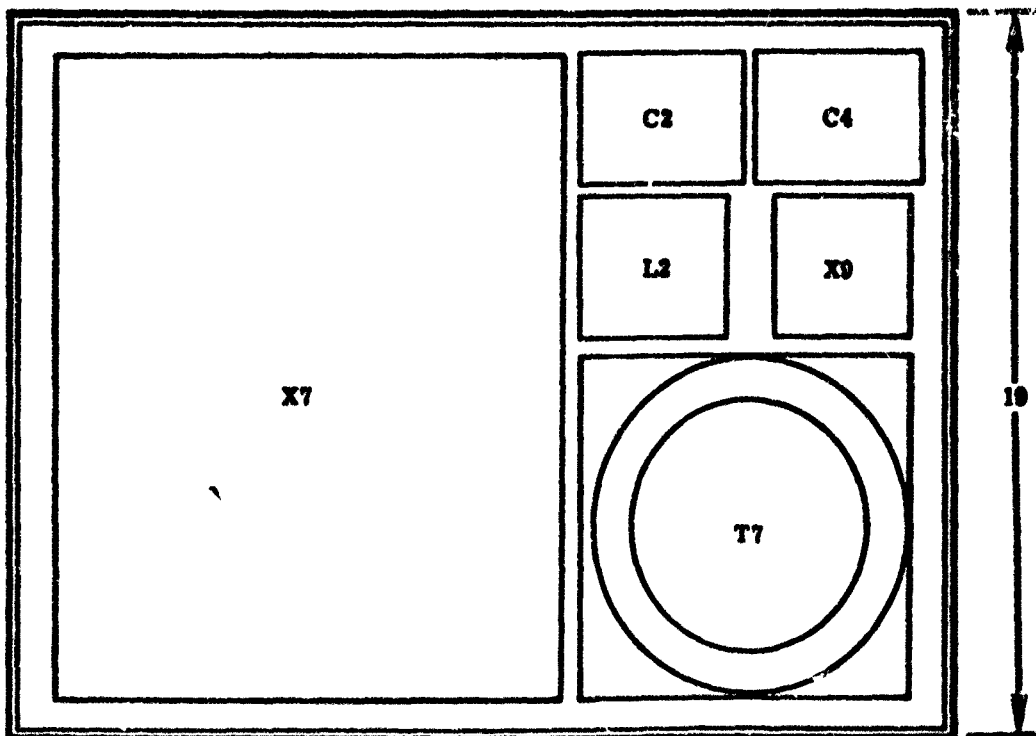


VIEW C-C





VIEW B-B



VIEW A-A

Figure 47. Preliminary Mechanical Design of 60 KW, 1 ϕ , 200 KC Static Tube Converter--Typical of 50 and 800 KC Designs

fluid jackets for the diodes and thyratrons. Optimum cooling for each of the transformers will be gained by mounting them back to back on a common cold plate with coolant ducts carrying fluid through each transformer.

Packaging for this concept is not too flexible because of the tube volumes and shapes. Tube outlines used in the design layout are of conventional units and are expected to become smaller in the future as advances are made in the state of art. Unit packaging is dependent to a great degree on the generator configuration and also the load configuration. Only a preliminary concept can be considered until more information is available on these parts of the total system. Components in a tube system are not as susceptible to radiation damage as semiconductor components and shielding is not too much of a problem.

Design of a 60 KW, three-phase, 200 KC converter is shown in Figure 48. 300 KW converters, both single-phase and three-phase, are shown in Figures 49 and 50.

THERMAL DESIGN

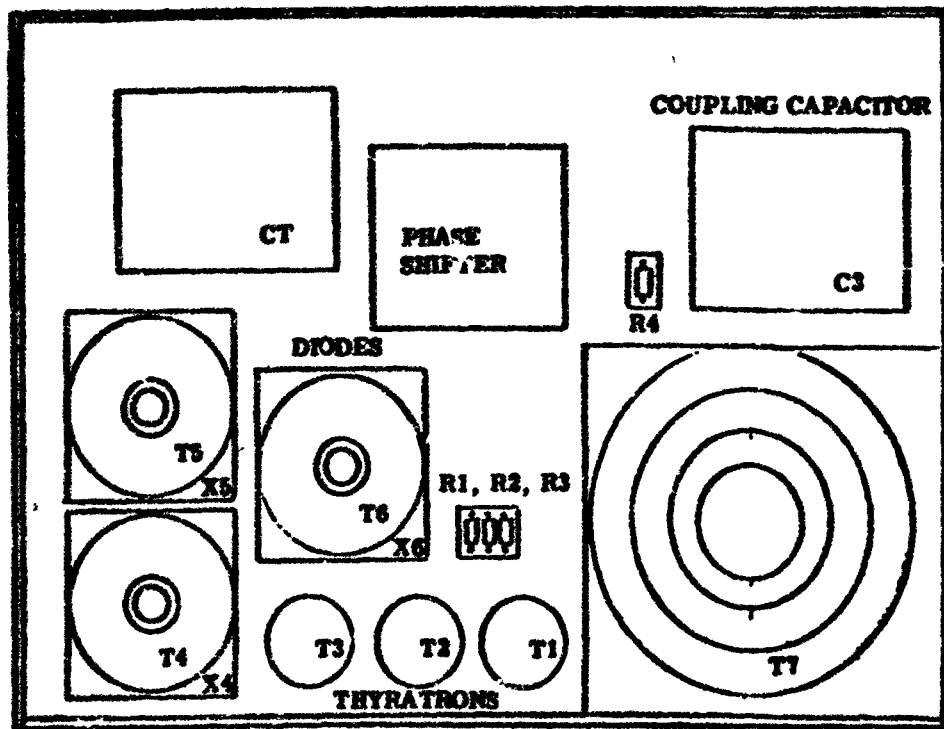
Most triode tubes operating in Class C mode are up to 80 per cent efficient and such efficiency is assumed in this converter unit. Ceramic-type tubes with exceptionally low driving power are being developed and some have capabilities up to 400°F maximum.

Figure 51 shows the total lbs/KW out for both single-phase and three-phase converters with outputs of 60 KW and 300 KW at 50 KC, 200 KC, and 800 KC frequency levels. The plotted curve indicates the system weight incurred at various temperature levels. Since the tube system is limited by temperature, the system operating point, as far as system weight is concerned, is assumed to be at the maximum tube operating temperature (400°F).

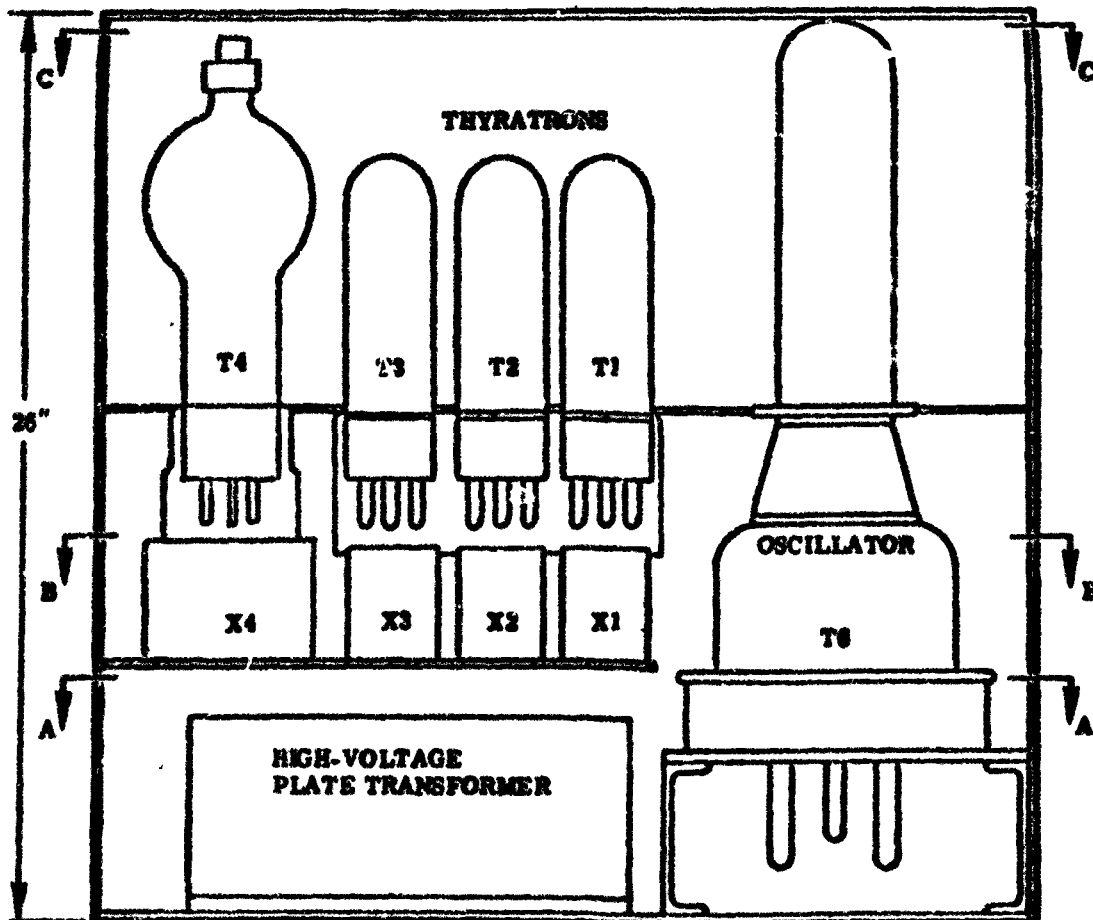
Design of the cooling system considers internal cooling ducts for each tube (or coolant jacket) and use of rugged ceramic tube types. Cold-plate shelving for cooling all the other components is also considered in addition to internal cooling ducts for each of the transformers. The possibility of using a liquid bath cooling technique, enclosing all the gas tubes and maintaining a common operating temperature has been considered, but has been rejected in favor of the ducted coolant system.

The tube cooling system, in general, must consist of a source of coolant, a feed-pipe system which carries the coolant through coolant pipes to the outlets of the oscillator tube and a radiator for heat dissipation to space. For check-out purposes, a provision for interlocking the coolant flow through each of the cooled elements with the power supply must be made. When the plate is at high potential above ground, the feed-pipe system should have good insulating qualities and proper design to reduce leakage current to a negligible value. The coolant system analysis will need to consider reaction of the coolant with the piping system in order that contamination of the coolant can be held to a minimum. Proper

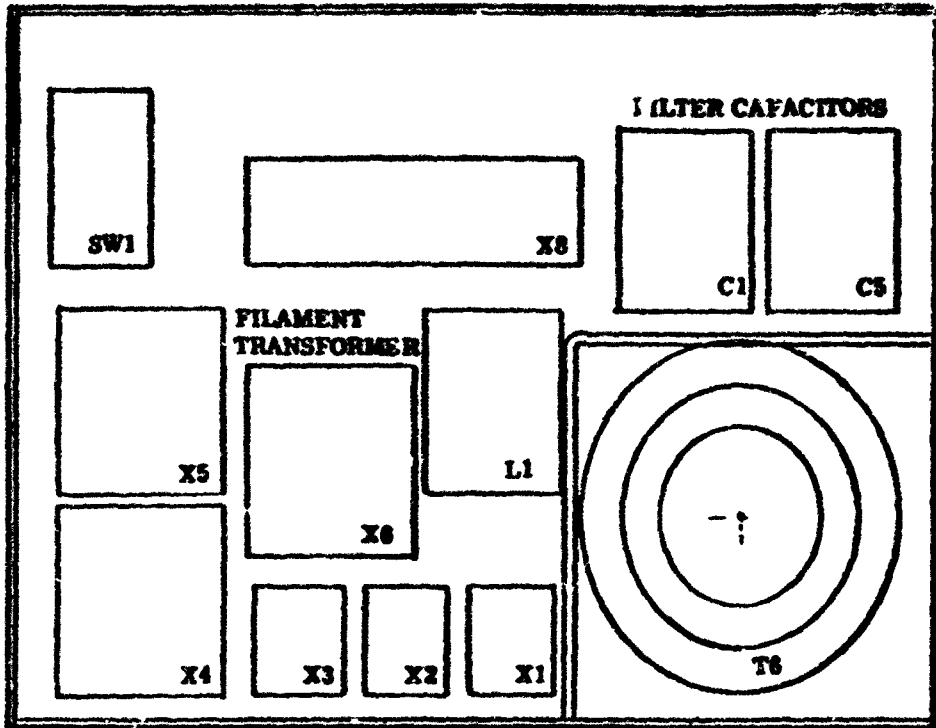
THIS PAGE HAS BEEN DELETED INTENTIONALLY.



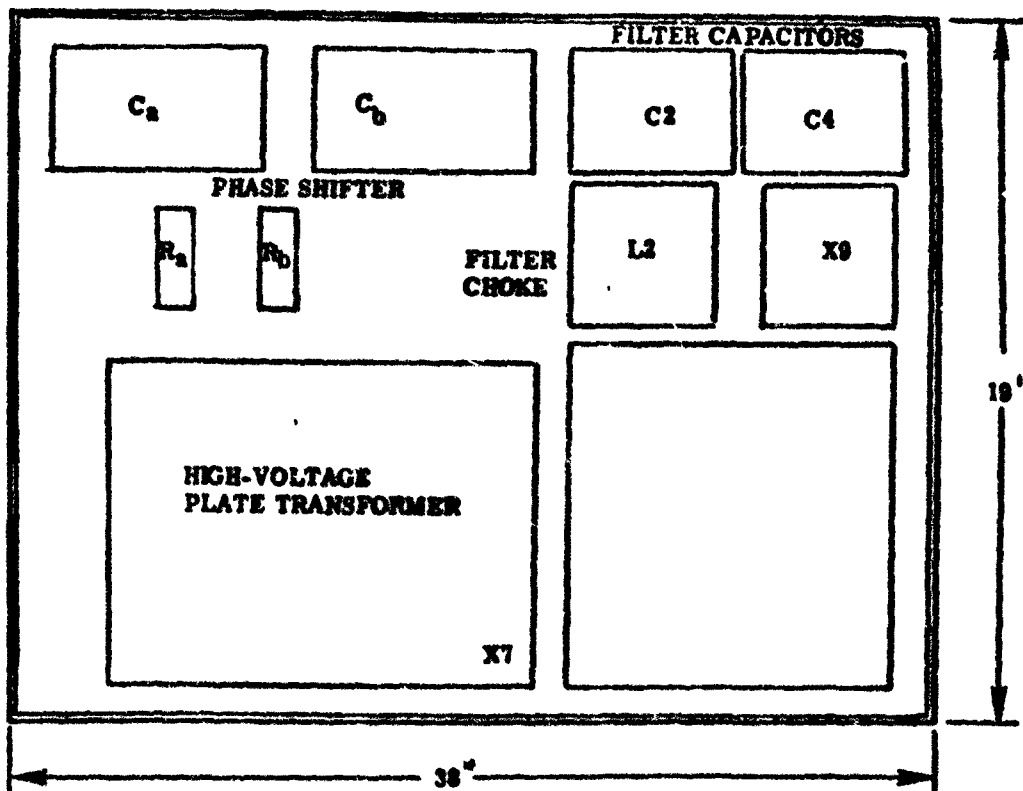
VIEW C-C



60 KW, 3 ϕ , 200 KC

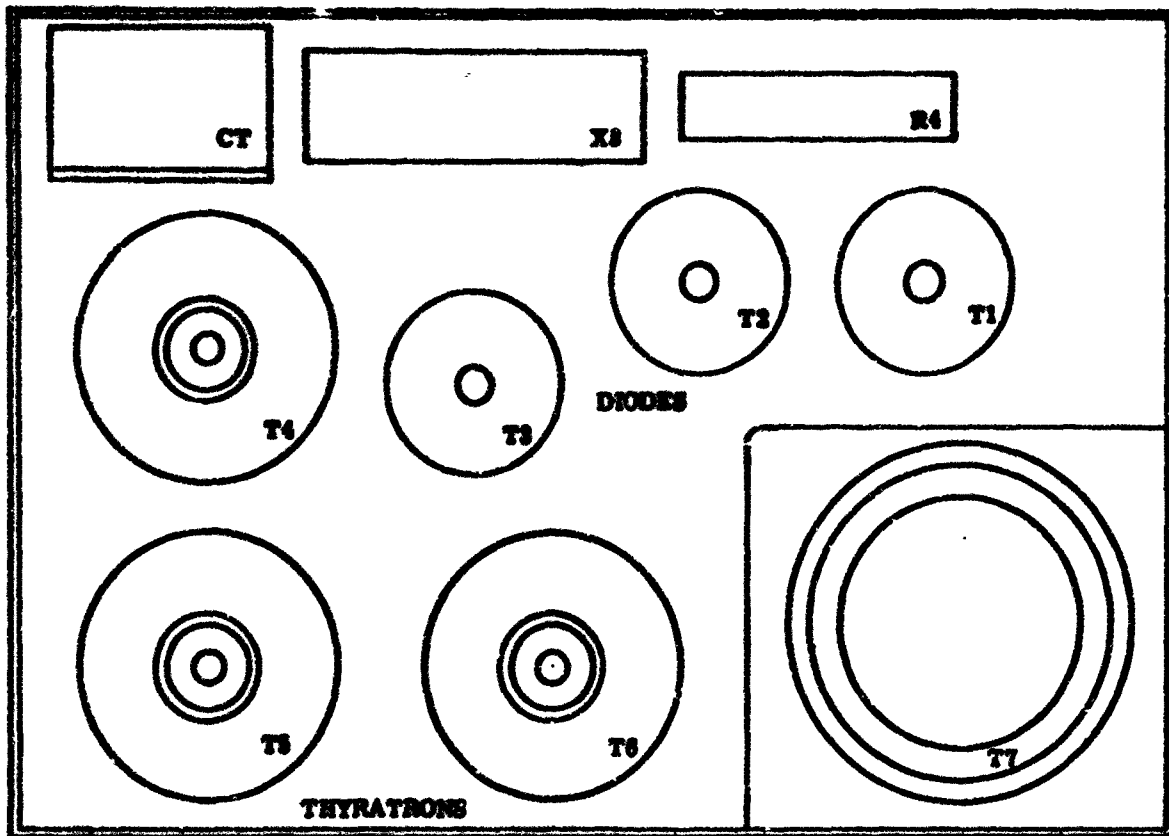


VIEW B-B

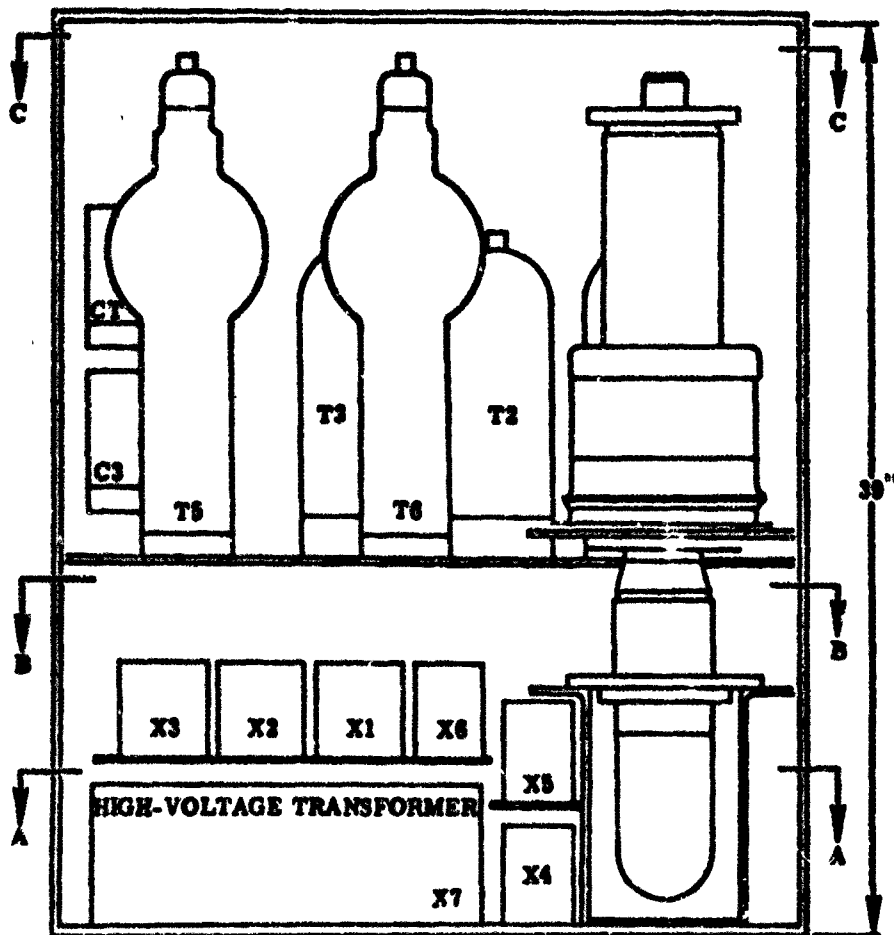


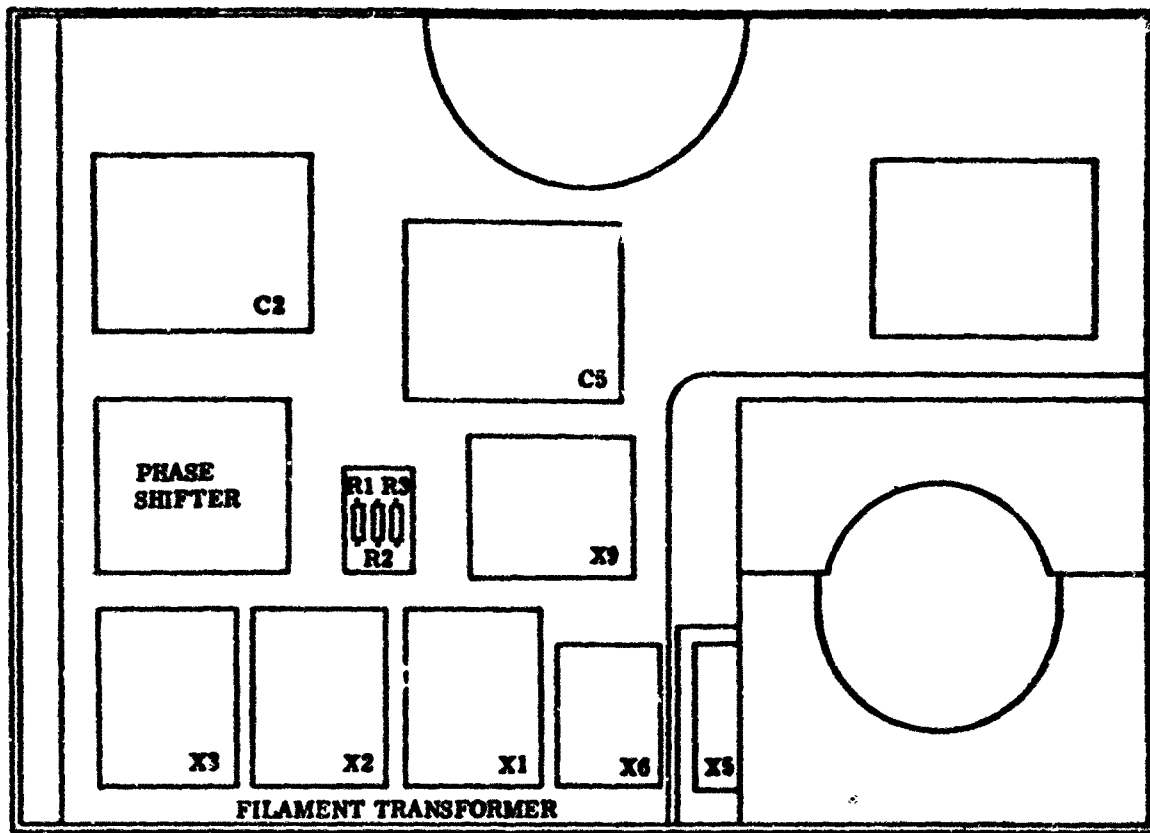
VIEW A-A

Figure 48. Preliminary Mechanical Design of 60 KW, 3 ϕ , 200 KC Static Tube, Converter--typical of 50 and 800 KC Designs

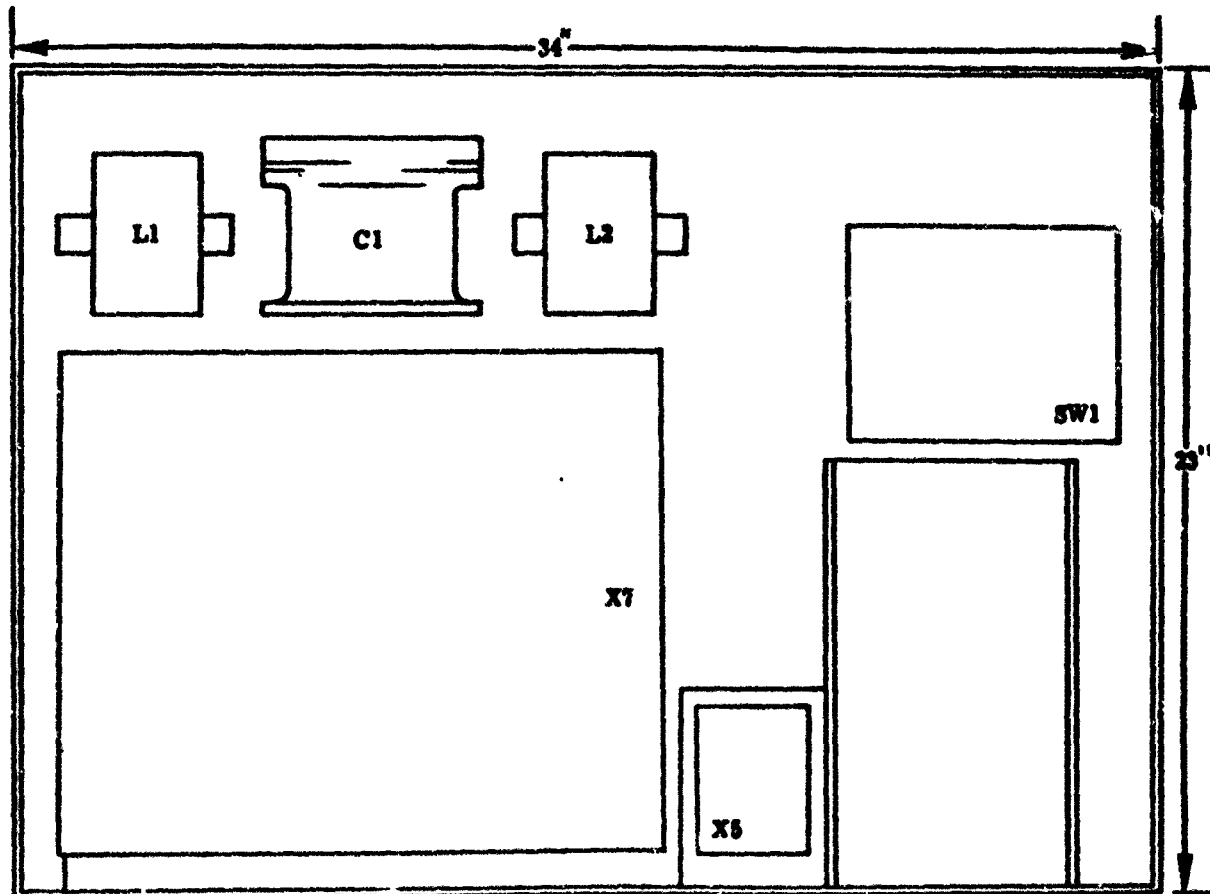


VIEW C-C



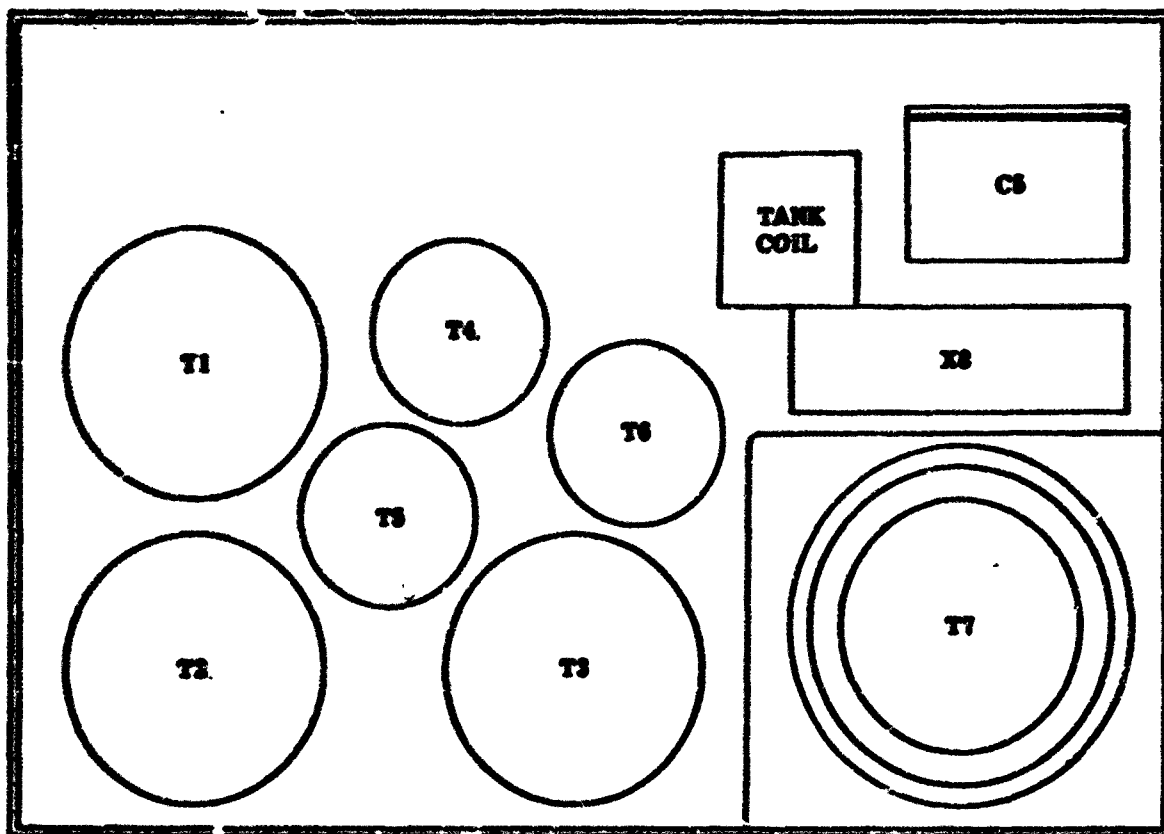


VIEW B-B

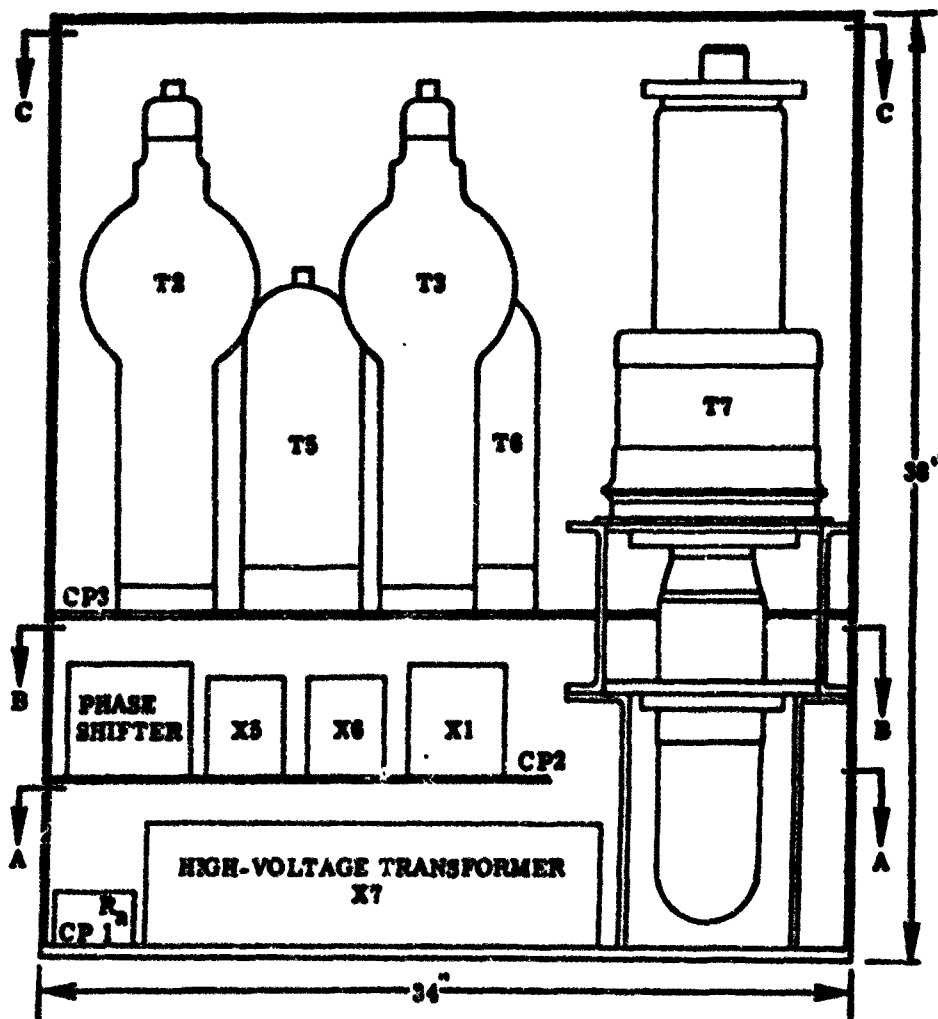


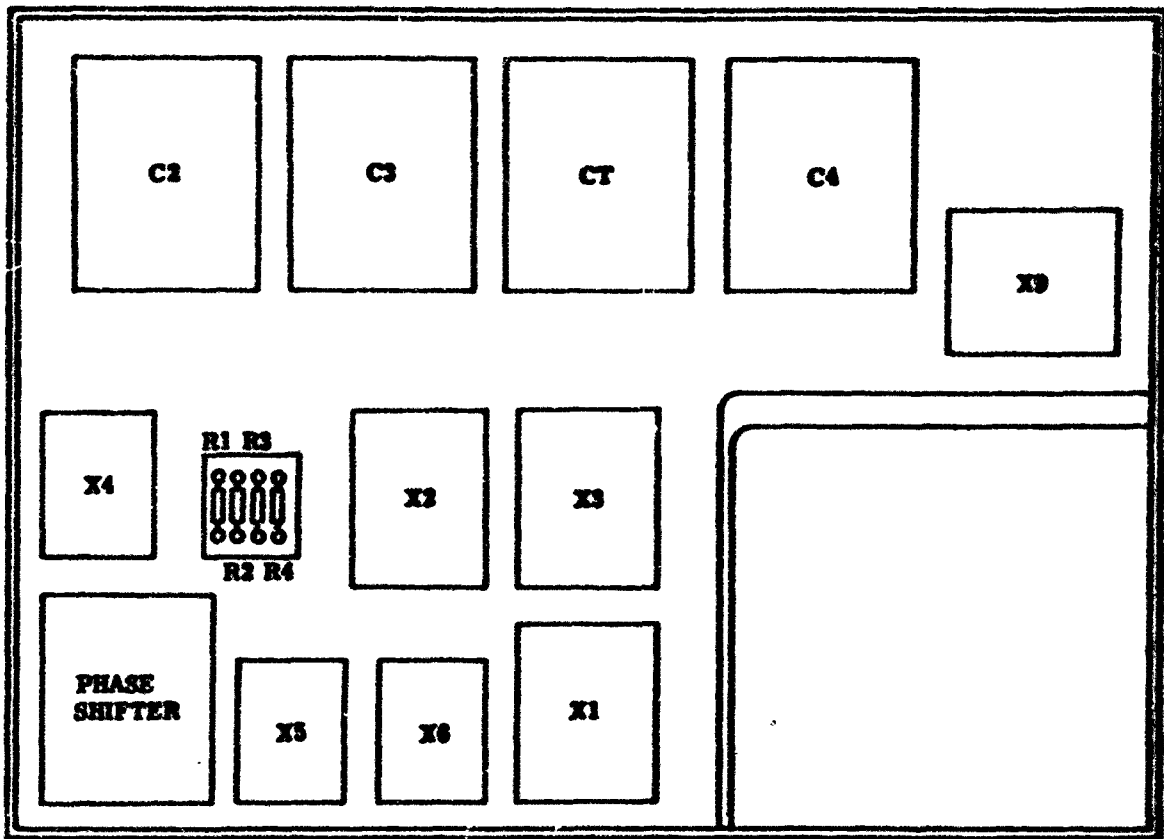
VIEW A-A

Figure 49. Preliminary Mechanical Design of 300 KW, 1 ϕ , 200 KC Static Tube Converter--Typical of 50 and 800 KC Designs

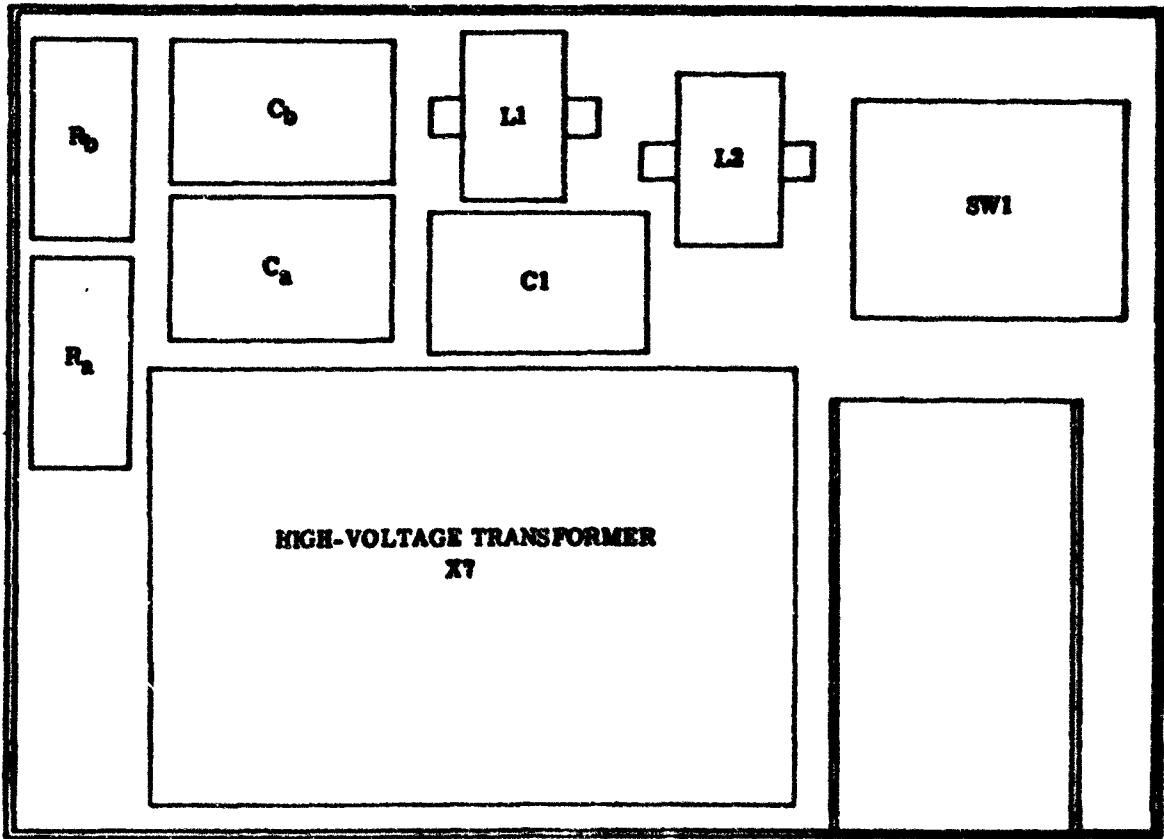


COLD PLATE
VIEW C-C





COLD PLATE NO. 2
VIEW B-B



VIEW A-A

Figure 50. Preliminary Mechanical Design of
300 KW, 3 ϕ , 200 KC Static
Tube Converter—Typical of
50 and 800 KC Designs

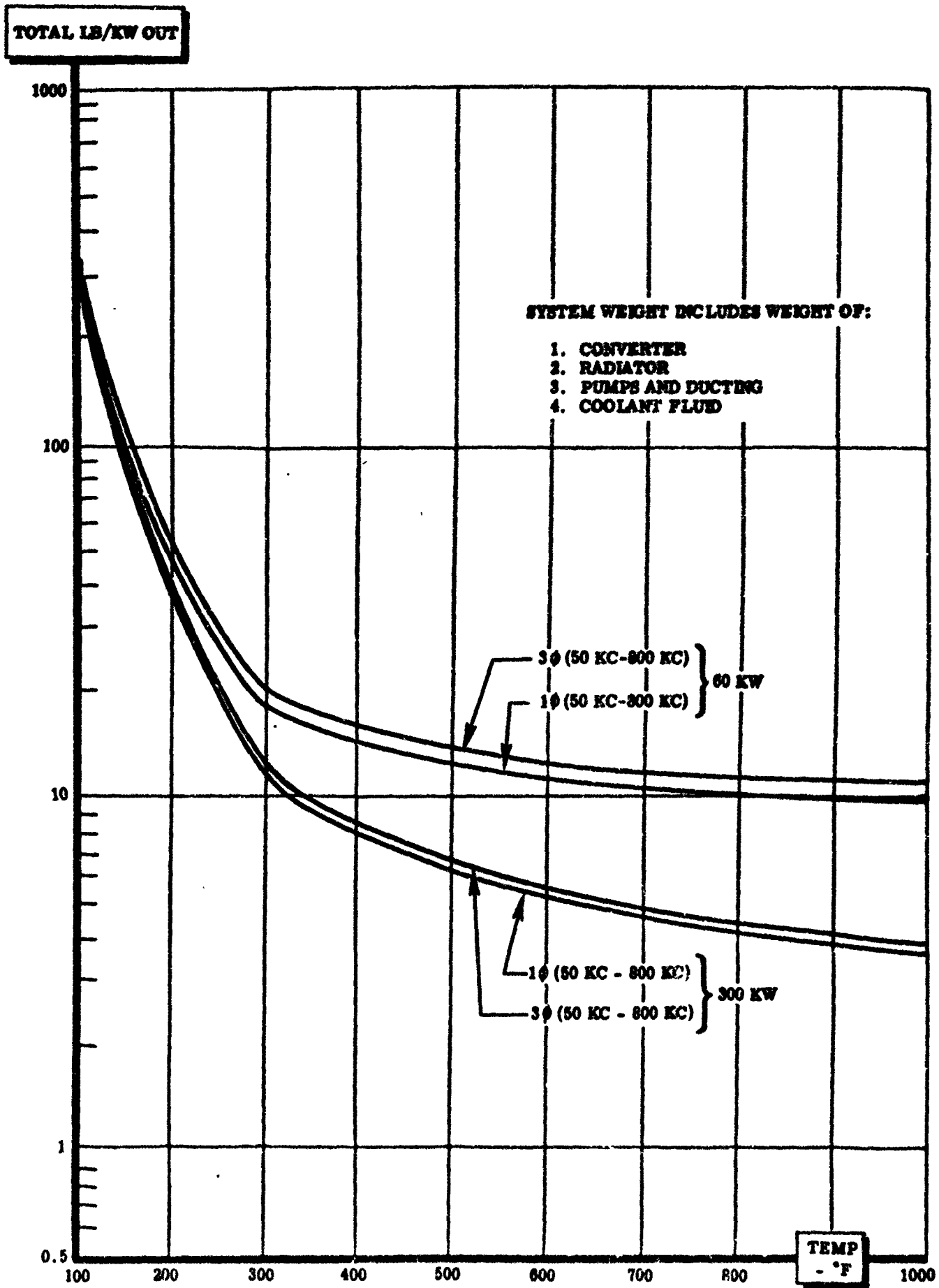


Figure 51. Analysis of System Weight vs. Temperature for Static Tube Converter

function of the coolant system is absolutely necessary in the static tube converter system. The heat of the tube filament will lead to tube destruction in a short time if coolant is not flowing. A method of preventing tube operation until coolant flow has started must be provided.

System cooling for the tube circuit converters was approached by computing the heat losses per component on each shelf. In the 60 KW converters the heat losses were concentrated roughly as 50 per cent of total losses in the oscillator (T7) and 50 per cent are distributed in three shelves. See Figure 52.

Assuming a coolant temperature rise (ΔT) of 50°C, parallel cooling can be applied to the shelves as one unit and the oscillator tube as another unit. The oscillator tube has a coolant jacket around it so that heat transfer is dependent upon the coolant flow rate and the coolant temperature rise (ΔT). The shelf on which the other units are mounted can be cooled by cold-plate techniques except where the thyratrons and diodes are mounted. A coolant jacket is planned for both the thyratrons and diodes with coolant flow and through the tube bases. Here again parallel cooling is used. The coolant flow (W_f) is controlled by using a form of the continuity equation

$$W_f = VA$$

where A is the area in square feet and V is the velocity in feet/second. W_f is now in terms of cubic feet per second and can be converted into weight/second. By inserting values for the coolant flow (W_f) required, using a velocity high enough to insure turbulent flow, the coolant tube area can be computed. The inlet coolant tube area is then determined by finding the sum of the individual areas. By keeping the sum of the areas constant, ΔP can be assumed to be equal to zero. The only ΔP encountered would be due to friction losses.

The 300 KW converter system thermal analysis is performed in the same manner except that the oscillator tube losses represent over 60 per cent of the total losses. A coolant flow diagram is shown in Figure 53.

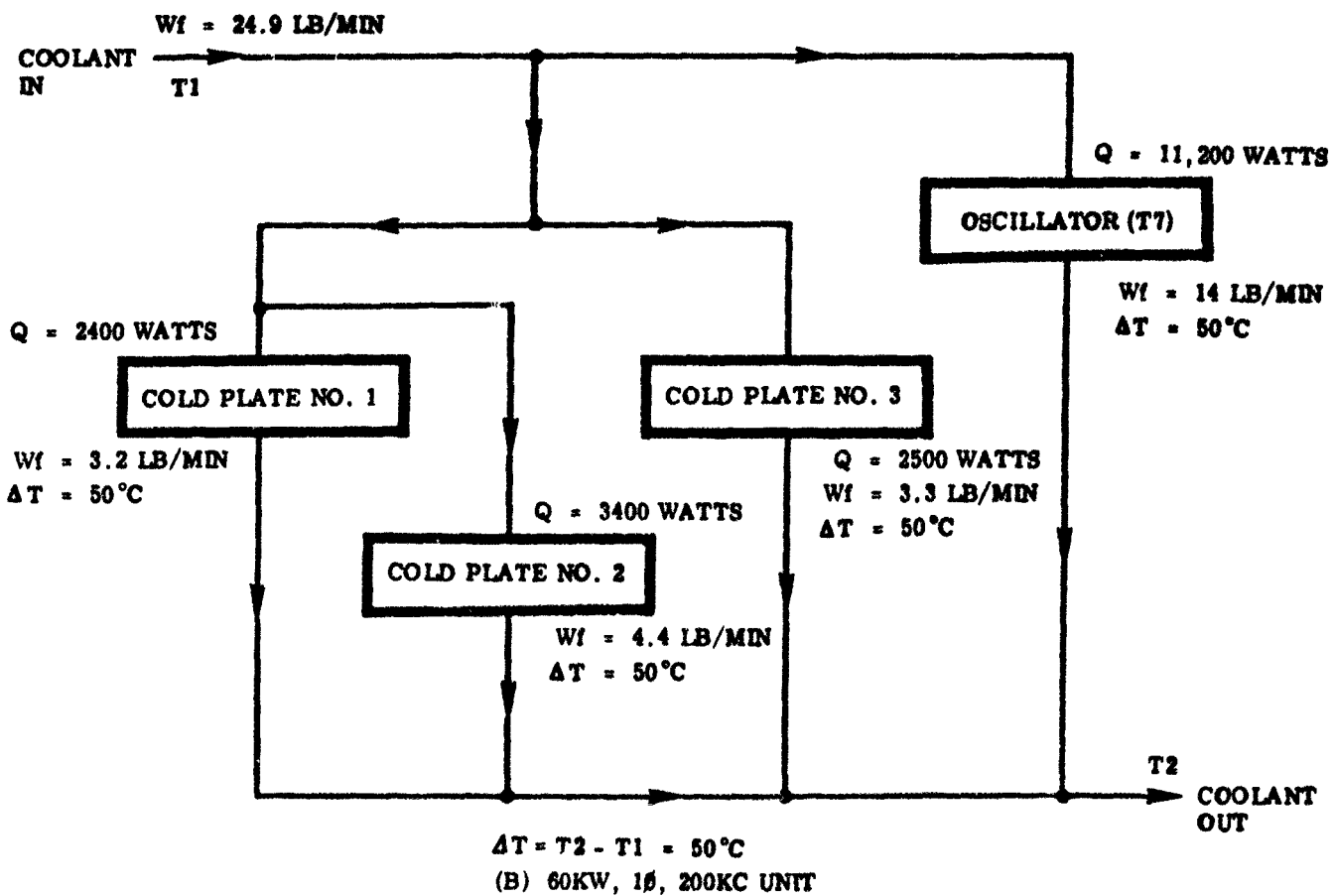
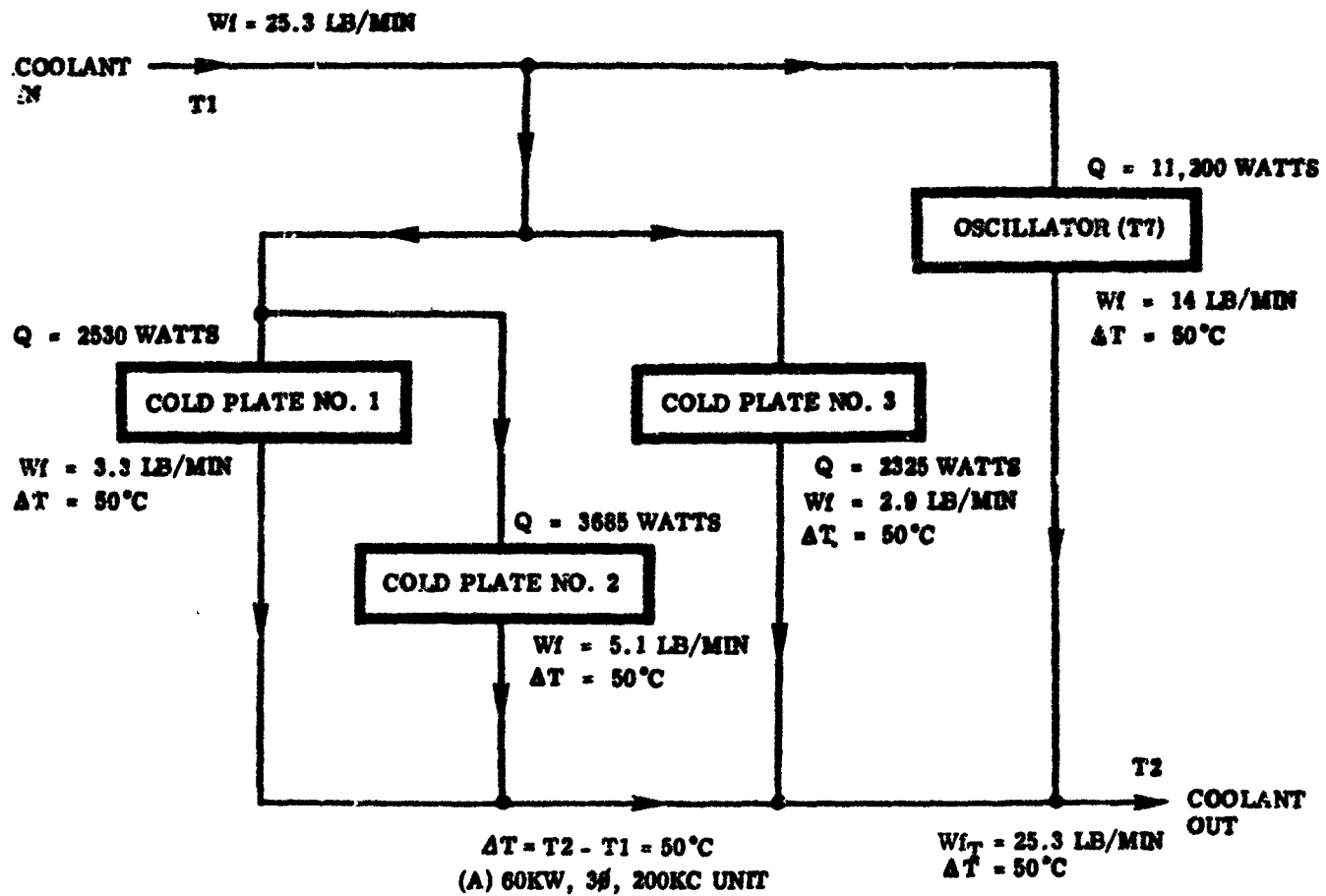


Figure 52. Thermal Flow Diagram for 60 KW Static Tube Converter Unit

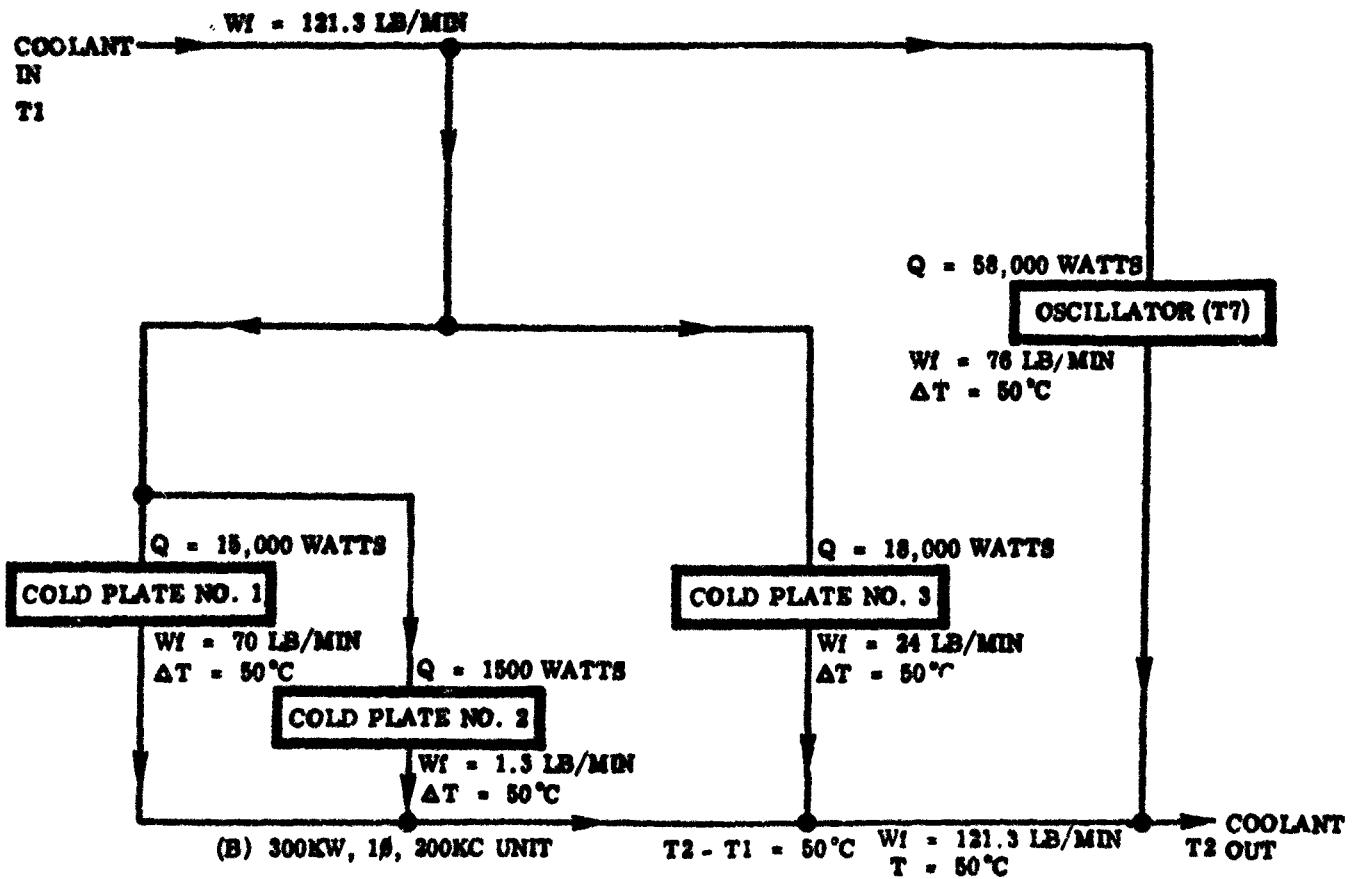
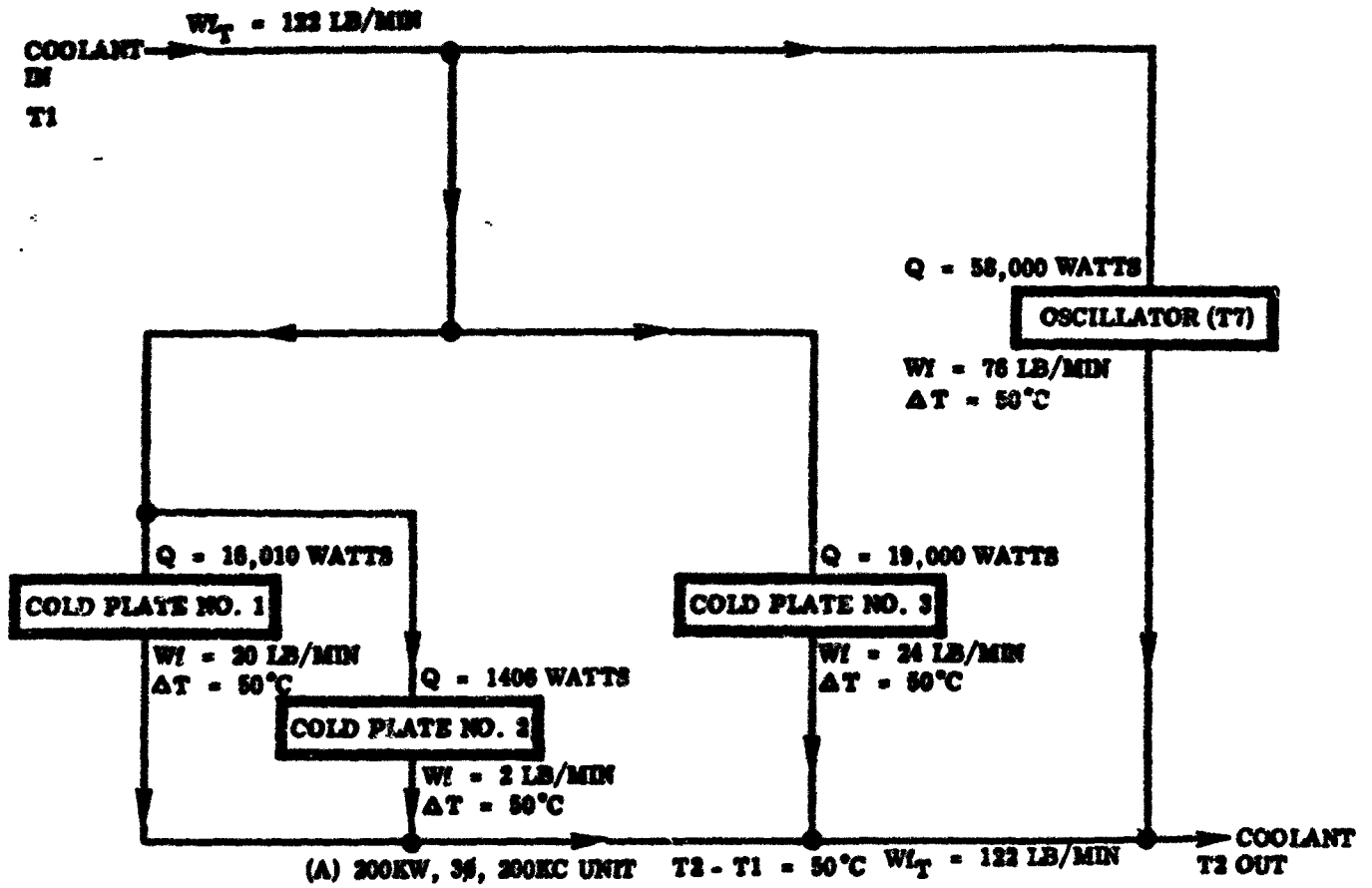


Figure 53. Thermal Flow Diagram of 300KW Static Tube Converter

MOTOR GENERATOR DESIGN CONCEPT

A 60 KW UNIT

The design of a motor-generator type of 60 KW converter has been based on:

Input - 60 KW, 1 KC, 43.6/75.8 volts, three-phase
Output - 10,100 volts, 50 to 200 KC, 1 ϕ and 3 ϕ

Figure 54 illustrates a particular converter concept in which a solid-rotor type of generator is used to generate high-frequency (50 KC to 200 KC), high-voltage power. The input frequency of 1 KC for the 60 KW converter requirement gives an operating speed of 30,000 rpm for a four-pole motor to drive the generator. This speed has been selected for the design speed.

Parametric data on weight, volume, losses, and efficiency for both 1 ϕ and 3 ϕ , 60 KW, converter designs for several frequencies are tabulated in Table 13. Parametric data has been derived on single-phase 50, 100, and 200 KC designs, and on a 50 KC and 200 KC three-phase design. Due to the number of poles required in an 800 KC generator design, the motor-generator concept has not been considered for the 800 KC converter requirement.

Since a three-phase generator requires three times as many stator slots as does a single-phase generator, a large size stator is required for the three-phase generator in order to accommodate the number of slots. In order to limit the rotor stress to the design value of 60,000 psi, it is necessary to construct the three-phase generator using a common shaft with three rotor sections on it. There are three separate stators in the design, and the poles of the rotor sections are displaced from each other by 120 electrical degrees. In effect, the three-phase output is achieved by installing three single-phase generators in a common frame with their voltage outputs in parallel, and their phase displacement such as to achieve three-phase power at the output terminals.

A 300 KW UNIT

Design details of a motor-generator type of converter unit to meet the 300 KW power conversion requirements of the Work Statement are similar to those of the 60 KW unit as shown in Figure 54. The basic difference other than power handling level is in a different input which is listed as follows:

Input - 300 KW, 3,200 cps, 120/208 V, 3 ϕ
Output - 50 to 200 KC, 10,100 V, 1 ϕ and 3 ϕ

As in the case of the 60 KW design, a motor-generator unit was not considered for the 800 KC requirement because of the extreme number of poles required for such a unit.

The motor for driving each of the generators is a 120 volt, 3,200 cps, three-phase synchronous solid-rotor type, turning at 24,000 rpm. Parametric data for a 300 KW converter (1 ϕ and 3 ϕ) is summarized in Table 14.

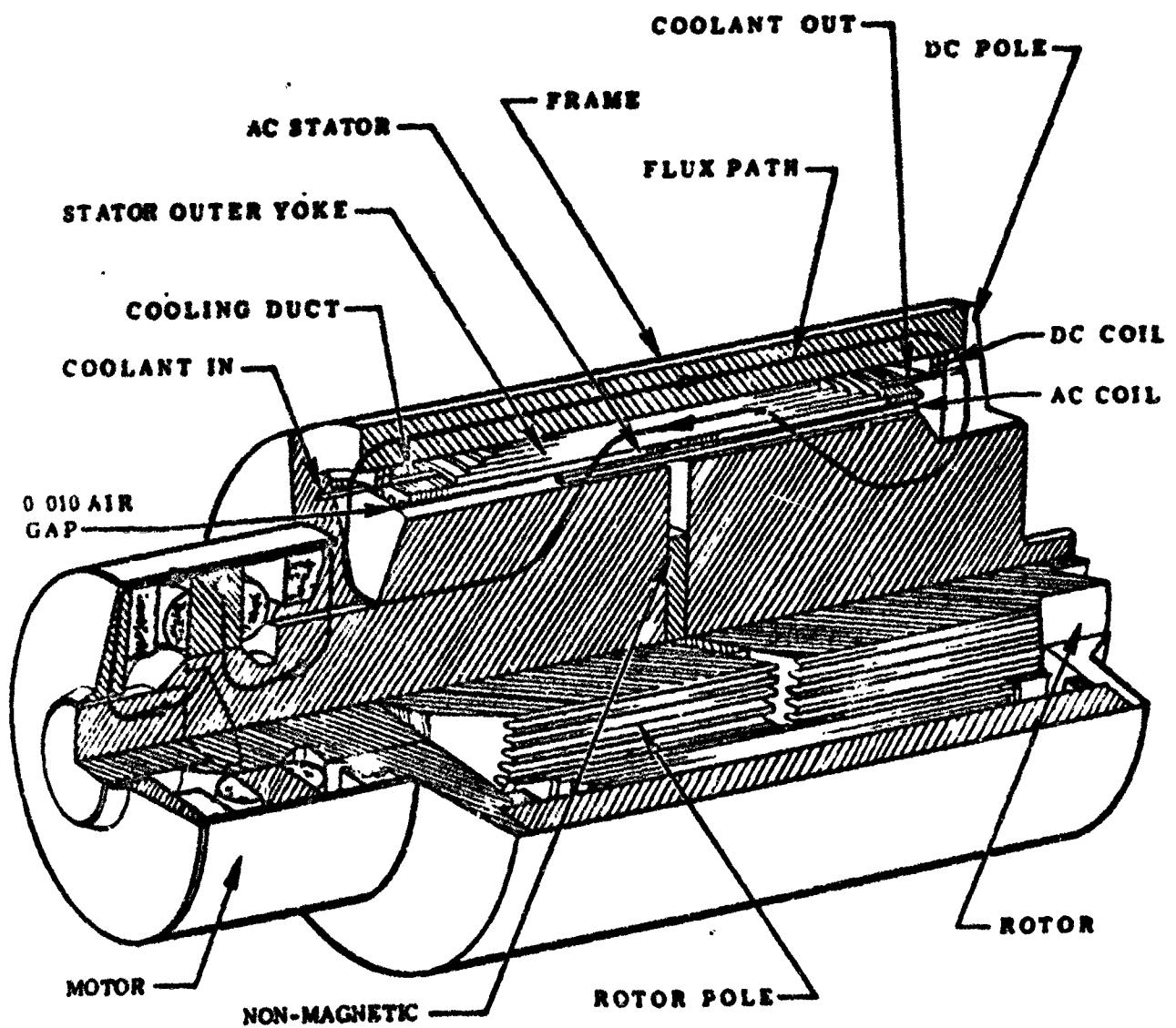


Figure 54. Motor Generator Unit (Perspective)

Table 13

Summary of 60 KW Motor-Generator Parametric Data

1φ	50 KC	100 KC	200 KC
WEIGHT (lbs.)	150	204	320
KW RAD (LOSSES)	10.1	11.5	13.5
KW OUT	49.9	48.5	46.5
EFFICIENCY (%)	81.8	81.8	77.5
LENGTH (Inches)	11.5	13.5	17.8
DIAMETER (Inches)	10	10.3	12.5
VOLUME (cu. ft.)	.52	.62	1.3
LBS/KW RAD	13.9	16.8	23.7
LBS/KW OUT	3.0	4.0	6.8
3φ	50 KC	200 KC	800 KC
WEIGHT (lbs.)	176	350	-
KW RAD (LOSSES)	10.1	13.8	-
KW OUT	49.9	46.2	-
EFFICIENCY (%)	83.2	77	-
LENGTH (Inches)	15.8	22	-
DIAMETER (Inches)	9.8	12	-
VOLUME (cu. ft.)	.65	1.4	-
LBS/KW RAD	17.4	25.4	-
LBS/KW OUT	3.5	7.6	-

NOTE: Values do not include cooling system weights.

Table 1k

Summary of 300 KW Motor-Generator Parametric Data

1φ	50 KC	100 KC	200 KC
WEIGHT (lbs.)	540	645	1,500
KW RAD (LOSSES)	49.5	51.0	52.8
KW OUT	250.5	249.0	247.2
EFFICIENCY (%)	83.5	83.0	82.4
LENGTH (Inches)	13.5	16.0	35.6
DIAMETER (Inches)	16.0	16.0	17.8
VOLUME (cu. ft.)	1.6	1.8	5.3
LBS/KW RAD	10.9	12.7	28.4
LBS/KW OUT	2.2	2.6	6.0
3φ	50 KC	200 KC	800 KC
WEIGHT (lbs.)	801	2,000	-
KW RAD (LOSSES)	48.6	60	-
KW OUT	251.4	240	-
EFFICIENCY (%)	83.8	80	-
LENGTH (Inches)	26.5	70	-
DIAMETER (Inches)	11	14	-
VOLUME (cu. ft.)	1.5	6.2	-
LBS/KW RAD	16.5	33.3	-
LBS/KW OUT	3.2	8.3	-

NOTE: Values do not include cooling system weights.

Mechanical details of 50 KC and 200 KC, single-phase converters are shown in the section which follows with a three-phase, 50 KC unit in which three separate generator sections are mounted on a common shaft. The three rotor and stator sections are displaced from each other by 120 electrical degrees to produce a three-phase voltage output.

GENERATOR DETAILS

Stator-Rotor Relationship

Figure 55 shows the relationship between rotor poles and stator slots for the proposed generator. The south poles of the rotor are displaced axially from the rotor north poles. The stator slots are so chosen that adjacent stator slots are located one for every three poles of the rotor (counting both north and south poles). A stator slot may have a maximum width of a pole pitch, the distance from the center of a north pole to the center of a south pole. This places the slots so that the induced voltages are in opposite directions in adjacent slots. Figure 55 shows cross sections through the generator.

Rotor - The rotor is made of a high-strength, solid magnetic material and the outer circumference is slotted to form poles similar to gear teeth. The teeth in one section are displaced 180 electrical degrees from the teeth in the other axially displaced section as shown in Figure 55. The depth of slot depends on the air gap between stator and rotor teeth and must be sufficient to reduce the flux from the space between poles to the stator to a low percentage of the flux from the teeth to the stator. The two sections of the rotor are spaced by a nonmagnetic material to minimize flux leakage between the north and south section.

The flux in the rotor is a DC flux and produces no loss during steady-state operation. A ripple flux in the pole tips will produce some losses; this loss may be reduced by reducing the stator slot opening to less than the width of a rotor tooth to prevent the flux from changing in the teeth.

Stator Iron Configuration - The stator iron is subjected to a pulsating flux of the generating frequency of a single polarity in each stator section. The flux also rotates in the yoke section of this lamination at a rate the same as the rotor speed (rpm) and is pulsating at the generating frequency. This material must be of low-loss magnetic material and of very thin laminations to minimize iron losses at high frequencies. The flux density must also be at reduced values to minimize losses at high frequencies. Ferrites are usable for this core, but limit the operating temperature to lower values than with nickel-iron alloys. Powdered metal cores made in thin laminations may also possibly be used for this core. The notches located in the outer periphery of this lamination is to provide for coolant fluid flow and are located at the source of heat generation.

Outer Yoke Configuration - The outer yoke carries the flux from the north stator section to the south stator section. The flux rotates in the outer yoke at the same speed (rpm) as the rotor is turning. It is an unchanging

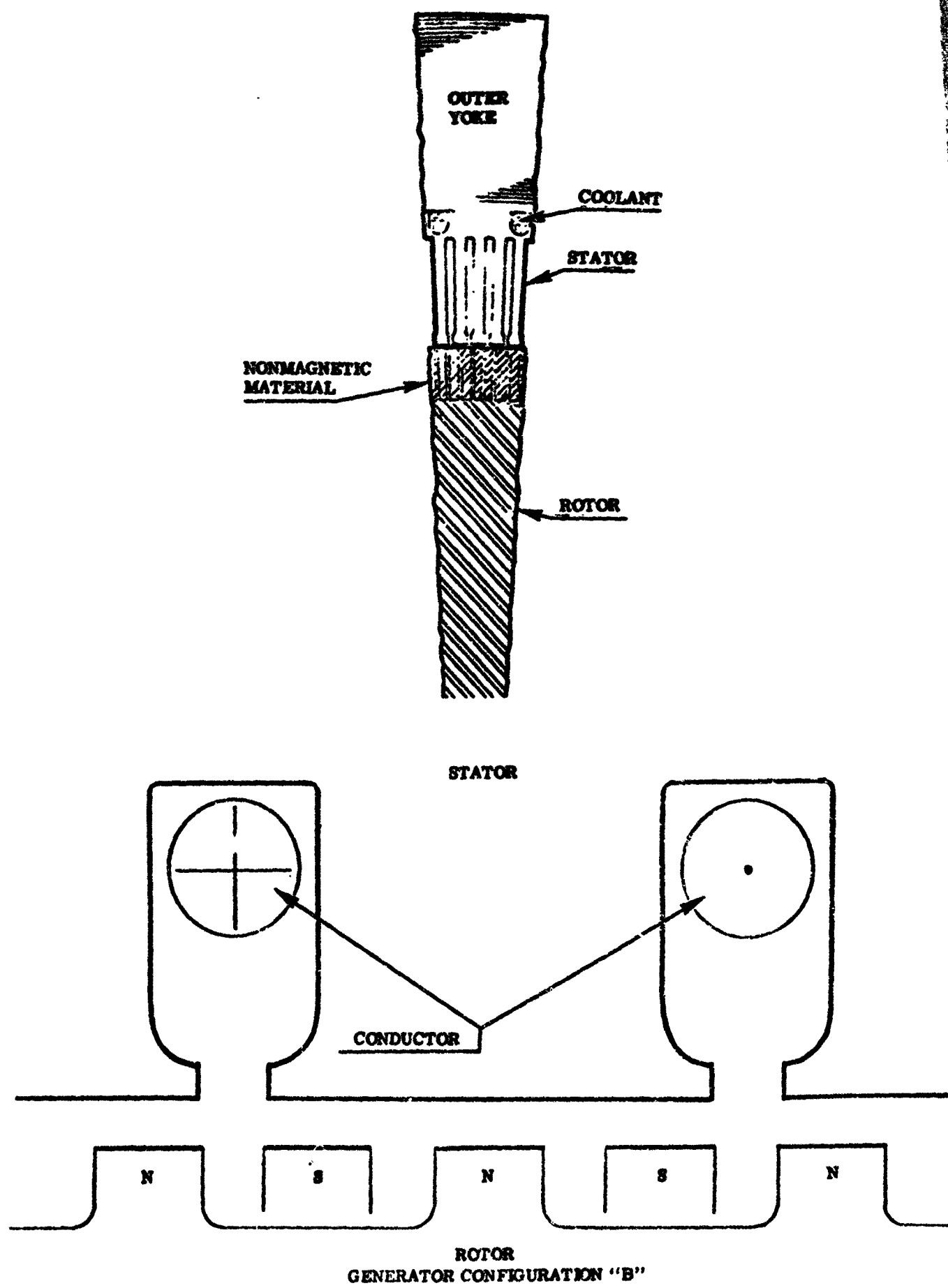


Figure 55. Details of Basic Generator Concept

or DC flux for any load condition. The outer yoke is shown as a tape wound core, and very little loss is generated as the outer yoke is laminated and the loss is generated by a constant spinning flux. The outer yoke lamination may be from a thicker and higher loss material than the stator iron and be operated at high flux densities.

Stator Air Gap - The stator air gap, clearance between rotor and stator, could be reduced to .001 inch and result in a more efficient electrical design and sufficiently large field MMF to compensate for demagnetizing stator MMF at 200 KC. The gap has been increased to 0.010 inch in consideration of practical manufacturing tolerances. Reducing this gap would result in a one to one-and-a-half per cent increase in efficiency.

Converter Drive Motor

The electric drive motor is a synchronous, solid-rotor NADYNE type. A solid-rotor type was chosen because its field winding is static and its efficiency and power factor are higher than an induction type of motor. The power factor may be adjusted to unity by adjusting the DC excitation power to the motor field coils. Its rotor speed is not limited other than by the limitations imposed by the strength of the steel used in the rotor construction. Solid-rotor NADYNE type motors have been built and tested and are identical to solid-rotor types of NADYNE generators.

At 1,000 cps input the motor is designed with four poles for 30,000 rpm. Motor design speeds of 60,000 rpm with two poles and 20,000 rpm with six poles are other possible combinations. The 60,000 rpm design would result in the minimum motor weight.

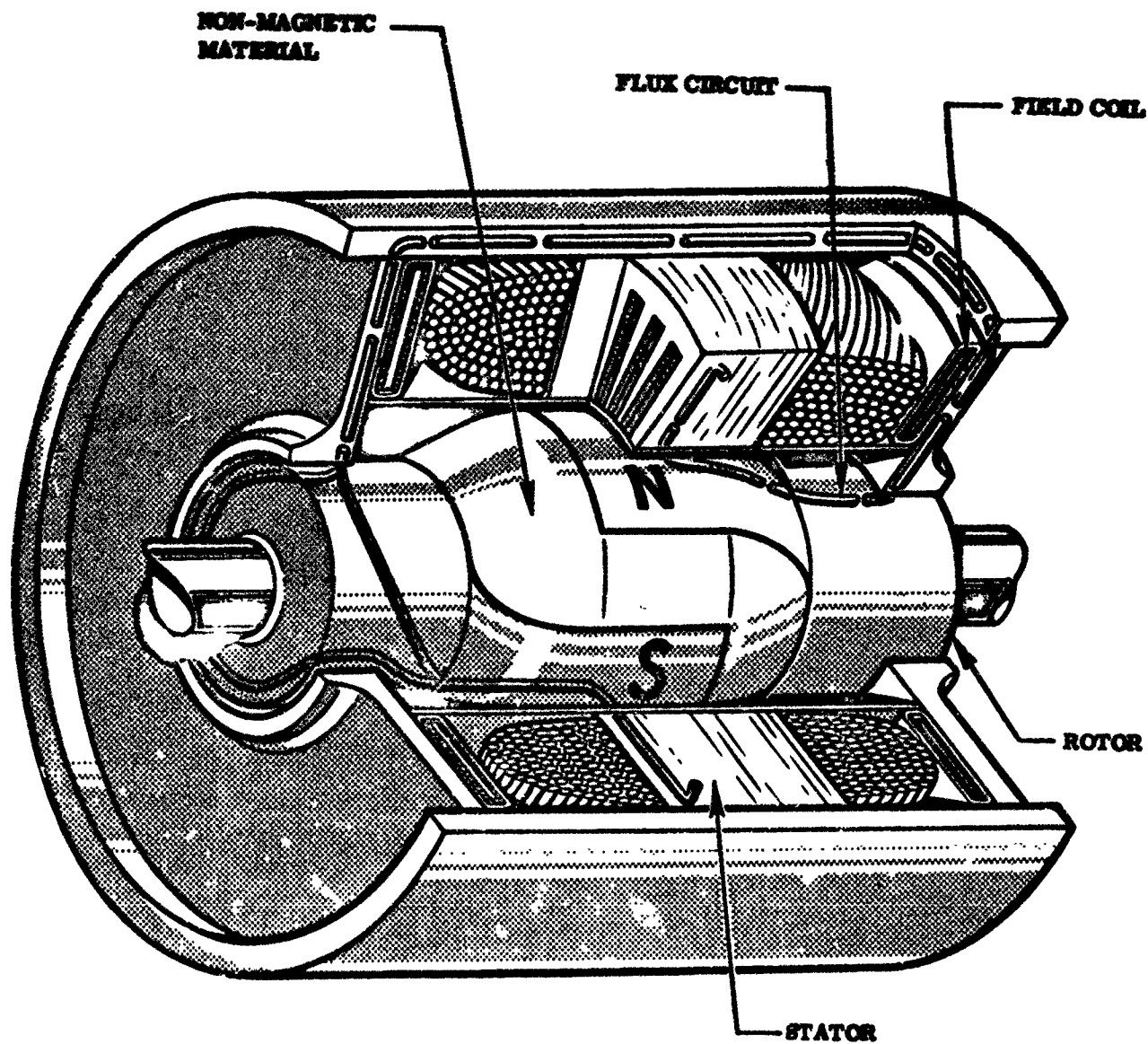
A detailed perspective drawing of the NADYNE synchronous motor (Figure 56) shows the physical arrangement of parts and magnetic flux circuit.

MECHANICAL DETAILS OF 60 KW CONVERTER

Details of the 60 KW converter are shown in the figures which follow for these configurations and design data is included in Tables 15 and 16.

1. 60 KW, 1 ϕ , 50 KC (Figure 57)
2. 60 KW, 1 ϕ , 100 KC (Figure 58)
3. 60 KW, 1 ϕ , 200 KC (Figure 59)
4. 60 KW, 3 ϕ , 50 KC (Figure 60)

As indicated in a previous section, this concept is not feasible for the 800 KC design because of the inability to get the required number of poles on the periphery of the rotor and stator. Rotor and stator configurations are to the dimensions shown on the drawings. Additional details are discussed in the section on Generator Details. The motor is a three-phase, 30,000 rpm, 1,000 cps unit and has a voltage rating to match the output of the SNAP 8 power system (43.6/75.8 volts AC). The same motor is used for each of the three frequency concepts.



NADYNE SYNCHRONOUS MOTOR

Figure 56. NADYNE Synchronous Motor Details

TABLE 15

60 KW MOTOR-GENERATOR 1ϕ DESIGN DATA

CONFIGURATION	50 KC	100 KC	200 KC
OPERATING SPEED	30,000 RPM		30,000 RPM
<u>WEIGHT (LBS)</u>			
Motor	60	60	60
Generator	70	124	240
Controls	10	10	10
Cooling (Structure)	5	5	5
Bearings	5	5	5
Total (Pounds)	<u>150</u>	<u>204</u>	<u>320</u>
STATOR LAMINATIONS (.0005")	HYMU 80	HYMU 80	HYMU 80
<u>GENERATOR LOSSES (WATTS)</u>			
Stator Iron	1480	1602	1610
Stator I ² R	760	2197	920
Field I ² R	940	165	3920
Windage (2PSIA)	145	350	1510
Stray Load 1%	600	600	600
Total (Watts)	<u>3925</u>	<u>4914</u>	<u>8560</u>
GENERATOR EFFICIENCY %	94	92.4	87.5
MOTOR EFFICIENCY %	88.5	88.5	88.5
CONVERTER EFFICIENCY %	83.1	81.8	77.5
<u>OTHER DATA</u>			
Avg. Stator Tooth Flux Density			
In Kilolines/Sq.Inch,	29.8	10.	15.8
In Gauss	4610	1550	2440
Stator Conductor Current Density			
In Amperes/Square Inch	6400	6400	6400
Field Conductor Current Density			
In Amperes/Square Inch	3500	3500	3500
Conductors	28 Ni-Clad Cu.		28 Ni-Clad Cu.
Curie Temperature °F	860°F	660°F	860°F

TABLE 16

60 KW MOTOR-GENERATOR DESIGN DATA (3 ϕ)

CONFIGURATION	50 KC 3 ϕ	200 KC 3 ϕ
OPERATIONG SPEED	30,000 RPM	30,000 RPM
<u>WEIGHT (LBS)</u>		
Motor	60	60
Generetor	96	270
Controls	10	10
Cooling (Structure)	5	5
Bearings	<u>5</u>	<u>5</u>
Total (Pounds)	176	350
STATOR LAMINATIONS (.0005")	HYMU 80	HYMU 80
<u>GENERATOR LOSSES (WATTS)</u>		
Stator Iron	595	1975
Stator I ² R	1435	1600
Field I ² R	658	3900
Windage (2PSIA)	265	1700
Stray Load 1%	<u>600</u>	<u>600</u>
Total (Watts)	3553	9775
GENERATOR EFFICIENCY %	94.1	83.0
MOTOR EFFICIENCY %	88.5	88.5
CONVERTER EFFICIENCY %	83.2	77.0
<u>OTHER DATA</u>		
Avg. Stator Tooth Flux Density	21.5	15.8
In Kilolines/Sq. Inch		
In Gauss	3330	2440
Stator Conductor Current Density		
In Ampere/Square Inch	4200	6400
Field Conductor Current Density		
In Ampere/Square Inch	3500	3500
Conductors	28 Ni-Clad Cu.	28 Ni-Clad Cu.
Curie Temperature °F	860°F	860°F

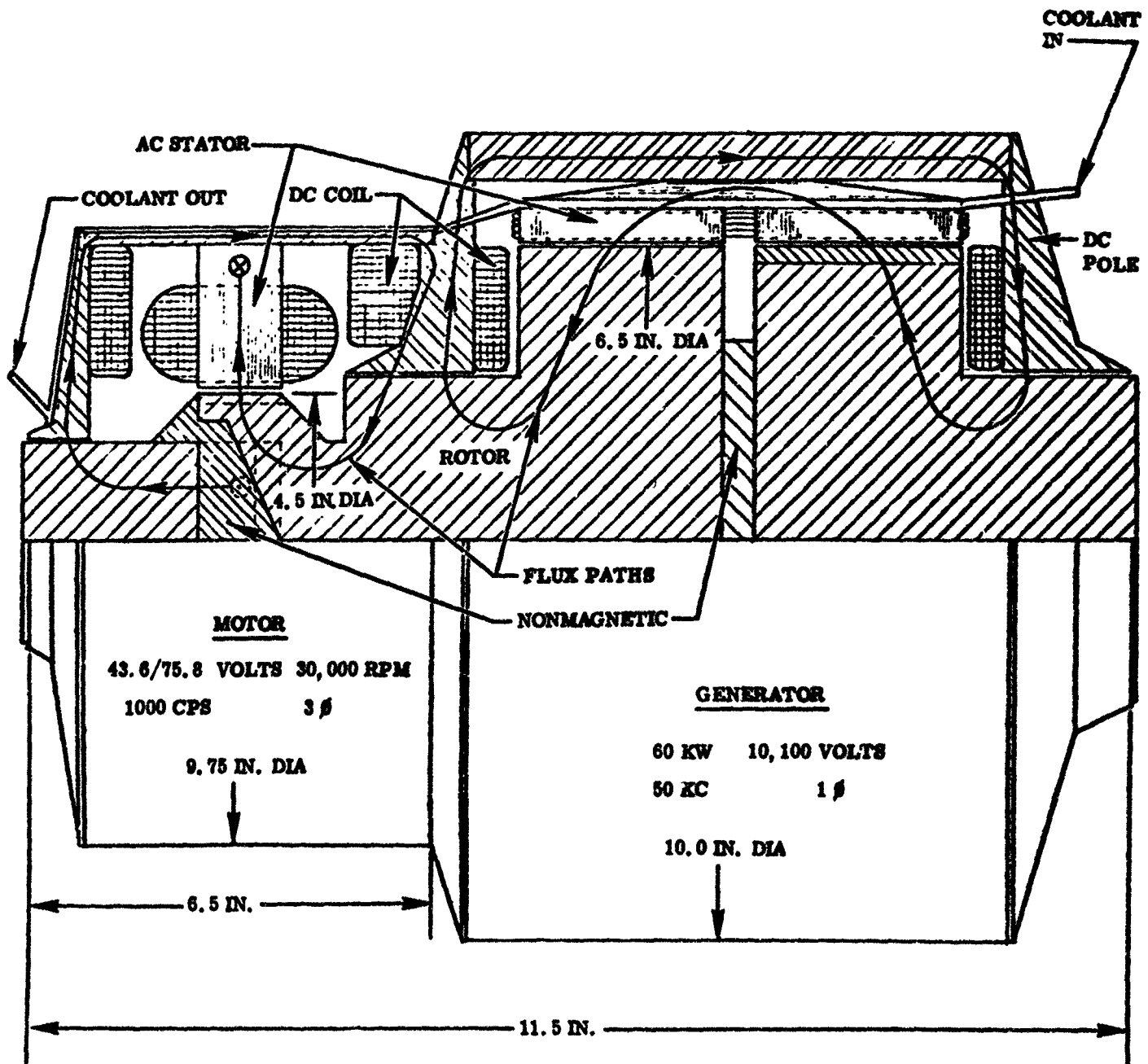


Figure 57. Preliminary Mechanical Design of 60 KW, 1φ, 50 KC Motor-Generator

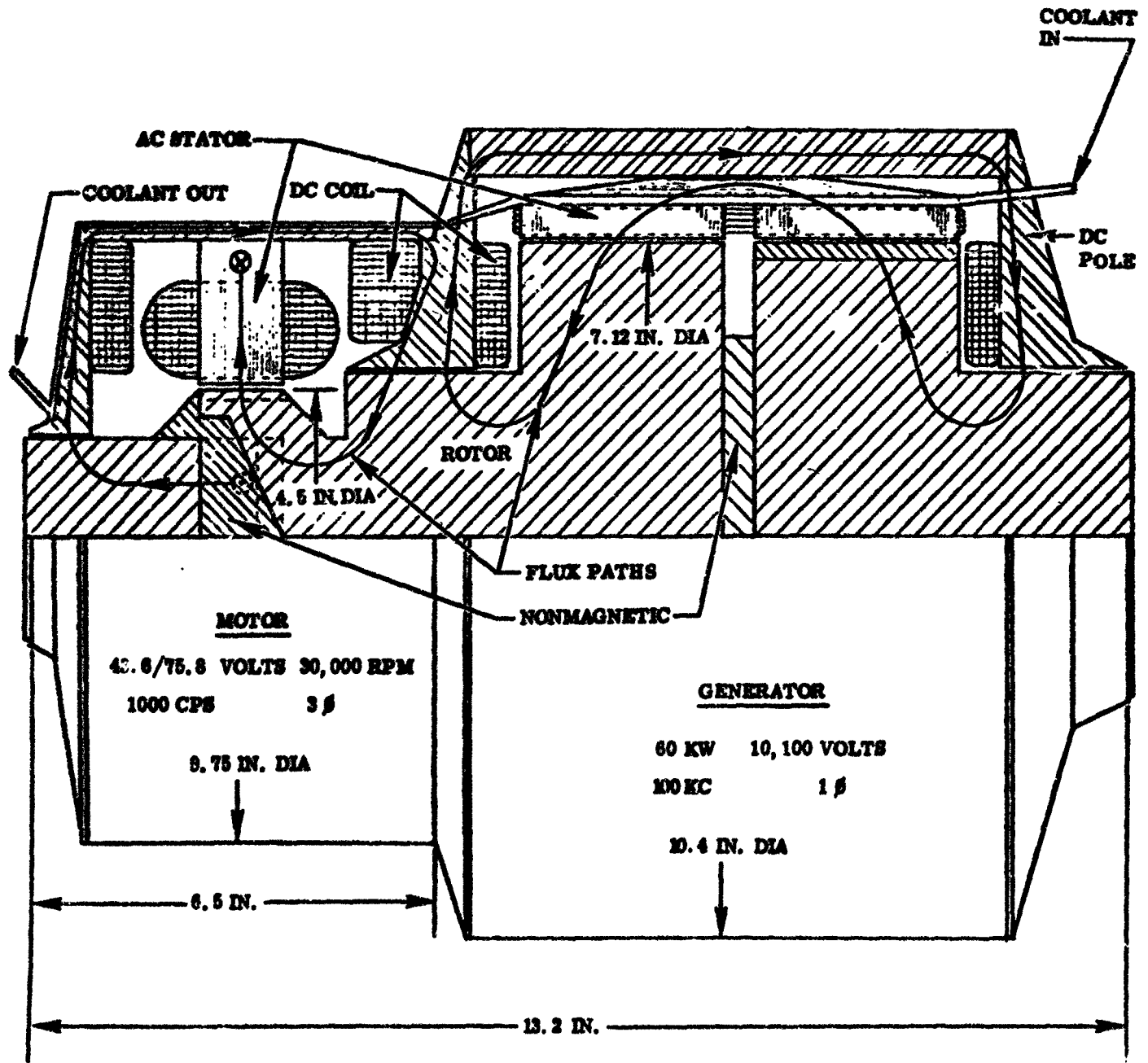


Figure 58. Preliminary Mechanical Design of 60 KW, 1 ϕ , 100 KC Motor-Generator

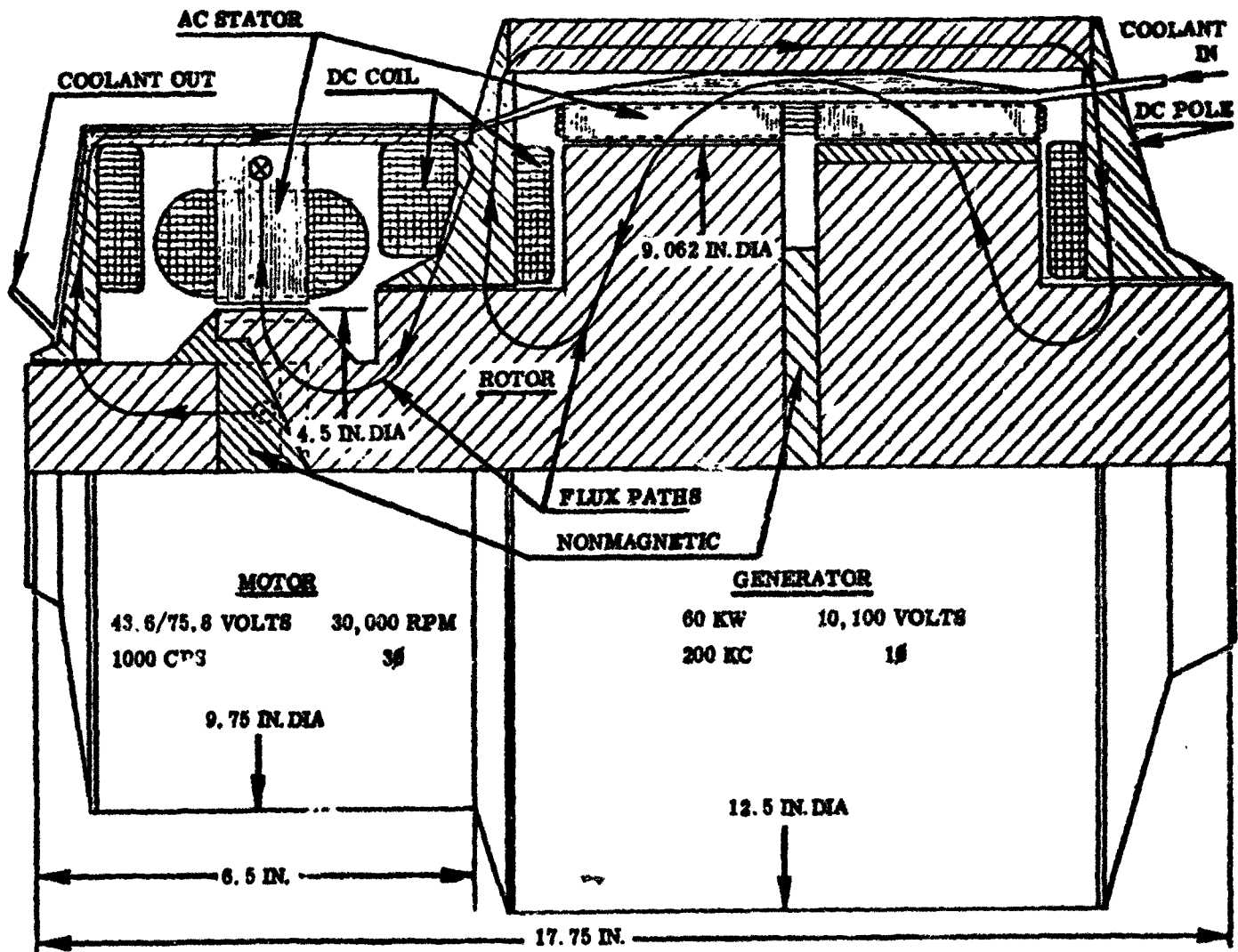


Figure 59. Preliminary Mechanical Design of 60 KW, 1φ, 200 KC Motor-Generator

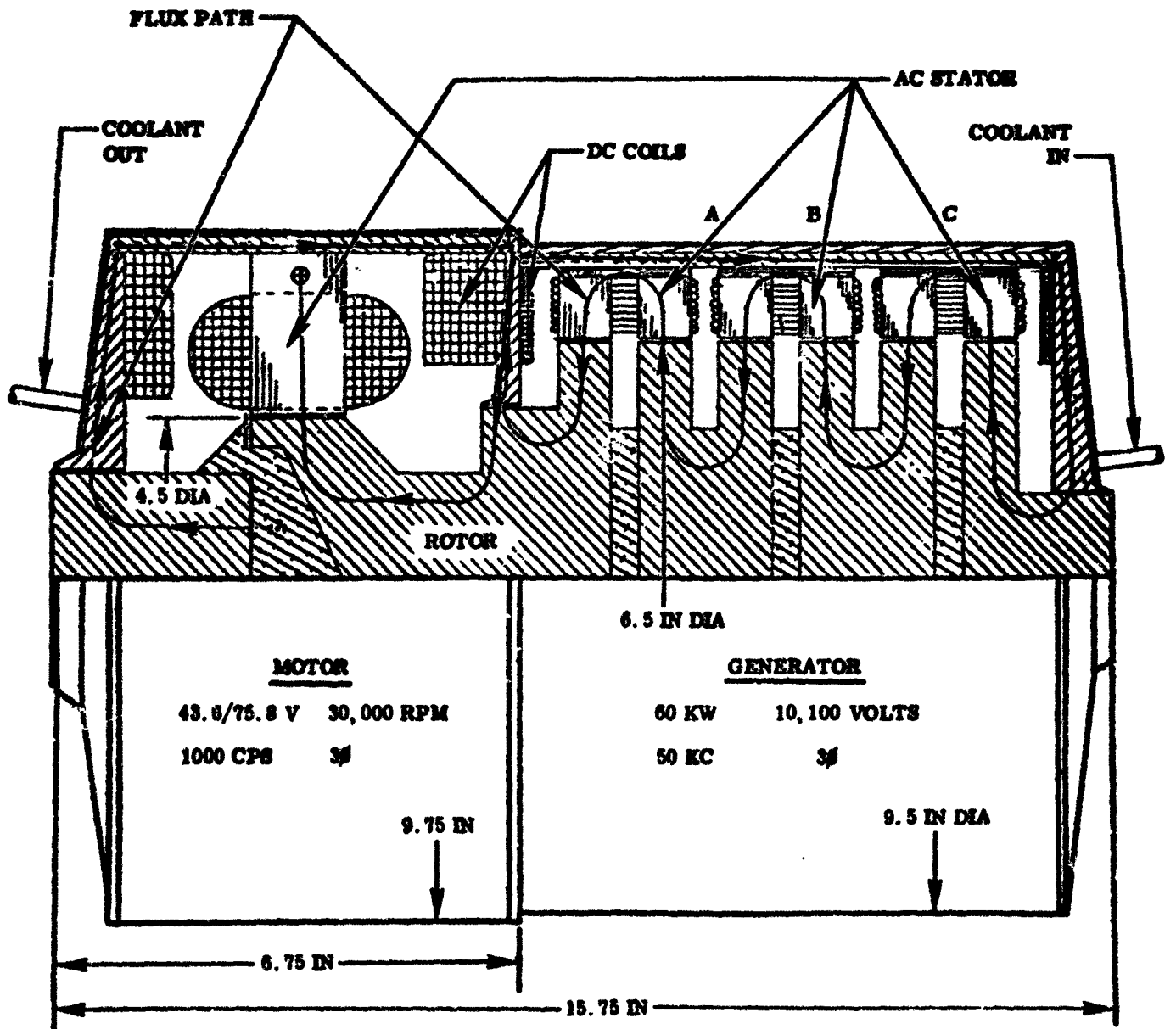


Figure 60. Preliminary Mechanical Design of 60 KW, 3 ϕ , 50 KC Motor-Generator

MECHANICAL DETAILS OF 300 KW CONVERTER

The 300 KW motor-generator design is similar to the 60 KW unit. Design details appear in the figures which follow for these configurations and parametric data is shown in Tables 17 and 18.

1. 300 KW, 1 ϕ , 50 KC (Figure 61)
2. 300 KW, 1 ϕ , 100 KC (Figure 62)
3. 300 KW, 1 ϕ , 200 KC (Figure 63)
4. 300 KW, 3 ϕ , 50 KC (Figure 64)

The inability to design a rotor and stator to contain the required number of poles makes the motor-generator concept not feasible for the 800 KC concept. Dimensions of the converters are shown on the face of the drawings and discussed in a previous section. The motor is a three-phase solid-rotor concept operating from the 120/208 volts AC output of the SPUR type of power system. The design is the same 24,000 rpm, 3,200 cps machine for each of the 300 KW converter units.

THERMAL ANALYSIS

The cooling system of the motor-generator unit is made up of thin parallel tubing located in the stator yoke. The parallel tubes then converge into a collection ring at each end. Due to the short length of coolant tubing, multiple coolant passes may be required in order to achieve a reasonable value of ΔT without resorting to unrealistically small tubing. Heat is removed from the stator to the coolant fluid by means of conduction. High-frequency generator units are capable of operating at temperatures in the 500°F to 800°F range. Figure 65 shows the effect of system operating temperature on generator system weight. Calculated electrical losses for a 50 KC, 100 KC, and 200 KC unit and other thermal design data including efficiencies for HYMU 80 materials are shown in Tables 15 through 18. Figure 66 is a coolant flow analysis for this system. Coolant flow rates and coolant temperature rise will vary from design to design of a given size of motor-generator. The iron losses are a function of flux density, iron volume, frequency, and material used in the laminations. Substitution of 48 alloy for the HYMU 80 reflected in the 200 KC, single-phase, 300 KW generator, Table 17, would increase the losses more than 3 KW. This would require increased coolant flow to maintain the same coolant ΔT .

Efficiency - Efficiency of the generator is reduced as the temperature of the generator iron increases. Figure 67 shows how the efficiency changes as a function of temperature for a 60 KW, 50 KC design. HYMU 80 material in .0005 inch laminations can be used to nearly 550°F stator iron surface temperatures with a calculated efficiency of 94 per cent (Table 15). Alloy 48 is shown on the efficiency versus temperature curve at a lower efficiency and has been considered for use because of its lower weight. If higher operating temperatures are required, the silicon irons will have

TABLE 17

300 KW MOTOR-GENERATOR DESIGN DATA (1 ϕ)

CONFIGURATION	50 KC 1 ϕ	100 KC	200 KC 1 ϕ
OPERATING SPEED	24,000 RPM	24,000 RPM	24,000 RPM
<u>WEIGHT (LBS.)</u>			
Motor	175	175	175
Generator	340	445	1300
Controls	11	11	11
Cooling (Structure)	7	7	7
Bearings	7	7	7
Total (Pounds)	<u>540</u>	<u>645</u>	<u>1500</u>
STATOR LAMINATIONS (.0005")	HYMU 80	HYMU 80	HYMU 80
<u>GENERATOR LOSSES (WATTS)</u>			
Stator Iron	10900	10,500	5600
Stator I ² R	2870	4,850	6430
Field I ² R	1285	200	3640
Windage (2PSIA)	633	1,700	4650
Stray Load 1%	3000	3,000	3000
Total (Watts)	<u>18188</u>	<u>20,250</u>	<u>23320</u>
GENERATOR EFFICIENCY %	94.4	93.8	93.2
MOTOR EFFICIENCY %	88.5	88.5	88.5
CONVERTER EFFICIENCY %	88.5	83.0	82.4
<u>OTHER DATA</u>			
Avg. Stator Tooth Flux Density	29.8	15.5	15.8
In Kilolines/Square Inch			
In Gauss	4,460	2,360	2,440
Stator Conductor Current Density	6,400	6,400	6,400
In Amperes/Square Inch			
Field Conductor Current Density	3,500	3,500	3,500
In Amperes/Square Inch			
Conductors	28 Ni-Clad Cu.		28 Ni-Clad Cu.
Curie Temperature $^{\circ}$ F	860	860	860

TABLE 18

300 KW MOTOR-GENERATOR DESIGN DATA (3φ)

CONFIGURATION	50 KC 3φ	200 KC 3φ
OPERATING SPEED	24,000 RPM	24,000 RPM
<u>WEIGHT (LBS.)</u>		
Motor	175	175
Generator	601	1800
Controls	11	11
Cooling (Structure)	7	7
Bearings	7	7
Total (Pounds)	<u>801</u>	<u>2000</u>
STATOR LAMINATIONS (.005")	HYMU 80	HYMU 80
<u>GENERATOR LOSSES (WATTS)</u>		
Stator Iron	4020	12655
Stator I ² R	6520	6800
Field I ² R	1240	1250
Windage	1295	1295
Stray Load 1%	3000	3000
Total (Watts)	<u>16075</u>	<u>25000</u>
GENERATOR EFFICIENCY %	94.6	91.6
MOTOR EFFICIENCY %	88.5	88.5
CONVERTER EFFICIENCY %	83.8	80
<u>OTHER DATA</u>		
Avg. Stator Tooth Flux Density In Kilolines/Sq. Inch	21.21	15.8
In Gauss	3300	2440
Stator Conductor Current Density in Amperes/Sq.Inch	6400	6400
Field Conductor Current Density In Amperes/Square Inch	3500	3500
Conductors	28 Ni-Clad Cu.	28 Ni-Clad Cu.
Curie Temperature °F	860°F	860°F

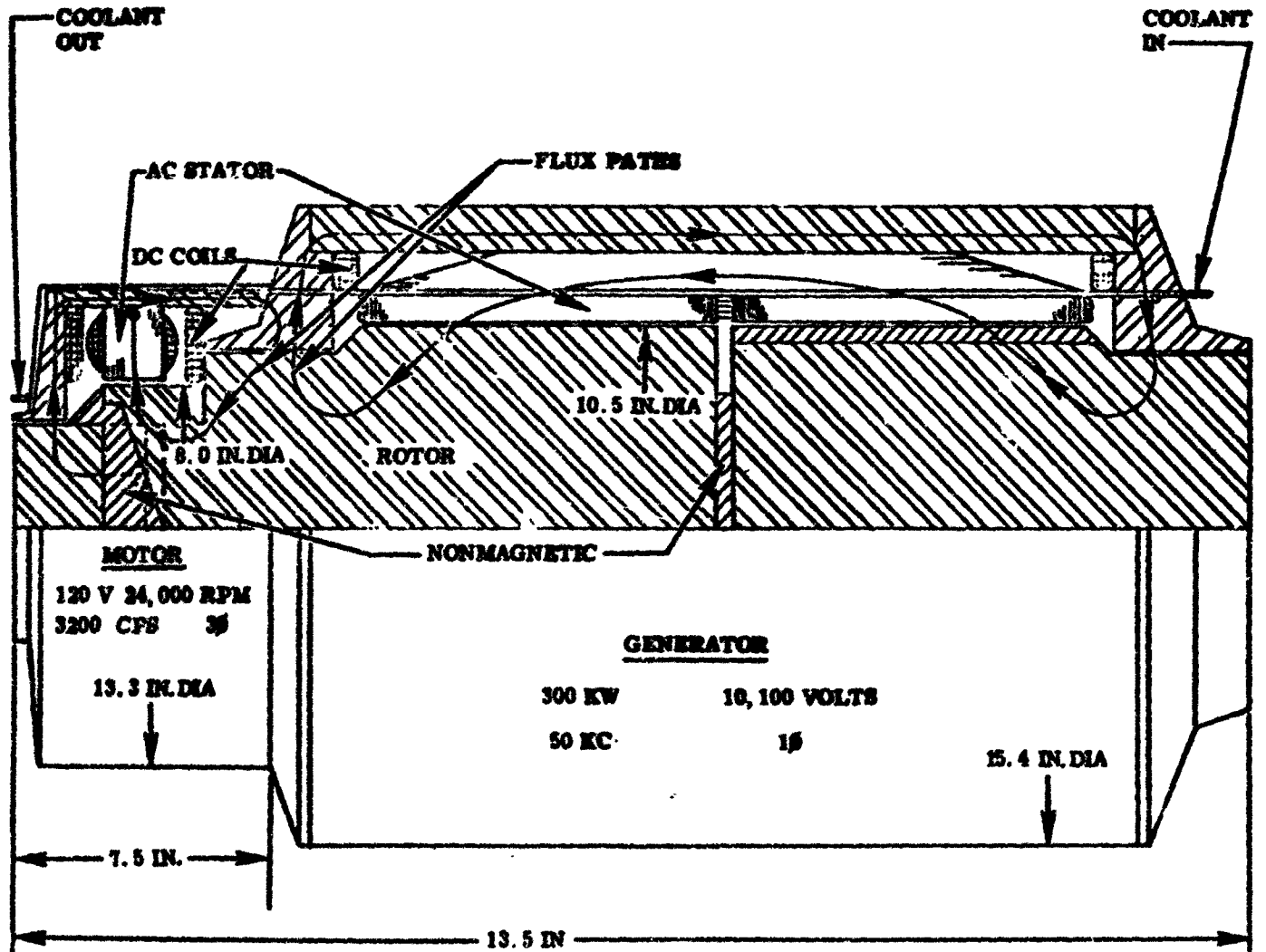


Figure 61. Preliminary Mechanical Design of 300 KW, 1ϕ
50 KC Motor-Generator

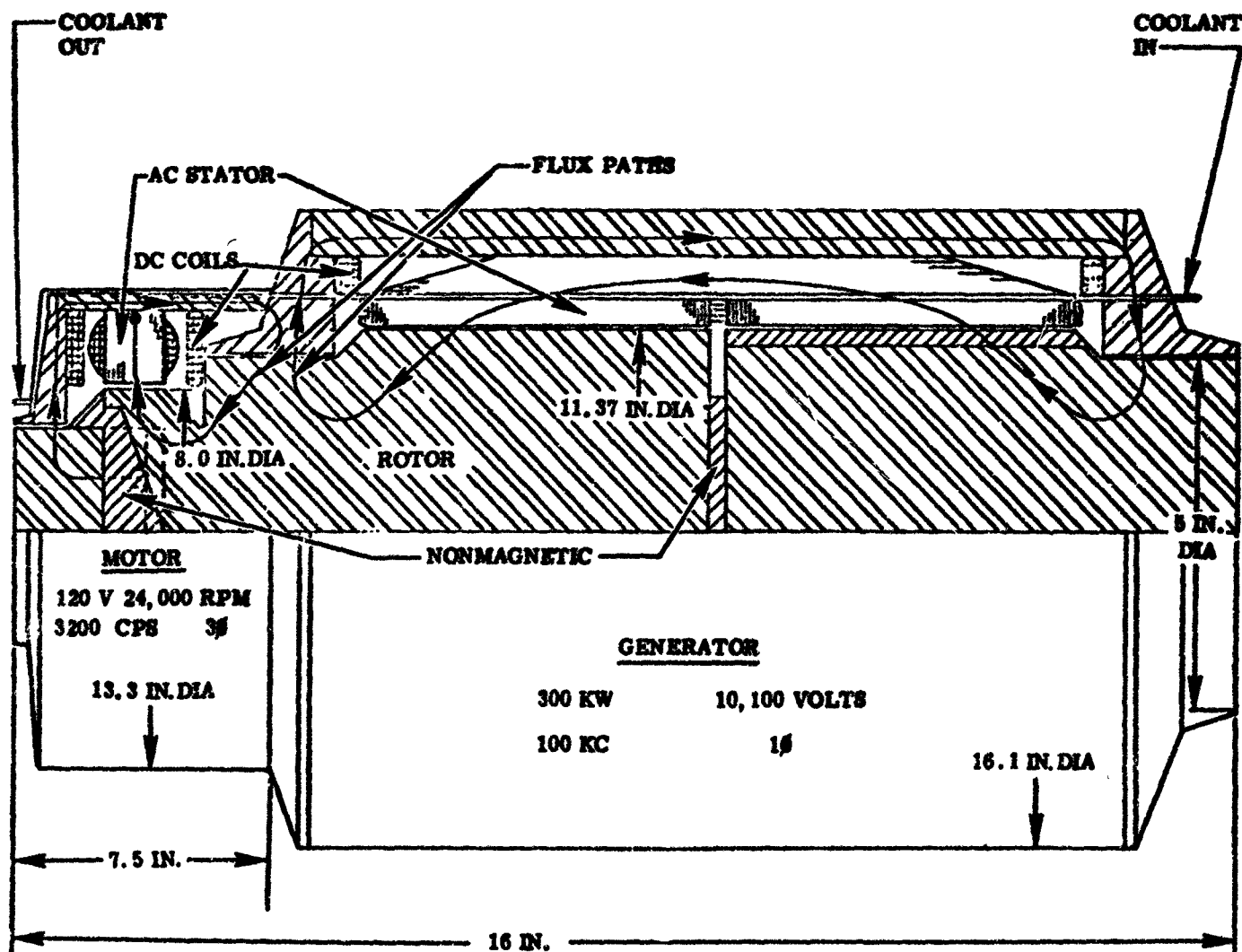


Figure 62. Preliminary Mechanical Design of 300 KW, 1φ, 100 KC Motor-Generator

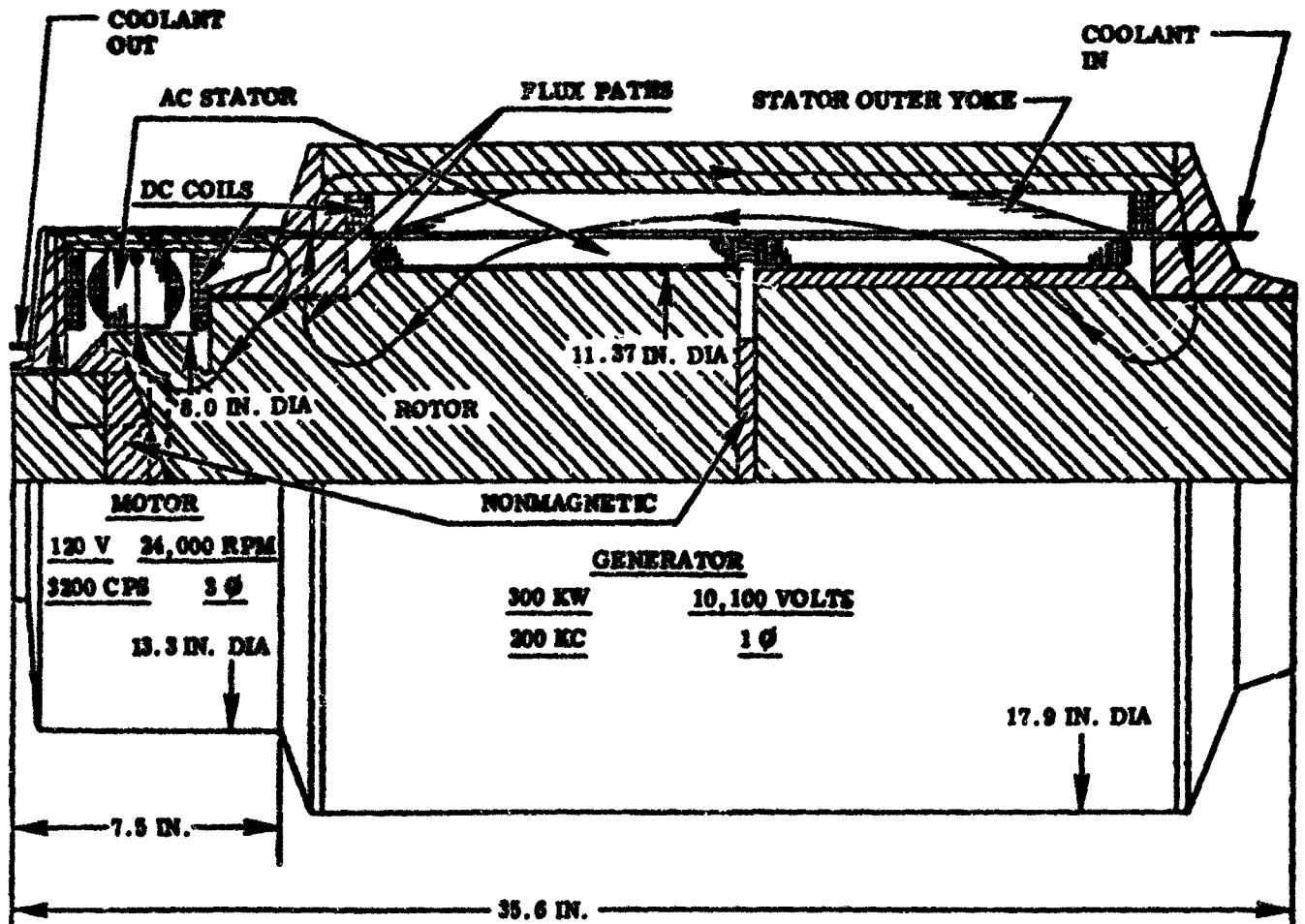


Figure 63. Preliminary Mechanical Design of 300 KW, 1 ϕ , 200 KC Motor-Generator

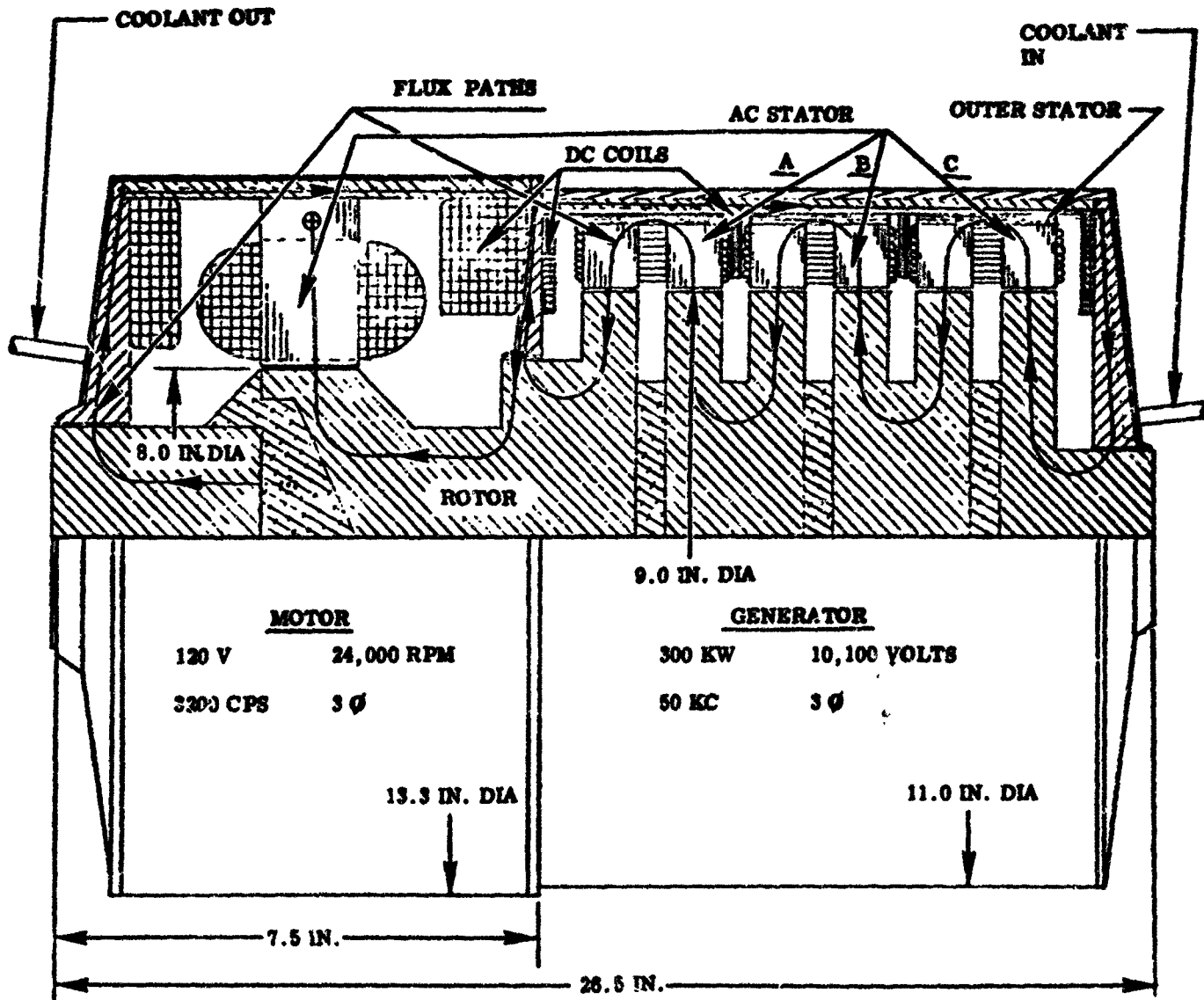


Figure 64. Preliminary Mechanical Design of 300 KW, 3 ϕ , 50 KC Motor-Generator

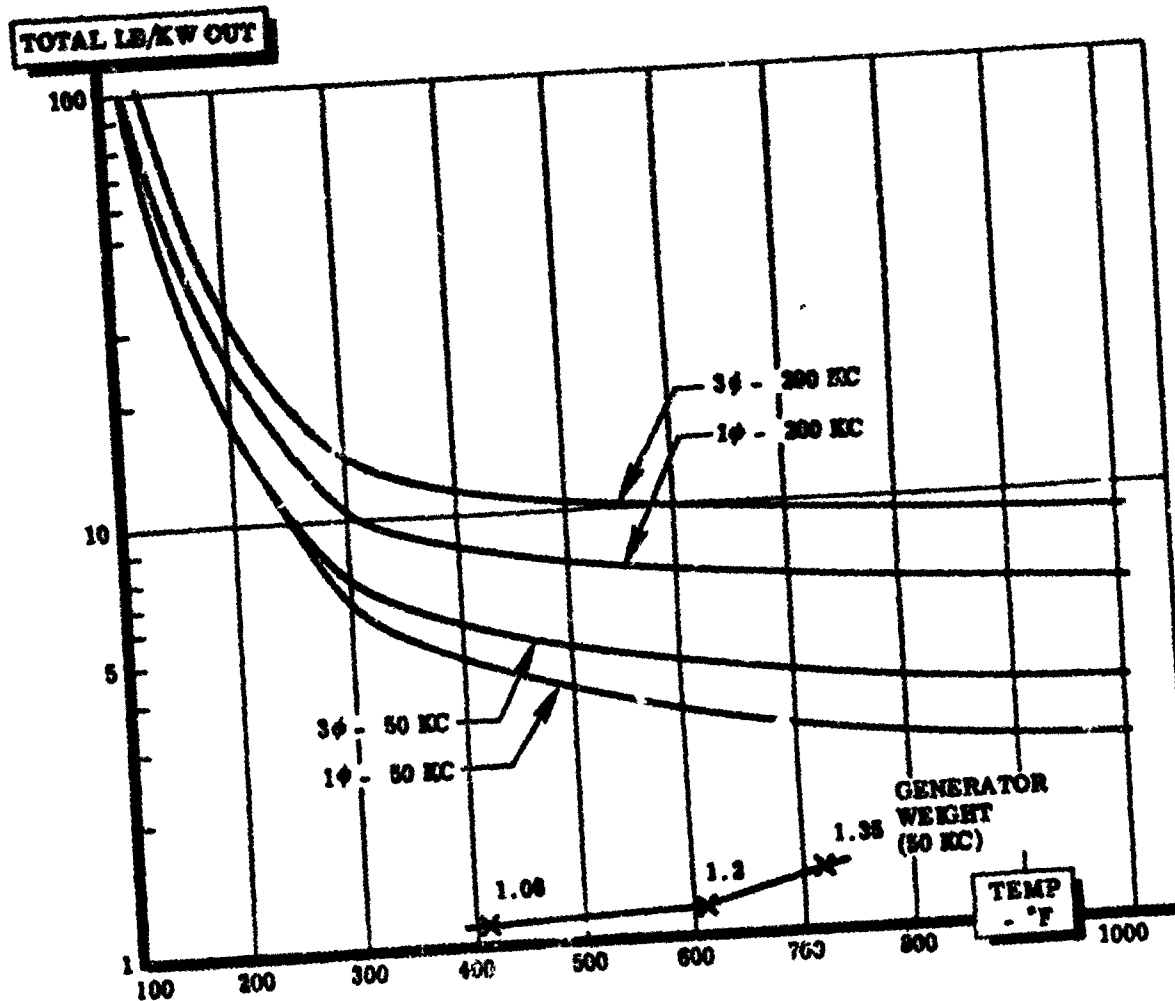
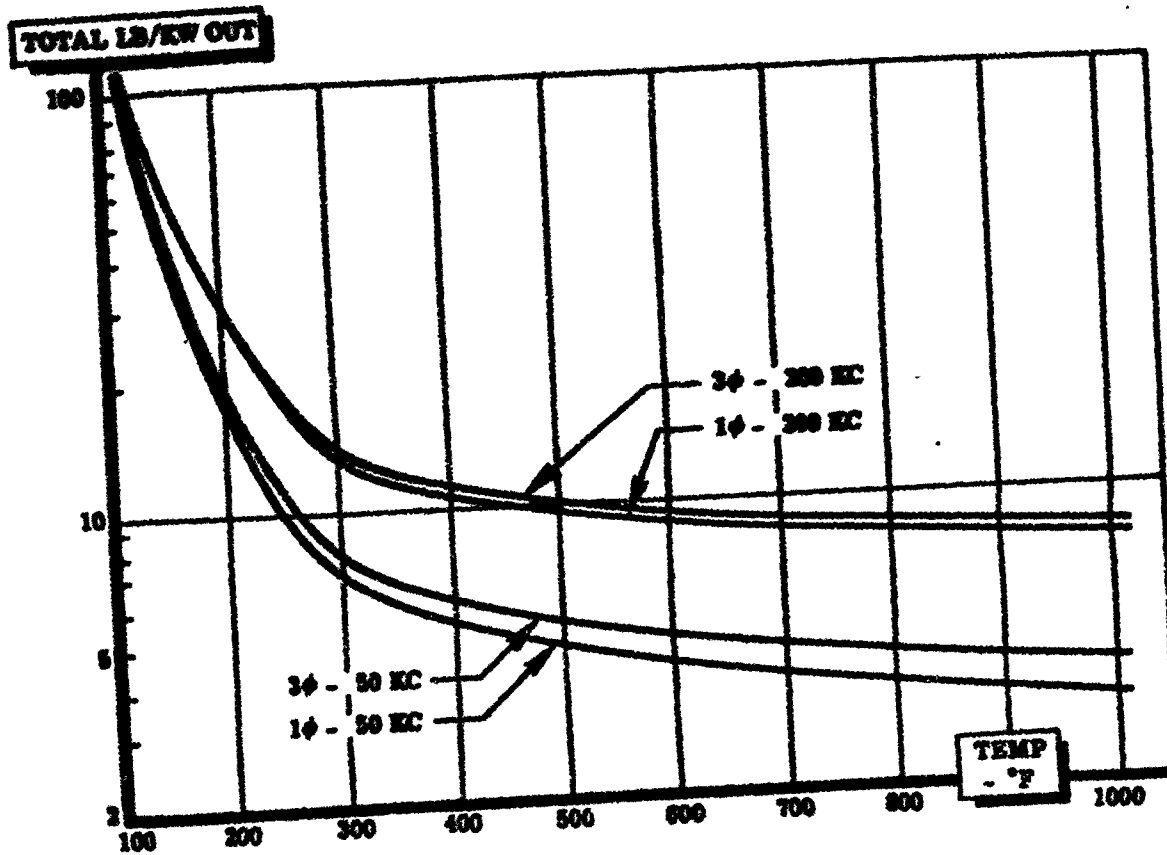
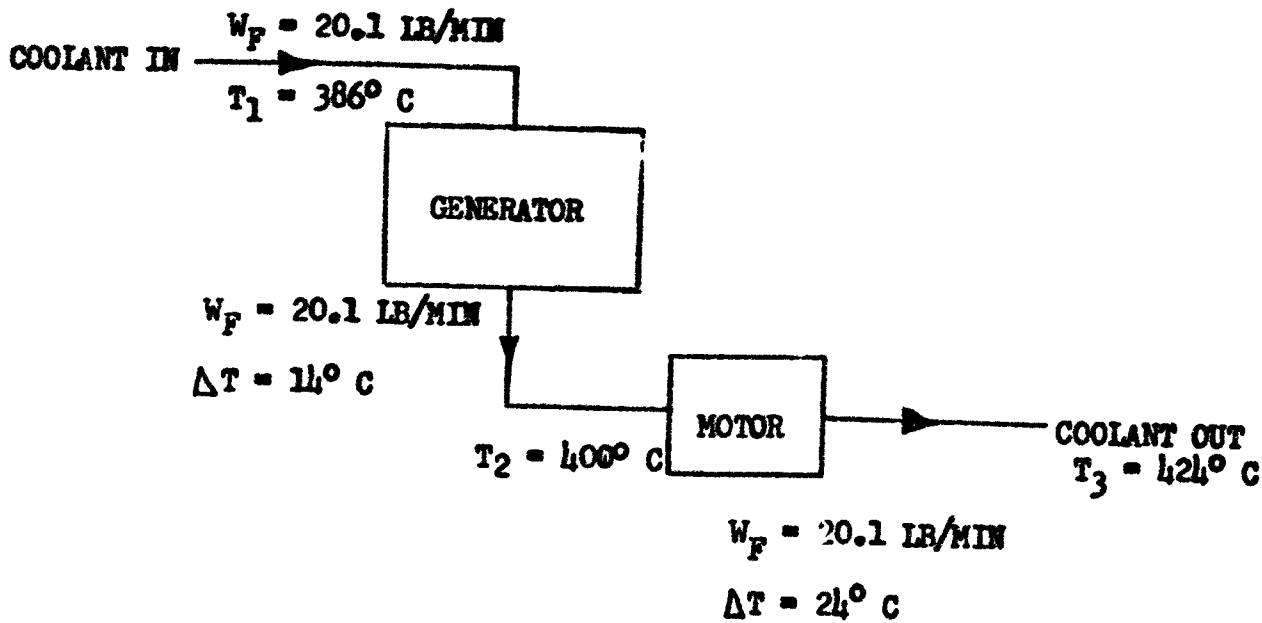
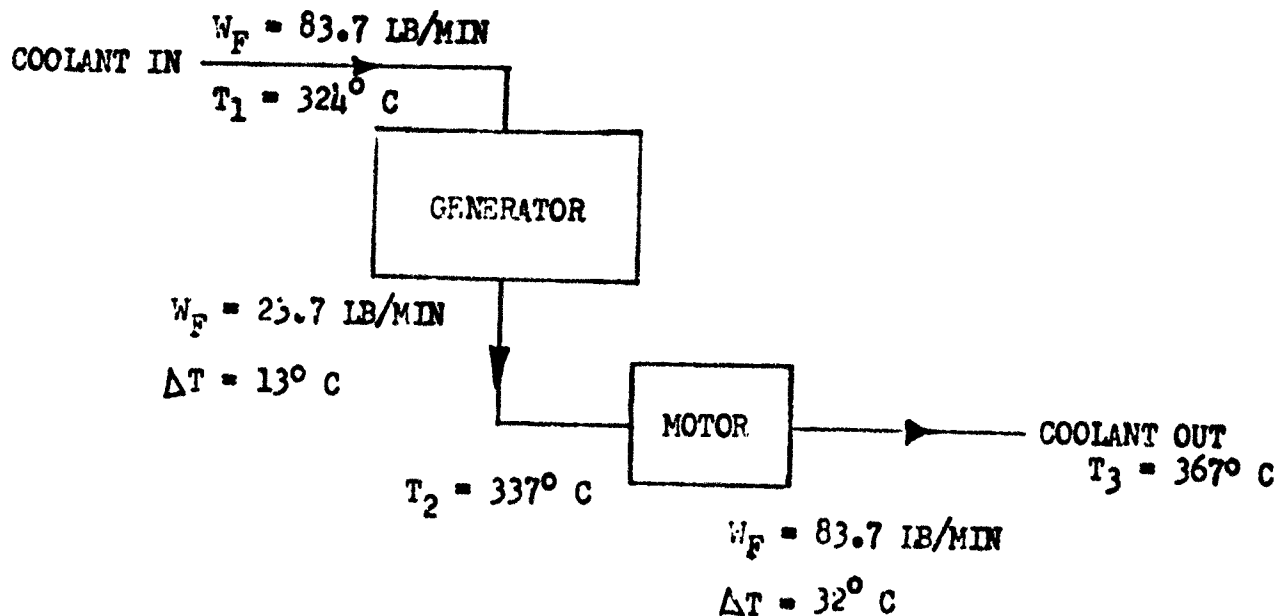


Figure 65. Analysis of System Weight vs. Temperature for Motor-Generator Converters



A 60 KW, SINGLE PHASE, 100 KC MOTOR-GENERATOR



B 300 KW, SINGLE PHASE, 50 KC MOTOR-GENERATOR

Figure 66. Thermal Flow Diagrams for 60 KW and 300 KW Motor-Generators

EFFICIENCY

EFFICIENCY VERSUS TEMPERATURE
90 KW, 50 KC, 30,000 RPM

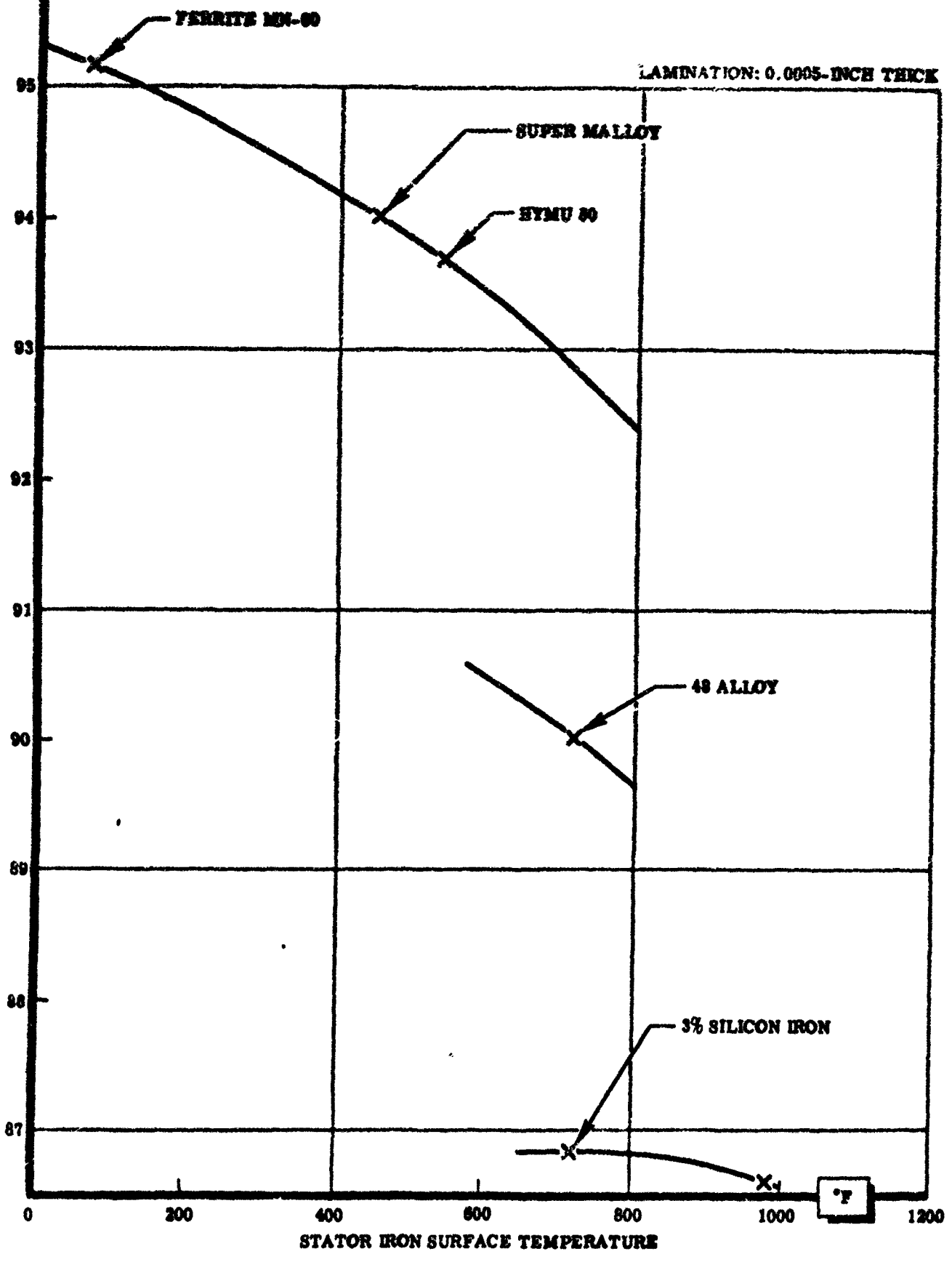


Figure 67. Efficiency versus Temperatures for Motor Generator Converters

to be used with resulting lower efficiencies. The efficiency versus weight curves for different magnetic materials (shown in section on 300 KW design) emphasizes the fact that there exists a maximum efficiency at a given frequency for each material. For any given material, weight may be varied for an increase in efficiency up to a maximum efficiency.

Stator Iron Losses - The iron losses at high frequencies (50 KC to 800 KC) become very important in the design of generators since they affect the temperature of the parts and the efficiency of the generator. The effect of frequency on iron losses, magnetic materials, and various lamination thicknesses are reviewed in a later section on materials. Only a limited amount of information exists on losses at the 50 to 200 KC level at elevated temperatures. Tests have been conducted as part of this program to determine the magnitude of these losses. Data is included in the experimental data section concerning this portion of the program and the magnitude of losses which can be expected at the higher frequencies.

Copper Losses - The conductor I^2R losses vary directly as a function of resistivity and the square of current density and indirectly with temperature. All the copper losses have been calculated for the same material resistivity and current density (see Table 15) in the stator winding and a lower current density in the field coils. These losses may be reduced by additional conductor material and weight. The increase in this loss due to increase in conductor resistance as a function of frequency (skin effect) can be minimized by using small diameter conductors in parallel.

Section III

HIGH FREQUENCY GENERATOR CONCEPT

OBJECTIVE

A portion of the program effort was devoted to investigation of conceptual designs for the generation of high frequency electrical power by rotary electromechanical machines and conversion techniques. (The high frequency term used in the discussion refers to a frequency higher than conventional power frequency and in the range of 50 KC to 800 KC). The mechanical shaft power available for use in this generator design was 500 hp at 24,000 rpm. The electrical power requirement was for 50 KC, 100 KC, and 200 KC, single-phase, 10,100 volts. Design objectives included efficiency of not less than 85 per cent and overall weight of 1,500 pounds. The shaft temperature was considered to be 1,000°F and the generator life expectancy objective was 10,000 hours.

BASIC DESIGN APPROACH

This generator design is similar to the generator design considered for use in the 300 KW motor-generator converter concept and is to be driven directly from a turbine. Figure 68 illustrates the basic generator concept considered for this 50 KC to 200 KC generator concept. The generator is a solid-rotor homopolar, inductor type operating at the specified 24,000 rpm. Note that the field windings are static and located on the stator. This particular type of machine was selected for this application after preliminary investigation of the various types of machines available for use. Analysis curves of frequency versus power output and estimated weight for this machine concept (Configuration B) are found in the section on Electromagnetic Generators. This type of solid-rotor generator possesses high rpm and high temperature capabilities, and is capable of operation above the 90 per cent efficiency level.

In comparing the weight of the generator in the converter system with this generator, the turbine driven generator system weight should be less than the weight of the motor-generator concept by the amount of motor weight required by the converter system. To be considered also is the fact that this generator design is based on a 500 hp input from the turbine which is really a 373 KW input. Performance and loss data for this design concept are summarized in Table 19 and 20 which follow for a 50 KC, 100 KC, and 200 KC high-frequency generator design. This data is based on inputs and outputs as shown in the block diagram which follows.

Specific details of a turbine driven generator to produce a 50 KC single-phase 10,100 volt output are shown in Figure 69. Figures 70 and 71 show pertinent details of the 100 KC and 200 KC designs. A thermal analysis follows the section on Mechanical Details.

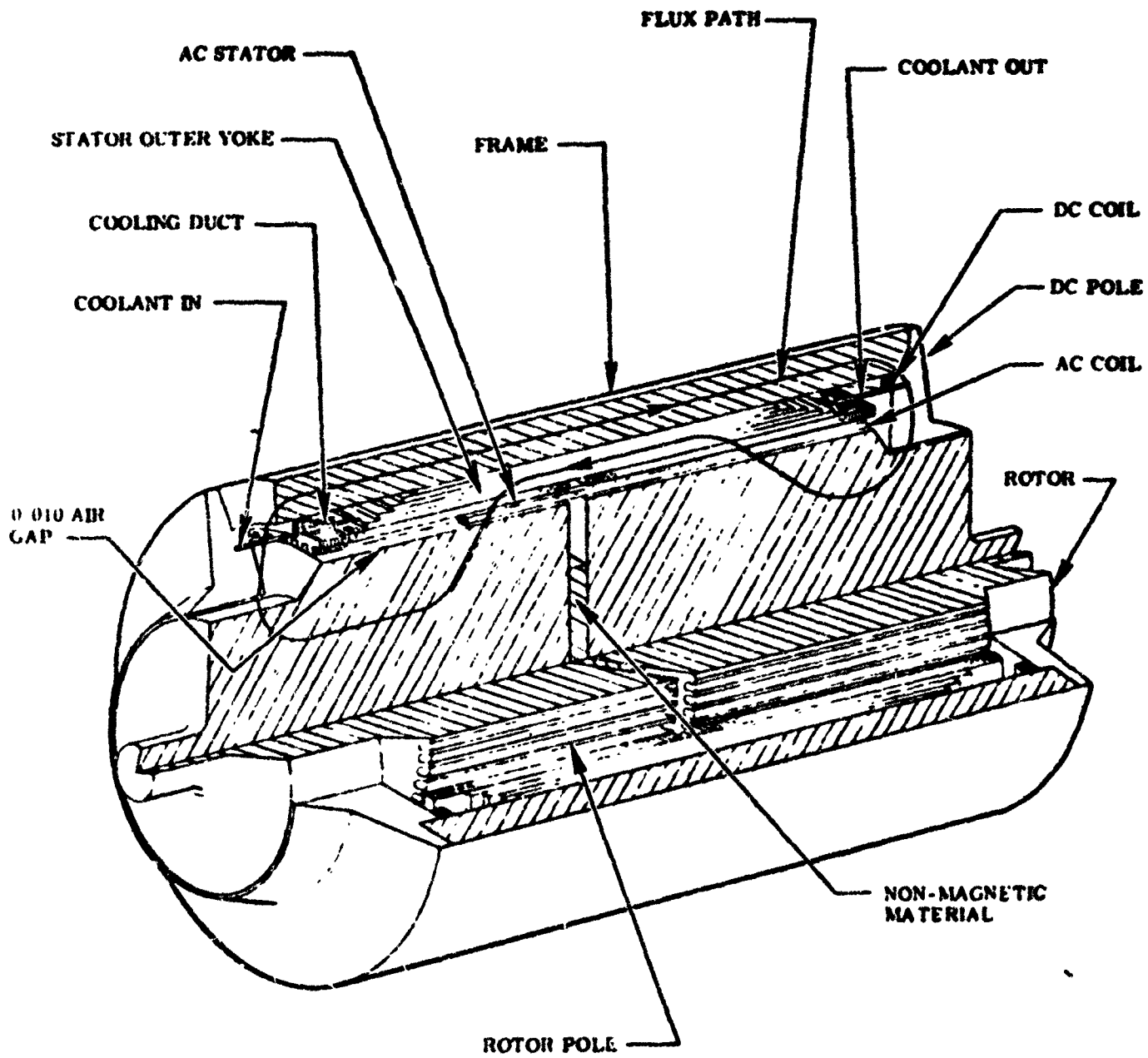


Figure 68. Basic High-Frequency Generator Configuration (Perspective)

TABLE 19**SUMMARY OF HIGH-FREQUENCY GENERATOR PARAMETRIC DATA**

1ϕ	50 KC	100 KC	200 KC
WEIGHT (lbs)	425	548	1525
KW RAD (Losses)	13.7	22.3	23.3
KW OUT	300	300	300
EFFICIENCY (%)	95.6	93.3	92.8
LENGTH (inches)	10.7	11	28
DIAMETER (inches)	15.8	16	17.9
VOLUME (cu. ft.)	1.2	1.3	4.1
LBS/KW RAD	31	24.6	67.2
LBS/KW OUT	1.43	1.83	5.08
NOTE: Values do not include cooling system weights			

TABLE 20
HIGH FREQUENCY GENERATOR DESIGN DATA
(300 KW)

	50 KC 1ϕ		100 KC 1ϕ	200 KC 1ϕ	
<u>Weight (lbs.)</u>					
Generator	400		523		1500
Controls	11		11		11
Cooling (Structure)	7		7		7
Bearings	7		7		7
Total (lbs.)	425		548		1525
	HYMU 80	48 ALLOY	HYMU 80	HYMU 80	48 ALLOY
<u>Lamination Materials</u>					
Thickness	.0005"	.0005"	.0005"	.0005"	.0005"
<u>Losses (Watts)</u>					
Stator Iron	5900	11300	12178	5600	8450
Stator I ² R	3240	3600	5028	6430	8700
Field I ² R	527	586	200	3640	3800
Windage	1019	1019	1870	4650	4650
Stray Load	3000	3000	3000	3000	3000
Total (Watts)	13686	19505	22,296	23,320	26,600
<u>Generator Efficiency (%)</u>	95.6	93.1	93.3	92.8	92.0
<u>Other Data</u>					
Aug. Stator Tooth Flux Density in Kilolines/Square Inch in Gausses	22.8	22.8	15.5	15.8	15.8
Stator Conductor Current Density in Amperes/Square Inch	3540	3540	2360	2400	2400
Field Conductor Current Density Amperes/Square Inch	6400	6400	6400	6400	6400
Conductor	28 NI	Clad Cu.			
Curie Temperature °F	860°	932°	860°	860°	932°

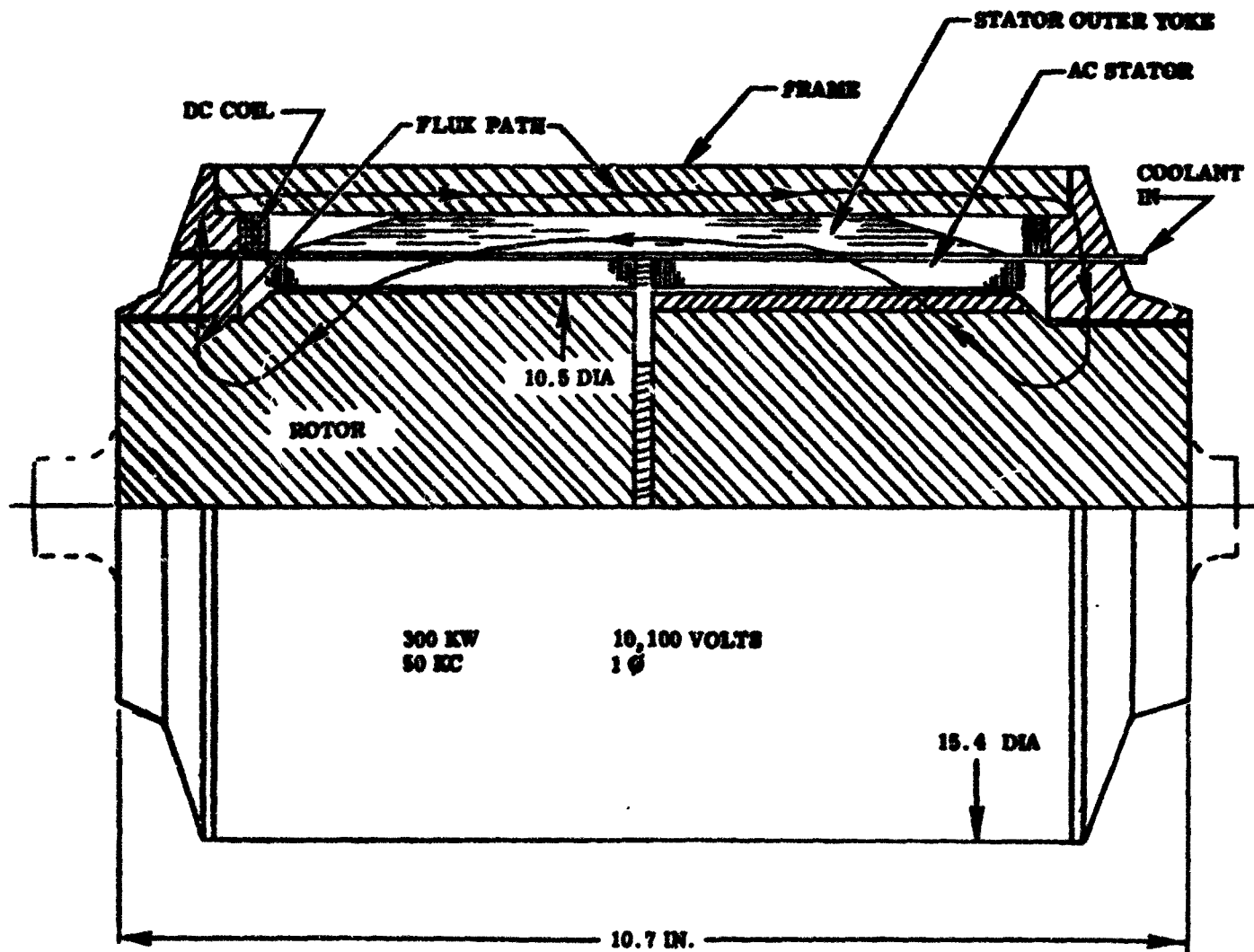


Figure 69. Preliminary Mechanical Design of a 50 KC High Frequency Generator

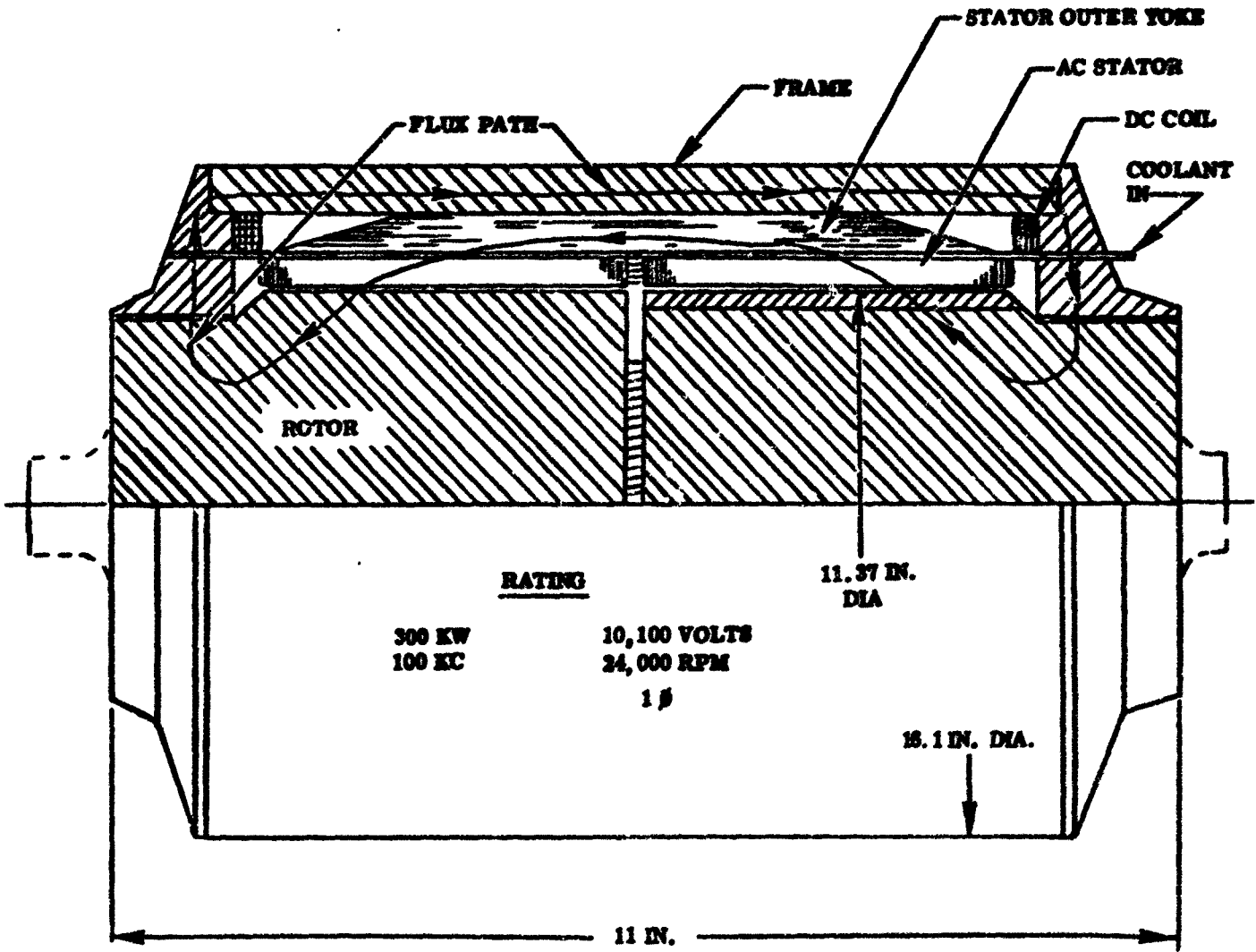
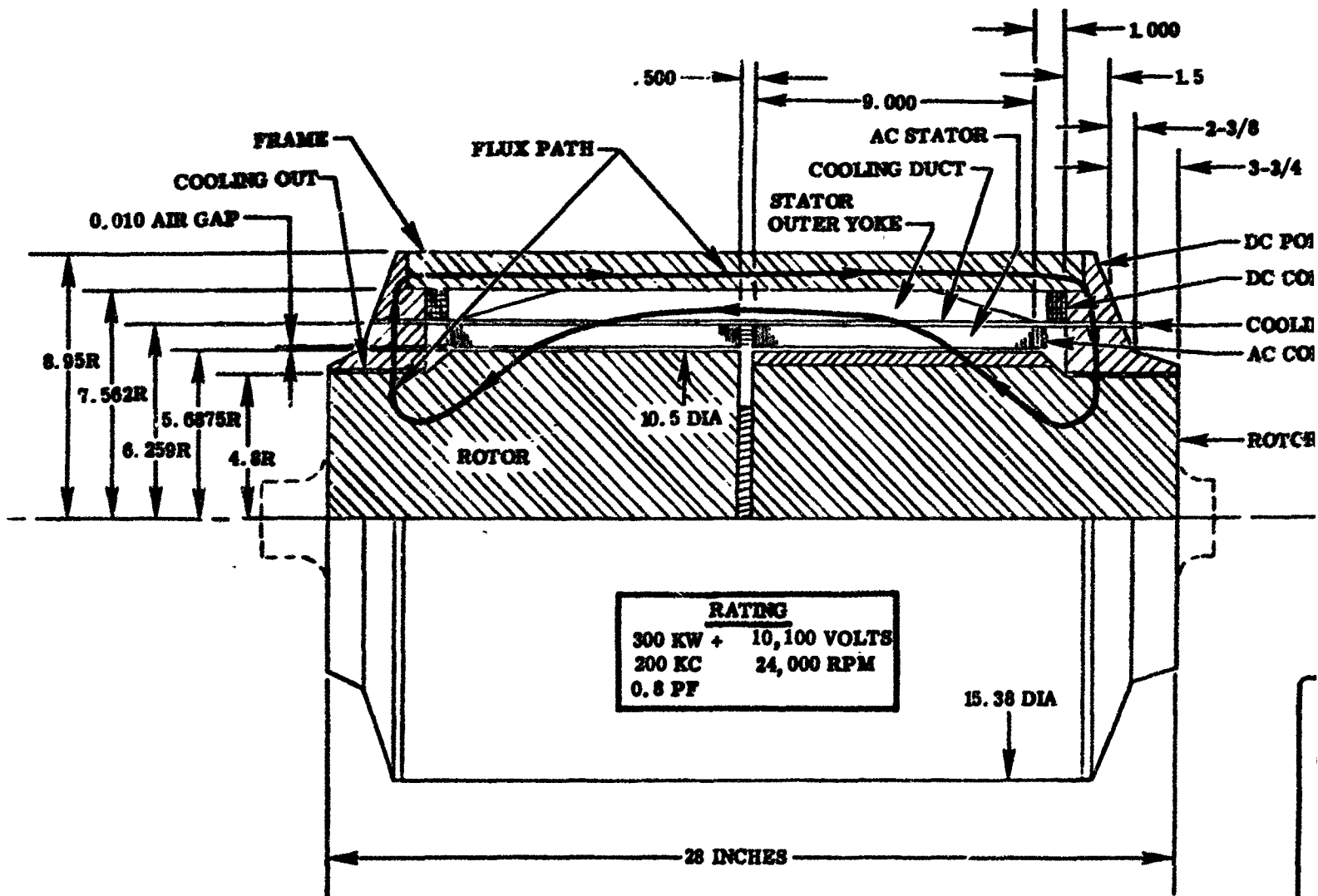
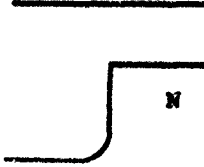


Figure 70. Preliminary Mechanical Design of a 100 KC High Frequency Generator



RATING	
300 KW +	10,100 VOLTS
200 KC	24,000 RPM
0.8 PF	

SECTION A - A



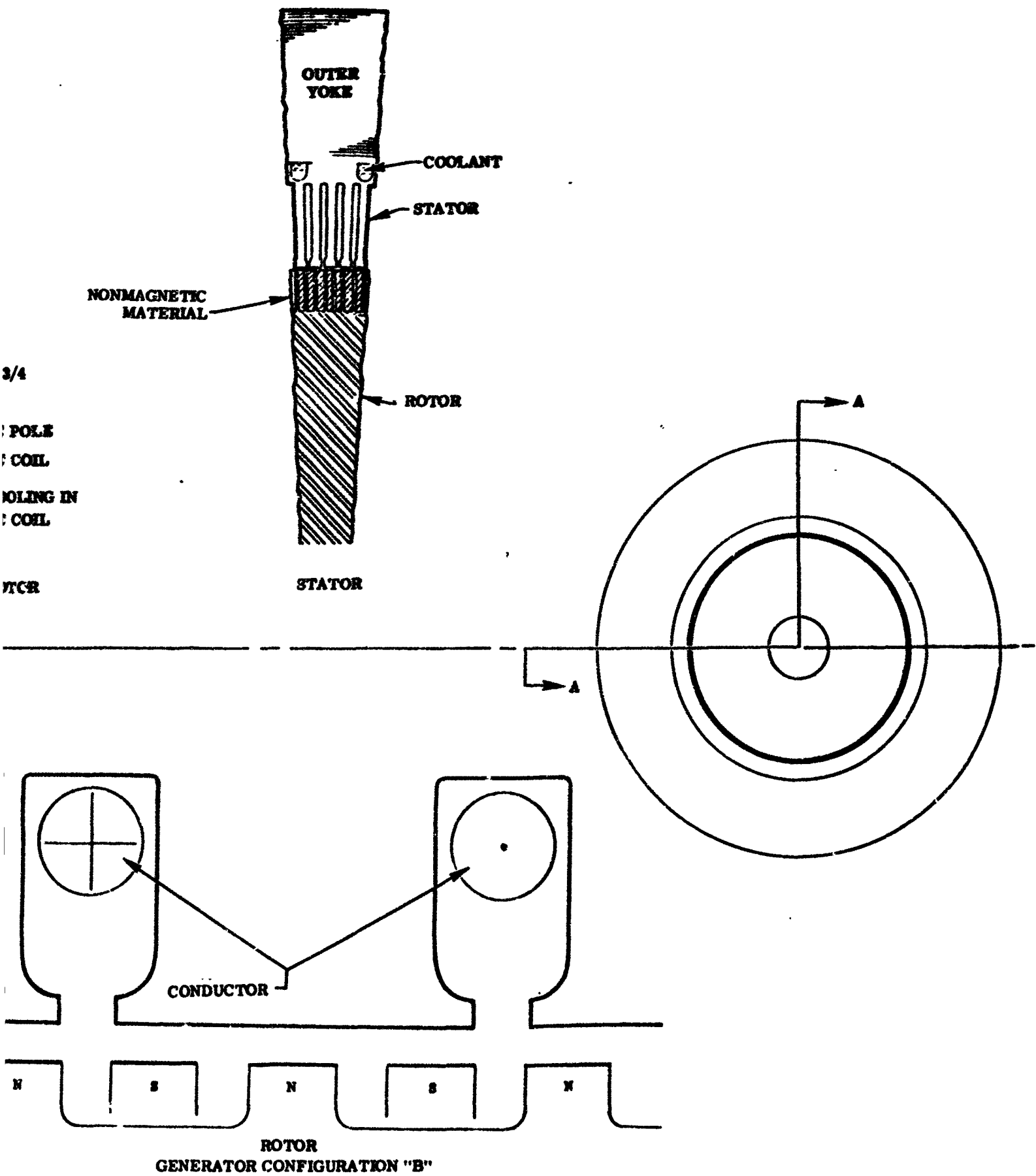
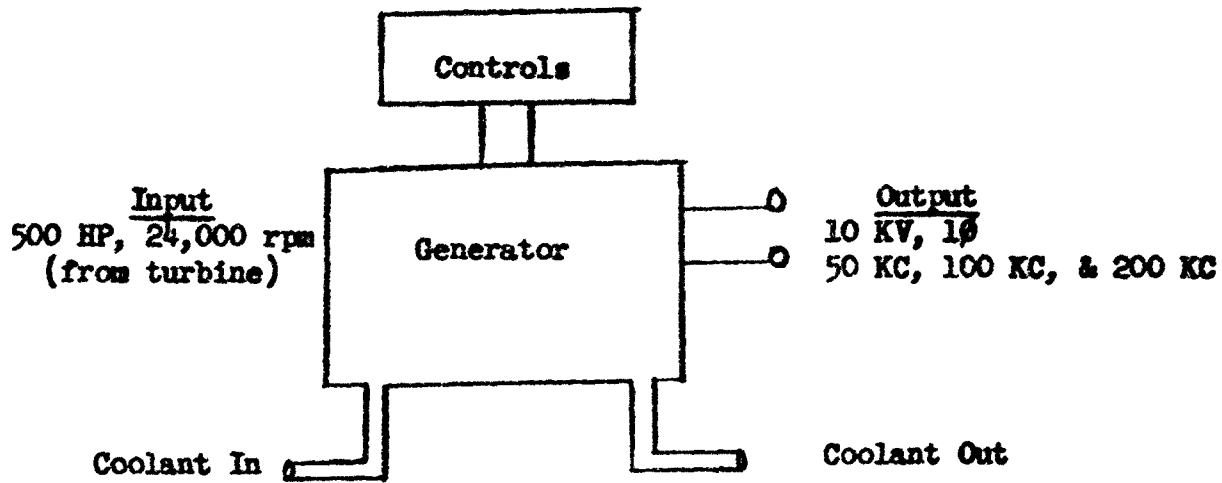


Figure 71. Preliminary Mechanical Design Details of a 200 KC High Frequency Generator



GENERATOR DETAILS

Stator Rotor Relationship

Figure 71 shows the relationship between rotor poles and stator slots for the proposed generator. The south poles of the rotor are displaced axially from the rotor north poles. The stator slots are so chosen that adjacent stator slots are located one for every three poles of the rotor (counting both north and south poles). A stator slot may have a maximum width of a pole pitch, the distance from the center of a north pole to the center of a south pole. This places the slots so that the induced voltages are in opposite directions in adjacent slots. A view of Figure 71 shows cross sections through the generator.

Rotor - The rotor is made of a high-strength, solid magnetic material and the outer circumference is slotted to form poles similar to gear teeth. The teeth in one section are displaced 180 electrical degrees from the teeth in the other axially displaced section as shown in Figure 71. The depth of a rotor slot depends on the air gap between stator and rotor teeth. The slot depth must be sufficient to reduce the flux from the slot to one stator to a low percentage of the flux from the teeth to the stator. The two sections of the rotor are spaced by a nonmagnetic material to minimize flux leakage between the north and south section.

The flux in the rotor is a DC flux and produces no loss during steady-state operation. A ripple flux in the pole tips will produce some losses; this loss may be reduced by reducing the stator slot opening to less than the width of a rotor tooth to prevent the flux from changing in the teeth.

Outer Yoke - The outer yoke carries the flux from the north stator section to the south stator section. The flux rotates in the outer yoke at the same speed (rpm) as the rotor is turning. It is an unchanging flux for any load condition. The outer yoke as shown in a tape wound core and very little loss is generated by a constant spinning flux. The outer yoke

lamination may be from a thicker and higher loss material than the stator iron, and could be operated at higher flux densities.

Stator Iron - The stator iron is subjected to a pulsating flux of the generating frequency of a single polarity in each stator section. The flux rotates in the yoke section of this lamination at a rate the same as the rotor speed (rpm) and is pulsating at the generating frequency. This material must be of a low-loss magnetic material and of very thin laminations to minimize iron losses at high frequencies. Laminations of .001 inches and .0005 inch thickness have been considered in this design. The flux density must also be at reduced values to minimize losses at high frequencies. Ferrites are usable for this core, but limit the operating temperature to lower values than are achievable with nickel-iron alloy laminated cores.

OTHER DETAILS

The most difficult area of generator manufacture is in the assembly of the AC stator section parts. As the use of thin laminations (.0005 to .001 in.) is desirable, methods for assembly of the laminations would have to be developed. One solution is to fabricate the laminations from .001 inch laminations which have been built up from bonded layers of thin lamination material in the sheet form. If this were done, then fabrication can easily be accomplished as if .010" thick laminations were being used. Other manufacturing operations may be accomplished using techniques which have been developed for manufacture of generators and motors for other applications.

The mounting and coupling of generator to turbine may be accomplished by presently developed methods and requires coordination with the turbine manufacturer.

THERMAL ANALYSIS

Cooling - The cooling system of the high-frequency generator unit is made up of thin parallel tubing located in the stator yoke. The parallel tubes converge into a collection ring at each end. Due to the short length of coolant tubing, multiple coolant passes may be required in order to achieve a reasonable value of ΔT without resorting to unrealistically small tubing. Heat is removed from the stator to the coolant fluid by means of conduction. High-frequency generator units are capable of operating at temperatures above 1,000°F, but designs considered here are based on coolant temperatures in the 500°F to 800°F range. As part of the generator system thermal analysis, data was plotted in Figure 72 to show the effect of system operating temperature on generator system weight. Calculated electrical losses for a 50 KC and 200 KC unit and other thermal design data, including efficiencies for 48 Alloy and HYMU 80 materials, are shown in Tables 19 and 20. Figure 73 is included to show coolant flow requirements for a typical 50 KC design. Coolant flow rates and coolant temperature rise will vary from design to design of a given size of generator. Since iron losses are a function of flux density, iron volume, frequency, and material used in the laminations, various magnetic materials must be considered in the design.

TOTAL LB/EW OUT

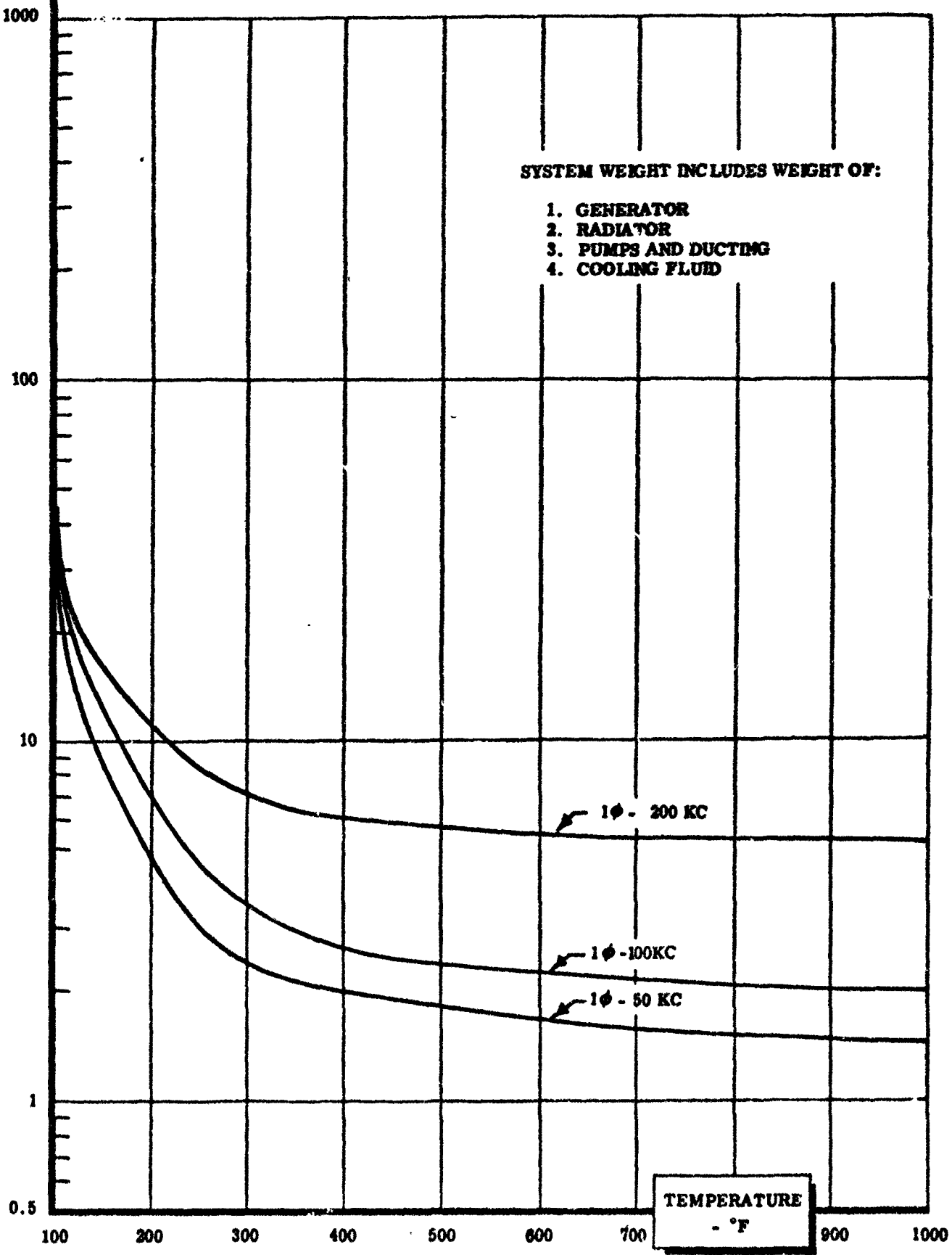


Figure 72. Analysis of System Weight vs. Temperature For High Frequency (50 to 200 KC) Generator

SINGLE PHASE, 50 KC GENERATOR (500 HP INPUT)

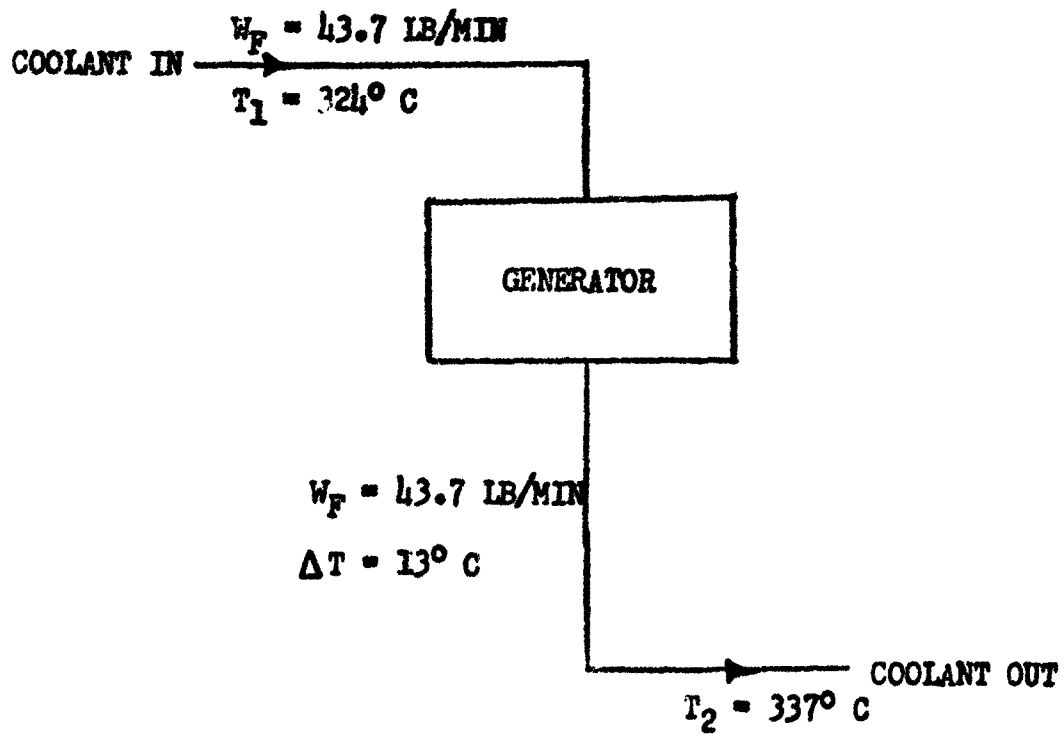


Figure 73. Thermal Flow Diagram for High Frequency Generator

Substitution of 48 alloy for the HYMU 80 in the 200 KC, single-phase, 300 KW generator as shown in Table 20, would increase the total losses by more than three KW. Such an increase would require increased coolant flow to maintain the same coolant ΔT .

Efficiency - Efficiency of the generator is reduced as the temperature of the generator iron increases. Figure 74 indicates the manner in which the efficiency changes as a function of temperature for a 300 KW, 200 KC design. HYMU 80 material in .0005 inch laminations can be used to nearly 600°F stator iron surface temperatures with a calculated efficiency of 93.3 per cent (Table 20). Alloy 48 is shown on the efficiency versus temperature curve at a lower efficiency and has been considered for use because of its lower weight. If higher operating temperatures are required, the silicon irons will have to be used with resulting lower generator efficiencies. Before a generator design can be finalized, effort must be expended to give an indication of efficiency versus weight trade-off potentials.

Efficiency Versus Weight - The calculated values of efficiency versus generator weight are plotted on Figure 75. These curves were obtained by varying magnetic flux densities. It can be seen that for a given frequency there exists a maximum value of efficiency which is also a function of magnetic material employed in the design. The highest efficiency can be achieved by using HYMU 80 in laminations of .0005 inch thickness.

At higher temperatures where materials like HYMU 80 lose their magnetic properties silicon steels are employed. The higher unit volume loss results in lower efficiencies for the generator.

Stator Iron Losses - The iron losses at high frequencies become very important in the design of generators as they affect the temperature of the parts and the efficiency of the generator. The effect of frequency on iron losses, magnetic materials, and various lamination thicknesses are reviewed in a later section on Materials. Only a limited amount of information exists on losses at the 50 to 200 KC level at elevated temperatures. Tests have been conducted as part of this program to determine the magnitude of these losses. Data is included in the experimental data section concerning this portion of the program and magnitude of losses which can be expected at the higher frequencies.

Copper Losses - The conductor I^2R losses vary as a function of temperature, resistivity, and the square of current density. All the copper losses have been calculated for the same material resistivity and current density (see Table 20) in the stator winding and a lower current density in the field coils. These losses may be reduced by additional conductor material and weight. The increase in this loss due to increase in conductor resistance as a function of frequency (skin effect) can be minimized by using small diameter conductors in parallel.

Weight Versus Temperature - The curves of weight versus temperature show that the higher the operating temperature, the larger the generator. The increase in size or weight with temperature results from an increase in

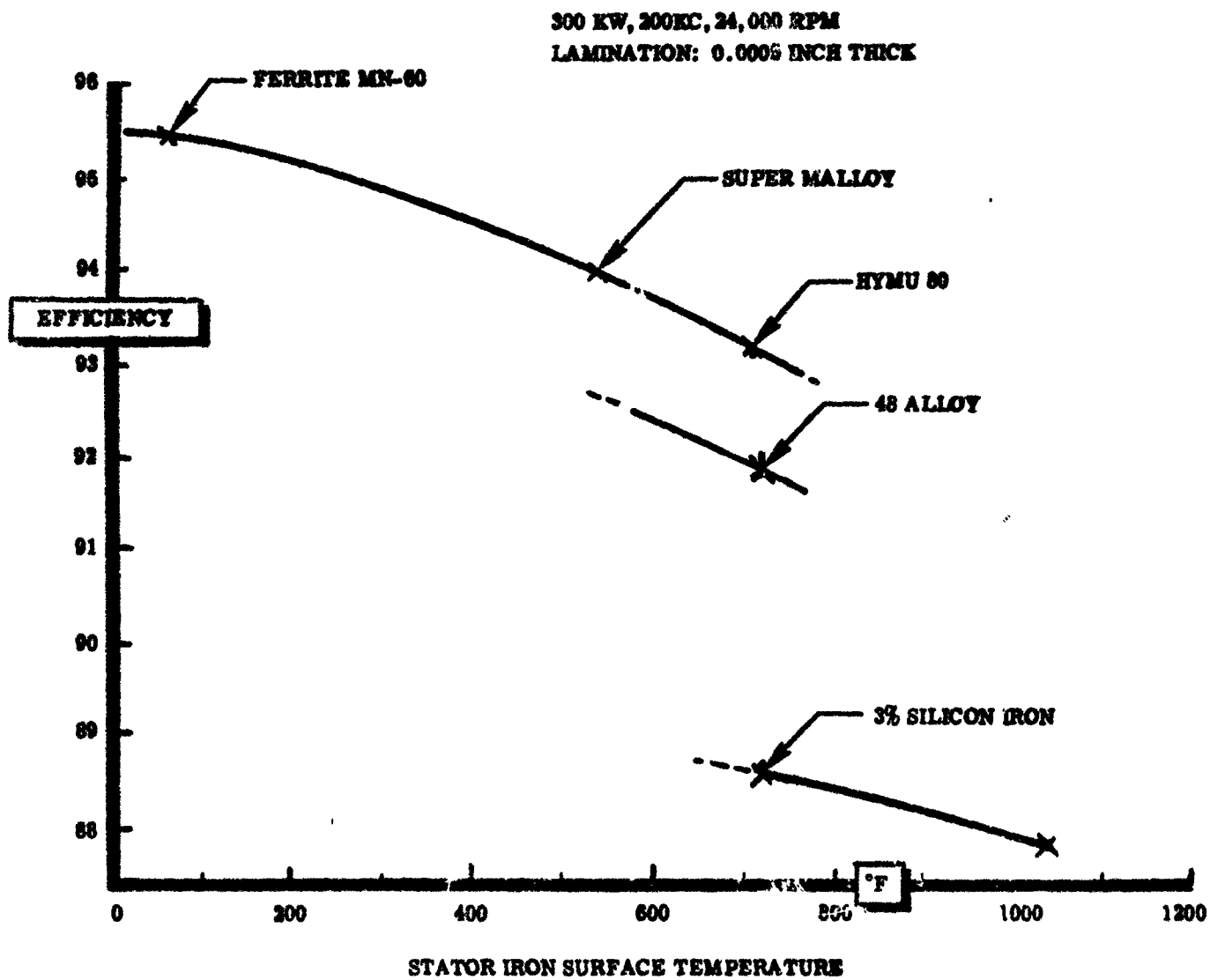


Figure 74. Efficiency vs. Temperature for High Frequency (50 to 200 KC) Generator

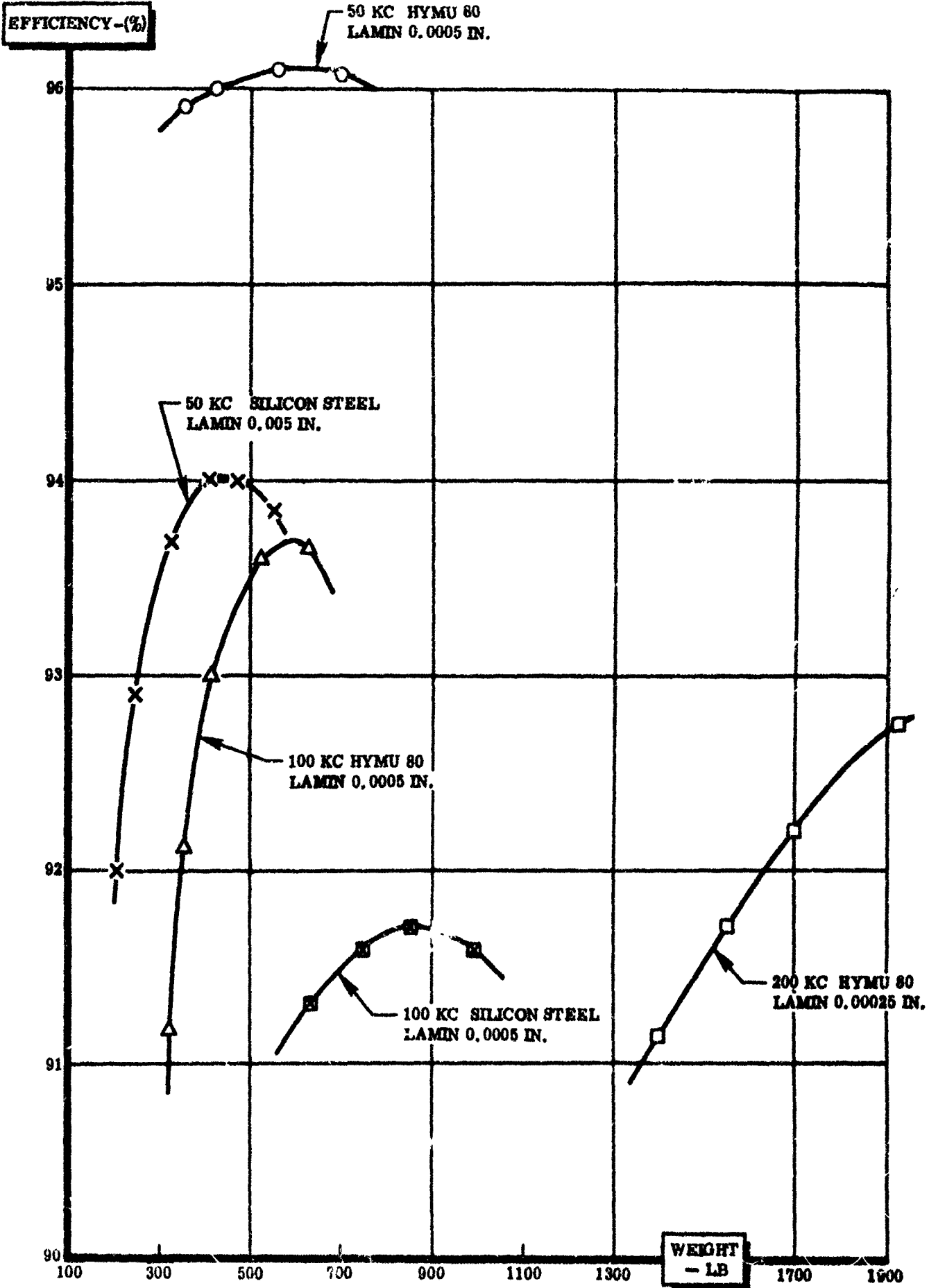


Figure 75. Efficiency vs. Weight for Various Generator Materials

magnetic material as a result of reduction in permissible operating flux density as temperature is increased for any given magnetic material. Lower weights can be obtained at the higher temperatures by changing to the use of higher loss materials which have higher allowable flux densities and Curie temperatures. As a result, the weight versus temperature has several slopes; one for each material considered, and can remain constant over a temperature range for high flux density material which is being utilized at a low value to minimize losses. Specific weight versus temperature curves for HYMU 80 and silicon steel are shown in Figures 76 and 77.

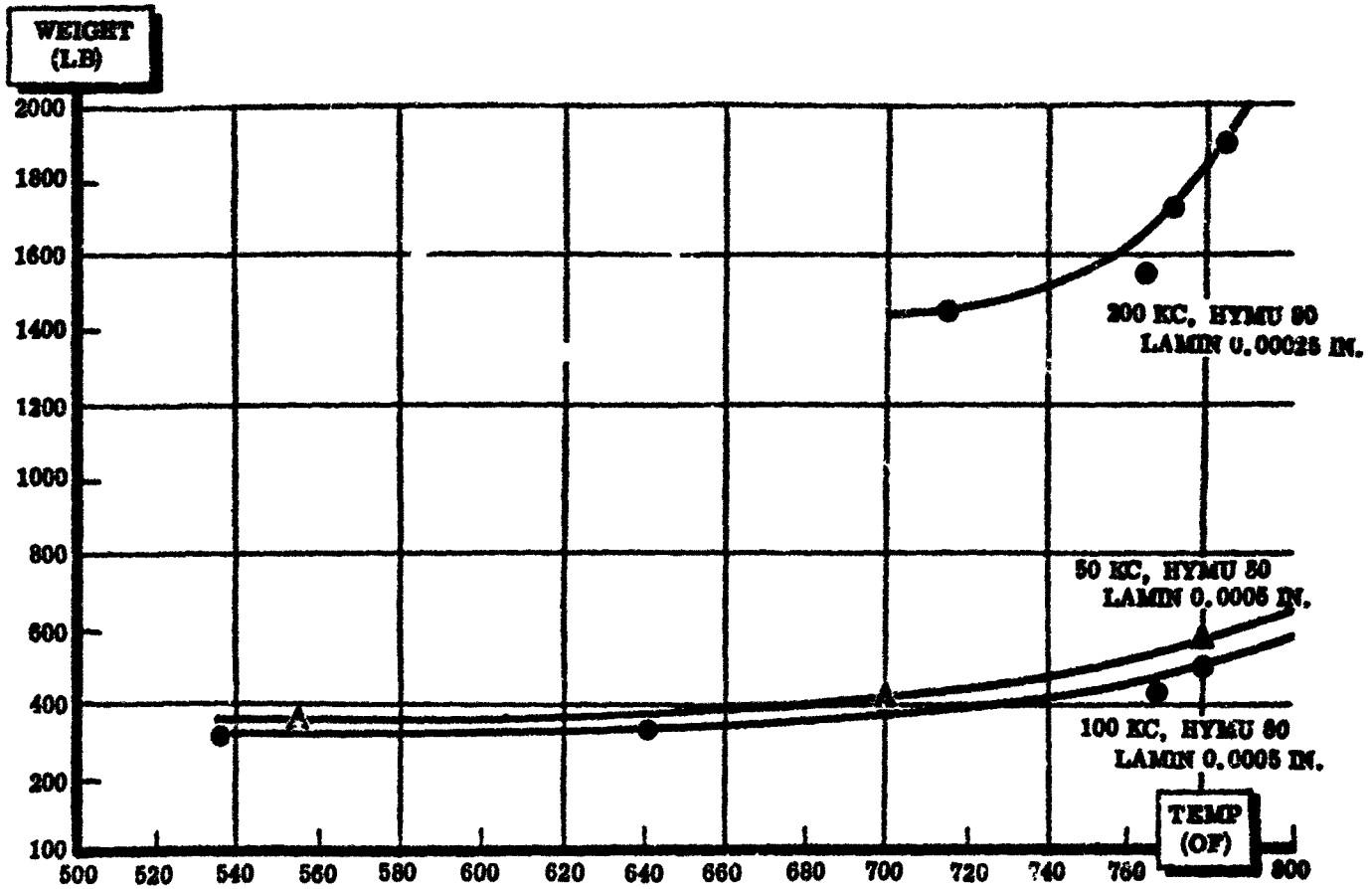


Figure 76. Weight vs. Temperature for HYMU 80 Material

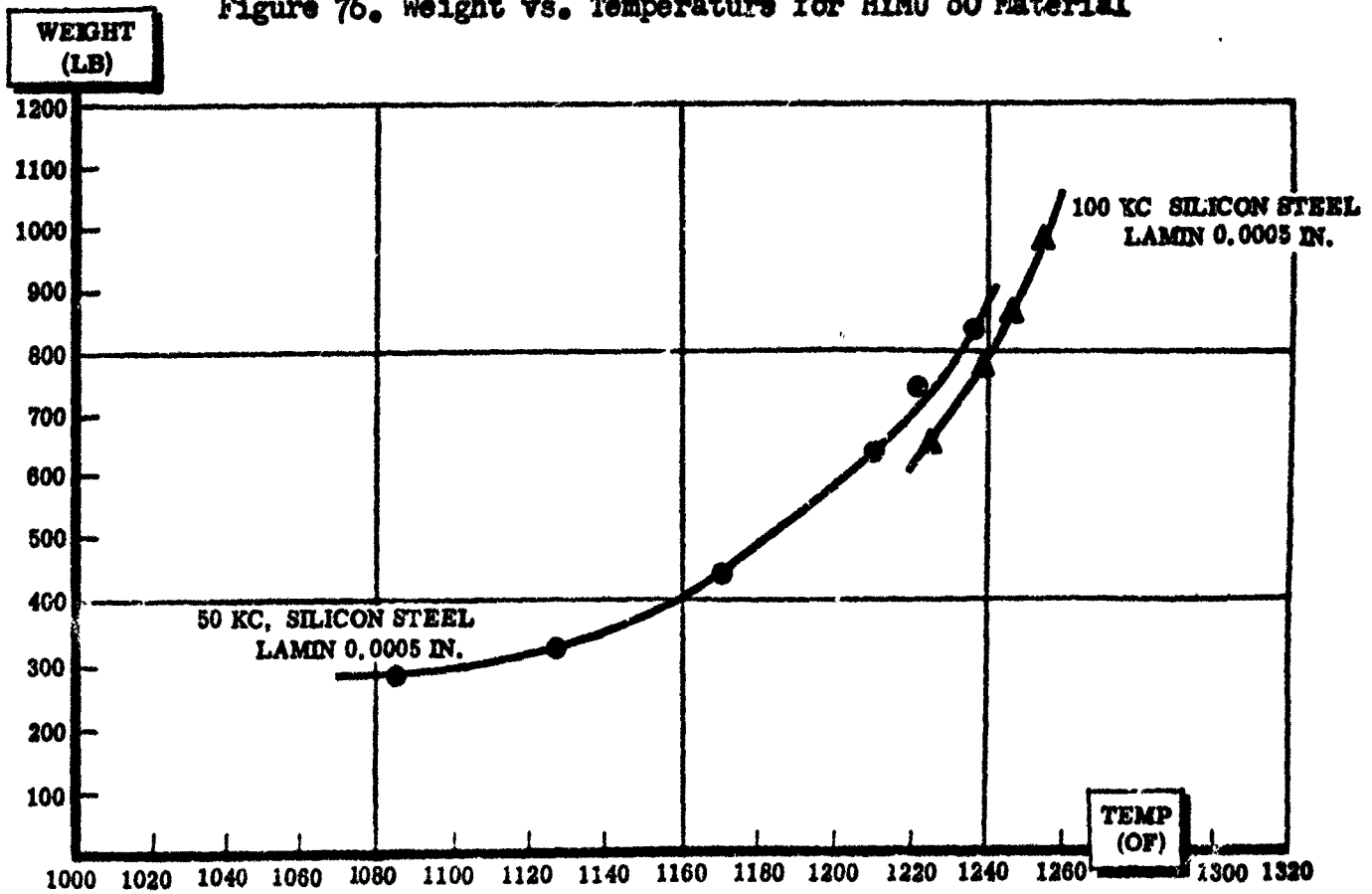


Figure 77. Weight vs. Temperature for Silicon Steel

Section IV

RELATED STUDIES

INTRODUCTION

This section is included in the report as additional information affecting the design of the converter and generator conceptual designs resulting from the study. This information supplements the information in the opening section of generation and conversion techniques and information contained in each of the conceptual design sections.

Specific information is divided into the following areas and a discussion of each is found in the section which follows:

1. Environment
2. Approach to system cooling
3. Analysis of materials
4. Radiation resistance of converter components
5. Reliability

ENVIRONMENT

Analytic studies have touched mainly on problems of temperature, radiation, corrosion, and vacuum. Others considered are listed below and involve prelaunch, natural and induced environmental conditions.

Pre-launch Environment

Corrosion
Extreme Temperature

Natural Environment

Ambient Temperature

High Vacuum

Solar Radiation

Ionized & Dissociated Gases

Van Allen Radiation

Nuclear Radiation

Induced Environment

Mechanical Vibration

Acoustic Vibration

Acceleration

Temperatures

Shock

ENVIRONMENT (NATURAL)

Ambient Temperature - Sources of heat which influence the ambient temperature in a major way are thermal radiation from direct sunlight and heat generated within the equipment itself. The solar constant is 2.0 calories/sq. cm-min. at the earth's mean distance from the sun. Since heating and cooling of equipment in space is by radiation only, the problem of controlling ambient temperature is a major one.

The effects of increased ambient temperature in power conversion equipment are:

1. Loss of mechanical integrity.
2. Leakage of sealed units, particularly at the union of dissimilar metals.
3. Material expansion, metal creep, and fatigue.
4. Material sublimation.

Design countermeasures involve use of absorptive and reflective surfaces, separation of equipment into temperature range categories, and use of radiation and conduction heat transfer cooling techniques. A standard consideration is the use of heat-resistant materials wherever possible.

High Vacuum - At 10 to 120 miles above the earth, atmospheric pressures represent partial space equivalent. Beyond 120 miles pressures are from 1.5×10^{-6} mm of Hg to an estimated 1.5×10^{-12} for outer space in the solar system.

Arc-over and corona discharge are to be considered in space in addition to boiling of liquids at lower temperatures, vibration problems due to lack of air for damping, explosive decompression of hermetically sealed units and sublimation and evaporation of inorganic materials. In sealed units that are not vacuum-tight, more volatile materials may evaporate from hotter parts and condense on colder ones as thin films. Outgassing can have corrosive, plating, and chemical effects. It is known that certain nylon, polyesters, and epoxies lose up to ten per cent of their weight per year in a vacuum at slightly above room temperatures.

Materials for use in a power conversion system must have low sublimation rates. Insulating materials must adequately provide protection from arc-over and corona discharge, as well as resist sublimation and also have high temperature capabilities.

Solar Radiation - For equipment that may undergo long exposure periods to solar radiation, extra shielding of semiconductor devices is required. The most significant effect of solar radiation appears to be on organic materials in the ultra-violet band below 2,400Å. Rubbers and polyesters are susceptible to damage.

Ionized and Dissociated Gases - These gases form at altitude as solar radiation changes chemical activity of normal gases. Hypersonic flight can also induce temperature extremes within a vehicle which can produce dissociation and ionization of gases. In altered or excited state, dissociated gases may have highly accelerated oxidation rates. These gases can do actual damage to equipment, e.g. monatomic oxygen reacts very readily and rapidly (forming oxide) with materials like Fe, Fe oxides and alloys, Cu, Ag, and many organic materials.

Design techniques to offset this environmental limitation include protective coatings for susceptible parts and sealing of compartment after all the air has been evacuated from both the compartment and individual packages.

Van Allen Radiation - Significant damage to semiconductors can be expected in magnetic and semiconductor devices only after prolonged exposure. For prolonged exposure times, shielding of this type of component is required. Figure 78 indicates the electron and proton intensity to be encountered in typical earth orbits.

Nuclear Radiation - Natural space radiation and neutrons, alpha, beta and gamma rays from primary and secondary power plants must be considered in power conversion unit design if resistors and semiconductors are used. Resistances decrease with releases of new current carriers or may increase with production of new scattering centers.

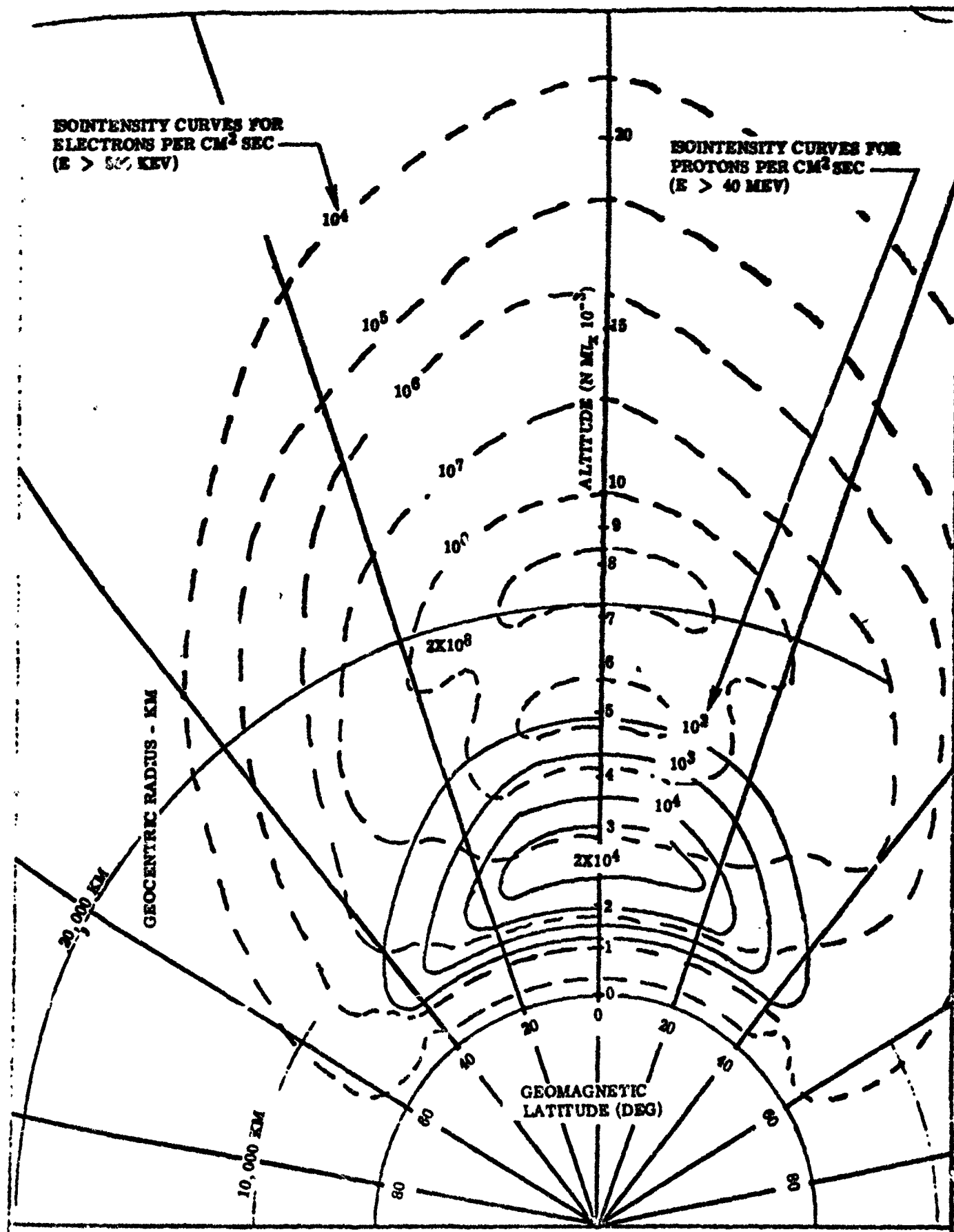
Shielding and selection of radiation - resistant components are measures to be used to offset the effects of nuclear radiation. Semiconductors must be protected from radiation. Recommended components to be used include; ceramic and subminiature tubes; ceramic, glass and mica capacitors; wire-wound resistors, ceramic and other organic insulators and glass-bonded mica connectors.

ENVIRONMENT (INDUCED)

Mechanical Vibration - Power conversion units designed for space vehicles with boost glide, low orbit flight profile, or restart capabilities may be subjected to frictional or combustion vibration problems. Otherwise, except for the launch environment no serious electrical or mechanical design problems are contemplated.

Methods which will aid in overcoming mechanical vibration include specifying the use of module type of packaging, particularly the solid or potted types, selection of equipment with high mass-area and high stiffness-mass ratios, requiring all free space in packages be filled with foam or denser materials, and requiring that all suspension mounts be of the isoelectric type.

Acoustic Vibration - Fluctuating sound pressure fields generated by rocket engines during the launch boost phase are of primary concern to designers of electronic components and other equipment for space vehicles. Of



secondary importance is boundary-layer turbulence. Acoustic stresses, which would occur only in very exceptional cases in space, never approach the intensity of those in the boost phase.

Some of the average sound levels commonly associated with space vehicle launches are:

1. Payload and nose-cone electronics of ballistic missiles and boosters, 155 db.
2. Booster compartment and pods at sides of booster, 165 db.

Generally the same design methods used to dampen mechanical vibration apply as countermeasures for eliminating acoustic vibration.

Acceleration - A potent threat to suspended units and elements during the launch and boost period are forces resulting from acceleration. Major sources of sustained acceleration for these converter units is booster propulsion during launch.

Predicted sustained launch and boost accelerations for space vehicles are 8 to 100 g's.

Here again measures taken to alleviate vibration problems will provide good solutions for acceleration problems. In general, substitution of solid devices and components for those in which dynamic balance or orientation is critical will solve the problem.

Temperature - The main induced thermal stresses affecting components in space vehicles are self-generated heat, frictional heating, and internal gradients. Damage to components and materials can also occur due to thermal shock at temperatures lower than the 800°F limited to the best items now available. Another formidable problem is posed by the internal heat expected from vehicles with nuclear engines. Design will involve considerable effort on radiation and conduction heat sinks since they are the most practical methods of heat transfer in space.

Shock - The problem posed here, similar to that noted previously for mechanical and acoustic vibration, is one of severe stresses which occurs only during the launch and boost phase. The difference between shock and vibration is one of degree. Shock can occur as abrupt change in magnitude or direction of velocity or in previously steady applied force. Levels at which it will occur depend on the type of vehicle flight profile and condition and methods of packaging. Shock level of 25 to 50 g's can be expected with booster separation raising this to 200 g's for one to two milliseconds.

APPROACH TO SYSTEM COOLING

THERMAL ANALYSIS

Radiation cooling of individual components has been eliminated from consideration for primary cooling because of the high ratio of area necessary to dissipate the heat directly to the total exposed surface area. Natural convection is automatically eliminated from consideration due to the zero-g-environment.

Conductive cooling is considered for each of the converter and generator units and the mechanical designs have proceeded with this in mind. The basic conduction equation

$$\dot{Q} = \frac{KA \Delta T}{L}$$

indicates the prerequisites of efficient heat transfer (large $\frac{\dot{Q}}{\Delta T}$). These prerequisites are:

1. Selection of material with high thermal conductivity, K.
2. Adequate cross-sectional area of heat flow, A.
3. Minimum heat transfer path, L.

The choice of material is limited to a few of the better conductors that have reasonable weights. The cross-sectional area is directly proportional to the weight of the conductor and this helps in determining this limitation. The heat transfer path length, L, that the heat must travel thus becomes a critical parameter in evaluating the success of conduction as the predominant mode of heat transfer. Emphasis will be placed on high-density packaging within the limits of electrical separation and component replaceability while maintaining full flexibility and reliability.

Figure 79 is part of the thermal analysis work accomplished during the study and shows the weight of the cooling system (radiator, fluid, pumps and piping) in lbs/KW of heat radiated to maintain different system operating temperatures.

Figure 80 shows a typical cooling system used for space applications and is representative of the system considered for each of the converter systems plus the high-frequency generator concept. It consists of pumps, piping, cooling fluid, and a radiator. The major weight producing component of the cooling system is the space radiator. In considering the design of a minimum weight radiator, simultaneous consideration of many factors is required. These include a variety of heat transfer problems, meteoroid protection, and radiator geometry effects. Figure 81 shows some aspects of the radiator design considered in arriving at a total system weight for the converter concepts and the high-frequency generator. Some of the basic assumptions are listed. A copper coating was assumed to be used to distribute the heat evenly between the tubes. The odd shape of the meteorite

TOTAL LB. KW_{RAD}

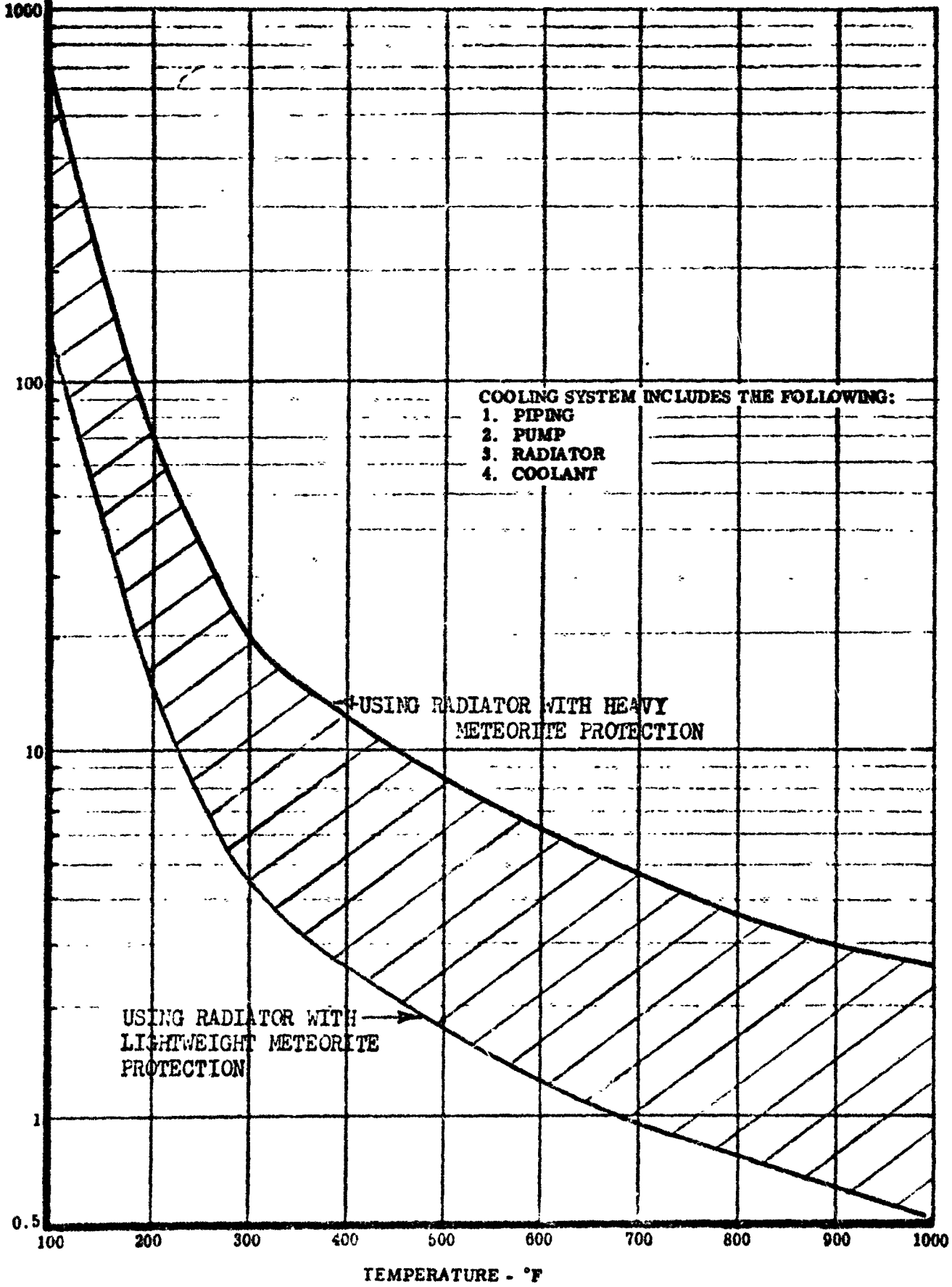


Figure 79. Analysis of Cooling System Weight Vs System Operating Temperature

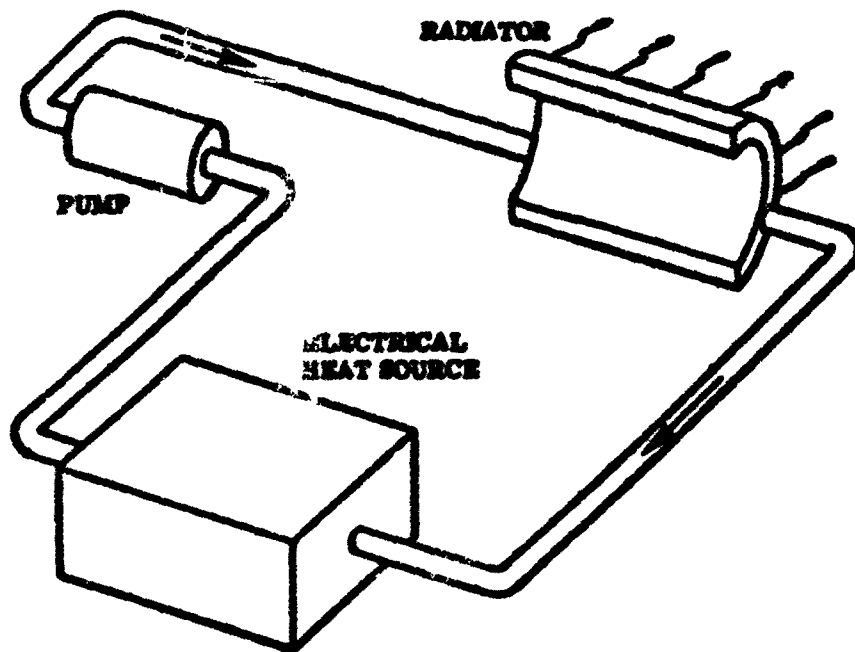
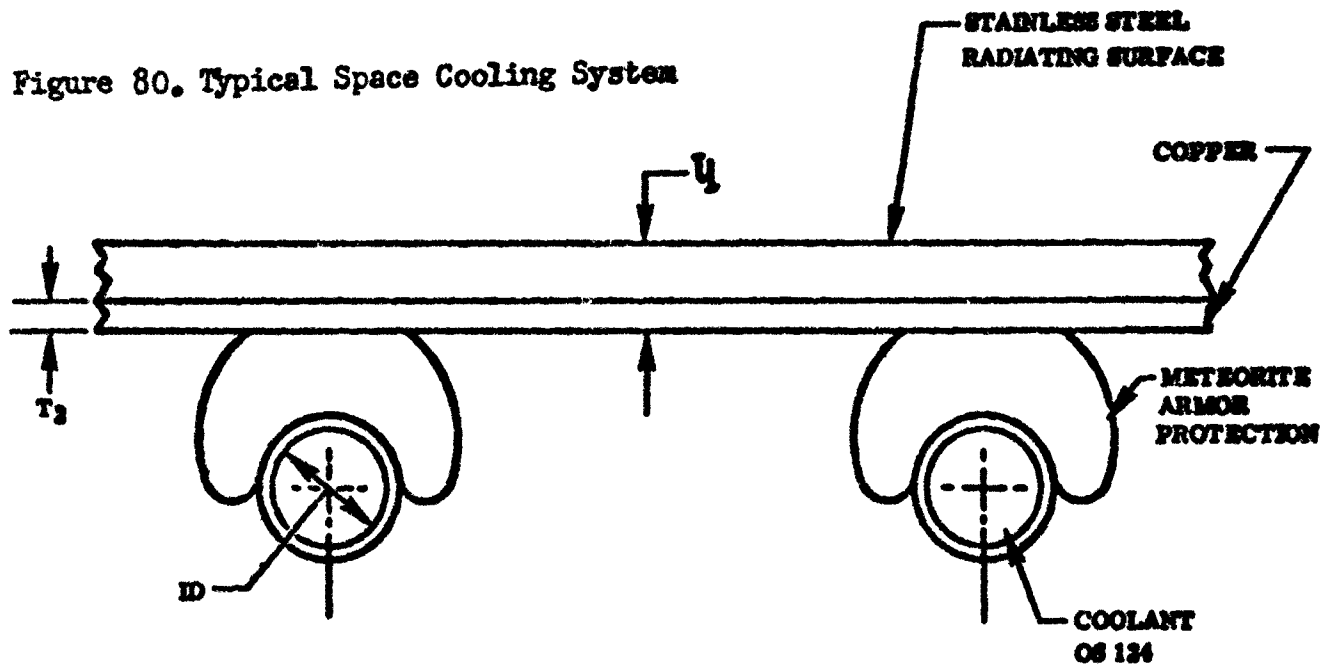


Figure 80. Typical Space Cooling System



TRADES-OFFS

- TUBE ID
- DISTANCE BETWEEN TUBES, D
- ARMOR THICKNESS
- COPPER THICKNESS, T_2
- NUMBER OF TUBES

ASSUMPTIONS

- FIN EMISSIVITY - 0.9
- FIN EFFECTIVENESS - 0.75
- RADIATOR $L/W = 2$

Figure 81. Space Radiator Technique
161

armor protection affords a constant thickness of heat exchanger material as protection for the tubes containing the coolant, regardless of the direction of an entering meteorite particle.

The major factor in determining the size, and therefore, weight of a space radiator is the coolant outlet temperature. Figure 82 shows how the radiator area per KW of heat radiated varies with coolant outlet temperature. By using the fact that radiator weight is directly proportional to its size and then adding the weight of fluid, pumps, and piping, the curve in Figure 79 was obtained. It shows the variation in total cooling system weight with changes in coolant outlet temperature. This particular curve is based on the use of OS-124 (Polyphenol Ether) as the cooling fluid. A second curve was added to show the cooling system weight when a lightweight, minimum meteorite protection radiator was used. The weight of the heavier cooling system has been used in all the analyses of this study because of a desire to be very realistic as far as the cooling system weight penalty is concerned. The trends in each case are the same.

By taking converter system weight and dividing it by the converter system losses, a weight/KW_{rad} figure is obtained. The cooling system weight/KW_{rad} from Figure 79 and the converter system weight/KW_{rad} are added and then multiplied by

$$\frac{1 - \eta_t}{\eta_t}$$

KW_{out} where η_t is the converter system efficiency at each temperature. This gives the total system weight as a function of temperature. The weight/KW_{rad} and weight/KW_{out} figures are computed so that a transistor system operating at 300°F and a motor-generator system operating at 800°F can be compared on an equal basis. System weight versus temperature results for the three converter systems are compared in the Summary Section at the beginning of the report. Curves showing the total system weight/KW_{out} as a function of temperature for each frequency are included in individual section.

ANALYSIS OF POSSIBLE COOLANTS

Coolants have been considered for several temperature ranges - 0° to 200°C, 200°C to 500°C, and over 500°C. A comparison of coolant properties was made in these three temperature ranges and is shown in the tables which follow.

Table 21 lists coolants considered in this study, along with some of their general properties. Studies were limited to liquid coolants since gaseous coolants for large power systems require bulky transport systems with resulting greater system weight. Among organic coolants the Coolanols, Aroclors, Skydrauls, and Pydrauls were rejected because of their poor radiation resistance. FC-75 (fluoro-chemical), water, and a water-ethylene glycol solution were rejected because of their low boiling points. These coolants would require a high pressure system at temperatures near 200°C.

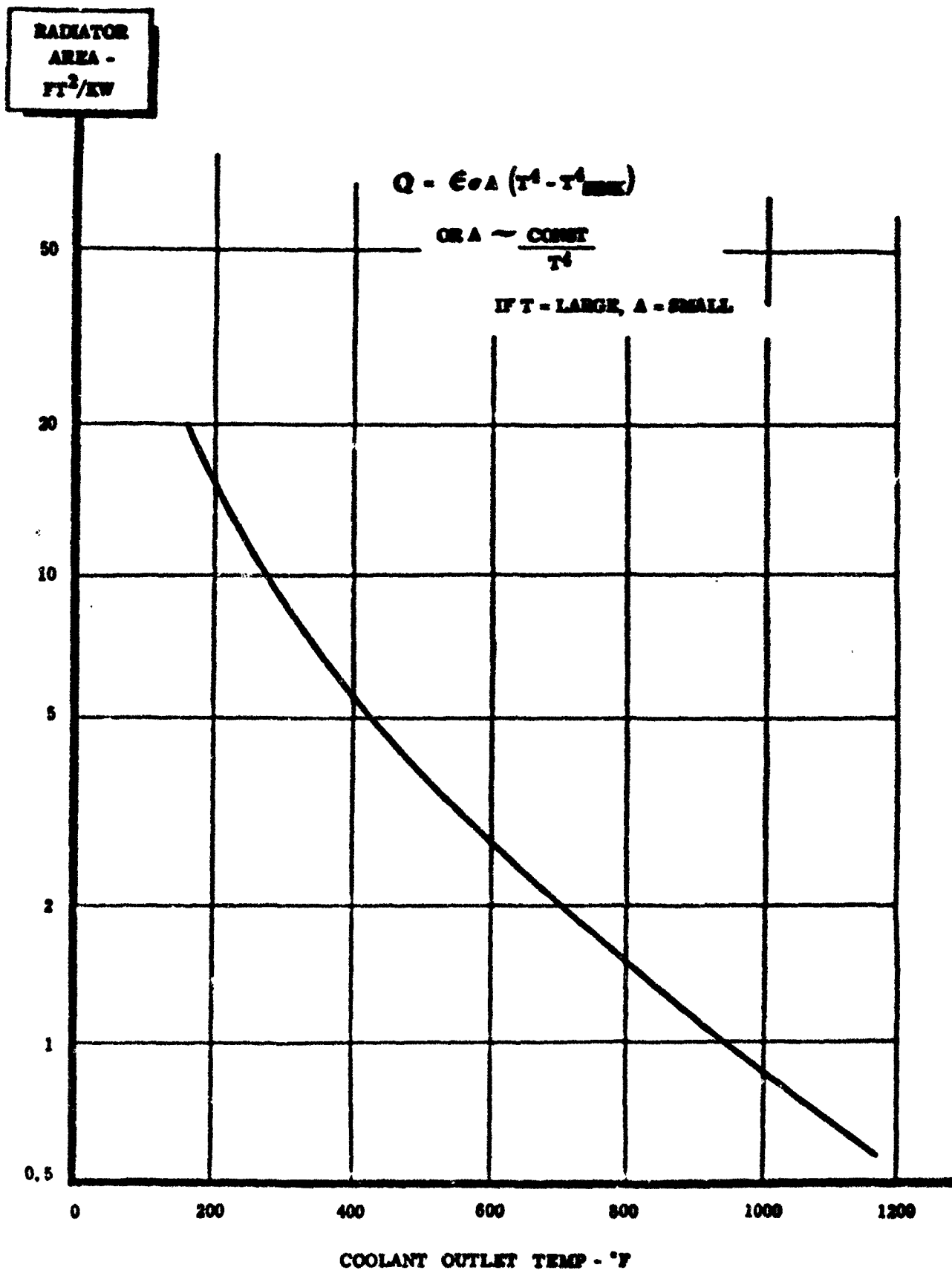


Figure 82. Analysis of Radiator Area vs. Temperature

TABLE 21

SUMMARY OF COOLANTS

COOLANT	TEMP. RANGE (°C)	DIELECTRIC PROPERTIES	RADIATION RESISTANCE	OTHER COMMENTS
Water	0-200	Poor		Corrosive, Low Boiling Point
Water-Ethylene Glycol	0-200	Poor		Corrosive, Low Boiling Point
FC-75**	0-200	Good		Low Boiling Pt.
Skydraul* [*]	0-200		Poor	
Pydraul* [*]	0-200		Poor	
Arcolors	0-200		Poor	
Coolanols	0-200		Poor	
Biphenyl	70-250	Good	Good	High Melting Point
Monoisopropyl Biphenyl (MIPB)	0-200	Good	Good	Recommended
Diisopropyl Biphenyl	0-200	Good	Good	Recommended
OS-124*	200-500	Good	Good	Recommended
Molton Salts	200-500	None	Good	
Liquid Sodium	200-500	None	Good	
Liquid Potassium	200-500	None	Good	
Sodium Potassium Eutectic Solution	200-500	None	Good	
Liquid Sodium	500	None	Good	Recommended
Liquid Potassium	500	None	Good	Low Specific Heat
Sodium Potassium Eutectic Solution	500	None	Good	Recommended
OS-124*	500			Unstable

* Registered Trade Mark - Monsanto Chemical Company
** Registered Trade Mark - Minnesota Mining & Manufacturing Company

Polyphenyls, thus far, have shown the best radiation resistance of organic coolants. Only monoisopropyl biphenyl (MIPB) and diisopropyl biphenyl (DIPB) have sufficiently low melting points to be fluid in the 0°C to 200°C range. MIPB was chosen as a typical coolant for further consideration in this temperature range.

In the 200°C to 500°C temperature range only OS-124, among the organic coolants considered, has sufficient thermal stability and a sufficiently high boiling point for use to 500°C without undue pressurization. OS-124 is a mixed-isomeric polyphenyl ether with the best thermal stability and widest fluid temperature range of any organic coolant. The liquid metal eutectic solution of sodium and potassium (NaK) was also considered for use in this temperature range.

Above 500°C the only coolant given serious consideration was eutectic NaK. It is possible to use OS-124 at temperatures near 600°C for short periods of time, but NaK is a better candidate as a coolant for temperatures above 500°C. Liquid sodium has much better cooling properties than eutectic NaK, but the eutectic has a wider fluid temperature range.

Other organic coolants are being developed which will have better properties than MIPB or OS-124, but information is limited and mostly unavailable. Organic coolant characteristics are shown in Table 22 with other inorganic coolants shown in Table 23.

Table 22 shows a variation in specific heat of two to one for the organic coolants over the temperature range of 0° to 1,000°F. Inorganic coolants have considerably less variation as shown in Table 23. For analysis purposes, the following specific heats are used in this study:

MIPB	0.464 BTU/LB	- F at 200°F
OS-124	0.5 BTU/LB	- F at 500°F
Eutectic NaK	0.21 BTU/LB	- F at 750°F

Each is assumed constant so that charts showing the development of fluid flow rate versus temperature rise for the coolants may be developed. These curves are formulated from the basic heat flow equation:

$$Q = W_f C_p \Delta T_f$$

where

Q = heat absorbed by a fluid

W_f = fluid flow rate

C_p = specific heat of fluid

ΔT_f = temperature rise of fluid

PROPERTIES OF ORGANIC COOLANTS

TEMPERATURE (F)	DENSITY (grams/cc)			SPECIFIC HEAT (BTU/#°F)			VAPOR PRESSURE (mm of Hg)		
	MIPB	DIPB	OS-124	MIPB	DIPB	OS-124	MIPB	DIPB	OS-124
0	1.015	0.990	-	0.371	0.335	-	-	-	-
80	-	-	1.204**	-	-	-	-	-	-
100	0.973	0.950	1.187	0.418	0.431	0.368	-	-	-
200	0.932	0.908	1.143	0.464	0.476	0.400	0.55	0.21	-
210	-	-	1.141	-	-	-	-	-	-
300	0.890	0.867	1.100	0.512	0.522	0.432	9.5	3.9	-
400	0.849	0.825	1.057	0.557	0.568	0.465	75	32	-
500	0.808	0.785	1.013	0.604	0.614	0.496	370	170	0.7
600	0.765	0.743	0.971	0.649	0.660	0.528	1300	610	5.3
700	0.725	0.703	0.926	0.697	0.705	0.560	5.3at	1850	26
800	0.680	0.660	0.880	0.742	0.750	0.593*	13.2at	16.6at	103
900	-	-	0.833*	-	-	0.626*	-	-	330
1000	-	-	0.783*	-	-	0.660	-	-	900*

* Extrapolations ** 68°F at - Atmospheres

GENERAL DATA	MIPB	DIPB	OS-124
Melting Point (°F)	-65	-24	40
Boiling Point (°F) (760 mm of Hg)	563-572	610-631	982
Flash Point (°F)	315	340	550
Fire Point (°F)	340	365	660
Thermal Stability (°F) Isoteniscope	-	-	847
Autoignition Temperature (°F)	850	850	1135
Thermal Conductivity (BTU/Hr-Ft ² -F)	.070	.068	.0658

TABLE 23

PROPERTIES OF INORGANIC COOLANTS

TEMPERATURE		DENSITY (# per cu. ft.)		SPECIFIC HEAT (BTU/#-F)		THERMAL CONDUCTIVITY (BTU/Hr.-Ft.-F)	
°C	°F	NA	NaK*	NA	NaK	NA	NaK
0	32	-	-	-	0.238	-	-
100	212	57.9	52.9	0.3305	-	49.71	14.1
104	215	-	-	-	-	-	-
170	334	-	-	-	-	-	-
200	392	-	-	0.3200	0.217	47.10	-
250	482	55.6	50.6	-	-	-	-
	572	-	-	-	-	43.76	-
400	752	53.3	48.4	0.3055	0.210	41.15	15.4
	932	-	-	-	-	38.61	-
550	1022	51.0	46.1	-	-	-	-
600	1112	-	-	0.2998	0.209	-	-
700	1292	48.7	43.9	-	-	-	-
800	1472	-	-	0.3030	0.213	-	-
OTHER DATA						NA	NaK
Melting Point (F)						208	12
Boiling Point (F) at 760 mm of Hg.						1621	1443
<p>*NaK - Eutectic Solution (22% NA, 78%K)</p> <p>Data from Reactor Handbook, Volume 2-Engineering; Chapter 2-2, Table 2.2.1, Pages 256 and 257; declassified edition published by Technical Information Service of United States, AEC, May, 1955.</p>							

Assuming the heat flow and specific heat constant, the variation of temperature rise with fluid flow may be plotted as a logarithmic curve or as a straight line curve on log-log paper. Figure 83 is a fluid-flow-rate versus fluid-temperature-rise for various values of heat flow for OS-124. From this curve, when the required heat rejection of any component is known, the combinations of possible coolant flow and temperature rise may be quickly and easily determined.

The convection temperature drop across the boundary layer film between a heated surface and the coolant is also important. Expressions for this drop are derived from a similar heat flow expression:

$$Q = h_c A_s \Delta T_c$$

where

h_c = convection film coefficient

A_s = convective surface area

ΔT_c = temperature drop through convection film

defining $Q = Q/A_s$, the above equation becomes

$$Q = h_c \Delta T_c$$

If nonboiling, turbulent forced-convection of organic liquid coolants in a cylindrical conduit is assumed, the film coefficient (h_c) may be determined from the expression:

$$N^M = 0.023 R_e^{.8} P_r^{.4}$$

where N^M = Nusselts' number = $\frac{h_c D}{k}$

R_e = Reynolds' number = $\frac{DG}{\mu}$

P_r = Prandtl number = $\frac{C_p \mu}{k}$

h_c = film heat transfer coefficient

D = conduit diameter

k = fluid thermal conductivity

G = fluid mass velocity $W_f / (\pi D^2/4)$

μ = fluid viscosity (absolute)

C_p = fluid specific heat

FLUID FLOW RATE -
LB/MINUTE

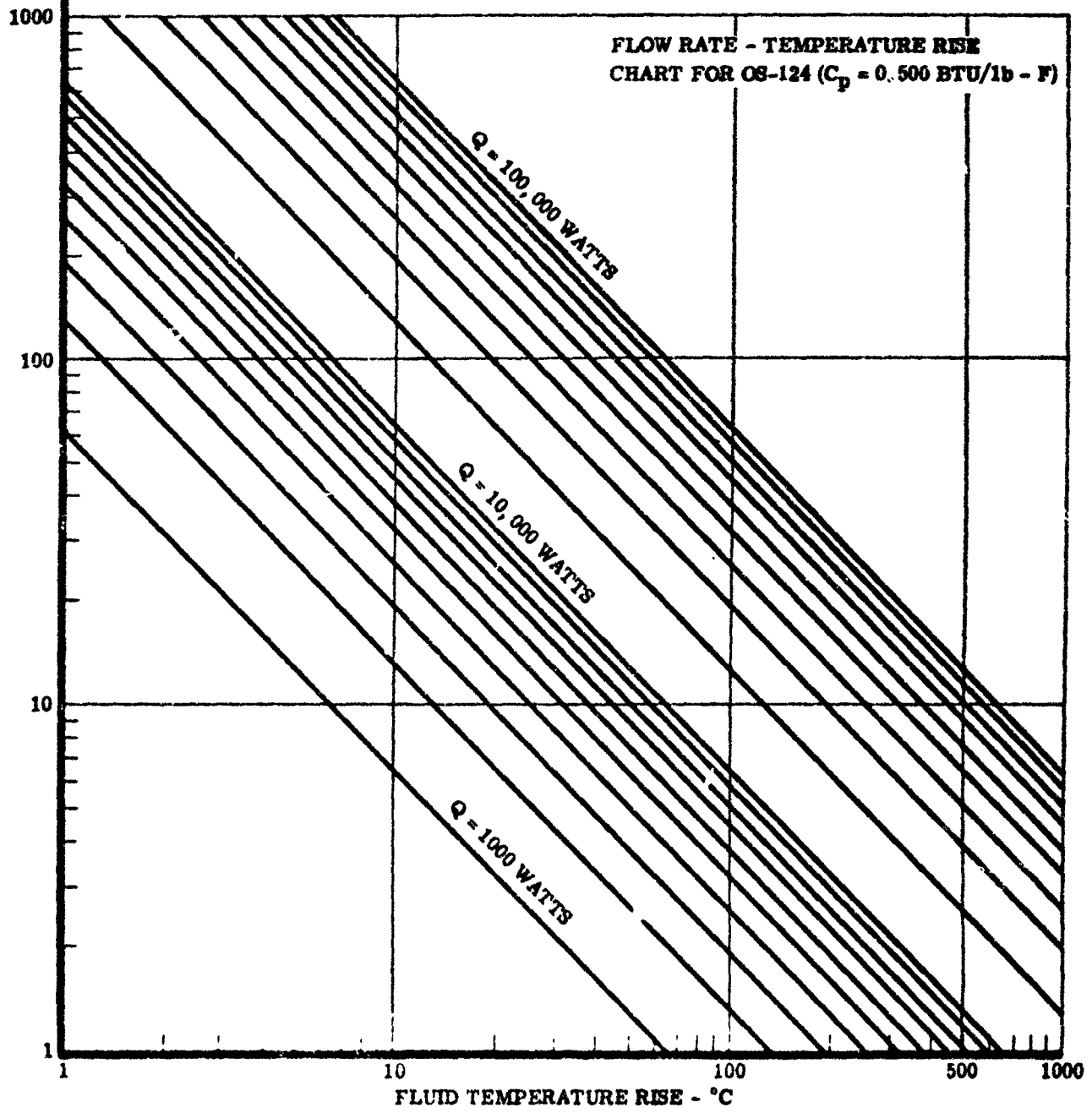


Figure 83. Fluid Flow Rate vs. Fluid Temperature Rise of OS-124

Substituting the relationship for N

$$h_c = .023 \frac{k}{D} (R_e)^{.8} (P_r)^{.4}$$

From Reynolds' number and the definition G , the diameter (D) is:

$$D = \frac{4W_f}{\mu R_e}$$

Substituting for D in the equation of h_c gives

$$h_c = \frac{.0181k}{W_f} (R_e)^{1.8} (P_r)^{.4}$$

The terms k, μ , and P_r are properties of the cooling fluid and are constant for a given type of fluid and temperature. Defining γ as a constant which includes k, μ , P_r , and the numerical values of the equation, the above equation becomes:

$$h_c = \frac{\gamma (R_e)^{1.8}}{W_f}$$

If the same conditions are imposed on the liquid metal coolants as imposed on the organic coolants, Nusselts' number for the liquid metals can likewise be obtained. In a similar fashion, the film heat transfer coefficient can be obtained.

TRANSFORMER COOLING

Because the numerous variables in transformer design are dependent on a particular design and/or application, only generalized cooling requirements have been considered. Transformer weight usually runs about .1 pound per cubic inch and convective heat dissipation from cooling surfaces will normally vary from 2.5 to 3.5 watts/sq. in. Where cooling is available from external surfaces only, the overall ΔT between transformer hot spots and coolant temperatures is normally about 200°F. This may be reduced to 70°-80° when the coolant is ducted between windings and directly along the core surfaces. For the larger units internal cooling ducts have been considered.

Figure 84 represents a cooling concept for each of the large transformers considered in this study. Coolant ducts rise upward through the windings and connect a lower cold-plate reservoir to the upper cold-plate reservoir. The coolant fluid is circulated in one side and out the other side to remove the excess heat resulting from losses in the transformer core material and its I^2R losses in the conductors. Heat sink material of both metal and conductive epoxy can be used to conduct the heat to basic structure and away from the transformer. In the case of transformer cooling, maximum use of the mounting shelf can be obtained by using the shelf as a heat sink.

The need may arise for isolating the transformer from the other system components, if it operates at a higher temperature than the other components.

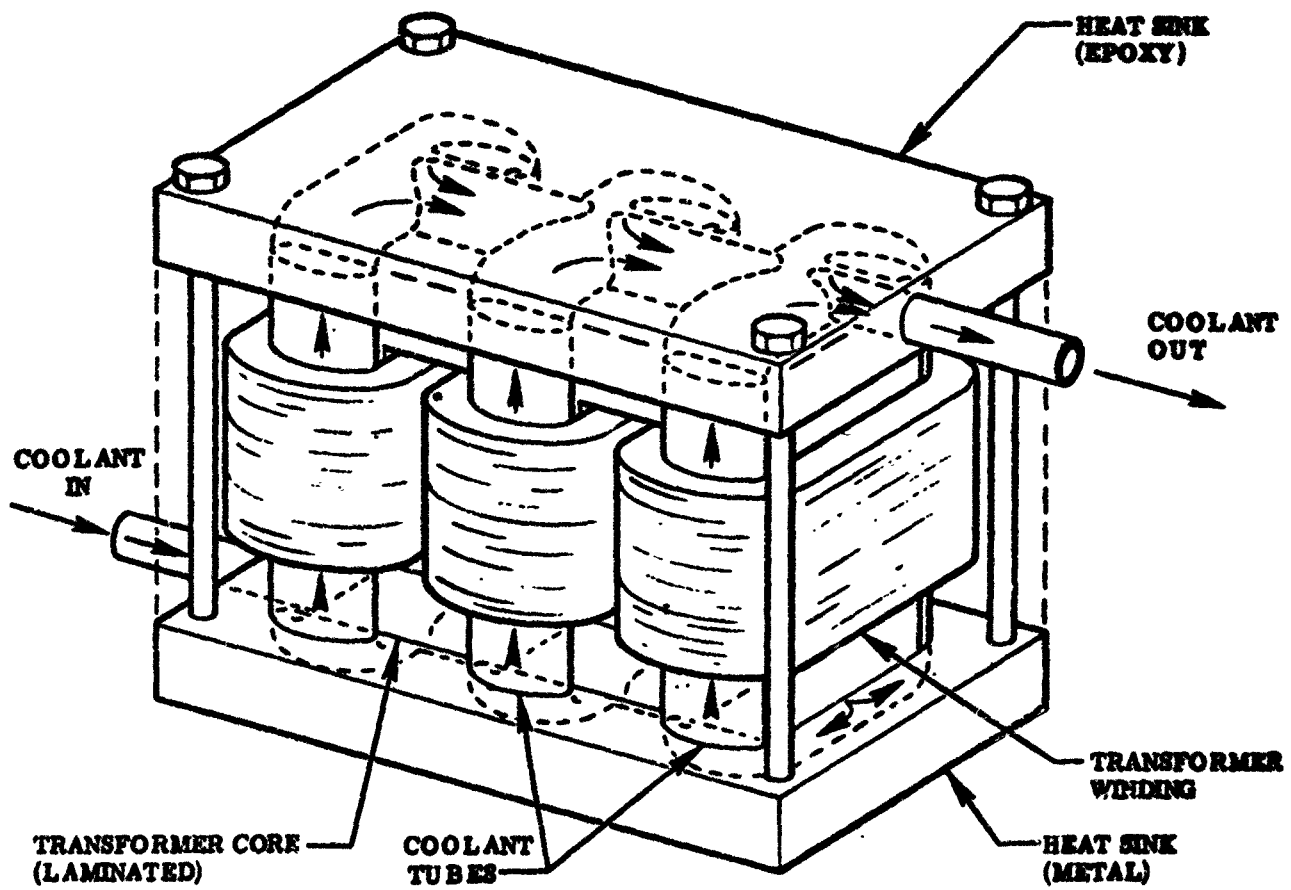


Figure 84. Typical Transformer Construction Showing Cooling Provisions

This isolation can be achieved by bonding an insulating sheet of mylar or glass fiber to the inside of the transformer case to serve as a heat shield.

TRANSISTOR COOLING

Transistors junction temperatures must be kept within certain limits to prevent failure and thermal runaway. In a space environment the only mode of heat transfer is radiation, either directly from the transistor or from a heat sink to which the transistor is thermally coupled. The surface area of a transistor is fairly small and can only provide a few milliwatts of direct radiative power whereas most high power transistors must dissipate over one hundred watts. Therefore, the problem resolves itself into an investigation of the thermal path between the transistor junction and the heat sink and making the thermal conductance as high as possible.

For purposes of a cooling analysis, it is assumed that all transistors will be mounted on a heat sink material which is part of a heat exchanger (cold-plate). Thermal design will consider thermal drop through electrical insulation, allowable junction temperatures of the transistors, and internal heat flow from each device to the heat exchanger. Figure 85 shows how a typical power transistor will be mounted in a heat sink. Two thermal paths are available: One from the case, through the top washer, to the heat sink and the other from the case through the stud and nut, through the bottom washer to the heat sink. Both paths are essentially in parallel.

The net thermal resistance desirably should be as low as possible. However, it is often necessary that the transistor be electrically insulated from the sink. This means that some sort of device, such as a washer, must be used to provide good thermal conductivity while serving as an electrical insulator. Further, if washers are to be used, they must have good mechanical properties to resist cranking when the nut on the transistor is tightened during mounting. Materials satisfying these specifications, to a greater or lesser degree, are beryllium oxide, mica, and aluminum oxide.

Figure 86 illustrates the increase in thermal resistance between the transistor case and the heat sink in a vacuum as compared with the resistance in air. In a vacuum the only mode of heat flow between the surfaces is conduction through the few discrete contact points; in air there is also the possibility of heat convection between the surfaces of heat conduction across the narrow air layer. The presence of a vacuum thus tends to amplify the cooling problem.

The increase in thermal resistance is due to the fact that surfaces are not perfectly smooth, and actually touch at only a limited number of points. The remainder of the space is nonconducting vacuum. Variables affecting the contact resistance include the pressure between the two surfaces, the smoothness of the surfaces, the materials themselves, and the possible addition of greases, solders, or some soft materials to fill the empty regions between the surfaces. Figure 86 illustrates the effect of surface pressure on contact resistance. The thermal resistance decreases linearly with surface pressure. The limiting factor in this case is the amount of pressure that the washer can withstand before cracking.

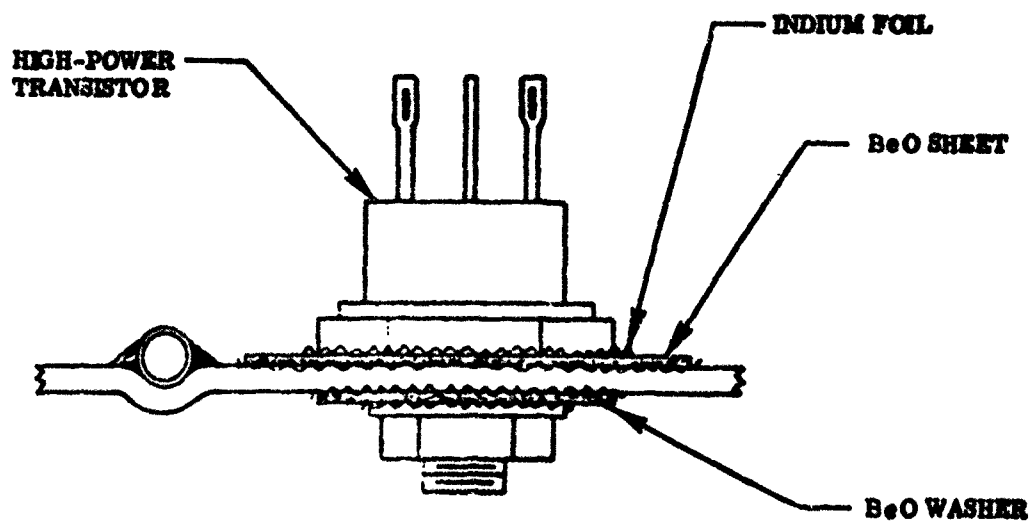
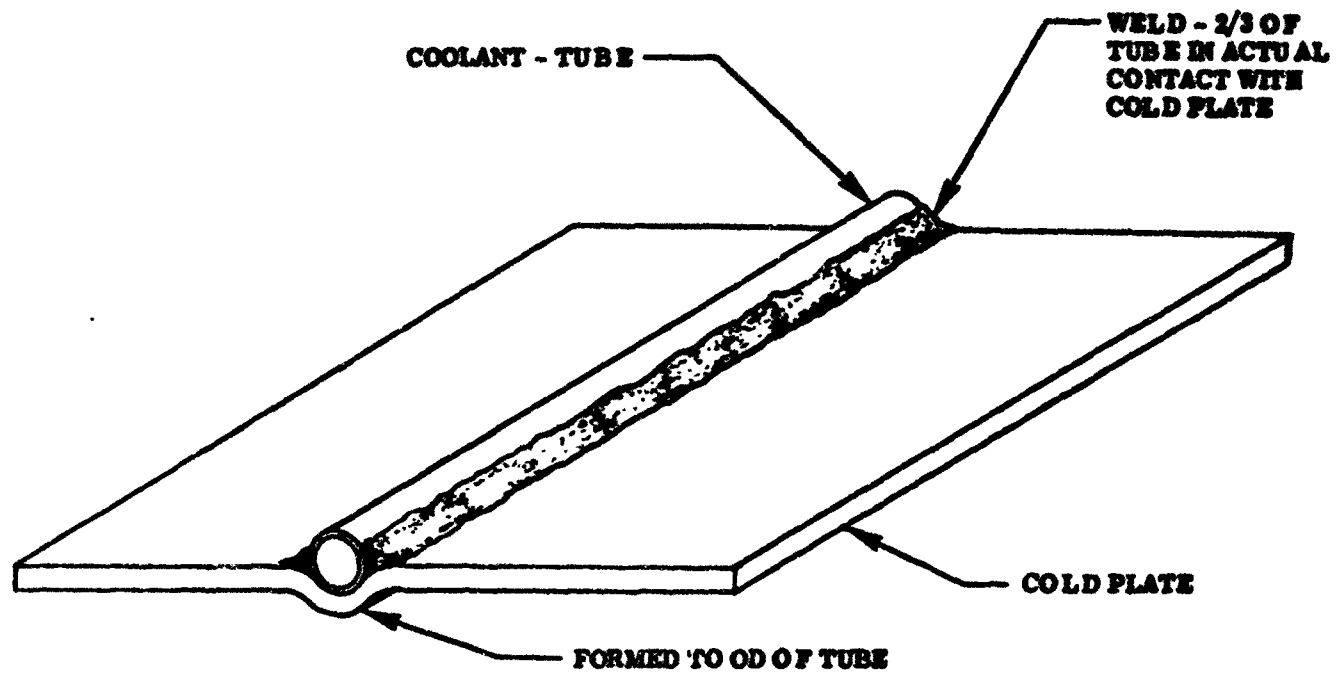


Figure 85. Transistor Cooling Concept
173

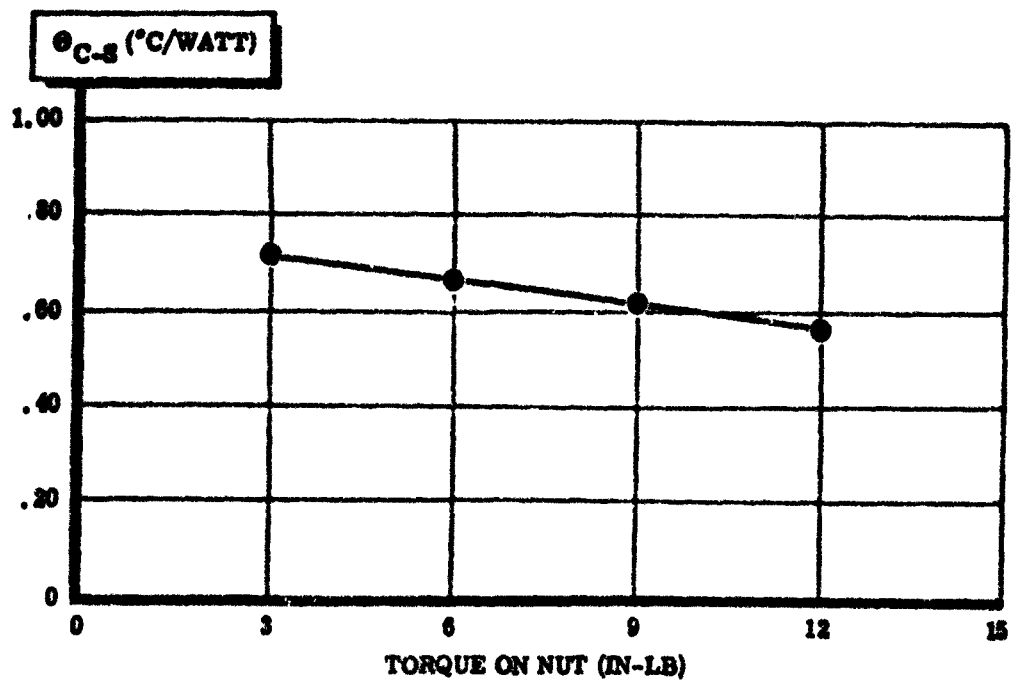
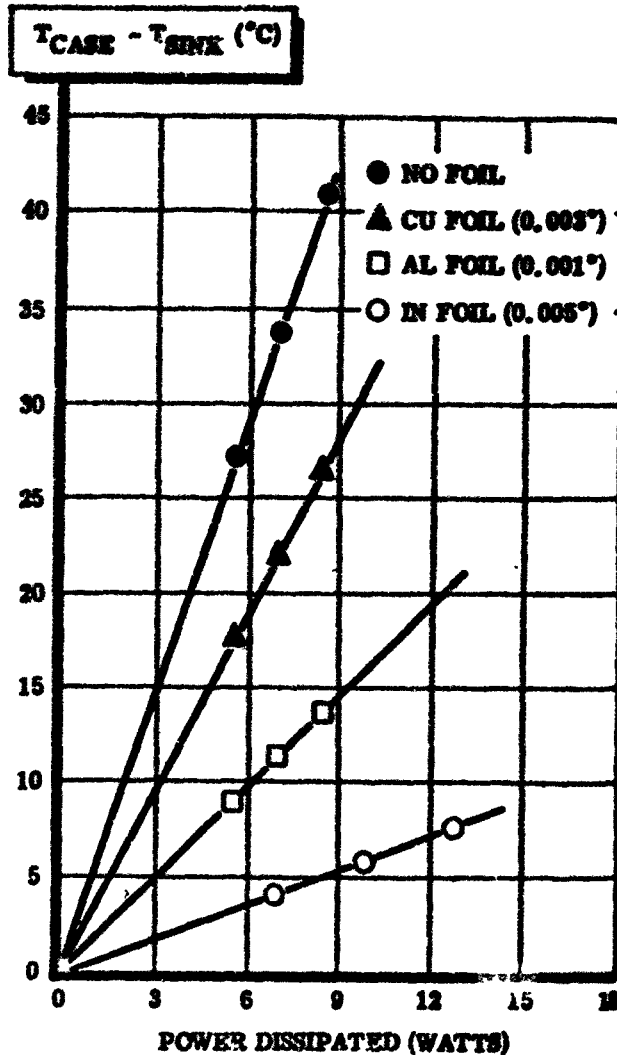
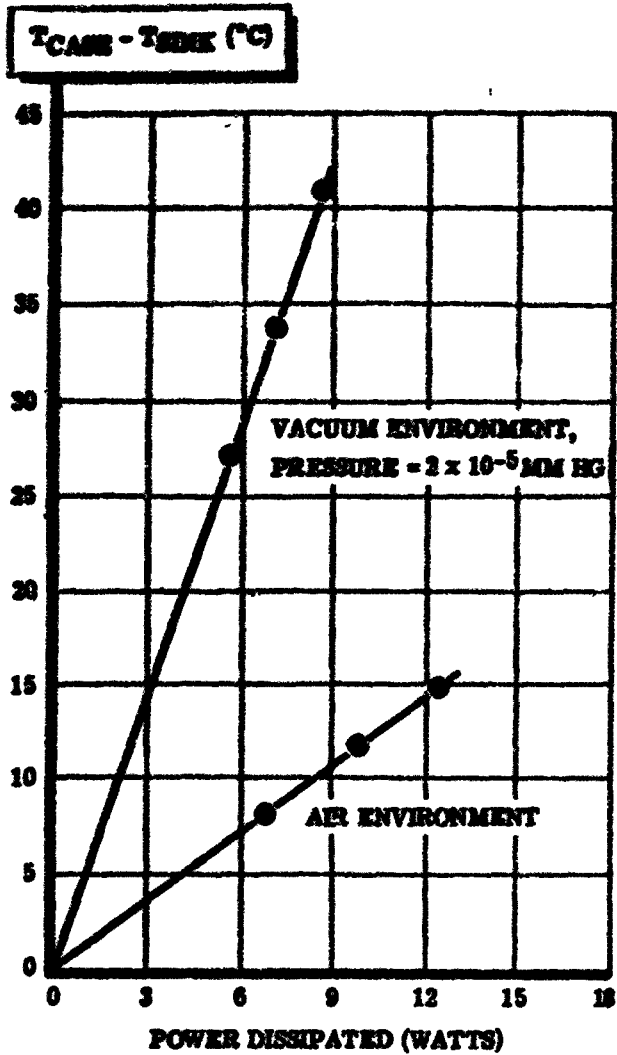


Figure 86. Transistor Mounting Considerations

Figure 86 illustrates the effect of using foils along the interfaces of the BeO washers in a vacuum environment to fill the void between the heat-conduction materials. In each case, a foil washer with the same surface dimensions as the BeO washer was placed between the transistor case and the top washer, between the top washer and the heat sink, and between the bottom washer and the heat sink. The graph shows that the use of any of the three interface materials lowered the thermal resistance from case to heat sink. Indium foil, however, proved most effective and lowered the thermal resistance to $0.61 \text{ }^{\circ}\text{C/watt}$, approximately $1/8$ of its value without interface material. Another method of reducing thermal contact resistance is to solder the surfaces together.

Generator Cooling - Many variables also enter into the thermal design problem for the rotary generator and converter concepts. Liquid coolant is considered in the cooling system design at temperatures between 500°F and $1,100^{\circ}\text{F}$. Stator cooling will be provided by ducts in the outer periphery. This system places the cooling fluid adjacent to the iron hot spots. The iron surface temperature referred to in the data tables is the temperature of the iron adjacent to the cooling fluid. The cooling fluid temperature will be less than the surface iron temperature by an amount depending on the coolant used in the system and the fluid flow rate in the ducts.

ANALYSIS OF MATERIAL

MAGNETIC MATERIAL CHARACTERISTICS

The frequencies considered for this study were 50 to 200 KC for the high frequency generator and 50 to 800 KC for the frequency converter units. Average coolant temperatures used in the design studies were in the 200 to 1,100°F range. Major determinants in the selection of magnetic materials for these conditions are the core and other losses at the design frequency and operating temperature, usable flux density at the design temperatures, and Curie point. Aspects of these determinants will be discussed in the section which follows with specific materials to be discussed later in this section.

Flux Density

The size of an electromagnetic device is directly related to the allowable flux density of its magnetic material. A magnetic material may have small core losses, but due to its low saturation flux density, a very large volume of material may be required to generate appreciable voltages. On the other hand, a magnetic material may have a very high saturation flux density, but its core losses may be prohibitively high. As an example, molypermalloy powdered cores have low core losses, but can carry only about 4,000 gauss of flux while oriented silicon steel laminations have much higher core losses, but can carry about 18,000 gauss without reaching saturation. It can, therefore, be seen that reducing the flux density in a design in order to reduce the core loss or to make possible the use of a material having lower losses may result in significant weight increases for a given power level and frequency. The wide range of maximum flux densities for various magnetic materials is shown on Figure 87.

At power frequencies the designer would ordinarily choose that material which provides the highest flux density, since less iron and copper are required and light weight can be achieved at high efficiencies. The efficiencies are high at power frequencies because the core losses are small compared with the total power output of the device.

A survey was made of the maximum flux density of various low-loss magnetic materials over the 100 to 800°C range. The results of this survey are shown in Figure 87. As can be seen in this figure, there is a decreasing maximum flux density in going to high temperature operation. Oriented-silicon steels are best for flux capability with low-loss ferrites being extremely temperature limited.

Losses in Ferromagnetic Materials

The core loss in a magnetic core is commonly divided into the eddy current loss, the hysteresis loss, and the residual loss. Eddy current losses are induced by varying magnetic fields in ferromagnetic materials (which are generally good conductors). On the other hand, hysteresis losses are due to the fact that all of the energy stored in a magnetic material is not returned to the circuit when the field is collapsed. Part of this energy is converted into heat in the process of aligning the domains in the ferromagnetic material. If the magnetization is carried through a

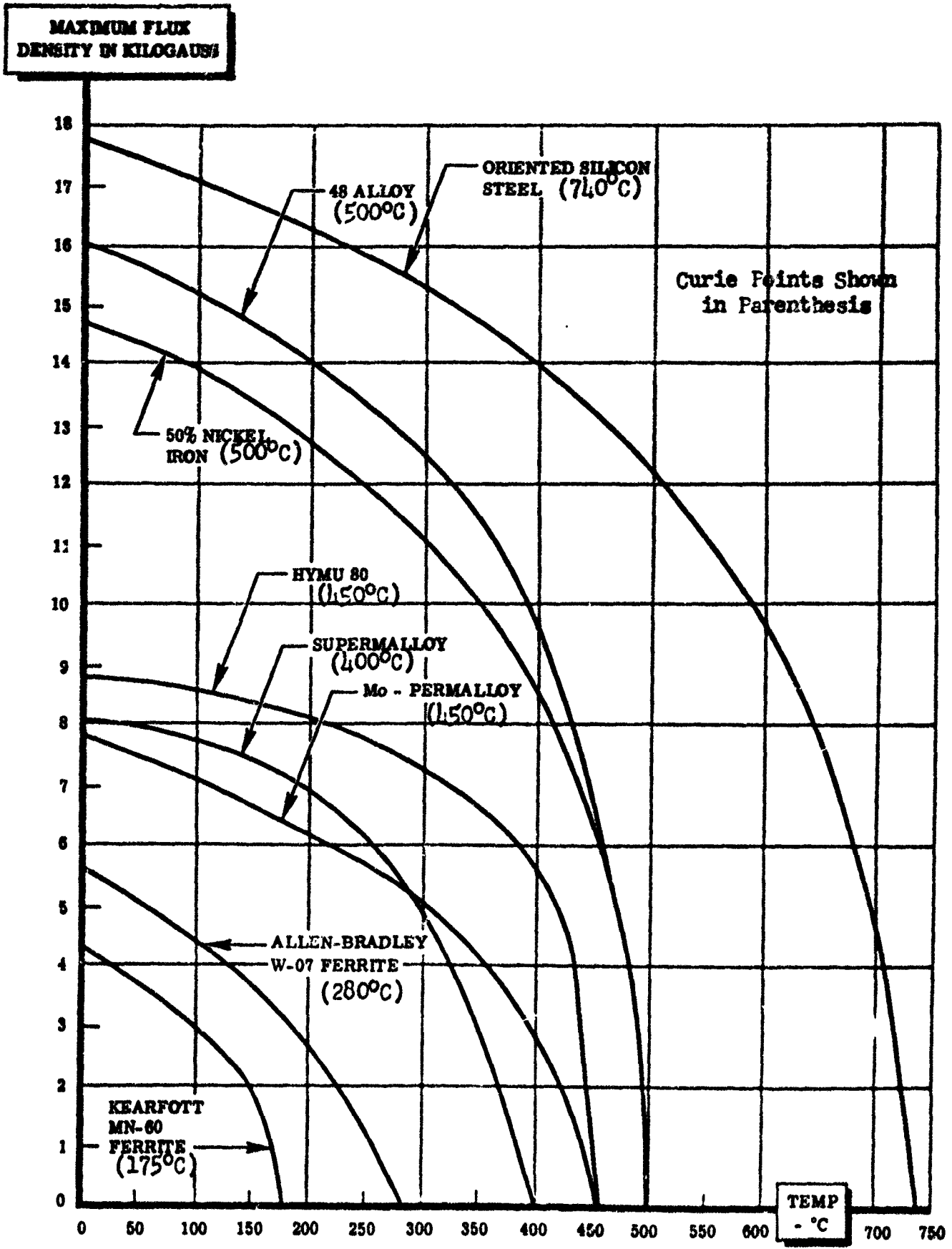


Figure 87. Flux Densities. Temperature for Various Materials

complete cycle of a magnetomotive force, the hysteresis loss is proportional to the area enclosed by the familiar B-H loop. Comparative B-H loops for Orthonal, 48 Alloy, and HYMU 80 are shown in Figure 86. It can be seen from a comparison of the areas covered by the loops of these materials that HYMU 80 has the lowest DC hysteresis loss. HYMU 80 retains this advantage at high frequencies as well.

All ferromagnetic material losses that cannot be attributed to either eddy current or hysteresis losses are classified as residual losses. The origin of these residual losses is not completely known, but they are associated with such phenomena as domain wall relaxation and domain wall resonance.

Even at low flux density applications, the residual losses contribute a large portion of the total core losses in ferrite materials. The rapid increase of residual losses with frequency as the ferromagnetic resonance is approached, results in an effective upper frequency limit for any given ferrite material.

The calculated power loss in ferromagnetic core subject to an alternating magnetizing force is the sum of the hysteresis and the eddy current losses. This power loss can be written:

$$P_c = \text{hysteresis loss} + \text{eddy current loss}$$

$$= K_1 h f B_{\text{Max}}^X + \frac{K_2 f^2 t^2 B_{\text{Max}}^2}{r}$$

where

h = hysteresis loss coefficient

f = frequency in cycles per second

B_{max} = maximum flux density in gaussses

X = hysteresis loss exponent

t = thickness of core laminations in mils

r = resistivity in microhm-centimeters

It can be seen from this equation that the eddy current loss can be reduced by reducing the thickness of the material or by going to a material having a higher resistivity. Figure 89 shows the effect of increasing the silicon content of electric steels on core loss, resistivity, and coercive force. The reduction in core loss is seen to be proportional to the silicon content. The hysteresis loss which is proportional to the coercive force, is also reduced by the increased silicon content.

As shown in the first term of P_c , the hysteresis loss should not vary with thickness, but actually this loss does vary to some extent due to differences in processing treatments. Also, the eddy current losses for a given grade do not vary exactly as the square of the thickness in the

21
22

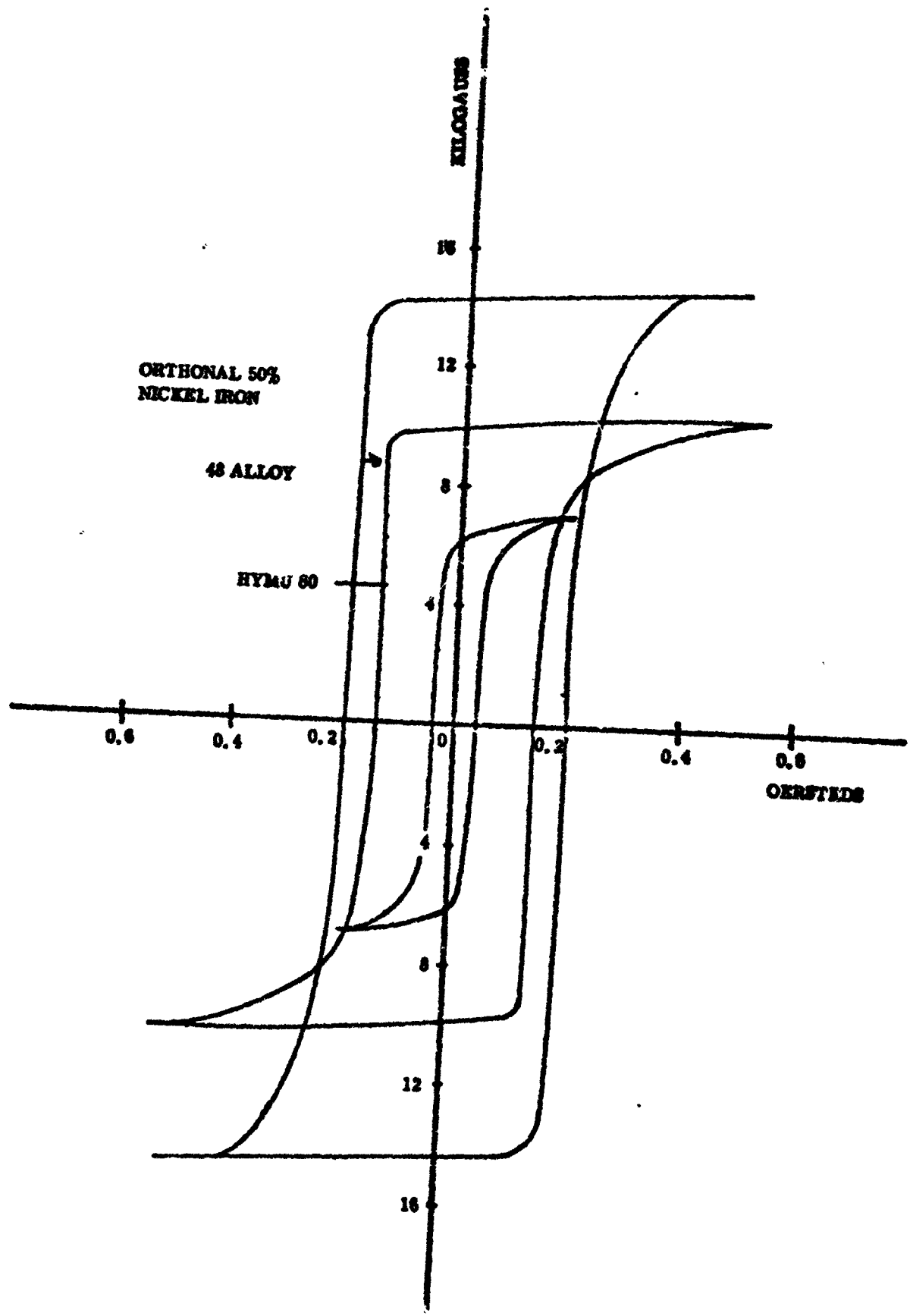


Figure 88. Hysteresis Loops of Various Magnetic Materials

**SATURATION FLUX DENSITY -
KILOGAUSS, PERCENT ELONGATION,
AND ELECTRICAL RESISTIVITY,
MICROHMS PER CUBIC CENTIMETER**

**COERCIVE FORCE IN OERSTEDS
AND CORE LOSS IN WATTS/LB
AT 90 CPS AND 10 KILOGAUSS**

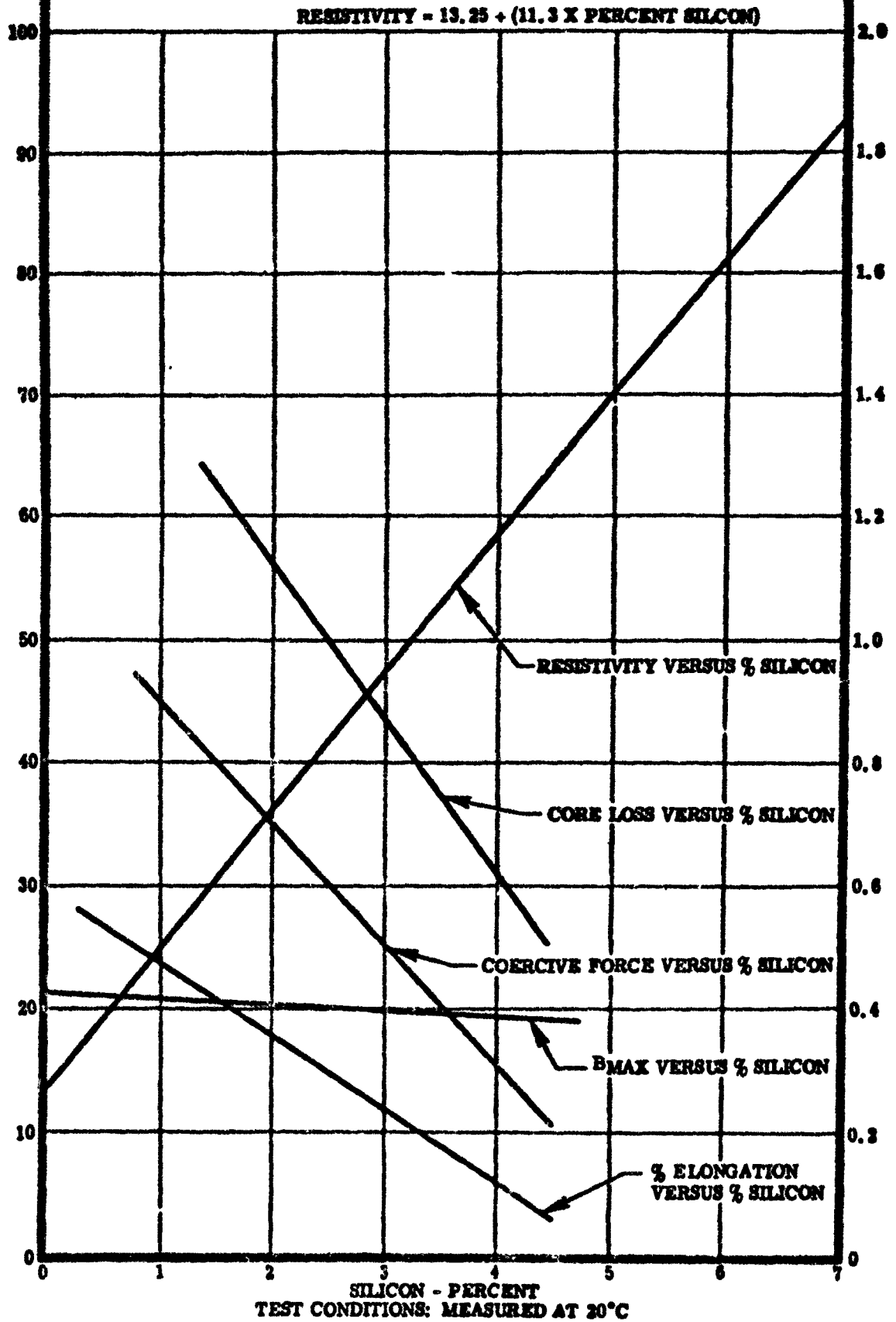


Figure 89. Variation of Physical and Magnetic Properties of Electrical Steels

thinner gages, but better agreement with the eddy current term above is had in the thicker gages. The effect of grain size and boundary conditions and minor thickness variations as well as slight differences in silica content are among the major factors causing this discrepancy.

The hysteresis loss is shown by the first term to increase linearly with frequency while the eddy current loss increases as the square of the frequency. As a result, although the hysteresis and eddy current losses are of the same order of magnitude at 60 cycles per second, the eddy currents at high frequencies are the major factor in determining the core loss. It is interesting to note that increasing temperature results in a small reduction in hysteresis loss. This is due to the fact that the saturation flux density and the coercive force are reduced as the temperature goes up. In the audio frequency range (500 to 15,000 cps) both the hysteresis and eddy current components of core loss become important and moderate magnetic flux density is required to reduce losses.

Above the audio frequency range, however, the eddy current component of the core loss becomes of primary importance not only to reduce core losses, but also to reduce the skin effect produced by eddy current shielding. Since the flux density in the ferromagnetic material is usually relatively large, and since the resistivity of ordinary electric steels is not extremely high, the induced eddy currents may become appreciable if means to minimize them are not taken. The eddy current loss in this case is of considerable importance in determining the efficiency, the temperature rise, and hence the rating of the electromagnetic device.

In addition to creating heat losses in the magnetic material, eddy currents screen or shield the individual sheets of magnetic material from the magnetic flux, and bring about a higher flux density near the center of the lamination than at the surface. The total flux tends to be crowded towards the center of the laminations, and the effective cross-sectional area of the magnetic material is reduced.

Core Loss Versus Frequency

The effect of operating frequency on core loss is shown in Figure 90. It can be seen here that the use of conventional oriented silicon steel material would result in comparatively high losses at 200 KC unless extremely thin laminations are used. The superiority of HYMU 80 is evident in these figures with respect to other low-loss materials. If thin steel laminations were used, the core losses could be reduced to levels approaching that of the ferrites without their disadvantage of a low operating temperature and flux density (see also Figure 91).

Hysteresis Loss

The hysteresis loss can be made small by the use of a material which has a hysteresis loop of small area. Although these loops would broaden out at higher frequencies, the relative advantage of HYMU 80 (and super-alloy) would continue to exist over more conventional materials such as 48 Alloy.

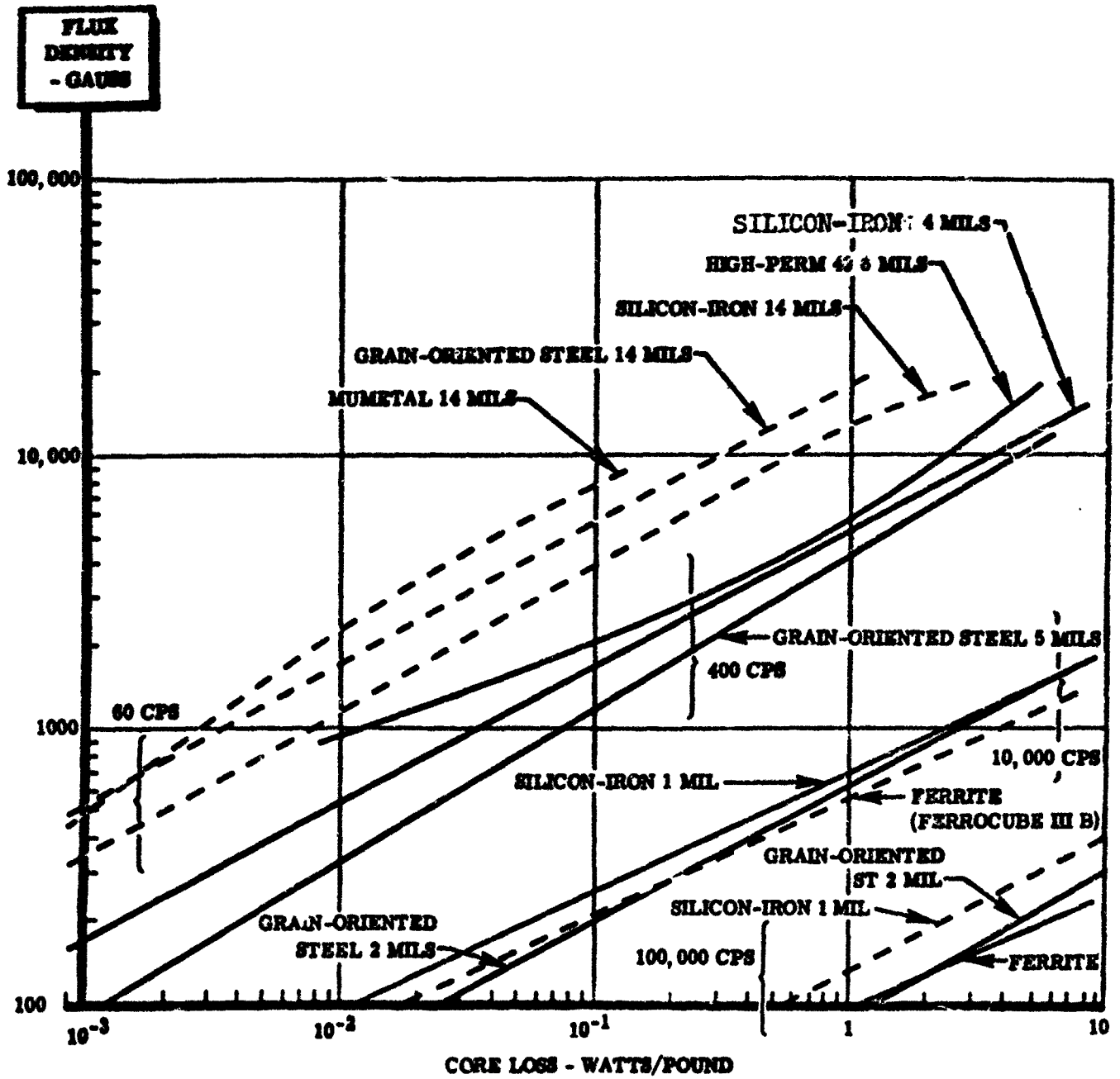


Figure 90. Flux Density vs. Core Loss for Various Materials

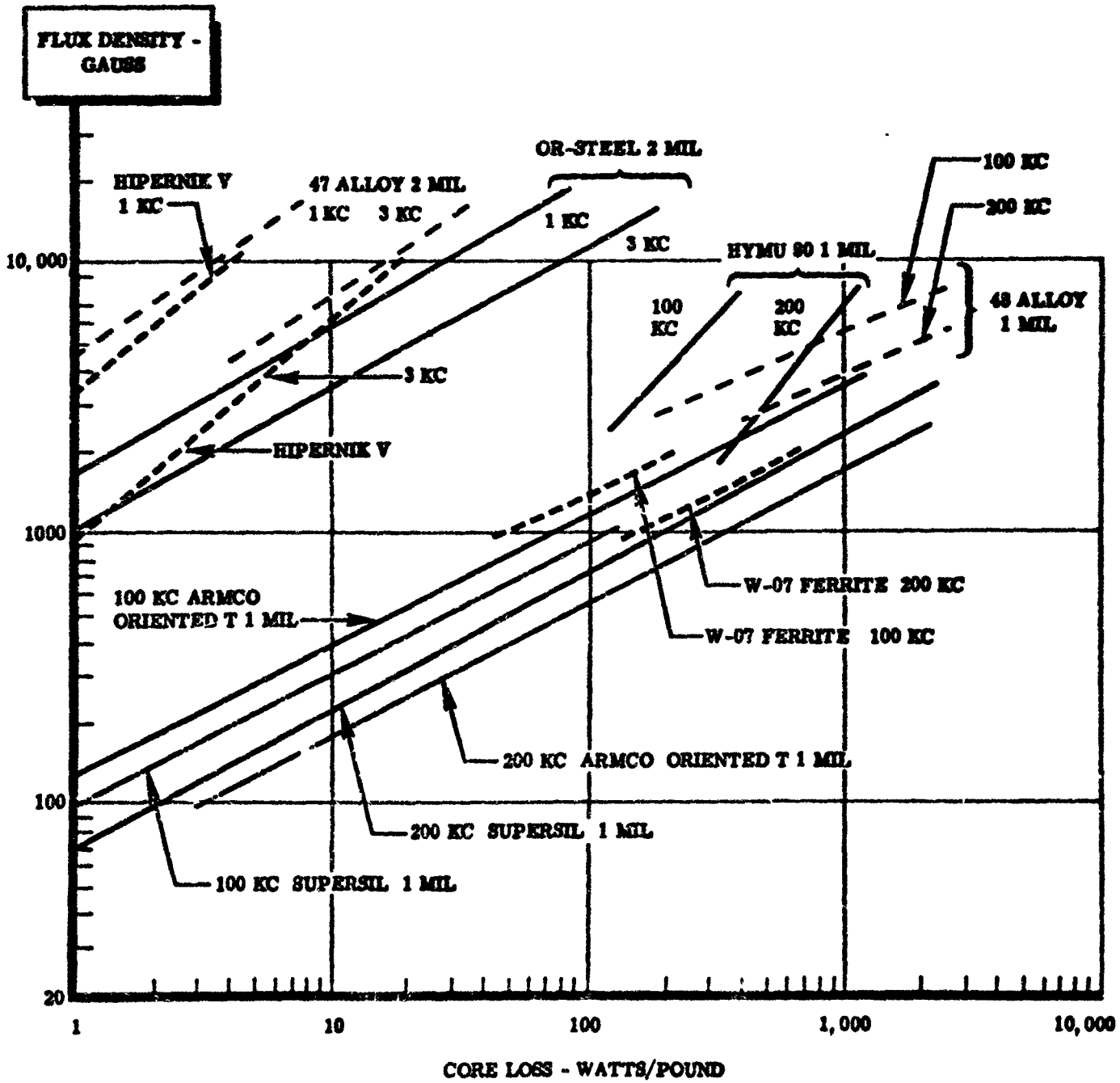


Figure 91. Flux Density vs. Core Loss for Various Materials

Core Loss Versus Temperature

Core loss data for high temperatures and low frequencies is available, but not much information is available on expected core losses in high-temperature, high-frequency devices. From the report of a previous study it is indicated that core losses at 550°C are reduced to about 60 per cent of room temperature values for various laminated core shapes. This variation did not appear to be a function of flux density.

Typical core loss versus flux density and core loss versus temperature curves at the low frequencies and high temperatures are shown in Figures 92A and 92B. The effect of temperature on total core loss (including both eddy current and hysteresis loss) at 1 KC frequency is shown in Figure 93A. In general, the core loss for both HYMU 80 and supermalloy drops off steadily with increasing temperature. The significant reduction in core loss in going from HYMU 80 to supermalloy is obvious from this data, but as shown in Figure 93A, supermalloy is both temperature and flux density limited. Figure 93B indicates that significant loss reductions are achieved by going from two mil to one mil materials and that even greater reduction could be achieved by using 1/2 mil or less laminations.

Curie Point

Care will have to be exhibited to insure that operating temperatures of both transformers and generators will not exceed the Curie point of the magnetic materials. The flux density value at which magnetic materials become saturated decreases until at the Curie temperature, approximately 750°C for silicon steel, it is totally nonmagnetic.

The range of maximum flux density for various magnetic materials and the corresponding Curie points for these materials are shown in Figure 87. The boundaries of these intersections point up the fact that increasing flux density is accompanied by generally higher Curie points.

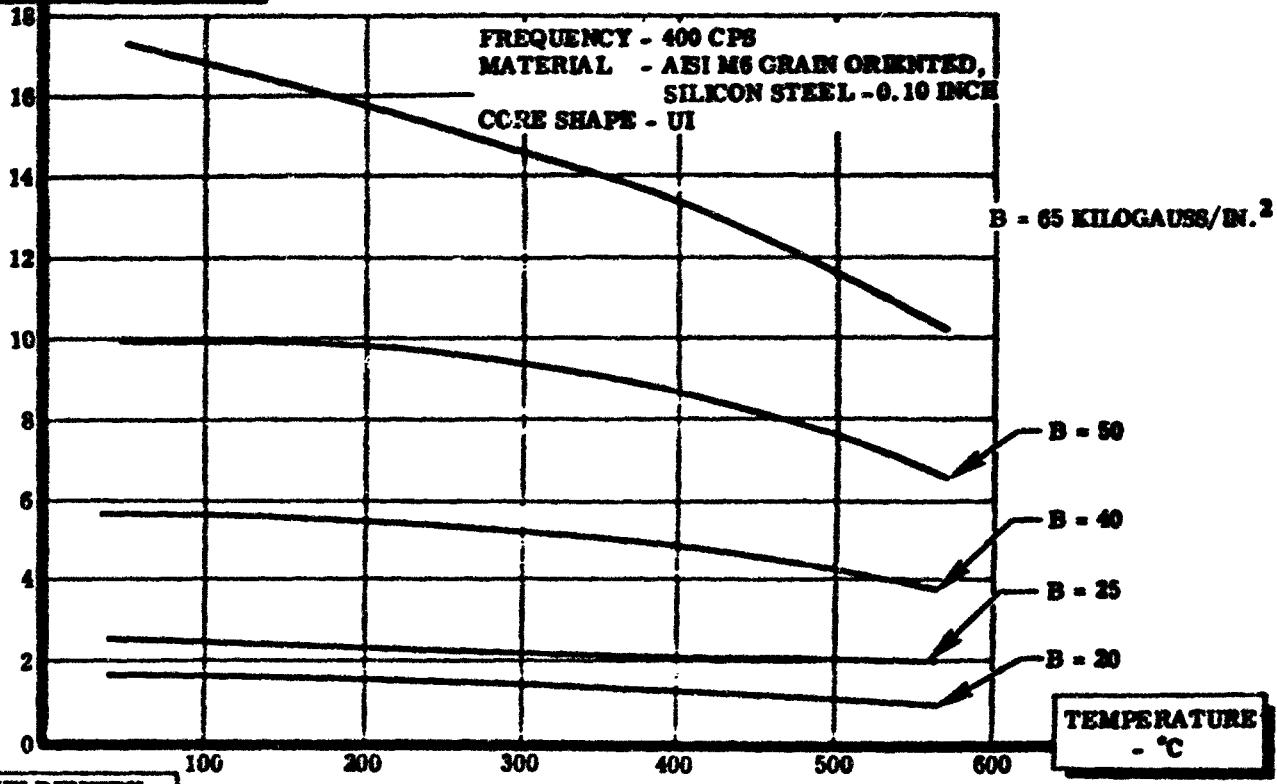
IRON LOSS DATA FOR GENERATOR DESIGNS

The iron loss data used in the various generator designs covered in this study is shown on Figure 94. These curves represent the best estimated from data available for the materials considered at the time the design calculations were performed.

It can be seen from this limited data that the use of conventional oriented silicon steel material would result in comparatively high losses at 200 KC unless extremely thin laminations are used. The superiority of HYMU 80 over other materials is evident in these figures with respect to other low-loss materials. If thin laminations are used, the core losses can be reduced to levels approaching that of the ferrites.

Loss calculations in this study have been based on data from these curves. Before detailed converter and generator designs for the high-frequency ranges specified in this study can be completed, it will be

CORE LOSS - WATTS / LB



FLUX DENSITY - KILOGAUSS/IN.²

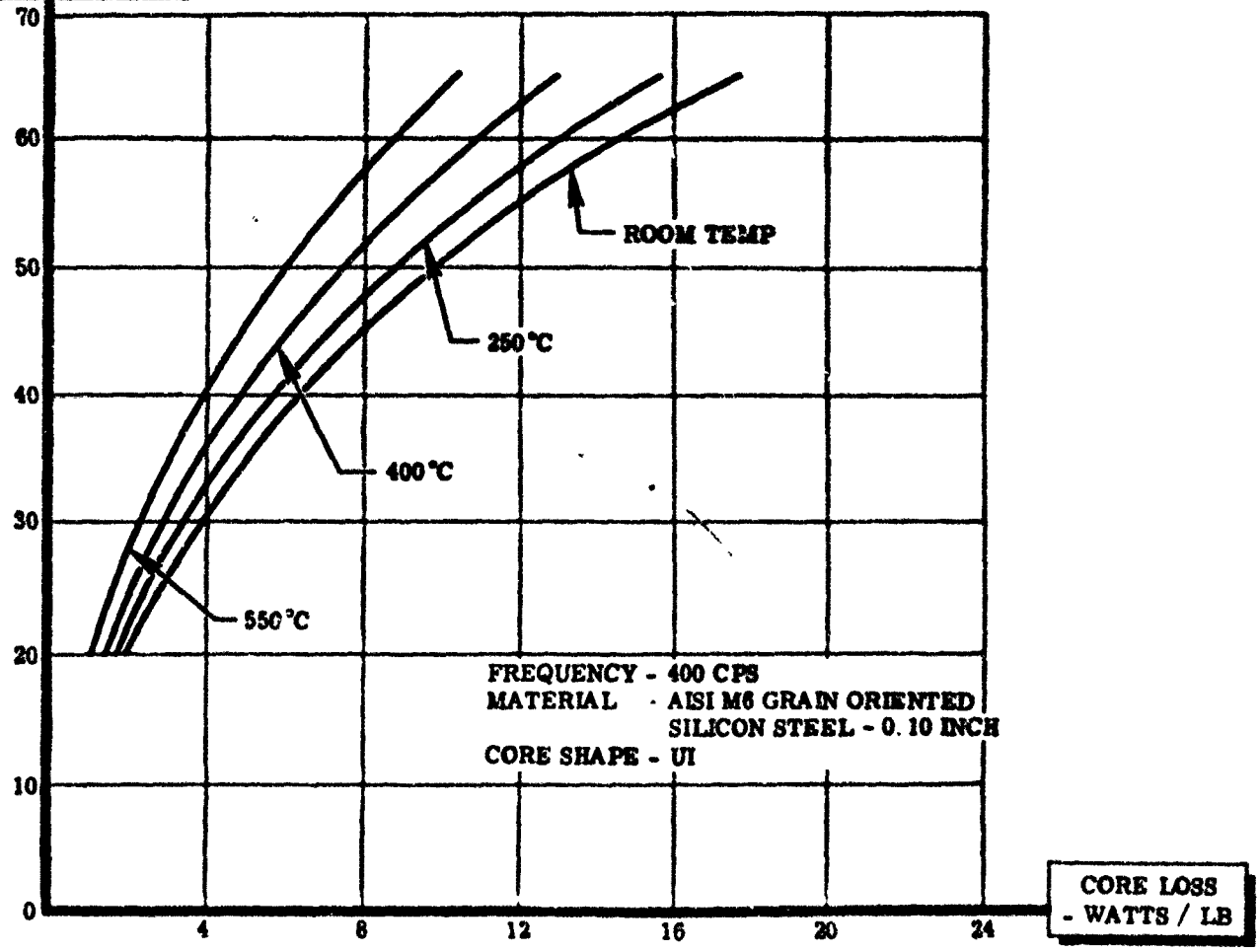
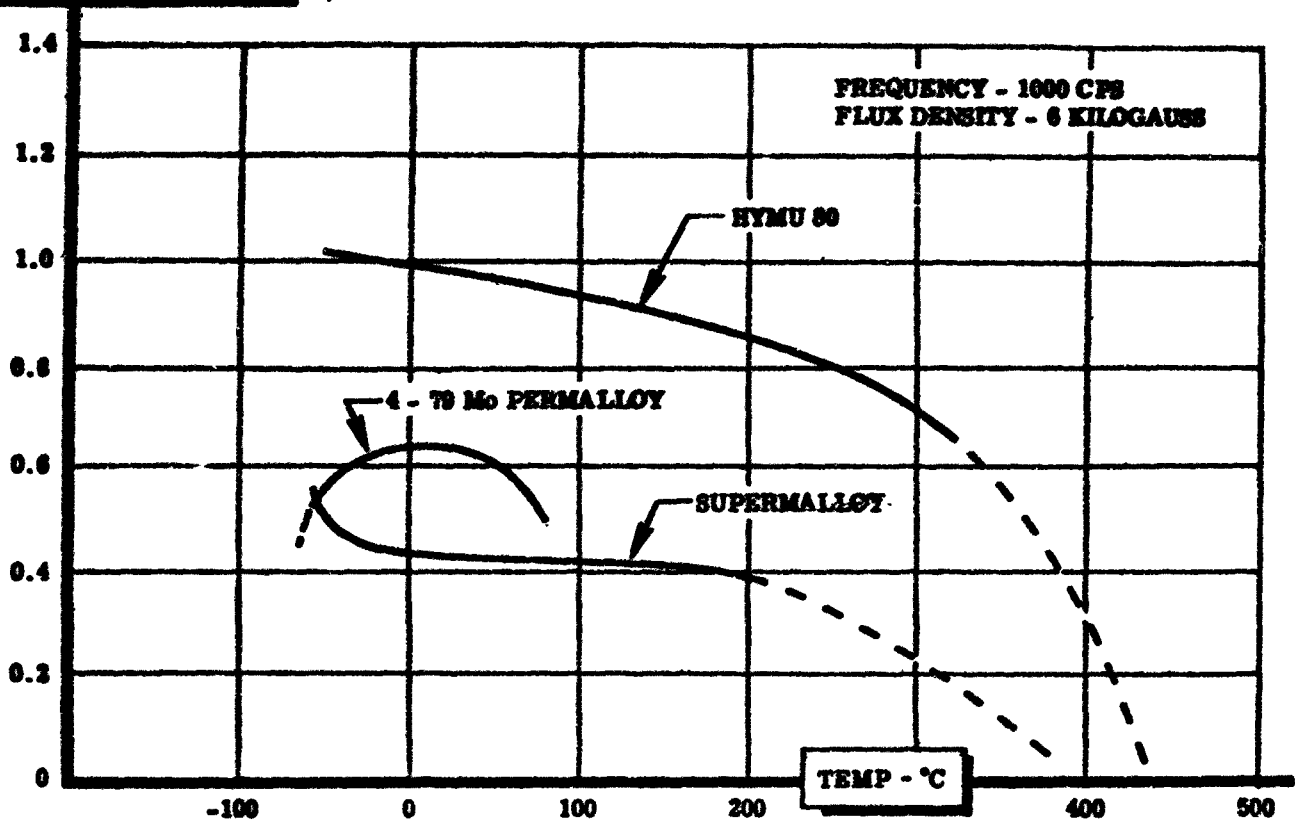


Figure 92. Core Loss vs Temperature and Flux Density for 3-1/4% Silicon Steel

CORE LOSS (WATTS/LB)



CORE LOSS - (WATTS / LB)

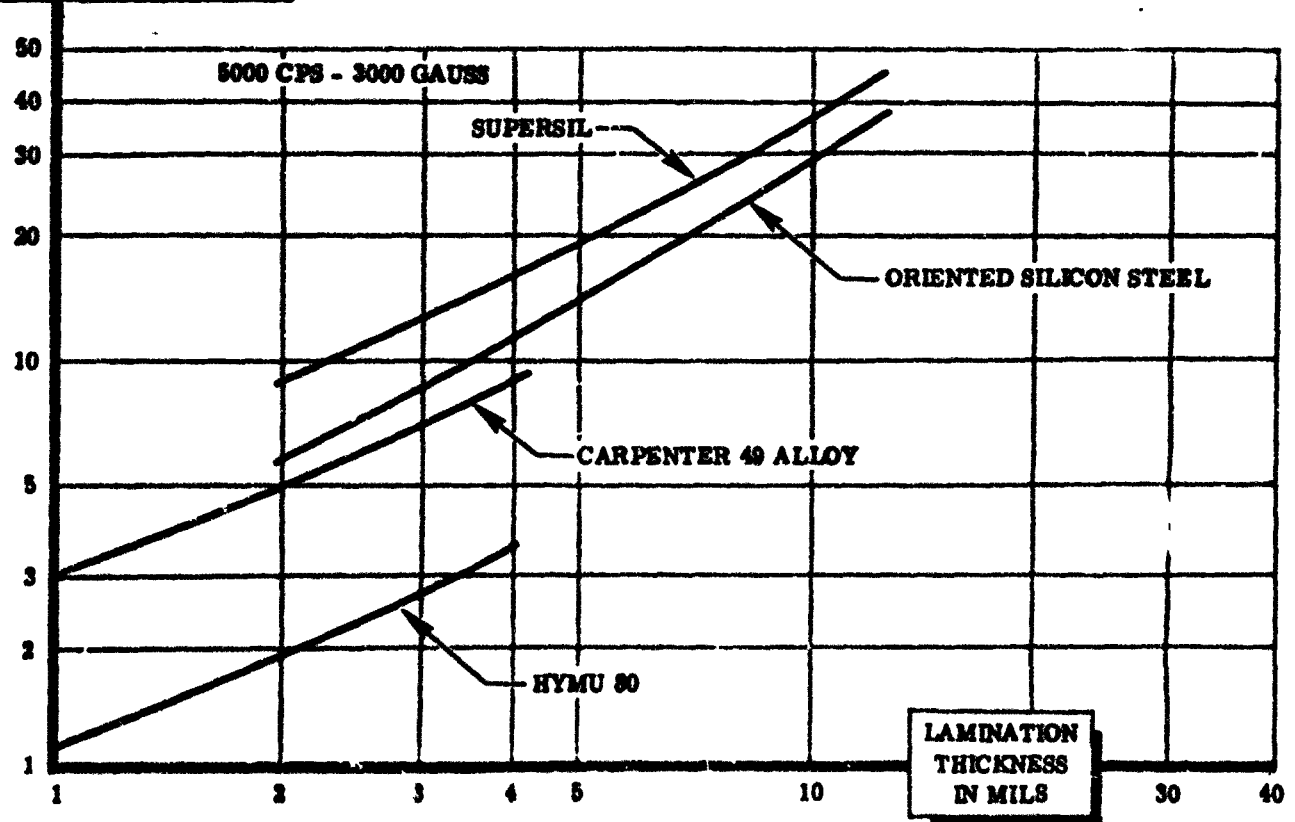


Figure 93. Core Loss vs. Temperature and Lamination Thickness

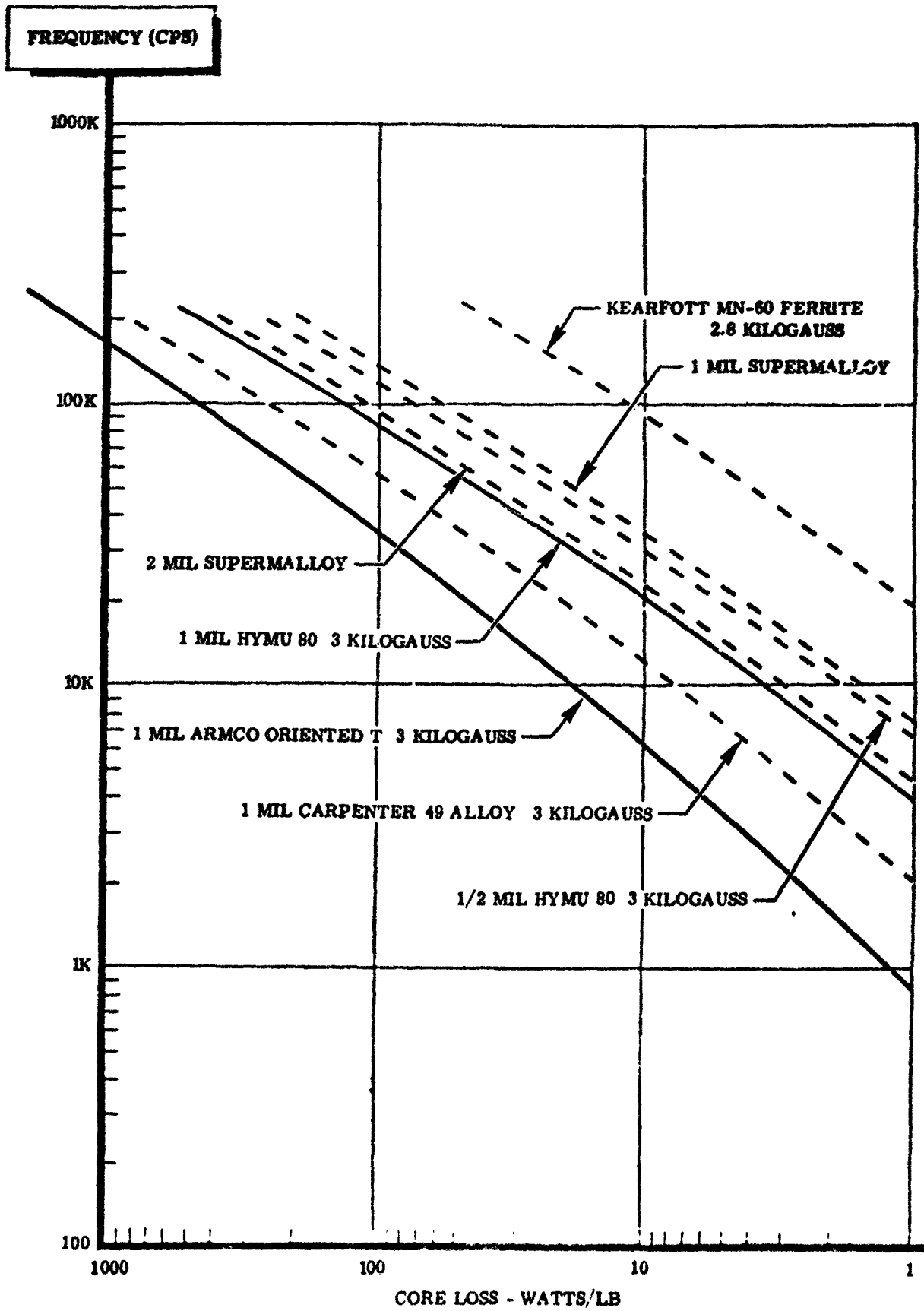


Figure 94. Iron Loss Data for Generator Designs

necessary to perform additional experiments to determine the magnitude of actual core losses to be encountered.

MATERIALS SELECTED

Selection of magnetic core material for the final transformer and generator designs will be based on standard design criterion with the additional requirement of stability of the magnetic properties in the specified environment. Based on Curie temperatures, cobalt alloys must be used if the magnetic components are to operate at the maximum temperature of 1,500°F. For a 1,000°F range, the choice is between Hiperco 27 or Hiperco 35 with Hiperco 27 being favored. If the maximum temperature of transformer operation is limited to 1,000°F, oriented-silicon-iron is recommended as the best material. Silicon-iron has been used in the preliminary transformer design calculations with HYMU 80 being considered for the high-frequency output transformers.

GENERATOR MATERIALS

Housing-low carbon steel

Stator - HYMU 80 or Alloy 48

Rotor - Nickel-maraging steel

Windings - Nickel clad copper, or ceramic coated copper for high temperatures.

Insulation - Ceramic slot liners or mica sheets backed with glass cloth.

TRANSFORMER MATERIALS

Cores - Silicon-iron (low frequency)
HYMU 80 (high frequency)

Windings - Nickel plated copper

Insulation - Synthamica asbestos compound

ROTOR MAGNETIC MATERIALS

Mechanical strength, as well as high saturation flux density, is an important consideration in the choice of magnetic materials for the generator rotor. Mechanical strength is of special importance since the centrifugal force at a design speed of 24,000 rpm is very high, and the use of material with a high yield strength at the design temperatures is essential. The wide range of saturation flux densities and yield strengths for various magnetic steels is shown on Figure 59. As a general rule, the harder and stronger the steel, the higher its coercive force and the lower its

saturation flux density. It should be noted, however, that the 18 nickel-maraging steels (recent development) have very high saturation flux density despite their higher yield strengths.

Since the magnetizing force is essentially constant under constant generator load, solid steel rotors are recommended for use in this design. The matter of low eddy current and hysteresis loss is of secondary consideration in the rotor. For this reason, a survey was made of commercial available materials having reasonably high yield strengths and saturation flux densities. The survey of materials is shown in Figure 95. In general, it can be said the materials having a high saturation flux density have a relatively low yield strength, and materials having a high yield strength have a low saturation flux density. Materials having both a high yield strength and a high saturation flux density are limited.

The Hiperco's and the Permendurs were eliminated from consideration in this study because of their long half-life when exposed to nuclear radiation.

Both AISI 4130 and 4340 are low-carbon, low-silicon steels that have found considerable use in the past for rotors. Of these two alloys, 4340 has somewhat higher yield strength at a slightly lower saturation flux density than 4130.

The one per cent Chromium low-carbon steel looks like an especially promising rotor material since its yield strength even in the annealed condition is high, and its yield strength in the hardened condition is almost double that of the ordinary steels used for high speed rotors.

Effect of Ambient Temperature on Yield Strength - In evaluating magnetic materials on the basis of their yield strength, the effect of ambient temperature on yield strength must be taken into consideration. As indicated on Figure 96, the 18 per cent nickel-maraging steels have a very high yield strength, but are useful over a smaller temperature range than either the low-carbon steels or Westinghouse Nivco-10. The corresponding usable temperature-yield strength range for other high strength materials is also shown on Figure 96.

WINDING MATERIALS

Conductors and conductor insulation for the transformer and generator windings at three performance levels, 500°F, 1,000°F, and 1,500°F were considered. Several insulations are available at the lower levels, but the choice is extremely limited at the 1,500°F level.

500°F Insulated Conductor System - Copper and aluminum conductors are available for use in transformer and generators. For equal current-carrying capacity, the volume of copper is less than that of aluminum. Aluminum electrical joints are fabricated more easily now than previously, and aluminum can now be handled quite easily.

SATURATION FLUX DENSITY - MEGAGAUS

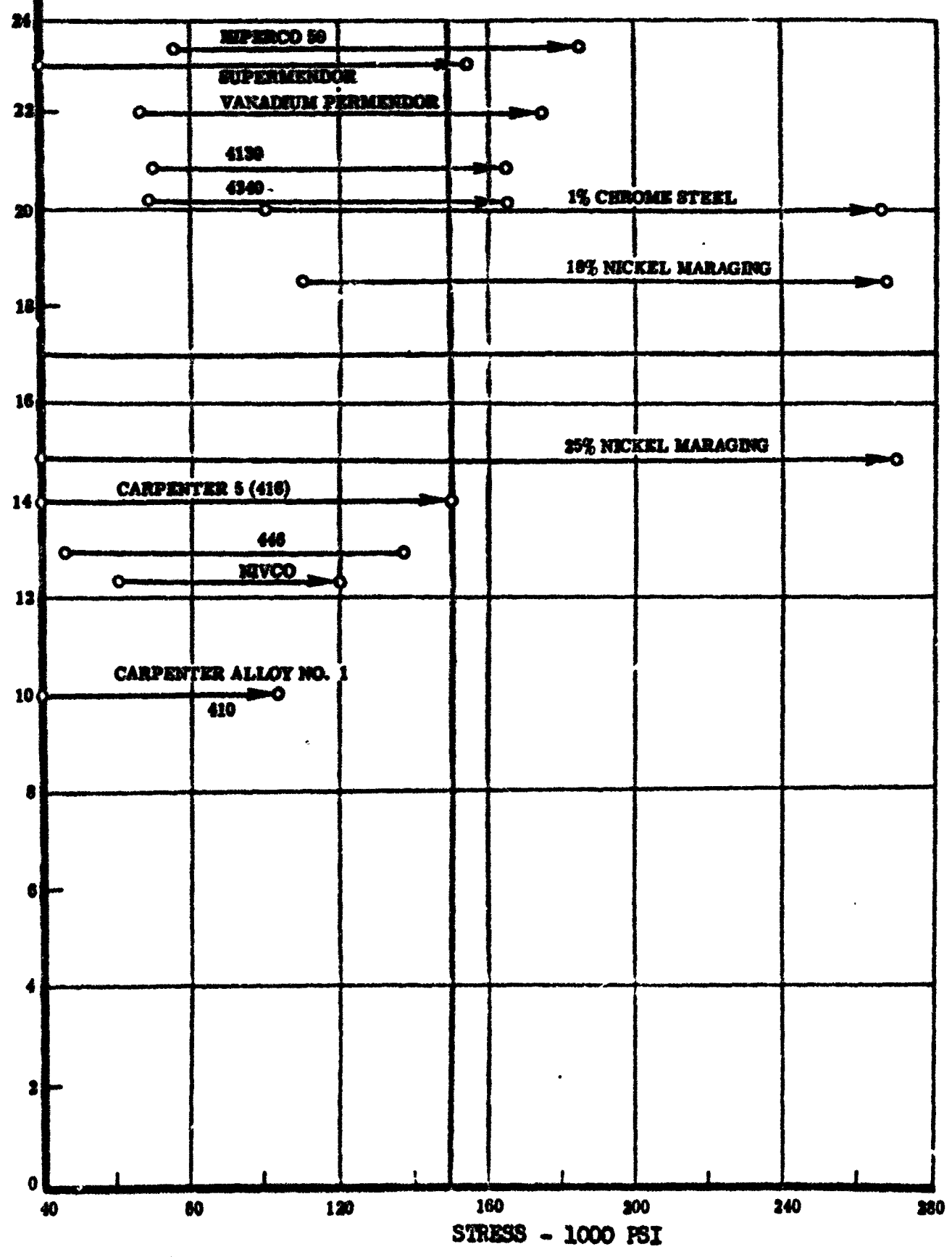


Figure 95. Comparison of Yield Strengths and Flux Densities

STRESS -
1000 PSI

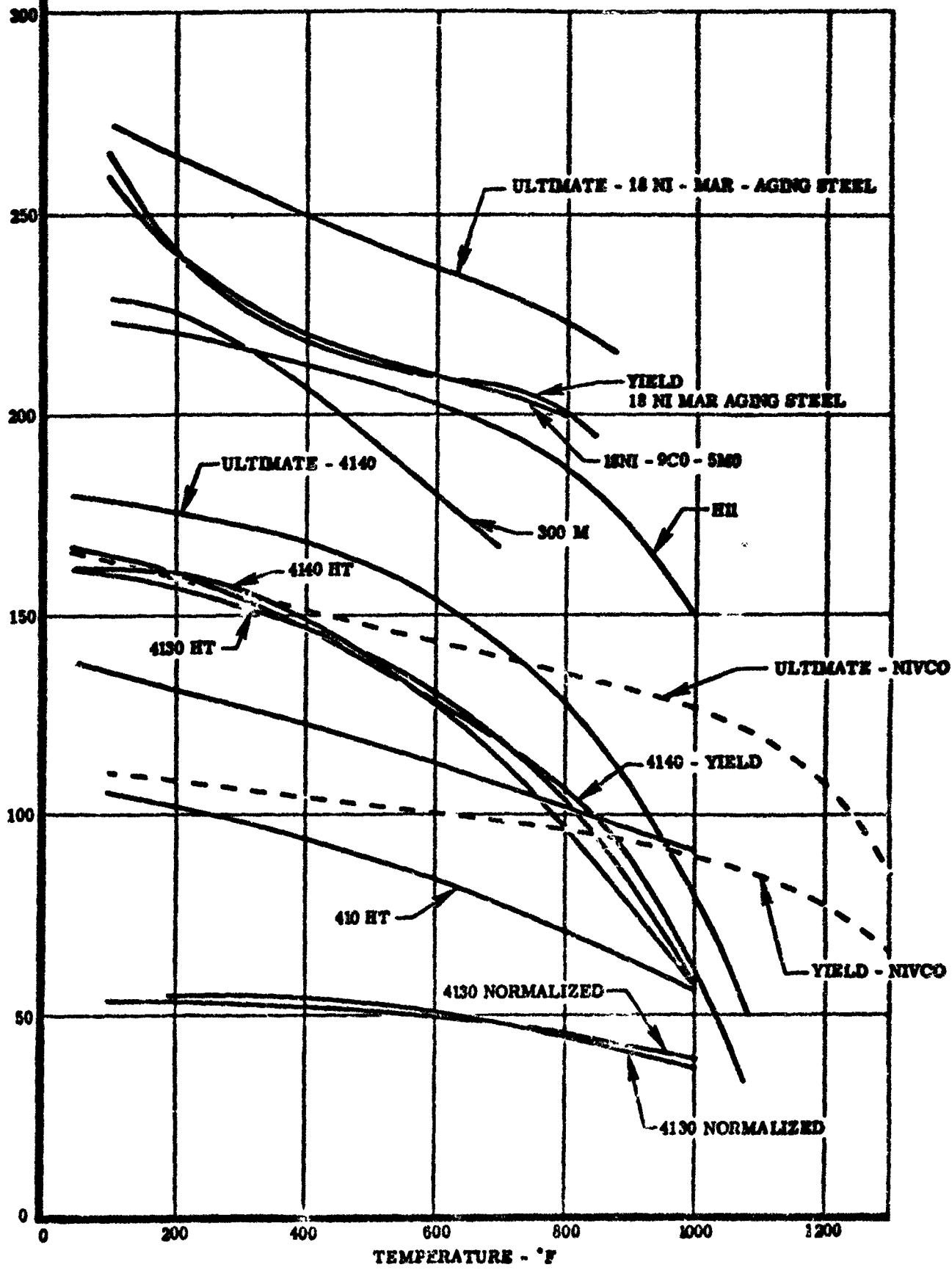


Figure 96. Yield Stress vs. Temperature for Magnetic Steels

1,000°F Insulated Conductor System - At the higher temperatures, copper conductors must be protected by a coating of oxidation resistant metal such as nickel. Cladding has the disadvantage of reducing the conductivity of copper, especially at the higher frequencies. Inorganic insulations must be considered at this temperature with special attention given to assembly of conductors and insulation.

1,500°F Insulated Conductor System - Stainless steel cladding or plating over copper appears to be the most suitable conductor design for 1,500°F. Refractory oxides appear to be the only insulations available for use. Fabrics and papers will probably be used as inter-layer material and as wrappings.

Magnet Wire - Magnet wires intended for use at elevated temperatures (as high as 850°C) and in intense nuclear radiation have been the subject of much industry research. The discussion which follows concerns several of the most available magnet wires.

In order to maintain reasonable conductivity, it is necessary to employ copper or silver. However, these metals must be protected from the oxidizing effects of the atmosphere. This has been done by the use of nickel cladding over the copper or silver. This technique works well up to about 400°C for copper. At higher temperatures, nickel can co-diffuse into the copper resulting in loss of conductivity. By comparison, silver and nickel do not exhibit harmful co-diffusion even at temperatures approaching the melting point of the silver. Stainless steel has also been used as a cladding over copper, and is useful up to 500°C. The size of the wire needs consideration in the choice of the conductor construction since diffusion proceeds in equal thicknesses of layers. Thus, fine wires exhibit marked loss of conductivity while large wires change slowly. Pure copper suffers from severe oxidation when exposed during high temperature insulation cure cycles and when exposed to chlorinated silicone coolant fluids.

Nickel Clad, Nickel Plated, and Stainless Steel Clad Wires - Nickel clad wire is a very acceptable material for use in stator windings operating up to about 900°F. However, there are problems associated with the use of nickel plated wires. The diffusion of the nickel and copper can cause a permanent change in the resistance of the material, particularly above 500°C. Coating elongation can also cause problems; for example, winding under excessive tension can produce a break in the coating and expose the conductor. Nickel plated wire offers little protection against oxidation.

Stainless clad copper or nickel clad copper with a ceramic-silicone coating is potentially useful where the operating temperatures do not exceed 750 to 840°F. Stainless steel clad copper wire shows unusual DC resistance stability even after exposure for 1,000 hours at 1,100°F. Unfortunately, electrical properties of this type of wire deteriorate rapidly at this ambient temperature.

Silver Clad Copper and Silver Wire - Silver clad copper wire is unsatisfactory for high temperature use since silver will migrate into the copper at elevated temperatures. Silver wire is more expensive than other forms of wire, but has

the advantage of good electrical conductivity at high temperatures, is ductile, and is readily joined by welding.

Ceramic Coated Copper Wire - Phelps Dodge manufactures a high temperature magnetic wire known as ceramic-eze, which is available in round sizes from 18 AWG through 36 AWG. This is a flexible, windable, abrasion resistant wire for use at temperatures up to 650°C. The total film buildup is on the order of 0.3 to 0.7 mils on all sizes of wire. The standard product is a 72 per cent copper, 28 per cent nickel clad conductor having a 72 per cent conductivity. For applications about 1,000°F, Phelps Dodge can furnish a 20 per cent nickel-clad silver conductor with their standard ceramic-eze coating. Ceramic-eze magnet wire has excellent chemical resistance. Acids and alkalies have no appreciable effect.

This insulation is also completely insoluble in water. Because the insulation is not completely vitreous, water will be absorbed on the surface and tenaciously held. For this reason it is recommended that the stator encapsulation system have a completely vitreous surface.

Glass-Served Copper Wire - Glass-served magnet wire employs a serving of glass fiber impregnated with inorganic binders and fillers. The insulation system consists of nickel plated copper wire covered with two layers of glass fiber. The composite is passed through a suspension of powdered mica and a phosphate solution and fired at 480°F. When suitably formulated, the insulation's resistance is equivalent to that of glass-served organic-coated wire.

Another glass-served system suitable for use at 930°F consists of two layers of glass impregnated with silicone resin. The silicone provides strength for winding and is subsequently volatilized by heating four hours at 930°F. This tends to make the glass somewhat fragile; however, if it is properly supported in the stator coil, it can remain undisturbed during mechanical stress. The glass serving adds about eight mils to the conductor diameter, and is compatible with most base conductor materials.

Magnet Wire Insulated with Glass Fiber and Organic Bonding Agent with Dispersed Ceramic Filler - The insulation consists of one or more servings bonded with a varnish in which ceramic or glass powder is thoroughly dispersed. The conductor is copper-core with an oxidation protective cladding. The varnish is completely fugitive when heated sufficiently. The ceramic or glass filler can then be fused or sintered to improve the mechanical and electrical characteristics of the insulation. This type of wire has a thermal rating of 650°C, and is available in round sizes 12 to 30 AWG with single or double servings.

INSULATION MATERIALS

Transformer and generator insulation is required to insulate electrical circuits from each other, from mechanical structure, and from the magnetic circuits. Two types of insulation are considered: A major insulation to provide electrical insulation, and a minor insulation whose function is mainly to add mechanical strength to the component.

the advantage of good electrical conductivity at high temperatures, is ductile, and is readily joined by welding.

Ceramic Coated Copper Wire - Phelps Dodge manufactures a high temperature magnetic wire known as ceramic-eze, which is available in round sizes from 18 AWG through 36 AWG. This is a flexible, windable, abrasion resistant wire for use at temperatures up to 650°C. The total film buildup is on the order of 0.3 to 0.7 mils on all sizes of wire. The standard product is a 72 per cent copper, 28 per cent nickel clad conductor having a 72 per cent conductivity. For applications about 1,000°F, Phelps Dodge can furnish a 20 per cent nickel-clad silver conductor with their standard ceramic-eze coating. Ceramic-eze magnet wire has excellent chemical resistance. Acids and alkalies have no appreciable effect.

This insulation is also completely insoluble in water. Because the insulation is not completely vitreous, water will be absorbed on the surface and tenaciously held. For this reason it is recommended that the stator encapsulation system have a completely vitreous surface.

Glass-Served Copper Wire - Glass-served magnet wire employs a serving of glass fiber impregnated with inorganic binders and fillers. The insulation system consists of nickel plated copper wire covered with two layers of glass fiber. The composite is passed through a suspension of powdered mica and a phosphate solution and fired at 480°F. When suitably formulated, the insulation's resistance is equivalent to that of glass-served organic-coated wire.

Another glass-served system suitable for use at 930°F consists of two layers of glass impregnated with silicone resin. The silicone provides strength for winding and is subsequently volatilized by heating four hours at 930°F. This tends to make the glass somewhat fragile; however, if it is properly supported in the stator coil, it can remain undisturbed during mechanical stress. The glass serving adds about eight mils to the conductor diameter, and is compatible with most base conductor materials.

Magnet Wire Insulated with Glass Fiber and Organic Bonding Agent with Dispersed Ceramic Filler - The insulation consists of one or more servings bonded with a varnish in which ceramic or glass powder is thoroughly dispersed. The conductor is copper-core with an oxidation protective cladding. The varnish is completely fugitive when heated sufficiently. The ceramic or glass filler can then be fused or sintered to improve the mechanical and electrical characteristics of the insulation. This type of wire has a thermal rating of 650°C, and is available in round sizes 12 to 30 AWG with single or double servings.

INSULATION MATERIALS

Transformer and generator insulation is required to insulate electrical circuits from each other, from mechanical structure, and from the magnetic circuits. Two types of insulation are considered: A major insulation to provide electrical insulation, and a minor insulation whose function is mainly to add mechanical strength to the component.

TABLE 2h

MAXIMUM TEMPERATURE OF TRANSFORMER INSULATIONS

MAJOR		MINOR		POTTING AND IMPREGNATING	
MATERIAL	TEMP	MATERIAL	TEMP	MATERIAL	TEMP
Tipersul	2200 F	Beryllia Oxides	4000 F	Tipersul	2200 F
		Alumina 99%	3540 F		
		Boron Silicides	2500 F		
		Tipersul	2200 F		
Synthamica			1550 F	Silicone Silicate Asbestos Compound	2000 F
		Isonica	1550 F	Silico Ceramic- Silicic Acid	2000 F
				Synthetic Mica Cement	2000 F
Quinorgo RA	1000 F	Isonica	1000 F	Lead-Oxide/Boric- Oxide Eutectic	1000 F
Samica	1000 F	Steatite at High Volt	1000 F		
Alkophos	1000 F				
Mica-Flakes- Silicone Bonded	500 F	Silicone Micarta	500 F	Silicone	500 F
Teflon	500 F	Micalex	500 F		

Magnetic Steel Insulation

Magnesia - During the processing of the core steel, a magnesium silicate is formed on the steel surface. Much of the steel has an additional phosphate type coating formed on it for greater insulation strength. These coatings, although very thin, are of high resistance, and are hard and abrasion resistant. They have the further advantage of extreme heat resistance and stability, and a smooth surface for handling ease.

Natural Oxide Finish - The low loss magnetic materials, such as supermalloy, HYMU 80, and Alloy 49 are composed of high content nickel alloys, and inter-lamination insulation can be achieved in the ordinary processing of these materials in the form of a natural oxide finish. A thin coating of Sterling 5-678 red core plate would provide additional protective material and reduce the effect of aging on core loss and excitation current.

Bonding of Stator Stack Laminations

Adhesives can be used to bond the ultra-thin stator laminations together, but they are too thin for any other type of fastening. Thermo-setting resin compounds are available which cure without the application of pressures, and which provide a strong bond between the surfaces while at the same time forming a dielectric layer between the parts they bond. A good example is Columbia Technical Corporations AC-523 adhesive which is rated for up to 350°C application. This material can be applied to the laminations over the oxide or varnish coating which provide the primary insulating coating.

Another type of material for bonding is an inorganic coating-cement composed essentially of ceramic fiber bonded with an air setting temperature resistant binder. It can be applied as a paste or by spray, dip or brush. The material has excellent thermal shock and has a rated use temperature of 2,300°F.

Encapsulation of Stator

The stator of a high-frequency generator will probably consist of low-loss high permeability laminations of from one to two mils thickness. Distortion is undesirable physically, but more important, it ruins the magnetic properties of the core. Slot windings must be rigidly supported in order to prevent conductor abrasion. For this reason the stator must be properly potted and encapsulated in the housing.

Potting and Embedding Compounds

Several air drying cements can be used for potting and embedding the stator at temperatures well over 930°F. Many of these materials were originally developed as high temperature thermal insulations for furnaces and thermocouples, but they can be used to electrically insulate and protect stator windings at high temperatures. Air drying cements are quite porous and tend to absorb moisture, but this would not be a great problem in a generator that is continuously operated at high temperature. The problem can be minimized with a suitable glaze or cement.

Fusion-Bonded Insulation System

The stator can be protected against the high operating temperature by coating or bonding the coils with an inorganic material which is sintered or bonded into place. The bond obtained with fusion bonded inorganic materials is better than that obtained with other high temperature materials and is most nearly similar to that obtained with the lower temperature plastics.

A process developed by Westinghouse Electric consists of the following steps:

1. Coating and/or potting the components with a porous material containing reactive components. This material is applied to the stator during winding as an interlayer coating and/or impregnated into the winding from a slurry, or solution.
2. Vacuum impregnating the stator assembly with certain glass compositions at high temperature. The best impregnants evaluated to date are a lead oxide-boric oxide eutectic ($88\text{PbO} - 12\text{Bi}_2\text{O}_3$) which reaches sufficient fluidity for vacuum impregnation at about $1,160^\circ\text{F}$, and a lead oxide - bismuth trioxide eutectic ($72\text{PbO} - 28\text{Bi}_2\text{O}_3$) which reaches sufficient fluidity at about $1,250^\circ\text{F}$.
3. Heat treating the assembly until the impregnant reacts with the potting compound and the internal inorganic insulation. During heating, the composition of the impregnant changes so as to improve the physical and electrical properties of the insulation system.

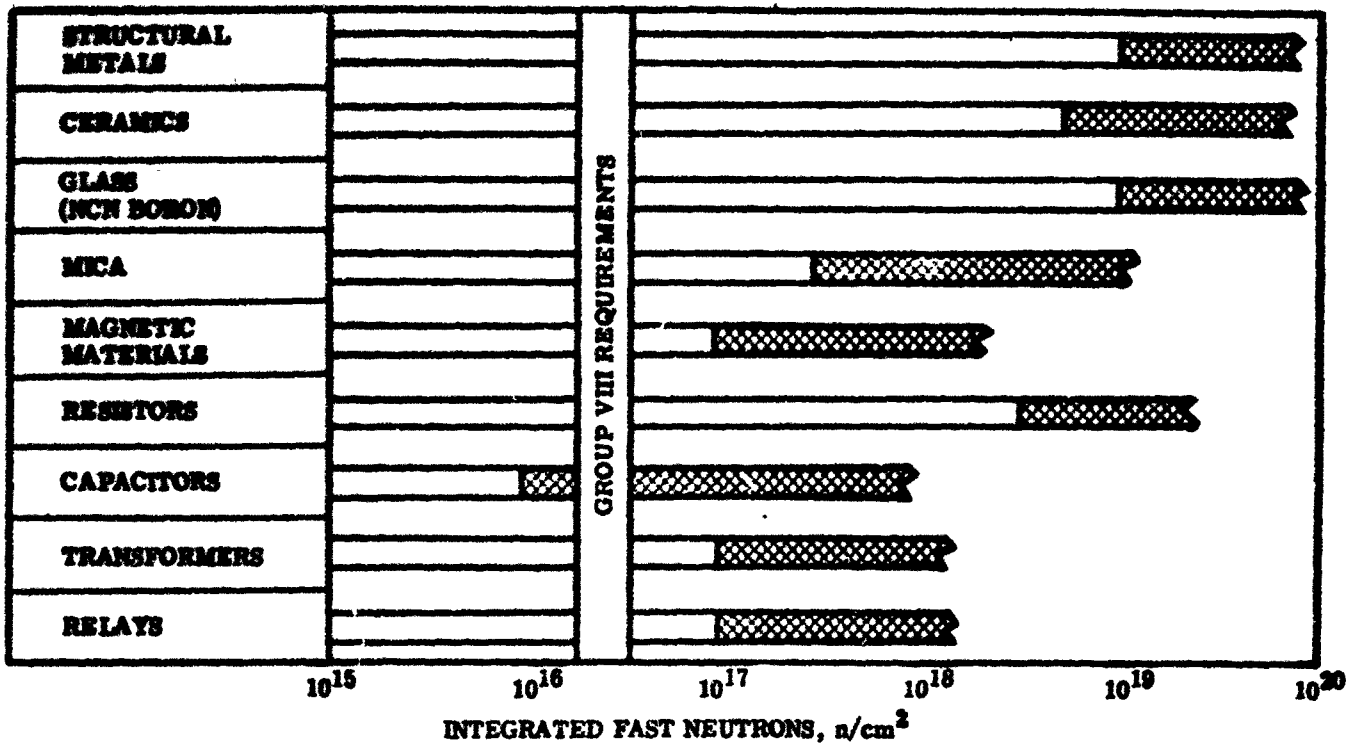
Phelps Dodge has developed a synthetic mica-aluminum phosphate encapsulation system that has performed satisfactorily at temperatures up to $1,200^\circ\text{F}$. This system requires a vitreous coating to be applied to the encapsulant in order to provide an overglazed surface.

RADIATION RESISTANCE OF CONVERTER COMPONENTS

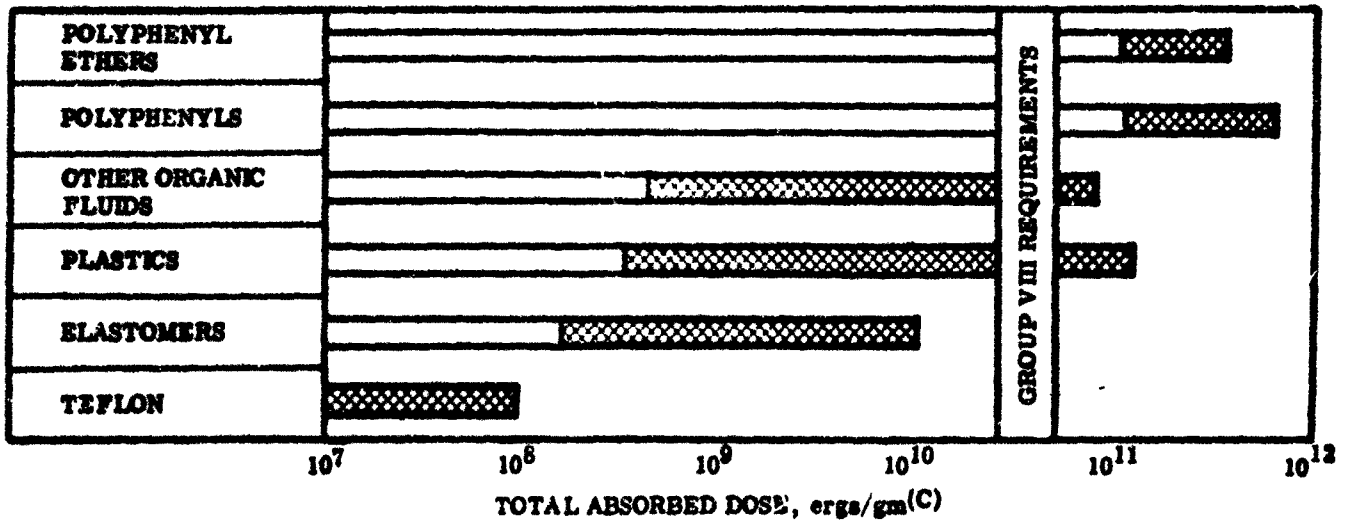
The radiation tolerance of generating system materials and subcomponents has been investigated in previous studies. The investigation was conducted through a literature survey of reported radiation effects on generating system type of materials. This study was hampered by the fact that most of the radiation testing of electrical components has utilized standard, off-the-shelf, low temperature equipment. Available data for high temperature equipment is limited.

A portion of the radiation resistant material was derived in connection with development of the HOTELEC generating system. A general summary of this information is presented graphically in Figure 97, and an expanded discussion on specific materials and components is presented in the sections which follow.

**MATERIALS PRIMARILY SENSITIVE
TO FAST NEUTRON OR DISPLACEMENT DAMAGE**



**MATERIALS PRIMARILY SENSITIVE TO
IONIZATION BY BOTH NEUTRONS AND GAMMAS**



KEY:
 NO SIGNIFICANT EFFECTS
 SOME EFFECTS BUT OFTEN USABLE

Figure 97. Relative Radiation Tolerance of Various Materials

The results of these studies lead to the evident conclusion that extreme high temperature capabilities and radiation resistance are generally synonymous. As a class, the organic or covalent compounds are less resistant than the inorganic and ionic compounds to the damaging effects of these two environmental conditions. The high temperature requirements of the power conversion system will eliminate most organic compounds from consideration as candidate materials, without the added factor of radiation induced damage. The single class of organic materials which will be considered is that of fluids for lubrication and heat transfer.

Structural Metals - Experimental evidence to date indicates that structural metals are quite resistant to nuclear radiation, although not all the useful or potential alloys suitable for nuclear-powered-air vehicle construction have been adequately investigated. On the basis of out-of-pile tests, fast neutrons in integrated flux levels above 10^{19} n/cm² represent the only reactor radiation that can significantly affect the properties of nonfissionable metals. This is considerably above the levels anticipated and thus no great problem is anticipated for structural metals.

Neutron effects in metals have been studied at integrated fluxes between 10^{15} and 10^{22} n/cm² (fast) at temperatures between 30 and 400°C. Such investigations have included carbon steels, stainless steels, aluminum alloys, nickel alloys, cobalt alloys, magnesium alloys, titanium, zirconium, molybdenum, tungsten, tantalum, copper and beryllium. Radiation effects in metals are analogous to those of cold work, but are less severe and by different mechanisms.

Electrical Insulating Materials - The failure of conventional electrical insulation in nuclear radiation environments is primarily due to the mechanical and physical deterioration of the materials rather than to gross changes in their dielectric properties. The ionizing effects of radiation in organic insulators lead to a series of complex chemical reactions which drastically alter the nature of the material. Elevated temperature, a common adjunct of a nuclear radiation environment, tends to advance the deterioration of organic materials.

Inorganic materials are, in general, much more resistant to radiation damage than are organic materials. This is due to the type of damage which occurs in the materials. Atomic displacements, which constitute only a small part of the damage in organic polymers, account for nearly all of the permanent damage in inorganic insulators. Ionization and excitation of atoms lead to no new bond formations so that the irradiation of inorganic substances leaves the material unaltered chemically. Since most inorganic insulators are stable ceramic oxides, radiation promotes no chemical reaction of the insulation with its environment.

There is, however, a strong photoconductive effect accompanying the irradiation of most inorganic ceramics. A large part of the energy of incident radiation is absorbed by electronic excitation and ionization. Although this excitation does not lead to bond breakage or formation, it does produce quasi-free electrons which are free to move under the influence of an electrical field. Since the mobility of charge carriers in inorganic compounds is higher than that in organic polymers, there is a corresponding difference in

the magnitude of the radiation induced photocurrent. This effect, however, is not expected to seriously impair the usefulness of inorganic insulators in a radiation field.

Atomic displacements lead to permanent changes in inorganic insulators which are manifested as changes in the lattice parameters, density, strength, and electrical properties. For crystalline bodies (crystalline quartz, Al_2O_3 , MgO , etc.) radiation bombardment results in lattice expansion and a corresponding decrease in density. However, the flux levels for this phenomena are considerably above the levels anticipated by this program.

The best experience indicates that most ceramic insulators, with the notable exception of glass, are satisfactory up to integrated fast fluxes of 10^{22} n/cm². Since the damage in inorganic insulators is due primarily to atomic displacements, gamma rays are not expected to offer much of a problem. It is true that the Compton electrons produced by gamma ray scattering will cause some atomic displacements, but experience with semiconductors indicates that this damage is small in comparison with that caused by fast neutrons.

In addition to the comparative radiation resistance of inorganic insulators, they possess much greater temperature stability than do organic materials. In fact, operation at elevated temperatures allows thermal annealing to take place, which lessens the amount of damage suffered by the inorganic materials.

Effects of Nuclear Radiation on Magnetic Materials - The magnetic properties of materials have been measured in many nuclear irradiation experiments. They have, however, been used primarily for following solid-state reactions and not for examining the effects of radiation on the properties of magnetic materials. Although little information is available concerning the basic mechanisms of radiation damage in magnetic materials, some insight may be gained from investigations of radiation effects in metals, alloys, and semiconductors. It would be expected that those properties of a ferromagnetic material that are structure sensitive, such as permeability, remanence, and coercive force, would be affected by radiation, while such nonstructure sensitive properties as the saturation magnetization would not be affected. Much of the available experimental information confirms the above statements and adds to the present understanding of radiation effects on materials in general.

The U. S. Naval Ordnance Laboratory has studied the effects of reactor irradiation on a number of magnetic materials including the following classes: High-nickel-iron alloys, 50 nickel-iron alloys, silicon irons, aluminum irons, and 2V Permendur. These materials were exposed to reactor flux levels up to 10^{17} n/cm² (fast). The associated gamma intensity (1 to 2 Mev) was approximately 3×10^7 rads, and the temperature was approximately 60°C. The following magnetic properties of the laminated and tapewound cores were measured before irradiation, during irradiation and after irradiation: (1) Normal DC induction curve and hysteresis loop, permeabilities, coercive force, remanence, and maximum induction at a field of 30 oersteds, and (2) AC induction curves and dynamic loops at 69 cycles and 400 cycles. Loss measurements at higher frequencies were made on the powder and ferrite cores before and after irradiation.

The high nickel-iron alloys, which have the higher permeabilities and the lowest coercive forces, changed the most upon irradiation. Their high permeabilities were drastically lowered and their low coercive forces were correspondingly raised. The properties of the 50 nickel-iron alloy change markedly, but not so much as those of the high nickel-irons. Silicon irons, aluminum irons, and 2V Permendur cores proved to be radiation resistant to the neutron and gamma exposures used, their changes in properties being small or negligible. The results of these experiments are summarized in Table 25.

Effects of Nuclear Radiation on Capacitors - The feasibility of using various types of capacitors in a radiation environment can be estimated from available information of a general nature. Figure 98A indicates the approximate amount of radiation that various capacitor types will withstand and still be operational. This information is not design data, but only an indication of the suitability of a particular type of capacitor.

The important and most obvious factor to consider in choosing a capacitor for use in a radiation environment is the choice of an inherently radiation-resistant material. Inorganic materials, such as mica, glass, and ceramics, exhibit the greatest resistance to radiation induced damage. Capacitors using these dielectrics have shown negligible damage after being exposed to integrated fluxes as great as 10^{16} n/cm² (fast) and greater than 10^{18} n/cm² (total).

Aluminum is the usual plate material for capacitors and causes little trouble because it is not subject to radiation damage at exposures usually encountered and its small neutron cross-section results in low residual activity. Several government sponsored programs are now under way for the development of high-temperature radiation-resistant capacitors to operate in a radiation environment and at temperatures as high as 500°C. The approach to this problem is to use new dielectric materials. Aluminum oxide, magnesium oxide and boron nitride are under consideration as dielectric materials with boron nitride presently receiving the most attention.

It is necessary to consider the total environment under which the unit must operate, that is, the intensity of and exposure time to radiation, temperature, humidity, and mechanical stresses. It must be known, at least approximately, how much variation in capacitor usually is exhibited in three ways: (1) Change in capacitance, (2) increase in dissipation factor, and (3) decrease in leakage resistance. The change in these characteristics at the peak radiation levels shown in Figure 98A may be sufficient to cause improper functioning of the unit. For example, an increase in leakage current usually accompanies exposure to gamma radiation as the result of gamma-induced ionization in air paths and in the dielectric material.

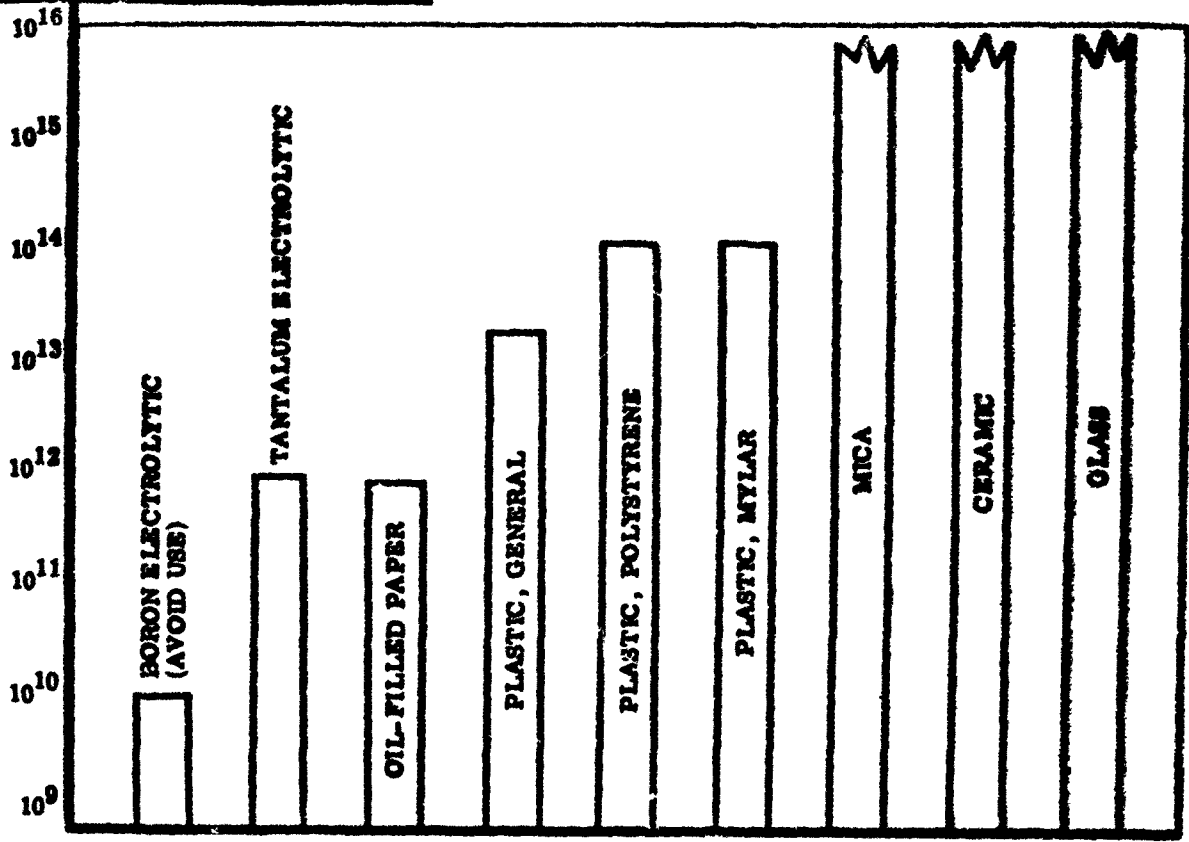
Effects of Nuclear Radiation on Resistive Components - It has been pointed out that nuclear radiation affects all components and materials in some way. The type and extent of damage observed in resistors depends upon the materials used, the interaction between materials, and the application of the resistors. Since some resistor applications are more critical than others, the proper selection of radiation-resistant resistors is an

TABLE 25

PERCENTAGE CHANGE IN D-C MAGNETIC PROPERTIES OF VARIOUS MAGNETIC ALLOYS
AS A RESULT OF IRRADIATION WITH APPROXIMATELY 10^{17} FAST N CM⁻²

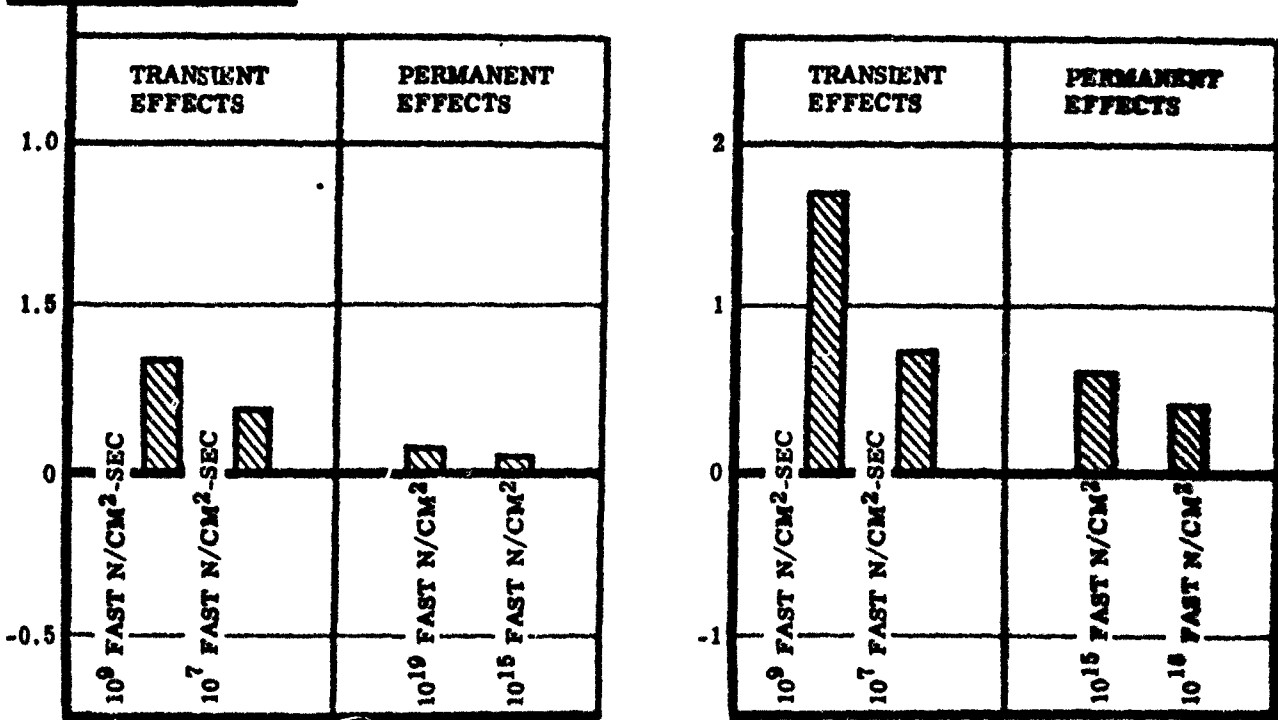
Material	Per Cent Change in Permeability (Induction of 20 Gauss)	Per Cent Change in Maximum Permeability	Per Cent Change in Coercive Force	Per Cent Change in Remanence	Per Cent Change in Loop Rectangularity
<u>High Nickel-Iron Alloys</u>					
Supermalloy	-93	-93	815	-38	-36
4-79 Mo Permalloy	-89	-79	403	-44	-44
Mumetal	-65	-38	158	-26	-23
<u>50 Nickel-Iron Alloys</u>					
48 nickel-iron	-70	-10	99	-26	-26
50 nickel-iron (oriented)	-31	15	-28	-24	-21
<u>Silicon Irons, Aluminum Irons, and 2V Permendur</u>					
3.5 silicon-iron	8	-1	6	1	1
3 silicon-iron (oriented)	18	1	-2	3	-1
3-1 silicon-alumi- num-iron	1	1	2	2	-1
16 aluminum-iron (ordered)	34	15	-8	8	13
16 aluminum-iron (disordered)	-4	-4	-2	--	--
2V Permendur	3	2	-2	-1	0

FAST NEUTRON EXPOSURE - $N \cdot CM^2$



A CAPACITORS

ESTIMATED PER CENT RESISTANCE CHANGE



B RESISTORS

Figure 98. Radiation Tolerance of Capacitors and Resistors

important initial step toward good design of systems that will function reliably when exposed to intense nuclear fields.

Presently available data provides a rough estimate of the relative stability of various types of resistors under nuclear radiation, but does not provide any basis for estimating damage thresholds. The relative radiation resistance of various types of fixed resistors in order of increasing sensitivity to radiation is as follows:

1. Wire wound.
2. Metal film.
3. Crystalline carbon film.
4. Carbon composition.
5. Borocarbon film.

High and low-temperature, precision-wire-wound resistors and power-type wire-wound resistors have been exposed to radiation up to approximately 1×10^{19} (nv)₀t and 5×10^{18} fast n/cm². The effects of radiation on the electrical parameters of all types of fixed wire-wound resistors are negligible. Regardless of manufacturer and of resistance value, the mean deviation in resistance attributable to radiation are approximately 0.05 per cent. Attempts to examine the transient effects have been unsuccessful because the changes during irradiation are less than the accuracy of the instrument used for measurement. Bar charts illustrating the comparative effects of reactor radiation on various types of resistors are shown in Figure 98B.

RELIABILITY

A preliminary study of converter and generator reliability has been conducted mainly to indicate relative reliability of the conceptual designs and indicate areas for future research. As part of the prototype unit design and prior to construction of a breadboard unit, converter reliability requirements will have to be determined and mean-time-to-failure (MTF) figures for each individual component of the converter established. A systematic listing of each component must be made as part of a conceivable failure analysis. In analyzing conceivable failures, all possibilities are considered and listed, both degenerative and catastrophic. The mission profile and environment on materials and components are listed for quick reference in determining failures induced by environmental stresses. Failure mechanisms-the "thing" which causes a failure-must also be listed if reliability of design is to be achieved. Oftentimes it is the most remote of failure mechanisms which leads to unit failure.

Consequence of failure on overall mission must be considered-especially performance which becomes degraded with the passage of time. Where failure of any type cannot be tolerated, alternate components operating in parallel or redundancy must be considered in the original designs. Methods of eliminating failures and reducing the effect of failures are other items to be considered as the basic design is formulated. All the above analysis must consider state-of-the-art components and known MTF figures. Where MTF figures are not known, testing to determine failure rates will be required.

Figure 99 gives an indication of the MTF required for a 10,000 hour mission and shows how the MTF increases greatly as the required reliability increases and also as mission time is increased.

Techniques which can be applied to achievement of reliability in conversion systems are:

1. Simplicity of design.
2. Use of preferred components with component derating and control of ambient environment.
3. Reduction of failure effects by redundancy and alternate modes.

Reliability of Static Transistor Converters

The reliability of a static transistor converter is directly dependent upon the life of the individual transistors. Simplicity of design is a necessity for long life along with control of ambient environment for the transistors. Derating of each of the transistors and use of redundant circuitry is planned in order to achieve a reasonable converter life. Shielding of the transistors from the radiation environment must be accepted as a firm requirement when SNAP 8 and SPUR type power sources are considered since all semiconductor devices are weak in radiation resistance.

Most life tests of power transistors relate reliability to temperature. It has been found that failure mechanisms other than temperature exist and

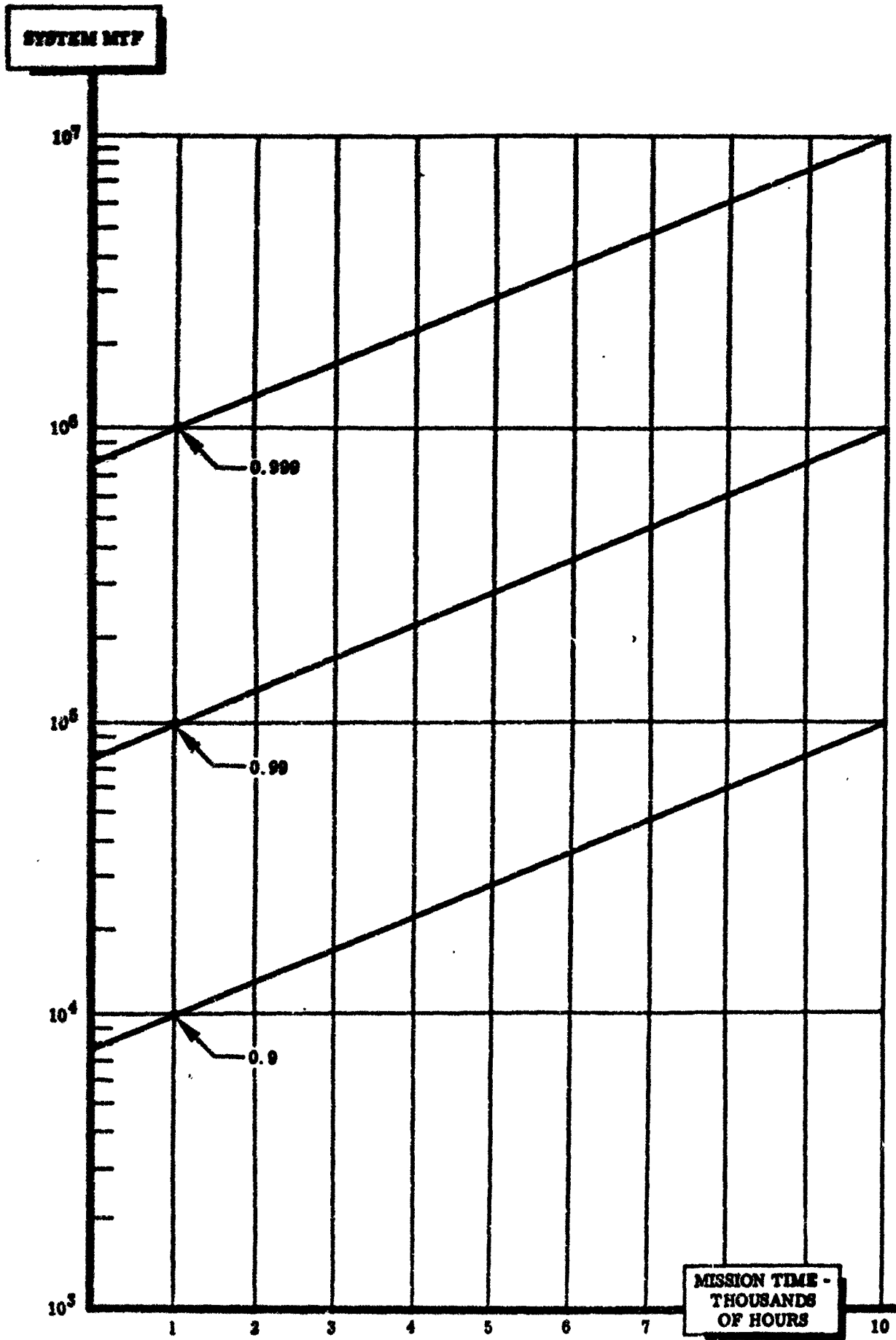


Figure 99. Reliability Required For Various Mission Times

one of these is called "secondary breakdown" of the collector, or a collector-to-emitter short. This breakdown is a characteristic of collector current and voltage wherein the current is concentrated at a point in the base, and the resulting temperature rise melts the base. Failures occur if energy per unit volume within the base becomes excessive. Maximum allowable energy is a function of both current and voltage in this instance. In actual use, the collector current and voltage have excursions which are functions of time, supply voltage, input signals, loads and other variables.

In design of the power chopper device, consideration must be given to these excursions, or transient surges, as well as the steady-state power dissipation for safe operation of the power transistor. The maximum steady-state power dissipation of the power transistor may be safely exceeded if the excursion time is short. "Safe-operating graphs" are prepared by transistor manufacturers and these may be used in obtaining good reliable transistor design.

Adequate cooling must be available at all times for each power transistor. Long converter life then is dependent also on design of the cooling system which circulates fluid through the heat sink mounting plate.

Reliability of Static Tube Converters

The basic components in the static tube converter fall into the following categories:

1. Tubes.
2. Transformers.
3. Controls.
4. Resistors and capacitors.
5. Wiring.
6. Coolant system.
7. Structure.

The most vulnerable components in this type of converter unit are the tubes. Design has been based on use of the latest in ceramic-type tubes operating in a derated mode to give maximum life. These ceramic tubes are rugged in design with greater life expectancies than conventional glass or metal types. Long life is dependent upon proper cooling at all times, protection against conditions of overvoltage and vibration, and proper warm-up and operating conditions. Input and output transformers can be very reliable if operated in a derated mode and with proper cooling. The same techniques apply to resistor and capacitor components and good reliability can be expected. Wire-wound resistors and capacitors using inorganic materials are best. Controls must be simple in order to be reliable. Redundant circuits can be considered in this particular design especially in the phase shifter portion of the circuit. Wiring and connections are important components of the converter, although not usually considered in a reliability analysis. Extreme environments of temperature, radiation, and vibration must be considered when selection of conductors is made.

Radiation-resistant conductors such as nickel-plated copper or stainless steel clad copper must be used in radiation and high-temperature environments for long life. Paralleled pumps and coolant flow paths are methods of achieving good coolant system reliability. Structure reliability must be inherent in the basic design.

Section V

EXPERIMENTAL STUDIES

MEASUREMENT OF CORE LOSSES

In designing the converter systems it was found that a substantial portion of the losses within each system occurred in the components containing magnetic materials, such as transformers and chokes, and the magnetic portions of the generators. This is largely a result of the high frequencies involved. Low frequency core loss curves were developed from known data and extrapolated to the higher frequencies. These are shown in the section on Materials under the core loss versus frequency discussions. These curves were used as a basis for each of the converter designs at 50 KC, 100 KC, 200 KC and the 800 KC level.

Several important results and observations were obtained from the experiments conducted in this portion of the program.

1. Numerous core loss assumptions made in preliminary designs were verified.
2. A flux density of 2300 gauss for high frequency core designs is feasible and this level was demonstrated at 500 KC, 100 KC and 200 KC levels.
3. Ferrite materials are temperature limited for this application, and even though they have very low loss characteristics, they can not be considered in high frequency transformer designs.
4. Core losses decrease with a decrease in lamination thickness.

This test program was conducted with the objectives of verifying the original assumed loss data for transformer and generator designs. At the same time, an evaluation of various magnetic materials at each of the high frequencies could be made. Both wound cores and molded cores were tested and a toroidal configuration was used for all these tests. The materials that were tested are listed as follows:

<u>Material</u>	<u>Number of Cores</u>	<u>Weight (Lbs)</u>	<u>OD(In.)</u>	<u>ID(In.)</u>	<u>Cross Section</u>	<u>Lamin Thick</u>
Silectron	2	.23	3.0	2.5	.5 x .25	1 mil
Supermalloy	2	.24	3.0	2.5	.5 x .25	1 mil
4-79 Mo-Permalloy	2	.238	3.0	2.5	.5 x .25	1 mil
Deltamax	2	.224	3.0	2.5	.5 x .25	1 mil
W-07 Ferrite	2	.10	3.0	2.5	.5 x .25	---

<u>Material</u>	<u>Number of Cores</u>	<u>Weight (lbs.)</u>	<u>OD(In.)</u>	<u>ID(In.)</u>	<u>Cross Section</u>	<u>Lamin Thick</u>
W-03 Ferrite	1	.16	2.375	1.625	.375x.375	--
M-60 Ferrite	2	.10	2.0	1.25	.375x.25	--
Carpenter 45-5 Alloy	1	.605	3.0	2.5	.5 x .5	2 mil

CORE LOSS VERSUS FREQUENCY

A summation of core loss magnitudes for the various materials tested at frequencies between 50 KC and 800 KC is found in Figures 100 and 101. This data has been taken from Tables 26 and 27 which are derived data from the core loss tests. Core losses were measured in the 2000 to 3000 gauss flux density range for each of the samples at the 50 KC, 100 KC and 200 KC levels. A limited output of the oscillator at the 800 KC level prevented achieving more than a 1100 to 1200 gauss flux density in measuring core losses at the 800 KC frequency.

MATERIALS TESTED

Specific cores tested during the program, as listed in a previous table, were of various materials generally used in transformer core designs. Each material is discussed in the section which follows.

Silectron - Silectron cores are manufactured from a highly grain-oriented, cold-rolled grade of 3% Silicon Steel. It has a high saturation flux density and lower core losses and exciting volt-amperes than regular silicon steels. The high degree of orientation obtained in Silectron permits operation of the core material at higher induction levels and can result in reduced component weight and size. The cores tested were tape-wound toroids of 1 mil Silectron material and each was enclosed in a nylon case and impregnated with grease.

No unusual results were obtained from the 50 KC tests. Both samples showed fairly low losses at this frequency and at 2330 gauss were below the saturation level of the material. At 100 KC, the core losses increased considerably, but distortion was not noticed at the 2330 gauss level. At 200 KC the losses doubled in magnitude and the output waveforms began to show distortion at the 2000 gauss level as seen in Figure 102A. The loss at 800 KC was less because the flux density was lower (the oscillator not being able to furnish sufficient power to produce more than approximately 600 gauss).

Supermalloy

Supermalloy is closely related to 4-79 Mo-Permalloy in composition and is one of the latest developments in high permeability nickel-iron alloys. It exhibits an extremely low hysteresis loss. Tape-wound cores are used in radar pulse transformers and for low-level magnetic amplifiers. The Supermalloy cores tested were tape-wound toroids of 1 mil laminations. They were

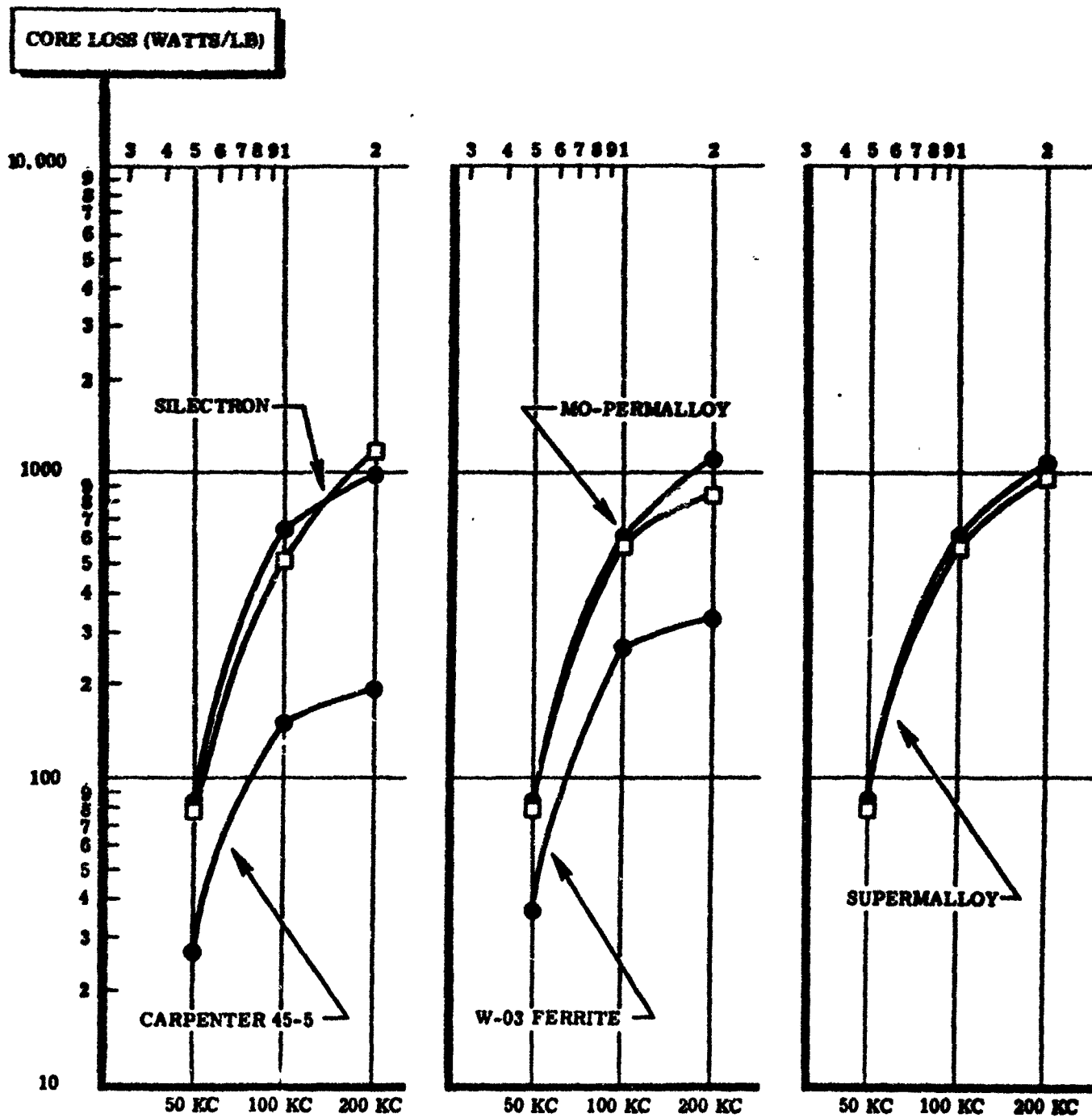


Figure 100. Core Loss vs. Frequency for Transformer materials

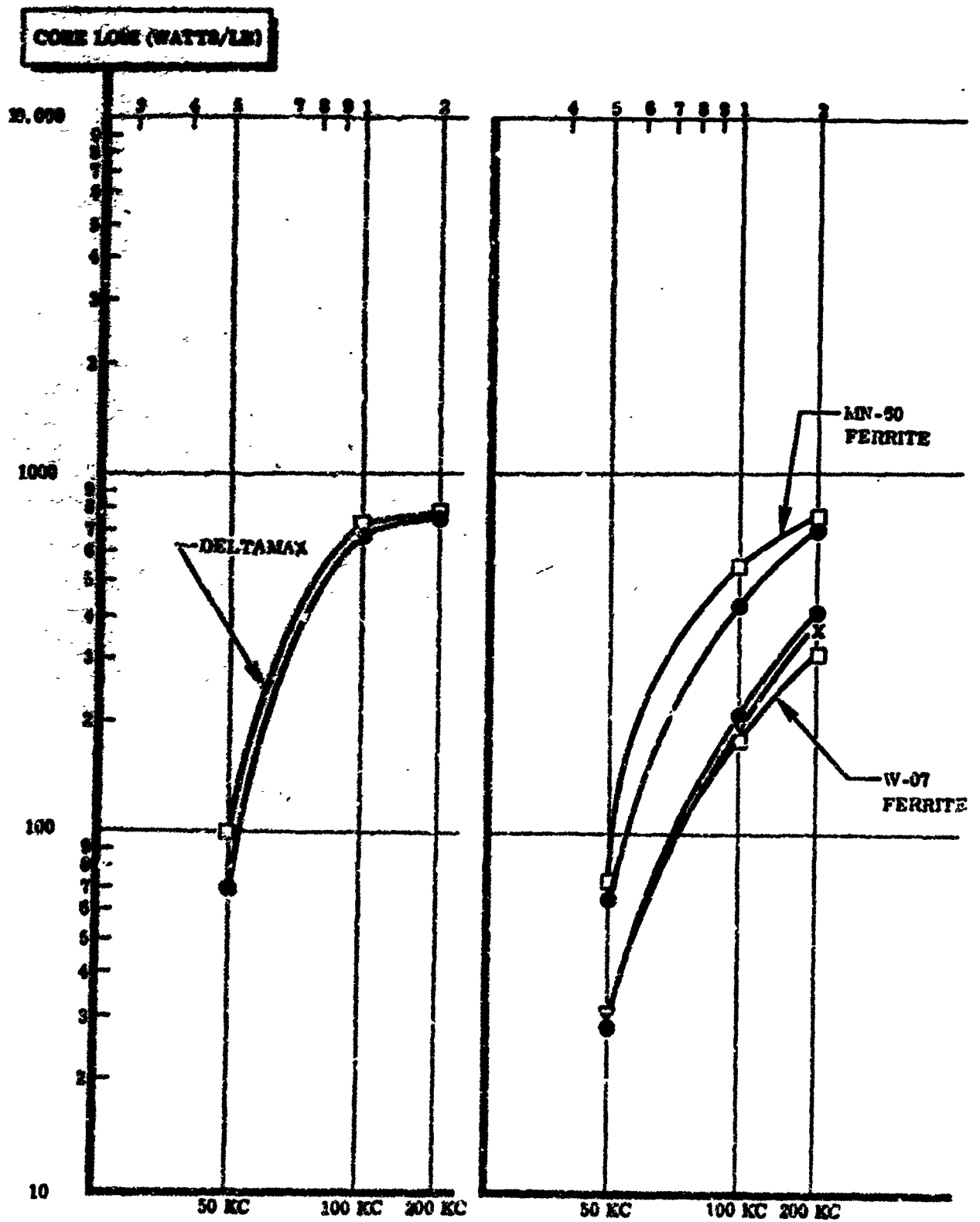


Figure 101. Core Loss vs. Frequency for Transformer Materials Including Ferrites

TABLE 26
PARAMETRIC DATA ON CORE TESTS

MATERIAL-SILECTRON

Sample Number	1				2			
Frequency (KC)	50	100	200	800	50	100	200	800
Core Loss (Watts/lb)	83.6	623	963	918	79.2	505	1150	1000
Flux Density (Gauss)	2180	2660	2000	625	2055	2130	1800	587

MATERIAL-SUPERMALLOY

Sample Number	1				2			
Frequency (KC)	50	100	200	800	50	100	200	800
Core Loss (Watts/lb)	84.2	627	1040	962	86.3	575	958	965
Flux Density (Gauss)	2120	2240	3360	945	2300	2130	3400	1010

MATERIAL-DELTAMAX

Sample Number	1				2			
Frequency (KC)	50	100	200	800	50	100	200	800
Core Loss (Watts/lb)	72.6	723	743	608	98.2	735	786	698
Flux Density (Gauss)	2147	3480	2810	705	2340	3425	3260	920

MATERIAL 4-79 MO-PERMALLOY

Sample Number	1				2			
Frequency (KC)	50	100	200	800	50	100	200	800
Core Loss (Watts/lbs)	82.7	617	1060	1000	80.6	578	804	975
Flux Density (Gauss)	2210	3680	3520	1060	2432	3220	3400	1100

TABLE 28

PARAMETRIC DATA ON CORE TESTS

MATERIAL MN-60 FERRITE (KEARFOOT)

Sample Number	1				2			
Frequency (KC)	50	100	200	800	50	100	200	800
Core Loss (Watts/lb)	64.2	422	711	1150	78.7	550	730	1230
Flux Density (Gauss)	2160	3695	2710	837	2025	3620	2680	785

MATERIAL W-07 FERRITE (ALLEN-BRADLEY)

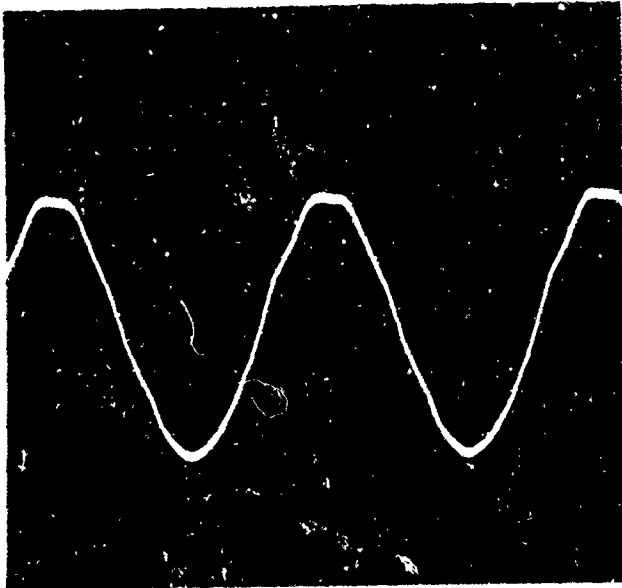
Sample Number	1				2			
Frequency (KC)	50	100	200	800	50	100	200	800
Core Loss (Watts/lb)	27.2	219	425	655	31.6	187	325	413
Flux Density (Gauss)	2140	3680	2910	1280	2265	3495	2784	1120

MATERIAL W-03 FERRITE (ALLEN-BRADLEY)

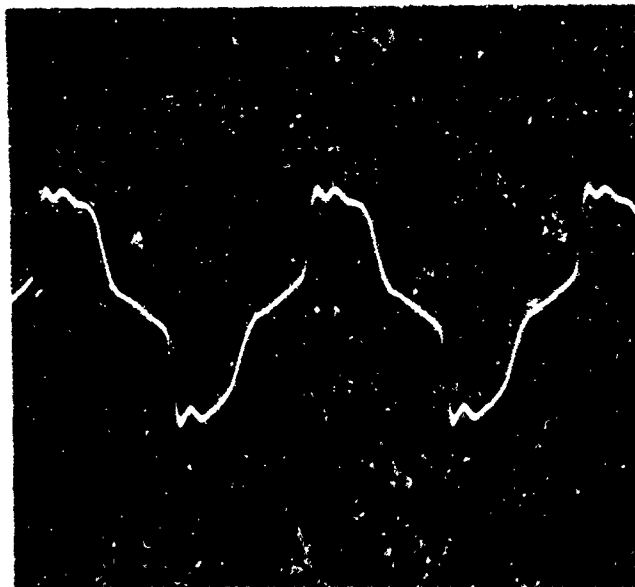
Sample Number	1			
Frequency (KC)	50	100	200	800
Core Loss (Watts/lb)	36.4	274	325	477
Flux Density (Gauss)	2050	3860	2940	887

MATERIAL CARPENTER ALLOY 45

Sample Number	1			
Frequency (KC)	50	100	200	800
Core Loss (Watts/lb)	2615	159	198	200
Flux Density	2740	2620	2340	1100



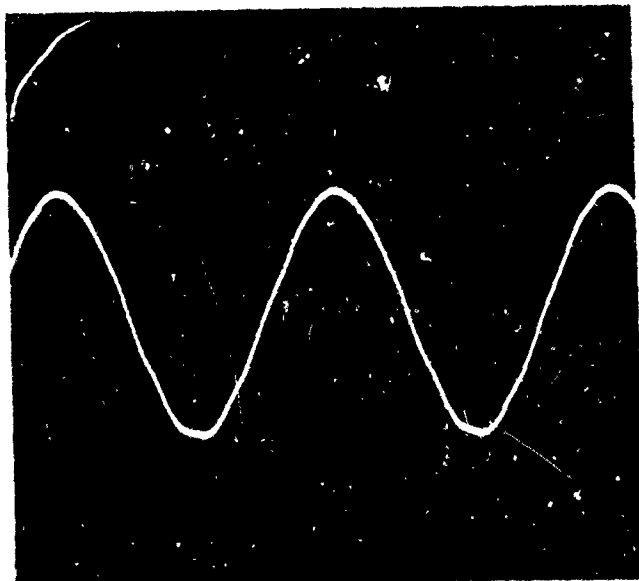
A SILECTRON 200 KC
2000 GAUSS



B SUPERMALLOY 200KC
3360 GAUSS



C MO-PERMALLOY 200 KC
3520 GAUSS



D DELTAMAX 200 KC
2810 GAUSS

Figure 102. Transformer Core Output Voltage Waveforms for Various Materials

nylon cased and impregnated with grease.

These samples at 50 KC had approximately the same losses at comparable flux densities as the Silectron cores and showed no sign of saturation at 50 KC. At 100 KC, the output waveshap began to show signs of core saturation. Increased distortion was evident in the output at the 200 KC level as shown in Figure 102B. No distortion was noticed in the output at approximately 1000 gauss and 800 KC, but this was due to operation at a point much below the saturation level for this frequency.

4-79 Mo-Permalloy

4-79 Mo-Permalloy is a 4% molybdenum, 79% nickel - and iron alloy. The material is not grain-oriented and is available in tapes of various thicknesses. Specific applications include cores for current transformers, pulse transformers, and wide-band communication transformers of many types. The cores tested were tape-wound toroids of 1 mil laminated material and were nylon encased and grease impregnated.

The 50 KC core loss tests indicated low losses for this material and no saturation in the 2200 to above 2400 gauss range. At 100 KC, the output waveshape was distorted, but the material was operating much above the 2330 gauss design level. (See Figure 102C). The same was true of operation at 200 KC where the flux density level was over 3500 gauss, and the losses were correspondingly heavier than at the 100 KC level. The response of the 4-79 Mo-Permalloy cores were quite similar to the Supermalloy cores.

Deltamax

Deltamax is a grain-oriented 50% nickel-iron alloy having a rectangular hysteresis loop and is used in saturable core reactors and particularly in magnetic amplifiers. It is available only in thin strip form and wound-core construction is generally used. Little AC data has been published on this material. The cores tested in this study were also tape-wound toroids of 1 mil material and were nylon encased and grease impregnated.

The core losses in Deltamax material followed the same trends as in the 4-79 Mo-Permalloy material. The major difference was in the output waveshapes (Figure 102D). Here the material demonstrates a much higher maximum flux density characteristic and no distortion was noticeable at 2810 gauss flux level (200 KC).

Carpenter 45-5 Alloy

Carpenter 45-5 is a nickel-chromium-iron alloy developed to match the thermal expansion of certain glasses. This core sample was one available for testing from our own materials laboratory and was tried along with the other samples. The material was a toroid also, but was rolled of 2 mil material. The sample had the lowest loss of any of the cores and this fact is attributed to the high resistivity of the 45-5 alloy material. The sample performed well at flux densities of over 2700 gauss at 50 KC and over 2300 gauss at 200 KC. At 200 KC, there appeared to be only slight distortion at the 2300 gauss level.

This is seen in Figure 103A. As in the other samples, operation at the 800 KC level was much below the maximum flux density level and also below the design level of 2300 gauss. However, observation of the output waveshape showed the core to be temperature sensitive. Output distortion increases slightly with increases in temperature.

Ferrites

All ferrite samples tested were molded rings. W-07 ferrite (Allen Bradley) is a low-loss material used for transformer cores, but is temperature limited for this particular application.

Both samples tested had lower losses than any of the tape-wound cores with the exception of the Carpenter 45-5 Alloy material. The core losses increased with frequency as with the other cores and core saturation was not evident at 50 KC at a flux level of 2140 gauss. The 200 KC tests were run at 2780 gauss and a slight degree of saturation was noticeable as shown in Figure 103B. On completion of the tests with this material, it was noticed that the cores were split in several places due to internal heating. Ferrite materials are peculiar in that they can reach extremely high internal temperatures while the exterior shows almost no noticeable change. The cracks produce air gaps and necessitate an increase in excitation current to sustain the same flux density levels as in the uncracked cores. The output waveform seemed unaffected by the air gap.

A W-03 Ferrite (Allen-Bradley) was tested, although only one sample of this material was available (donated by the supplier). Maximum flux density appeared to be above 3500 gauss at the 100 KC level and noticeable distortion was present in the output waveform at the 200 KC level. (See Figure 103C). An oscillatory or "ringing" effect was noticeable at both the 100 KC and 200 KC levels.

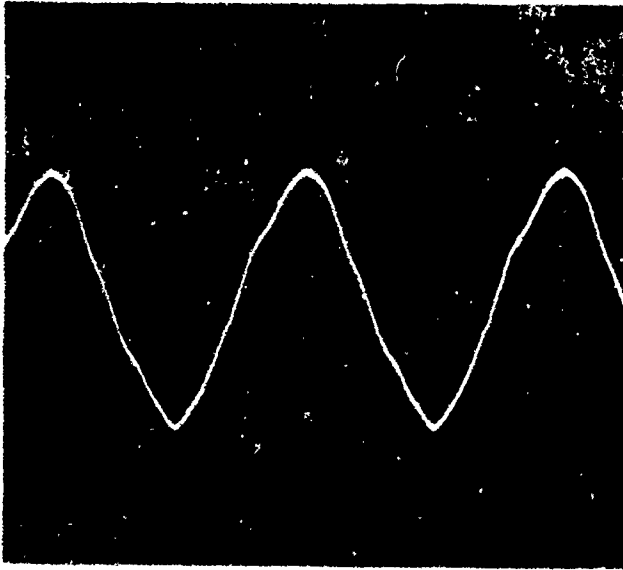
MN-60 Ferrite (Kearfott)

MN-60 ferrite is also a low-loss material and like the other ferrites, it is temperature limited.

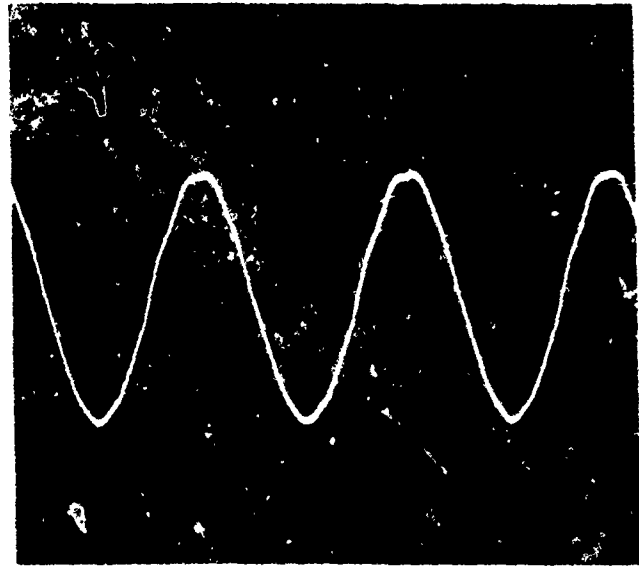
The core losses increased with frequency in these samples as in the others, but were the highest of the ferrites tested. The losses were of the same magnitude as the tape wound cores. Ringing was noticed in this sample also as shown in Figure 103D, which shows a waveshape at the 200 KC level and at 2680 gauss. This core also split under the influence of high internal temperatures resulting from core losses.

LABORATORY SETUP

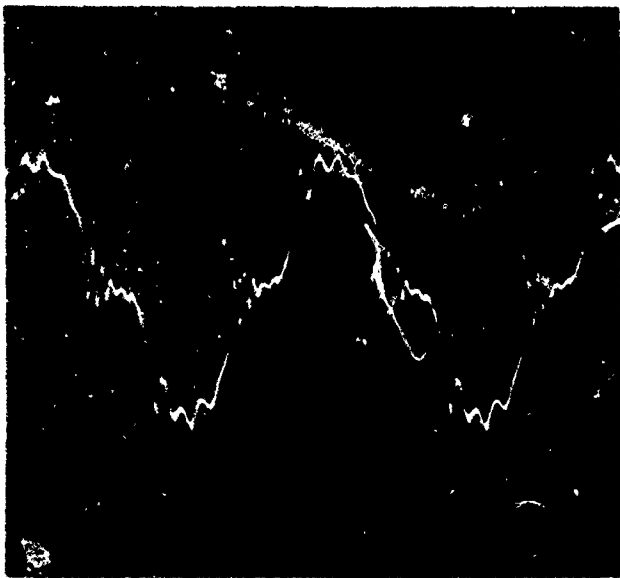
Two different laboratory set-ups were used to obtain the core loss data. The 50 KC test circuit is shown in Figure 104A. Figure 105 is a view of the laboratory set-up. This method for deriving 50 KC data provides for direct reading of the core losses, but is limited to frequencies below 80 KC due to the instrumentation involved. For the 100 KC, 200 KC and 800 KC tests,



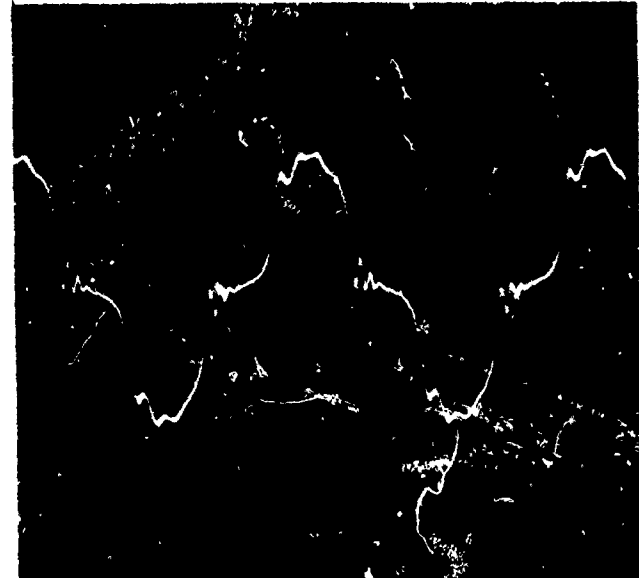
A CARPENTER ALLOY 45 200 KC
2340 GAUSS



B W-07 FERRITE 200 KC
2780 GAUSS

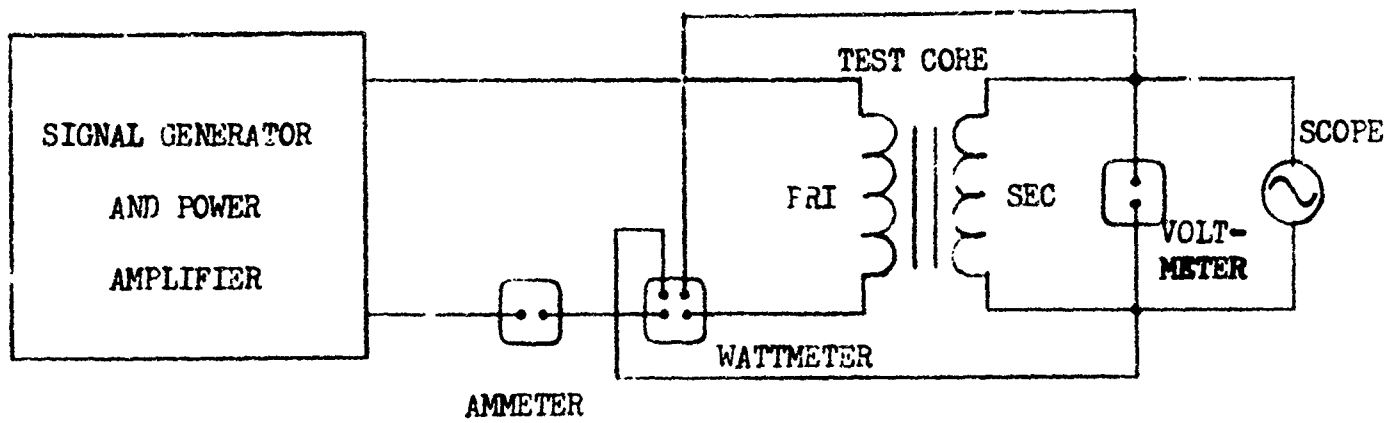


C W-03 FERRITE 200 KC
2940 GAUSS

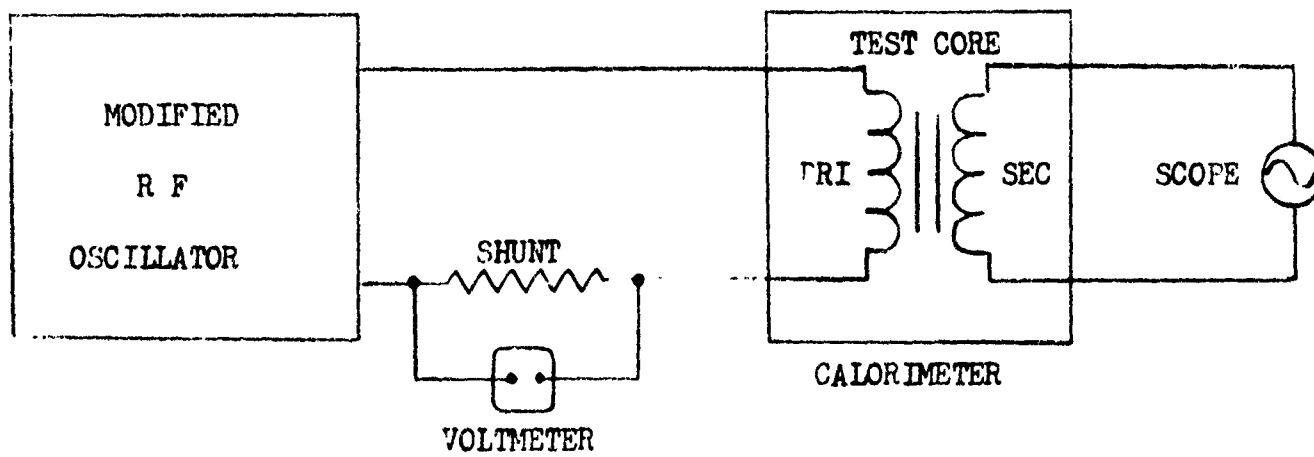


D MN-60 FERRITE 200 KC
2680 GAUSS

Figure 103. Transformer Core Output Waveforms (Including Ferrites)



A 50 K C TEST CIRCUIT



B 100 TO 800 K C TEST CIRCUIT

Figure 104. Laboratory Test Circuits



Figure 105. Laboratory Test Setup (50 KC Core Loss Testing)

The test circuit of Figure 10bB was used. The actual test set-up is shown in Figures 106 and 107. A standard oscillator circuit was modified for the tests and provided 500 watts of RF power to the cores. The amount of loss was obtained by a heat substitution method. The calorimeter temperature versus time characteristics were first recorded using a known voltage level. Each core was then placed in the calorimeter and the starting and final temperatures and the elapsed time were recorded. This data was compared with the calibration curves and the wattage loss was obtained.

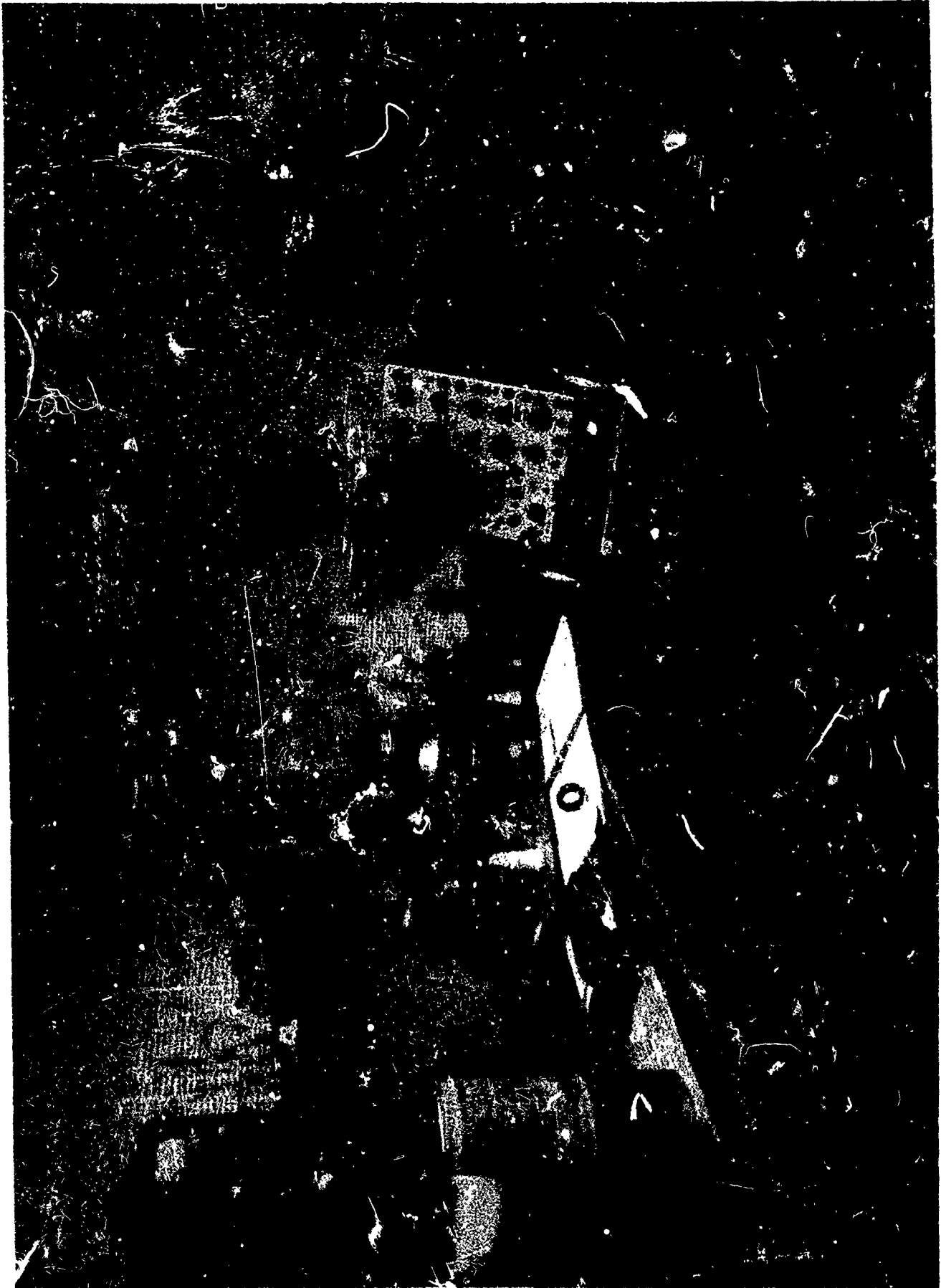


Figure 106. Laboratory Test Setup (100 KC to 800 KC Core Loss Testing)

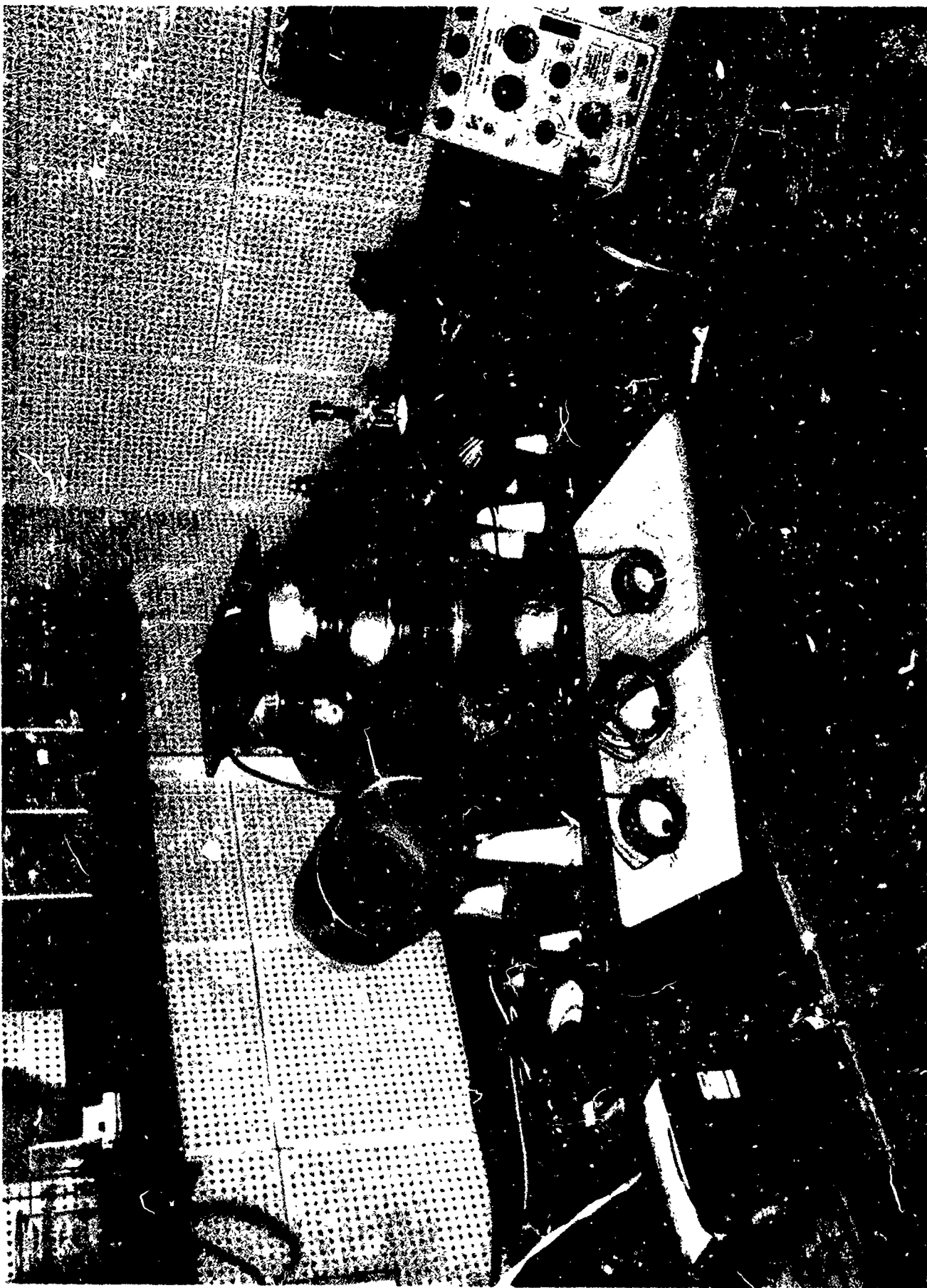


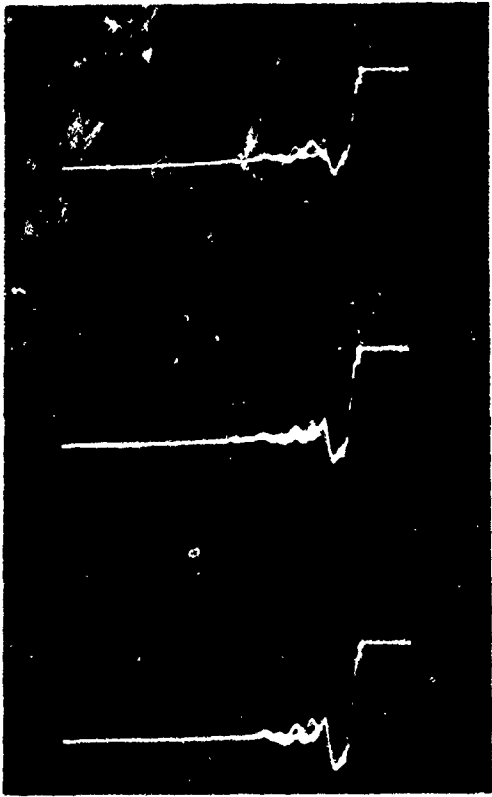
Figure 107. Laboratory Test Setup Showing Transformer Cores

TRANSISTOR CHARACTERISTICS IN PARALLEL OPERATION

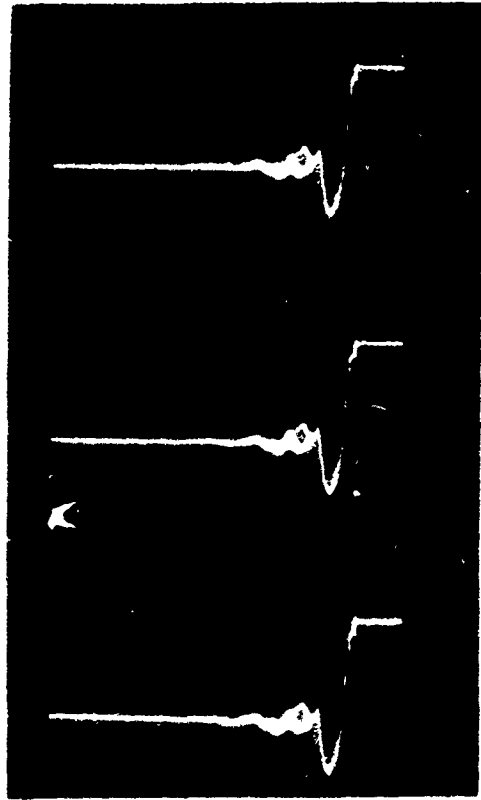
It has been found that parallel operation of new high power semiconductor devices with their fast switching speeds lend themselves quite readily to high frequency power conversion applications. In the past transistors have not had the power capacity applicable to most needs. With the advent of new devices their feasibility has become more promising. Although these new devices have good switching characteristics when operated separately, their operation in parallel was not clearly defined. The purpose of these tests was to determine current sharing and switching characteristics for parallel operation of power transistors.

Conclusions:

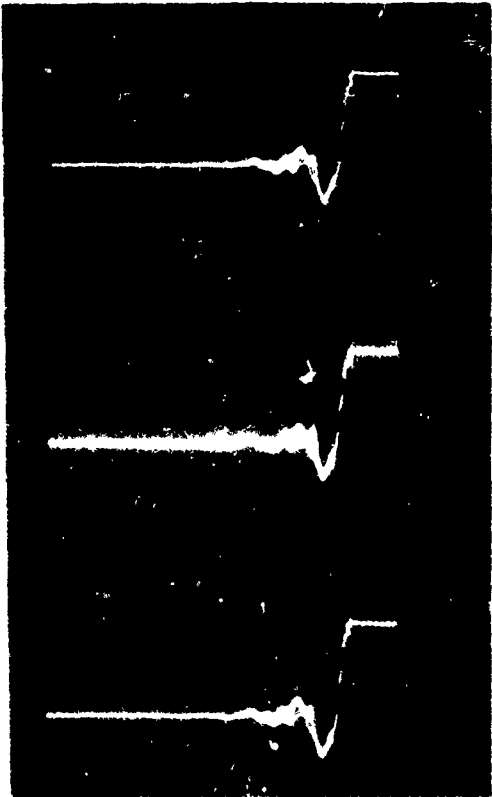
The results of the transistor tests did illustrate the feasibility of utilizing semiconductor devices in parallel operation for high power application. The frequency response figures pointed out that the transistor outputs were almost exact representations of the input for various frequencies. Comparing the frequency response oscillographs, one can see that less distortion existed at 100 and 200 KC than at 800 KC. It was concluded that the transistor capacitance created this problem. In the final design a semiconductor would be chosen which has the proper characteristics for the selected design. By observation of the data in Table 28 and Figure 108 it can be seen that conditions can be created which will cause the paralleled units to share current equally. In summation, it can be said that the characteristics of parallel transistor operation were defined, and the results demonstrated their feasibility for power applications.



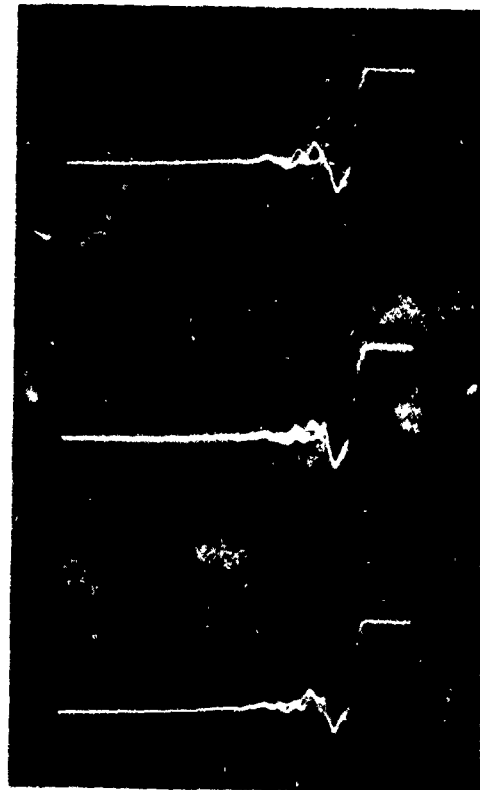
A $0.5 \frac{\mu\text{sec}}{\text{cm}}$



B $0.5 \frac{\mu\text{sec}}{\text{cm}}$



C $0.5 \frac{\mu\text{sec}}{\text{cm}}$



D $0.5 \frac{\mu\text{sec}}{\text{cm}}$

Figure 108. Current Sharing Waveforms

TABLE 28

CURRENT SHARING RESULTS

<u>UNIT NO.</u>	<u>RESISTANCE ($r_e + r_f$)(ohms)</u>	<u>VOLTAGE AT 35A (Volts)</u>	<u>VOLTAGE AT 70A (Volts)</u>
1.	0.182	0.180	
2.	0.181	0.180	0.355
3.	0.183	0.185	0.355
4.	0.180	0.178	0.360
5.	0.180	0.178	0.355
6.	0.180	0.178	0.355
7.	0.179	0.178	0.355
8.	0.179	0.178	0.355
9.	0.183	0.178	0.355
10.	0.181	0.185	0.362
11.	0.179	0.183	0.360
12.	0.175	0.180	0.358
13.	0.178	0.172	0.350
14.	0.179	0.175	0.350
15.	0.179	0.175	0.350
16.	0.181	0.180	0.360
17.	0.181	0.180	0.361
18.	0.181	0.178	0.360
19.	0.180	0.180	0.360
20.	0.179	0.181	0.363
21.	0.180	0.182	0.365
22.	0.182	0.182	0.365
23.	0.182	0.185	0.368
24.	0.177	0.183	0.365
25.	0.177	0.180	0.362
26.	0.180	0.180	0.362
27.	0.182	0.180	0.362
28.	0.181	0.185	0.368
29.	0.179	0.182	0.360
30.	0.178	0.180	0.355
31.	0.179	0.180	0.356
32.	0.180	0.180	0.356
33.	0.182	0.183	0.360
34.	0.181	0.185	0.365
35.	0.180	0.184	0.365
		0.184	0.364

TEST PROCEDURE

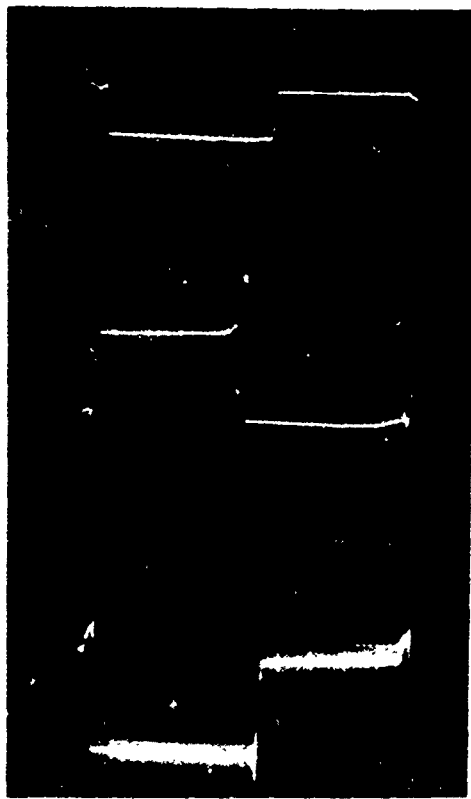
The tests were all directed to prove feasibility of power switching and proper current sharing. To illustrate current sharing the emitter resistance and voltage of all units in parallel was recorded for a given input voltage and frequency. Also, the waveform of 12 sample units (out of 35) was obtained. The latter was to insure equal turn-on-time. Frequency response tests were also performed. These consisted of holding a constant output with a variable input frequency and recording the emitter signal with various combinations of parallel devices.

In Table 25 one can observe the current sharing test results. This test served to prove that each semiconductor was carrying approximately the same amount of emitter current. Thirty-five units were switched on and the collector voltage was set at a negative 25 volts. A negative DC input was adjusted until the load current was 35 amperes. The value of emitter potential was then recorded. This was done again for a load current of 70 amperes. From the data of emitter voltage and resistance an emitter current was obtained for each device. In comparing these values it was demonstrated that the semiconductors were sharing current properly.

Data for Figure 108 was obtained in approximately the same manner as above. In this case the only change was the DC input was removed and a 50 KC square wave was inserted. Sample waves are shown in the illustration to demonstrate that each device had approximately the same rise time. This was to insure that individual units were not drawing more current than others in the transient period between off and on. Since all the signals appeared similar, it was believed that twelve samples would be sufficient.

By observation of Figures 109 through 111 one can see the frequency characteristics. In these tests the input frequency was varied from 10 to 200 kilocycles per second for five, ten and twenty parallel units. The waveforms of frequency response are shown in a similar manner. In each Figure A₁, B₁, C₁, and D₁, are the inputs to the parallel group. Also, A₂, B₂, C₂, and D₂, represent the emitter signal with approximately one ampere per device. A₃, B₃, C₃, and D₃, are emitter signals with about two amperes per device. It was intended that the oscillographs shown would demonstrate switching time and offer a comparison between input and output wave forms.

In the figures of frequency response a certain amount of ringing was detected at turn-on and turn-off. This was attributed to inductance in the long connection leads of the test set-up. A final design would have proper component placement and added capacitive reactance to compensate for any inductive components in the circuit. A slight blurr, as shown in Figure 111 (A3), appears on some of the oscillographs. This came about from the switching of external environmental test equipment in the immediate area causing transient loads on the input power at the instant the photo was taken.

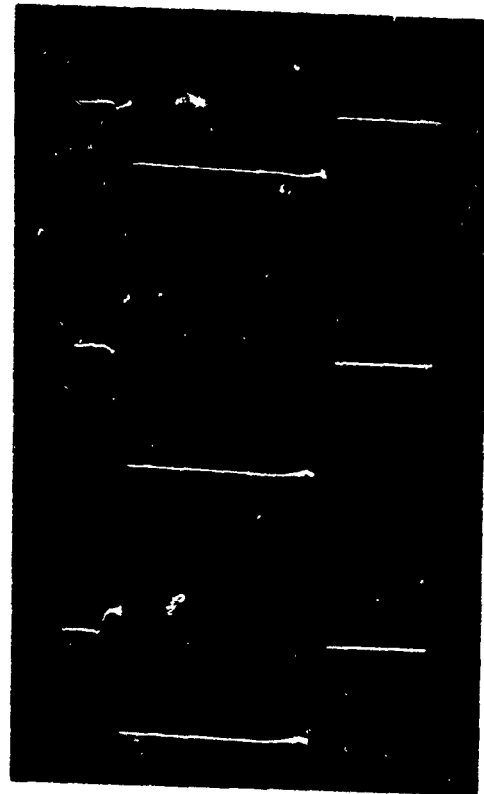


A 10 KC $\frac{25 \mu\text{sec}}{\text{cm}}$

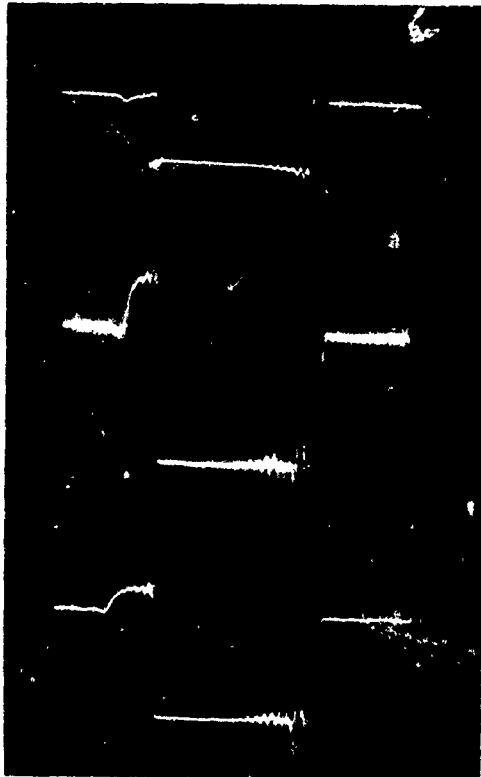
1 0.5 Volts/cm 1

2 0.1 Volts/cm 2

3 0.2 Volts/cm 3



B 20 KC $\frac{4 \mu\text{sec}}{\text{cm}}$

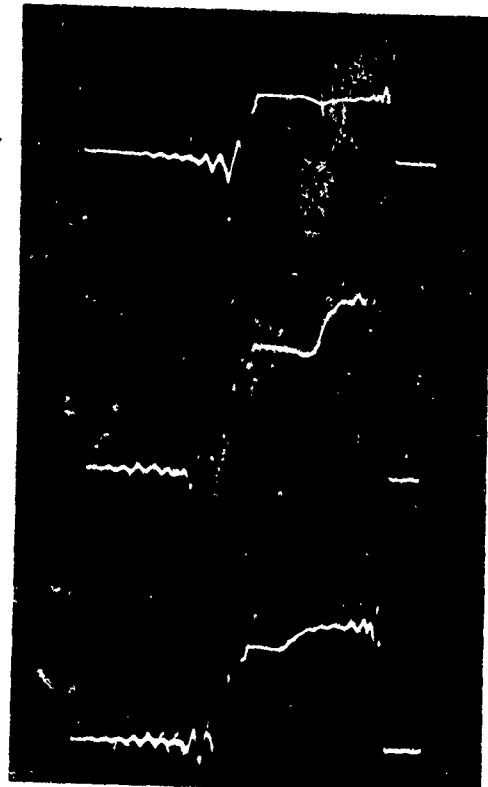


C 50 KC $\frac{2 \mu\text{sec}}{\text{cm}}$

1 0.5 Volts/cm 1

2 0.1 Volts/cm 2

3 0.2 Volts/cm 3



D 100 KC $\frac{1 \mu\text{sec}}{\text{cm}}$

Figure 109A. Frequency Response Waveforms (5 Parallel Transistors)

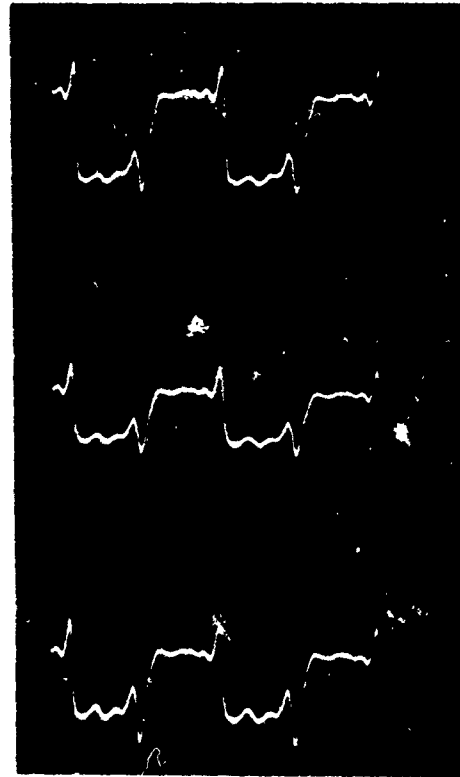


1 0.5 Volts/cm 1

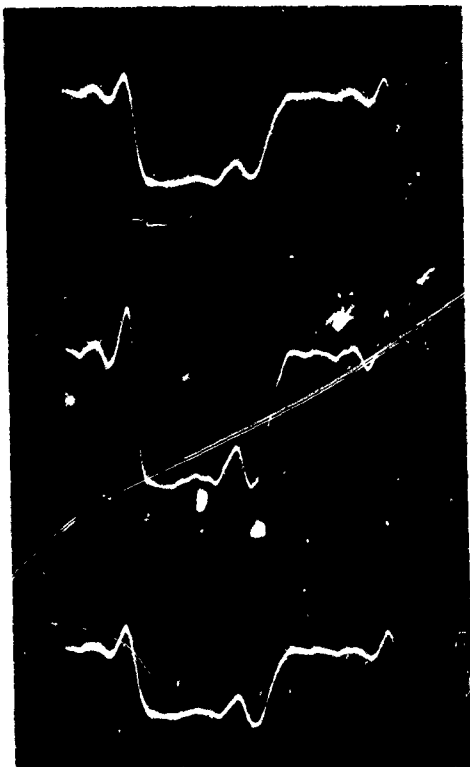
2 0.2 Volts/cm 2

3 0.5 Volts/cm 3

A 200 KC $0.5 \mu\text{sec/cm}$



B 400 KC $0.5 \mu\text{sec/cm}$

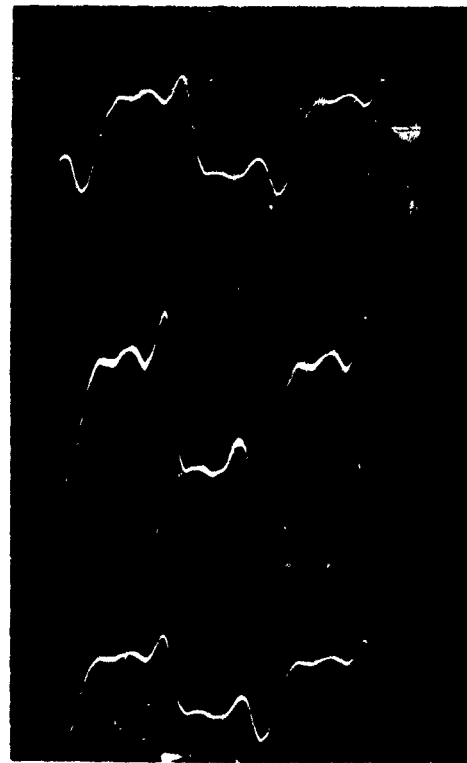


1 0.5 Volts/cm 1

2 0.2 Volts/cm 2

3 0.5 Volts/cm 3

C 600 KC $0.2 \mu\text{sec/cm}$



D 800 KC $0.2 \mu\text{sec/cm}$

Figure 109B. Frequency Response Waveforms (5 Parallel Transistors)

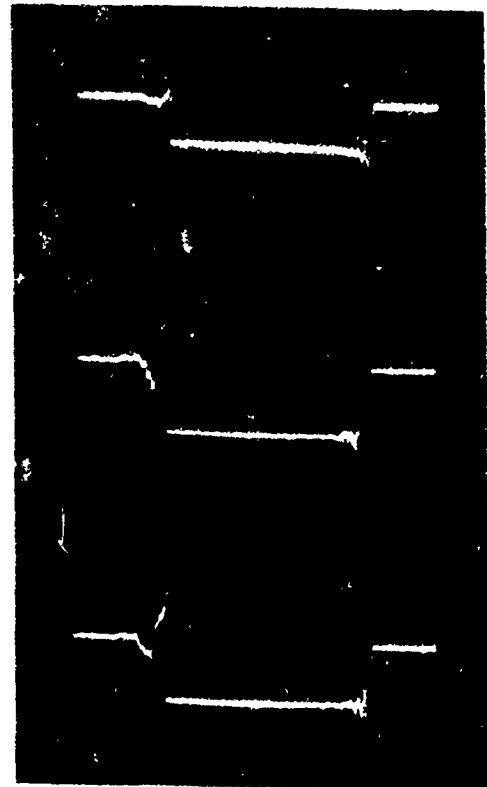


A 10 KC $25 \frac{\mu\text{sec}}{\text{cm}}$

1 0.5 Volts/cm 1

2 0.1 Volts/cm 2

3 0.2 Volts/cm 3



B 20 KC $4 \frac{\mu\text{sec}}{\text{cm}}$



C 50 KC $2 \frac{\mu\text{sec}}{\text{cm}}$

1 0.5 Volts/cm 1

2 0.1 Volts/cm 2

3 0.2 Volts/cm 3



D 100 KC $1 \frac{\mu\text{sec}}{\text{cm}}$

Figure 110A. Frequency Response Waveforms (10 Parallel Transistors)

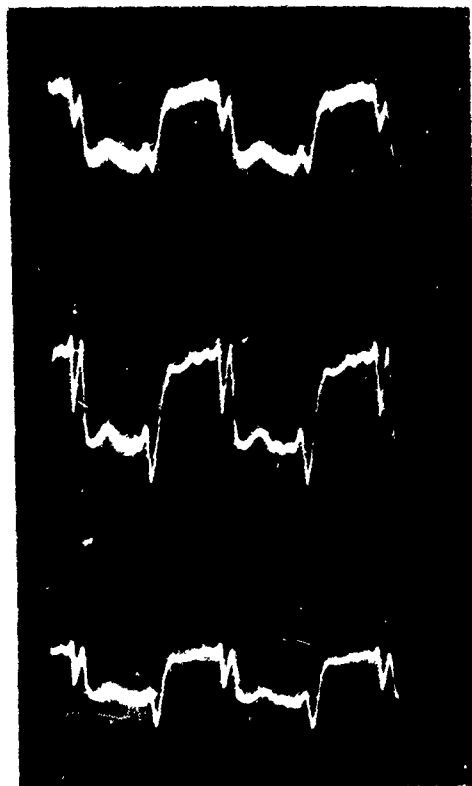


A 200 KC $0.5 \mu\text{sec/cm}$

1 $0.5 \frac{\text{Volts}}{\text{cm}}$

2 $0.2 \frac{\text{Volts}}{\text{cm}}$

3 $0.5 \frac{\text{Volts}}{\text{cm}}$

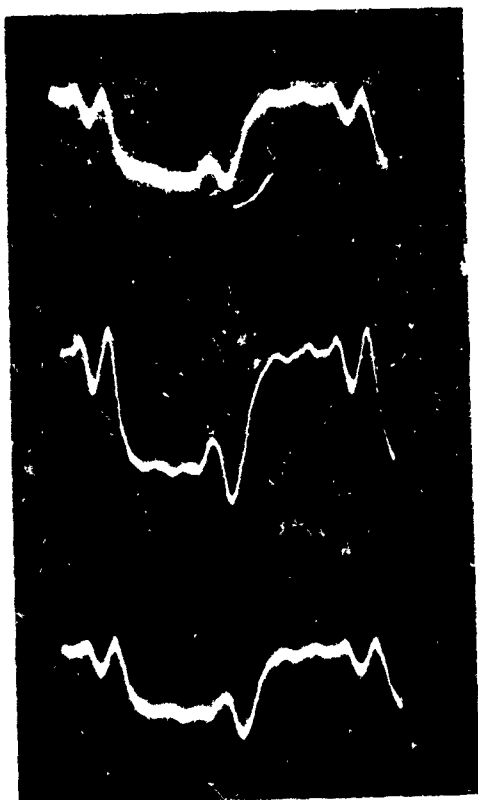


B 400 KC $0.5 \mu\text{sec/cm}$

1

2

3

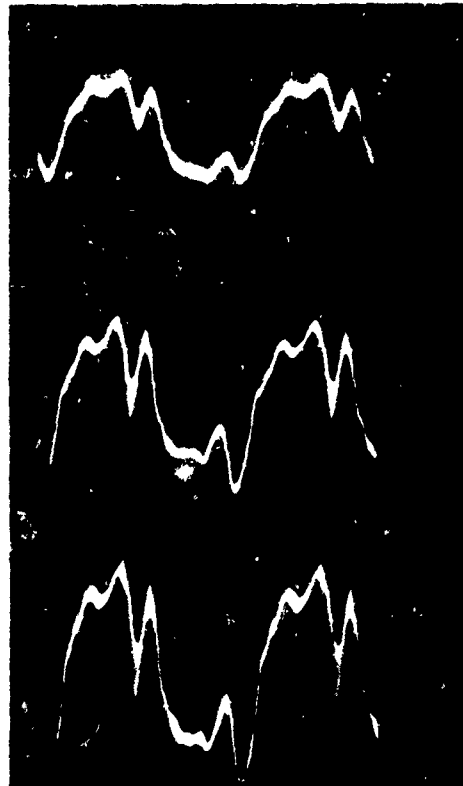


C 600 KC $0.2 \mu\text{sec/cm}$

1 $0.5 \frac{\text{Volts}}{\text{cm}}$

2 $0.2 \frac{\text{Volts}}{\text{cm}}$

3 $0.5 \frac{\text{Volts}}{\text{cm}}$



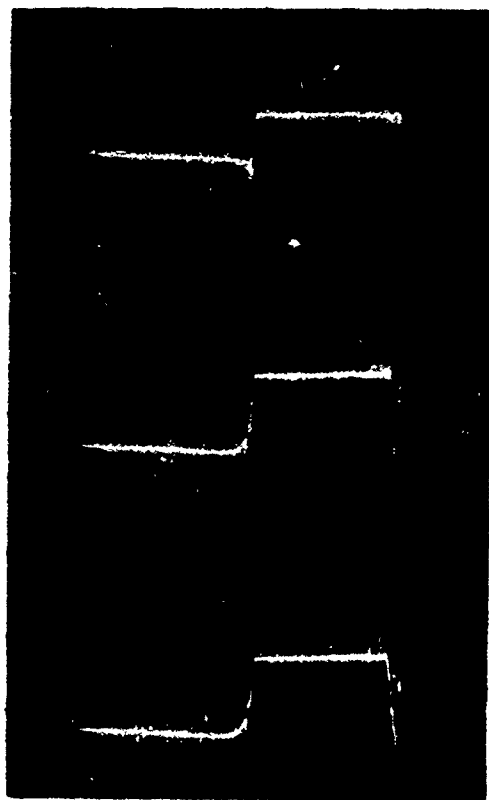
D 800 KC $0.2 \mu\text{sec/cm}$

1

2

3

Figure 110B. Frequency Response Waveforms (10 Parallel Transistors)

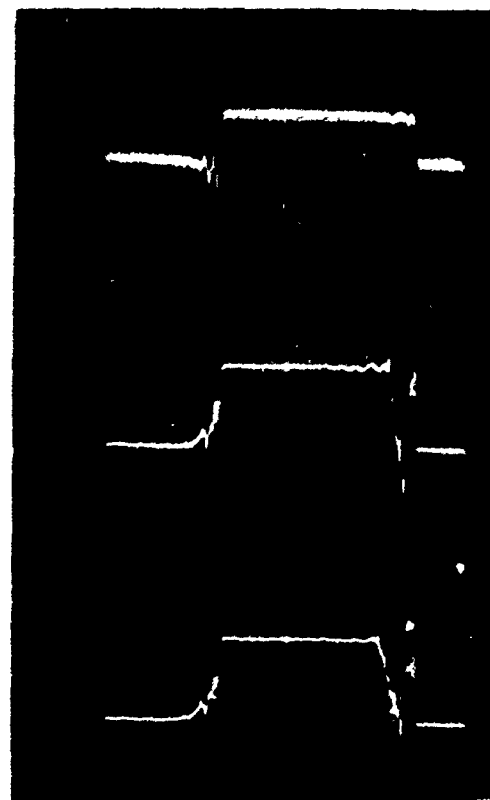


1 0.5 Volts 1
cm

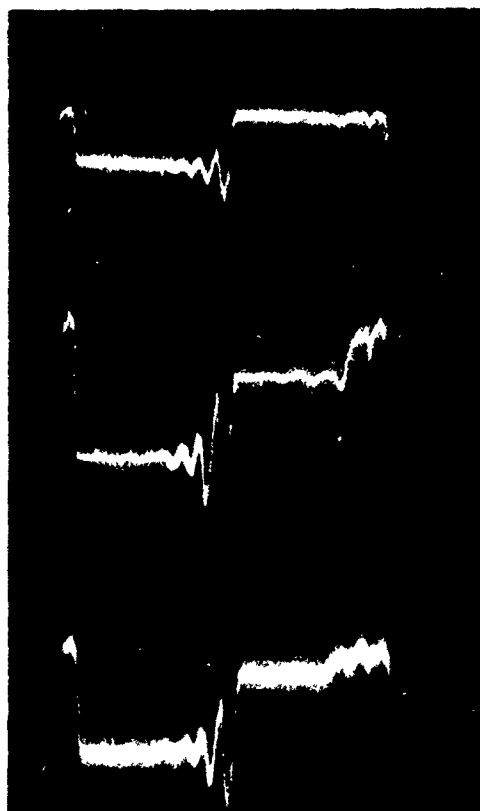
2 0.1 Volts 2
cm

3 0.2 Volts 3
cm

A 10 KC $25 \mu\text{sec}$
cm



B 20 KC $4 \mu\text{sec}$
cm



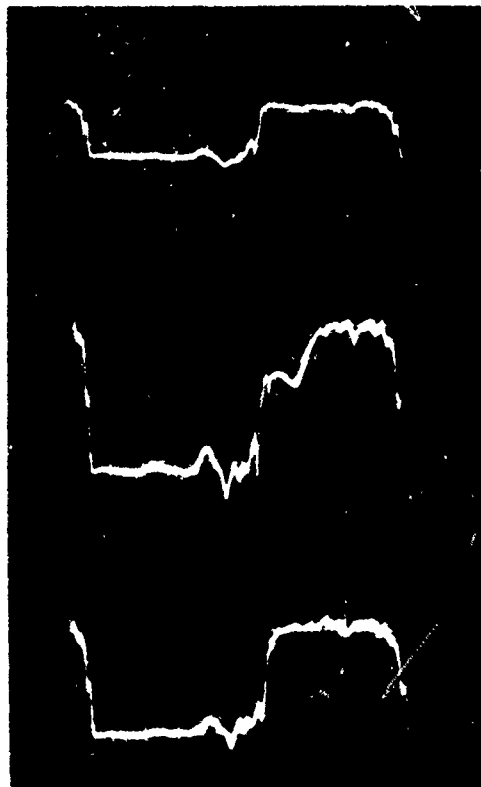
1 0.5 Volts
cm

2 0.1 Volts
cm

3 0.2 Volts
cm

C 50 KC $2 \mu\text{sec}$
cm

Figure 111A. Frequency Response Waveforms (20 Parallel Transistors)

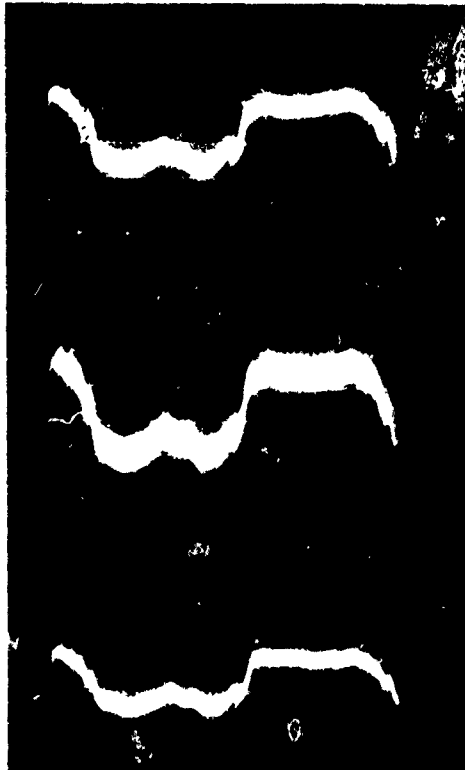


1 $0.5 \frac{\text{Volts}}{\text{cm}}$

2 $0.2 \frac{\text{Volts}}{\text{cm}}$

3 $0.2 \frac{\text{Volts}}{\text{cm}}$

A 100 KC $1 \frac{\mu\text{sec}}{\text{cm}}$



1 $0.5 \frac{\text{Volts}}{\text{cm}}$

2 $0.1 \frac{\text{Volts}}{\text{cm}}$

3 $0.5 \frac{\text{Volts}}{\text{cm}}$

B 200 KC $0.5 \frac{\mu\text{sec}}{\text{cm}}$

Figure 111B. Frequency Response Waveforms (20 Parallel Transistors)

The transient over-shoot spikes, as shown in Figure 109B (A1), were a result of fast rise time in conjunction with the transistor internal capacitance. These spikes were diminished as the current through the device was increased. This can be seen by comparing Figure 109B (C2) and (C3). Also, since the spikes did appear on the input, another remedy would be the addition of zener diode clipping networks on the input.

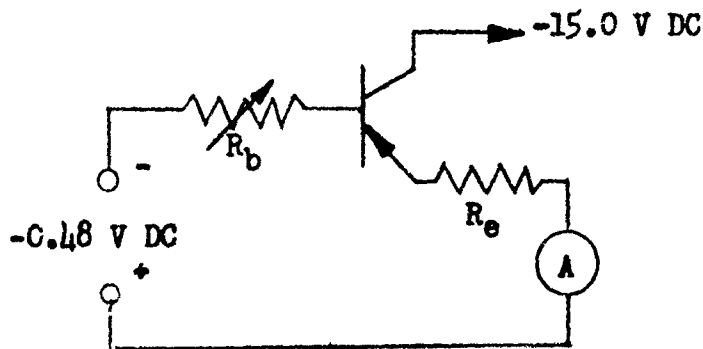
It was observed that the output was a closer approximation of the input for larger emitter currents. This can be seen by comparing signals 1, 2 and 3 of the frequency response figures. It is believed this resulted from an increase in current causing the transistor to be operating in a more linear region of its operating characteristics.

In comparison of the oscillographs, it was observed that as the number of devices in parallel was increased the input waveform was distorting, and in turn, the output did too. This was a result of the input impedance of the parallel networks decreasing as the number of devices was increased which caused a mis-match of the driver output impedance to the network input impedance. Proper impedance matching in the final design would correct this situation, once a frequency was decided upon.

TEST SETUP

The circuit schematic used for these tests is shown in Figure 112. The transistors were 2N1907 from Texas Instruments. A brief description is as follows: An input from a square wave generator is directed to a driver circuit where current amplification is obtained. Variable capacitor C_1 is for the purpose of speeding up the rise time of the square wave for different input frequencies. Capacitor C_2 was to decouple any AC signals from the DC supply. The square wave was then directly coupled to the parallel transistors through a bank of six switches. Switches were used in order that different parallel combinations could be obtained. A common connection was made between all the semiconductors to one common load, and the other side of the load went to the negative terminals of the DC supply. All emitter resistances were connected to a common point which was returned to the positive terminal of the DC supply.

The emitter resistances (R_e) were constant for all transistors. A value of 0.1 ohms was used. In order to insure current sharing, the base resistance (R_b) for each device was fixed at a value dependent upon each specific amplification (B) factor. The circuit shown below was used to determine this resistance.



R_b was adjusted for a current of one ampere in the emitter leg. This was done for each unit.

Figure 113 illustrates the completed layout used for the test. Base resistors, emitter resistor and switches were mounted on a separate breadboard. Connections are then made to transistor sockets mounted on a copper plate. The transistors are then inserted into the sockets from the back side of the plate. Copper tubes were brazed to the copper plate between the semiconductors. These tubes were connected to two manifolds for the purpose of conducting water to cool the devices. Since the cooling plate was copper, the units were mounted directly to the plate and the plate was used as the common collector connection.

Figures 114 and 115 show the complete bench setup. The carbon pile load is shown in the foreground of Figure 110. Table 29 lists the instrumentation utilized for the tests. All equipment was calibrated prior to starting of tests. It was believed that this setup would prove sufficient to define the parallel operating characteristics desired.

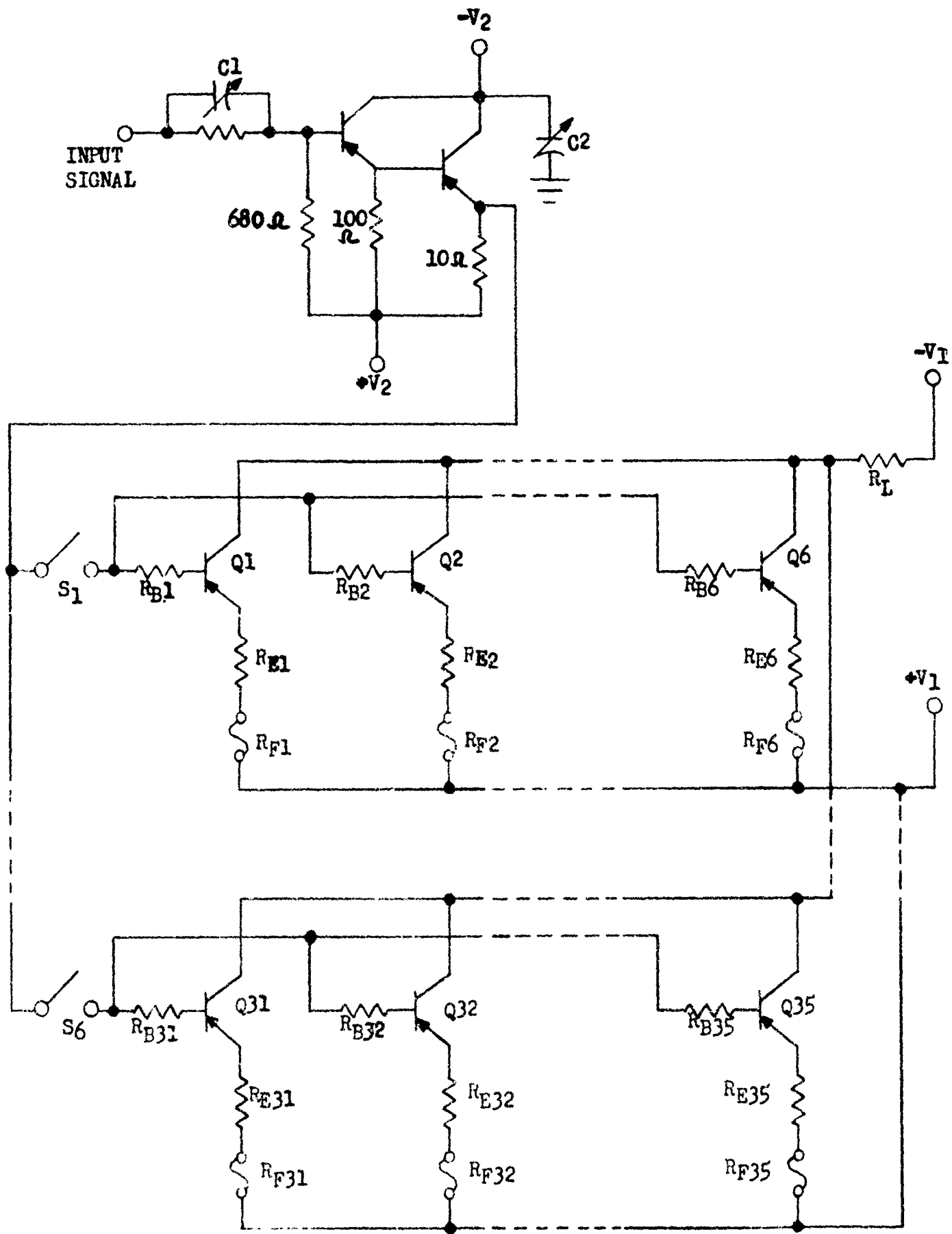


Figure 112. Test Circuit Schematic

TABLE 29
TEST INSTRUMENTATION

<u>INSTRUMENT</u>	<u>MANUFACTURER</u>	<u>MODEL NUMBER</u>	<u>RATED ACCURACY</u>
V.T.V.M.	Hewlett-Packard	410B	3% of full scale
Wheatstone Bridge	Leeds & Northrop	Type RN	1% of full scale
Oscilloscope	Tektronix	Type 535	3% of full scale
Square Wave Gen- erator	Hewlett-Packard	211A	
D.C. Power Supply	Con Avionics	Y 50-2	
D.C. Power Supply	N.J.E. Corp.	CR-36-20	
D.C. Power Supply	Generator Equipment	R300-28	
D.C. Ammeter	Westinghouse	Type NX-35	3% of full scale
Differential D.C.- A.C. Voltmeter	John Fluke Co.	803	± 0.05%



Figure 113. Test Setup Showing Mounted Transistors

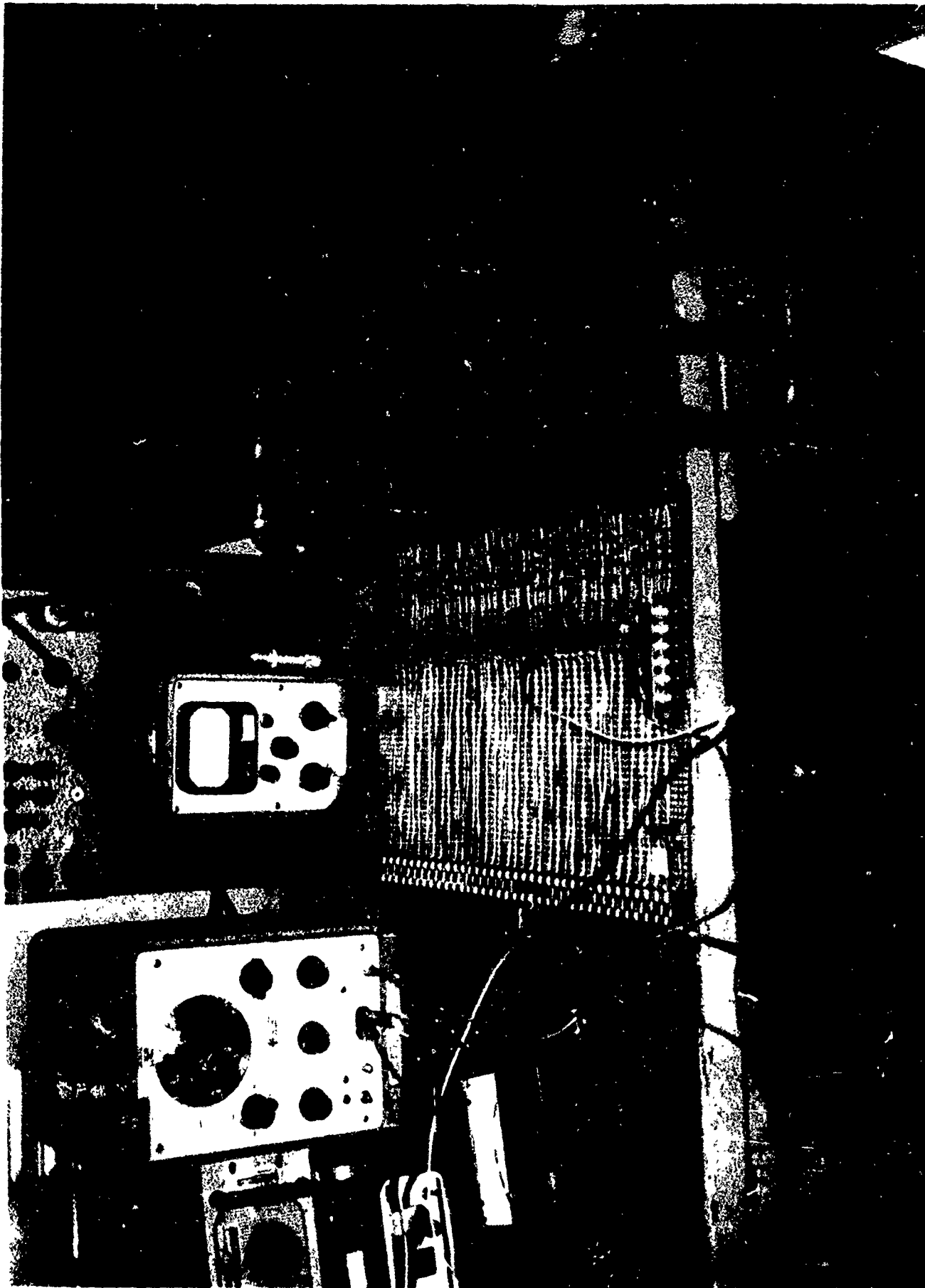
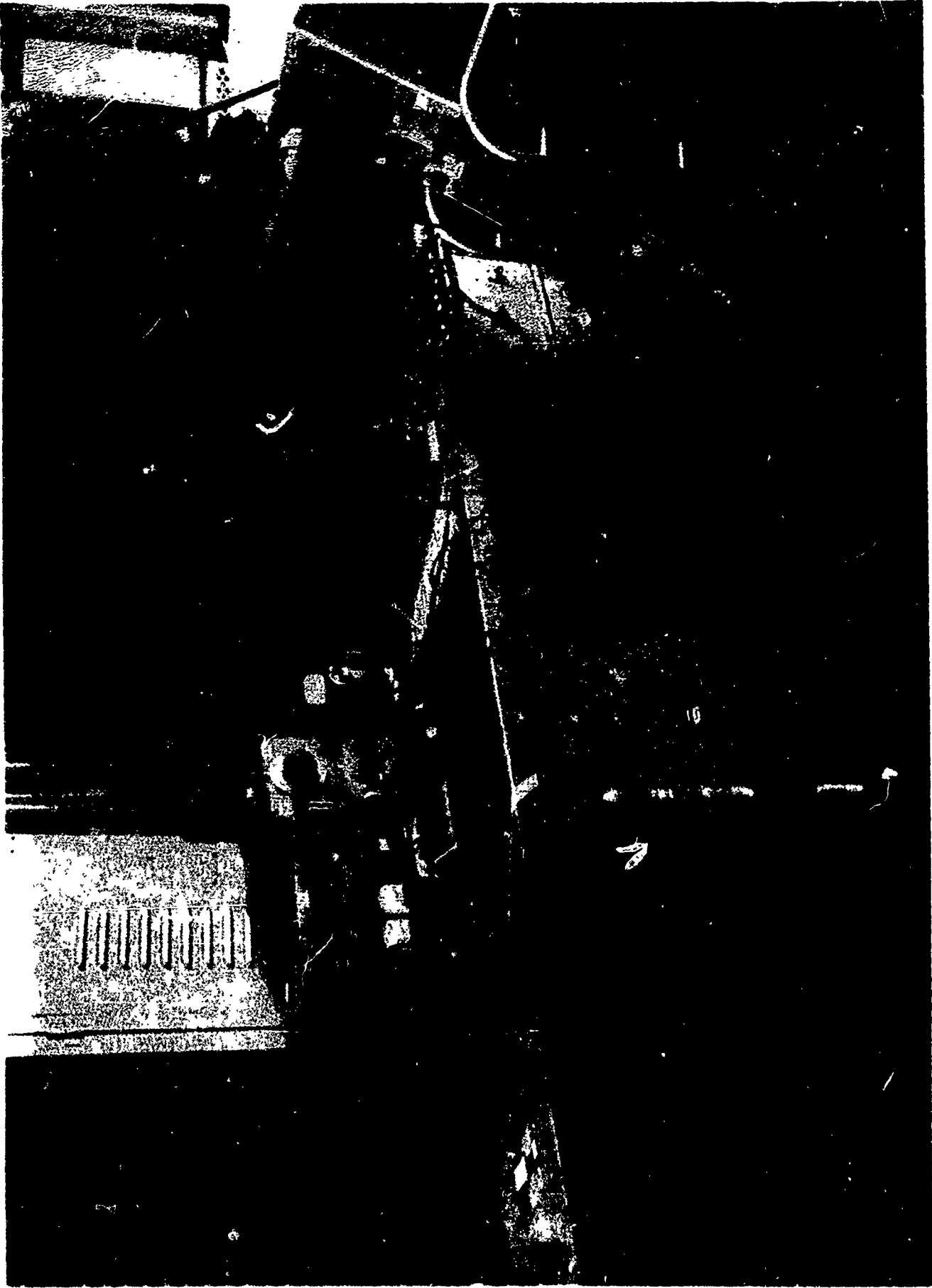


Figure 114. Test Setup Showing Transistors and Instrumentation



AREA

STAT

gram

Figure 115. Transistor Test Setup Showing Power Supplies

SECTION VI

CONCLUSIONS AND RECOMMENDATIONS

CONCLUSIONS

Conclusions reached at the end of the study program are:

1. Three techniques are feasible for converting SNAP 8 (60 KW) and SPUR (300 KW) types of power to high-voltage, high-frequency power suitable for electromagnetic engine use.
 - a. Static transistor techniques.
 - b. Static tube oscillator technique.
 - c. Motor-generator unit.
2. Of the three techniques analyzed during the program, the static transistor converter was lightest in weight and most efficient, as shown in Figures 1 and 2 in the Program Summary section.
3. The motor-generator concept is competitive with the static transistor unit at the 50 KC frequency, but becomes less appealing at the higher frequencies.
4. The static tube converter concept possesses both high-voltage and high-frequency capabilities. The overall efficiency of the tube system is below the design objective and inherent limitations of vacuum tubes prevent much improvement in this area. There is doubt as to the reliability of such a system in a space environment.
5. It is possible to produce the high-voltage, high-frequency power (10,100 volt, 50 KC to 200 KC) using an electromagnetic generator driven directly from a turbine. The technique involves use of a high speed (up to 30,000 rpm) solid-rotor machine in which the field windings are mounted in the stator section. Efficiencies of this type of generator fall in the 92 to 95 per cent range and weights are below the design objective of 1,000 pounds. Specific data is shown in Figures 3 and 6 in the Program Summary section.

AREAS FOR FUTURE RESEARCH

STATIC TRANSISTOR CONVERTER

Very preliminary tests performed in the experimental portion of the program to determine the response of transistors in parallel verified the power

chopper technique. Areas recommended for research include:

1. Further testing on the laboratory test specimens to determine maximum safe output levels for the power transistors and to determine (as much as possible) the reliability of the units in continuous operation.
2. Building of a converter unit, 60 KW, if possible, using the latest silicon power transistors in a prototype of the unit detailed in the report. (The test specimens used lower priced germanium transistors.) Test this unit with a specific engine load to determine load matching, power handling, effect of transient, throttling and other integrated system characteristics.
3. Analyze the power chopper technique, as analyzed in the study for an electromagnetic engine, for possible use in an AC to DC converter for ion engine use.

STATIC TUBE CONVERTER

Research in tube power converters should be performed in the following areas:

1. Optimizing a tube power converter to a specific existing electromagnetic propulsion engine design. The high-frequency power for most known electromagnetic propulsion engine research today is furnished by laboratory type r-f generator systems.
2. Building a prototype (breadboard) of a tube power converter (scaled down perhaps) to match a specific existing electromagnetic propulsion engine and testing to verify load matching, power handling, and other characteristics of the integrated system.

MOTOR-GENERATOR

Research proposed in this area includes:

1. Building of a breadboard 60 KW motor-generator unit to produce a 10,100 volt, 50 KC output using the solid-rotor technique analyzed during this study and detailed in the report. Research on materials, including bearing and seals, has proceeded to the point where this type of machine is feasible for a 60 KW, high-frequency design. (Machines at this power level at 1 - 3 KC are presently under development).

HIGH FREQUENCY GENERATOR

Research in the area of high-frequency generator techniques really parallels any work that might be performed in the area of a high-frequency motor-generator research. Specific research which should be performed in either area, and which would benefit both is:

1. Building a high speed, multi-pole generator unit using a solid-rotor technique to produce a high-voltage, high-frequency output. Such a unit would prove-out the high frequency capability of such a concept. With bearing, seal, magnetic material, and other component technologies now available for use in this type of generator, a prototype unit could quite easily be built for test and evaluation.

BIBLIOGRAPHY

Electromagnetic Generators

1. Electromagnetics, John D. Kraus, McGraw-Hill Publication.
2. Design of Electrical Apparatus, John Kuhlman, John Wiley Publication.

Electrostatic Generators

1. Thompson-Ramo-Wooldridge, Inc., and Atomics International, Advanced Space Propulsion Systems, WADC TR-59-365 Vol. II.
2. Trump, J. G., "Electrostatic Sources of Electric Power," Electrical Engineering, June 1947.
3. McCoy, F. J., Coenraads, C. N., & Denholm, A. S., "The Design of Electrostatic Generators for Operation in Space," ARS Paper 2052-61 presented in October, 1961.

Magnetic Multiplier

1. William McMurray, "Magnetic Frequency Multipliers and their Rating," July, 1957, AIEE Paper 57-91.
2. George W. Dick, "Symmetrical Frequency Multiplier Circuits," AIEE Paper 60-66, May, 1960.

Transformer

1. "Research and Development of New Design Methods for Power Transformers," G. A. Forsles, L. J. Stratton, H. Garluno, Final Report, March, 1956.
2. "Size Reduction of Air-Borne Transformers," AIEE Paper 57-1013, Ray E. Lee, January, 1958.

Semiconductor Design

1. Sorensen, Albert A., "Design Techniques for Static Inverter," Electrical Manufacturing, January, 1960.
2. Motto, J. W., Jr., "Gate Turnoff Controlled Rectifiers Simplify DC Power Supply Design," Military Systems Design, December, 1963.
3. Switching Transistor Handbook, Motorola, Inc., 1963.
4. Silicon Controlled Rectifier Manual, General Electric Co.

Static (Tube) Converter Design

1. Induction Heating, P. G. Simpson
2. RCA Electron Tube Handbook (HB-3) Transmitting Tube Section.
3. Reference Data for Radio Engineers, Fourth Edition, ITT Corporation

Generator Techniques

1. ASD TDR-62-472, Development of High Temperature Aircraft Electrical System, ASD Contract AF33(600)-35489.

2. Magnetic Circuits and Transformers, EE Staff at MIT, Technical Press Publication.

Environment and Cooling

1. Jakob, M., and Hawkins, G., "Elements of Heat Transfer," Third Edition, edited by Wiley and Sons.
2. Mandish, J. J., "Basic Analysis of Liquid Cooling Systems," Electronic Design, August 16, 1963.
3. John, J. E. A., and Hilliard, J. J., Power Transistor Cooling in a Space Environment, NASA TND-1753.
4. Katz, L., "Heat Design for Electronic Equipment," Electromechanical Design, December, 1963.
5. Streeter, V. L., Fluid Mechanics, edited by McGraw-Hill Book Co.
6. "Thermal and Atmospheric Control Study (USAF) Contract AF33(616)-7635, AF33(657)-8953, AF33(616)-8323.

Materials

1. WADC Technical Report 59-348, Ultra High Temperature (500°C) Power Transformers and Inductors, AF33(616)-5579.
2. WADC Technical Report 57-492, Vol. I, Ultra High Temperature Miniaturized Power Transformers and Inductor Materials, Vol. I, Electronics Components Lab, Contract AF33(616)-3623.
3. ASD TDR-62-477, Development of High Temperature Aircraft Electrical System, ASD Contract AF33(600)-35489.

Electromagnetic Propulsion Technique

1. William Corliss, "Propulsion Systems for Space Flight," McGraw-Hill Book Company.
2. A. S. Penfold and D. L. Curtis, "A Single-Phase Induction Plasma Accelerator," AIAA Paper 63012-63.
3. G. Fonda-Bonardi, "Development Potential of the Plasma Engine," AIEE Paper CP 62-1291.

APPENDIX

TRANSFORMER DESIGN TECHNIQUES

ANALYSIS OF SCR POWER CONVERTER

TRANSISTOR POWER CAPABILITIES

TRANSFORMER DESIGN TECHNIQUES

TRANSFORMER DESIGN FACTORS

The key factors in power transformer design are the selection of a core or lamination, the distribution of core and copper losses, and the purposeful design for the temperature rise and regulation requirements.

Core - Design of the transformers to be used in these power converter concepts has been based on a core type of device using laminations of the following material types: (See section of Materials for additional information).

Silicon - Iron	(1 mil)	1-3 KC
HYMU 80	(1 mil)	50-800 KC

Ferrite cores have been considered for use in this application, but they are limited because of their low Curie temperature.

Basic construction, both 1-phase and 3-phase is as shown in Figure 84. The coolant tubes are mounted flush with the core and tend to fill the gap between the winding and the core. For any given application, reduction of the cross-sectional area of the core requires a related increase in the number of turns of wire to produce the same flux density. This has a number of consequences. The core window area must be increased to accommodate the larger number of turns. The weight of wire and wire losses increase while the weight of iron and core losses decrease. A square cross section area has been assumed.

Laminations - In order to reduce the eddy current losses within the transformer core, it is necessary to use a core of thin laminated material. Lamination thicknesses as low as 1/8 Mil have been used in communication work, and in this way magnetic cores can be obtained that have fairly low loss even at high frequencies. One mil laminations are considered in these transformer designs. Additional tests should be performed on cores using available half-mil lamination.

Losses - With the flux densities fixed in core and copper, the minimum total loss transformer is the one for which the core loss is approximately equal to the copper loss at full load. Such a transformer will have maximum efficiency at full load.

The loss per pound for the transformer cores have been determined from Figures 90 and 91 for each of the designs. Copper loss has been directly calculated in each instance from the winding resistances and current through the winding.

Design Equations - Flux densities for each of the transformer designs were taken as 90,000 lines (13,750 gauss) for the 1 and 3.2 KC designs

and 15,000 lines (2330 gauss) for the 50 KC to 800 KC design. Current density in the copper windings was established at 1500 amperes/sq. in.

Transformer design has been based on the following equation:

$$\text{The induced voltage, } E = 4.44(f)(t)BA_c 10^{-8} \text{ volts} \quad (1)$$

$$I = (A)(s_c) \quad (2)$$

where f = frequency (cps)

A = 1500 amperes/sq.in.

t = number of turns

B = flux density (lines/sq.in.)

s_c = conductor cross sectional area

A_c = area of core section

I = current (amperes)

In the design of each transformer, ϕt was easily derived when the turns ratio was established by the voltage requirements and the converter frequency was selected. Total flux becomes:

$$\phi_t = \frac{E_h \times 10^8 \text{ lines}}{4.44(f)(t_h)} \quad (3)$$

Where $\phi_t = BA_c$, E_h = high voltage and t_h = number of turns in high voltage coil

With ϕ_t known, A_c was determined. The current in the high voltage winding was determined by

$$I_h = \frac{\text{KVA} \times 10^{-3} \text{ amperes}}{E_h} \quad (4)$$

And in the low voltage windings,

$$I_l = \frac{t_h \times I_h \text{ amperes}}{t_l} \quad (5)$$

The cross sectional area of the conductor for the high voltage and low voltage windings is

$$s_{ch} = \frac{I_h \text{ sq.in. (high)}}{A} \quad (6)$$

$$s_{cl} = \frac{I_r}{A} \text{ sq.in. (low)} \quad (7)$$

To obtain the desired ratio of core loss to copper loss, core window dimensions were chosen to

$$h/W = 3$$

where: h_w = window height and W_w = window width

The copper space factor, f_s , that is, the ratio of the net copper area in the window to the area of the window, varies with the capacity of the transformer and with the voltage of the windings. Values for f_s used for various transformers in designs was .36 for the three phase designs and .12 to .16 for the single phase designs.

For single phase transformers, the area of the window

$$h_w W_w = \frac{2(s_{ch} t_h)}{f_s} \text{ sq.in.} \quad (8)$$

and for three phase core type transformers

$$h_w W_w = \frac{4(s_{ch} t_h)}{f_s} \text{ sq.in.} \quad (9)$$

Core weight is calculated then from the volume of the core block minus the volume of the window area times the specific density of the core material. Wire weight was easily calculated by multiplying turns by the mean diameter of a single turn times cross-sectional area of the wire.

As discussed earlier in the section of Transformers in the preliminary concept portion of this report, the frequency level at which power is transformed plays a significant part in determining the weight of a transformer. In each of the converter design concepts, the voltage transformation (step-up) was made after the frequency change, in order to gain the weight advantage which comes with transformation at the higher frequencies. In the converter designs where a power supply in the output stage was required, the transformer weight was a significant part of the total weight.

ANALYSIS OF SCR FREQUENCY POWER CONVERTER

A 60 KW SCR CONVERTER DESIGN

A silicon controlled rectifier power converter is shown in Figure 116. Parametric data is summarized in Table 30. The design of the SCR converter is based on the free running power chopper. The design was based on the future availability of an SCR capable of switching 150 amperes of current and able to withstand blocking voltages up to 600 volts.

The 43.6/75.8, 3 ϕ , 1,000 cycle power is applied to the full wave bridge composed of diodes CR1 to CR6. The pulsating DC is smoothed by filter choke L_1 and capacitors C_1 and C_2 . The filtered DC is then applied to the anode of CR7 to CR10 through the current balancing reactor L_2 . Upon application of the DC voltage, capacitor C_2 starts to charge through resistor R_1 toward the applied voltage level. When the voltage across C_2 reaches the breakdown value of D_1 , D_1 starts to conduct applying a positive-going pulse to the SCR's CR1 to CR10 gates, causing them to conduct. The load current (600 amps) is applied through the primary of T_1 to the ground returns. At the same instant CR7 to CR10 starts to conduct, capacitor C_3 starts to charge through resistor R_2 . When the voltage across C_3 reaches the breakdown value of D_2 , D_2 starts to conduct applying a negative-going pulse to SCR CR7 to CR10 gates causing them to return to their blocking state. The cycle then repeats at a rate determined by the charging time constant of C_2 - R_1 and C_3 - R_2 . Resistors R_3 - R_6 are inserted in the SCR gate circuit to insure that each SCR will turn on at the same time. Inductor L_2 is used to force each SCR to share the same amount of current.

The frequency limitation of present SCR devices is such as to prevent operation in excess of 35,000 cps. However, it is anticipated that future developments in semi-conductor technology will produce SCR's capable of operating frequencies approaching 1,000,000 cps.

Comparison of SCR Static Converter and the Transistor Static Converter

A comparison of the SCR static converter with the transistor converter for a 60 KW, 50 KC, 1 ϕ unit shows that the SCR converter is approximately 20 pounds heavier. Additional weight is due to the current balancing reactor required to assure equal current division between SCR's. The SCR converter is more efficient than the transistor converter due mainly to the fact that SCR's are capable of handling more power per device than transistors. However, the transistor is capable of higher operating frequencies.

The SCR's used in the converter design are presently not available, but should be available in the near future. An examination of the SCR preliminary schematics shows that the SCR converter contains a lot less components than the transistor converter, and therefore, should be more reliable.

A few basic design differences between the SCR and transistor converters exist which affect the number of components used. The frequency stability

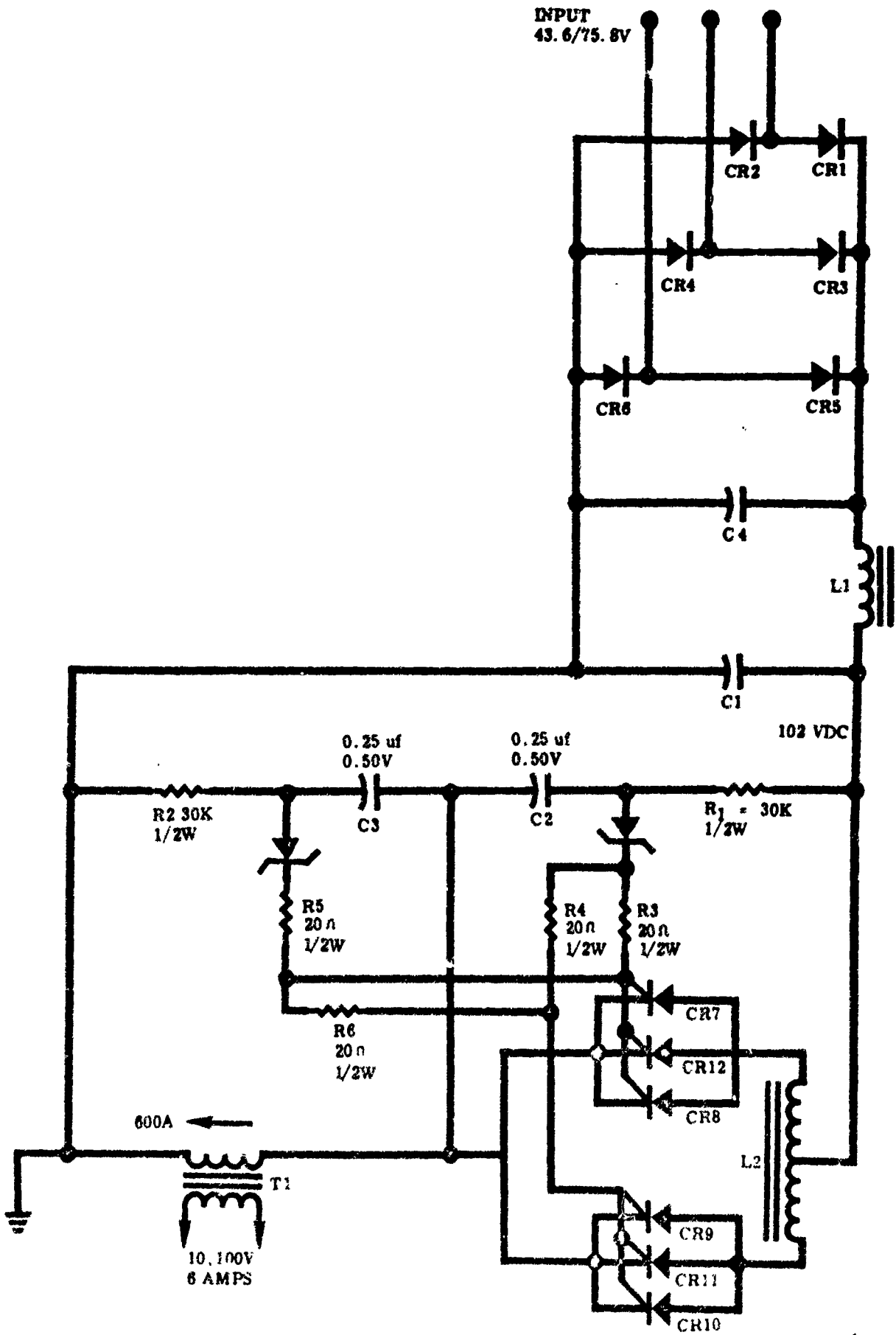


Figure 116. Schematic of 60 KW, 50 KC SCR Inverter
253

TABLE 30
 PRELIMINARY COMPONENT LIST FOR
 60 KW STATIC (SCR) CONVERTER 10

NO.	COMPONENTS	WT - LBS	LOSS - WATTS
	<u>Power Supply</u>		
6	Rectifier Semiconductor	3.0	1140.
2	Capacitor, Filter	.5	---
1	Filter Choke	18.0	3520.
	<u>Switching Section</u>		
6	Resistor	.01	3.
2	Capacitor Tuning	.3	---
	Diodes, Breakover (Shockley)	.2	0.5
1	Transformer Output	13.0	680.
6	Silicon Controlled Rectifier	3.0	600.
1	Current Balancing Reactor	8.3	600.
	Mounting Plate & Enclosure	35.0	
	Cooling Ducts	3.0	
	Controls	10.0	
	Wire & Hardware	18.0	
	TOTALS	172.3	6843.5

of the transistorized converter is controlled by an oscillator whereas the SCR converter frequency is controlled by the charging and discharging of an RC network. If extreme frequency control were required, the SCR converter could employ an oscillator similar to the one used in the transistorized converter, thereby increasing the total component count.

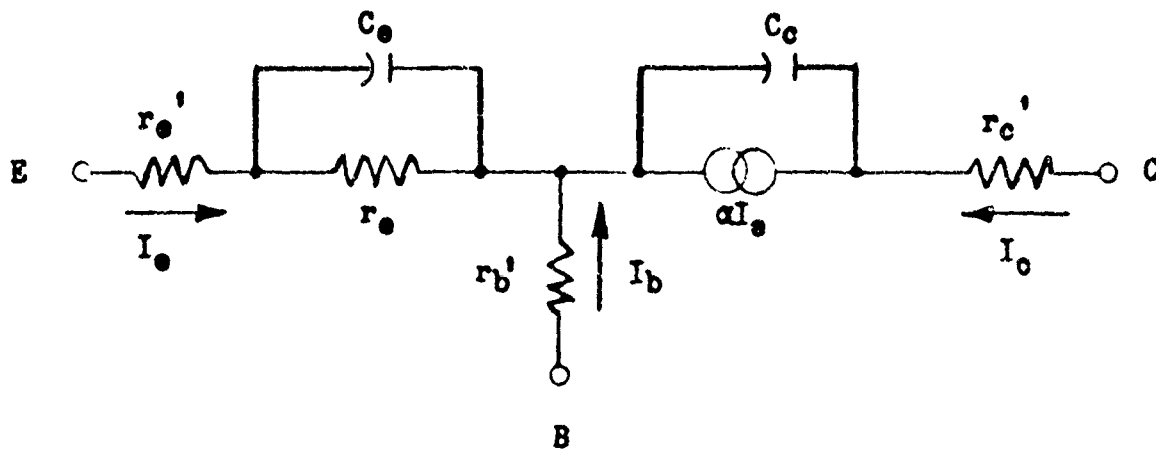
TRANSISTOR POWER CAPABILITIES

The design of the transistorized power converter was based on the availability of a transistor capable of switching 100 amps of current with a voltage rating of 500 volts and a frequency capability of 1 megacycle. Although this type of device is not presently on the market it should be available in 5 to 7 years through normal development. Consultation with several of the leading transistor research engineers has led to the conclusion that these devices can be made available sooner with an accelerated development program. The problems associated with development of these devices are discussed in the section which follows.

The mesa transistor developed in 1956 initiated high-frequency power transistor development, and although it has largely been replaced by the planar configuration, the mesa type of transistor still has the important advantage of high-voltage and high-current capability. First, high collector breakdown voltage, difficult to realize in shallow planar devices is readily obtainable in the larger mesa junctions. Secondly, by comparison with planar junctions, substantially larger mesa junction areas are economically feasible due to their relative freedom from contamination-induced defects such as phosphorus "pipe." Figure 117 shows the power frequency-material interrelationship (1963) for semiconductors. Power capability in the 50 - 800 KC range is limited to a 1 KW maximum (which is the product of voltage and current).

If we review some of the basic design theories of power transistors, we find that the theories consist of the original junction transistor theory of Shockley plus a collection of analysis attempting to improve upon this theory. Most of these theories are multi-dimensional and non-linear, and although these theories serve as a qualitative guide, they fall short of a precise quantitative theory.

Let us look at the T-equivalent circuit representations of a power transistor as shown below.



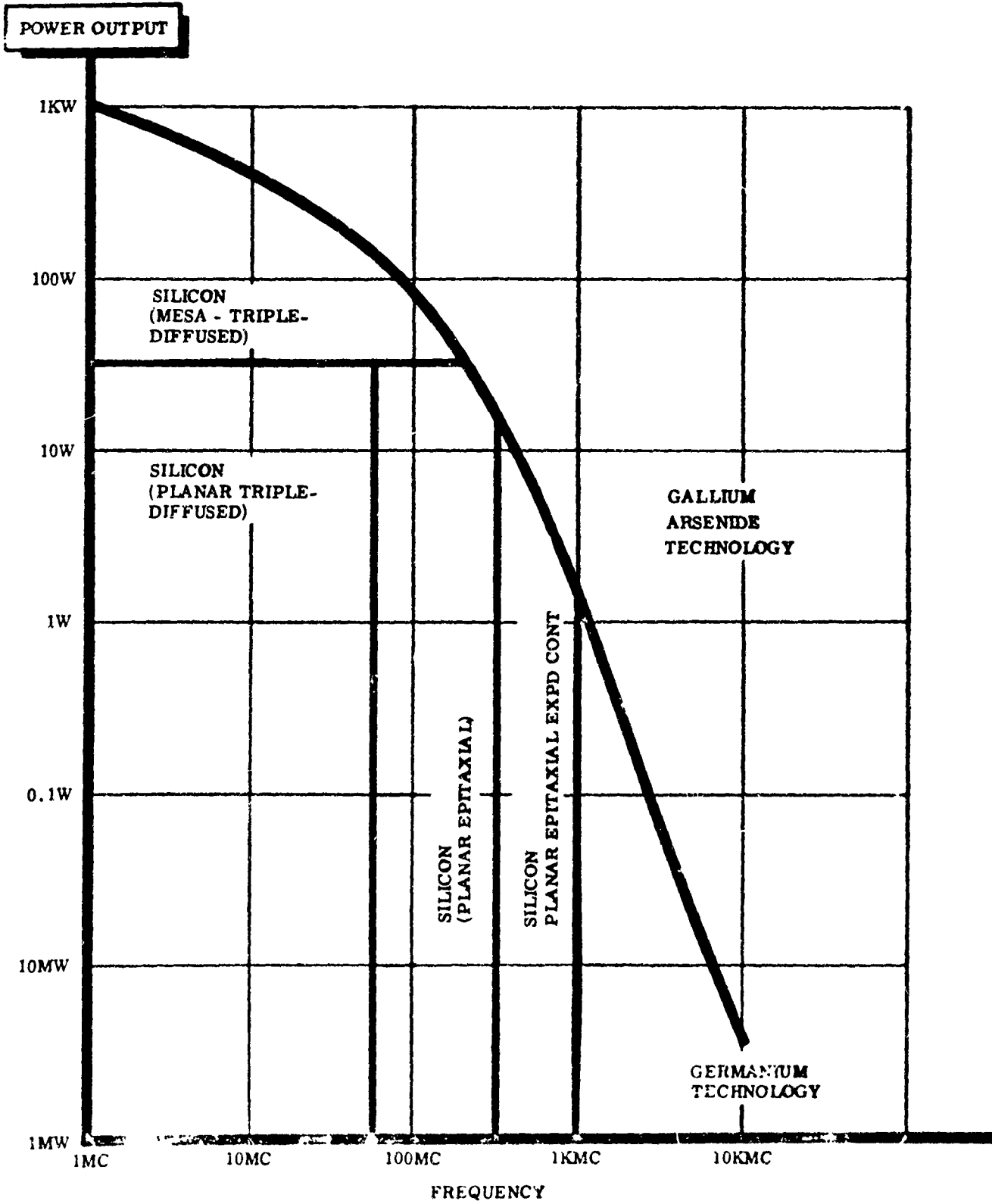


Figure 117. Power-Frequency-Material Relationship (1963)

We can write an expression for a figure of merit of a transistor, and if we use the power-gain bandwidth squared product, we will have an expression relating the high frequency performance of a transistor to the product of certain device parameters.

$$G_p (BW)^2 \frac{f_b}{4} \approx \frac{1}{\frac{1}{A_{f_0}} + \frac{1}{f_c} + \frac{1}{f_e}} \quad \text{where} \quad A_{f_0} = \frac{A_0}{1 + j f / f_{a_0}}$$

and

$$f_b = \frac{1}{2\pi r_b' C_c} \quad f_c = \frac{1}{2\pi (r_e' + r_e + r_c') C_c}$$

$$f_e = \frac{1}{2\pi r_e C_e}$$

where

A_0 = low frequency gain

r_e' = emitter parasite resistance

r_b' = base parasite resistance

C_c = collector junction capacitance

$r_e = \frac{26}{I_e (M_a)}$

r_c' = collector resistance

G_p = power gain

BW = bandwidth

f_b = base frequency

f_c = collector frequency

f_e = emitter frequency

C_e = emitter capacitance

If we rewrite the equation and substitute values for $A_{f_0} + f_b + f_e$ the equations take the form

$$G_p (BW)^2 = \left(\frac{1}{2\pi r_b' C_c} \right) \left(\frac{A_{f_0}}{1 + 2\pi(r_e + r_e' + r_c')C_c A_{f_0} + 2\pi C_e A_{f_0} r_e} \right)$$

This expression shows that the frequency response is dependent on certain RC time constants in the T-equivalent circuit.

Now, if we relate the geometry of a device to its effect on the transistor parameters, we note the following effects:

1. For high-current density the active volume will be much smaller than the total available volume due to the "edge effect." The current flow will be concentrated at the emitter edge. Therefore, the major power dissipation will take place at the collector junctions opposite the emitter edge. The active cross-sectional area of the transistor for high-current densities is proportional to the emitter edge length $2L$ and not to the emitter area.
2. Junction capacitances are, to a first order approximation, proportional to the geometry areas involved, and are, therefore, proportional to L .
3. Parasitic resistances are inversely proportional to the cross-sectional area of the material through which the current flows. Applying the geometry-parameter relationships to low-power, high frequency, devices with linear geometry, or interdigitated constructions. The scaling-up process is limited so far by the size of a semiconductor junction that can be produced that is free from contaminant-induced defects.

Now consider several design parameters that arise from the foregoing considerations.

1. For high current gain, the base must be thin.
2. To reduce effects of high-current density, utilize thin bases with low resistivity material. Maintain emitter efficiency close to unity by means of heavy emitter doping.
3. For low base resistance, the base layer should be thick.
4. For high collector to base breakdown voltage, utilize high resistivity in the base regions.

From these considerations we notice several conflicting parameters which result in the necessity of trading off high-voltage for high current or vice-versa. Present day requirements have been for the high current capability. The problem of obtaining increased power handling capabilities (higher current and higher voltage in the same unit) can be solved by material processing refinements and the use of different diffused structures such as the NPIN structure.

Distribution List for Final Report
for Contract AF33(657)-11049

<u>No of Copies</u>	<u>Activities at WPAFB</u>
1	FTDE 3A(Capt. R. J. Smith)
10	APIP-3 (Capt. H. L. Briggs)
1	AFIT (Library)
1	SEPRR (Library)
1	SEPR (Technical Reports Division)

Other U.S. Government Agencies

30	Defense Documentation Center Cameron Station Alexandria, Virginia
1	Power Information Center Moore School Building 200 South 33rd Street Philadelphia 4, Pennsylvania
1	NASA, Lewis Research Center Space Electrical Power Office Attn: Mr. Ernest Koutnik Cleveland 35, Ohio
2	Scientific and Technical Information - Facility Attn: NASA Representative (SAK/DL) P. O. Box 5700 Bethesda, Maryland 20014
37	OTS Stock 1200 South Eads Street Arlington, Virginia
1	Director Air University Library Maxwell AFB, Alabama

Distribution List for Final Report
for Contract AF33(657)-11049
(Continued)

No. of Copies

Other U.S. Government Agencies

1

U.S. Army Signal R&D Laboratory
Attn: SIGRA/IS-PS, Mr. A. F. Daniel
Fort Monmouth, New Jersey

1

Electrical Power Branch
Engineering Research Development Lab.
Attn: Mr. E. F. Cogswell
Fort Belvoir, Virginia

1

Army Research Office
Department of the Army
Room 3D442, Pentagon
Washington 25, D.C.

1

Director
U.S. Army Engineering Research and
Development Laboratory
Attn: Technical Documents Center
Fort Belvoir, Virginia

1

Bureau of Naval Weapons (Code RR-24)
Department of the Navy
Washington 25, D.C.

1

Office of Naval Research
Department of the Navy
Washington 25, D.C.

1

Bureau of Ships (Code 660)
Department of the Navy
Washington 25, D.C.

1

Naval Research Laboratory
Attn: B. J. Wilson
Washington 25, D.C.

Non-Government Organization

1

Lewis Allen Company
Attn: Arnold Bergson
427 East Stewart Street
Milwaukee, Wisconsin

1

Radio Corporation of America
224 North Wilkinson Street
Dayton 2, Ohio

1

Westinghouse Electric Company
32 North Main Street
Dayton, Ohio

Distribution List for Final Report
for Contract AF33(657)-11049
(Continued)

No. of Copies

1

Litton Systems, Inc.
Space Sciences Laboratory
Attn: Emil L. De Graeve
336 North Foothill Road
Beverly Hills, California

1

General Electric Corporation
Attn: Eugene L. Bartels
118 West First Street
Dayton 2, Ohio

1

Bendix Corporation
Red Bank Division
Attn: E. L. Badwick
Eatontown, New Jersey 07724